**ANNÉE 2013**

**THÈSE / UNIVERSITÉ DE RENNES 1**

*sous le sceau de l'Université Européenne de Bretagne*

pour le grade de

**DOCTEUR DE L'UNIVERSITÉ DE RENNES 1**

*Mention : Biologie*

**Ecole doctorale Vie-Agro-Santé**

présentée par


# Anne-Sophie DUMAS

Préparée à l'unité mixte de recherche 6553 Ecobio
Ecosystème, Biodiversité, Evolution
CNRS-Université de Rennes 1


---

# Mécanismes moléculaires de tolérance des plantes aux xénobiotiques: Application à la phytoremédiation des Hydrocarbures Aromatiques Polycycliques (HAPs)

**Thèse soutenue à Rennes**
**le 5 décembre 2013**

devant le jury composé de :

**Jacques BOURGUIGNON**
Ingénieur chercheur, CEA Grenoble / *rapporteur*

**Bertrand HIREL**
Directeur de recherche, INRA-AgroParisTech / *rapporteur*

**Malika AINOUCHE**
Professeur, Université de Rennes 1 / *examinateur*

**Alain BOUCHEREAU**
Professeur, Université de Rennes 1 / *examinateur*

**Gérard GAILLARD**
Executive Vice-President, Axson / *examinateur*

**Anis LIMAMI**
Professeur, Université d'Angers / *examinateur*

**Abdelhak EL AMRANI**
Maître de conférence, Université de Rennes 1 / *directeur de thèse*

**Richard BERTHOME**
Chargé de recherche, INRA Toulouse / *co-directeur de thèse*

**Remerciements**

Je tiens à remercier en premier lieu la société Axson Coatings et le groupe Axson pour avoir financé le projet ; en particulier Mr Gérard Gaillard, vice-président exécutif, pour avoir lancé le projet, Mr Denys Delcourt pour avoir effectué le suivi de la thèse, Mme Aline Fontaine pour tout l'aspect administratif et enfin Mr Pascal Frichot pour son aide pour son aide sur le terrain.

J'adresse tous mes remerciements à Mr Bourguignon et Mr Hirel pour avoir accepté d'être les rapporteurs de cette thèse ainsi qu'à Mme Ainouche, Mr Bouchereau et Mr Limami pour leur rôle d'examinateur.

Un gros merci à mes encadrants, Richard Berthome et Abdel El Amrani, pour m'avoir accompagnée dans cette aventure qu'est la thèse.

Merci à l'ensemble des gens de l'UMR Ecobio en particulier Delphine Bernard, pour son soutien et sa grande aide dans les expérimentations ; Valérie Gouesbet et Louis Parize pour leur appui technique que ce soit sur le terrain ou au labo ; les stagiaires (Morgan et Jérôme) qui ont fait un gros boulot sur le terrain. Merci à Morgane pour m'avoir aidée à prendre mes repères au sein du labo et puis avoir partagé café, bureau et soutien moral mutuel ! Moez, Rahma, Maria-Dolores et Mounir pour avoir partagé bureaux et labos. Le reste de l'équipe MOB (ancienne ou présente) pour les pauses midi, thé… Julie, Paula, Julien, Mathieu … mais aussi Alexandra et Anne-Antonella et tous les autres ! Merci à Agnès Schermann de m'avoir recueillie pour la fin de ma rédaction avant que je ne sois « sans bureau fixe ». Un grand merci à l'ensemble de l'équipe MOB puis à toutes les autres personnes d'Ecobio que j'ai pu côtoyer à un moment ou à un autre durant ma thèse.

Je tiens aussi à remercier l'ensemble des personnes travaillant à l'URGV pour leur accueil, leur aide et leurs parties de volley qui ont rendu mes quelques semaines dans leur labo très agréables.

Un gros merci à Emile Jardé et Laurent Jeanneau pour leur aide précieuse pour les analyses de HAPs.

Un coucou à toi Aurore pour avoir affirmé que « 2013, année de la thèse », c'est vrai mais après 10 ans tu sais beaucoup de chose !!

Enfin un gros merci à ma famille, mes parents et ma petite sœur (qui n'est plus si petite) pour leur soutient durant cette période de ma vie. Reste à voir ce qui va venir pour la suite…

« La souris est un animal qui, tué en quantité suffisante et dans des conditions contrôlées, produit une thèse de doctorat. »

**Woody Allen**

# Sommaire

*Chapitre 1 : Introduction générale* 11

Partie 1: Gestion des sols pollués 13
1. Introduction 13
2. Des régulations pour contrôler les pollutions 13
3. Les hydrocarbures aromatiques polycycliques (HAPs) 17
4. Les techniques de décontamination des sols pollués par les HAPs 20
5. Conclusion 27

Partie 2: Mécanismes moléculaires et physiologiques de la biotransformation des Hydrocarbures Aromatiques Polycycliques (HAPs) par les microorganismes et les plantes 29
Préambule 29
Abstract 33
1. Introduction 35
2. Microbial PAHs degradation 37
3. PAHs metabolization by plants 47
4. Strategies to improve PAHs bioremediation technologies 54
5. Conclusion 59
Bibliography 63

Partie 3: Les sucres solubles : des molécules-clés impliquées dans la tolérance aux stress abiotiques chez les plantes supérieures 75
1. Introduction 75
2. Les stress abiotiques modifient la teneur en sucres solubles chez les végétaux 76
3. Sucres et signalisation 78
4. Rôle des sucres dans la phytoremédiation 80
5. Conclusion 83

Partie 4 : Travail de thèse 84

*Chapitre 2 : Etude des modifications développementales, transcriptomiques et métabolomiques induites par le stress provoqué par le phénanthrène* 89

Préambule 91

Abstract 95

1. Introduction 97

2. Material and methods 101
2.1. Plant material and growth conditions 101
2.2. Measurement of seedling growth and development 101
2.3. Fluorescence microscopy 102
2.4. Transcriptome studies 102
2.5. Statistical Analysis of Microarray Data 103
2.6. ANOVA analysis 103
2.7. Biological pathways enrichiment 104
2.8. Clustering 104
2.9. cDNA Synthesis and Quantitative Real-Time PCR (qRT-PCR) 105
2.10. Targeted analysis of metabolites 106

3. Results-discussion 107
3.1. Phenanthrene altered plant development in a dose dependant manner 107
3.2. Phenanthrene uptake and localization in Arabidopsis 111
3.3. Transcriptome analysis of early plant response to phenanthrene exposure 113

4. Conclusion 135

**Literature cited** 195

**Préambule** 205

**Abstract:** 209

**1. Introduction** 211

**2. Material and methods** 213
- **2.1. Plant material and growth conditions** 213
- **2.2. Measurement of plant growth and development** 214
- **2.3. Fluorescence microscopy** 214
- **2.4. Phenanthrene quantification** 215
- **2.5. Targeted analysis of metabolites** 216
- **2.6. Transcriptome studies** 216
- **2.7. Statistical Analysis of microarray data** 217
- **2.8. Biological pathways enrichment** 218
- **2.9. Microarrays data validation by quantitative Real-Time PCR (qRT-PCR)** 218

**3. Results and discussion** 219
- **3.1. Sucrose induced tolerance to phenanthrene injury** 219
- **3.2. Cellular and histological localization of phenanthrene under protective sucrose condition** 223
- **3.3. Sucrose reconfigured transcriptomic and metabolomic profile under phenanthrene-induced stress** 227

**4. Conclusion** 241

**Bibliography** 305

***Chapitre 4 : Approche expérimentale pour l'amélioration de la phytoremédiation naturelle des HAPs: mise en place et conception d'un site pilote.*** *311*

**1. Introduction** 313

**2. Matériel et méthodes** 315
- **2.1. Mise en place du système expérimental** 315
- **2.2. Apports en saccharose et entretien du site** 316
- **2.3. Suivi du site pilote** 317
- **2.4. Echantillonnage et dosages des HAPs** 318
- **2.5. Analyses statistiques** 318

**3. Résultats-discussion** 319
- **3.1. Suivi du développement de la végétation sur le site pilote** 319
- **3.2. Estimation des capacités de stockage des HAPs par les 3 espèces végétales** 323
- **3.3. Les HAPs restant dans les sols après 21 mois de traitement** 329

**4. Conclusion et perspectives** 337

***Chapitre 5 : Conclusion générale et perspectives*** *351*

***Bibliographie*** *359*

# **Chapitre 1 :**
# Introduction générale

# Partie 1: **Gestion des sols pollués**

## 1. Introduction

Aujourd'hui, le développement durable est l'une de nos préoccupations majeures. Ce concept a été défini pour la première fois en 1987 comme « un développement qui répond aux besoins du présent sans compromettre la capacité des générations futures à répondre aux leurs » (Giddings et al., 2002). Le développement durable combine à la fois le développement économique avec l'équité sociale et la préservation de l'environnement. Le développement de l'agriculture moderne et l'industrialisation ont permis d'améliorer le niveau de vie de la population mais ont aussi engendré de nombreux problèmes environnementaux. Les marées noires, les rejets industriels, l'utilisation incontrôlée des pesticides et des fertilisants, la gestion des déchets domestiques et industriels qui ont eu lieu par le passé posent actuellement de nombreux problèmes.

## 2. Des régulations pour contrôler les pollutions

Afin de contrôler ces pollutions, des mesures ont dû être prises par les autorités dans un cadre de protection de l'environnement. En effet, dés 1989, les Etats-Unis mettent en place le premier texte à visée environnementale pour la protection de l'eau : « the Refuse Act for water protection » (Cowdrey, 1975). Le parlement européen a promulgué sa première loi environnementale en 1958, dans le premier traité de la Communauté Economique Européenne (CEE) (Jans and Vedder, 2008).

Pour gérer au mieux les sols pollués, des niveaux-seuils de régulation (RGV=regulatory guidance value) ont été mis en place par la plupart des nations. Ces valeurs sont des recommandations qui permettent aux autorités locales de mettre en place des règlementations pour la gestion des sites contaminés (Jennings, 2012).

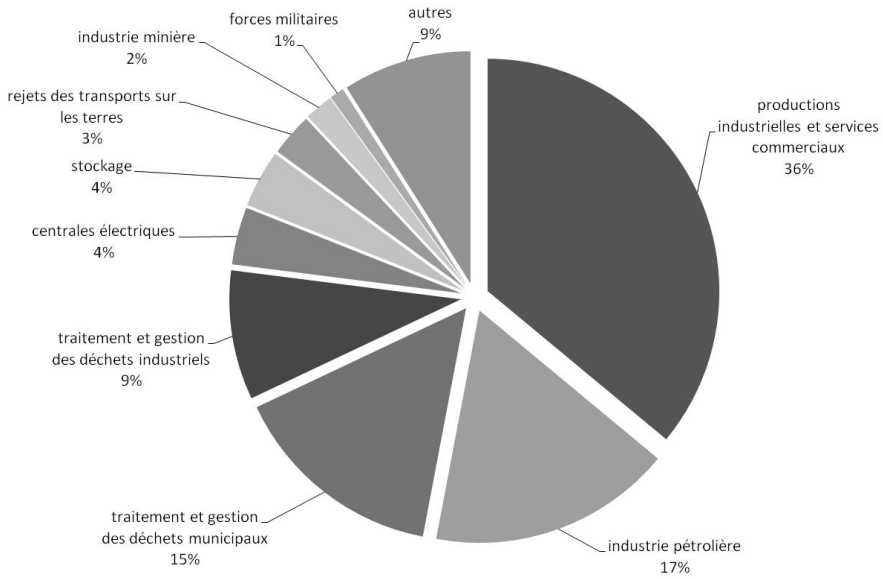


**<u>Figure 1</u> : Ensemble des activités responsables de la pollution des sols en Europe** (EEA, 2011a)

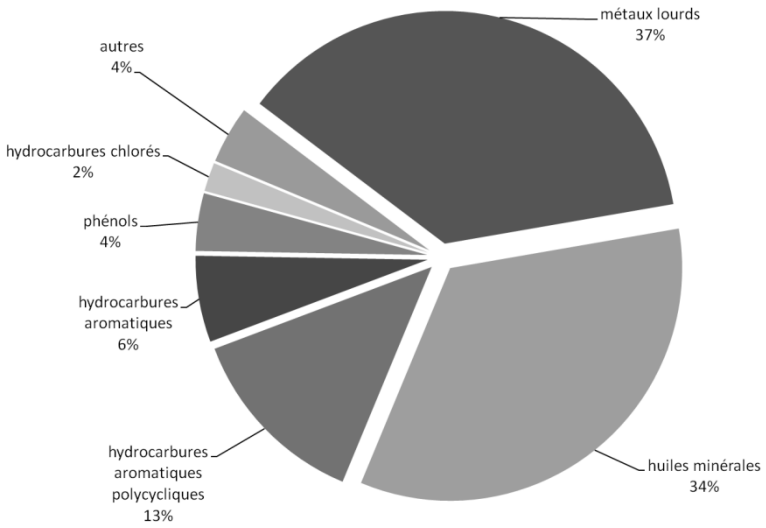


**<u>Figure 2</u>**

**: Ensemble des polluants affectant les sols et les eaux souterraines en Europe** (EEA, 2011b)

La régulation de la gestion de l'environnement a conduit à la création d'agences gouvernementales telles que l'Agence Américaine pour l'Environnement (USEPA) en 1970 et de l'Agence Européenne pour l'Environnement (EEA) en 1990. Leur rôle est de guider, d'informer, de prévenir et d'interagir avec les institutions gouvernementales et scientifiques ainsi qu'avec le monde industriel et agricole mais aussi avec l'ensemble de la population.

L'EEA regroupe 32 pays : les 27 Etats-membres de l'Union Européenne (UE) ainsi que l'Islande, le Liechtenstein, la Norvège, le Suisse et la Turquie. L'ensemble des données disponibles sur les pollutions des sols et des eaux souterraines, de ces pays, ont été collectées et publiées par l'EEA. En Europe, la production industrielle et les services commerciaux ainsi que l'industrie pétrolière et le traitement des déchets industriels et municipaux sont à l'origine de plus de ¾ des pollutions de sol (Fig. 1). Ces données soulignent l'impact négatif des activités humaines sur l'environnement.

De plus, les métaux lourds, les huiles minérales et les hydrocarbures aromatiques polycycliques (HAPs) représentent la majorité (84%) des polluants retrouvés dans les sols et eaux souterraines en Europe (Fig. 2). Le pétrole est la source de l'essentiel des pollutions de par la production d'huile minérale, d'HAPs et d'hydrocarbures aromatiques.

Actuellement, l'évaluation des sites pollués (nombre, types de pollution, état des lieux) est réalisée uniquement à un niveau national mais aucune base de données n'a été crée afin d'évaluer à l'échelle mondiale l'ampleur des sols pollués (nombre, localisation, répartition, mesures prises par les autorités…) et ce même si les Nations Unies ont développé un programme environnemental en 1972.

Lors de la conférence de Rio de Janeiro sur l'Environnement et le Développement (1992), les Nations Unies ont créé le principe du « pollueur-payeur » obligeant ainsi les responsables de pollutions à payer les frais de dépollution et de traitement du site pollué (UN, 1992). Ce principe a été adopté par le parlement européen en 2004 avec la directive (directive 2004/35/CE) sur la responsabilité environnementale (UE, 2004). Cette directive a été transposée dans la loi française en 2008 (Parlement Français, 2008). L'USEPA a aussi mis en place cette directive (EPA, 1996).

**Tableau 1: Liste des 16 HAPs appartenant à la liste des polluants prioritaires de l'USEPA**

| Nom | Structure | Formule | Solubilité dans l'eau | PM (g/mol) |
|---|---|---|---|---|
| Acénaphthène | 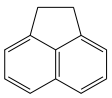 | $C_{12}H_{10}$ | 3,92mg/L | 154.21 |
| Acénaphtylène | 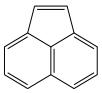 | $C_{12}H_8$ | 3,927mg/L | 152.20 |
| Anthracène | 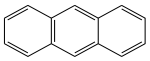 | $C_{14}H_{10}$ | 1,3mg/L | 178.23 |
| Benzo[a]anthracène | 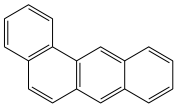 | $C_{18}H_{12}$ | 1,3mg/L | 228.29 |
| Benzo[a]pyrène | 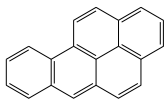 | $C_{20}H_{12}$ | 1,8mg/L | 252.31 |
| Benzo[b]fluoranthène | 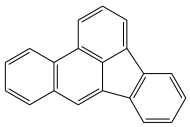 | $C_{20}H_{12}$ | 0,0061mg/L | 252.31 |
| Benzo[g,h,i]Perylène | 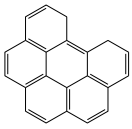 | $C_{21}H_{16}$ | 0,00026mg/L | 268.35 |
| Benzo[k]fluoranthène | 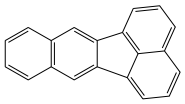 | $C_{20}H_{12}$ | 0,00076mg/L | 252.31 |
| Chrysène | 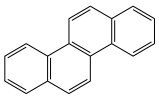 | $C_{18}H_{12}$ | 3,9mg/L | 228.29 |
| Dibenzo[a,h]anthracène | 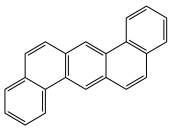 | $C_{22}H_{14}$ | 0,0006mg/L | 278.35 |
| Fluoranthène | 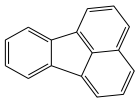 | $C_{16}H_{10}$ | 0,062mg/L | 202.26 |
| Fluorène | 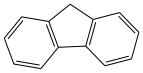 | $C_{13}H_{10}$ | 1,8mg/L | 166.22 |
| Indéno[1,2,3cd]pyrène | 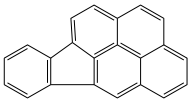 | $C_{22}H_{12}$ | 0,062mg/L | 276.33 |
| Naphtalène | 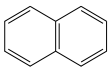 | $C_8H_{10}$ | 32mg/L | 128.19 |
| Phénanthrène | 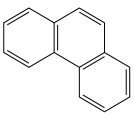 | $C_{14}H_{10}$ | 1,2mg/L | 178.23 |
| Pyrène | 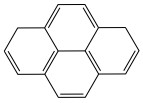 | $C_{16}H_{10}$ | 0,135mg/L | 202.26 |

L'agence américaine pour l'enregistrement des substances toxiques et des maladies qui leur sont associées (ASTDR, USA) établit, tous les deux ans, la liste des polluants nécessitant une action prioritaire de dépollution. Cette liste se base sur des critères tels que la fréquence, la toxicité et l'exposition potentielle de l'homme. De plus, l'USEPA a classé 16 HAPs sur sa liste des polluants nécessitant une action prioritaire (Tableau 1) (Wilson and Jones, 1993). Cette liste a été reprise comme référence par de nombreux autres pays.

## 3. Les hydrocarbures aromatiques polycycliques (HAPs)

Les HAPs constituent une vaste classe de composés organiques. Ces molécules peuvent être formées naturellement par les volcans ou les feux de forêts mais elles sont surtout produites par les activités industrielles et humaines.

### 3.1. Caractéristiques physico-chimiques des HAPs

Les HAPs sont constitués uniquement d'atomes de carbone et d'hydrogène assemblés en au moins deux cycles accolés.

Ils sont classés en deux catégories : les alternants qui ne contiennent que des cycles benzéniques (composés chacun de 6 atomes de carbone) et les non-alternants qui sont formés de cycles benzéniques mais aussi de cycles avec un nombre impair d'atomes de carbone.

Si les cycles sont assemblés de façon linéaire, alors le HAP est un acène comme, par exemple, l'anthracène (Tableau 1).

Les HAPs sont souvent classés en fonction de leur poids moléculaire : les HAPs avec deux ou trois cycles sont les HAPs à faible poids moléculaire (LMW HAPs= low molecular weight HAPs) alors que les HAPs avec quatre cycles ou plus sont les HAPs à fort poids moléculaire (HMW HAPs= high molecular weight HAPs) (Mrozik et al., 2003). Leur poids moléculaire influe

fortement sur leurs caractéristiques physico-chimiques comme leur solubilité dans l'eau. Les HMW HAPs, plus gros, sont beaucoup moins solubles dans l'eau que les LMW HAPs (Tableau 1).

De nombreux HAPs contiennent une région appelée « bay-region » et une région appelée « k-region » (Fig. 3) qui sont fortement réactives aussi bien chimiquement que biologiquement. Par exemple, les époxydes formés au niveau de la « k-region » sont bien plus carcinogènes que les HAPs à partir desquels ils ont été formés (Samanta et al., 2002; Mrozik et al., 2003).

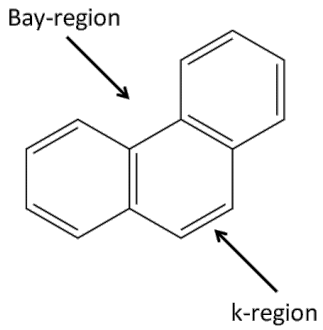


**<u>Figure 3</u>: Représentation des régions "bay-region" et "k-region" sur la molécule du phénanthrène**

Les propriétés physico-chimiques des HAPs dépendent de la structure de la molécule. Les HAPs sont fortement hydrophobes et possèdent un spectre d'absorption qui dépend du milieu dans lequel la molécule est étudiée.

Habituellement les HAPs fluorescent après avoir été exposés aux UV. Chaque HAP a son spectre d'émission spécifique qui dépend donc de la structure de la molécule. Presque tous les HAPs sont phosphorescents mais cette phosphorescence ne peut pas être détectée à température ambiante dans un milieu fluide (Dabestani and Ivanov, 1999).

### 3.2. Effets toxiques d'une exposition aux HAPs

Les HAPs sont des polluants organiques persistants (POP) qui sont présents dans l'atmosphère sous forme gazeuse ou particulaire mais aussi dans les sols, les sédiments et les boues. La carcinogénicité de cette famille de molécule a été évaluée et diffère en fonction du type de HAPs.

L'homme est exposé aux HAPs de différentes manières telles que l'inhalation, l'ingestion et le contact par la peau. De plus, il a été montré par Bjoerseth (1983) que la présence d'HAPs dans l'alimentation peut être due aussi bien à une contamination de la chaîne alimentaire qu'aux procédés de fumage et de cuisson des aliments. D'autre part, une étude américaine a révélé que 70% des HAPs reçus par une personne non-fumeuse provient de son alimentation en particulier des céréales, des huiles et matières grasses mais aussi des fruits, des légumes et des sucres. La viande, le poisson, le lait et les boissons ne sont à l'origine que d'un faible apport (Ramesh et al., 2004).

De nombreuses études ont montré que l'exposition de l'homme aux HAPs en milieu industriel et l'occurrence de cancers sont liés. La durée d'exposition (nombre d'années de travail dans ce milieu), le type de molécule, la dose reçue sont autant de paramètres qui sont pris en considération par les autorités pour les études sur l'impact des HAPs sur la santé (Boffetta et al., 1997).

L'effet allergène des HAPs a aussi été démontré. En effet, les émissions routières d'HAPs accentuent directement l'irritation allergique (Schober et al., 2007).

Ramesh et al. (2004) ont montré que les HAPs sont responsables de problèmes neurologiques, reproductifs et développementaux. L'exposition d'une femme enceinte aux HAPs a de nombreux effets sur son bébé. En effet, l'enfant sera plus prédisposé à développer des symptômes respiratoires et de l'asthme à l'âge de 12-24 mois (Miller et al., 2004; Jedrychowski et al., 2005). Les HAPs ont aussi un rôle important dans les premières semaines de grossesse. Une exposition à de fortes doses de HAPs augmente le risque de retard de croissance pour l'enfant (Dejmek et al., 2000). Certaines études ont établi un lien entre une exposition aux HAPs prénatale et un développement cérébral altéré. Des enfants exposés *in-*

*utero* aux HAPs présentent un retard dans leur développement cérébral à l'âge de trois ans et un QI plus bas que la moyenne à l'âge de cinq ans (Perera et al., 2009).

Les HAPs augmentent le risque de développer certains cancers comme celui du poumon (Smith et al., 2000; Armstrong et al., 2004), du sein (Rundle et al., 2000), de l'œsophage (Kamangar et al., 2005), du pancréas (Ojajärvi et al., 2000), de l'estomac (Ward et al., 1997), du colon (Sivaraman et al., 1994), de la vessie (Bonassi et al., 1989; Clavel et al., 1994), de la peau (Bizub et al., 1986), de la prostate (Rybicki et al., 2006) et du col de l'utérus (Mancini et al., 1999).

## 4. Les techniques de décontamination des sols pollués par les HAPs

Il existe deux types de traitement des sols : les techniques *in-situ* (Fig. 4A) qui traitent directement le sol pollué et les techniques *ex-situ* (Fig. 4B) qui nécessitent une excavation du sol avant son traitement. Le traitement *ex-situ* peut être fait dans une unité de traitement installée directement sur le site ou dans un centre spécialisé. En France, en 2008, 24% des terres étaient traitées *in-situ*, 21% *ex-situ* directement sur le site et 55% *ex-situ* dans un centre de traitement (ADEME, 2011).

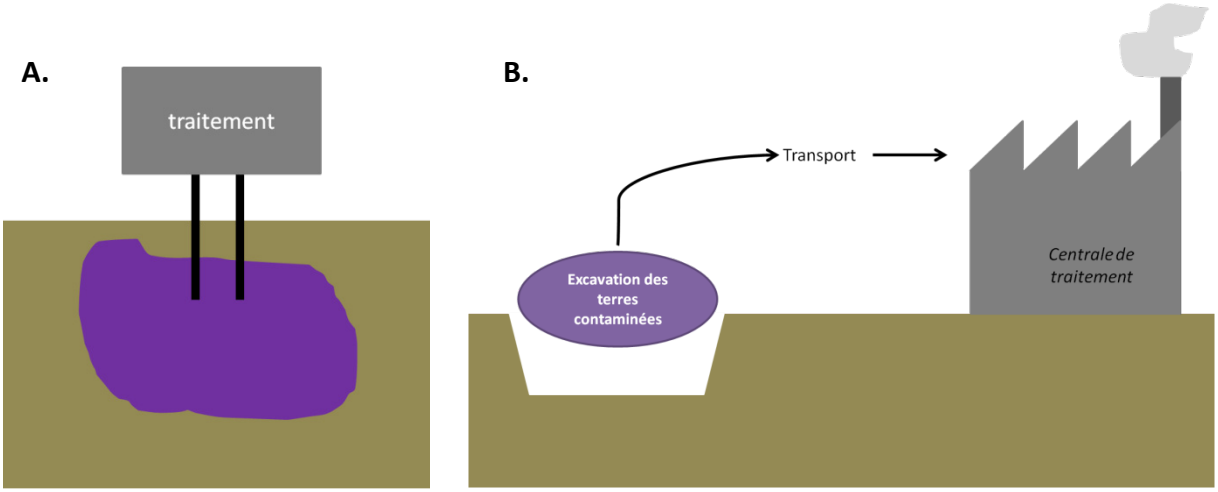


**Figure 4: Principes des traitements *in-situ* (A) et *ex-situ* (B).**
Dans les techniques *in-situ,* le sol pollué (en violet) est traité directement alors que les techniques *ex-situ* demandent une excavation des terres contaminées qui sont dépolluées dans une centrale de traitement.

## 4.1. Les techniques de traitement *in-situ*

### *4.1.1. Par voie biologique*

Le bioventing consiste en un apport d'oxygène dans le sol afin de stimuler la dégradation naturelle des HAPs par les microorganismes. C'est l'une des techniques parmi les moins coûteuses (entre 5 et 35€/t traitée) et qui est bien perçue par l'opinion générale. Cette technique reste tout de même lente tout en utilisant des processus naturels (ADEME, 2011).

Il est aussi possible d'améliorer la biodégradation naturelle des HAPs en stimulant l'activité des microorganismes naturellement présents dans le sol par la circulation de solutions nutritives dans le sol contaminé. Cette technique a un des coûts de mise en place parmi les plus faibles (entre 20€ et 75€/t traitée) (FRTR, 2002).

La phytoremédiation est une technique biologique de traitement des sols qui utilise les plantes, leur microflore associée ainsi que les techniques agronomiques pour diminuer la pollution environnementale. On peut distinguer (Pilon-Smits, 2005) :

- La rhizofiltration : les racines filtrent les eaux polluées (Fig. 5A). Les parties aériennes des plantes (les feuilles, en particulier) peuvent aussi servir de filtre de l'air (Fig. 5B).
- La phytoextraction/phytoaccumulation : la plante agit comme une « pompe » et extrait puis stocke directement les polluants du sol sans les modifier ni les conjuguer (Fig. 5C).
- La phytodégradation : la plante seule est capable d'absorber puis de dégrader totalement ou en partie le polluant (Fig. 5C).
- La phytovolatilisation : la plante est capable de libérer le polluant absorbé dans le sol ou un dérivé dans l'atmosphère (Fig. 5C).
- La phytostabilisation : la plante permet de piéger le polluant au niveau de ses racines et d'en diminuer la mobilité, ce qui empêche donc la propagation du polluant notamment dans les eaux souterraines (Fig. 5C).
- La phytostimulation/rhizodégradation : les plantes libèrent des exsudats ou des enzymes qui stimulent l'activité des microorganismes du sol et donc la transformation biochimique du polluant (Fig. 5C).

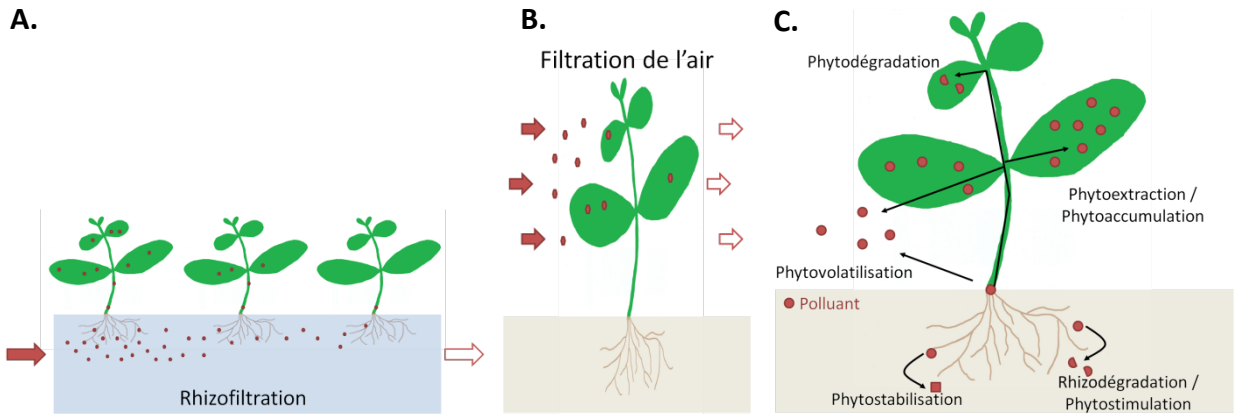


**<u>Figure 5</u>: Les technologies de phytoremediation pour la décontamination du sol, de l'eau et de l'air** (d'après Pilon-Smits, 2005).

Alors que la phytovolatilisation et la rhizofiltration sont des procédés permettant d'éliminer aussi bien des polluants organiques qu'inorganiques, la phytostabilisation et la phytoaccumulation sont des techniques plutôt adaptées pour les polluants inorganiques tels que les métaux lourds, grâce à l'utilisation de plantes hyperaccumulatrices (Marmiroli et al., 2006). La phytodégradation et la rhizodégradation sont des stratégies parfaitement adaptées aux polluants organiques tels que les HAPs (Ghosh and Singh, 2005).

La popularité de la phytoremédiation est liée à son bon rapport coût/efficacité (en moyenne 30€/m² traité) et à sa bonne perception par la population, car elle est considérée comme une « technologie verte ». Même si la phytoremédiation présente de nombreux avantages, cette technique de dépollution a tout de même quelques limites qui doivent être prises en compte. En effet, c'est un procédé plutôt lent qui dépend des propriétés du sol et des conditions climatiques ; il est plus approprié pour des pollutions peu profondes car son efficacité est limitée par la longueur des racines.

### *4.1.2. Par des procédés physico-chimiques*

Le confinement est une technique permettant de séparer physiquement le sol pollué du reste de l'environnement. Cette technique n'est pas permanente car elle ne permet pas d'éliminer le polluant du sol contaminé. Cette stratégie permet d'éviter la propagation de la pollution (Henner et al., 1997). Cette technique a un faible coût de revient compris entre 35€ et 60€ par tonne traitée (ADEME, 2011).

L'oxydation chimique consiste en l'injection d'un oxydant sous forme liquide ou de gaz dans le sol, de façon à ce qu'il soit en contact direct avec le polluant. Le polluant va être ainsi transformé sous une forme moins toxique ou plus facilement biodégradable. Cette méthode peut aussi s'utiliser *ex-situ* et son coût est compris entre 40€ et 90€ par mètre cube de sol traité (FRTR, 2002).

Le lavage des terres sur site consiste en une extraction des polluants en lavant les terres polluées avec de l'eau ou des solvants. Cette technique peut aussi être utilisée sur des sols excavés. Le coût de cette technique a été évalué entre 15€ et 60€ par tonne de terre traitée (FRTR, 2002; ADEME, 2011).

Il est aussi possible d'extraire les polluants du sol par évaporation. Une pompe à vide est utilisée afin de créer un gradient de pression/concentration qui induit la volatilisation en phase gazeuse du polluant qui est enlevé du sol grâce à des puits d'extraction. Cette technique est une des plus coûteuses : son coût de mise en place est estimé entre 300€/t et 1100€/t (FRTR, 2002).

La stabilisation physico-chimique *in-situ* consiste en une réaction chimique ou physique qui diminue la mobilité du polluant. Cette technique, comme le confinement, ne permet pas d'éliminer le polluant du sol et présente un coût relativement élevé d'environ 80€ par tonne qui peut monter jusqu'à 100€/t (ADEME, 2011).

#### *4.1.3. Par des traitements thermiques*

Les techniques thermiques permettent l'élimination des polluants en chauffant le sol pollué afin d'améliorer la désorption du polluant puis de le volatiliser ou l'extraire. Les vapeurs sont récupérées et traitées. Pour traiter une tonne de terre avec cette technique, il faut compter environ 80€.

### 4.2. Les traitements *ex-situ*

Les techniques *ex-situ* requièrent une excavation préalable des terres polluées, ce qui ajoute des frais de mise en place supplémentaires.

#### *4.2.1. Par des procédés biologiques*

Dans les biopiles, les terres polluées sont mélangées avec des amendements puis stockées dans des zones de traitement imperméables. Cette technique utilise les microorganismes afin de dégrader le polluant. C'est une technique à faible coût (environ 50€/t), facile à mettre en œuvre mais qui, comme pour l'ensemble des techniques de dégradation par voie biologique, est relativement lente (ADEME, 2011).

Le compostage consiste à mélanger le sol contaminé avec des amendements organiques et des agents de charge. Il est important avec cette technique d'avoir une bonne gestion des paramètres physico-chimiques du compost afin d'améliorer la dégradation du polluant. Le coût de revient de cette technique est estimé entre 500€ et 600€ par mètre cube traité (FRTR, 2002).

Le landfarming utilise les pratiques agronomiques afin de stimuler la dégradation du polluant. Les terres contaminées sont excavées et puis étalées en couches qui sont régulièrement labourées et enrichies afin d'optimiser au maximum la biodégradation du

polluant (Al-Awadhi et al., 1996; Atagana, 2004; Maila and Cloete, 2004). Le coût total de cette technique n'a pas été évalué mais on estime qu'il faut moins de 75€ par mètre cube de terre afin de mettre en place cette méthode de dépollution.

Il est aussi possible de traiter des terres polluées dans des bioréacteurs. Afin de traiter un mètre cube de terre avec cette technique, il faut compter entre 100 et 150€.

### *4.2.2. Par des procédés physico-chimiques*

L'extraction chimique consiste en un extracteur dans lequel les terres polluées sont mélangées avec un solvant afin de solubiliser le polluant. La solution solvant/polluant ainsi obtenue est placée dans un séparateur qui permet de séparer le solvant et le polluant. Ensuite, le polluant est traité et le solvant peut être réutilisé. L'utilisation d'huiles végétales comme solvant pour extraire les HAPs a été étudiée car ces huiles sont des solvants d'extraction non-toxiques, économiquement rentables et biodégradables (Gan et al., 2009).

L'oxydoréduction chimique est la conversion, par ajout d'un agent oxydant, d'un polluant en une forme moins hasardeuse ou moins dangereuse. Cette technique peut être aussi mise en place *in-situ* (cf. oxydation chimique). Le coût de cette technique est très variable et est compris entre 150€ et 500€ par mètre cube de terre traité (FRTR, 2002).

Les techniques de séparation permettent de concentrer les terres polluées par des procédés chimiques ou physiques tels que la gravité, le magnétisme ou le tamisage afin d'éliminer le polluant du sol.

Le lavage des terres est une technique consistant à extraire les polluants des terres en les lavant avec de l'eau ou des solvants. Cette méthode de traitement est aussi exploitée *in-situ*. L'efficacité de cette technique dépend de du type de solvant utilisé et du ratio terre/solvant appliqué. Un mélange avec 75% de cyclohexane et 25% d'éthanol s'est avéré être

le plus adapté pour éliminer les HAPs à cause de son efficacité et de sa sûreté (Gan et al., 2009). Cette technique coûte entre 50€ et 150€ par mètre cube de terre traité (FRTR, 2002).

Les procédés de stabilisation physico-chimiques utilisés *ex-situ* sont les mêmes que ceux mis en place *in-situ* mais dans ce cas-là ils sont appliqués sur sol excavé. Le coût de cette technique est d'environ 70€ par tonne de terre traitée (ADEME, 2011).

### *4.2.3. Par des méthodes thermiques*

L'incinération est l'utilisation de hautes températures comprises entre 870°C et 1200°C afin de brûler en présence d'oxygène les déchets dangereux tels que les terres polluées. C'est l'une des techniques les plus chères à mettre en place avec un coût situé autour de 330€ par tonne de terre traitée. L'impact écologique de ce type de traitement est important mais cette technique reste malgré tout une des plus efficaces notamment en termes de durée de traitement (ADEME, 2011).

La pyrolyse est une décomposition chimique induite dans les matériaux organiques par la chaleur en absence d'oxygène. Cette technique, un peu moins coûteuse que l'incinération, a un coût estimé à environ 250€ par tonne traitée (ADEME, 2011).

La désorption thermique consiste en la volatilisation de l'eau et du polluant organique qui sont ensuite transportés dans un système de traitement des gaz. Cette technique est la méthode de traitement thermique *ex-situ* la moins chère avec un coût allant de 35€ à 190€ par mètre cube traité (FRTR, 2002).

## 5. Conclusion

Avec l'augmentation du nombre de sites pollués dans le monde, les autorités ont dû prendre des mesures afin de prévenir les risques de pollution et pour traiter les sites pollués, ce qui a conduit à la création du principe du « pollueur-payeur ». Ce principe est appliqué par l'ensemble des pays membres de l'Organisation de Coopération et de Développement Economique (OCDE) et de l'Union Européenne. Avec ces nouvelles règles, il s'est avéré nécessaire de développer des techniques de traitement.

Parmi les xénobiotiques les plus répandus, les HAPs représentent un intérêt majeur en raison de leur dangerosité pour la santé humaine. De nombreuses méthodes ont été développées afin de décontaminer les environnements pollués par ces molécules. Ces techniques ont toutes leurs avantages et leurs inconvénients. Leur utilisation dépend de nombreux facteurs économiques et techniques. Même si les méthodes *ex-situ* sont actuellement les plus utilisées, les technologies *in-situ* représentent un atout considérable et apportent de nouvelles solutions souvent plus économiques afin de dépolluer l'environnement.

# Partie 2: **Mécanismes moléculaires et physiologiques de la biotransformation des Hydrocarbures Aromatiques Polycycliques (HAPs) par les microorganismes et les plantes**

**Préambule**

L'ingénierie écologique a permis l'émergence de nouvelles technologies telles que la bioremédiation et la phytoremédiation pour nettoyer les pollutions de l'environnement.

Cette introduction sous forme d'article de synthèse résume les dernières connaissances acquises sur les mécanismes moléculaires et physiologiques impliqués dans la biotransformation des hydrocarbures aromatiques polycycliques (HAPs) par les microorganismes du sol et les plantes.

Alors que la plupart des articles de synthèse portent soit sur les microorganismes, soit sur les plantes seules, cet article de synthèse aborde les interactions microbiennes notamment au niveau de la rhizosphère. En effet, les racines des plantes libèrent une grande variété de molécules contrôlant ainsi les populations fongiques et bactériennes, qui jouent un rôle central dans la dégradation des HAPs et d'autres molécules complexes.

L'émergence des approches globales, telles que la métagénomique, la transcriptomique, la métabolomique et la protéomique, sera discutée en mettant l'accent sur comment les approches « -omiques » ont permis de comprendre les mécanismes de bioremédiation afin d'améliorer les stratégies écologiques pour dépolluer les environnements contaminés par les HAPs.

**Title:** Molecular and physiological mechanisms of the biotransformation of PAHs by plants and microorganisms: contribution of “omics” approaches

**Authors:** Anne-Sophie Dumas[1], Richard Berthomé[2], Lukas Y. Wick[3] and Abdelhak El Amrani[1]

[1]Université de Rennes 1, CNRS/UMR 6553, Ecosystèmes-Biodiversité-Evolution, 35042 Rennes cedex, France.

[2]Laboratoire des Interactions Plantes Micro-organismes (LIPM), UMR INRA 441/CNRS 2594, CS 52627, 31326 CASTANET TOLOSAN CEDEX, France.

[3]Helmholtz Centre for Environmental Research – UFZ, Department of Environmental Microbiology, Permoserstraße 15, D-04318 Leipzig, Germany.

**Corresponding author**: Abdelhak El Amrani (abdelhak.elamrani@univ-rennes1.fr)

**Abstract**

The understanding of genetic and metabolic plasticity of leaving organisms to degrade and accumulate pollutants, allowed the emergence of new technologies such as bioremediation and phytoremediation to clean up environmental pollution. This review summarizes recent knowledge of molecular and physiological mechanisms involved in Polycyclic Aromatic Hydrocarbons (PAHs) biotransformation by micro-organisms and plants. Whereas most of available reviews have focused on PAHs degradation by either plants or micro-organisms separately, this review intends to address the interactions of plants and microbial consortia, present in the rhizosphere. Indeed, plant roots release exudates containing manifold signaling molecules controlling bacterial and fungal populations. These complex populations play a pivotal role in the degradation of high-molecular weight PAHs and other complex molecules. Emerging integrative approaches, such as metagenomic, transcriptomic, metabolomic and proteomic studies, are discussed, emphasizing on how 'omics' approaches bring new insights to decipher molecular mechanisms of PAHs degradation. This knowledge will help to set up integrative bioremediation strategies taking into account the rhizosphere population community and plants.

**Key-words:** PAHs metabolization, pollution, molecular mechanisms, 'omics'-approaches, bioremediation, phytoremediation.

## 1. Introduction

Polycyclic aromatic hydrocarbons (PAHs) constitute a large class of persistent and toxic organic compounds; they are generated from different anthropogenic and industrial processes and accidents such as crude oil spills. Their molecular structure contains two or more assembled aromatic rings. Thereby, they are classified into low-molecular weight PAHs (LMW; two to three rings) and high-molecular weight PAHs (HMW; more than three rings) (Mrozik et al., 2003).

In 2011, the Agency for Toxic Substances and Disease Registry (ATSDR, USA) ranked PAHs number 9 on the "CERCLA priority list of hazardous substances" with respect of their frequency, toxicity, human exposure and need of decontamination. Sixteen of the most prevalent PAHs thereby have been classified on the Priority Pollutant List of the USEPA (Wilson and Jones, 1993).

In order to overcome environmental concerns due to PAHs pollution in natural ecosystems, several implementations have been developed for soil treatment: (1) soil can directly be treated *in-situ* or (2) removed before being treated in a treatment center (*ex-situ* treatment), requiring excavation and transport. Traditionally, physico-chemical (solvent extraction, supercritical fluid extraction), chemical (chemical oxidation, photocatalytic degradation, electrokinetic remediation) and thermal (incineration, thermal desorption, thermally enhanced soil vapor extraction) techniques are used to remove PAHs from a contaminated soil (Gan et al., 2009). These techniques are efficient but expensive and impact the environment. Recently, ecological engineering approaches emerged as an alternative to these technologies (Mitsch, 2012). They use the ability of the environment to auto-restore itself with the natural action of living organisms. Indeed, it is common to define bioremediation and phytoremediation as the use of micro-organisms and plants, respectively, to clean up polluted environment. Accordingly, it is of high interest to understand the mechanisms involved in PAHs degradation by these organisms.

In this review, we summarize molecular mechanisms involved in PAHs metabolization by soil micro-organisms and plants and discuss their role in order to improve phyto- and bioremediation approaches of PAHs contaminated environments.

**Table 1: Different set-ups used in bioremediation**

| | Name | description | references |
|---|---|---|---|
| *in-situ* | Bioventing | This method consist in bringing oxygen into the soil to enhance natural degradation of the contaminant by micro-organism | Lee & Swindoll, 1993; Masten & Davies, 1997; Frutos et al., 2010 |
| | Enhanced Bioremediation | The activity of naturally occurring microbes is stimulated by circulating water-based solutions through contaminated soils contaminants | Liebeg & Cutright, 1999 |
| | Landfarming | This technique uses agronomical techniques to stimulate the degradation of the contaminant (mixing, aeration, moisture and nutrients additions) | Al-Awadhi et al., 1996; Atagana, 2004; Hansen et al., 2004 |
| *ex-situ* | Bioreactors | This technique uses naturally occurring micro-organisms (i.e. native micro-organisms population of the soil) or inoculated strains with specific metabolic capacities towards the PAH found in the soil to be treated. The bioreactor are designed in order to provide the best medium (nutrients, pH, temperature, oxygenation) for the microbial activity | Pinelli et al. 1997; Janikowski et al. 2002; Mohan et al. 2006 |
| | Composting | It consists in mixing the contaminated soil which was excavated with bulking agents and organic amendments. A good management of the physical and chemical parameters of the compost is essential for the success of this technology | ANTIZAR-LADISLAO, LOPEZ-REAL, and BECK 2004 |

## 2. Microbial PAHs degradation

Aerobic microbial PAHs degradation has been intensively studied and showed to require molecular oxygen to initiate the enzymatic attack (Cerniglia, 1992). Contrary, in anaerobic condition nitrate and sulfate are used as terminal electron acceptors, and has been observed only in enriched cultures (Al-Turky, 2009). In addition, little is known on the processes involved (Haritash and Kaushik, 2009). Hence, in this review, we will focus our analyses mainly on aerobic degradation.

This natural process has been used to remove man-made PAHs contamination from the environment. Indeed, technologies listed in table 1 are mostly used to enhance microbial activities. It has been shown that bacteria, fungi and algae share a common pathway for PAHs catabolism. The first step involves the action of a mono or a dioxygenase which introduces atoms of oxygen in the ring forming cis-dihydrodiols. This step implies that PAHs are taken up by the cells. Then, the oxidation of the cis-dihydrodiols forms aromatic dihydroxy compounds that are channeled through the ortho- or the meta cleavage pathway (Johnsen et al., 2005; Haritash and Kaushik, 2009).

### 2.1. Molecular and biochemical pathways of bacterial PAHs degradation

Till now, most studied bacteria strains degrading PAHs have been isolated from contaminated soil (Haritash and Kaushik, 2009). They belong mainly to a limited number of taxonomic groups such as *Sphingomonas*, *Burkholderia*, *Pseudomonas* and *Mycobacterium* (Johnsen et al., 2005). Indeed, several strains degrading LMW PAHs such as phenanthrene, and HMW such as benzo[a]pyrene, pyrene, acenaphthene, fluorene, anthracene and fluoranthene have been well described (Smith, 1990; Samanta et al., 2002). According to these works, efficient PAHs-degrading strains are likely to be oligotrophic, and are able to highly express genes involved in PAHs catabolism (Johnsen et al., 2005). Overall, it has been shown that enzymes involved in PAHs degradation are often coded by genes located in plasmid DNA. Interestingly several genes were found to be a part or flanked by transposon or transposon like-

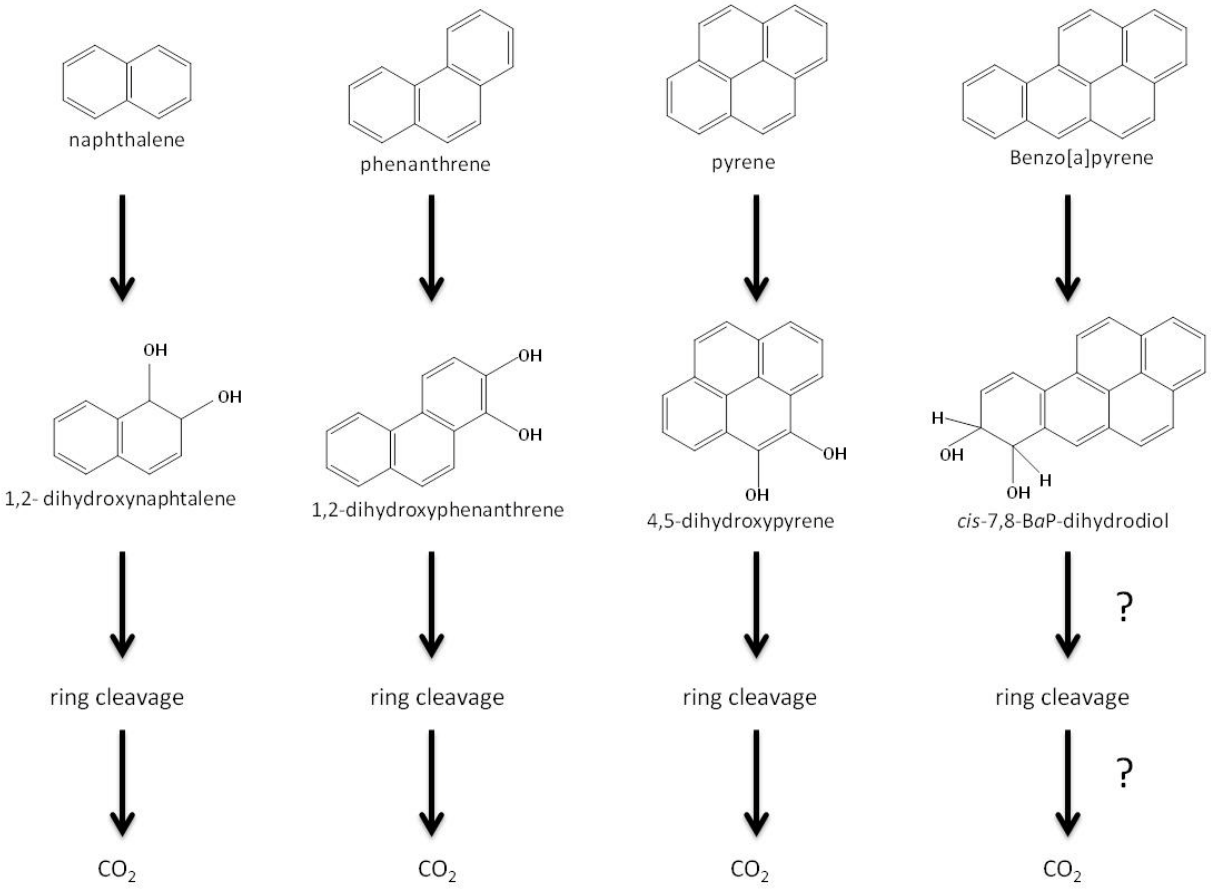


**<u>Figure 1</u>: Degradation pathways of different PAH by bacteria**

sequences, which suggested that plasmid encoded genes may have high spread activity among different bacterial population. Following are summarized some examples of PAHs degradation pathways identified in bacteria.

- Degradation of naphthalene: Naphthalene degradation is well known because it is the simplest and most soluble PAH. Most of the bacteria degrading naphthalene are from *Pseudomonas* genus. The degradation pathway by *Pseudomonas* was firstly described by Davies and Evans (1964) and is presented in figure 1. The first step is the oxidation of naphthalene by the introduction of both oxygen atoms into the aromatic cycle to form *cis*-1,2-dixydroxy-1,2-dihydronaphthalene by the dioxygenases. The dihydrodiol is then converted to 1,2-dihydroxynaphtalene by the naphthalene(+)-*cis*-dihydrodiol dehydrogenase and then goes under ring cleavage.

- Degradation of phenanthrene: Phenanthrene degradation pathways were described for *Pseudomonas*, *Mycobacterium*, *Arthrobacter*, *Aeromonas*, *Acidovorax*, *Sphingomonas, Staphylococcus* and *Nocardia* genera (Mrozik et al., 2003). *Staphylococcus* sp. Strain PN/Y can use phenanthrene as a sole source of energy. The complete pathway of phenanthrene degradation has been identified for this bacterium (Mallick et al., 2007). This pathway will be described here as an example of phenanthrene degradation by bacteria (Fig. 1). PN/Y initiates the degradation of phenanthrene by a dioxygenation at the C-1 and C-2 position leading to the formation of *cis*-1,2-dihydroxyphenanthrene which goes under a dehydrogenation to form the corresponding diol. Several reactions lead to the formation of catechol which after a ring cleavage goes into the TCA cycle.
  According to the different genus of bacteria, the degradation pathway can vary. The main differences are in the first step during the dioxygenation which can be on the C-1/-2 and on the C-3/-4 positions.

- Degradation of pyrene: Pyrene is a HMW PAHs which has been used as a model compound for HMW PAHs. Bacteria degrading this molecule are mainly members of the *Mycobacterium* and *Rhodococcus* genera. *Mycobacterium vanbaalenii* was reported as the first mineralizing pyrene strain. Kim et al. (2007) described a complete and integrated pyrene degradation using a combination of metabolite identification and genomic and proteomic analyses. Proteomic data and the genome sequence led to the identification of potential enzymes involved in the pyrene mineralization pathway shown in figure 1.

- Degradation of benzo[a]pyrene: Benzo[a]pyrene (BaP) is a HMW-PAHs which degradation has been observed for the genus *Mycobacterium*, *Pseudomonas* and *Bacillus* (Schneider et al., 1996; Kanaly and Harayama, 2000; Mrozik et al., 2003; Lily et al., 2009). Even little is known about bacterial HMW-PAHs degradation, the pathway of BaP degradation by Mycobacterium sp. Strain RJGII-135 is partially described (Fig. 1). BaP degradation starts by the dioxygenation of the molecule at the C-4/5 or C-7/8 or C-9/10 positions leading to the formation of the corresponding dihydrodiol. Then the dihydrodiol goes under ring cleavage. The complete mineralization pathway remains unknown.

Conventionally, PAHs degradation pathways have been elucidated using straightforward "step-by-step" techniques that include analytical chemistry, biochemical characterization for experimental identification of metabolic intermediates and key enzymes. Even if these approaches allowed deciphering several metabolic processes and mechanisms involved in PAHs degradation, most of the metabolic involved steps remains poorly understood.

Interestingly, high-throughput "-omics" approaches clearly revitalized the study of the PAHs catabolism and allowed to bring a global view of the process for PAHs polluted sites. Although, recent reviews listed proteomic approaches that have been used to study bacterial degradation of PAHs (Kim et al., 2007; Loh and Cao, 2008; Kim et al., 2009b), few reports described the real bacterial catabolic diversity of the environment and the *in-situ* functional characterization of catalytic activities.

In parallel, the use of stable isotope probing (SIP) could help to identify bacteria degrading PAHs and the proteins involved in such metabolic pathways. SIP is a method that consists in introducing $^{13}C$-labeled substrate, in our case PAHs, into cellular biomarkers such as proteins or DNA and in identifying populations that have integrated the labeled elements. Recently, DNA-based SIP has been already used to identify bacteria degrading phenanthrene, pyrene and naphthalene (Singleton et al., 2005; Singleton et al., 2007; Jones et al., 2011).

In other hand, focused screening using DNA library generated from metagenomic approaches and specific enzymatic activities, such as oxygenases, and their ability to produce yellow or blue coloration depending on the subtract used when expressed in *Escherichia coli* have been also carried out to better understand PAHs catabolism (Vilchez-Vargas et al., 2010). As an exemple, Brennerova et al. (2009) identified several dioxygenase activities in the community of a contaminated site. Interestingly, their results strongly suggested that the effective degradation of a mixture of aromatic compounds could be achieved through a complementary and a community balanced catalytic power against diverse derivatives.

### 2.2. Biochemical pathways of fungal PAHs degradation: an underestimated system?

Several fungi are known to degrade naphthalene, pyrene, phenanthrene, benzo[a]pyrene, fluoranthene, chrysene. In other hand, mycelial fungi such as *Aspergillus*, *Cladosporium*, *Cunninghamella*, *Penicillium*, *Phanerochaete*, *Pleurotus*, *Syncephalastrum* and yeasts like *Candida*, *Rhodotorula*, *Saccharomyces*, *Torulopsis* are PAHs-degrading fungi found in soil (Zhanf et al., 2006).

In contrast to bacteria, most fungi do not use PAHs as sole source of carbon, but they are significantly involved in PAHs degradation through the production of metabolites with higher water solubility which could enhance microbial activity in the soil (Cerniglia, 1997).

White-rot fungi are able to degrade a wide range of PAHs because of the lignin-degrading system encoded by their genome. *Pleurotus ostrateatus* is a good example of white-rot fungus for which metabolism of phenanthrene degradation is well described (Bezalel et al., 1996b).

However, fungal degradation of PAHs remains poorly understood even if several fungi have been identified as PAHs degraders.

We summarized below known metabolic pathways of fungus PAHs degradation.

- Degradation of phenanthrene*:* Among fungus*, Pleurotus oestreatus* has been described to be able to completely mineralize phenanthrene (Bezalel et al., 1996a; Bezalel et al., 1996b) (Fig. 2). The first step in phenanthrene mineralization is the $0_2$ incorporation by the cytochrome P450 monooxygenases (Bezalel et al., 1997). The phenanthrene 9,10-oxide formed is transformed by epoxide hydrolases leading to the synthesis of phenanthrene trans-9,10-dihydrodiol. The involvement of the lignolitic system in the ring cleavage system remains unclear even if experiments with [$^{14}$C]phenanthrene show its mineralization by the formation of $^{14}CO_2$.

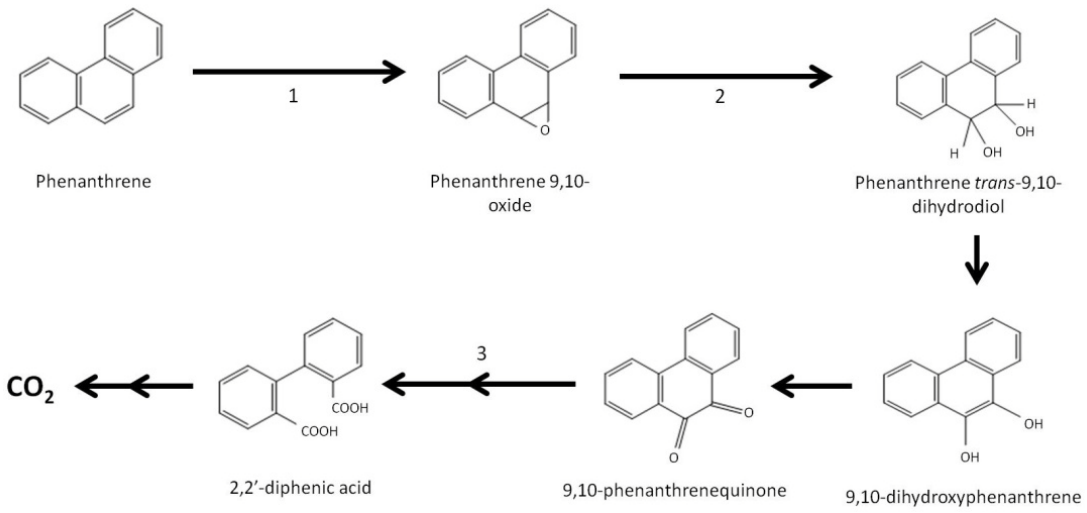


**Figure 2: Proposed pathway for phenanthrene degradation by *P. ostrateus***

1, Cytochrome P450; 2, Epoxyde hydrolase; 3, Ring cleavage enzymes. (adapted from Bezalel et al., 1996a; Bezalel et al., 1996b; Bezalel et al., 1997)

- Degradation of other PAHs: The white rot fungi *Bjerkandera* sp. strain BOS55 has been identified to mineralize benzo[a]pyrene but this mineralization is not really efficient and is, most of the time, not complete (Kotterman et al., 1998).

6 cytochromes P450 monooxygenases of the white rot basidiomycetes *Phanerochaete chrysosporium* have been characterized. These enzymes are able to oxidize pyrene, benzo[a]pyrene and phenanthrene which is the first step in PAHs mineralization by micro-organisms (Syed et al., 2010).

Indigenous fungi from a former gasworks site belonging to the *Penicillium* genus are able to use pyrene as the sole carbon source (Saraswathy and Hallberg, 2002).

But, in most described cases degradation of some PAHs is incomplete and could stop after the oxidative step leading to form dead-end products that can sometimes be metabolized by bacteria or have a negative effect on the microbial population of the soil (Andersson and Henrysson, 1996; Andersson et al., 2003).

### 2.3. Metabolic pathway of algae PAHs degradation

Algal biodegradation of PAHs is useful and has been developed for remediation of aquatic environment. Indeed, prokaryotic and eukaryotic algae, green algae and diatoms are known to metabolize naphthalene (Cerniglia et al., 1980).

Benzo[a]pyrene can be metabolized by marine algae (Warshawsky et al., 1995) within 5 to 6 days and by the freshwater green alga *Selenastrum capricornutum, Scenesdemus acutus* and *Ankistrodesmus reinhardtii* through a dioxygenase pathway to dihydrodiols (Fig. 3) (see Warshawsky et al. 1995). Fluoranthene and pyrene (individually or in mixture) have been reported to be metabolized by *Chlorella vulgaris*, *Scenedesmus platydiscus*, *Scenedesmus quadricauda* and *Scenedesmus capricornutum* (Lei et al., 2007).

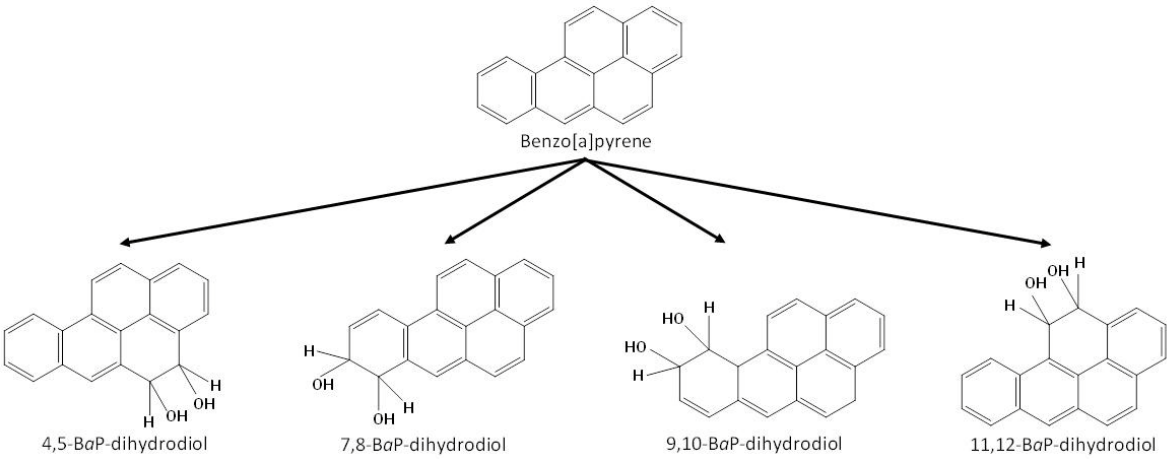


**<u>Figure 3</u>: Proposed dioxygenase pathway for benzo[a]pyrene (B*a*P) degradation by freshwater green algae.**

The dioxygenation of the benzo[a]pyrene is performed by a dioxygenase enzyme system leading to the formation of dihydrodiol.

Numerous studies showed that algae are suitable for PAHs bioremediation and acts co-metabolically with bacteria (Haritash and Kaushik, 2009). An *in-vitro* study with contaminated soil was carried out using algae *Filamentus chlorophyte* for PAHs removal. The soil with algae was flooded and showed a reduction of more than 90 % of the level of PAHs (Edema et al., 2011). These results showed the potential of algae mediated remediation especially in flooded conditions. Degradation pathways have been partially characterized at least for *Ankistrodesmus reinhardtii,* and several studies showed that the first step was identical to bacteria and fungi leading to the formation of diols (Cerniglia et al., 1980; Narro et al., 1992; Warshawsky et al., 1995).

## 2.4. PAHs involved meta-cleavage pathways in soil micro-organisms communities: incidence of consortium

Most of the available data explaining molecular and biochemical mechanisms involved in PAHs degradation has been obtained by laboratory studies using isolated pollutant-degrading micro-organisms or model strains. However, it is still misunderstood how such complex molecules are degraded by soil microbial communities.

*In-situ* technologies have used indigenous mixture of micro-organisms containing several strains of bacteria, fungi and algae which could act as a consortium. The interaction between the members of a consortium seems to be determinant for the PAHs degradation.

Indeed, Juhasz et al. (2000) used a mixture of five bacteria strains in their bioremediation techniques. Boonchan et al. (2000) showed that a fungal–bacterial consortium can degrade benzo[a]pyrene whereas the fungus or the bacteria cannot degrade it alone. These results suggest that there is a mutually dependent relationship between the fungus and the bacteria during the benzo[a]pyrene degradation as it has been as well proposed for bacterial consortium by Brennerova et al. (2009). Furthermore, Trzesicka-Mlynarz and Ward (1995) previously found that a consortium of four fluoranthene-degrading bacteria was more efficient than any individual isolate. It has been suggested that the pre-oxydation of the benzo[a]pyrene performed by the fungus might increase the bioavailability to the bacterial community. Unlike bacteria development, mycelia spread ubiquitously in the soil, penetrate air-water interfaces and cross over air-filled pores between the bacteria and contaminants. In air-filled soil, enhanced homogenization of bacteria and contaminants can be achieved by bridging physical air gaps with fungal hyphae thus enabling substrate-directed mobilization of bacteria along chemical gradients.

Recent studies demonstrated that mycelial dispersal networks influence both the microbial transport and the translocation of polycyclic aromatic hydrocarbons (Furuno et al., 2010; Kohlmeier et al., 2005). They showed that mycelial networks (i) act as effective dispersal networks for both undirected and chemotactic mobilization of contaminant degrading bacteria (termed by authors as ‘fungal highways’), (ii) increase the mobility of a wide range of PAHs due to their translocation in their cytoplasmic streaming (‘fungal pipelines’) with transport rates of

about 0.02 to 1.1 pmol ≙ 4 to 200 pg) per hypha per hour over a distance of 1 cm (figure 4) (Furuno et al., 2012), and thus improve the accessibility of bacteria to soil contaminants and, concomitantly, their biodegradation (Schamfuß et al., 2013a). Given their ubiquity and length of up to 1000 m.g-1 dry soil mycelial networks, fungus appear to play a significant role for the ecology of PAHs biodegradation in contaminated ecosystems (Harms et al., 2011).

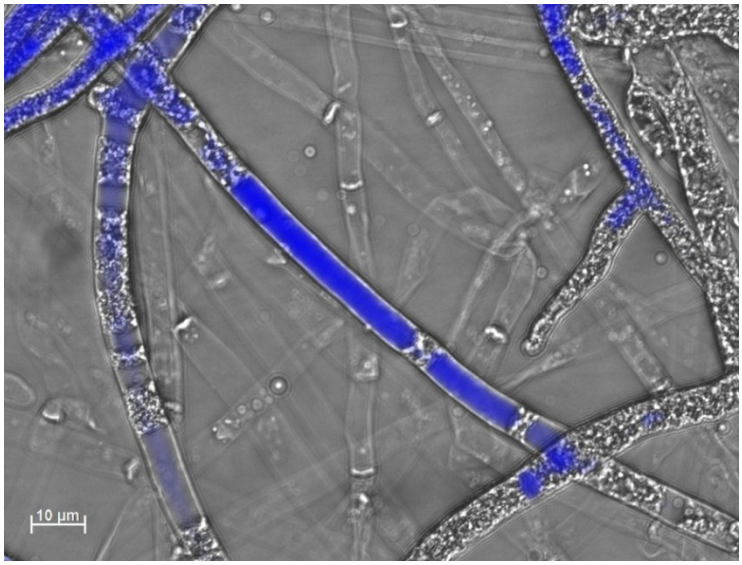


**Figure 4: Overlay of a transmission light and fluorescence micrograph (DAPI filter setting) depicting vesicle-bound FLU within hyphae of *P. ultimum* growing over MMA**

(Magnification 630x, bar 10 micro m). Micrograph by: S. Schamfuß and L.Y. Wick, UFZ.

Such data highlight the importance of the complementarities, both at the ecological and metabolic level, of the micro-organisms consortium, each component of the mixture being able to catalyze and use different PAHs derivatives.

Sequencing the 16S rDNA and analyzing the PCR-DGGE profiles, HuiJie et al. (2011) demonstrate that the degradation efficiency of a PAHs mixture depends on bacterial strains constituting the consortium and on the type of PAHs found in the contaminated soil. But it remains difficult to identify which species is doing what in a polluted environmental condition. However, such study might be of high interest and could contribute to bring solutions allowing the restoration of bacterial communities often perturbed in polluted soil.

Recently, Guazzaroni et al. (2013) used a metagenomic and a proteomic approaches to identify the strains compositions of communities, their capacity to metabolize PAHs and relative protein abundance, in a soil chronically contaminated by PAHs with or without biostimulation. Results indicate that biostimulation clearly improve soil PAHs decontamination but also strongly modify bacterial communities. Interestingly, metagenomic analyses of highly contaminated aromatic hydrocarbons site, revealed strong enrichment of genes encoding extradiol dioxygnenase, and high diversity and abundance of meta-cleavage pathways, suggesting that micro-organisms communities evolved and acquired selective advantage towards aromatic hydrocarbons degradation (Brennerova et al., 2009).

## 3. PAHs metabolization by plants

### 3.1. Molecular mechanisms Involved in plants PAHs detoxification

Description of PAHs absorption by plant organs has been addressed only for one PAH model: the phenanthrene. Alkio et al. (2005) showed that *Arabidopsis thaliana* was able to absorb and internalize phenanthrene. Thereby, its quantification using a GC-MS and the fluorescence characteristics of phenanthrene provides evidence that it was accumulates in plants tissues. Additional data based on fluorescence microscopy observations indicated that phenanthrene accumulates in trichomes of 14 and 21-day-old plants leaves. But it remains unclear if trichomes are an entry point for phenanthrene present in the air or a storage point of the phenanthrene absorbed by the roots and transported to leaves to prevent its toxicity.

Zhan et al. (2010) also studied the absorption of phenanthrene by roots using wheat as plant model. They showed that phenanthrene uptake involved two biological mechanisms: (i) a fast passive diffusion occurring just after the transfer of wheat in the phenanthrene supplemented medium and (ii) a slow active absorption mediated by a transporters that still have to be characterized.

Contrasting with numerous studies describing mechanisms involved in PAHs degradation by bacteria, fungus and algae, little is known about the mechanisms of PAHs metabolization and accumulation in plants.

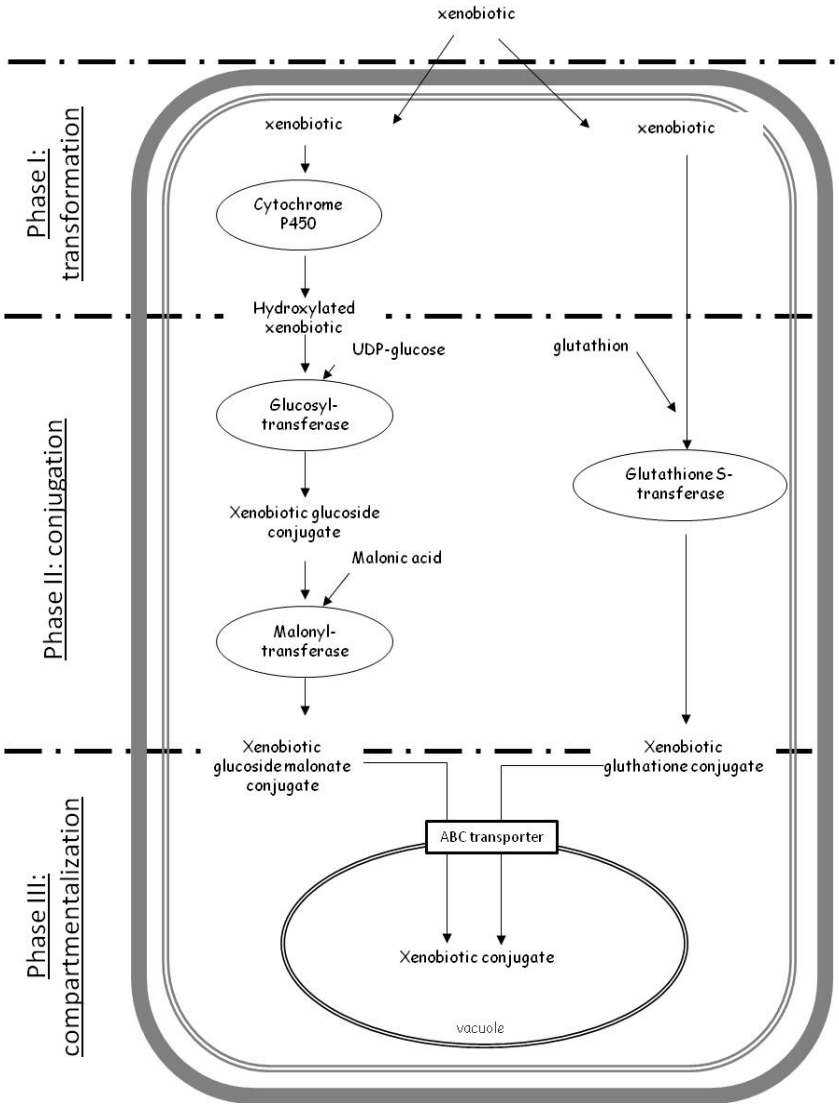


**Figure 5: Representation of the plant detoxification system**

*This model is set in three phases. (i) Transformation: xenobiotics are chemically modified using oxidation, reduction, or hydrolysis, this stage involved cytochrome P450 (CYP). (ii) Conjugation: the xenobiotics are conjugates to endogenous molecules. Glycosyltransferases (UGT) transfer nucleotide-diphosphate-activated sugars like UDP-glucose to low-molecular-weight substrates. The glycosylated xenobiotic is also conjugated with malonic acid by malonyltransferases (MT). The conjugation step can also be performed by the gluthatione-S-transferases (GST) by attaching the tripeptide gluthatione to xenobiotics. (iii) Compartmentalization: The conjugated xenobiotic is transferred to the vacuole or the cell wall by the ATP-binding cassette (ABC) transporters.*

However a “green-liver” model (Fig. 5) was proposed for plant organic pollutants detoxification mechanisms by Sandermann Jr (1992). It corresponds to an analogy of the detoxification system described in the mammalian liver. Processes involved in this model have been divided into two steps: (i) detection and signaling, (ii) transport and biotransformation (Sandermann Jr., 1992; Coleman et al., 1997; Edwards et al., 2011). Edwards et al. (2005) also proposed that “the whole expressed genome responsible for the detection, transport and detoxification of xenobiotics in the cell” constitute the xenome. However, even if general models of xenobiotics detoxification by plants are proposed, experimental data demonstrating that they can be applied to plant PAHs detoxification are still missing.

Despite the detection and signaling steps in plant are still unknown, enzymatic activities involved in the green-liver model, and encoded by genes that might belong to the xenome have been proposed. The transformation step which consists in making the xenobiotic more water soluble has been proposed to involve cytochromes P450 (CYPs). Indeed, these enzymes contribute to the phenanthrene degradation in fungi (Bezalel et al., 1996b; Syed et al., 2010). Additionaly, the glycosyltransferases (UGT), the gluthatione-S-transferases (GST) and the malonyltransferases (MT) participate to the conjugation step whereas ATP-binding cassette (ABC) transporters are involved in the compartmentalization step. Except for MT, reported to be encoded by two genes in *Arabidopsis thaliana* (Taguchi et al., 2010), all other components of the green-liver model are encoded by multigenic families. In *A. thaliana*, 244 CYP, 55 GST, 107 UGT and 120 ABC transporters have been respectively annotated (Dixon and Edwards, 2010; Bak et al., 2011; Edwards et al., 2011a)

Among the most promising studies performed to understand molecular mechanisms involved in PAHs remediation, a transcriptomic analysis on 21-days old *Arabidopsis* plants grown *in vitro* on a media supplemented with phenanthrene, showed that phenanthrene treatment induces expression of genes encoding proteins mostly involved in oxidative stress regulation or production (Weisman *et al*. 2010). The authors suggested that following the uptake, the phenanthrene might be oxidized by mono- or di-oxygenases, like the CYP, creating an increase in the reactive oxygen species (ROS) level which is responsible for the oxidative stress. However, it was still unclear if oxidative stress results from the activities linked to the phenanthrene detoxification or if it is an indirect consequence of its own or derivatives phytotoxicity.

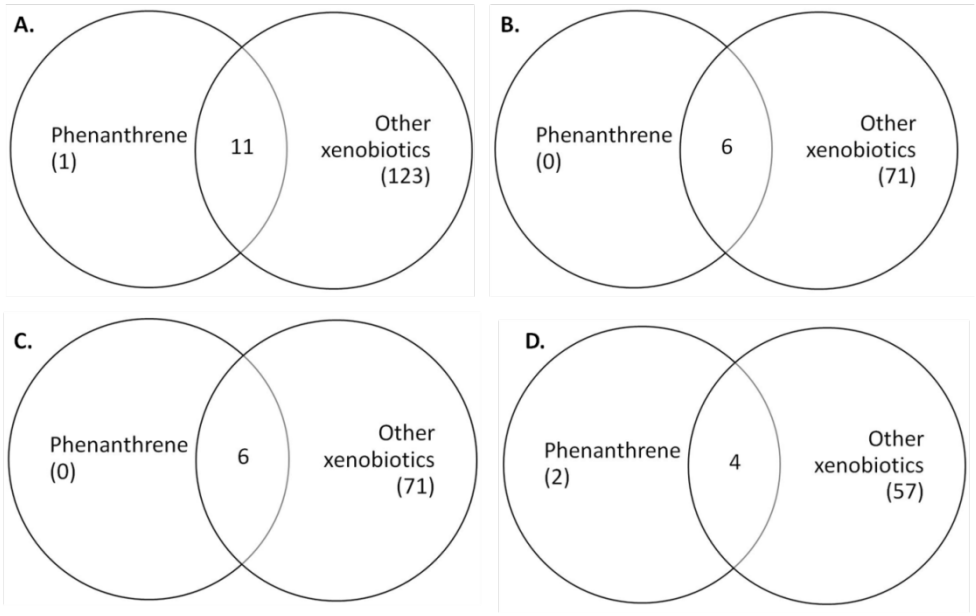


**Figure 6: Venn diagram depicting the number of *Arabidopsis* differentially expressed genes compared between data published in Weisman et al. (2010) and the list of potential genes belonging to the xenome extracted from available public data of wide-genome analysis carried out in the presence of xenobiotics experiment. Comparison of cytochromes P450 (A), glutathione-S-transferases (B), glycosyltransferases (C) and ATP-binding cassette transporters (D).**

Zhan *et al*. (2010) suggested that several physiological changes might occur very rapidly after phenanthrene exposure. To gain a better understanding of the mechanisms involved in the putative molecular processes involved in PAHs metabolization in plants, it was of high interest to focus on highly regulated genes involved within the few hours after the plant have been transferred to medium supplemented with PAHs. Hence, we performed a genome wide analysis using CATMA array after a short term phenanthrene exposure (data not shown).

Preliminary data indicated that the plant response could be divided in three phases: 1) an early response occurring within the first 30 min in which plant seems to sense phenanthrene rapidly, as genes mainly involved in perception and signalization are differentially expressed within the first 30 minutes, 2) a phase of reaction observed after 2h to 8h of incubation, characterized by regulation of genes involved in detoxification, 3) and a third exhausting phase from 8h where many differentially expressed genes are involved in repression of the secondary metabolism, this later being closely related to those described by Weisman *et al.* (2010).

During this last phase, late plant responsiveness to PAHs was characterized by the induction of numerous genes often regulated in plant response to stresses. In other hand, since no comparative data are available about the specific xenome induced after exposure of PAHs, it is reasonable to speculate that there are common genes shared with other xenobiotic.

Hence, we initiated a preliminary analysis where we collected all information available in public data bases carried out on the xenobiotic. These wide-genome analyses were collected from experiment using aluminum (Goodwin and Sutter, 2009), atrazine (Ramel et al., 2007), BOA (benzoxazolin-2(3H)-one) (Baerson et al., 2005), cadmium (Herbette et al., 2006), PCB (Polychlorinated biphenyl) (Jin et al., 2011), phenol (Xu et al., 2012), selenium (Van Hoewyk et al., 2008) and TNT (trinitrotoluene) (Landa et al., 2010) as xenobiotics. Then we have established a list of all the genes encoding a potential xenome protein (CYP, UGT, MT, GST and ABC transporters) that appeared differentially expressed in at least one transcriptomic analyses after *Arabidopsis* exposure to cited xenobiotics. We have confronted this list to the data obtained by Weisman et al. (2010) and found out that most potential xenome genes involved in phenanthrene detoxification are commonly regulated in other experiments, except for one cytochrome P-450 (AT5G47990) and two ATP-binding cassette transporters (AT1G51500 and AT5G44110) (Fig. 6). These findings suggest that plant xenobiotics detoxification shared

## **Table 2**: List of potential plants for phytoremediation of PAHs

| Molecule | Common name | Scientific name | Results obtained | References |
|---|---|---|---|---|
| anthracene | Poplar | *Populus nigra L. cv. Loenen* | oxidation of anthracene at a higher rate than in an unplanted soil, presence of products of anthracene degradation in the soil | Ballach et al., 2003 |
| benzo[a]pyrene | tall fescue | *Festuca arundinacea* | Residual benzo[a]pyrene lower in soil with plants (44%) than in the absence of plants (53%) | Banks et al., 1999 |
| benzo[b] fluoranthene | arrowhead | *Sagitaria latifolia* | 69-83% of benzo[b]fluoranthene removed after 13 months | Euliss et al., 2008 |
| | eastern gamagrass | *Tripsacum dactyloides* | 61-68% of benzo[b]fluoranthene removed after 13 months | |
| | Poplar | *Populus spp.* | 33-48% of benzo[b]fluoranthene removed after 13 months | |
| | sedge | *Carex stricta* | 79-86% of benzo[b]fluoranthene removed after 13 months | |
| | switch grass | *Panicum virgatum* | 71-79% of benzo[b]fluoranthène removed after 13 months | |
| | willow | *Salix exigua* | 41-69% of benzo[b]fluoranthène removed after 13 months | |
| fluoranthene | arrowhead | *Sagitaria latifolia* | 81-90% of fluoranthene removed after 13 months | Euliss et al., 2008 |
| | eastern gamagrass | *Tripsacum dactyloides* | 84-92% of fluoranthene removed after 13 months | |
| | Poplar | *Populus spp.* | 62-81% of fluoranthene removed after 13 months | |
| | sedge | *Carex stricta* | 91-95% of fluoranthene removed after 13 months | |
| | switch grass | *Panicum virgatum* | 92-97% of fluoranthene removed after 13 months | |
| | willow | *Salix exigua* | 62-95% of fluoranthene removed after 13 months | |
| naphthalene | tall fescue | *Festuca arundinacea* | mineralization of [$^{14}$C]naphthalene greater than in bulk soil | Siciliano et al., 2003 |
| phenanthrene | pea<br>soybean<br>sunflower<br>wheat | *Pisum sativum*<br>*Glycine max*<br>*Helianthus annuus*<br>*Triticum aestivum* | significant diminution of the phenanthrene in the growth medium | Liste & Alexander, 1999 |
| | white clover | *Trifolium repens* | 81.79–91.80% removal of phenanthrene in 60 days | Xu et al., 2006 |
| | | *Miscanthus giganteus* | almost 98% of phenanthrene disappeared | Técher et al., 2012 |
| | corn | *Zea mays* | 92.1% of phenanthrene removed from soil in 60 days | Xu et al., 2006 |
| pyrene | arrowhead | *Sagitaria latifolia* | 72-91% of pyrene removed after 13 months | Euliss et al., 2008 |
| | eastern gamagrass | *Tripsacum dactyloides* | 80-94% of pyrene removed after 13 months | |
| | Poplar | *Populus spp.* | 52-79% of pyrene removed after 13 months | |
| | sedge | *Carex stricta* | 72-91% of pyrene removed after 13 months | |
| | switch grass | *Panicum virgatum* | 71-79% of pyrene removed after 13 months | |
| | willow | *Salix exigua* | around 70% of pyrene removed after 13 months | |
| | dill<br>pepper<br>radish | *Anathum graveolens*<br>*Capsicum annuum*<br>*Raphanus sativus* | 52-68% of the total pyrene extractable has disappeared after 28 days | Liste & Alexander, 2000 |
| | jack pine<br>red pine | *Pinus banksiana*<br>*Pinus resinosa* | around 60% of the pyrene removed from the soil at 57 days | |
| | oat | *Avena sativa* | diminution of 62% of pyrene in soil after 56 days | |
| | rape | *Brassicca napus* | diminution of 78% of pyrene in soil after 56 days | |
| | | *Miscanthus giganteus* | around 70% of pyrene disappeared | Técher et al., 2012 |
| | corn | *Zea mays* | 88.36% of pyrene removed from soil in 60 days | Xu et al., 2006 |
| | rye grass | *Lolium perenne* | degradation rates of pyrene after 60 days: 70.39%-80.72% | |
| | white clover | *Trifolium repens* | 62.33–88.12% of the total pyrene had disappeared in 60 days | |
| total PAH | alfalfa | *Medicago sativa* | a reduction of 57% in total PAH concentration after 6 months | Pradhan et al., 1998 |
| | eelgrass | *Zostera marina* | decrease of 73% of the total PAH content | Hueseman et al., 2009 |
| | Salt marsh plants | *Spartina alterniflora* | detection of PAH in roots and shoots | Watts et al., 2006 |
| | switch grass | *Panicum virgatum* | a reduction of 57% in total PAH concentration after 6 months | Pradhan et al., 1998 |
| | willow | *Salix viminalis* L. 'Orm' | 23% of reduction of total PAH content in 1.5 years | Vervaeke et al., 2003 |

common molecular futures. Nevertless, PAHs exposure involved specific genes. Indeed, the identification and the functional characterization of these specific genes will bring new insights about specific detoxification pathway of the PAHs.

### 3.2. Adapted plant species to PAHs contaminated environment

Even if molecular mechanisms associated to the PAHs metabolization by plants are still under study, number of species have been described to grown on PAHs contaminated soil and to reduce their level in their environment. These species could be considered as potentially degrading PAHs molecules and might be useful for phytoremediation.

Screening of plant species involved in PAHs remediation is often realized *in vitro* using soil or growth medium contaminated with single PAH or a mixture of the 16 PAHs that are on the Priority Pollutant List of the USEPA (Table 1) as a total PAHs content. Mostly, studies evaluate the quantity of PAHs removed from the soil by plant compared to unplanted soil or the amount of PAHs absorbed by the plant to identify plants species adapted for phytoremediation. Table 2 listed potential PAHs degrading plants. Nevertheless, it remains difficult to identify the best plant for PAHs phytoremediation because plants do not remove each PAHs molecule at identical rate. Even if in general, LMW-PAHs are preferentially degraded, higher level of HMW-PAHs degradation rates were observed when combining several plant species compared to each plant alone (Xu et al., 2006; Cheema et al., 2010).

## 4. Strategies to improve PAHs bioremediation technologies

### 4.1. Plant-microbe cooperation enhance PAHs degradation : Rhizodegradation

Rhizodegradation (Fig. 7) is the convergence between phytoremediation and microbial bioremediation strategies which leads to a more efficient approach of sustainable remediation technology (Cunningham et al., 1995; Salt et al., 1995; Schnoor et al., 1995; Alkorta and Garbisu, 2001).

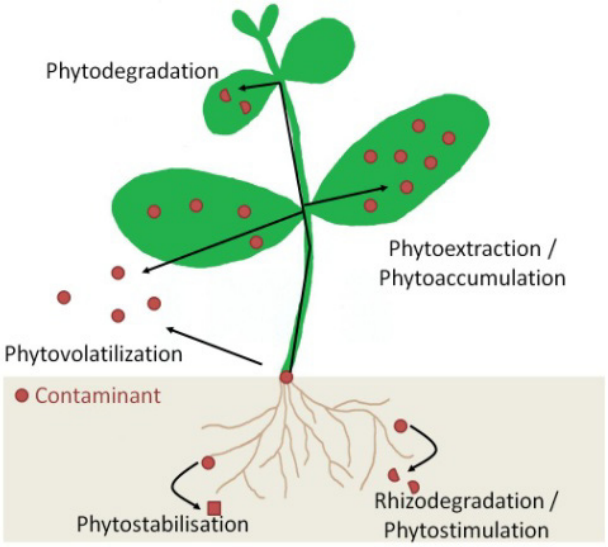


**Figure 7: Phytoremediation technologies for decontamination of soil** (adapted from Pilon-Smits, 2005).

Field studies mainly showed that rhizodegradation take a predominant place in the process of phytoremediation. Muratova et al. (2003) showed that plants increase the total number of micro-organisms in PAHs-contaminated soil while unplanted soil showed less variety of PAHs degraders. Rhizoremediation occurs naturally because roots release a myriad of compounds, such as flavonoids (Ma et al., 2010) or some fatty acids (Yi and Crowley, 2007), which increase microbial growth and PAHs degradation activity. Indeed, studies have shown that for the initial ring hydroxylation of PAHs, micro-organisms could use roots exudates as a carbon source for the catabolism of HMW-PAHs like benzo[a]pyrene during rhizodegradation (Rentz et al., 2005).

Planted soil with linoleic acid containing plants showed enhanced biodegradation of PAHs compared to unplanted soil. However, its mode of action is still unclear. Liste and Alexander (2000b) found that there is a higher concentration of phenanthrene and pyrene in rhizosphere of some plant species (soybean and rice). It was suggested that plants are responsible for the movement of the PAHs into the root zone, where microbial activity is especially intense. In the *Spartina* rhizosphere, 37 PAHs degrading aerobic bacterial communities were found whereas only 11 were found in unplanted sediment (Launen et al., 2007). Besides chemical compounds released from roots, their growth and death also mechanically enhance PAHs oxidation by allowing soil aeration (Gerhardt et al., 2009).

### 4.2. Endophytes-assisted phytoremediation: another plant-microbe interaction

The use of bacteria and fungi living within the plant tissues, termed endophytes, present several advantages compared to the free rhizospheric micro-organisms: they are easier to control and they may possibly cause a concentration gradient of the PAHs within the plant tissues, between the organs where the endophytes were localized and the other parts of the plant (Doty, 2008). It may be argued that this strategy may protect meristematic and photosynthetic tissues in order to allow plants to maintain high level of growth, photosynthesis and production of energy, required for protection and cell repair in PAHs induced stress conditions.

Endophytic bacteria showing high tolerance to PAHs and able to use PAHs as sole source of carbon were identified in willow (Doty, 2008). In other hand, some endophytic fungus such *Ceratobasidum stevensii* found in *Bischofia polycarpa* was also able to degrade about 90% of the phenanthrene after 10 days of growth (Dai et al., 2010).

Results obtained by Germaine *et al.* (2009) strongly support that the engineering of PAHs metablizing endophytes, which enhance phytoremediation, constitute a promising strategy. Indeed, they showed that the engineered naphthalene-degrading endophytic strain of *Pseudomonas putida*, an efficient colonizer of plants (pea, annual ryegrass), named VM1441(pNAH7), enhances plant tolerance to naphthalene. Plants containing this endophyte

had a higher naphthalene degradation rate in soil. Indeed, 68% of naphthalene was removed from the soil with inoculated peas compared to unplanted soil, 40% and 37% more when compared to uninoculated plants or to the inoculum alone, respectively.

The use of these new technologies are clearly promising but many efforts have to be done in order to identify and characterize endophytes associated to PAHs degradation, and to better understand the mechanisms involved in these beneficial interactions.

### 4.3. New tools to improve phyto- and bioremediation

Although micro-organisms play a major role in soil decontamination, PAHs degradation efficiency is limited by (1) the distribution of the cells/communities providing suitable catabolic activity, and (2) the spatio-temporal distribution of catabolically interacting microorganisms. In order to improve soil remediation, it is hence of high interest to understand how microbial populations are distributed in the soil and their role in PAHs degradation activity. Recently, "-omics" approaches emerged as new technologies to address such questions (Desai et al, 2010).

Contrary to classical approaches, metagenomic studies allowed the identification and the monitoring of PAHs degrading microbial populations in the soil. For instance, Layton et al. (2012) were able to monitor the evolution of *Pseudomonas fluorescens* HK44 , its ability to degrade PAHs in the soil following its inoculation, and its impact on the indigenous bacterial population (Layton et al., 2012). Likewise, microbial population dynamic and efficiency of bioremediation processes were monitored also using DNA microarrays (Bae and Park, 2006). Interestingly, pyrosequencing and qPCR assays (Desai et al., 2010) allowed the identification of PAHs degrading bacteria which did not grow on artificial media. In addition, Singleton et al. (2012) successfully monitored bacteria population growing on PAHs contaminated soils, in reactors. They studied the impact of factors such as oxygenation, nutriments, soil depth and duration of treatment, on the bacteria strains development. These promising technologies will bring a global and integrative view about how microbial consortia colonize and adapt to PAHs contaminated ecosystems.

In other hand, recent advances in plant high throughput technologies provide opportunities to decipher mechanisms involved in plant response to PAHs pollution. These global approaches correspond to genome wide association mapping, transcriptomic, metagenomic, proteomic and metabolomic analyses. Indeed, identification of events or actors involved in the perception, absorption, transformation, conjugation and compartmentalization/transport of PAHs should help to create plants enabling a more efficient remediation of pollutants.

Moreover, this knowledge could either allow the improvement of natural occurring methods or the production of transgenic plants harboring an enhanced tolerance to xenobiotics. Several successful incorporation of prokaryotic genes into plants have already been realized especially for decontamination of explosives (Abhilash et al., 2012). Studies using "-omics" approaches designed to investigate the phytoremediation of PAHs still be sparse but will clearly increase in the next future.

Genes degrading PAHs have been identified in bacteria (e.g. Kim et al., 2007; Peng et al., 2008) and fungus (e.g. Syed et al., 2010). They can lead to the creation of transgenic plants to be used for PAHs remediation. As an example, a fungal glutathione-S-transferase gene was introduced into tobacco plants (Dixit et al., 2011). The transgenic plants obtained showed an increased tolerance and higher uptake and metabolization of naphthalene.

Organic pollutants such PAHs are known to be phototoxic and poorly bio-available. Another approach to enhance their phytoremediation would be to use transgenic plants secreting PAHs-degrading enzymes. Even if this strategy is achieved for organic pollutants such as bisphenol A, pentachlorophenol, 2,3-dihydroxybiphenyl and 1-chlorobutane (Doty, 2008), such approaches have not been used for PAHs phytoremediation yet.

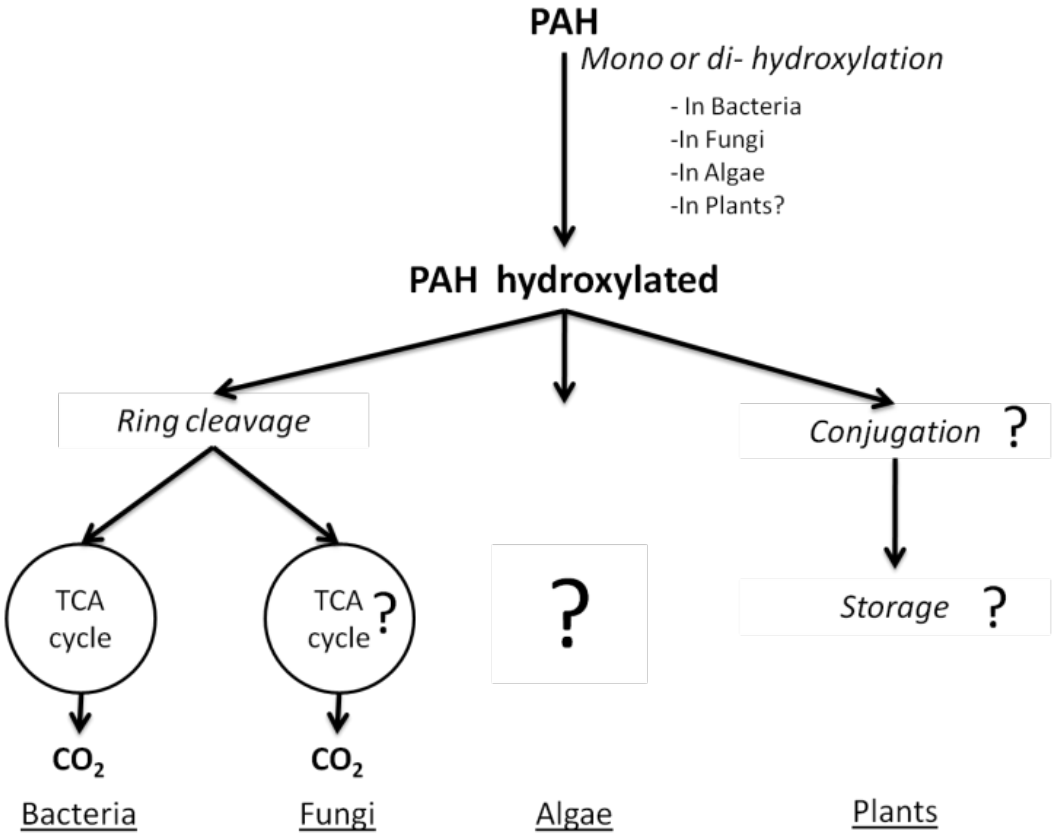


**Figure 8: Common and specific PAHs degradation pathways in bacteria, fungi, algae and plants**

## 5. Conclusion

PAHs pollution is a worldwide problem and affects all the components of natural ecosystem. Toxic effects of these molecules conduct most countries to create a regulation of PAHs emissions in the environment. The toxic effects of PAHs and the general concerns highlight the importance of the decontamination of PAHs-contaminated sites.

There is a large variety of decontamination methods ranging from traditional techniques (chemical or thermal) to green technologies. Bioremediation and phytoremediation, classified as green technologies, use the natural capacity of living organisms (plant, fungus, bacteria or algae) to clean up PAHs in the environment. Even if these technologies are slower than thermal treatment, they are easy to set up and demand low capital investment. Moreover, these methods fit in the framework of sustainable development and are widely accepted.

Still far, bacterial remediation is the most developed bioremediation technology and present different strategies that can be set up *in-situ* or *ex-situ*. Indeed, PAHs degradation pathways by bacteria are described and fairly well known. Besides, the PAHs metabolization pathways in fungi and algae are partly described, PAHs degradation in plants was observed but mechanisms involved still have to be identified, even if models of xenobiotic metabolization have been proposed, these processes remain poorly understood.

The emergence of "-omics" tools will help, in the next future, to elucidate the processes of PAHs degradation in plants and also in micro-organisms. Using metabolomic, proteomic and genomic tools, a complete overview of the degradation pathway should be elucidated and could highlight specific events or actors involved in the degradation of PAHs.

Bioremediation technologies are well perceived and promising. Recent metagenomic data show that an efficient PAHs degradation is done mainly by consortium of organisms.

**Table 3: List of different combination of remediation technologies**

| | Molecules | Technologies used | Results | References |
|---|---|---|---|---|
| combination of biological techniques and agricultural practice | phenanthrene benzo[a] pyrene | soil amendment and bioremediation | Optimization of the carbon source, C/N ratio, soil moisture and aeration conditions are important to enhance PAHs degradation. | Teng et al., 2010 |
| | total PAHs | biosurfactant (ramnolipids), microbial degradation, phytoremediation | Degradation by the combined techniques is 251.83% greater than phytoremediation alone. Better degradation of HMW PAHs. | Zhang et al., 2010 |
| | | phytoremediation + landfarming + biodegradation | enhance PAHs removal of 100% more than landfarming, 50% more than bioremediation and 45% more than phytoremediation | Huang et al., 2004 |
| | | phytoremediation+ pig manure vermicompost (PMVC) | PMVC increased the shoot and root dry biomasses of S. alfredii by 2.27- and 3.93-fold, PMVC+plants have a higher degradation rate of PAHs than plants or PMVC alone. | Wang et al., 2012 |
| combination of chemical and biological techniques | benzo[a] pyrene | ozonation fallowed by bioremediation | ozonation+bioremediation remove 75-82% of benzo[a]pyrene whereas bioremediation alone remove 35% of the PAHs in 30 days | Russo et al., 2012 |
| | phenanthrene pyrene | solid-liquid 2 phases extraction then bioremediation in a reactor | 80% of the original mass of PAHs in the soil has been extracted and after a 14 d period approximately 78%, 62% and 36% of phenanthrene, pyrene, and fluoranthene, respectively, had been desorbed from the polymer and degraded at a laboratory scale. | Rehmann et al., 2008 |
| | total PAHs | solvent pretreatment (acetone or ethanol) then bioremediation | When the soil is pre-treated with solvents, the biodegradation rate of total PAHs is twice the rate without treatment. no difference between the solvents used was observed | Lee et al., 2001 |
| | | biodegradation in reactors fallowed by ozonation | shortened the soil remediation from 2-3 months to 1 week | Derudi et al., 2007 |
| | | Modified Fenton oxidation and bioremediation as post-treatment | The bioremediation treatment increase up to 10% PAHs degradation compared to the natural attenuation which is usually used after Fenton oxidation. This study shows the compatibility of the 2 treatments. | Venny et al., 2012 |

To enhance PAHs degradation, it seems important to use different organisms that can act at different stage of the degradation (Fig. 8). Moreover, it is of high interest to understand the mechanisms involved and to improve their efficiency. In order to optimize these techniques, different approaches have been used.

The most promising is the combination of phytoremediation and microbial remediation. The combination of rhizodegradation with chemical (ozonation) or biological (biosurfactant) treatments is also feasible (table 4) and creates the best conditions for soil decontamination. The use of genetically modified plants or micro-organisms for soil decontamination is also a promising alternative in term of increasing decontamination efficiency.

**Bibliography**

**Abhilash, P.C., Powell, J.R., Singh, H.B. and Singh, B.K.** (2012) Plant–microbe interactions: novel applications for exploitation in multipurpose remediation technologies. *Trends in Biotechnology*, **30**, 416–420. Available at: [Accessed November 15, 2012].

**Al-Awadhi, N., Al-Daher, R., EINawawy, A. and Salba, M.T.** (1996) Bioremediation of oil-contaminated soil in Kuwait. I. landfarming to remediate oil-contaminated soil. *Journal of Soil Contamination*, **5**, 243–260. Available at: [Accessed December 3, 2012].

**Alkio, M., Tabuchi, T.M., Wang, X. and Colón-Carmona, A.** (2005) Stress responses to polycyclic aromatic hydrocarbons in *Arabidopsis* include growth inhibition and hypersensitive response-like symptoms. *Journal of Experimental Botany*, **56**, 2983–2994.

**Alkorta, I. and Garbisu, C.** (2001) Phytoremediation of organic contaminants in soils. *Bioresource Technology*, **79**, 273–276. Available at: [Accessed July 16, 2012].

**Andersson, B.E. and Henrysson, T.** (1996) Accumulation and degradation of dead-end metabolites during treatment of soil contaminated with polycyclic aromatic hydrocarbons with five strains of white-rot fungi. *Appl Microbiol Biotechnol*, **46**, 647–652. Available at: [Accessed April 11, 2013].

**Andersson, B.E., Lundstedt, S., Tornberg, K., Schnürer, Y., Öberg, L.G. and Mattiasson, B.** (2003) Incomplete degradation of polycyclic aromatic hydrocarbons in soil inoculated with wood-rotting fungi and their effect on the indigenous soil bacteria. *Environmental Toxicology and Chemistry*, **22**, 1238–1243. Available at: [Accessed April 11, 2013].

**Antizar-Ladislao, B., Lopez-Real, J. and Beck, A.** (2004) Bioremediation of Polycyclic Aromatic Hydrocarbon (PAH)-Contaminated Waste Using Composting Approaches. *Critical Reviews in Environmental Science and Technology*, **34**, 249–289. Available at: [Accessed December 3, 2012].

**Atagana, H.I.** (2004) Bioremediation of creosote-contaminated soil in South Africa by landfarming. *J. Appl. Microbiol.*, **96**, 510–520.

**Bae, J.-W. and Park, Y.-H.** (2006) Homogeneous versus heterogeneous probes for microbial ecological microarrays. *Trends in Biotechnology*, **24**, 318–323. Available at: [Accessed November 15, 2012].

**Baerson, S.R., Sánchez-Moreiras, A., Pedrol-Bonjoch, N., Schulz, M., Kagan, I.A., Agarwal, A.K., Reigosa, M.J. and Duke, S.O.** (2005) Detoxification and Transcriptome Response in *Arabidopsis* Seedlings Exposed to the Allelochemical Benzoxazolin-2(3H)-one. *J. Biol. Chem.*, **280**, 21867–21881. Available at: [Accessed September 19, 2012].

**Bak, S., Beisson, F., Bishop, G., Hamberger, B., Höfer, R., Paquette, S. and Werck-Reichhart, D.** (2011) Cytochromes P450. *The Arabidopsis Book*, e0144. Available at: [Accessed September 19, 2012].

**Ballach, H.-J., Kuhn, A. and Wittig, R.** (2003) Biodegradation of anthracene in the roots and growth substrate of poplar cuttings. *Environmental Science and Pollution Research*, **10**, 308–316. Available at: [Accessed January 9, 2013].

**Banks, M.K., Kulakow, P., Schwab, A.P., Chen, Z. and Rathbone, K.** (2003) Degradation of crude oil in the rhizosphere of Sorghum bicolor. *Int J Phytoremediation*, **5**, 225–234.

**Banks, M.K., Lee, E. and Schwab, A.P.** (1999) Evaluation of Dissipation Mechanisms for Benzo[a]pyrene in the Rhizosphere of Tall Fescue. *Journal of Environmental Quality*, **28**, 294–298. Available at: [Accessed January 9, 2013].

**Bezalel, L., Hadar, Y. and Cerniglia, C.E.** (1997) Enzymatic Mechanisms Involved in Phenanthrene Degradation by the White Rot Fungus Pleurotus ostreatus. *Appl Environ Microbiol*, **63**, 2495–2501. Available at: [Accessed November 14, 2012].

**Bezalel, L., Hadar, Y. and Cerniglia, C.E.** (1996) Mineralization of Polycyclic Aromatic Hydrocarbons by the White Rot Fungus Pleurotus ostreatus. *Appl. Environ. Microbiol.*, **62**, 292–295. Available at: [Accessed November 13, 2012].

**Bezalel, L., Hadar, Y., Fu, P.P., Freeman, J.P. and Cerniglia, C.E.** (1996) Metabolism of phenanthrene by the white rot fungus Pleurotus ostreatus. *Appl Environ Microbiol*, **62**, 2547–2553. Available at: [Accessed October 26, 2012].

**Boonchan, S., Britz, M.L. and Stanley, G.A.** (2000) Degradation and Mineralization of High-Molecular-Weight Polycyclic Aromatic Hydrocarbons by Defined Fungal-Bacterial Cocultures. *Appl. Environ. Microbiol.*, **66**, 1007–1019. Available at: [Accessed December 3, 2012].

**Brennerova, M.V., Josefiova, J., Brenner, V., Pieper, D.H. and Junca, H.** (2009) Metagenomics reveals diversity and abundance of meta-cleavage pathways in microbial communities from soil highly contaminated with jet fuel under air-sparging bioremediation. *Environ Microbiol*, **11**, 2216–2227. Available at: [Accessed February 28, 2013].

**Cerniglia, C.E.** (1992) Biodegradation of polycyclic aromatic hydrocarbons. *Biodegradation*, **3**, 351–368. Available at: [Accessed October 29, 2012].

**Cerniglia, C.E.** (1997) Fungal metabolism of polycyclic aromatic hydrocarbons: past, present and future applications in bioremediation. *J Ind Microbiol Biotech*, **19**, 324–333. Available at: [Accessed November 13, 2012].

**Cerniglia, C.E., Baalen, C.V. and Gibson, D.T.** (1980) Metabolism of Naphthalene by the Cyanobacterium Oscillatoria sp., Strain JCM. *J Gen Microbiol*, **116**, 485–494. Available at: [Accessed January 8, 2013].

**Cheema, S.A., Imran Khan, M., Shen, C., Tang, X., Farooq, M., Chen, L., Zhang, C. and Chen, Y.** (2010) Degradation of phenanthrene and pyrene in spiked soils by single and combined plants cultivation. *Journal of Hazardous Materials*, **177**, 384–389. Available at: [Accessed January 9, 2013].

**Coleman, J., Blake-Kalff, M. and Davies, E.** (1997) Detoxification of xenobiotics by plants: chemical modification and vacuolar compartmentation. *Trends in Plant Science*, **2**, 144–151. Available at: [Accessed October 16, 2012].

**Cunningham, S.D., Berti, W.R. and Huang, J.W.** (1995) Phytoremediation of contaminated soils. *Trends in Biotechnology*, **13**, 393–397. Available at: [Accessed November 6, 2012].

**Dai, C., Tian, L., Zhao, Y., Chen, Y. and Xie, H.** (2010) Degradation of phenanthrene by the endophytic fungus Ceratobasidum stevensii found in Bischofia polycarpa. *Biodegradation*, **21**, 245–255.

**Derudi, M., Venturini, G., Lombardi, G., Nano, G. and Rota, R.** (2007) Biodegradation combined with ozone for the remediation of contaminated soils. *European Journal of Soil Biology*, **43**, 297–303. Available at: [Accessed January 11, 2013].

**Desai, C., Pathak, H. and Madamwar, D.** (2010) Advances in molecular and "-omics" technologies to gauge microbial communities and bioremediation at xenobiotic/anthropogen contaminated sites. *Bioresource Technology*, **101**, 1558–1569. Available at: [Accessed November 14, 2012].

**Dixit, P., Mukherjee, P.K., Sherkhane, P.D., Kale, S.P. and Eapen, S.** (2011) Enhanced tolerance and remediation of anthracene by transgenic tobacco plants expressing a fungal glutathione transferase gene. *Journal of Hazardous Materials*, **192**, 270–276. Available at: [Accessed December 3, 2012].

**Dixon, D.P. and Edwards, R.** (2010) Glutathione Transferases. *Arabidopsis Book*, **8**. Available at: http://www.ncbi.nlm.nih.gov/pmc/articles/PMC3244946/ [Accessed September 19, 2012].

**Doty, S.L.** (2008) Enhancing phytoremediation through the use of transgenics and endophytes. *New Phytol.*, **179**, 318–333. Available at: [Accessed June 8, 2012].

**Edema, C.U., Idu, T.E. and Edema, M.O.** (2011) Remediation of soil contaminated with polycyclic aromatic hydrocarbons from crude oil. *African Journal of Biotechnology*, **10**, 1146–1149. Available at: [Accessed December 3, 2012].

**Edwards, R., Brazier-Hicks, M., Dixon, D.P. and Cummins, I.** (2005) Chemical Manipulation of Antioxidant Defences in Plants. In J. A. Callow, ed. *Advances in Botanical Research*. Academic Press, pp. 1–32. Available at: http://www.sciencedirect.com/science/article/pii/S0065229605420017 [Accessed October 11, 2012].

**Edwards, R., Dixon, D.P., Cummins, I., Brazier-Hicks, M. and Skipsey, M.** (2011) New Perspectives on the Metabolism and Detoxification of Synthetic Compounds in Plants. In P. Schröder and C. D. Collins, eds. *Organic Xenobiotics and Plants*. Plant Ecophysiology. Springer Netherlands, pp. 125–148. Available at: http://www.springerlink.com/content/w47665207215u483/abstract/ [Accessed September 14, 2012].

**Euliss, K., Ho, C., Schwab, A.P., Rock, S. and Banks, M.K.** (2008) Greenhouse and field assessment of phytoremediation for petroleum contaminants in a riparian zone. *Bioresource Technology*, **99**, 1961–1971. Available at: [Accessed January 9, 2013].

**Frutos, F.J.G., Escolano, O., García, S., Babín, M. and Fernández, M.D.** (2010) Bioventing remediation and ecotoxicity evaluation of phenanthrene-contaminated soil. *Journal of Hazardous Materials*, **183**, 806–813. Available at: [Accessed November 30, 2012].

**Furuno, S., Foss, S., Wild, E., Jones, K.C., Semple, K.T., Harms, H. and Wick, L.Y.** (2012) Mycelia Promote Active Transport and Spatial Dispersion of Polycyclic Aromatic Hydrocarbons. *Environ. Sci. Technol.*, **46**, 5463–5470. Available at: [Accessed April 11, 2013].

**Furuno, S., Päzolt, K., Rabe, C., Neu, T.R., Harms, H. and Wick, L.Y.** (2010) Fungal mycelia allow chemotactic dispersal of polycyclic aromatic hydrocarbon-degrading bacteria in water-unsaturated systems. *Environ. Microbiol.*, **12**, 1391–1398.

**Gan, S., Lau, E.V. and Ng, H.K.** (2009) Remediation of soils contaminated with polycyclic aromatic hydrocarbons (PAHs). *Journal of Hazardous Materials*, **172**, 532–549. Available at: [Accessed September 20, 2012].

**Gerhardt, K.E., Huang, X.-D., Glick, B.R. and Greenberg, B.M.** (2009) Phytoremediation and rhizoremediation of organic soil contaminants: Potential and challenges. *Plant Science*, **176**, 20–30. Available at: [Accessed November 6, 2012].

**Germaine, K.J., Keogh, E., Ryan, D. and Dowling, D.N.** (2009) Bacterial endophyte-mediated naphthalene phytoprotection and phytoremediation. *FEMS Microbiology Letters*, **296**, 226–234. Available at: [Accessed December 3, 2012].

**Goodwin, S. and Sutter, T.** (2009) Microarray analysis of <i>Arabidopsis</i> genome response to aluminum stress. *Biologia Plantarum*, **53**, 85–99. Available at: [Accessed September 19, 2012].

**Guazzaroni, M.-E., Herbst, F.-A., Lores, I., *et al.*** (2013) Metaproteogenomic insights beyond bacterial response to naphthalene exposure and bio-stimulation. *ISME J*, **7**, 122–136. Available at: [Accessed January 11, 2013].

**Hansen, L.D., Nestler, C., Ringelberg, D. and Bajpai, R.** (2004) Extended bioremediation of PAH/PCP contaminated soils from the POPILE wood treatment facility. *Chemosphere*, **54**, 1481–1493.

**Haritash, A.K. and Kaushik, C.P.** (2009) Biodegradation aspects of Polycyclic Aromatic Hydrocarbons (PAHs): A review. *Journal of Hazardous Materials*, **169**, 1–15. Available at: [Accessed August 9, 2012].

**Harms, H., Schlosser, D. and Wick, L.Y.** (2011) Untapped potential: exploiting fungi in bioremediation of hazardous chemicals. *Nature Reviews Microbiology*, **9**, 177–192. Available at: [Accessed December 3, 2012].

**Herbette, S., Taconnat, L., Hugouvieux, V., *et al.*** (2006) Genome-wide transcriptome profiling of the early cadmium response of *Arabidopsis* roots and shoots. *Biochimie*, **88**, 1751–1765. Available at: [Accessed September 19, 2012].

**Hoewyk, D. Van, Takahashi, H., Inoue, E., Hess, A., Tamaoki, M. and Pilon-Smits, E.A.H.** (2008) Transcriptome analyses give insights into selenium-stress responses and selenium tolerance mechanisms in Arabidopsis. *Physiol Plant*, **132**, 236–253. Available at: [Accessed September 19, 2012].

**Huang, X.-D., El-Alawi, Y., Penrose, D.M., Glick, B.R. and Greenberg, B.M.** (2004) A multi-process phytoremediation system for removal of polycyclic aromatic hydrocarbons from contaminated soils. *Environ. Pollut.*, **130**, 465–476.

**Huesemann, M.H., Hausmann, T.S., Fortman, T.J., Thom, R.M. and Cullinan, V.** (2009) In situ phytoremediation of PAH- and PCB-contaminated marine sediments with eelgrass (Zostera marina). *Ecological Engineering*, **35**, 1395–1404. Available at: [Accessed January 9, 2013].

**HuiJie, L., CaiYun, Y., Yun, T., GuangHui, L. and TianLing, Z.** (2011) Using population dynamics analysis by DGGE to design the bacterial consortium isolated from mangrove sediments for biodegradation of PAHs. *International Biodeterioration & Biodegradation*, **65**, 269–275. Available at: [Accessed December 3, 2012].

**Janikowski, T., Velicogna, D., Punt, M. and Daugulis, A.** (2002) Use of a two-phase partitioning bioreactor for degrading polycyclic aromatic hydrocarbons by a Sphingomonas sp. *Appl Microbiol Biotechnol*, **59**, 368–376. Available at: [Accessed December 3, 2012].

**Jin, X.-F., Shuai, J.-J., Peng, R.-H., *et al.*** (2011) Identification of candidate genes involved in responses of *Arabidopsis* to polychlorinated biphenyls based on microarray analysis. *Plant Growth Regulation*, **65**, 127–135. Available at: [Accessed September 19, 2012].

**Johnsen, A.R., Wick, L.Y. and Harms, H.** (2005) Principles of microbial PAH-degradation in soil. *Environmental Pollution*, **133**, 71–84. Available at: [Accessed August 9, 2012].

**Jones, M.D., Crandell, D.W., Singleton, D.R. and Aitken, M.D.** (2011) Stable-isotope probing of the polycyclic aromatic hydrocarbon-degrading bacterial guild in a contaminated soil. *Environmental Microbiology*, **13**, 2623–2632. Available at: [Accessed April 11, 2013].

**Juhasz, A.L., Stanley, G.A. and Britz, M.L.** (2000) Degradation of High Molecular Weight PAHs in Contaminated Soil by a Bacterial Consortium: Effects on Microtox and Mutagenicity Bioassays. *Bioremediation Journal*, **4**, 271–283. Available at: [Accessed December 3, 2012].

**Kanaly, R.A. and Harayama, S.** (2000) Biodegradation of High-Molecular-Weight Polycyclic Aromatic Hydrocarbons by Bacteria. *J. Bacteriol.*, **182**, 2059–2067. Available at: [Accessed August 7, 2012].

**Kim, S.-J., Kweon, O. and Cerniglia, C.E.** (2009) Proteomic applications to elucidate bacterial aromatic hydrocarbon metabolic pathways. *Current Opinion in Microbiology*, **12**, 301–309. Available at: [Accessed November 16, 2012].

**Kim, S.-J., Kweon, O., Jones, R.C., Freeman, J.P., Edmondson, R.D. and Cerniglia, C.E.** (2007) Complete and integrated pyrene degradation pathway in Mycobacterium vanbaalenii PYR-1 based on systems biology. *J. Bacteriol.*, **189**, 464–472.

**Kohlmeier, S., Smits, T.H.M., Ford, R.M., Keel, C., Harms, H. and Wick, L.Y.** (2005) Taking the fungal highway: mobilization of pollutant-degrading bacteria by fungi. *Environ. Sci. Technol.*, **39**, 4640–4646.

**Kotterman, M.J.J., Vis, E.H. and Field, J.A.** (1998) Successive Mineralization and Detoxification of Benzo[a]pyrene by the White Rot FungusBjerkandera sp. Strain BOS55 and Indigenous Microflora. *Appl. Environ. Microbiol.*, **64**, 2853–2858. Available at: [Accessed November 13, 2012].

**Landa, P., Storchova, H., Hodek, J., Vankova, R., Podlipna, R., Marsik, P., Ovesna, J. and Vanek, T.** (2010) Transferases and transporters mediate the detoxification and capacity to tolerate trinitrotoluene in Arabidopsis. *Funct. Integr. Genomics*, **10**, 547–559. Available at: [Accessed September 19, 2012].

**Launen, L.A., Dutta, J., Turpeinen, R., Eastep, M.E., Dorn, R., Buggs, V.H., Leonard, J.W. and Häggblom, M.M.** (2007) Characterization of the indigenous PAH-degrading bacteria of Spartina dominated salt marshes in the New York/New Jersey Harbor. *Biodegradation*, **19**, 347–363. Available at: [Accessed November 9, 2012].

**Layton, A., Smart, A.E., Chauhan, A., *et al.*** (2012) Ameliorating Risk: Culturable and Metagenomic Monitoring of the 14 Year Decline of a Genetically Engineered Microorganism at a Bioremediation Field Site. *OMICS: Journal of Bioremediation and Biodegradation*, **9**. Available at: http://www.osti.gov/energycitations/product.biblio.jsp?osti_id=1047016 [Accessed January 11, 2013].

**Lee, M.D. and Swindoll, C.M.** (1993) Bioventing for in situ remediation. *Hydrological Sciences Journal*, **38**, 273–282. Available at: [Accessed November 30, 2012].

**Lee, P.-H., Ong, S.K., Golchin, J. and Nelson, G.L. (Sam.** (2001) Use of solvents to enhance PAH biodegradation of coal tar-. *Water Research*, **35**, 3941–3949. Available at: [Accessed January 10, 2013].

**Lei, A.-P., Hu, Z.-L., Wong, Y.-S. and Tam, N.F.-Y.** (2007) Removal of fluoranthene and pyrene by different microalgal species. *Bioresource Technology*, **98**, 273–280. Available at: [Accessed October 26, 2012].

**Liebeg, E.W. and Cutright, T.J.** (1999) The investigation of enhanced bioremediation through the addition of macro and micro nutrients in a PAH contaminated soil. *International Biodeterioration & Biodegradation*, **44**, 55–64. Available at: [Accessed December 3, 2012].

**Lily, M.K., Bahuguna, A., Dangwal, K. and Garg, V.** (2009) Degradation of Benzo [a] Pyrene by a novel strain Bacillus subtilis BMT4i (MTCC 9447). *Brazilian Journal of Microbiology*, **40**, 884–892. Available at: [Accessed August 9, 2012].

**Liste, H.-H. and Alexander, M.** (2000a) Accumulation of phenanthrene and pyrene in rhizosphere soil. *Chemosphere*, **40**, 11–14. Available at: [Accessed November 7, 2012].

**Liste, H.-H. and Alexander, M.** (2000b) Plant-promoted pyrene degradation in soil. *Chemosphere*, **40**, 7–10. Available at: [Accessed July 3, 2012].

**Liste, H.-H. and Alexander, M.** (1999) Rapid Screening of Plants Promoting Phenanthrene Degradation. *Journal of Environmental Quality*, **28**, 1376–1377. Available at: [Accessed November 7, 2012].

**Loh, K.-C. and Cao, B.** (2008) Paradigm in biodegradation using Pseudomonas putida—A review of proteomics studies. *Enzyme and Microbial Technology*, **43**, 1–12. Available at: [Accessed February 28, 2013].

**Ma, B., He, Y., Chen, H., Xu, J. and Rengel, Z.** (2010) Dissipation of polycyclic aromatic hydrocarbons (PAHs) in the rhizosphere: synthesis through meta-analysis. *Environ. Pollut.*, **158**, 855–861.

**Mallick, S., Chatterjee, S. and Dutta, T.K.** (2007) A novel degradation pathway in the assimilation of phenanthrene by Staphylococcus sp. strain PN/Y via meta-cleavage of 2-hydroxy-1-naphthoic acid: formation of trans-2,3-dioxo-5-(2'-hydroxyphenyl)-pent-4-enoic acid. *Microbiology (Reading, Engl.)*, **153**, 2104–2115.

**Masten, S.J. and Davies, S.H.R.** (1997) Efficacy of in-situ for the remediation of PAH contaminated soils. *Journal of Contaminant Hydrology*, **28**, 327–335. Available at:.

**Mitsch, W.J.** (2012) What is ecological engineering? *Ecological Engineering*, **45**, 5–12. .

**Mohan, S.V., Kisa, T., Ohkuma, T., Kanaly, R.A. and Shimizu, Y.** (2006) Bioremediation technologies for treatment of PAH-contaminated soil and strategies to enhance process efficiency. *Rev Environ Sci Biotechnol*, **5**, 347–374. Available at: [Accessed December 3, 2012].

**Mrozik, A., Piotrowska-Seget, Z. and Łabuzek, S.** (2003) Bacterial degradation and bioremediation of polycyclic aromatic hydrocarbons. *Polish Journal of Environmental Studies*, **12**, 15–25.

**Muratova, A., Hübner, T., Tischer, S., Turkovskaya, O., Möder, M. and Kuschk, P.** (2003) Plant--rhizosphere-microflora association during phytoremediation of PAH-contaminated soil. *Int J Phytoremediation*, **5**, 137–151.

**Narro, M.L., Cerniglia, C.E., Baalen, C. Van and Gibson, D.T.** (1992) Metabolism of phenanthrene by the marine cyanobacterium Agmenellum quadruplicatum PR-6. *Appl Environ Microbiol*, **58**, 1351–1359. Available at: [Accessed January 8, 2013].

**Peng, R.-H., Xiong, A.-S., Xue, Y., Fu, X.-Y., Gao, F., Zhao, W., Tian, Y.-S. and Yao, Q.-H.** (2008) Microbial biodegradation of polyaromatic hydrocarbons. *FEMS Microbiology Reviews*, **32**, 927–955. Available at: [Accessed December 3, 2012].

**Pinelli, D., Fava, F., Nocentini, M. and Pasquali, G.** (1997) Bioremediation of a polycyclic aromatic hydrocarbon-contaminated soil by using different aerobic batch bioreactor systems. *Journal of Soil Contamination*, **6**, 243–256. Available at: [Accessed December 3, 2012].

**Pradhan, S.P., Conrad, J.R., Paterek, J.R. and Srivastava, V.J.** (1998) Potential of Phytoremediation for Treatment of PAHs in Soil at MGP Sites. *Journal of Soil Contamination*, **7**, 467–480. Available at: [Accessed November 5, 2012].

**Ramel, F., Sulmon, C., Cabello-Hurtado, F., Taconnat, L., Martin-Magniette, M.-L., Renou, J.-P., Amrani, A.E., Couée, I. and Gouesbet, G.** (2007) Genome-wide interacting effects of sucrose and herbicide-mediated stress in *Arabidopsis thaliana*: novel insights into atrazine toxicity and sucrose-induced tolerance. *BMC Genomics*, **8**, 450. Available at: [Accessed September 19, 2012].

**Rehmann, L., Prpich, G.P. and Daugulis, A.J.** (2008) Remediation of PAH contaminated soils: Application of a solid–liquid two-phase partitioning bioreactor. *Chemosphere*, **73**, 798–804. Available at: [Accessed December 5, 2012].

**Rentz, J.A., Alvarez, P.J.J. and Schnoor, J.L.** (2005) Benzo[a]pyrene co-metabolism in the presence of plant root extracts and exudates: Implications for phytoremediation. *Environmental Pollution*, **136**, 477–484. Available at: [Accessed November 5, 2012].

**Russo, L., Rizzo, L. and Belgiorno, V.** (2012) Ozone oxidation and aerobic biodegradation with spent mushroom compost for detoxification and benzo(a)pyrene removal from contaminated soil. *Chemosphere*, **87**, 595–601. Available at: [Accessed December 5, 2012].

**Salt, D.E., Blaylock, M., Kumar, N.P.B.A., Dushenkov, V., Ensley, B.D., Chet, I. and Raskin, I.** (1995) Phytoremediation: A Novel Strategy for the Removal of Toxic Metals from the Environment Using Plants. *Nature Biotechnology*, **13**, 468–474. Available at: [Accessed November 6, 2012].

**Samanta, S.K., Singh, O.V. and Jain, R.K.** (2002) Polycyclic aromatic hydrocarbons: environmental pollution and bioremediation. *Trends in Biotechnology*, **20**, 243–248. Available at: [Accessed August 7, 2012].

**Sandermann Jr., H.** (1992) Plant metabolism of xenobiotics. *Trends in Biochemical Sciences*, **17**, 82–84. Available at: [Accessed October 4, 2012].

**Saraswathy, A. and Hallberg, R.** (2002) Degradation of pyrene by indigenous fungi from a former gasworks site. *FEMS Microbiology Letters*, **210**, 227–232. Available at: [Accessed November 20, 2012].

**Schamfuß, S., Neu, T.R., Harms, H., Meer, J.R. van der, Tecon, R. and Wick, L.Y.** (2013) Mycelial Networks Enhance the Bioavailability of PAH in Water Unsaturated Environments. *Environmental Science & Technology*.

**Schneider, J., Grosser, R., Jayasimhulu, K., Xue, W. and Warshawsky, D.** (1996) Degradation of pyrene, benz[a]anthracene, and benzo[a]pyrene by Mycobacterium sp. strain RJGII-135, isolated from a former coal gasification site. *Appl. Environ. Microbiol.*, **62**, 13–19. Available at: [Accessed November 13, 2012].

**Schnoor, J.L., Licht, L.A., McCutcheon, S.C., Wolfe, N.L. and CARREIRA, L.H.** (1995) Phytoremediation of Organic and Nutrient Contaminants. *Environ. Sci. Technol.*, **29**, 318A–323A. Available at: [Accessed November 6, 2012].

**Siciliano, S.D., Germida, J.J., Banks, K. and Greer, C.W.** (2003) Changes in Microbial Community Composition and Function during a Polyaromatic Hydrocarbon Phytoremediation Field Trial. *Appl. Environ. Microbiol.*, **69**, 483–489. Available at: [Accessed January 9, 2013].

**Singleton, D.R., Hunt, M., Powell, S.N., Frontera-Suau, R. and Aitken, M.D.** (2007) Stable-isotope probing with multiple growth substrates to determine substrate specificity of uncultivated bacteria. *Journal of Microbiological Methods*, **69**, 180–187. Available at: [Accessed April 11, 2013].

**Singleton, D.R., Jones, M.D., Richardson, S.D. and Aitken, M.D.** (2012) Pyrosequence analyses of bacterial communities during simulated in situ bioremediation of polycyclic aromatic hydrocarbon-contaminated soil. *Appl. Microbiol. Biotechnol.*

**Singleton, D.R., Powell, S.N., Sangaiah, R., Gold, A., Ball, L.M. and Aitken, M.D.** (2005) Stable-Isotope Probing of Bacteria Capable of Degrading Salicylate, Naphthalene, or Phenanthrene in a Bioreactor Treating Contaminated Soil. *Appl. Environ. Microbiol.*, **71**, 1202–1209. Available at: [Accessed April 11, 2013].

**Smith, M.R.** (1990) The biodegradation of aromatic hydrocarbons by bacteria. *Biodegradation*, **1**, 191–206.

**Syed, K., Doddapaneni, H., Subramanian, V., Lam, Y.W. and Yadav, J.S.** (2010) Genome-to-function characterization of novel fungal P450 monooxygenases oxidizing polycyclic aromatic hydrocarbons (PAHs). *Biochemical and Biophysical Research Communications*, **399**, 492–497. Available at: [Accessed November 20, 2012].

**Taguchi, G., Ubukata, T., Nozue, H., Kobayashi, Y., Takahi, M., Yamamoto, H. and Hayashida, N.** (2010) Malonylation is a key reaction in the metabolism of xenobiotic phenolic glucosides in *Arabidopsis* and tobacco. *The Plant Journal*, **63**, 1031–1041. Available at: [Accessed February 1, 2013].

**Técher, D., Laval-Gilly, P., Henry, S., *et al.*** (2011) Contribution of Miscanthus x giganteus root exudates to the biostimulation of PAH degradation: An in vitro study. *Science of The Total Environment*, **409**, 4489–4495. Available at: [Accessed November 8, 2012].

**Técher, D., Laval-Gilly, P., Henry, S., Bennasroune, A., Martinez-Chois, C., D'Innocenzo, M. and Falla, J.** (2012) Prospects of Miscanthus x giganteus for PAH phytoremediation: A microcosm study. *Industrial Crops and Products*, **36**, 276–281. Available at: [Accessed November 8, 2012].

**Teng, Y., Luo, Y., Ping, L., Zou, D., Li, Z. and Christie, P.** (2010) Effects of soil amendment with different carbon sources and other factors on the bioremediation of an aged PAH-contaminated soil. *Biodegradation*, **21**, 167–178. Available at: [Accessed December 5, 2012].

**Trzesicka-Mlynarz, D. and Ward, O.P.** (1995) Degradation of polycyclic aromatic hydrocarbons (PAHs) by a mixed culture and its component pure cultures, obtained from PAH-contaminated soil. *Can. J. Microbiol.*, **41**, 470–476.

**Al-Turky, A.I.** (2009) Microbial polycyclic aromatic hydrocarbons degradation in soil. *Research Journal of Environmental Toxicology*, **3**, 1–8.

**Venny, Gan, S. and Ng, H.K.** (2012) Modified Fenton oxidation of polycyclic aromatic hydrocarbon (PAH)-contaminated soils and the potential of bioremediation as post-treatment. *Science of The Total Environment*, **419**, 240–249. Available at: [Accessed December 5, 2012].

**Vervaeke, P., Luyssaert, S., Mertens, J., Meers, E., Tack, F.M.. and Lust, N.** (2003) Phytoremediation prospects of willow stands on contaminated sediment: a field trial. *Environmental Pollution*, **126**, 275–282. Available at: [Accessed November 8, 2012].

**Vilchez-Vargas, R., Junca, H. and Pieper, D.H.** (2010) Metabolic networks, microbial ecology and "omics" technologies: towards understanding in situ biodegradation processes. *Environmental Microbiology*, **12**, 3089–3104. Available at: [Accessed November 15, 2012].

**Wang, K., Zhang, J., Zhu, Z., Huang, H., Li, T., He, Z., Yang, X. and Alva, A.** (2012) Pig manure vermicompost (PMVC) can improve phytoremediation of Cd and PAHs co-contaminated soil by Sedum alfredii. *J Soils Sediments*, **12**, 1089–1099. Available at: [Accessed December 5, 2012].

**Warshawsky, D., Cody, T., Radike, M., Reilman, R., Schumann, B., LaDow, K. and Schneider, J.** (1995) Biotransformation of benzo[a]pyrene and other polycyclic aromatic hydrocarbons and heterocyclic analogs by several green algae and other algal species under gold and white light. *Chemico-Biological Interactions*, **97**, 131–148. Available at: [Accessed August 13, 2012].

**Watts, A.W., Ballestero, T.P. and Gardner, K.H.** (2006) Uptake of polycyclic aromatic hydrocarbons (PAHs) in salt marsh plants Spartina alterniflora grown in contaminated sediments. *Chemosphere*, **62**, 1253–1260.

**Weisman, D., Alkio, M. and Colón-Carmona, A.** (2010) Transcriptional responses to polycyclic aromatic hydrocarbon-induced stress in *Arabidopsis thaliana* reveal the involvement of

hormone and defense signaling pathways. *BMC Plant Biol*, **10**, 59. Available at: [Accessed September 19, 2012].

**Wilson, S.C. and Jones, K.C.** (1993) Bioremediation of soil contaminated with polynuclear aromatic hydrocarbons (PAHs): A review. *Environmental Pollution*, **81**, 229–249. Available at: [Accessed October 26, 2012].

**Xu, J., Su, Z.-H., Chen, C., *et al.*** (2012) Stress responses to phenol in *Arabidopsis* and transcriptional changes revealed by microarray analysis. *Planta*, **235**, 399–410. Available at: [Accessed September 21, 2012].

**Xu, S.Y., Chen, Y.X., Wu, W.X., Wang, K.X., Lin, Q. and Liang, X.Q.** (2006) Enhanced dissipation of phenanthrene and pyrene in spiked soils by combined plants cultivation. *Science of The Total Environment*, **363**, 206–215. Available at: [Accessed November 8, 2012].

**Yi, H. and Crowley, D.E.** (2007) Biostimulation of PAH Degradation with Plants Containing High Concentrations of Linoleic Acid. *Environ. Sci. Technol.*, **41**, 4382–4388. Available at: [Accessed December 4, 2012].

**Zhan, X.-H., Ma, H.-L., Zhou, L.-X., Liang, J.-R., Jiang, T.-H. and Xu, G.-H.** (2010) Accumulation of phenanthrene by roots of intact wheat (Triticum acstivnm L.) seedlings: passive or active uptake? *BMC Plant Biology*, **10**, 52. Available at: [Accessed November 5, 2012].

**Zhang, J., Yin, R., Lin, X., Liu, W., Chen, R. and Li, X.** (2010) Interactive Effect of Biosurfactant and Microorganism to Enhance Phytoremediation for Removal of Aged Polycyclic Aromatic Hydrocarbons from Contaminated Soils. *Journal of Health Science*, **56**, 257–266.

**Zhang, X.-X., Cheng, S.-P., Zhu, C.-J. and Sun, S.-L.** (2006) Microbial PAH-Degradation in Soil: Degradation Pathways and Contributing Factors. *Pedosphere*, **16**, 555–565. Available at: [Accessed October 26, 2012].

# Partie 3: **Les sucres solubles : des molécules-clés impliquées dans la tolérance aux stress abiotiques chez les plantes supérieures**

## 1. Introduction

En tant qu'organismes cessiles, les plantes sont soumises aux changements de leur environnement et doivent donc mettre en place des processus qui leur permettent de s'adapter à ces modifications. Seules les plantes capables de développer cette capacité à s'adapter ont pu survivre à cette sélection naturelle et se propager. Ces conditions de stress modifient le développement des plantes en affectant plusieurs processus cellulaires tels que le développement, la photosynthèse, le métabolisme des lipides et des sucres, l'expression des gènes, l'équilibre osmotique. Ces perturbations affectent profondément le fonctionnement des plantes entrainant une inhibition de leur croissance.

Une des conséquences les plus communes des stress abiotiques est la production de dérivés actifs de l'oxygène (ROS) dont l'accumulation crée un stress oxydant. Les ROS sont produites continuellement au sein de la plante de par la photosynthèse et la respiration mais leur niveau reste faible grâce à la prise en charge par le système antioxydant. L'augmentation du niveau des ROS due à un stress abiotique est un moyen de signaler à l'ensemble de la plante les modifications dans l'environnement et de provoquer des changements au niveau métabolique. Une accumulation de ces molécules peut causer des dommages cellulaires pouvant aller jusqu'à la mort cellulaire (Foyer and Noctor, 2005).

Les plantes sont des organismes autotrophes et photosynthétiques qui sont capables de produire et de consommer les sucres. Cependant, les sucres ne sont pas seulement des ressources métaboliques et des composés structuraux, ils jouent de nombreux rôles notamment de signalisation et de protection vis-à-vis des stress abiotiques (Rolland et al., 2002; Rosa et al., 2009; Wind et al., 2010).

Le saccharose est un disaccharide représentant la forme majoritaire sous laquelle les sucres sont transportés chez les végétaux supérieurs. Comme la plupart des sucres solubles, il a aussi des caractéristiques autres que métaboliques et induit l'initiation de voies signalétiques qui modifient l'expression des gènes et l'adaptation physiologique de la plante (Wind et al., 2010).

## 2. Les stress abiotiques modifient la teneur en sucres solubles chez les végétaux

Les plantes doivent s'adapter aux modifications de leur environnement et doivent donc modifier leur métabolisme afin de gérer au mieux ces changements. Ces perturbations, en provoquant une situation de stress abiotique, peuvent entrainer des modifications du métabolisme primaire. Plusieurs études ont notamment montré que, en condition de stress, la concentration en saccharose de la plante est modifiée (Rosa et al., 2009). Ainsi, le stress salin provoque chez le riz une accumulation des sucres solubles, ainsi que d'autres métabolites, afin de rétablir la balance osmotique (Dubey and Singh, 1999). De plus, dans ces conditions, l'activité de la Sucrose Phosphate Synthase (SPS) est augmentée, conduisant à une accumulation de saccharose suite à la dégradation de l'amidon.

Un déficit en eau induit, lui-aussi, une accumulation des sucres solubles chez les plantes. Cette accumulation peut être liée à la diminution de la teneur en eau des cellules végétales (Hsiao, 1973).

Cette accumulation des sucres a été observée chez le coton au niveau des feuilles (Timpa et al., 1986). Alors qu'en condition d'irrigation, les cultivars sensibles et résistants ne présentent pas de différence dans leur teneur en saccharose, la comparant des cultivars sensibles et des cultivars résistants à un déficit en eau, a permi à ces auteurs de montrer que, chez les cotons résistants, la teneur en saccharose est la même en condition de stress ou d'irrigation normale alors que ce n'est pas le cas pour les plantes sensibles. Cette étude a donc montré que le transport du saccharose n'a pu se dérouler normalement chez les cultivars sensibles.

D'autre part, chez des plantes fourragères de zone tropicale, le saccharose peut aussi jouer un rôle dans l'ajustement osmotique en condition de stress hydrique mais cet effet est moindre comparé à d'autres osmolytes (Ford and Wilson, 1981).

Un stress lié à une inondation crée également des modifications dans la teneur en sucre : les sucres s'accumulent dans les parties aériennes alors que les racines présentent un déficit chez l'épicéa et le mélèze (Islam and Macdonald, 2004). Ce résultat montre qu'il y a une interruption du transport des sucres des organes sources (les feuilles) aux organes puits (les racines) probablement due aux conditions d'hypoxie liées à l'inondation.

La présence de métaux lourds (nickel et cadmium) a induit, chez le riz, une accumulation des sucres, notamment du saccharose, au niveau des parties aériennes (Moya et al., 1993). Cette augmentation de la teneur en sucres n'est pas liée à une augmentation de l'activité photosynthétique puisque cette dernière est inhibée par les métaux lourds. Etant donné que la croissance racinaire du riz en présence de cadmium et de nickel est inhibée, il est possible que la répartition entre source et puits soit modifiée avec une accumulation des sucres dans les organes sources, ce qui pourrait souligner une absence de transport ou une inhibition du transport des sucres.

Chez l'épinard, Guy et al. (1992) ont montré qu'une période de froid (3°C) induit l'accumulation de saccharose. Le premier intérêt peut être purement métabolique : le stock de saccharose sert de réserve énergétique facilement utilisable et transportable vers les organes qui en ont besoin. L'accumulation du saccharose est souvent corrélée avec la tolérance au froid car il peut aussi servir de cryoprotecteur, empêchant la formation de glace au sein des cellules. D'autre part, un stress dû à de basses températures induit aussi un stress hydrique impliquant donc l'accumulation d'osmolytes tels que le sucre.

De manière générale, quel que soit le stress, on observe une accumulation de sucres dans les plantes qui peut être due à deux facteurs, pas forcément indépendants : (i) un changement osmotique ou (ii) une rupture du transport des sucres entre les organes puits et les organes sources.

## 3. Sucres et signalisation

La perception des sucres (« sugar sensing ») résulte de l'interaction entre une molécule de sucre et une protéine-perceptrice couramment appellée « sensor » ce qui permet l'induction de voie de signalisation. En effet, les sucres solubles agiraient comme des phytohormones afin de contrôler l'expression de gènes impliqués dans diverses voies biologiques (Gupta and Kaur, 2005; Gonzali et al., 2006; Rosa et al., 2009). Price et al. (2004) et Thum et al. (2004) ont montré que les sucres modulent une grande variété de gènes impliqués dans les principaux processus cellulaires: le métabolisme des sucres et de l'azote, le métabolisme secondaire, la transduction de signal, le transport des métabolites et la réponse aux stress.

Pour les hexoses, plus particulièrement le glucose, deux systèmes de perception des sucres, coexistant chez les plantes, ont été proposés. Le premier système dit « hexokinase (HXK) dépendant » nécessite la phosphorylation des sucres par l'hexokinase qui joue le rôle de percepteur du signal. Le second système dit « hexokinase indépendant » ne nécessite pas cette étape de phosphorylation. Un récepteur spécifique du glucose, l'hexokinase 1 (HXK 1) a été identifié permettant une meilleure caractérisation du système HXK-dépendant (Ramon et al., 2008).

D'autre part, plusieurs voies de régulation spécifiques au saccharose ont été identifiées.

Le saccharose régule le développement des plantes, notamment au niveau du système racinaire. MacGregor et al. (2008) ont montré que le saccharose modifie l'architecture racinaire en induisant le développement de racines secondaires. La mise en évidence de l'effet signalétique du saccharose sur le développement racinaire a été réalisée grâce à l'application de saccharose sur les parties aériennes. Cette étude a permis de montrer le rôle important des échanges d'informations entre les parties aériennes et les parties racinaires.

Le saccharose réprime la traduction du facteur de transcription bZIP11 entrainant des modifications dans le métabolisme des acides aminés. Le peptide de contrôle du saccharose (SC-peptide), en présence de fortes teneurs en saccharose, inhibe la traduction du facteur de transcription bZIP11 en bloquant le ribosome sur l'ARN messager (ARNm) (Rahmani et al., 2009).

La nitrate reductase 1 (NR1) est connue comme étant activée par la lumière. Cheng et al. (1992) ont montré que le saccharose provoquait une accumulation des ARNm de la NR1, de la même manière que la lumière. Cette action régulatrice du saccharose sur la NR1 permet à la plante de gérer ses réserves en limitant l'action de l'enzyme quand la teneur en sucres est faible. De plus, les auteurs signalent qu'ils ont obtenu le même résultat en substituant le saccharose par le glucose, soulevant l'hypothèse selon laquelle le saccharose n'agirait pas directement mais par l'intermédiaire d'autres métabolites tels que les sucres phosphorylés. D'autre part, ce travail permet de mettre en évidence le lien entre la régulation du métabolisme carboné et celle du métabolisme azoté chez les plantes qui sont, tous deux, dépendant du stade de développement de la plante, du type de cellule et des conditions environnementales (Coruzzi and Zhou, 2001). En condition de stress azoté, on observe, comme dans de nombreux autres stress, une accumulation des sucres (saccharose, glucose et fructose) aussi bien dans les parties aériennes que dans les parties racinaires (Krapp et al., 2011), ce qui met bien en évidence un lien étroit entre carbone et azone chez les plantes.

Karthiketan et al. (2007) ont mis en relation la réponse à un déficit en phosphate et la réponse aux sucres. La présence de saccharose, même à très faible concentration, dans le milieu de culture permet d'augmenter le niveau des transcrits des gènes induits par une privation de phosphate. Par contre, en l'absence de saccharose dans le milieu, ces gènes ne sont pas exprimés. Ces gènes peuvent être aussi régulés par d'autres sucres solubles (glucose, fructose) mais à un niveau réduit.

L'accumulation des anthocyanes a souvent été observée pour des plantes qui ont poussé sur des milieux contenant du saccharose. Solfanelli et al. (2006) ont montré que le saccharose agit comme une molécule-signal sur la voie des anthocyanes : le saccharose induit le facteur de transcription PAP1 qui stimule les gènes de biosynthèse des flavonoïdes. De plus, cette voie de régulation semble être spécifique du saccharose car ni le fructose, ni le glucose n'ont permis d'augmenter le niveau d'ARNm de PAP1.

Plusieurs transporteurs ont été identifiés comme étant spécifiquement régulés par le saccharose. Le saccharose a un effet sur ses propres transporteurs : il régule le niveau d'expression des gènes codant pour SUT2 (Barker et al., 2000) et inhibe l'activité de SUT1 en faisant cesser le transport du saccharose (Wind et al., 2010).

L'action signalétique directe ou indirecte du saccharose se retrouve donc à plusieurs niveaux du fonctionnement de la plante : au niveau du développement de par son influence sur l'architecture racinaire et de la physiologie de par son action sur le métabolisme primaire, sur le métabolisme secondaire et sur les transporteurs.

L'étude des mécanismes moléculaires spécifiques de la signalisation pour une molécule telle que le saccharose est très difficile car ce dernier peut être rapidement hydrolisé en glucose et fructose. A ce stade des connaissances, peu de choses sont connues quant aux mécanismes de perception et de transduction du signal. Chiou et Bush (1998), Barker et al. (2000) et Sivitz (2008) ont suggéré que la fonction « sensor » du saccharose serait assurée par un transporteur de ce dernier. Cependant, aucune donnée expérimentale n'a jusqu'à présent confirmé cette hypothèse.

## 4. Rôle des sucres dans la phytoremédiation

### 4.1. Conjugaison avec des sucres solubles pour la modification de la toxicité et l'élimination des polluants organiques

Les polluants organiques sont des molécules chimiques toxiques pour les organismes vivants. Au cours de l'évolution des systèmes de détoxification ont été mis en place selon différentes stratégies adaptatives. En effet, un modèle de détoxification des xénobiotiques chez les plantes a été proposé en s'inspirant du système de détoxification du foie des mammifères (cf. partie 2, Figure 4). Ce modèle, appelé « green-liver », se décompose en 3 étapes : (i) une étape de transformation, (ii) une étape de conjugaison et (iii) une étape de compartimentalisation (Sandermann Jr., 1992; Edwards et al., 2011b).

Dans ce modèle, le glucose sous forme d'UDP-glucose peut servir comme conjugué dans la deuxième étape de détoxification grâce à l'action des glycosyltransferases (UGT) qui conjuguent le groupement glucosyl au xénobiotique organique. Cette étape de glycosylation permet de rendre le xénobiotique moins toxique et plus hydrosoluble ainsi que de le stabiliser (Jones and

Vogt, 2001). Chez *Arabidopsis thaliana*, 107 UGT ont été identifiées (Edwards et al., 2011b). Cette famille multigénique est impliquée dans le métabolisme secondaire mais aussi dans la tolérance aux polluants organiques (Jones and Vogt, 2001).

Après une présélection basée sur des considérations chimiques et structurales, (Meßner et al., 2003) ont identifié la capacité de plusieurs UGT d'Arabidopsis, appartenant aux sous-familles E et L, de conjuguer le 2,4,5-trichlorophénol (TCP) avec de l'UDP-glucose. UGT84B1, UGT72E2 et UGT75D1 ont montré la plus forte affinité vis-à-vis de ce polluant. D'autre part, ces enzymes semblent aussi intervenir dans la voie de synthèse des lignines, ce qui montre un chevauchement entre le métabolisme des plantes et les voies de détoxification (Meßner et al., 2003). Par contre, toutes les UGT des plantes ne présentent pas d'activité face au TCP. En effet, aucune activité de conjugaison n'a pu être détectée pour l'UGT80A2 par exemple.

L'aniline chlorée 3,4-dichloroalanine (DCA) est un xénobiotique issu de la synthèse des pesticides. La conjugaison de ce xénobiotique avec un UDP-glucose a été observée chez *Arabidopsis* (Lao et al., 2003). Une fois conjugué, le xénobiotique est rapidement exporté des racines vers le milieu environnant (Lao et al., 2003). Des études supplémentaires ont permis de caractériser quelle enzyme catalysait cette réaction. Loutre et al. (2003) ont montré que l'UGT72B1 était l'enzyme qui conjugue le DCA et qu'elle présente aussi une activité pour d'autres anilines chlorées et même pour des phénols comme le TCP, ce qui met en évidence le large spectre d'action de cette enzyme. L'UGT72B1 est à la fois une *O*-glucosyltransferase (OGT) et une *N*-glucosyltransferase (NGT), ce qui la rend unique au sein des UGT. Afin de comprendre le fonctionnement de ces deux types d'activité, la structure et la fonction de cette enzyme a été caractérisée et cette UGT présente une activité OGT et NGT vis-à-vis du DCA (Brazier-Hicks et al., 2007).

Les UGT permettent grâce à la conjugaison de limiter les effets toxiques des xénobiotiques. Leur activité est caractérisée pour de nombreux polluants organiques. De plus, leur large spectre de substrat permet de penser que ces enzymes peuvent conjuguer de nombreux autres xénobiotiques organiques tels que les hydrocarbures, par exemple. Selon le modèle du « green-liver » (Sandermann Jr., 1992), le xénobiotique glycosylé est transporté dans la vacuole par les transporteurs à ATP Binding Cassette. Les travaux de Taguchi et al. (2010) sur les composés

phénoliques glycosilés ont permis de mettre en évidence une étape de malonylation du composé phénolique glycosilé précédant l'étape de compartimentalisation du modèle du « green-liver ».

### 4.2. Les sucres jouent un rôle prédominant dans la tolérance au stress oxydant

Les ROS sont des molécules fortement réactives qui peuvent provoquer la destruction complète des cellules (Mittler et al., 2004). Les organismes ont donc dû mettre en place des systèmes permettant de moduler l'action des ROS. Ces systèmes antioxydants prennent naturellement en charge les ROS produites par la photosynthèse et la respiration. Cependant, en condition de stress abiotique (xénobiotiques, ozone, métaux, salinité), on assiste à une accumulation des ROS car le système antioxydant n'arrive plus à prendre en charge les ROS produites (Keunen et al., 2013).

Les sucres solubles, notamment le fructose, le glucose et le saccharose, ont un double rôle vis-à-vis des ROS : ils entrent dans les voies métaboliques produisant des ROS mais ils ont aussi un effet protecteur face à ces molécules.

Des études ont montré que le saccharose et le glucose (à un niveau moindre) confèrent une meilleure tolérance à l'atrazine, un herbicide qui cause la production d'oxygène triplet (Sulmon et al., 2004; Sulmon et al., 2006). Les études réalisées sur l'effet du saccharose en présence d'atrazine ont permis de montrer que le saccharose semble avoir un effet signalétique sur le système antioxydant. L'apport de saccharose permet d'inhiber la voie métabolique des pentoses phosphates, ce qui limite l'effet des ROS (Couée et al., 2006).

D'autre part, de nombreuses études semblent mettre en évidence l'action des sucres en tant que molécules antioxydantes (Ende and Valluru, 2009; Bolouri-Moghaddam et al., 2010; Ende and Peshev, 2013; Keunen et al., 2013). Des essais biochimiques *in-vitro* ont permis de montrer que le saccharose a un pouvoir antioxydant mais cela n'a pas encore pu être vérifié *in-planta.*

Les sucres jouent un rôle primordial dans la gestion du stress oxydant et des ROS par les plantes, soit directement en tant que molécules antioxydantes ou indirectement en tant que molécule signal. Même si de nombreuses études montrent le rôle protecteur des sucres en conditions de stress oxydant, peu de choses sont actuellement connues sur les mécanismes précis d'action du sucre.

## 5. Conclusion

Les sucres sont des molécules-clés dans le fonctionnement général des plantes. Ils interviennent à différents niveaux et ne sont pas seulement des métabolites. Leur action en condition de stress abiotique est très large. Ils peuvent agir en tant qu'osmo-protecteur (Ende and Peshev, 2013), protecteurs contre les ROS, dans les voies de signalisation ce qui montre que les sucres ont un rôle clé dans le fonctionnement des plantes.

Les études portant sur l'effet du sucre en conditions de stress ont été réalisées notamment sur des effets climatiques mais peu de choses sont connues quant à l'effet des sucres sur un stress causé par un xénobiotique et rien n'est connu sur les effets du stress liés à des polluants industriels tels que les HAPs. Il paraît intéressant donc de s'intéresser à l'effet des sucres solubles sur les stress causés par les polluants organiques notamment les HAPs qui sont connus comme étant générateur de stress oxydant (Liu et al., 2009). D'autre part, Sulmon et al. (2006) ont montré lors d'un essai en pots que la phytoaccumulation de l'atrazine est améliorée par un apport de saccharose, montrant le potentiel d'un amendement en saccharose pour favoriser la phytoremédiation des polluants organiques d'un sol pollué.

# Partie 4 : **Travail de thèse**

Une collaboration a été mise en place entre l'Université de Rennes 1 et l'entreprise Axson-Coatings afin d'évaluer la faisabilité et l'efficacité d'un système de dépollution des HAPs par les plantes d'un site industriel contaminé par les HAPs. C'est dans le cadre d'une convention industrielle de formation par la recherche (CIFRE) que mon projet de thèse a été mis en place.

Le projet porte sur la compréhension des mécanismes de phytoremédiation aussi bien à l'échelle moléculaire qu'*in-situ,* avec une partie réalisée au laboratoire au sein de l'Unité Mixte de Recherche Ecobio (Rennes) et une partie réalisée sur un site pilote qui se situe à Aubevoye (Eure, France).

Des études réalisées au sein de l'UMR Ecobio ont permis de mettre en évidence le rôle protecteur du saccharose dans le processus de tolérance à un herbicide, l'atrazine (Sulmon et al., 2004; Sulmon et al., 2006; Ramel et al., 2007; Ramel et al., 2009). Ces études ont montré le rôle du saccharose dans la réponse à un stress oxydant. D'autre part, le saccharose stimule aussi l'accumulation de l'atrazine dans les plantes (Sulmon et al., 2007a). Ces travaux suggèrent fortement qu'un amendement en saccharose peut améliorer la tolérance des plantes à des polluants organiques, et favoriser sa phytoaccumulation.

L'apport de saccharose apparait donc comme un moyen facile et non dangereux pour l'environnement de stimuler la phytoremédiation d'un polluant organique. A ce stade des recherches, il apparaissait intéressant de voir si le saccharose permet de stimuler la phytoremédiation et de protéger les plantes face à d'autres composés organiques néfastes tels que les HAPs.

Mon travail de thèse s'est articulé autour de trois grandes questions :

(i) La première partie de mon travail a porté sur l'étude des effets des HAPs sur les plantes. Plus particulièrement, ce travail a eu pour objectif d'étudier les mécanismes impliqués dans la réponse des plantes aux HAPs, de déterminer si ces dernières mettent en œuvre des processus de détoxification et d'identifier des acteurs et voies cruciales impliquées dans ce processus pouvant, à moyen terme, faire l'objet de caractérisation fonctionnelle. Cette étude a été réalisée en conditions contrôlées avec la plante modèle *Arabidopsis thaliana* et le phénanthrène, en tant que HAP modèle. L'ensemble des expérimentations a été effectué dans un milieu de culture sans apport de saccharose, contrairement à ce qui est fait précédemment dans d'autres travaux, puisque les résultats obtenus dans notre équipe montrent qu'il a un effet protecteur contre l'atrazine. Les effets du phénanthrène ont été évalués à plusieurs niveaux : d'abord au niveau du développement de la plante sur les parties aériennes et racinaires, ensuite au niveau cellulaire, de son transcriptome, et de son métabolome. Pour les analyses transcriptomiques et métabolomiques, j'ai analysé les effets à court terme (après quelques heures d'incubation) afin d'étudier les premiers évenemments qui sont mis en place et qui sont succeptibles d'apporter des informations précieuses pour comprendre l'induction des différents mécanismes de tolérance. De plus, Zhan et al. (2010) ont montré que le phénanthrène est rapidement absorbé par les plantes. D'autre part les seules données de transcriptome disponibles pour la réponse des plantes au phénanthrène correspondent à des incubations longues, ce qui pourrrait interférer avec des processus de mise en place de senéscence.

(ii) La deuxième partie de mon travail porte sur l'effet protecteur du saccharose en condition de stress induit par le phénanthrène. En effet, les résultats préliminaires obtenus dans le cadre d'un stage de master ont montré que le saccharose permet aux plantes d'*Arabidopsis* de supporter des concentrations de phénanthrène supérieures aux plantes contrôles. Le travail réalisé dans cette partie est parallèle à celui réalisé lors de l'étude des effets du phénanthrène sur les plantes. Dans cette

partie, je me suis intéressée aux effets du saccharose en présence de phénanthrène sur le développement de la plante. Ensuite, une analyse du transcriptome m'a permis de comprendre les effets du sucre en condition de stress et en conditions de culture « standards » mais aussi de voir comment la présence de saccharose modifie l'activité transcriptionnelle de différents groupes de gènes impliqués dans les stresses ou codant pour les gènes impliqués dans le xénome. Mais aussi du métabolome de la plante en présence de phénanthrène. Enfin, j'ai cherché à savoir si un apport de saccharose modifiait l'absorption et la répartition du phénanthrène dans les plantes.

(iii) La dernière partie de mon travail concerne l'utilisation des connaissances obtenues au laboratoire sur un système simple et contrôlé, pour l'amélioration de la phytoremédiation sur un site expérimental. En effet, cette étude *in-situ* porte sur deux grands axes : la comparaison de divers couverts végétaux (arbres, herbacées et aucune végétation plantée) qui permet de chercher quel est l'espèce végétale la plus efficace pour la dépollution des sols et l'étude des effets du saccharose sur la tolérance des plantes aux HAPs dans un écosystème complexe, où coexistent plusieurs communautés microbiennes.

Le manuscrit est organisé de la façon suivante :

- Le chapitre 2 est une présentation de l'ensemble de mes résultats sur l'effet du phénanthrène à court terme sur la plante modèle *Arabidopsis thaliana*.
- Le chapitre 3 décrit l'effet du saccharose en condition de stress lié au phénanthrène.
- Dans le quatrième chapitre, les résultats d'un essai de phytoremédiation sur un site industriel sont présentés.
- Le dernier chapitre est une conclusion générale sur l'ensemble de mon travail.

La partie 2 du chapitre d'introduction a été rédigée en anglais sous forme d'un article de synthèse qui vient d'être soumise au journal Plant Science. Les chapitres 2 et 3 sont rédigés en anglais sous forme d'articles scientifiques dans le but d'une soumission future

# Chapitre 2 : **Etude des modifications développementales, transcriptomiques et métabolomiques induites par le stress provoqué par le phénanthrène**

**Préambule**

Au cours de leur évolution, les organismes sessiles tels que les végétaux supérieurs ont développé des mécanismes moléculaires et physiologiques qui leur permettent de s'adapter aux modifications de leur environnement. En effet, en condition de stress abiotique, les mécanismes de signalisation et le contrôle de l'expression des gènes jouent un rôle majeur pour le maintien du fonctionnement cellulaire.

Les sucres solubles, en particulier le saccharose, ont un impact considérable en condition de stress abiotique et, de par leur action signalétique, modulent fortement la réponse de la plante au stress oxydant (Bolouri-Moghaddam et al., 2010; Keunen et al., 2013). Or, la majorité des études *in-vitro* portant sur les effets d'un stress abiotique, notamment celles sur les effets du phénanthrène (un HAP), sont réalisées sur des milieux supplémentés en saccharose, modifiant ainsi la réponse réelle de la plante au stress. Nous avons donc décidé de travailler en condition d'absence de source carbonée dans le milieu de culture.

D'autre part, Zhan et al. (2010) ont montré que les plantes sont capables d'absorber très rapidement le phénanthrène grâce à un transporteur actif. Ces résultats montrent l'importance des premières heures de contact entre le xénobiotique et les plantes dans la réponse de la plante au xénobiotique.

Dans cet article, nous avons utilisé des approches de transcriptomique et de métabolomique afin de déterminer les premières modifications au niveau du métabolisme et de l'expression des gènes impliquées dans la réponse à un stress induit par le phénanthrène, un produit dangereux issu des activités humaines. Ce travail avait également pour objectif d'identifier des acteurs impliqués dans les étapes précoces de perception et de gestion de ce polluant par la plante. En effet, leur caractérisation fonctionnelle de ces acteurs permettra d'évaluer s'ils pourrontt être utilisés dans des approches biotechnologiques destinées à améliorer le processus de phytorémédiation. Lors de cette étude, les résultats obtenus, nouveaux, montrent que les plantes détectent rapidement la présence du phénanthrène puisque, dés 30 minutes d'incubation, des modifications apparaissent au niveau de la transcription de gènes impliqués principalement dans les voies de signalisation. Les gènes de détoxification et de gestion du stress oxydant, très probalement induits par le phénanthrène, sont régulés plus tardivement jusqu'à 8 heures de

traitement. Enfin, après 8h d'exposition, de très nombreux genes impliqués dans les métabolismes primaires et secondaires sont réprimés alors que ceux intervenant dans les processus de glycolyse, de fermetation et de réponse aux stress sont induits. L'intégration des données de dosage de metabolites montre une forte accumulation d'acides aminés et de sucres solubles, qui sont des indicateurs d'un fonctionnement de la plante en déclin. Le statut énergétique semble être un facteur limitant qui conduit à l'épuisement, lors de la troisième phase de notre modèle.

**Running title**: Deciphering the early plant response to phenanthrene

**Title**: New insights into the early *Arabidopsis thaliana* response to phenanthrene exposure

**Authors**:

Anne-Sophie Dumas[2,*] (anne-sophie.dumas@univ-rennes1.fr)

Evangelos Barbas[1,a,*] (vbarbas@for.auth.gr)

Guillem Rigaill[1] (rigaill@evry.inra.fr)

Delphine Bernard[2,b] (Delphine.Bernard@univ-brest.fr)

Ludivine Taconnat[1] (taconnat@evry.inra.fr)

Abdelhak El Amrani[2,] † (abdelhak.el-amrani@univ-rennes1.fr)

Richard Berthomé[1,c,] †(rberthome@toulouse.inra.fr)

[1]INRA, UMR 1165, Unité de Recherche en Génomique Végétale (URGV), CNRS, ERL 8196, UEVE, 91057, Evry cedex, France.

[2]CNRS, Université de Rennes 1, UMR 6553, Ecosystèmes-Biodiversité-Evolution, 35042 Rennes cedex, France.

Current addresses

a: Laboratory of Forest Genetics and Tree Breeding, AUTH, University Campus, 54124 Thessaloniki, Greece

b : Laboratoire de Génétique Moléculaire et de Génétique Epidémiologique, INSERM U1078, 46, rue Felix Le Dantec, CS 51819, 29218 Brest Cedex 2, France

c : Laboratoire des Interactions Plantes Micro-organismes (LIPM), UMR INRA 441/CNRS 2594, CS 52627, 31326 CASTANET TOLOSAN CEDEX, France

† Corresponding autors:

Richard Berthomé (rberthome@toulouse.inra.fr), tel (33) 5.61.28.55.09

**Abstract**

Along their evolution, sessile organisms such as higher plants developed molecular and physiological plasticity to cope with environmental cues. Under abiotic stress, signaling mechanisms and control of gene expression play a major role to maintain cellular homeostasis and plant development. In this paper, we used transcriptomic and metabolomic analysis to decipher the early events involved in phenanthrene induced stress, a hazardous polycyclic aromatic hydrocarbon of natural and anthropogenic origins. Our results, are consistent with the earlier studies performed on phenanthrene or others xenobiotics and add a new resolution level by dissecting early plant response during a kinetic ranging from 30m minutes to 24h of treatment. Plant response can be divided in three phases: i) plant sense phenanthrene rapidly, as genes mainly involved in perception and signalization, were differentially expressed within the first 30 minutes, ii) a reaction phase after 2h to 8h of incubation, characterized by regulation of genes involved in detoxification, iii) and a third exhausting phase from 8h where many differentially expressed genes are involved in repression of the secondary metabolism. This study also allowed the identification of new early regulated phenanthrene dependent genes that could be good candidates for further functional characterizations and development of strategies of molecular avoidance for phenanthrene.

**Key words**: PAH, Arabidopsis, transcriptome, metabolome, xenome, natural xenobiotic

## 1. Introduction

Polycyclic aromatic hydrocarbons (PAHs) constitute a large class of organic pollutants (POPs) present in the atmosphere in either a gaseous or a particulate form. These chemicals are ultimately deposited within the soil, silt and sediments. The common sources of PAHs in the environment are from both natural (volcanoes eruptions, forest and rangeplant fires) and anthropogenic sources (Haritash and Kaushik, 2009)(1). Human activities generate PAHs through the incomplete combustion processes of organic material such as biomass or of carbon-based fuels as well as from the release of petroleum into the environment (Ravindra et al., 2008; Katsoyiannis et al., 2011; Callén et al., 2012)(2-4). They are highly resistant to biological degradation as their structure contains two or more benzenes rings. There is a concern with these compounds as they are present throughout the environment, and have been shown to have adverse effects on human health since some of them have been described to be carcinogenic, mutagenic or endocrine disrupting compounds (Luch, 2005; Gammon and Santella, 2008; Balabanič et al., 2011)(5-7).

Risks associated to PAHs pollution can be partially overcome by their removal from soil using chemical, physical or thermal treatments. These techniques are efficient but expensive. In addition, they impact the environment and often transfer the pollutant from one compartment to another (Gan et al., 2009)(8). Alternatives emerged with “green technologies” which use of the environment ability to transform the pollutant in a less hazardous compound by the natural action of living organisms (Mitsch, 2012)(9). The development of these green approaches, including bioremediation and phytoremediation tools, brought focus on factors affecting PAHs remediation efficiency. Environmental conditions, plant species used, nature of microbes and plants interactions in the soil, and nature of the pollutant to be degraded have been demonstrated to modulate PAHs remediation (Cheema et al., 2010; Furuno et al., 2010; Furuno et al., 2012; Schamfuß et al., 2013b)(10-13). As for heavy metals or explosives detoxification approaches already in use, improvements in the PAHs bioremediation systems might come from the studies of plant-microbes interactions in the soil and genetic engineering of plants able to stimulate these interactions and/or degrade PAHs (Rylott et al., 2011; Bhargava et al., 2012; Panz and Miksch, 2012; Shim et al., 2013)(14-17). Promising results have been obtained with the engineering a naphthalene-degrading endophytic strain *Pseudomonas putida*

VM1441(pNAH7) that efficiently colonized plants (pea, annual ryegrass) and enhanced plant tolerance to naphthalene (Germaine et al., 2009). Tobacco plants expressing a fungal gluthatione-S-transferase also showed an increased tolerance, higher uptake and transformation of naphthalene (Dixit et al., 2011).

Development of such innovative tools for PAHs phytoremediation remains rare, mainly because cellular and molecular mechanisms involved in plant response to PAHs and their putative uptake and metabolization by the plants are still largely unknown; contrasting with numerous studies performed to elucidate mechanisms involved in PAHs degradation by bacteria, fungus and algae (Cerniglia, 1992; Warshawsky, Cody et al. 1995; Bezalel, Hadar et al. 1997; Kotterman, Vis et al. 1998; Mrozik *et al.*, 2003; Johnsen *et al.*, 2005; Kim *et al.*, 2007; Syed, Doddapaneni et al. 2010). General models for plant xenobiotics detoxification have been based on an analogy of the xenobiotic detoxification system described in the mammalian liver (Sandermann Jr., 1992; Edwards et al., 2005)(18, 19). Edwards et al. (2005) also proposed that "the whole expressed genome responsible for the detection, signalization, transformation, conjugation, compartmentalization and transport of xenobiotics or derivatives in the cell" constitute the xenome.

The phenanthrene, used as PAH model, has been shown to be taken up by both *Arabidopsis* (Alkio et al., 2005)(20) and wheat roots (Zhan et al., 2010)(21) then gone on to be internalized, implying this pollutant or its derivatives being transported in the plants. Moreover, some PAHs were metabolized in cell cultures of different plant species and proposed to be conjugated to soluble sugar or link to glutathione (Sandermann Jr. et al., 1984; Kolb and Harms, 2000)(22, 23). Interestingly, Zhan et al (2010) have shown that the uptake of phenanthrene by roots occurs in a fast passive diffusion just after the transfer of wheat in the phenanthrene supplemented medium and in a slow active absorption probably mediated by a transporter, after 2 hours of incubation. Hence, these observations suggested that the phenanthrene absorption, and its putative transformation, might be quickly regulated by the plant. Physiological, cellular and molecular investigations of plant response to PAHs have been carried out, mostly on long-term expositions to phenanthrene (14-30 days) (Alkio et al., 2005; Liu et al., 2009; Weisman et al., 2010a)(20, 24, 25). After phenanthrene treatments, a concentration dependent reduction of plants size, roots length, chlorophyll content and a delay to set seeds are observed. Phenanthrene induces organelle

structure alteration, up-regulation of antioxidant activities and morphological deformations that could be linked to tissue necrosis (Alkio et al., 2005; Liu et al., 2009)(20, 25). This data sheds light on some features shared between plant responses to phenanthrene, other abiotic stress and pathogen hypersensitive response (HR). More particularly, the production of reactive oxygenes species (ROS) appear to play an important role in stress related phenotypes observed following phenanthrene treatment (Liu et al., 2009)(25). Transcriptional analyses of the plant response to long exposure to phenanthrene support this hypothesis. Weisman et al (2010) proposed that through its putative oxidation by mono- or di-oxygenases, that have to be identified the phenanthrene might trigger an increase in the reactive oxygen species (ROS) level and induce expression of genes encoding proteins mostly involved in oxidative stress regulation or production. However, for phenanthrene it remains unclear if oxidative stress and cell death result from detoxification activities or if it is an indirect consequence of phenanthrene or derivatives phytotoxicity since cell death only appears in location where it accumulates.

ROS are natural byproducts of various metabolic pathways generated in many compartments including organelles, peroxisomes, the endoplasmic reticulum and the plasma membrane. Plant use low levels of ROS as early signaling molecule to restrict pathogen invasion, induce program cell death or regulate stomata closure (Wang and Song, 2008; Zurbriggen et al., 2010)(26, 27). However, the balance between production and scavenging of ROS is disturbed, under various abiotic stress conditions such as UV-radiation, ozone, intense light, drought, decrease or increase in temperature, mechanical stress and xenobiotics stress, leading to irreversible damages that could result in tissue or organ necrosis. To fight against increased levels of ROS, plants use a battery of enzymatic activities and buffering processes (Choudhury et al., 2013)(28). Among them, soluble-sugars originate as true ROS scavengers in plant (Keunen et al., 2013)(29) and also as a tool to improve phytoremediation efficiency through the limitation of ROS production in xenobiotic stress conditions. Exogenous soluble sugars supply, particularly sucrose, has been shown to confer a high level of tolerance to atrazine in *Arabidopsis* (Sulmon et al., 2004; Sulmon et al., 2007a; Sulmon et al., 2007b)(30-32). Interestingly, transcriptome analysis revealed that sensitivity and sucrose-induced tolerance to atrazine were also associated to important modifications of gene expression related to ROS defence mechanisms as for results obtained by Weisman

et al. (2010) in case of long term exposure to phenanthrene (Ramel et al., 2007; Ramel et al., 2009)(33, 34). However, all published data on the plant response to phenanthrene were carried out in medium containing sucrose. As a result the use of these mediums do not allow to discriminate if differential gene expression and process associated to ROS production and scavenging were the result of phenanthrene treatment alone or the consequence of sucrose-induced protection.

In order to characterize mechanisms involved in the phytoremediation process and to decipher molecular determinant of phenanthrene induced injury, a time course genome wide analysis and metabolome profiling were carried out. As sucrose may deeply change genes expression and plant responses, this whole study was performed using sucrose free medium. Results obtained in this study begin to unfold the early events involved in phenanthrene responses. Our results showed that plant response can be divided in three phases: i) Phenanthrene is detected rapidly by plants as genes mainly involved in perception and signalization, were differentially expressed within the first 30 minutes, ii) a reaction phase is observed 2h to 8h after incubation and is characterized by the regulation of genes involved in detoxification, iii) After 8h of exposure to phenanthrene, numerous genes involved photosynthesis, primary and secondary metabolism are repressed, whereas genes mainly involved in glycolysis, fermentation, redox and stress metabolisms are up-regulated. Integration of metabolites titration data indicates a strong accumulation of amino acids and soluble sugars, indicators of functional declines that might lead the exhaustion of the plant. Energy status appears to be the crucial limiting factor that leads the plant to the third phase of our model.

## 2. Material and methods

### 2.1. Plant material and growth conditions

Seeds of *Arabidopsis thaliana* ecotype Columbia-0 (Col-0) were used in all the experiments. Seeds were surface sterilized for 10 min with a solution containing 10% (v/v) commercial bleach (BAYROL France SAS, Dardilly, France) ) diluted in 95° ethyl alcohol and 0.05% (v/v) Teepol 610 (SERVA Electrophoresis GmbH, Heidelberg, Germany). Seeds were rinsed thoroughly with 95° ethyl alcohol and dried overnight in a sterile hood Seeds were sown on half-strength Murashige and Skoog solid medium (MS/2) containing 0.8% (W/V) agar-agar type E (SIGMA ALDRICH) supplemented with phenanthrene solved in dimethylsulfoxide (DMSO) or DMSO alone used as control. Seeds were germinated in a growth chamber (16-h light/8-h dark cycle 4000 lux, 22°C, 70% hygrometry) after cold treatment for 48 h at 4°C. Phenanthrene stock solution was at 700mM and in each experiment, controls were prepare adding identical volume of DMSO.

### 2.2. Measurement of seedling growth and development

For root measurement and fresh weight determination, seeds were sown on MS/2 solid medium supplemented with 0, 50, 100, 200 and 400µM of phenanthrene or with DMSO alone as control. Plants were cultivated vertically on square Petri dishes (15x15cm). Primary roots were measured after 10 days of growth using digital photographs acquisitions and Image J v 1.45s software (Abramoff et al., 2004)(73). For each condition, primary root length was measured for 30 independents plants. For rosette fresh weight measurements, plantlets were grown horizontally on circle Petri dishes. Shoots were separated from the roots and weighted after 30 days of growth. Shoots from three plants for two distinct replicates were harvested. Results represent the mean with the standard error (SE). Statistical analyses were carried on using the t-Test in the R software (team RDC, 2013)(74). Levels of chlorophyll were determined using the equations given by Lichtenthaler and Wellburn (1983)(75). Shoots samples previously weighted were ground and incubated for 10 minutes in 80% acetone at room temperature under stirring. Absorbance of these extracts

was measured at three wavelengths (663 nm, 646 nm and 470 nm). Results were given as the mean of the 6 measurements with the standard error (SE). Data were analyzed using the t.Test in the R software (team RDC, 2013)(74).

### 2.3. Fluorescence microscopy

Analysis were performed at the Imagif plateform, in the Cellular Biology Pole, (CNRS,Gif sur Yvette, France). *Arabidopsis* plantlets used were grown on MS/2 medium for 15 days and then transferred at stage 1.04 (Boyes et al., 2001)(76) on MS/2 medium containing 200µM of phenanthrene or the same volume of DMSO. In order to facilitate the transfer, plants were grown vertically. A sterile and transparent plastic film was applied to the contaminated medium in order to avoid any contact of the vegetative parts of the plantlets with the medium. After 5 days of phenanthrene treatment, leaves and roots from 5 independent plantlets harvested on 3 different petri dishes were observed with a Zeiss LSM510 META microscope under UV-light (excitation 364nm and acquisition with 32 channels between 362nm and 704nm). Data were acquired using Zen2008 software developed by Zeiss (Germany).

### 2.4. Transcriptome studies

Microarray analysis was carried out at the Research Unit in Plant Genomics in Evry, France, using the CATMA version 5 array containing 31776 gene-specific tags corresponding to 22,089 genes from *Arabidopsis* (Crowe et al., 2003; Hilson et al., 2004)(50, 51). Total RNA extractions from two independent biological replicates were performed using the QIAGEN RNAeasy plant minikit according to the manufacturer's instructions. Each biological replicate was composed of *Arabidopsis* plantlets grown *in-vitro* for 15 days on solid MS/2 medium and transferred at stage 1.04 (Boyes et al., 2001)(76) on liquid MS/2 medium containing 200µM of phenanthrene or the same volume of DMSO. Each biological replicates includes phenanthrene-treated and control plants. Each sample corresponding to 30 plants pooled were harvested after 30 min, 2-, 4-, 8- and 24h of incubation. For all comparisons performed

(Supplemental Figure 1 A), the experiment was done using the dye-switch technique. The labeling of antisense amplified RNA with Cy3-dUTP or Cy5-dUTP (Perkin-Elmer-NEN Life Science Products), the hybridization to the slides, and the scanning were performed as described by Lurin et al. (2004)(77).

### 2.5. Statistical Analysis of Microarray Data

Experiments were designed in collaboration with the Bioinformatic and Predictive Genomics group at the Research Unit in Plant Genomics in Evry, France. Specific statistics were developed to analyze CATMA hybridizations. For each array, the raw data include the logarithm of median feature pixel intensity (in log base 2) at wavelengths of 635 nm (red) and 532 nm (green). No background was subtracted. The normalization method used was described by Lurin (2004)(77). Differentially expressed genes were determined by performing a paired t-test on the log ratios averaged on the dye switch. A trimmed variance was calculated from spots that did not display extreme variance. The raw P values were adjusted by the Bonferroni method, which controls the family-wise error rate (with a type I error equal to 5%). We also adjusted the raw P values to control a false discovery rate using Benjamini-Yetkutieli at a level of 1%. Nonetheless, in the CATMA analysis pipeline, family-wise error rate proved to be the best solution to balance the estimated number of false positives and false negatives (Ge et al., 2003)(78). As described by Gagnot et al. (2008), when the Bonferroni P value was lower than 0.05, the gene was declared differentially expressed (Gagnot et al., 2008)(79). The complete data set is given as Supplemental Tables 1.

### 2.6. ANOVA analysis

Normalized intensities for each dye-switch experiment were recovered. A sample is characterized by the time-point of the experiment (0h, 2h, 4h, 8h or 24h), the treatment (none or phenanthrene), the dye used for the experiment (red or green) and the array on which the sample was hybridized (numbered from 1 to 28). For a given gene, we denote $Y_{tpda}$ the expression level of the gene at time-point *t*, with the treatment *p*, using the dye *d* and on

the array *a*. We studied two linear models. The first (see model 1) considers an additive effect of time ($\alpha_t$) and the treatment ($\beta_p$) without interaction. The second model (see model 2) considers an additive effect of time ($\alpha_t$) and the treatment ($\beta_p$) and an interaction between the two ($\gamma_{tp}$). In both model we take into account a potential array effect ($\delta_a$). We only analyzed genes for which all 56 data-points were available, in other words genes without missing values.

$Y_{tpda} = \mu + \alpha_t + \beta_p + \delta_a + \varepsilon_{tpda}$ (model 1)

$Y_{tpda} = \mu + \alpha_t + \beta_p + \gamma_{tp} + \delta_a + \varepsilon_{tpda}$ (model 2)

For each gene the parameters of model 1 and 2 were fitted using ordinary least squares. Model 1 has 22 residual degrees of liberty and model 2 only 18. For each gene we used a Fisher test to test the hypothesis H0 that model 1 is true, against the alternative H1 that model 2 is true. We accounted for multiple testing issues using the Benjamini-Hochberg procedure. We considered that genes with an adjusted p-value of less than 5% have an interaction between time and treatment. All these analysis were performed with the R software (team RDC, 2013)(74). Data corresponding to selected genes are presented in Supplemental Table III.

### 2.7. Biological pathways enrichiment

Lists of genes, with an adjusted p-value of less than 5% have an interaction between time and treatment, were recovered for 30 min, 2-, 4-, 8-, and 24h comparisons. Biological pathways significantly over-represented in lists of differentially expressed genes were identified with the classification superviewer tool of the university of Toronto website (http://bar.utoronto.ca/ntools/cgi-bin/ntools_classification_superviewer.cgi) using MAPMAN classification as a source (Provart T., 2003)(80).

### 2.8. Clustering

Hierarchical clustering using Pearson correlation as distance calculation were performed. on the Genevestigator Web site (https://www.genevestigator.com/gv/) using

our top list (Table II) and selections of data corresponding to stress, biotic and chemical perturbation.

### 2.9. cDNA Synthesis and Quantitative Real-Time PCR (qRT-PCR)

The qRT-PCR validation was carried on 11 genes being found to be differentially regulated in phenanthrene treated and control samples described in the microarray section.. Primers were designed using the online software Primers3 (Rozen and Skaletsky, 2000)(81) (http://frodo.wi.mit.edu/, optimal temperature of 60°C, Supplemental Table VI). The primer pairs were first tested on a dilution series of genomic DNA (5, 0.5, 0.05, and 0.005ng) to generate a standard curve and assess their PCR efficiency, which ranged between 90% and 110%. RT was performed on 1µg of total RNA with oligo(dT) primer (18-mer) and the SuperScript II RNase $H^-$ reverse transcriptase according to the manufacturer's instructions (Invitrogen). In every run, at least three replicates PCRs were done for each cDNAs. For each gene investigated using qPCR, a dilution series covering 3 orders of magnitude (1, 1/10 and 1/100) of the cDNA stock solution was prepared. Three replicates of each of the three standards were used in qPCR experiment together with three no-template controls. qPCR was performed in 5 µL, with 0.5 µL of RT reaction (1/100 dilution), 900 nM final concentration of each primer pair, and 2,5µL of MESA GREEN qPCR MasterMix Plus for SYBR® Assay (Eurogentec). Corresponding minus-RT controls were performed with each primer pair. All reactions were performed with the CFX384 Touch™ Real-Time PCR Detection System (Bio-Rad) as follows: 95°C for 5 min; 40x95°C for 10 s and 60°C for 30 s ; and a dissociation step to discriminate primer dimers from the PCR product. Using CFX Manager™ Software version 3.0 provided by the manufacturer, the optimal cycle threshold (Ct) was determined from the dilution series, with the raw expression data derived. Six housekeeping genes were assessed in this experiment, and the two best control genes, consistently expressed, were selected to calculate the average normalization factor: *AT4G13615* and *AT5G21090* for each sample pair. Normalized (Norm) $\Delta$Ct for each differentially expressed gene was calculated as following: Norm $\Delta$Ct = - (raw$\Delta$Ct - Norm factor). Microarray data from this article were deposited at Gene Expression Omnibus (http://www.ncbi.nlm.nih.gov/geo/), accession no. GSE48181) and at CATdb

(http://urgv.evry.inra.fr/CATdb/; Project: AU10-04_phytoremediation) according to the "Minimum Information About a Microarray Experiment" standards.

## 2.10. Targeted analysis of metabolites

Analysis were realized at the CORSAIRE platform (Biogenouest, INRA UMR 1349 IGEPP, Le Rheu, France). *Arabidopsis* plants used for this analysis were grown on MS/2 medium for 15 days and then transferred at stage 1.04 (Boyes et al., 2001)(76) on liquid MS/2 medium containing 200µM of phenanthrene or the same volume of DMSO. After 24 hours of incubation, plants were harvested, frost in liquid nitrogen, lyophilized and ground. A total of 10mg of dry plant material was extracted in 500µL of extraction solvent and 250µL of chloroform. The extraction solvent is composed of 5% of methanol and 95% of beta amino benzoic acid (10mM) – adonitol (20mM) concentrated solution. Samples were shaken 10 min at room temperature then 500µL of ultra pure water were added. All samples were vortexed for 30s and then centrifugated for 5 min at 12000g and 15°C. The entire liquid phase was transferred to a new tube. For amino acids analysis, 50µL of the extract was dried under vacuum and 50µL of water were added. Samples were derivated using the AccQTag method (Waters) and analyzed by Ultra Performance Liquid Chromatography (UPLC, Waters). For the sugars, organic acids, alcohol and ammonium quantification, 50µL of the extract supplemented with 50µL of internal standard were dried under vacuum. 50µL of methoxamine in pyridine (concentration 20mg/mL) were added to the dried samples which were incubated 90min at 30°C. 50µL of MSTFA (N-Methyl-N-(trimethylsilyl)trifluoroacetamide) were added to each sample which are incubated for 30min at 37°C and than analyzed by GC-MS.

## 3. Results-discussion

### 3.1. Phenanthrene altered plant development in a dose dependant manner

In order to estimate the phenanthrene concentration to be used in our time course analysis and to evaluate its effect on plant development, we investigate the toxicity level of phenanthrene on Arabidopsis. As sucrose has been described as a true ROS scavenger which might act as a signaling molecule modifying plant responses to abiotic responses, these tests were performed on a sucrose free medium. For this purpose, plants were germinated on MS/2 medium, supplemented with 0-, 50-, 100-, 200- and 400µM of phenanthrene. When phenanthrene treatment does not exceed 24h, no macroscopic alterations were induced. However, compared to the control, plants grown for 10 to 30 days on phenanthrene supplemented medium showed altered phenotypes and differences in shoots fresh weight, primary roots length and leaf chlorophyll content, the later well known to be a good indicator of photosynthetic activity, stress and nutrient state (Alena Torres Netto, 2005)(35) (Figure 1).

Thirty days of phenanthrene exposure clearly inhibits the development of plant shoots even at the lower phenanthrene concentration. Plant development was reduced in a dose-dependent manner. The strongest effect was observed at 200µM and 400µM. Plant growth variation was observed with some plants unable to grow. This variation was ever higher at 400µM. Moreover, whereas small plants remained green at 200µM, all of them were chlorotic at 400µM (Figure 1A). In parallel, the mean shoot fresh weight of all treatments were significantly different from the control and decreased by 31%, 57%, 58% and 83% at 50µM, 100µM, 200µM and 400µM of phenanthrene, respectively (Figure 1B). Chlorophyll content, of 30-day-old plants confirmed the chlorotic macroscopic phenotypes observed as it only significantly decrease at 400µM of phenanthrene when compared to the control (Figure 1C). A significant decrease in primary root length was also observed between the untreated plants and those grown on phenanthrene supplemented medium, excepted at 50µM of phenanthrene. At 100µM, 200µM and 400µM of phenanthrene, the primary roots length was reduced about 13%, 55% and 48% in comparison to the control, respectively (Figure 1D). In high salinity stress conditions, toxic effects of salts within the plant lead to inhibition of many biochemical and physiological processes such as nutrient uptake and

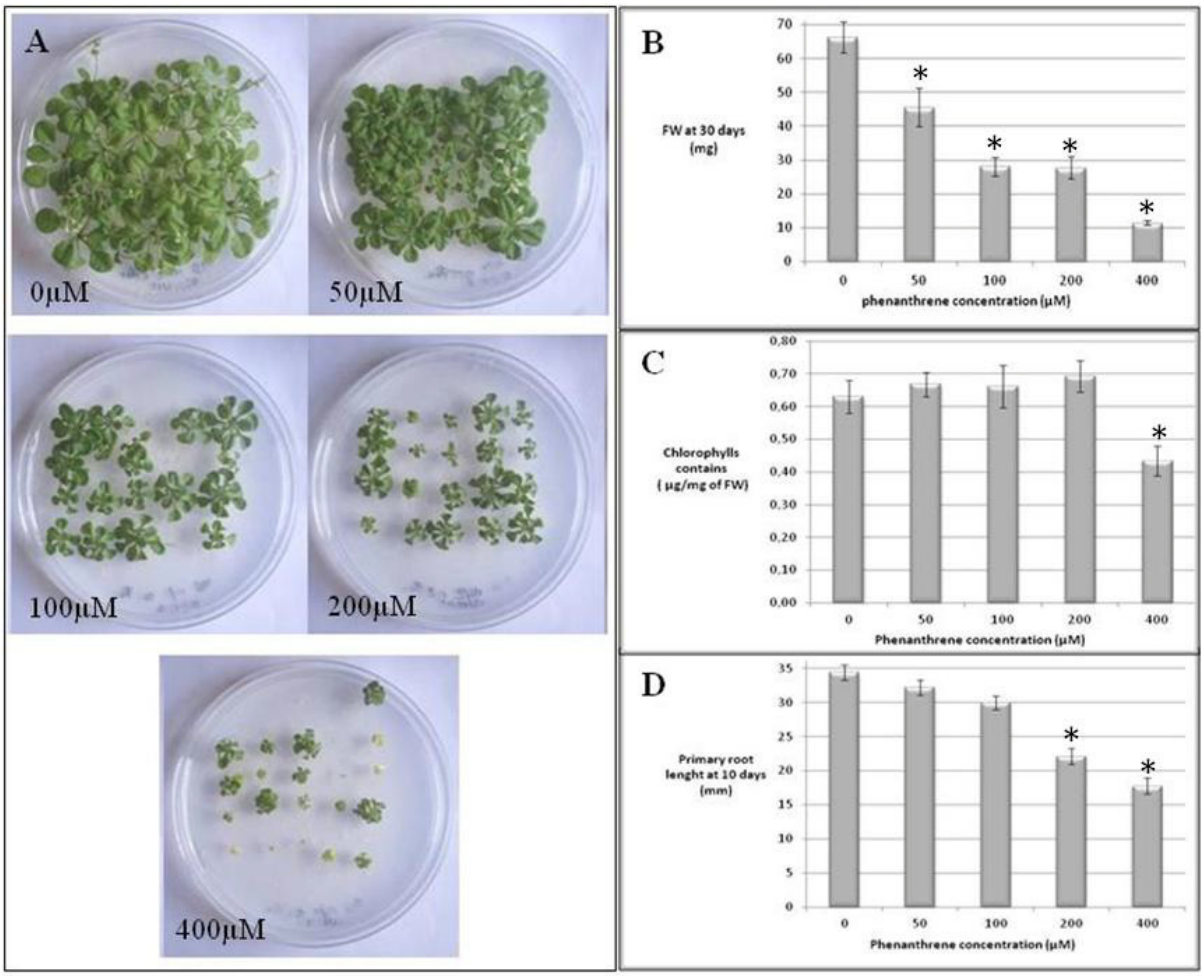


**<u>Figure 1</u>: Impact of increasing concentrations of phenanthrene on plant development.**

*Arabidopsis thaliana* plantlets were grown on MS/2 sucrose free medium supplied with 0- (DMSO), 50-, 100-, 200- or 400µM of phenanthrene. 30-days old plantlets were phenotyped (**A**) and harvested to measure their fresh weight (**B**) and chlorophyll contents (**C**). Plantlets were also grown vertically and primary root length measured after 10 days of growth (**D**). The values presents are the means of 30 independents measurements and error bars represent SE. *indicates significant difference between treated and control plants (p-value≤0,05).

assimilation. As a consequence, plant development is altered; shoot growth being more affected as it is more sensitive to salt toxicity than roots growth (Carillo et al., 2011)(36). Phenanthrene uptake and toxicity might induce similar phenomena. Hence, our data showed that shoot growth is more affected than root growth at 50µM. Moreover, the strongest decrease of shoot growth observed at 400µM could be due to the concomitant effects of phenanthrene toxicity and the limited nutrient availability linked to the root growth reduction.

Our results showing a phenanthrene concentration dependent inhibition of roots and shoots development are in accordance with data previously described by Alkio et al. (2005) and Liu et al. (2009) (20, 25). However, several differences were observed in our conditions such as chlorotic phenotypes at 400µM, absence of HR like necrosis on leaves, phenotypic plasticity in the progeny within the same treatment and an absence of saturation of the response between 200- and 400µM of phenanthrene. Rather than differences due to the experimental conditions, we propose that these discrepancies could be linked to the effect of exogenous sucrose supply, with soluble-sugar emerging as true ROS scavengers in plant and limit ROS production in atrazine stress conditions (Sulmon et al., 2006; Sulmon et al., 2007a; Sulmon et al., 2007b)(30-32). A common point with many biotic and abiotic stresses in plant is also the change of bioenergetic status for which plants are mainly dependent on photosynthesis. Abiotic stress such as drought and high salinity toxicity lead to the inhibition of photosynthetic activities. Down regulation of genes involved in photosynthesis also appear to be a common feature of plant response to numerous biotic stresses (Bilgin et al., 2010; Ana Sofia Duque, 2013)(37, 38). In our conditions, at phenanthrene concentrations over 200µM, the lack of sucrose would not enable 30 days old plants to face ROS overproduction associated to phenanthrene metabolism, leading to alteration of photosynthetic activity and ultimately to a decrease of chlorophyll content and the appearance of chlorotic phenotypes. Considering these observations, early incidence of phenanthrene on plant was studied using 200µM phenanthrene concentration.

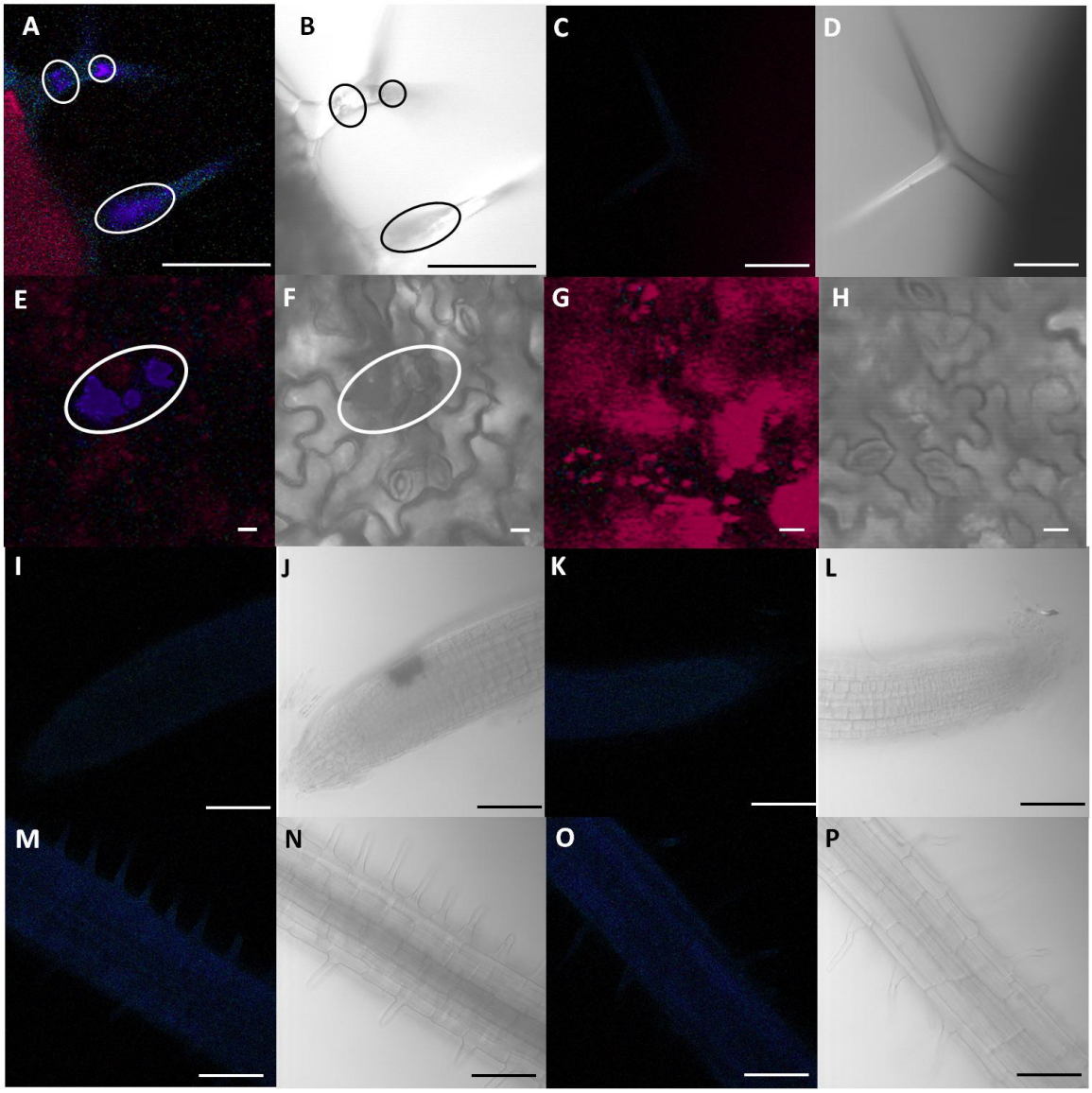


**<u>Figure 2</u>: Observations of phenanthrene fluorescence in 20-days-old plantlets.**

Plants were grown 15 days on MS/2 sucrose free medium and then transferred for 5 days on a identical medium supplemented with 0.2mM of phenanthrene (A, B, E, F, I, J, M and N) or DMSO as control (C, D, G, H, K, L, O and P). Pictures A to D are an observation of the trichomes, E to H of the underside of the leaves, I to L of the apex of the primary root and M to P of the root hairs of the primary root. 2 consecutives photos (A-B, C-D …) represent the same area. A, C, E, G, I, K, M and O are observations made under UV light and B, D, F, H, J, L, N and P with transmission. Circles show the localization of phenanthrene. All bar scales represent 100µm except for pictures E to H where it represents 10µm.

### 3.2. Phenanthrene uptake and localization in Arabidopsis

To validate phenanthrene uptake from solid medium in our experimental conditions, gas chromatography and mass spectrometry analysis were performed and confirmed that phenanthrene accumulates only in plants grown on 200µM phenanthrene compared to the control (data not shown).

Using its specific fluorescence spectra under UV light, phenanthrene was also detected *in vivo* in plants tissues. The third leaf and primary root of 15 days old plantlets transferred five days before on solid medium supplemented with 200µM phenanthrene or DMSO were observed (Figure 2).

In control plants, fluorescence was neither detected in leaves nor in roots (Figure 2 C, D, G, H, K, L, O, P). For phenanthrene treated plants, specific fluorescence was only detected in leaves (Figure 2A, B, E, F), not in roots (Figure 2 I, J, M, N). At the adaxial side of leaves, trichomes were the only fluorescent cells detected, signal appearing to be concentrated as bright spots in specific parts of the trichomes (Figure 2 A, B). At the abaxial side of leaves, these spots harbor different shape and seem to be stuck on the epidermis surface (Figure 2 E, F). Our results are consistent with those previously described by Alkio et al. (2005) even if they do not detect the fluorescent signal at the abaxial side of leaves.

In our experiment, we used a transparent sterile plastic film applied to the contaminated medium in order to avoid any contact of the aerial parts of the plants transferred to the medium. This specific device and fluorescent microscopy data strongly suggest that phenanthrene could be absorbed, at least partially from roots, transported and accumulated in specialized cells in leaves. Indeed, Zhan et al (2010) showed, using hydroponic experiments, that the phenanthrene uptake by wheat roots is not only due to a passive diffusion as suggested by Alkio et al. (2005) but also to an active phenanthrene specific symport system. Surprisingly, specific phenanthrene fluorescence was not observed in roots (Figure 2 I, M). An explanation could be that a portion of phenanthrene rapidly moves up to the upper part of the plant. This is in accordance with the adaxial xyleme and the trichome rich adaxial side of *Arabidopsis* leaves (Chitwood et al., 2007). As the majority of organic contaminants absorbed by plants undergoes enzymatic transformation such as reduction, oxidation or hydrolysis that reduce their toxicity and allow their conjugation (Kvesitadze et al., 2009), these processes might also modify their UV absorbance spectra,

making them much more difficult to detect, except in specific locations where they are compartmentalized.

Moreover, even if most of the PAHs are characterized by their low volatility, some studies indicate that phenanthrene is relatively volatile (Sitaras et al., 2004; Schreiber et al., 2008). Thus, in airless conditions such as Petri dishes, we could not exclude that a portion of phenanthrene is volatilized and absorbed by leaves through stomata. Interestingly, in Arabidopsis, most of the stomata are localized at the abaxial side of leaves where bright fluorescent spots were observed (Figure 2 E). In this case, absorption of volatile phenanthrene would also enable its localization in trichome. Obviously, its localization would be expected in most of the stomata, and it is clearly not the case. Alternatively, these fluorescent spot could also correspond to excretion of non-transformed phenanthrene; rather rare process of organic contaminants elimination happening at high concentration of xenobiotic (Kvesitadze et al., 2009). In Arabidopsis, the function of trichome, unicellular and non-glandular, is poorly understood. They are believed to be part of physical defenses but several line of evidence suggests there are involved in detoxification process of heavy metals. In the Zinc hyperaccumulator accession *Arabidopsis hallieri*, trichomes contains by far the largest concentration of Zinc and Cadmiun, metals being localized in specific subcellular compartment at the base of the trichome, as it seems to be the case for phenanthrene or derivatives in our observations (Figure 2 A) (Küpper et al., 2000). In addition, total glutathione content of trichome have been shown to be more than 300-fold higher than in other epidermal cells. Overexpression of metallothioneins in *Arabidopsis* transgenics demonstrates that glutathione are expressed in trichomes, suggesting that trichome functions as a compartment enabeling conjugation and sequestration of heavy metals (Gutiérrez-Alcalá et al., 2000; Guo et al., 2003). Moreover, overexpression of a cystein in Arabidopsis, Atcys-3A, increased level of GSH in leaves in the presence of cadmium and improved its accumulation in trichomes (Domínguez-Solís et al., 2004). In others species such *Nicotiana tabaccum,* trichomes can function as glandular organs and have been demonstrate to participate to heavy metals detoxification through the formation of metal/calcium crystals actively excreted (Choi et al., 2001; Sarret et al., 2006).

The present observations and previous data obtained by Alkio et al (2005) also support that phenanthrene is absorbed and highlighted the role of trichomes in the compartmentalization of native or phenanthrene derivatives and their putative excretion.

## 3.3. Transcriptome analysis of early plant response to phenanthrene exposure

### 3.3.1. *Global gene expression studies*

In their natural environment, plants are often subject to external factors, biotic and/or abiotic, causing stress that could strongly affect their development. Additionally plants have also to cope with increasing concentrations of pollutants of both natural and anthropogenic origins, define as natural xenobiotics, among which polycyclic aromatic hydrocarbons constitute a large family. Plants have been shown to be an essential component in the ecological process of phytoremediation leading to the accumulation, the partial or complete degradation and decomposition of pollutants. Hence, the study of plant response to xenobiotics offers the opportunity to engineer efficient ecological detoxification tools. This has been done for phenanthrene at the physiological level as well as, through transcriptome analysis, for only long term treatments (Alkio et al., 2005; Liu et al., 2009; Weisman et al., 2010). Plant response to long term exposure involves metabolic pathways that regulate ROS but also processes linked to plant response to pathogens.

Based on the Sandermann's green liver concept, Edwards et al. (2011) defined the plant xenome as "the biosystem responsible for the detection, transport and detoxification of xenobiotics in the plant cell" (Sandermann Jr., 1992; Skipsey et al., 2011). Analogies with xenobiotics detoxification in mammalian liver suggest that molecular mechanisms in the plant xenome would be involved in two phases: i) early perception and the signaling and ii) the transport and the biotransformation of the xenobiotic. However, even if the model of detoxification of xenobiotic by plants have been proposed, data demonstrating that these processes play a role in PAHs detoxification are still missing.

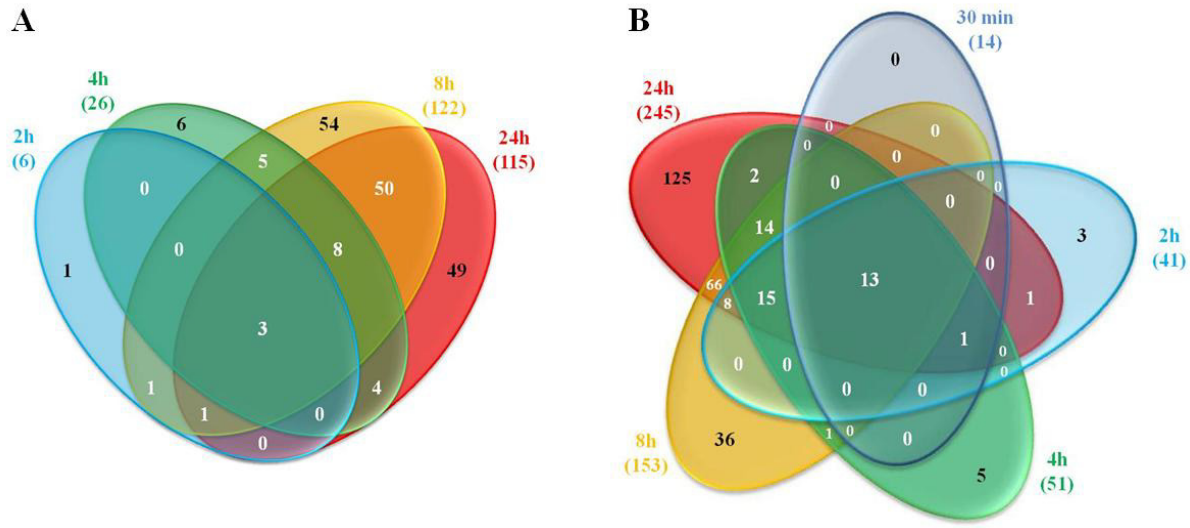


**Figure 3: Venn diagram of the total number of differentially expressed genes, selected by ANOVA analysis (p-value < 0.05), showing an interaction between time and treatment.**

Lists of compared genes correspond to down-regulated (**A**) and up-regulated genes (**B**) obtained in comparisons between phenanthrene treated samples and control samples at 30 minutes, 2h, 4h, 8h and 24h. Differentially expressed genes used are listed in Supplemental Table III were selected by statistical analysis based on the Bonferroni method using a p-value cut-off of 0.05. Transcriptome data corresponding to hybridizations performed are available in Supplemental Table I.

In order to identify the early molecular events of the plant response to phenanthrene, 15-day-old plantlets grown on solid medium were transferred in liquid media containing either 200µM of phenanthrene or DMSO as control. The transcriptome analysis was performed using CATMA version 5 array containing 31776 gene-specific tags corresponding to 22,089 genes from *Arabidopsis* (Crowe et al., 2003; Hilson et al., 2004). The experimental design was set up to compare 0 minutes to 30 minutes, 30 minutes to 2h, 2h to 4h, 4h to 8h and 8h to 24h of incubation in phenanthrene and DMSO (8h-24h comparison is missing) and to compare phenanthrene treatment to control at each kinetic point (Supplemental Figure 1 A). Two independent biological replicates were performed. Overall, within the comparisons between phenanthrene treated to control samples, 1262 genes were differentially expressed, 58, 130, 174, 650 and 897 genes being differentially expressed at 30 min, 2 h, 4 h, 8 h and 24 h, respectively. Using real time RT-PCR, we confirmed expression changes for 11 genes analysed (Supplemental Figure. 2).

### 3.3.2. *Plant response to phenanthrene is fast and can be separated in two phases*

An ANOVA analysis was performed on selected differentially expressed genes showing an interaction between time and treatment. Lists of genes corresponding to comparisons between phenanthrene-treated and control samples at 30 minutes, 2h, 4h, 8h and 24h are shown in supplemental Table III and were used for further analysis.

A total of 467 genes were recovered, with 14, 47, 77, 275 and 360 genes differentially expressed after 30 minutes, 2h, 4h, 8h and 24h of phenanthrene treatment, respectively. All the 14 differentially expressed genes at 30 minutes were up-regulated. In general for the other comparisons, up-regulated genes represent the majority of the gene whose expression is modified, (41/47, 51/77, 153/275, 245/360 for 2h, 4h, 8h, 24h comparisons, respectively). If we look at each point of the time course, we can observe an increase in the number of genes differentially expressed between 30 minutes-4h and 8-24h, even stronger trend if we consider the entire gene regulated without ANOVA selection (58, 130, 174, 650 and 897). This result might reflect a sequential response of the plant to phenanthrene. This response

seems to be composed of an early and short phase from 30 minutes to 4h and second phase from 8h to 24h.

Lists of genes whose expression was modified at each time point of the kinetic were compared using Venn diagrams to identify the genes which were specifically induced or repressed after phenanthrene treatment (Figure 3, A-B). Among differentially expressed genes, only five genes encoding a plant thionin, a putative aspartyl protease, the cytochrome P450 protein CYP704B1, the glycosyl hydrolase ATXYN1 and the senescence protein ATWI-12 (*AT1G58370, AT1G66100*, *AT1G69500, AT3G10985, AT5G48430,*) displayed opposing regulation. Strikingly, this regulation occurs between 4h and 24h of treatments for three of them. Few genes are specifically differentially up or down-regulated for 30 minutes, 2h and 4h comparisons (0/3/5 and 0/1/6), contrasting with 8h and 24h comparisons (36/125 and 44/59). Interestingly, 13 out of the 14 genes early up-regulated after 30 minutes are found in common to all comparisons, amount of the corresponding transcript increasing in time. The high number of common gene, differentially up- or down- regulated, between 8h and 24h (66 and 50 respectively) confirm that same pathways are regulated by the plant in response to phenanthrene after 8h and 24h.

Venn diagram analysis performed on differentially expressed genes without ANOVA selection confirms these results (supplementary Figure 1 B, C). Table I shows the 20 mostly differentially expressed genes, when available, for the kinetically different regulated genes.

### 3.3.3. *Biological processes regulated in response to phenanthrene treatment*

Larcher proposed that physiological response to stress may involved three phases: i) the alarm phase corresponding to early events enabling the perception and the signaling of the stress by the plants; ii) the resistance phase where functional alterations are observed and have to be counteracted to avoid iii) the exhaustion phase (Larcher, 2003).

Even if early events of perception and signaling of xenobiotic are poorly understood, the molecular processes and metabolic pathways involved in their detoxification, which can be assimilated to the resistance phase, have been well described in animal and extrapolated to plants based on the Sandermann's the green liver concept (Sandermann Jr., 1992;

Kvesitadze et al., 2009; Skipsey et al., 2011). The detoxification involves the transformation of the xenobiotics, perfomed by cytochrome P450 (CYP450), peroxidases, phenoloxidases, ascorbatoxidase and catalase. These pollutants undergo oxidation, reduction or hydroxylation to make them more water soluble. Then the conjugation of the xenobiotics to endogenous molecules is realized by transferases such as Glutathione S-transferase (GST), glucuronozyl-O-transferase, malonyl-O-transferase, or glucosyl-O-transferase Glycosyltransferases (UGT). Finally, during the compartmentalization, the conjugated xenobiotic is transferred to the vacuole or the cell wall by ABC transporters.

If we only consider the differentially expressed gene selected using ANOVA analysis and the functional classes in which they are involved in, primary and secondary metabolisms are over-represented. Despite this result, 54 regulatory genes such as transcription factors, receptor kinase and protein phosphatase also showed modified expression during the kinetic in response to phenanthrene treatment. However, in our top lists (Table I), only 11 regulatory genes are listed, 9 up-related and 2 down-regulated. Interestingly, 5 of the most differentially expressed genes are regulated after 30 minutes of treatment whereas all the others, including down-regulated genes, have their expression modified after 8h or 24h. These 5 genes code for three transcriptions factors whose differential expression gradually increase in time, except for *ATMYB4* (*AT4G38620*) showing its highest differential expression at 30 minutes. The two others genes code for a receptor-like kinase protein (RLK) (*AT5G48540*) and the phosphofructokinase 7 (PFK7) (*AT5G56630*) suggesting a fast induction of the glycolysis metabolism after 30 minutes. Such peculiar differential expression pattern for these 5 genes suggests they could be involved in the early phase of sensing and signalization of the phenanthrene by the plant. The RLK would constitute a good candidate of receptor putatively able to bind phenanthrene. This action fits well the model of chemical ligand binding to receptor, described in the case of ABA sensing and suitable for chemical stress such as heavy metal or nutritent depletion stress (Verslues and Zhu, 2005).

**Table I: The most differentially expressed genes during the time course in phenantrene treated plants.** Of all the differentially expressed genes, a maximum of 20 genes for each different response pattern are listed. AGI identifiers and gene annotation in bold face correspond to genes involved in the "xenome". Expression changes are given as log2. Expression changes in bolt correspond to genes differentially expressed at the significant threshold of Bonferroni p-value<0.05.

| AGI ID | Gene annotation | 30 min | 2h | 4h | 8h | 24h |
|---|---|---|---|---|---|---|
| ***Rapid up-regulation after 30min of treatment and stay up-regulated throughout the kinetic*** | | | | | | |
| AT1G70800 | EHB1__Calcium-dependent lipid-binding (CaLB domain) family protein | **0.64** | **1.23** | **1.91** | **1.97** | **1.19** |
| AT4G38620 | ATMYB4_MYB4__myb domain protein 4 | **3.51** | **2.19** | **2.30** | **2.18** | **1.94** |
| AT2G47950 | unknown protein | **1.49** | **2.27** | **2.27** | **2.65** | **1.91** |
| AT5G48540 | receptor-like protein kinase-related family protein | **1.42** | **2.44** | **3.27** | **3.48** | **3.51** |
| AT5G59820 | RHL41_ZAT12__C2H2-type zinc finger family protein | **1.19** | **1.63** | **2.14** | **2.70** | **2.50** |
| AT2G16900 | *Arabidopsis* phospholipase-like protein (PEARLI 4) family | **0.98** | **1.68** | **1.67** | **1.61** | **2.16** |
| AT1G68620 | alpha/beta-Hydrolases superfamily protein | **0.93** | **2.18** | **1.68** | **2.77** | **2.70** |
| AT5G56630 | PFK7__phosphofructokinase 7 | **0.91** | **1.59** | **2.41** | **1.54** | **2.53** |
| AT3G22840 | ELIP_ELIP1__Chlorophyll A-B binding family protein | **0.89** | **1.40** | **2.19** | **1.70** | **2.38** |
| AT1G63840 | RING/U-box superfamily protein | **0.83** | **1.80** | **1.64** | **2.10** | **2.16** |
| AT2G36590 | ATPROT3_ProT3__proline transporter 3 | **0.79** | **1.42** | **1.93** | **1.80** | **2.24** |
| AT4G39670 | Glycolipid transfer protein (GLTP) family protein | **0.73** | **1.26** | **1.01** | **1.42** | **2.13** |
| AT4G27657 | unknown protein | **0.70** | **1.26** | **1.10** | **1.75** | **0.74** |
| AT4G15248 | B-box type zinc finger family protein | **1.39** | **1.75** | **1.04** | 0.35 | **1.63** |
| ***Genes differentially up-regulated after 2h and stayed high*** | | | | | | |
| AT2G35980 | ATNHL10_NHL10_YLS9__Late embryogenesis abundant (LEA) hydroxyproline-rich glycoprotein family | 0.56 | **1.72** | **1.96** | **1.81** | **2.34** |
| AT3G22600 | Bifunctional inhibitor/lipid-transfer protein/seed storage 2S albumin superfamily protein | 0.16 | **1.68** | **1.96** | **1.36** | **1.96** |
| AT4G25640 | ATDTX35_DTX35_FFT__detoxifying efflux carrier 35 | 0.27 | **1.66** | **1.40** | **1.98** | **2.11** |
| **AT3G21560** | **UGT84A2__UDP-Glycosyltransferase superfamily protein** | 0.52 | **1.48** | **2.21** | **1.60** | **1.93** |
| AT1G74010 | Calcium-dependent phosphotriesterase superfamily protein | 0.46 | **1.39** | **1.68** | **1.32** | **2.50** |
| AT1G75040 | PR-5_PR5__pathogenesis-related gene 5 | 0.21 | **1.32** | **1.50** | **1.71** | **1.75** |
| AT1G30700 | FAD-binding Berberine family protein | 0.48 | **1.26** | **1.06** | **1.56** | **2.28** |
| AT3G04300 | RmlC-like cupins superfamily protein | 0.37 | **1.25** | **1.73** | **2.08** | **2.25** |

| AGI ID | Gene annotation | 30 min | 2h | 4h | 8h | 24h |
|---|---|---|---|---|---|---|
| AT1G18980 | RmlC-like cupins superfamily protein | 0.20 | **1.16** | **1.55** | **1.57** | **1.59** |
| AT1G76980 | unknown protein | 0.51 | **1.15** | **1.67** | **1.78** | **1.85** |
| AT5G54500 | FQR1__flavodoxin-like quinone reductase 1 | 0.47 | **1.12** | **1.14** | **1.50** | **1.79** |
| AT1G74450 | Protein of unknown function (DUF793) | 0.41 | **1.09** | **1.16** | **1.06** | **1.10** |
| AT3G04000 | NAD(P)-binding Rossmann-fold superfamily protein | 0.06 | **0.95** | **1.16** | **1.53** | **1.23** |
| AT1G27120 | Galactosyltransferase family protein | 0.00 | **0.91** | **2.00** | **2.30** | **2.45** |
| AT2G17500 | Auxin efflux carrier family protein | -0.20 | **0.80** | **1.19** | **1.79** | **1.20** |
| ***Genes differentially up-regulated from 4 h of treatment*** | | | | | | |
| **AT1G78340** | **ATGSTU22_GSTU22__glutathione S-transferase TAU 22** | 0.04 | 0.56 | **1.62** | **1.75** | **1.69** |
| **AT1G17170** | **ATGSTU24_GST_GSTU24__glutathione S-transferase TAU 24** | 0.06 | 0.39 | **1.57** | **2.00** | **2.05** |
| AT3G51660 | Tautomerase/MIF superfamily protein | 0.10 | 0.75 | **1.47** | **1.80** | **2.27** |
| **AT5G36270** | **similar to DHAR2, glutathione dehydrogenase (ascorbate)** | 0.00 | 0.55 | **1.38** | **1.56** | **1.74** |
| **AT4G15480** | **UGT84A1__UDP-Glycosyltransferase superfamily protein** | 0.18 | 0.47 | **1.27** | **1.02** | **1.40** |
| **AT1G78380** | **ATGSTU19_GST8_GSTU19__glutathione S-transferase TAU 19** | 0.10 | 0.69 | **1.23** | **1.45** | **1.49** |
| AT2G29500 | HSP20-like chaperones superfamily protein | 0.16 | 0.29 | **1.15** | **1.11** | **1.53** |
| AT1G75030 | ATLP-3_TLP-3__thaumatin-like protein 3 | 0.19 | 0.59 | **1.13** | **1.45** | **1.35** |
| **AT1G75270** | **DHAR2__dehydroascorbate reductase 2** | 0.36 | 0.78 | **1.09** | **1.60** | **1.49** |
| **AT1G64900** | **CYP89_CYP89A2__cytochrome P450, family 89, subfamily A, polypeptide 2** | -0.03 | 0.33 | **1.08** | **1.16** | **1.19** |
| AT3G13520 | AGP12_ATAGP12__arabinogalactan protein 12 | 0.17 | 0.57 | **1.08** | **1.39** | **0.88** |
| **AT2G12190** | **Cytochrome P450 superfamily protein** | -0.04 | 0.43 | **1.04** | **0.97** | **0.96** |
| AT4G13180 | NAD(P)-binding Rossmann-fold superfamily protein | 0.28 | 0.29 | **1.03** | **1.07** | **1.39** |
| **AT1G05680** | **UGT74E2__Uridine diphosphate glycosyltransferase 74E2** | 0.14 | -0.05 | **1.01** | **1.80** | **0.83** |
| AT2G48140 | EDA4__Bifunctional inhibitor/lipid-transfer protein/seed storage 2S albumin superfamily protein | 0.02 | 0.74 | **1.20** | **0.73** | 0.40 |
| **AT3G09270** | **ATGSTU8_GSTU8__glutathione S-transferase TAU 8** | -0.12 | 0.41 | **1.15** | 0.26 | **1.09** |
| AT1G23490 | ARF1_ATARF_ATARF1_ATARFA1A__ADP-ribosylation factor 1 | 0.48 | 0.76 | **1.04** | 0.64 | **1.32** |
| **AT1G58370** | **ATXYN1_RXF12__glycosyl hydrolase family 10 protein / carbohydrate-binding domain-containing protein** | 0.17 | 0.64 | **1.13** | 0.08 | **-0.86** |

| AGI ID | Gene annotation | 30 min | 2h | 4h | 8h | 24h |
|---|---|---|---|---|---|---|
| ***Genes differentially up-regulated after 8h of treatment*** | | | | | | |
| AT5G22140 | FAD/NAD(P)-binding oxidoreductase family protein | 0.30 | 0.02 | 0.76 | **2.15** | **1.97** |
| AT3G44190 | FAD/NAD(P)-binding oxidoreductase family protein | 0.03 | 0.21 | 0.95 | **2.05** | **2.01** |
| AT2G23110 | Late embryogenesis abundant protein, group 6 | 0.45 | 0.78 | 0.51 | **1.87** | **2.04** |
| AT5G64250 | Aldolase-type TIM barrel family protein | -0.01 | 0.35 | 0.59 | **1.62** | **1.55** |
| AT3G28210 | PMZ_SAP12__zinc finger (AN1-like) family protein | 0.36 | 0.52 | 0.98 | **1.60** | **2.09** |
| AT1G75280 | NmrA-like negative transcriptional regulator family protein | 0.15 | 0.62 | 0.86 | **1.56** | **1.37** |
| AT4G24160 | alpha/beta-Hydrolases superfamily protein | -0.01 | 0.40 | 0.59 | **1.52** | **1.25** |
| AT3G10500 | anac053_NAC053__NAC domain containing protein 53 | 0.12 | 0.77 | 0.66 | **1.48** | **1.16** |
| AT2G01180 | ATLPP1_ATPAP1_LPP1_PAP1__phosphatidic acid phosphatase 1 | 0.20 | 0.33 | 0.95 | **1.44** | **1.97** |
| AT5G54206 | similar to 12-oxophytodienoate reductase OPR1 | 0.17 | 0.15 | 0.29 | **1.41** | **2.04** |
| **AT2G29460** | **ATGSTU4_GST22_GSTU4__glutathione S-transferase tau 4** | 0.12 | 0.52 | 1.00 | **1.37** | **0.95** |
| **AT4G34131** | **UGT73B3__UDP-glucosyl transferase 73B3** | 0.33 | 0.38 | 0.89 | **1.31** | **1.38** |
| AT1G05670 | Pentatricopeptide repeat (PPR-like) superfamily protein | 0.20 | 0.02 | 0.71 | **1.30** | **0.69** |
| AT1G77120 | ADH_ADH1_ATADH_ATADH1__alcohol dehydrogenase 1 | -0.18 | 0.54 | 0.25 | **1.30** | **1.02** |
| AT2G21620 | RD2__Adenine nucleotide alpha hydrolases-like superfamily protein | -0.01 | 0.75 | 0.94 | **1.28** | **1.82** |
| AT1G66580 | RPL10C_SAG24__senescence associated gene 24 | 0.32 | 0.45 | 0.63 | **1.26** | **1.44** |
| AT2G36950 | Heavy metal transport/detoxification superfamily protein | 0.21 | 0.45 | -0.10 | **1.26** | **1.01** |
| AT1G72490 | unknown protein | -0.09 | 0.20 | 0.02 | **1.25** | **1.10** |
| AT1G67600 | Acid phosphatase/vanadium-dependent haloperoxidase-related protein | 0.01 | 0.45 | 0.50 | **1.25** | **1.07** |
| AT5G27760 | Hypoxia-responsive family protein | 0.14 | 0.47 | 0.83 | **1.19** | **1.43** |
| ***Genes differentially up-regulated after 24 h of treatment*** | | | | | | |
| AT1G65290 | mtACP2__mitochondrial acyl carrier protein 2 | 0.13 | 0.06 | 0.13 | 0.34 | **2.63** |
| AT4G37990 | ATCAD8_CAD-B2_ELI3_ELI3-2__elicitor-activated gene 3-2 | 0.07 | 0.30 | 0.34 | 0.00 | **2.43** |
| AT5G25260 | SPFH/Band 7/PHB domain-containing membrane-associated protein family | -0.10 | -0.06 | 0.30 | 0.04 | **2.07** |
| AT2G18690 | unknown protein | 0.11 | 0.70 | 0.54 | 0.66 | **1.98** |

| AGI ID | Gene annotation | 30 min | 2h | 4h | 8h | 24h |
|---|---|---|---|---|---|---|
| AT4G12490 | Bifunctional inhibitor/lipid-transfer protein/seed storage 2S albumin superfamily protein | 0.22 | 0.07 | 0.66 | 0.28 | **1.90** |
| AT1G14870 | AtPCR2_PCR2__PLANT CADMIUM RESISTANCE 2 | -0.03 | 0.51 | 0.03 | 0.48 | **1.76** |
| AT2G23150 | ATNRAMP3_NRAMP3__natural resistance-associated macrophage protein 3 | -0.17 | -0.16 | 0.01 | 0.59 | **1.69** |
| AT2G17740 | Cysteine/Histidine-rich C1 domain family protein | -0.03 | -0.15 | 0.66 | 0.20 | **1.67** |
| AT1G66090 | Disease resistance protein (TIR-NBS class) | 0.36 | 0.29 | 0.66 | 0.55 | **1.67** |
| AT5G06320 | NHL3__NDR1/HIN1-like 3 | -0.28 | 0.11 | -0.08 | 0.31 | **1.60** |
| AT2G29350 | SAG13__senescence-associated gene 13 | -0.17 | 0.17 | 0.82 | 0.59 | **1.55** |
| AT1G13330 | AHP2__*Arabidopsis* Hop2 homolog | 0.00 | -0.09 | 0.69 | 0.36 | **1.55** |
| AT5G13320 | GDG1_GH3.12_PBS3_WIN3__Auxin-responsive GH3 family protein | -0.10 | -0.25 | 0.11 | -0.07 | **1.54** |
| AT5G17380 | Thiamine pyrophosphate dependent pyruvate decarboxylase family protein | 0.04 | 0.03 | 0.35 | 0.65 | **1.48** |
| AT2G20142 | Toll-Interleukin-Resistance (TIR) domain family protein | 0.06 | 0.05 | 0.21 | 0.23 | **1.47** |
| AT4G26200 | ACS7_ATACS7__1-amino-cyclopropane-1-carboxylate synthase 7 | 0.22 | -0.01 | 0.18 | 0.26 | **1.44** |
| AT1G74710 | ATICS1_EDS16_ICS1_SID2__ADC synthase superfamily protein | 0.05 | -0.19 | 0.14 | -0.09 | **1.41** |
| AT4G11890 | Protein kinase superfamily protein | 0.10 | 0.19 | -0.04 | 0.56 | **1.38** |
| AT5G25250 | SPFH/Band 7/PHB domain-containing membrane-associated protein family | 0.07 | 0.00 | 0.28 | 0.40 | **1.38** |
| AT1G26380 | FAD-binding Berberine family protein | 0.24 | 0.24 | 0.34 | 0.43 | **1.38** |
| | ***Genes differentially down-regulated from 2 h of treatment and stayed low*** | | | | | |
| AT1G26810 | GALT1__galactosyltransferase1 | -0.13 | **-1.16** | **-1.71** | **-1.65** | **-1.79** |
| AT3G19450 | ATCAD4_CAD_CAD-C_CAD4__GroES-like zinc-binding alcohol dehydrogenase family protein | 0.03 | **-0.82** | **-1.22** | **-1.74** | **-1.74** |
| AT5G48930 | HCT__hydroxycinnamoyl-CoA shikimate/quinate hydroxycinnamoyl transferase | -0.20 | **-1.17** | **-1.11** | **-1.50** | **-1.18** |
| | ***Genes differentially down-regulated from 4 h of treatment and stayed low*** | | | | | |
| AT1G08630 | THA1__threonine aldolase 1 | 0.06 | -0.54 | **-1.81** | **-0.92** | **-1.62** |
| AT1G43160 | RAP2.6__related to AP2 6 | 0.02 | -0.57 | **-1.57** | **-1.16** | **-0.99** |
| AT5G49730 | ATFRO6_FRO6_FRO6__ferric reduction oxidase 6 | -0.05 | -0.27 | **-1.35** | **-0.79** | **-1.46** |
| AT5G25460 | Protein of unknown function, DUF642 | -0.03 | -0.55 | **-1.30** | **-1.72** | **-1.41** |

| AGI ID | Gene annotation | 30 min | 2h | 4h | 8h | 24h |
|---|---|---|---|---|---|---|
| AT4G29905 | unknown protein | 0.00 | 0.29 | **-1.16** | **-0.76** | **-1.83** |
| AT1G05240 | Peroxidase superfamily protein | 0.08 | 0.19 | **-1.07** | **-1.48** | **-0.91** |
| AT4G23400 | PIP1;5_PIP1D__plasma membrane intrinsic protein 1;5 | -0.29 | -0.16 | **-1.06** | **-0.99** | **-1.50** |
| AT1G69100 | Eukaryotic aspartyl protease family protein | 0.13 | -0.04 | **-1.06** | **-1.21** | **-1.03** |
| AT5G01210 | HXXXD-type acyl-transferase family protein | 0.05 | -0.78 | **-1.65** | **-1.37** | -0.38 |
| AT2G45960 | ATHH2_PIP1;2_PIP1B_TMP-A__plasma membrane intrinsic protein 1B | -0.17 | -0.11 | **-1.14** | **-0.77** | -0.37 |
| AT1G65930 | cICDH__cytosolic NADP+-dependent isocitrate dehydrogenase | -0.03 | -0.29 | **-1.13** | **-0.96** | -0.56 |
| AT4G14040 | EDA38_SBP2__selenium-binding protein 2 | 0.21 | -0.31 | **-1.01** | **-0.70** | -0.60 |
| AT1G64370 | unknown protein | -0.15 | -0.22 | **-1.01** | **-0.77** | -0.16 |
| ***Genes differentially down-regulated from 8 h of treatment and stayed low*** | | | | | | |
| AT3G03780 | ATMS2_MS2__methionine synthase 2 | 0.15 | -0.55 | -0.50 | **-1.66** | **-2.22** |
| AT4G22210 | LCR85__low-molecular-weight cysteine-rich 85 | -0.16 | -0.27 | -0.69 | **-1.56** | **-1.27** |
| AT4G15390 | HXXXD-type acyl-transferase family protein | 0.08 | -0.44 | -0.70 | **-1.39** | **-1.54** |
| AT3G59970 | MTHFR1__methylenetetrahydrofolate reductase 1 | 0.02 | -0.54 | -0.40 | **-1.30** | **-1.06** |
| AT2G44160 | MTHFR2__methylenetetrahydrofolate reductase 2 | 0.20 | -0.28 | -0.52 | **-1.28** | **-0.95** |
| AT5G39210 | CRR7__chlororespiratory reduction 7 | -0.09 | 0.14 | -0.58 | **-1.27** | **-0.89** |
| AT3G19820 | CBB1_DIM_DIM1_DWF1_EVE1__cell elongation protein / DWARF1 / DIMINUTO (DIM) | 0.07 | -0.11 | -0.45 | **-1.27** | **-1.15** |
| AT1G29600 | Zinc finger C-x8-C-x5-C-x3-H type family protein | -0.10 | -0.15 | -0.19 | **-1.22** | **-1.02** |
| AT4G12545 | Bifunctional inhibitor/lipid-transfer protein/seed storage 2S albumin superfamily protein | -0.03 | 0.28 | -0.70 | **-1.20** | **-1.66** |
| AT1G11860 | Glycine cleavage T-protein family | 0.00 | -0.16 | -0.32 | **-1.17** | **-1.14** |
| AT3G60320 | Protein of unknown function (DUF630 and DUF632) | 0.03 | -0.18 | -0.72 | **-1.10** | **-0.77** |
| AT5G24760 | GroES-like zinc-binding dehydrogenase family protein | -0.04 | -0.50 | -0.34 | **-1.08** | **-1.19** |
| AT5G17920 | ATCIMS_ATMETS_ATMS1__Cobalamin-independent synthase family protein | 0.13 | -0.26 | -0.41 | **-1.06** | **-0.99** |
| AT3G06350 | EMB3004_MEE32__dehydroquinate dehydratase, putative / shikimate dehydrogenase, putative | -0.11 | -0.25 | -0.62 | **-1.03** | **-0.85** |
| AT3G16390 | NSP3__nitrile specifier protein 3 | 0.06 | 0.20 | 0.30 | **-1.03** | **-1.02** |
| AT1G29560 | Zinc finger C-x8-C-x5-C-x3-H type family protein | 0.15 | -0.38 | -0.45 | **-1.00** | **-0.93** |
| AT5G03300 | ADK2__adenosine kinase 2 | 0.16 | -0.30 | 0.03 | **-0.99** | **-0.94** |

| AGI ID | Gene annotation | 30 min | 2h | 4h | 8h | 24h |
|---|---|---|---|---|---|---|
| AT1G80830 | ATNRAMP1_NRAMP1_PMIT1__natural resistance-associated macrophage protein 1 | -0.02 | -0.46 | -0.93 | **-0.99** | **-0.75** |
| AT4G14890 | FdC2__2Fe-2S ferredoxin-like superfamily protein | -0.10 | -0.19 | -0.48 | **-0.97** | **-1.01** |
| AT5G65010 | ASN2__asparagine synthetase 2 | -0.03 | 0.07 | -0.15 | **-0.97** | **-0.84** |
| ***Genes only differentially down-regulated after 24 h of treatment*** | | | | | | |
| AT5G36910 | THI2.2__thionin 2.2 | -0.16 | 0.04 | -0.38 | 0.21 | **-1.73** |
| AT2G25510 | unknown protein | -0.09 | 0.23 | 0.11 | -0.40 | **-1.52** |
| **AT1G17190** | **ATGSTU26_GSTU26__glutathione S-transferase tau 26** | -0.01 | -0.19 | 0.32 | -0.31 | **-1.41** |
| AT3G16450 | JAL33__Mannose-binding lectin superfamily protein | 0.00 | 0.28 | -0.51 | -0.67 | **-1.30** |
| AT4G35100 | PIP2;7_PIP3_PIP3A_SIMIP__plasma membrane intrinsic protein 3 | 0.01 | 0.10 | -0.81 | -0.67 | **-1.26** |
| AT3G28270 | Protein of unknown function (DUF677) | -0.26 | 0.46 | 0.25 | -0.57 | **-1.26** |
| AT5G51720 | 2 iron, 2 sulfur cluster binding | -0.06 | -0.25 | -0.17 | -0.38 | **-1.24** |
| AT5G24420 | PGL5__6-phosphogluconolactonase 5 | 0.00 | 0.05 | -0.32 | -0.02 | **-1.20** |
| AT4G13870 | ATWEX_ATWRNEXO_WEX_WRNEXO__Werner syndrome-like exonuclease | -0.02 | 0.10 | 0.61 | -0.34 | **-1.19** |
| AT3G02380 | ATCOL2_COL2__CONSTANS-like 2 | -0.11 | -0.60 | -0.41 | 0.04 | **-1.15** |
| AT4G16980 | arabinogalactan-protein family | 0.07 | -0.10 | -0.84 | -0.54 | **-1.14** |
| AT3G45140 | ATLOX2_LOX2__lipoxygenase 2 | -0.12 | 0.51 | 0.51 | -0.24 | **-1.11** |
| AT1G12090 | ELP__extensin-like protein | -0.06 | -0.04 | -0.52 | -0.33 | **-1.08** |
| AT1G54000 | GLL22__GDSL-like Lipase/Acylhydrolase superfamily protein | 0.03 | -0.28 | -0.77 | -0.55 | **-1.06** |
| AT5G58260 | NdhN__oxidoreductases, acting on NADH or NADPH, quinone or similar compound as acceptor | 0.04 | -0.01 | -0.14 | -0.58 | **-1.05** |
| AT3G16420 | JAL30_PBP1__PYK10-binding protein 1 | -0.04 | 0.07 | 0.01 | -0.64 | **-1.02** |
| AT3G16440 | ATMLP-300B_MEE36_MLP-300B__myrosinase-binding protein-like protein-300B | -0.24 | 0.21 | -0.37 | -0.38 | **-0.91** |
| AT3G15850 | ADS3_FAD5_FADB_JB67__fatty acid desaturase 5 | -0.21 | -0.01 | -0.68 | -0.06 | **-0.91** |
| AT3G01480 | ATCYP38_CYP38__cyclophilin 38 | 0.07 | 0.01 | -0.76 | -0.54 | **-0.88** |
| AT3G11170 | AtFAD7_FAD7_FADD__fatty acid desaturase 7 | 0.03 | -0.12 | -0.30 | -0.63 | **-0.87** |

To identify differentially expresses genes involved in the xenobiotic detoxification processes, we then recovered AGI identifiers of all CYP450, GST, glycosyl transferase and ABC transporters from the TAIR website (http://www.arabidopsis.org/browse/genefamily/) to constitute a gene list of the putative plant xenome.

Comparing this list to our study reveals that 36 differentially expressed genes belongs to the xenome (Supplemental Table III). These genes have mainly their expression modified from 4h of treatment. Moreover, in our top list (Table I), 16 out 36 are among the highest differentially regulated genes, one being specifically up-regulated after 2h of treatment whereas 11 are differentially up-regulated after 4h. This result suggest that early plant response to phenanthrene follows the Larcher's model (Larcher, 2003). Indeed, after 30 minutes of treatments, the plant seems to sense phenanthrene and induce a cascade of regulation and signalization that leads, in a second phase, to the induction of detoxification processes, mainly between 2h and 4h of treatment.

To identify biological processes which are mostly and significantly regulated by the plant in response to phenanthrene at each time point of our kinetic, lists of genes corresponding to each comparison, were analysed using the classification superviewer tool from the Bio-Array Ressource for Plant Biology (http://www.bar.utoronto.ca/ntools/cgi-bin/ntools_classification_superviewer.cgi) using the MAPMAN classification as source (Figure 4). For up-regulated genes, the number of pathways in which genes are significantly over-represented gradually increase in time, pathways affected from 2h of treatment staying induced at the other kinetic points.

After only 30 minutes of treatment, glycolysis metabolism is induced. At 2h, miscellaneous pathways is induce as for 4h of treatment with the redox metabolism in more. Interestingly, genes corresponding to miscellaneous pathway whose expression is modified in our study encode proteins such as UDP-glycosyltransferase, nitrilase and cytochrome P450, proteins that might be involved in transformation and conjugation of phenanthrene. This analysis seems to confirm that the plant might adapt its response to phenanthrene after 4h of treatment since numerous pathways in which differentially expressed genes are over-represented are induced at 8h and remain regulated at 24h. These pathways include transport, stress, RNA, redox, protein, miscellaneous, hormone, glycolysis and fermentation metabolisms. Compared to up-regulated genes, genes whose steady state expression

decreased were clearly over-represented in different functional classes, mostly involving primary and secondary metabolisms (amino acid , C1, lipid, tetrapyrrole synthesis, metal handling, co-factor and vitamins, TCA, etc). As for up-regulated genes, number of pathways repressed increase in time, pathways affected from 2h of treatment staying repressed at the other kinetic points. Moreover, modification in the plant response after 4h is also illustrated by the increased number of pathways in which differentially repressed genes are significantly over-represented.

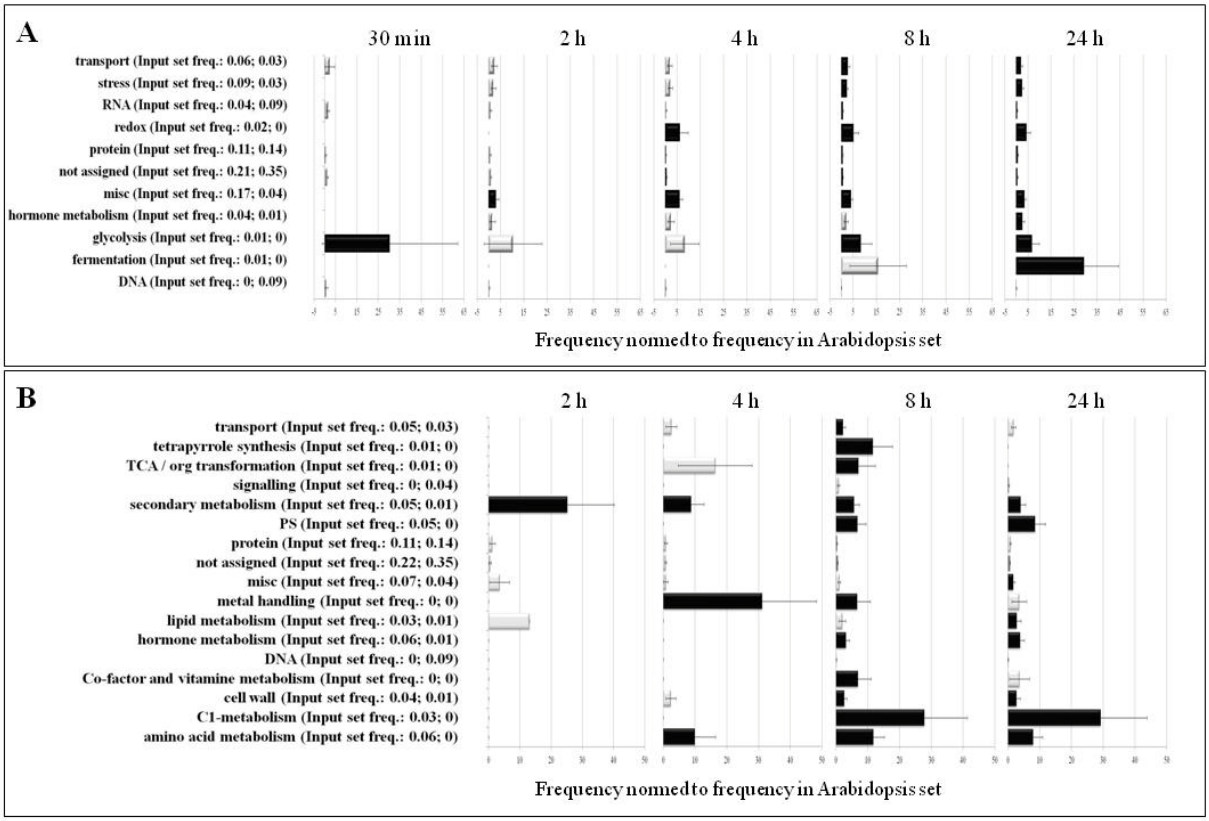


**<u>Figure 4</u>: Biological pathways with significant over-representation of up- (A) and down- (B) regulated genes (P-values < 0.05) after 30 min, 2 h, 4 h, 8 h and 24 h of incubation in phenanthrene-treated plants.**

Functional enrichment for differentially expressed genes analyzed using the classification superviewer tool from the Bio-Array Resource for Plant Biology (http://www.bar.utoronto.ca/ntools/cgi-bin/ntools_classification_superviewer.cgi) using the MapMan classification as the source. Significant pathways are in bold. PS, Photosynthesis. Misc, miscellaneous.

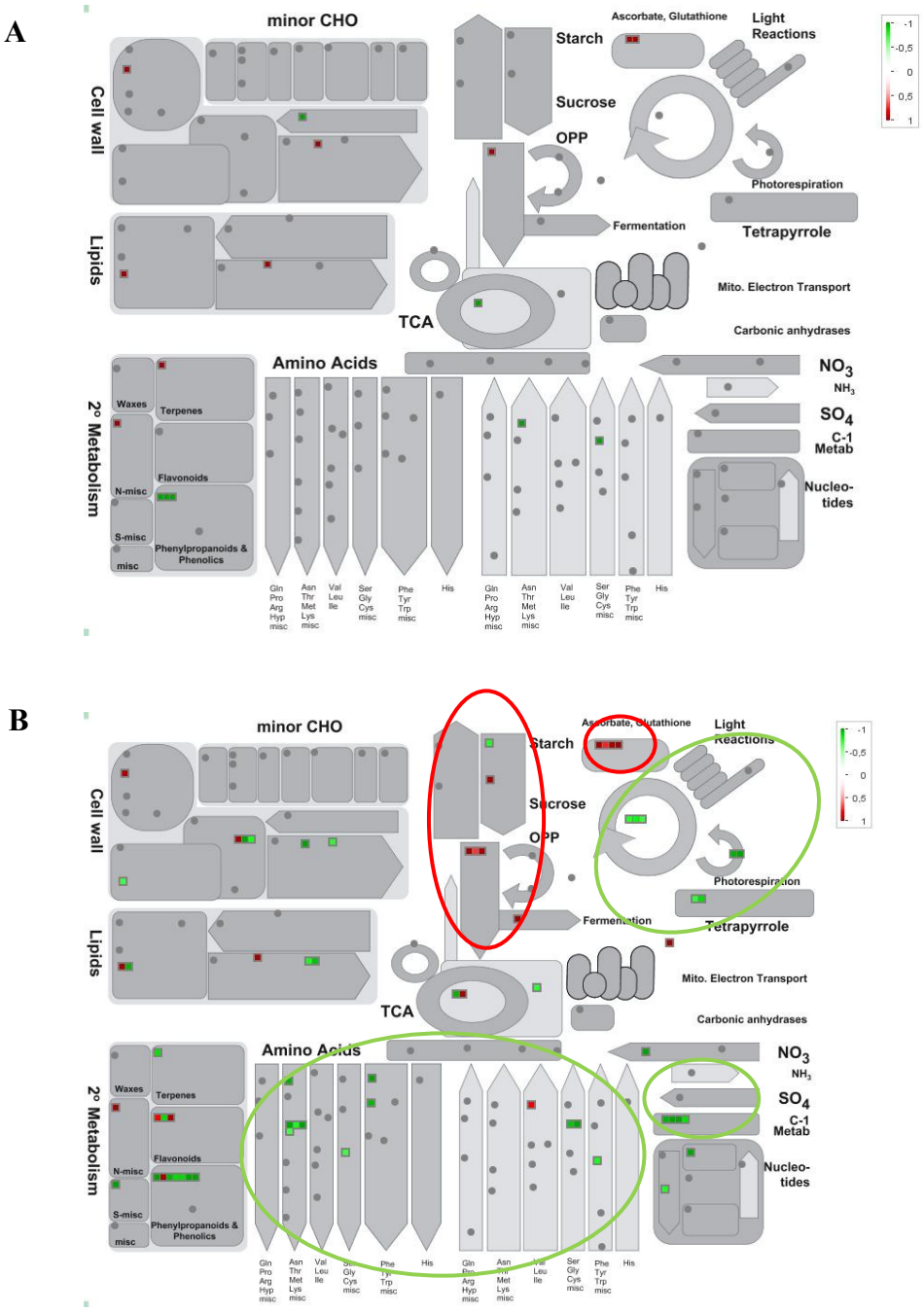


**<u>Figure 5</u>: Metabolic gene expression changes at 4 h (A) and 8h (B) of incubation with 0,2mM phenanthrene analyzed by the MapMan tool.**

Ratios are given for comparisons phenanthrene-treated to control samples.

### 3.3.4. *Integration of metabolite data, metabolic changes revealed*

We used the MAPMAN tool to analyse and compare gene expression changes during our time-course. This tool allows the detail visualization and comparison of individual differentially expressed genes onto metabolic pathways.

As an example of recovered information, Figure 5 presents an overview of general metabolism evolutions highlighted for 4h and 8h comparisons. Genes lists corresponding to 4h and 8h comparisons were chosen due to the strong differences in the number of differentially expressed genes that might reflect a modification of plant response to phenanthrene. All the differences at 8h were also confirmed for the 24h kinetic point (Supplemental Figure 3 A).

A first difference was observed for genes involved in light reactions and photorespiration. Whereas no genes are regulated at 4h, some genes involved in the Calvin cycle and photorespirations are repressed at 8h. These changes are in accordance with the known physiological responses to early abiotic stress, well described by Duque et al. (2013). Despite differences in early perception and signalling events between abiotic stress, early stress responses often reduce photosynthetic efficiency, repress transport metabolism or induce accumulation of metabolites and/or uptake-translocation of ions. The stress generated by phenanthrene, proposed by Weisman et al. (2010), originates from its transformation might reduce energy production or increase energy demand to be overcome, as for other abiotic stresses. Consequently, the resulting unbalanced bioenergetic status might affect many other metabolisms.

The glycolysis metabolism produce ATP but also pyruvate for TCA cycle and reductants, such as NADH. Due to the photosynthesis performance reduction, it is not surprising that the number of genes differentially up-regulated involved in glycolysis increase after 8h and 24h.. Some genes involved in ethanolic fermentation are also up-regulated after 24h. These genes encoding alcohol deshydrogenase (ADH) and pyruvate decarboxylase (PDC) have been shown to be hypoxically induced in maize (Ellis et al., 1999). Induction of glycolytic pathway and ethanolic fermentation are part of a strategy developed by the plant to maintain the energy status through the regeneration of NADH in case of oxygen deprivation.

**Table 2: Metabolites levels in plants after 24h of phenanthrene treatment.** Data are given as the ratio of untreated plants (control). Metabolite contents were determined by GC-MS and HPLC. Data are means of three independent replicates. Citrate, galactinol, galactose, gentibiose, hydroxypiroline, maltose, mannitol, mannose, melibiose, quinate, sorbitol, succinate and trehalose were not detected in both conditions.

Color code (%)

| <20 | 20-49 | 50-80 | 81-119 | 120-200 | 201-300 | >300 |
|---|---|---|---|---|---|---|

| Compounds | phenathrene treated plants<br>% of untreated plants |
|---|---|
| Amino acids | |
| Alpha-Alanine (Ala) | 245% |
| Arginine (Arg) | 132% |
| Asparagine (Asn) | 140% |
| Aspartate (Asp) | 123% |
| Beta-Alanine | 10% |
| Cystine | 150% |
| GABA | 173% |
| Glutamate (Glu) | 125% |
| Glutamine (Gln) | 146% |
| Glycine (Gly) | 140% |
| Histidine (His) | 121% |
| Isoleucine (Ile) | 227% |
| Leucine (Leu) | 233% |
| Lysine (Lys) | 151% |
| Methionine (Met) | 144% |
| Methylcysteine | 55% |
| Ornithine | 111% |
| Phenylalanine (Phe) | 159% |
| Proline (Pro) | 159% |
| Serine (Ser) | 164% |
| Threonine (Thr) | 169% |
| Tryptophan (Trp) | 174% |
| Tyrosine (Tyr) | 127% |
| Valine (Val) | 185% |
| Alcohols | |
| Adonitol | 132% |
| Myo-inositol | 131% |
| Organic acids | |
| Fumarate | 0% |
| Malate | 76% |
| Sugars | |
| Fructose | 115% |
| Glucose | 110% |
| Sucrose | 184% |
| Inorganic acid | |
| Ammonium | 77% |

Moreover, stresses that alter the production of ROS and unbalanced antioxidant networks generate $O_2$ deprevation. Through its transformation, phenanthrene could strongly affect the plant antioxidant balance and consequently stimulates glycolysis and fermentation metabolisms. However, $O_2$ deprivation could also results from hypoxic or anoxic conditions. In our study, seedlings were incubated in liquid media before being harvested for transcriptome analysis during which these conditions might have happened. To exclude this possibility, we compared our gene lists to genes differentially regulated by anoxia, hypoxia, and O2 deprivation in the seedlings/shoots of *Arabidopsis* microarray datasets (Pucciariello et al., 2012) and showed that only 3 genes are found in common (Supplemental Table V).

Another difference was observed for genes involved in amino acid synthesis and nucleotide synthesis, only down-regulated at 8h and 24h. Nevertheless, amino acid titration after 24h of phenanthrene treatment suggested the opposite since amino acid accumulates (Table II). This result could be explains by the induction of proteolysis metabolism with increased number of genes whose expression is up-regulated after 8h and 24h of treatment (Supplemental Figure 3 B, Supplemental Figure 4 B). Numerous biochemical studies showed that allosteric enzymes are feedback inhibited by the amino acid they synthesize (Galili, 1995). Accumulation of amino acids in phenanthrene treated plant, due to active proteolysis from 8h to 24h, might reflect a similar situation, feedback inhibition of amino acids synthesis resulting in down-regulation of genes involved in this metabolism. Similar regulations have been described for nucleotides and could explain the repression of genes involved in nucleotide synthesis and C1-metabolism (Zrenner et al., 2006).

Kinetic expression changes of genes classified in the xenome, involved in secondary and the redox metabolisms, shown in Table I and Figure 4, are also supported by visualization of our gene lists onto metabolic pathways (Supplemental Figure 3 and 4). Surprisingly, metabolites titration revealed that sucrose, fructose and glucose accumulate in phenanthrene treated plants at 24h. This result is in accordance with our transcriptome results since numerous known sugar-inducibled genes, such as senescence associated genes (Paul and Pellny, 2003), are differentially up-regulated at 24h. Sugars function as metabolic resources and structural constituents of cells, but also act as signals regulating various processes associated

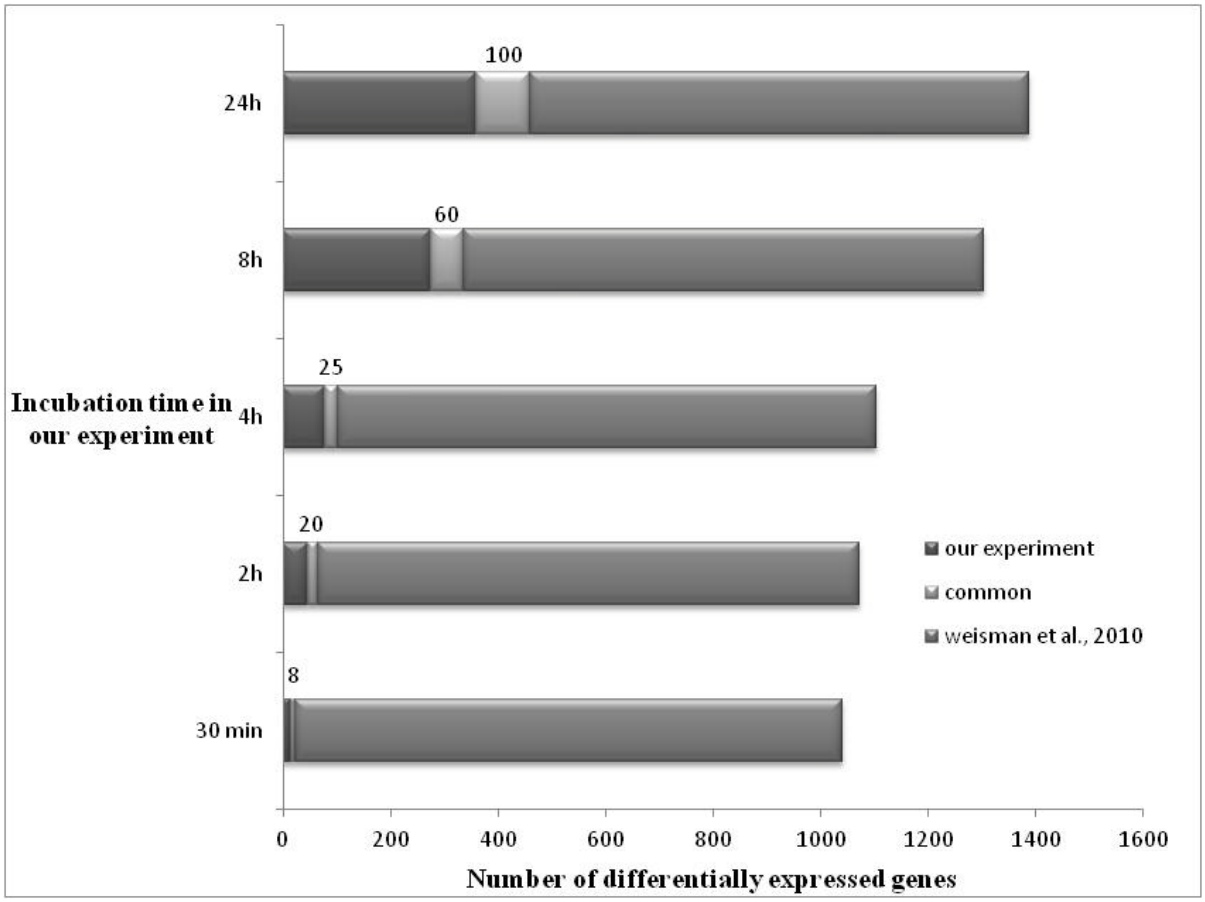


**Figure 6: Number of differentially expressed genes found in our experiment, in Weisman et al. (2010) and shared between both experiments.**

Numbers above histograms represent the number of differentially expressed genes that are common in both experiments at each kinetic point. 14, 45, 77, 275 and 360 genes found to be differentially expressed in our study after 30 minutes, 2h, 4h, 8h and 24h of treatments with phenanthrene, respectively, were compared to the 1027 differentially expressed genes from the Weisman's (2010) study (24).

with plant growth and development. Accumulation of soluble sugar has also been reported during different biotic and abiotic stress related to oxidative stress (Couée et al., 2006).

### 3.3.5. *Comparison with public available microarray data*

We first compared the transcriptome data obtained in our study with the only published data on the transcriptome response towards phenanthrene (Supplemental Table V) (Weisman et al., 2010). Weisman et al (2010) performed their transcriptome analysis on 21 days old plants grown on a solid medium supplemented with 250µM of phenanthrene and sucrose. The authors were able to identify PAH-specific response genes involved in xenobiotics detoxification (GST, UGT, CYP450), ROS detoxification mechanisms and also phytohormons metabolism.

In our study approximately 23% (109 out of 467) of the differentially expressed genes were found in common. The majority of these genes have their expression modified after 24h of incubation (100; 27,7%) and are identically differentially regulated at 24h.

Even if some genes belong to important functional classes that characterize the Weisman's transcriptome data (miscellaneous, redox, stress), they are less represented in our study. This is especially the case for genes involved in redox metabolism (ascorbate oxydase, peroxidise, catalase) and pathogen defence response. These discrepancies can be easily explained by differences in the experimental set up used. Indeed, Weisman et al (2010) studied a long term effect of the phenanthrene whereas we studied the 30 minutes-24h plants response.

Hence, results were expected and the fact that most of common genes belongs to our last time point (24h) make sense. However, we cannot exclude that differences could be linked to the scavenger effect of the sucrose, added in the medium in Weisman et al (2010) experiments, or simply to the selectivity of the ANOVA analysis. To test this last hypothesis, we compare the lists of differentially expressed genes obtained before the ANOVA analysis to the Weisman's genes list (data not shown). About 21% of genes (271/1262) were found in common, 24% (215/895) being in common with genes differentially expressed at 24h suggesting that ANOVA analysis do not contribute to differences between studies.

We then compared our differentially expressed genes lists to others transcriptome data sets of analysis performed to study the effect of xenobiotics such as aluminum (60), atrazine (Ramel et al., 2007), BOA (benzoxazolin-2(3H)-one) (Baerson et al., 2005), cadmium (Herbette et al., 2006), PCB (Polychlorinated biphenyl) (Jin et al., 2011), phenol (Xu et al., 2012) selenium (Van Hoewyk et al., 2008) and TNT (trinitrotoluene) (Landa et al., 2010) on higher plants. Differentially expressed genes considered had to be found in common with our genes lists in at least one of all the studies and in one time point in experiments with several time point. Overall, 77,7% (363 out of 467) of differentialy expressed genes were found in common. To summarized, theses comparisons showed that our work is in accordance with the earlier studies performed to decipher the plant response to phenanthrene and to other xenobiotics. Despite differences in gene expression observed between the types of xenobiotics studied, underlying specific molecular responses, this comparison led to the identification of a list of 363 genes, early regulated during phenanthrene exposure, corresponding to a gene network differentially expressed in response to xenobiotic (Supplemental Table V). Among these genes, a consensus group of 36 genes has been classified in the plant ”xenome” and are involved in transformation (CYP450), conjugation (GST, UGT, malonyl transferase) and compartmentalisation (ABC transporters) (Supplemental Table III and V). We thus add a new resolution level by deciphering early response to phenanthrene exposure using a detailed kinetic analysis. In addition, our study adds new phenanthrene regulated genes (Supplemental Tables V) to the present knowledge.

In a second step, we compared the main differentially expressed genes (our study, Table I) with transcriptome data from public genevestigator database to identify either similarities with other transcriptome analysis obtained in response to abiotic, biotic and chemical stimuli (Supplemental Figure 5).

A hierarchical clustering analysis was performed using our top list of differentially regulated genes and all selected data sets. Clustering obtained showed a rather identical pattern of expression of differentially expresses genes from our top list in either abiotic stress conditions (cold, drought, salt and hypoxia stress) or biotic (plant response to pathogenic virus, fungi and bacteria) or chemical stress conditions (Supplemental Figure 5 A, B, C). This result strongly suggest that in response to xenobitotics plant use a common gene

network regulated in response to secondary entities also produced in other biotic or abiotic stress condition as proposed by Ramel et al. (2012) for xenobiotic. In the “biotic selection” (Supplemental Figure 5 B) several experiments showed an opposite regulation pattern. They mainly correspond to comparisons between plants responses to non-pathogenic pathogens such as the mutant bacteria *Pseudomonas syringae pv tomato hrcC*-, deficient in the type III secretion system and unable to infect plant (Deng et al., 1998), and the avirulent mutant bacteria *Pseudomonas syringae pv tomato AvrRpm1,* unable to induce specific resistance associated to the RPS2 plant resistance protein but triggering defence responses after pathogen recognition (Kim et al., 2009). This observation reflect that genes regulated in all these biotic stress may participate in pathogen-associated molecular patterns triggered immunity, mechanism in which photosynthesis seems to play a crucial role (Göhre et al., 2012) as for abiotic stress (Ana Sofia Duque, 2013). Hierarchical clustering with chemical stress experiments enables us to constitute a “chemical selection” inclucing the Weisman’s transciptome data. Even if most of the experiments clustered correspond to plant response to pesticides and herbicides without well described molecular effects on plant, the results obtained confirm that our top list of differentially expressed genes is relevant and representative of plants responses to xenobiotics. These clustering results support that ROS play a major role in the early plant response to phenanthrene since our top list clustered with experiments associated to non enzymatic lipid peroxidation by ROS (phytoprostane A1) (Sattler et al., 2006) or stimulating ROS production (ozone treatment, hydrogen peroxide). Furthermore, similar genes expression pattern observed with a study using fenclorim, known to increase the gluthatione conjugation of the herbicide pretilachlor (Wu et al., 1996) confirm that detoxification process have been activated in our study.

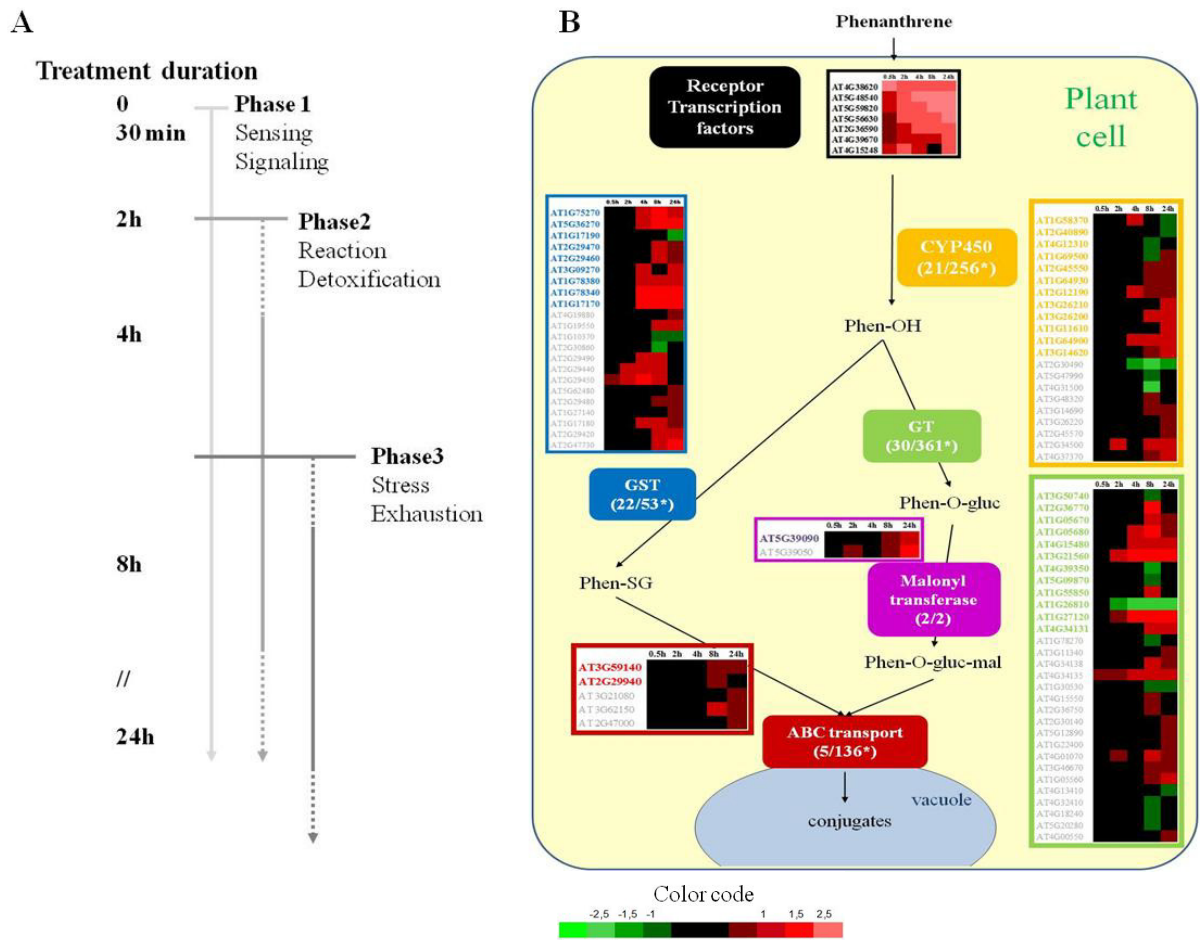


**Figure 7: Proposed model of early plant response to phenanthrene exposure.**

(**A**) Kinetic representation of the early plant response to phenanthrene. Following the sensing and the signalization of the phenanthrene within the first 30 minutes (phase 1), plant induces from 2h to 24h the expression of genes involved in defence response and detoxification of phenantrene (phase 2). Between 4 and 8h numerous indicators (gene expression and metabolites accumulation) suggest functional declines (phase 3).

(**B**) Representation of genes identified to be involved in the sensing, the signaling and the "xenome" according to the model described by Edwards et al. (2011). Numbers indicate the number of genes belonging to each family, differentially expressed in our study, compared to the total number of genes classified in each family. *: gene members of each family were retrieved from the TAIR website (http://www.arabidopsis.org/browse/genefamily/). Genes in bold face in each family correspond to differentially expressed genes selected after ANOVA analysis.

.

## 4. Conclusion

This analysis of the early responses of 15 day old *Arabidopsis* plantlets to phenanthrene exposure adds a new resolution level to previous studies on adult plants by dissecting early plant response during a kinetic ranging from 30m minutes to 24h of treatment. Our study is consistent with the earlier studies performed on phenanthrene or others xenobiotics and allowed us to identify a list of 363 genes found in common between our study and at least one of the others works. This study adds new early regulated phenanthrene dependent genes, differently expressed within the first 24h exposure to phenanthrene, Some of them, rapidly expressed after 30min of incubation, are among the most highly differentially expressed genes of the study and correspond to receptor kinase, kinase and transcription factors that could participate to the primary sensing and signalling events preceding detoxification of the phenanthrene. Thus, these genes are good candidates for further functional characterization and development of strategies of molecular avoidance for phenanthrene. A consensus group of 36 genes has been classified in the plant ”xenome” and are putatively involved in transformation (CYP450), conjugation (GST, UGT, malonyl transferase) and compartmentalization (ABC transporters). Eleven of them are also highly up-regulated after 4h of phenanthrene and may be considered in future studies to improve detoxification efficiency.

This study reveals rapid changes in gene expression that might correspond to an adaptive strategy developed by the plant to sense the phenanthrene and activates molecular process devoted to detoxify the pollutant. In a model presented in Figure 7 A, we proposed that the early plant response to phenanthrene could be finally divided in 3 phases. 1) A first phase of sensing and signaling within the first 30 minutes of treatment. Genes encoding receptor, transcription factors and kinase are differentially expressed and continuously regulated during the kinetic (Figure 7 B). 2) A reaction phase with genes involved the putative transformation, conjugation and compartmentalization of phenanthrene have they expression mainly up-regulated from 2 to 8h, some of them being expressed until 24h. Enzymatic activities of proteins encoded by these genes could contribute to increase the level of ROS and thus unbalanced the antioxidant status of cells. Clustering analysis of our top list of differently expressed genes indicates that these genes

are also similarly regulated in numerous transcriptome data sets corresponding to study of plants response to biotic, abiotic or chemical stress. Some of these experiments, using hydrogen peroxide, ozone or molecule that has to be in contact with oxygen singlets to induce similar expression patterns, support this hypothesis. If not counteracted, these free radicals can induce irreversible injuries. Some genes, such as *pfk7*, involved in the glycolysis metabolism, were up-regulated during the first 30 minutes and were continuously over-represented at the other kinetic points suggesting a strong energy and/or reductant demand within the first hours of exposure in order to restore homeostasis. Genes involved in phosynthesis metabolism were also down-regulated after 8h of treatment with phenanthrene. This result suggests that photosynthesis performance declines probably before. However, it remains difficult to known if it is the increase of energy demand or the reduction of energy production, through the repression of the expression genes involved in of the photosynthesis metabolism, that lead to an altered bioenergetics status. However, up-regulation of genes induced in fermentation metabolism at 24h support these decrease biological performances. Thus, energy status appears to be the crucial limiting factor that leads the plant to the third phase of our model. 3) After 8h of exposure to phenanthrene, numerous genes involved in primary and secondary metabolism are repressed, whereas genes mainly involved in glycolysis, fermentation, redox and stress metabolisms are up-regulated. Integration of metabolites titration data indicates a strong accumulation of amino acids and soluble sugars, indicators of functional declines that might lead the exhaustion of the plant.

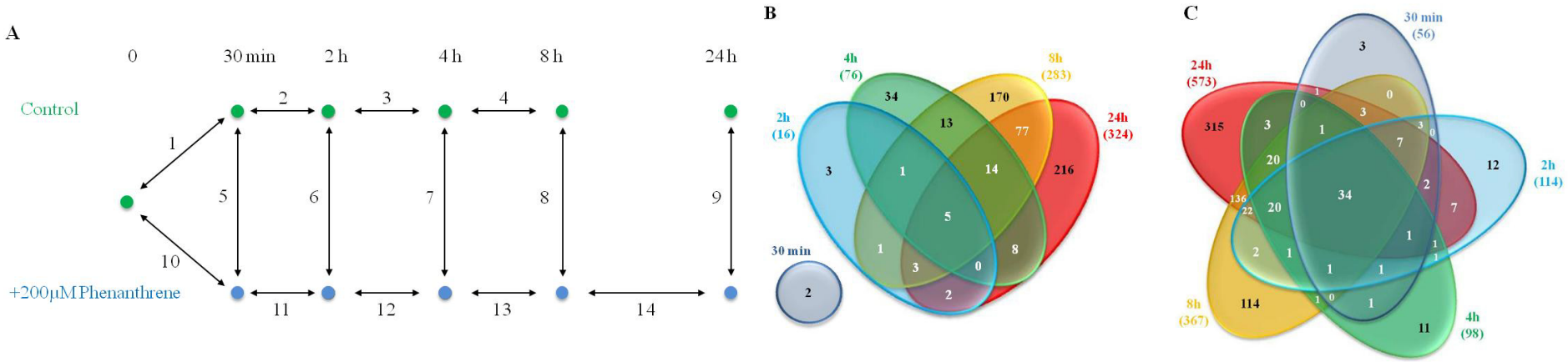


**Supplemental Figure 1:** (**A**) Schematic representation of the experimental procedure for transcriptome profiling of the *Arabidopsis* response to phenanthrene. Fourteen comparisons (1–14) of control and treated plants with 200µM phenanthrene were performed at five time points (30min, 2 h, 4 h, 8 h and 24 h). Double arrows point to the dye-switch hybridization described in material and method section for the two biological replicates used. In comparisons 1-4, RNAs from control plants from conditions 0, 30 min, 2 h and 4 h were hybridized on the same array with RNAs from control plants in the same condition at 30 min, 2 h, 4 h, 8 h respectively. In comparisons 5-9, RNAs from control plants at 30 min, 2 h, 4 h, 8 h and 24 h were hybridized with RNAs from phenanthrene-treated plants corresponding to the same kinetic point. In comparisons 10-14, RNAs from phenanthrene-treated plants at 0, 30 min, 2 h, 4 h and 8 h were hybridized on the same array with RNAs from treated plants in the 30 min, 2 h, 4 h, 8 h and 24h conditions respectively. (**B**, **C**) Venn diagram showing the total number of differentially expressed genes (p-value < 0.05). Lists of compared genes correspond to down-regulated (B) and up-regulated genes (C) obtained in comparisons between phenanthrene treated samples and control samples at 30 minutes, 2h, 4h, 8h and 24h.

Differentially expressed genes used are listed in Supplemental Table II. Transcriptome data corresponding to hybridizations performed are available in Supplemental Table 1.

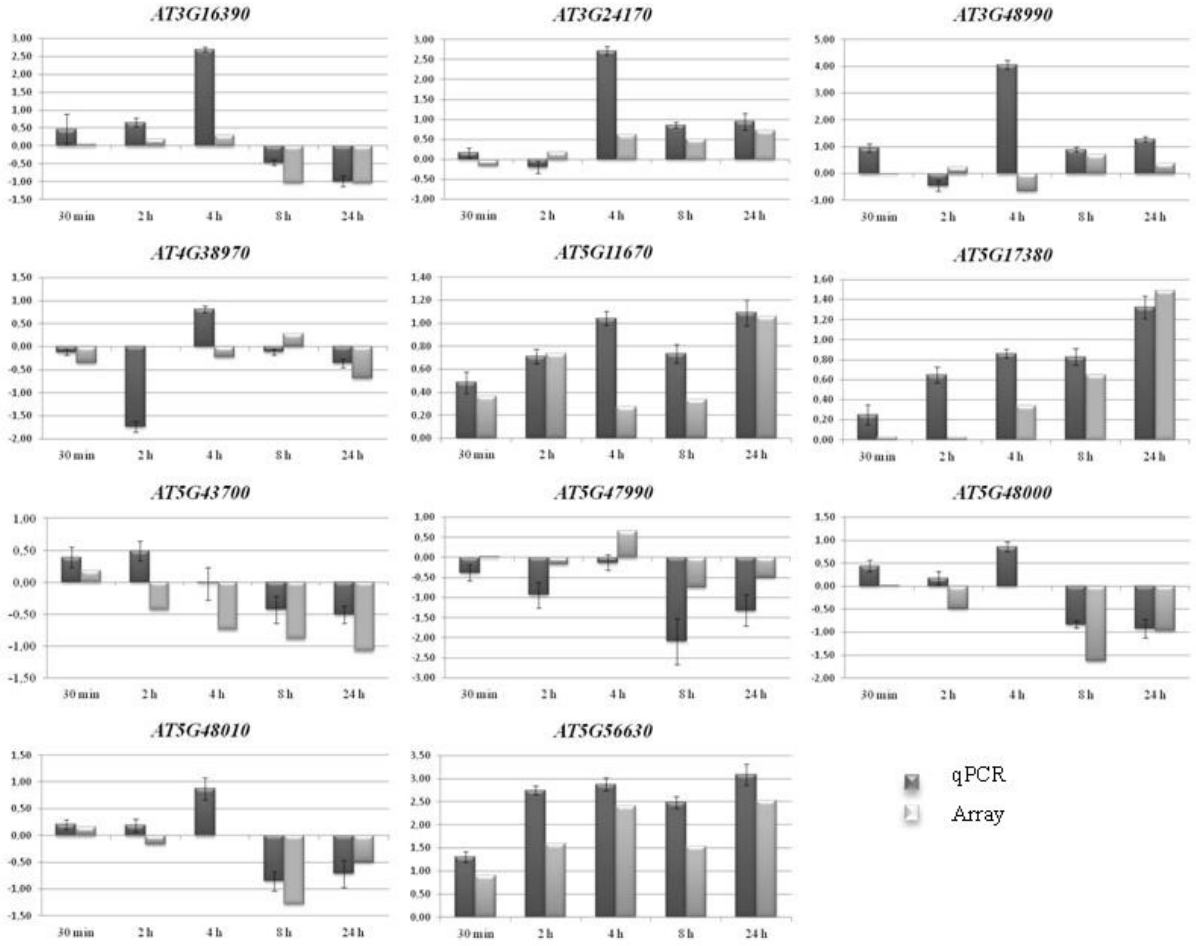


**Supplemental Figure 2:** QPCR validations of transcriptome data**.** The $\log_2$ ratios from CATMA microarray experiments and subsequent validation by qPCR ($\Delta C_t$) samples for 30 min, 2 h, 4 h, 8 h and 24 h comparisons for 11 selected transcripts. QPCR $\Delta C_t$ values are means ±SE of 3 replicates. Normalized $\Delta$Ct for each differentially expressed gene were calculated as following: Norm $\Delta$Ct =-(( $C_{t1}$-$C_{t2}$)-NF) where the NF corresponds to the average normalization factor calculated on the basis of results obtained for two best control genes chosen to be consistently expressed on CATMA microarray experiments in all samples compared (*AT4G13615* and *AT5G21090*).

**A**

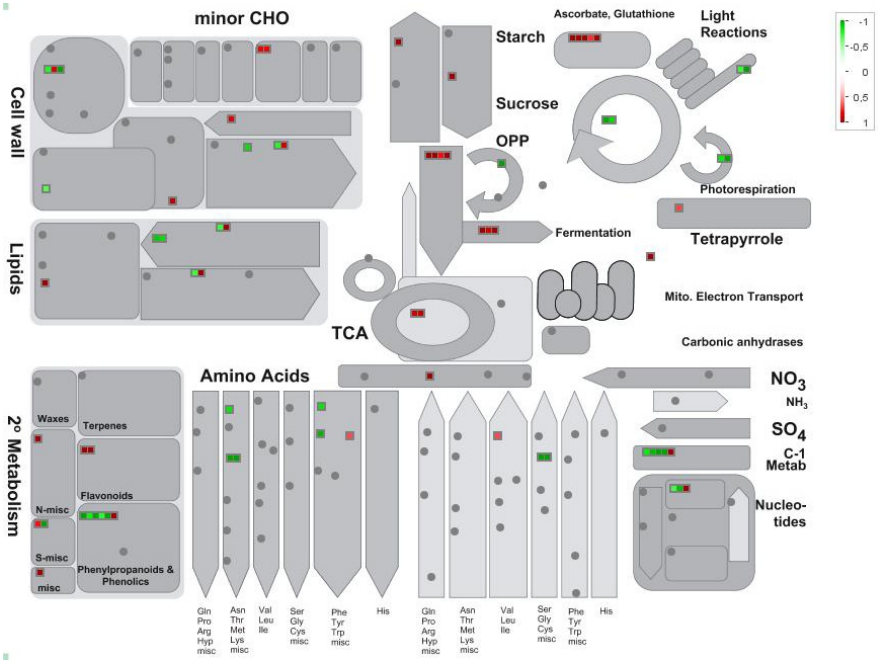


**B**

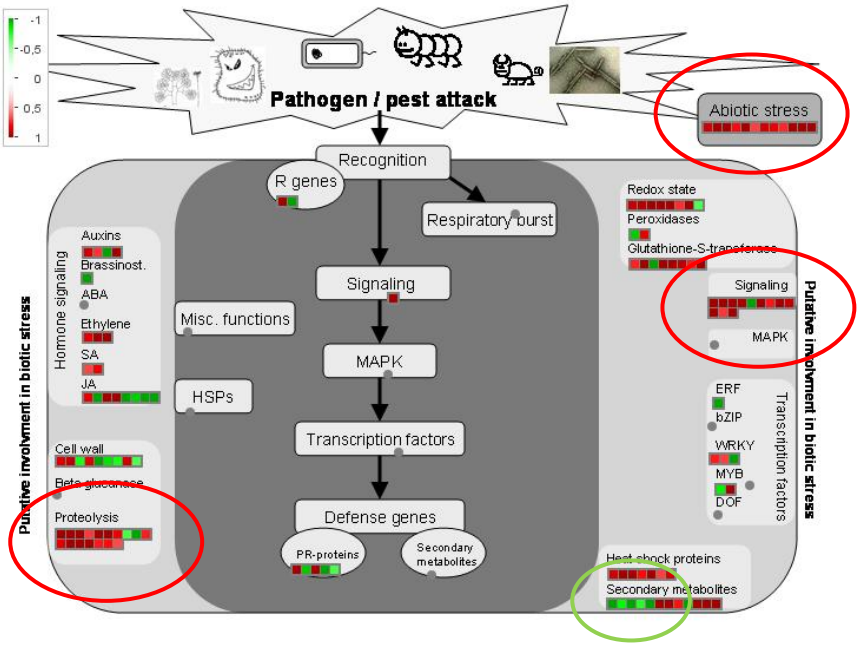


**<u>Supplemental Figure 3</u>:** Metabolic gene expression changes (**A**), and biotic gene expression overview (**B**), after 24 h of 0,2mM phenanthrene treatment, analyzed by the MapMan tool. Ratios are given for comparisons phenanthrene treated to control samples.

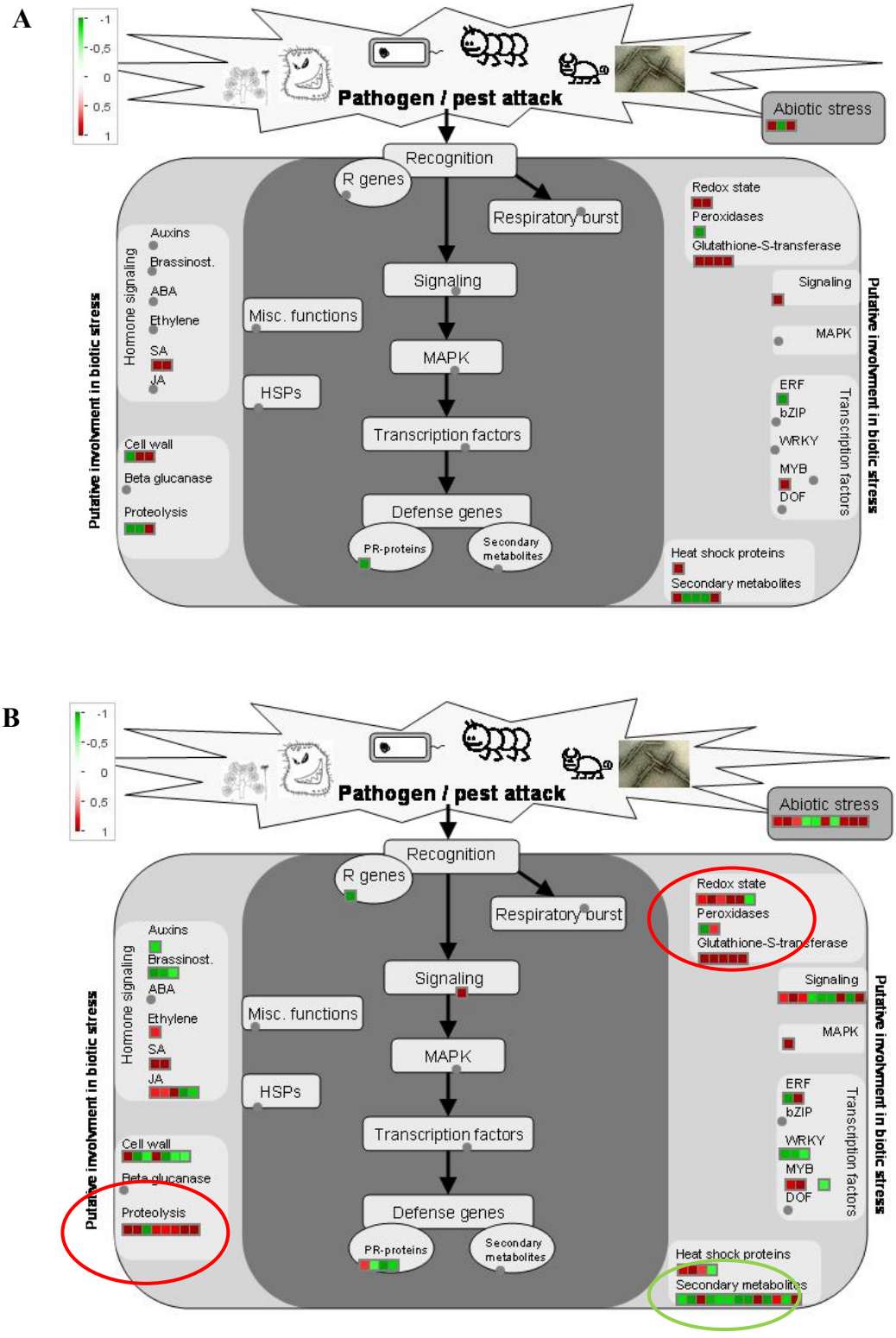


**Supplemental Figure 4:** Biotic stress genes expression changes after 4h (**A**) and 8h (**B**) of incubation with 0,2mM phenanthrene, analyzed by the MapMan tool. Ratios are given for comparisons phenanthrene treated to control samples.

## A: Abiotic selection

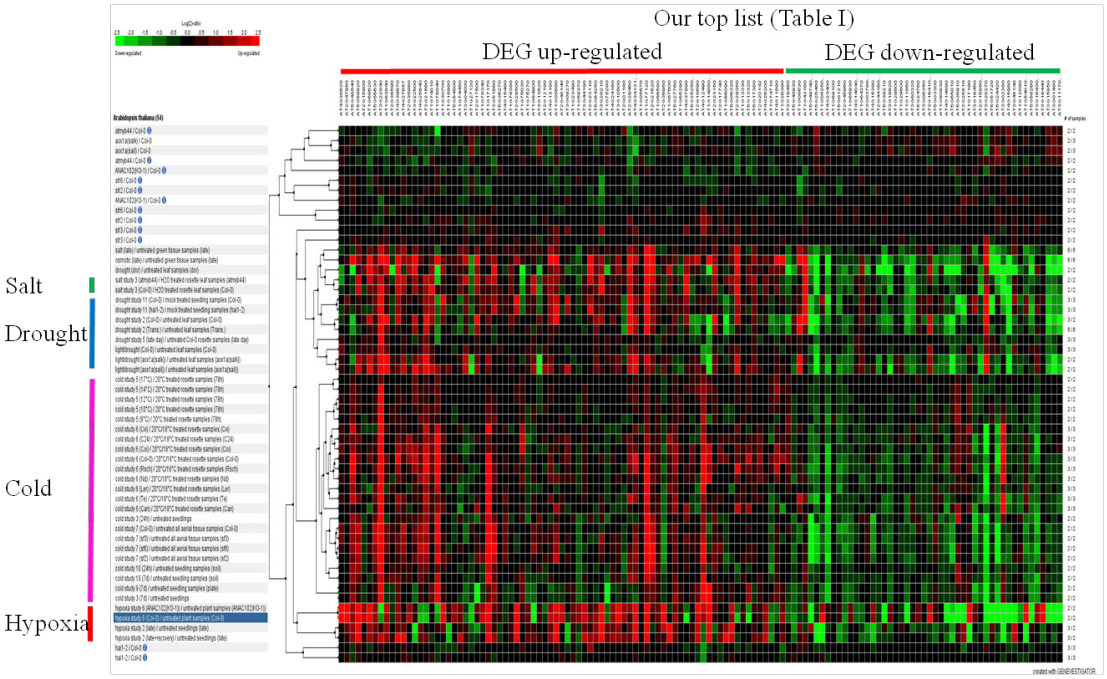


## B: biotic selection

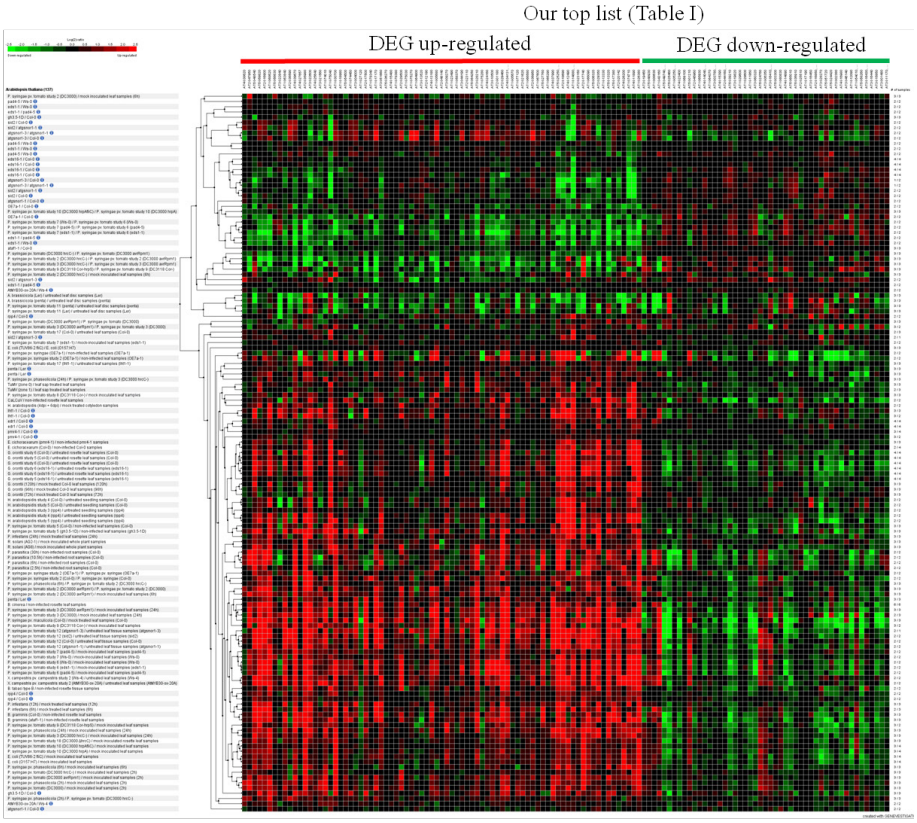


Wild type, mutant and transgenic plants response to mutated avirulent or non pathogenic bacteria and fungus

Wild type, mutants and transgenic response to pathogens: virus, bacteria, fungi

## C: Chemical selection

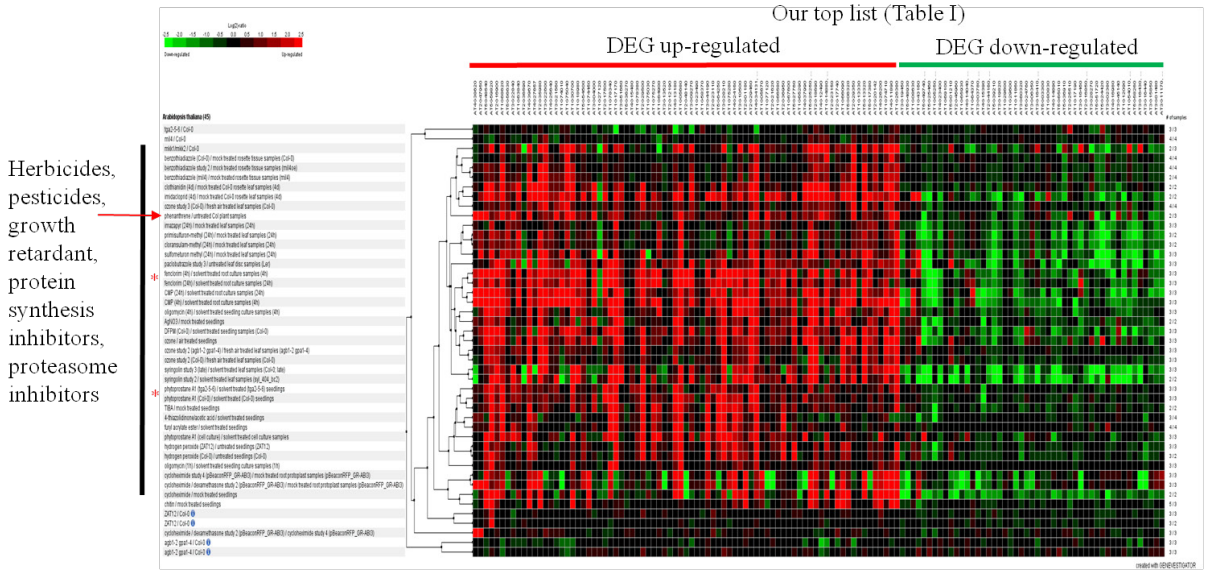


**Supplemental Figure 5:** Clustering analysis within Genevestigator public data. Clustering analysis was performed using our top list of differentially regulated genes (Table I) using the clustering tool available at www.genenvestigator.com. (**A**) clustering using subset "Abiotic selection", (**B**) clustering using subset "Biotic selection", (**C**) clustering uisng subset "chemical selection". → Weisman et al (2010) study (24).*, Denclorim and phytoprostane A1 examples cited in the article.

**Supplemental Table I:** Transcriptome data obtained for each comparisons performed. Differentially regulated genes, in bold face, were selected by statistical analysis based on the Bonferroni method using a P value cut-off of 0.05.
*(cf. electronic data)*

**Supplemental Table II:** Genes found to be differentially expressed in all the comparisons between phenenthrene-treated and control plants (hybridizations 5-9). Among the 1262 differentially expressed genes corresponding to annotated genes, 58, 130, 174, 650 and 897 genes were expressed at 30 min, 2 h, 4 h, 8 h and 24 h respectively. ns: not significantly differentially expressed. *Arabidopsis* annotation from TAIR, called TAIR10 (most recent versions as of 21 September 2012). Expression changes are given as log2. Expression changes in bolt correspond to genes differentially expressed at the significant threshold of Bonferroni p-value<0.05. ns, not significant.

| CATMA identifier | AGI identifier | Gene annotation | 30 min | 2h | 4h | 8h | 24h |
|---|---|---|---|---|---|---|---|
| CATMA4A26290_N | AT4G24570 | DIC2__dicarboxylate carrier 2 | **-0.68** | ns | ns | ns | ns |
| CATMA1B43120 | AT1G52000 | Mannose-binding lectin superfamily protein | **-0.65** | ns | ns | ns | ns |
| CATMA_GFT_02704 | AT1G70800 | EHB1__Calcium-dependent lipid-binding (CaLB domain) family protein | **0.64** | **1.23** | **1.91** | **1.97** | **1.19** |
| CATMA4A09435 | AT4G09460 | AtMYB6_MYB6__myb domain protein 6 | **0.64** | **0.91** | ns | **0.75** | ns |
| CATMA1A16850 | AT1G17830 | Protein of unknown function (DUF789) | **0.64** | ns | ns | ns | ns |
| CATMA4C42498 | AT4G25810 | XTH23_XTR6__xyloglucan endotransglycosylase 6 | **0.64** | **0.91** | ns | **0.97** | **1.60** |
| CATMA1C71994 | AT1G65360 | AGL23__AGAMOUS-like 23 | **0.65** | ns | ns | ns | ns |
| CATMA1A59790 | AT1G70530 | CRK3__cysteine-rich RLK (RECEPTOR-like protein kinase) 3 | **0.66** | **0.97** | ns | **1.13** | **1.68** |
| CATMA5A02320 | AT5G03210 | AtDIP2_DIP2__unknown protein | **0.68** | **1.31** | **1.34** | **0.92** | **1.03** |
| CATMA1A37730 | AT1G44750 | ATPUP11_PUP11__purine permease 11 | **0.69** | ns | **1.15** | ns | ns |
| CATMA5A04100 | AT5G04930 | ALA1__aminophospholipid ATPase 1 | **0.69** | **1.07** | **1.11** | **1.18** | **1.39** |
| CATMA5A12830 | AT5G14602 | Unknown protein | **0.70** | ns | **1.07** | **0.71** | **0.86** |
| CATMA4A29300 | AT4G27657 | unknown protein | **0.70** | **1.26** | **1.10** | **1.75** | **0.74** |
| CATMA2A35995 | AT2G37710 | RLK__receptor lectin kinase | **0.70** | **1.23** | **1.85** | **1.45** | **2.34** |
| CATMA5A22300 | AT5G24655 | LSU4__response to low sulfur 4 | **0.72** | **0.90** | **1.71** | **1.02** | **1.13** |
| CATMA5A30810 | AT5G35580 | Protein kinase superfamily protein | **0.72** | ns | ns | **0.98** | **0.92** |
| CATMA4A41020 | AT4G39670 | Glycolipid transfer protein (GLTP) family protein | **0.73** | **1.26** | **1.01** | **1.42** | **2.13** |
| CATMA3A52920 | AT3G59900 | ARGOS__auxin-regulated gene involved in organ size | **0.73** | ns | ns | ns | **0.83** |
| CATMA2A27835 | AT2G29450 | AT103-1A_ATGSTU1_ATGSTU5_GSTU5__glutathione S-transferase tau 5 | **0.73** | **1.09** | **1.55** | **1.35** | ns |
| CATMA1A00730 | AT1G01720 | ANAC002_ATAF1__NAC (No Apical Meristem) domain transcriptional regulator superfamily protein | **0.73** | ns | ns | **0.80** | **0.86** |
| CATMA4D01770 | AT4G34135 | UGT73B2__UDP-glucosyltransferase 73B2 | **0.76** | **0.85** | **1.25** | **1.04** | **1.45** |
| CATMA3A21990 | AT3G22060 | Receptor-like protein kinase-related family protein | **0.78** | **1.28** | **1.15** | **1.81** | **1.47** |
| CATMA2A34820 | AT2G36590 | ATPROT3_ProT3__proline transporter 3 | **0.79** | **1.42** | **1.93** | **1.80** | **2.24** |
| CATMA1A41790 | AT1G50740 | Transmembrane proteins 14C | **0.80** | **0.99** | ns | **0.75** | **0.96** |
| CATMA1A08840 | AT1G09970 | LRR XI-23_RLK7__Leucine-rich receptor-like protein kinase family protein | **0.81** | **0.99** | ns | ns | **1.34** |
| CATMA1A53060 | AT1G63840 | RING/U-box superfamily protein | **0.83** | **1.80** | **1.64** | **2.10** | **2.16** |
| CATMA2A42510 | AT2G44080 | ARL__ARGOS-like | **0.86** | ns | ns | **0.86** | **1.07** |
| CATMA3A25100 | AT3G25250 | AGC2_AGC2-1_AtOXI1_OXI1__AGC (cAMP-dependent, cGMP-dependent and protein kinase C) kinase family protein | **0.87** | **1.03** | **1.33** | **0.83** | **0.84** |
| CATMA3A22775 | AT3G22840 | ELIP_ELIP1__Chlorophyll A-B binding family protein | **0.89** | **1.40** | **2.19** | **1.70** | **2.38** |
| CATMA4A28990 | AT4G27410 | ANAC072_RD26__NAC (No Apical Meristem) domain transcriptional regulator superfamily protein | **0.89** | **1.26** | ns | **1.27** | ns |
| CATMA5A52440 | AT5G56630 | PFK7__phosphofructokinase 7 | **0.91** | **1.59** | **2.41** | **1.54** | **2.53** |
| CATMA1A58000 | AT1G68620 | alpha/beta-Hydrolases superfamily protein | **0.93** | **2.18** | **1.68** | **2.77** | **2.70** |
| CATMA1A50830 | AT1G61750 | Receptor-like protein kinase-related family protein | **0.94** | **1.03** | **1.20** | **0.77** | **1.01** |
| CATMA1A09000 | AT1G10140 | Uncharacterised conserved protein UCP031279 | **0.98** | **0.89** | ns | **1.02** | **0.79** |
| CATMA2A15560 | AT2G16900 | Arabidopsis phospholipase-like protein (PEARLI 4) family | **0.98** | **1.68** | **1.67** | **1.61** | **2.16** |
| CATMA1A42160 | AT1G51090 | Heavy metal transport/detoxification superfamily protein | **1.04** | **1.17** | ns | **0.98** | ns |
| CATMA4C42802 | AT4E19530 | Unknown protein | **1.06** | **1.16** | **1.64** | **0.79** | **0.91** |
| CATMA1A59680 | AT1G70420 | Protein of unknown function (DUF1645) | **1.13** | **1.33** | **1.15** | **1.53** | **1.41** |
| CATMA5C64297 | AT5G18140 | Chaperone DnaJ-domain superfamily protein | **1.13** | **1.12** | **1.36** | **1.27** | **1.30** |
| CATMA1C71184 | AT1G13245 | DVL4_RTFL17__ROTUNDIFOLIA like 17 | **1.14** | **0.87** | ns | **0.98** | **0.69** |
| CATMA1A22270 | AT1G23200 | Plant invertase/pectin methylesterase inhibitor superfamily | **1.18** | **2.10** | **2.56** | **2.05** | **2.54** |
| CATMA5A55595 | AT5G59820 | RHL41_ZAT12__C2H2-type zinc finger family protein | **1.19** | **1.63** | **2.14** | **2.70** | **2.50** |
| CATMA1A67660 | AT1G78600 | BBX22_DBB3_LZF1_STH3__light-regulated zinc finger protein 1 | **1.25** | **1.35** | **1.41** | **1.26** | **1.72** |
| CATMA2A04740 | AT2G05940 | RIPK__Protein kinase superfamily protein | **1.25** | **1.34** | **1.28** | **1.17** | **1.58** |
| CATMA3A52950 | AT3G59940 | Galactose oxidase/kelch repeat superfamily protein | **1.26** | **1.54** | ns | **1.59** | **1.56** |
| CATMA5A22310 | AT5G24660 | LSU2__response to low sulfur 2 | **1.29** | **1.56** | **2.35** | **1.94** | **2.06** |
| CATMA1A14680 | AT1G15670 | Galactose oxidase/kelch repeat superfamily protein | **1.31** | **0.89** | ns | ns | **1.09** |
| CATMA5A09430 | AT5G10695 | unknown protein | **1.33** | **1.32** | **1.18** | **1.36** | **1.78** |
| CATMA1A16150 | AT1G17147 | VQ motif-containing protein | **1.33** | **1.95** | **1.40** | **1.99** | **1.37** |
| CATMA1A38140 | AT1G47240 | ATNRAMP2_NRAMP2__NRAMP metal ion transporter 2 | **1.35** | **1.40** | **1.22** | **1.65** | **1.73** |
| CATMA2A42550 | AT2G44140 | Peptidase family C54 protein | **1.37** | **3.64** | **2.33** | **3.21** | **3.13** |
| CATMA4A15850 | AT4G15248 | B-box type zinc finger family protein | **1.39** | **1.75** | **1.04** | ns | **1.63** |
| CATMA5A44520 | AT5G48540 | receptor-like protein kinase-related family protein | **1.42** | **2.44** | **3.27** | **3.48** | **3.51** |
| CATMA2A46390 | AT2G47950 | unknown protein | **1.49** | **2.27** | **2.27** | **2.65** | **1.91** |
| CATMA1A51800 | AT1G62690 | unknown protein. | **1.52** | **1.81** | **2.07** | **2.12** | **2.83** |
| CATMA2A15423 | AT2G16720 | ATMYB7_ATY49_MYB7__myb domain protein 7 | **1.62** | **1.25** | ns | **0.75** | **0.88** |

| CATMA identifier | AGI identifier | Gene annotation | 30 min | 2h | 4h | 8h | 24h |
|---|---|---|---|---|---|---|---|
| CATMA3A12420 | AT3G13310 | Chaperone DnaJ-domain superfamily protein | **1.64** | **1.64** | **1.29** | **1.87** | **1.84** |
| CATMA4A40092 | AT4G38620 | ATMYB4_MYB4__myb domain protein 4 | **3.51** | **2.19** | **2.30** | **2.18** | **1.94** |
| CATMA1A19670 | AT1E21210 | unknown protein | ns | ns | ns | ns | **-0.71** |
| CATMA1A00310 | AT1G01320 | Tetratricopeptide repeat (TPR)-like superfamily protein | ns | ns | ns | **-1.14** | ns |
| CATMA1A00460 | AT1G01470 | LEA14_LSR3__Late embryogenesis abundant protein | ns | ns | ns | ns | **1.04** |
| CATMA1C71011 | AT1G01790 | ATKEA1_KEA1__K+ efflux antiporter 1 | ns | ns | ns | **-0.74** | ns |
| CATMA1A00950 | AT1G01960 | EDA10__SEC7-like guanine nucleotide exchange family protein | ns | ns | ns | **-0.96** | ns |
| CATMA1A01610 | AT1G02660 | alpha/beta-Hydrolases superfamily protein | ns | ns | **-1.18** | ns | ns |
| CATMA1D02499 | AT1G03230 | Eukaryotic aspartyl protease family protein | ns | ns | ns | ns | **0.69** |
| CATMA1C71037 | AT1G03700 | Uncharacterised protein family (UPF0497) | ns | **0.96** | ns | ns | ns |
| CATMA1A03115 | AT1G04270 | RPS15__cytosolic ribosomal protein S15 | ns | ns | ns | ns | **-0.67** |
| CATMA1A03260 | AT1G04430 | S-adenosyl-L-methionine-dependent methyltransferases superfamily protein | ns | ns | ns | **-0.78** | ns |
| CATMA1A03520 | AT1G04680 | Pectin lyase-like superfamily protein | ns | ns | ns | ns | **-0.75** |
| CATMA1A03570 | AT1G04770 | Tetratricopeptide repeat (TPR)-like superfamily protein | ns | ns | **1.00** | **0.71** | **0.90** |
| CATMA1A03970 | AT1G05100 | MAPKKK18__mitogen-activated protein kinase kinase kinase 18 | ns | ns | ns | **0.99** | ns |
| CATMA_GFT_02501 | AT1G05240 | Peroxidase superfamily protein | ns | ns | **-1.07** | **-1.48** | **-0.91** |
| CATMA1C71047 | AT1G05340 | unknown protein | ns | ns | ns | **0.80** | **1.12** |
| CATMA1C71051 | AT1G05560 | UGT1_UGT75B1__UDP-glucosyltransferase 75B1 | ns | ns | ns | **0.90** | **1.12** |
| CATMA1C71052 | AT1G05575 | unknown protein | ns | ns | ns | **1.21** | ns |
| CATMA1A04670 | AT1G05670 | Pentatricopeptide repeat (PPR-like) superfamily protein | ns | ns | ns | **1.30** | **0.69** |
| CATMA_GFT_00023 | AT1G05680 | UGT74E2__Uridine diphosphate glycosyltransferase 74E2 | ns | ns | **1.01** | **1.80** | **0.83** |
| CATMA1C71064 | AT1G06290 | ACX3_ATACX3__acyl-CoA oxidase 3 | ns | ns | ns | **0.69** | **0.74** |
| CATMA1A05580 | AT1G06550 | ATP-dependent caseinolytic (Clp) protease/crotonase family protein | ns | ns | ns | **-0.77** | ns |
| CATMA1A05615 | AT1G06570 | HPD_HPPD_PDS1__phytoene desaturation 1 | ns | ns | **-1.23** | ns | ns |
| CATMA1A06010 | AT1G06950 | ATTIC110_TIC110__translocon at the inner envelope membrane of chloroplasts 110 | ns | ns | ns | **-0.77** | ns |
| CATMA1A06190 | AT1G07135 | glycine-rich protein | ns | ns | ns | ns | **0.66** |
| CATMA1A06330 | AT1G07280 | Tetratricopeptide repeat (TPR)-like superfamily protein | ns | ns | ns | **-0.92** | ns |
| CATMA1A06470 | AT1G07400 | HSP20-like chaperones superfamily protein | ns | ns | **1.24** | **1.18** | **1.23** |
| CATMA1A06876 | AT1G07890 | APX1_ATAPX01_ATAPX1_CS1_MEE6__ascorbate peroxidase 1 | ns | ns | ns | ns | **0.87** |
| CATMA1A06950 | AT1G07985 | Expressed protein | ns | ns | ns | **0.74** | ns |
| CATMA1C71101 | AT1G08360 | Ribosomal protein L1p/L10e family | ns | ns | ns | ns | **-0.74** |
| CATMA1A07491 | AT1G08540 | ABC1_ATSIG1_ATSIG2_SIG1_SIG2_SIGA_SIGB__RNA polymerase sigma subunit 2 | ns | ns | ns | **-0.78** | ns |
| CATMA1A07550 | AT1G08630 | THA1__threonine aldolase 1 | ns | ns | **-1.81** | **-0.92** | **-1.62** |
| CATMA1A07793 | AT1G08920 | ESL1__ERD (early response to dehydration) six-like 1 | ns | ns | ns | **0.73** | **0.81** |
| CATMA1A07895 | AT1G09070 | (AT)SRC2_SRC2__soybean gene regulated by cold-2 | ns | ns | ns | **1.78** | **1.70** |
| CATMA1A07930 | AT1G09130 | ATP-dependent caseinolytic (Clp) protease/crotonase family protein | ns | ns | ns | **0.87** | ns |
| CATMA1C71120 | AT1G09340 | CRB_CSP41B_HIP1.3__chloroplast RNA binding | ns | ns | ns | ns | **-0.70** |
| CATMA1C71124 | AT1G09400 | FMN-linked oxidoreductases superfamily protein | ns | ns | ns | **0.74** | **1.08** |
| CATMA1C71125 | AT1G09500 | NAD(P)-binding Rossmann-fold superfamily protein | ns | ns | ns | **0.98** | ns |
| CATMA1A08395 | AT1G09530 | PAP3_PIF3_POC1__phytochrome interacting factor 3 | ns | ns | ns | **-0.79** | ns |
| CATMA1A09190 | AT1G10340 | Ankyrin repeat family protein | ns | ns | ns | ns | **0.93** |
| CATMA1C71141 | AT1G10370 | ATGSTU17_ERD9_GST30_GST30B_GSTU17__Glutathione S-transferase family protein | ns | ns | ns | **-0.71** | **-0.78** |
| CATMA1A09850 | AT1G10960 | ATFD1_FD1__ferredoxin 1 | ns | ns | ns | **-0.70** | ns |
| CATMA1C71155 | AT1G11610 | CYP71A18__cytochrome P450, family 71, subfamily A, polypeptide 18 | ns | ns | ns | ns | **1.12** |
| CATMA1A10860 | AT1G11850 | unknown protein | ns | ns | ns | ns | **-0.72** |
| CATMA1A10870 | AT1G11860 | Glycine cleavage T-protein family | ns | ns | ns | **-1.17** | **-1.14** |
| CATMA1A10930 | AT1G11910 | APA1_ATAPA1__aspartic proteinase A1 | ns | ns | ns | ns | **0.84** |
| CATMA1A11060 | AT1G12010 | 2-oxoglutarate (2OG) and Fe(II)-dependent oxygenase superfamily protein | ns | ns | ns | **-0.72** | **-0.80** |
| CATMA1A11135 | AT1G12090 | ELP__extensin-like protein | ns | ns | ns | ns | **-1.08** |
| CATMA1A11765 | AT1G12780 | ATUGE1_UGE1__UDP-D-glucose/UDP-D-galactose 4-epimerase 1 | ns | ns | **-1.06** | ns | ns |
| CATMA1A11780 | AT1G12800 | Nucleic acid-binding, OB-fold-like protein | ns | ns | ns | **-0.82** | ns |
| CATMA1A11900 | AT1G12900 | GAPA-2__glyceraldehyde 3-phosphate dehydrogenase A subunit 2 | ns | ns | ns | ns | **-0.89** |
| CATMA1A12340 | AT1G13330 | AHP2__Arabidopsis Hop2 homolog | ns | ns | ns | ns | **1.55** |
| CATMA1A13090 | AT1G14120 | 2-oxoglutarate (2OG) and Fe(II)-dependent oxygenase superfamily protein | ns | ns | **1.08** | ns | ns |
| CATMA1C71197 | AT1G14130 | 2-oxoglutarate (2OG) and Fe(II)-dependent oxygenase superfamily protein | ns | ns | ns | **1.04** | **0.86** |
| CATMA1A13300 | AT1G14290 | SBH2__sphingoid base hydroxylase 2 | ns | ns | ns | ns | **-0.82** |
| CATMA1A13550 | AT1G14540 | Peroxidase superfamily protein | ns | ns | ns | ns | **0.75** |
| CATMA1C71209 | AT1G14870 | AtPCR2_PCR2__PLANT CADMIUM RESISTANCE 2 | ns | ns | ns | ns | **1.76** |
| CATMA1A13910 | AT1G14880 | AtPCR1_PCR1__PLANT CADMIUM RESISTANCE 1 | ns | ns | ns | ns | **0.66** |
| CATMA1A14290 | AT1G15290 | Tetratricopeptide repeat (TPR)-like superfamily protein | ns | ns | ns | **-0.97** | ns |

| CATMA identifier | AGI identifier | Gene annotation | 30 min | 2h | 4h | 8h | 24h |
|---|---|---|---|---|---|---|---|
| CATMA1A14450 | AT1G15415 | The protein encoded by this gene was identified as a part of pollen proteome by mass spec analysis. It has weak homology to LEA (late embryo abundant) proteins. | ns | ns | ns | **0.74** | ns |
| CATMA1A14525 | AT1G15500 | Encodes protein phosphatase 2A (PP2A) B'gamma subunit. Targeted to nucleus and cytosol. ATNTT2__TLC ATP/ADP transporter | ns | ns | ns | **-0.69** | ns |
| CATMA1C71226 | AT1G15750 | TPL_WSIP1__Transducin family protein / WD-40 repeat family protein | ns | ns | ns | **0.78** | ns |
| CATMA1A14990 | AT1G15930 | Ribosomal protein L7Ae/L30e/S12e/Gadd45 family protein | ns | ns | ns | ns | **-0.71** |
| CATMA1A15040 | AT1G16030 | Hsp70b__heat shock protein 70B | ns | ns | ns | ns | **0.70** |
| CATMA1A15340 | AT1G16350 | Aldolase-type TIM barrel family protein | ns | ns | ns | **-0.74** | ns |
| CATMA1A15380 | AT1G16390 | ATOCT3_OCT3__organic cation/carnitine transporter 3 | ns | ns | ns | ns | **-0.83** |
| CATMA1A15690 | AT1G16720 | HCF173__high chlorophyll fluorescence phenotype 173 | ns | ns | **-1.31** | ns | ns |
| CATMA1C71257 | AT1G17170 | ATGSTU24_GST_GSTU24__glutathione S-transferase TAU 24 | ns | ns | **1.57** | **2.00** | **2.05** |
| CATMA1C71258 | AT1G17180 | ATGSTU25_GSTU25__glutathione S-transferase TAU 25 | ns | ns | **1.50** | **1.07** | **0.99** |
| CATMA1A16200 | AT1G17190 | ATGSTU26_GSTU26__glutathione S-transferase tau 26 | ns | ns | ns | ns | **-1.41** |
| CATMA1A16230 | AT1G17220 | FUG1__Translation initiation factor 2, small GTP-binding protein | ns | ns | ns | **-0.85** | ns |
| CATMA1A16880 | AT1G17860 | Kunitz family trypsin and protease inhibitor protein | ns | ns | ns | **1.10** | **1.06** |
| CATMA1A16990 | AT1G18020 | FMN-linked oxidoreductases superfamily protein | ns | ns | ns | **0.92** | ns |
| CATMA1A17300 | AT1G18290 | unknown protein | ns | ns | ns | ns | **-0.83** |
| CATMA1C71277 | AT1G18390 | Protein kinase superfamily protein | ns | ns | ns | ns | **0.82** |
| CATMA1A17560 | AT1G18510 | TET16__tetraspanin 16 | ns | ns | ns | **1.26** | ns |
| CATMA1A17615 | AT1G18570 | AtMYB51_BW51A_BW51B_HIG1_MYB51__myb domain protein 51 | ns | ns | ns | **-0.74** | ns |
| CATMA1A17740 | AT1G18700 | DNAJ heat shock N-terminal domain-containing protein | ns | ns | ns | **0.77** | **0.83** |
| CATMA1A17860 | AT1G18810 | phytochrome kinase substrate-related | ns | ns | ns | **-1.27** | ns |
| CATMA1B17945 | AT1G18880 | NRT1.9__Major facilitator superfamily protein | ns | ns | ns | ns | **0.76** |
| CATMA1A18010 | AT1G18980 | RmlC-like cupins superfamily protein | ns | **1.16** | **1.55** | **1.57** | **1.59** |
| CATMA1A18090 | AT1G19050 | ARR7__response regulator 7 | ns | ns | ns | **-0.72** | ns |
| CATMA1A18130 | AT1G19100 | Histidine kinase-, DNA gyrase B-, and HSP90-like ATPase family protein | ns | ns | ns | **-0.69** | ns |
| CATMA1A18260 | AT1G19220 | ARF11_ARF19_IAA22__auxin response factor 19 | ns | ns | ns | ns | **0.82** |
| CATMA1A18400 | AT1G19380 | Protein of unknown function (DUF1195) | ns | ns | ns | ns | **0.87** |
| CATMA_GFT_02523 | AT1G19550 | Glutathione S-transferase family protein | ns | ns | ns | **1.05** | **1.20** |
| CATMA1A18780 | AT1G19770 | ATPUP14_PUP14__purine permease 14 | ns | ns | **-1.01** | ns | ns |
| CATMA1A19470 | AT1G20470 | SAUR-like auxin-responsive protein family | ns | ns | ns | **0.71** | ns |
| CATMA1A19955 | AT1G20900 | AHL27_ESC_ORE7__Predicted AT-hook DNA-binding family protein | ns | ns | ns | ns | **-1.02** |
| CATMA1C71316 | AT1G21000 | PLATZ transcription factor family protein | ns | ns | ns | **0.73** | ns |
| CATMA1A20325 | AT1G21270 | WAK2__wall-associated kinase 2 | ns | ns | ns | ns | **0.74** |
| CATMA1A20370 | AT1G21320 | nucleotide binding;nucleic acid binding | ns | ns | ns | **-0.70** | ns |
| CATMA1A20530 | AT1G21480 | Exostosin family protein | ns | ns | ns | **-0.77** | **-1.08** |
| CATMA1A20650 | AT1G21570 | unknown protein | ns | ns | ns | **-1.57** | ns |
| CATMA1A20760 | AT1G21670 | unknown protein. | ns | **0.97** | ns | **1.20** | **1.79** |
| CATMA1A20815 | AT1G21720 | PBC1__proteasome beta subunit C1 | ns | ns | ns | **0.74** | ns |
| CATMA1A20840 | AT1G21750 | ATPDI5_ATPDIL1-1_PDI5_PDIL1-1__PDI-like 1-1 | ns | ns | ns | ns | **0.93** |
| CATMA1C72301 | AT1G22350 | unknown protein | ns | ns | ns | ns | **0.76** |
| CATMA1C71339 | AT1G22400 | ATUGT85A1_UGT85A1__UDP-Glycosyltransferase superfamily protein | ns | ns | ns | ns | **0.81** |
| CATMA1C71343 | AT1G22500 | AtATL15_ATL15__RING/U-box superfamily protein | ns | ns | ns | **0.88** | ns |
| CATMA1A21725 | AT1G22640 | ATMYB3_MYB3__myb domain protein 3 | ns | ns | ns | ns | **-0.83** |
| CATMA1A21785_N | AT1G22710 | ATSUC2_SUC2_SUT1__sucrose-proton symporter 2 | ns | ns | ns | **0.87** | **1.27** |
| CATMA1C71357 | AT1G22840 | ATCYTC-A_CYTC-1__CYTOCHROME C-1 | ns | ns | ns | ns | **0.70** |
| CATMA1A21975 | AT1G22920 | AJH1_CSN5A_JAB1__COP9 signalosome 5A | ns | ns | ns | ns | **-0.87** |
| CATMA1A22180 | AT1G23120 | Polyketide cyclase/dehydrase and lipid transport superfamily protein | ns | ns | ns | **-0.76** | ns |
| CATMA1A22430 | AT1G23350 | Plant invertase/pectin methylesterase inhibitor superfamily protein | ns | ns | **-1.13** | **-0.69** | ns |
| CATMA1C71370 | AT1G23490 | ARF1_ATARF_ATARF1_ATARFA1A__ADP-ribosylation factor 1 | ns | ns | **1.04** | ns | **1.32** |
| CATMA1A22740 | AT1G23880 | NHL domain-containing protein | ns | ns | ns | ns | **0.78** |
| CATMA1A22750 | AT1G23890 | NHL domain-containing protein | ns | ns | ns | **1.26** | ns |
| CATMA1A22830 | AT1G23980 | RING/U-box superfamily protein | ns | ns | ns | ns | **0.75** |
| CATMA1A23910 | AT1G25260 | Ribosomal protein L10 family protein | ns | ns | ns | ns | **-0.74** |
| CATMA1C71401 | AT1G26380 | FAD-binding Berberine family protein | ns | ns | ns | ns | **1.38** |
| CATMA1A24650 | AT1G26410 | FAD-binding Berberine family protein | ns | ns | ns | ns | **0.66** |
| CATMA1A24860 | AT1G26630 | ATELF5A-2_ELF5A-2_FBR12__Eukaryotic translation initiation factor 5A-1 (eIF-5A 1) protein | ns | ns | ns | ns | **1.36** |
| CATMA1A24990 | AT1G26761 | Arabinanase/levansucrase/invertase | ns | ns | **-1.09** | ns | ns |
| CATMA1A25030 | AT1G26810 | GALT1__galactosyltransferase1 | ns | **-1.16** | **-1.71** | **-1.65** | **-1.79** |
| CATMA1A25300 | AT1G27080 | NRT1.6__nitrate transporter 1.6 | ns | ns | ns | ns | **0.88** |
| CATMA1A25350 | AT1G27120 | Galactosyltransferase family protein | ns | **0.91** | **2.00** | **2.30** | **2.45** |
| CATMA1A25370 | AT1G27140 | ATGSTU14_GST13_GSTU14__glutathione S-transferase tau 14 | ns | ns | ns | ns | **0.79** |
| CATMA1A25440 | AT1G27190 | Leucine-rich repeat protein kinase family protein | ns | ns | ns | **1.96** | ns |
| CATMA1A26000 | AT1G27760 | ATSAT32_SAT32__interferon-related developmental regulator family protein / IFRD protein family | ns | ns | ns | **0.69** | **0.76** |
| CATMA1A27020 | AT1G29050 | TBL38__TRICHOME BIREFRINGENCE-LIKE 38 | ns | ns | ns | **-0.77** | ns |

| CATMA identifier | AGI identifier | Gene annotation | 30 min | 2h | 4h | 8h | 24h |
|---|---|---|---|---|---|---|---|
| CATMA1A27110 | AT1G29140 | Pollen Ole e 1 allergen and extensin family protein | ns | ns | ns | ns | **0.75** |
| CATMA1A27180 | AT1G29200 | O-fucosyltransferase family protein | ns | ns | ns | ns | **-0.85** |
| CATMA1A27260 | AT1G29280 | ATWRKY65_WRKY65__WRKY DNA-binding protein 65 | ns | ns | ns | **-0.95** | ns |
| CATMA1C71449 | AT1G29310 | SecY protein transport family protein | ns | ns | ns | ns | **0.68** |
| CATMA1A27510 | AT1G29560 | Zinc finger C-x8-C-x5-C-x3-H type family protein | ns | ns | ns | **-1.00** | **-0.93** |
| CATMA1A27550 | AT1G29600 | Zinc finger C-x8-C-x5-C-x3-H type family protein | ns | ns | ns | **-1.22** | **-1.02** |
| CATMA1A27560 | AT1G29630 | 5'-3' exonuclease family protein | ns | ns | ns | **-0.80** | **-0.72** |
| CATMA1D00214 | AT1G29910 | AB180_CAB3_LHCB1.2__chlorophyll A/B binding protein 3 | ns | ns | ns | ns | **-1.15** |
| CATMA1D00215 | AT1G29920 | AB165_CAB2_LHCB1.1__chlorophyll A/B-binding protein 2 | ns | ns | ns | ns | **-0.89** |
| CATMA1A28300 | AT1G30270 | ATCIPK23_CIPK23_LKS1_PKS17_SnRK3.23__CBL-interacting protein kinase 23 | ns | ns | ns | **0.69** | ns |
| CATMA1A28370 | AT1G30360 | ERD4__Early-responsive to dehydration stress protein (ERD4) | ns | ns | **-1.15** | ns | **-0.89** |
| CATMA1A28550 | AT1G30530 | UGT78D1__UDP-glucosyl transferase 78D1 | ns | ns | ns | **-0.85** | **-0.67** |
| CATMA1A28670 | AT1G30620 | HSR8_MUR4_UXE1__NAD(P)-binding Rossmann-fold superfamily protein | ns | ns | ns | ns | **1.01** |
| CATMA1A28750 | AT1G30700 | FAD-binding Berberine family protein | ns | **1.26** | **1.06** | **1.56** | **2.28** |
| CATMA1A29810 | AT1G31580 | CXC750__ECS1 | ns | ns | ns | **-1.12** | ns |
| CATMA1A30210 | AT1G31940 | unknown protein | ns | ns | ns | **0.81** | ns |
| CATMA1A30550 | AT1G32200 | ACT1_ATS1__phospholipid/glycerol acyltransferase family protein | ns | **-0.84** | ns | ns | **-0.74** |
| CATMA1A31040 | AT1G32700 | PLATZ transcription factor family protein | ns | ns | ns | **-0.69** | ns |
| CATMA1A31170 | AT1G32870 | ANAC013_ANAC13_NAC13__NAC domain protein 13 | ns | ns | ns | ns | **0.70** |
| CATMA1C71521 | AT1G32940 | ATSBT3.5_SBT3.5__Subtilase family protein | ns | ns | ns | ns | **1.06** |
| CATMA1C71522 | AT1G32960 | ATSBT3.3_SBT3.3__Subtilase family protein | ns | ns | ns | ns | **1.27** |
| CATMA1A31460 | AT1G33110 | MATE efflux family protein | ns | ns | ns | **0.85** | ns |
| CATMA1A31830 | AT1G33560 | ADR1__Disease resistance protein (CC-NBS-LRR class) family | ns | ns | ns | ns | **0.70** |
| CATMA1C71536 | AT1G33590 | Leucine-rich repeat (LRR) family protein | ns | ns | ns | **0.73** | **1.43** |
| CATMA1A31880 | AT1G33610 | Leucine-rich repeat (LRR) family protein | ns | ns | ns | **1.70** | **1.78** |
| CATMA1A32330 | AT1G34047 | Defensin-like (DEFL) family protein | ns | ns | ns | **0.82** | **0.82** |
| CATMA1A32770 | AT1G34440 | unknown protein | ns | ns | ns | ns | **-0.75** |
| CATMA1A32980 | AT1G34630 | FUNCTIONS IN: molecular_function unknown; INVOLVED IN: biological_process unknown; LOCATED IN: cellular_component unknown; EXPRESSED IN: 25 plant structures; EXPRESSED DURING: 15 growth stages; BEST Arabidopsis thaliana protein match is: Mitochondrial import inner membrane translocase subunit Tim17/Tim22/Tim23 family protein (TAIR:AT5G51150.1); (source: NCBI BLink). | ns | **1.06** | ns | ns | ns |
| CATMA1A33100 | AT1G34790 | TT1_WIP1__C2H2 and C2HC zinc fingers superfamily protein | ns | ns | ns | **-0.73** | ns |
| CATMA1C71568 | AT1G35350 | EXS (ERD1/XPR1/SYG1) family protein | ns | ns | ns | ns | **0.95** |
| CATMA1A33690 | AT1G35515 | HOS10_MYB8__high response to osmotic stress 10 | ns | ns | ns | **-0.73** | ns |
| CATMA1A34330 | AT1G36230 | unknown protein | ns | ns | ns | **-0.84** | ns |
| CATMA_GFT_02596 | AT1G36580 | BEST Arabidopsis thaliana protein match is: short-chain dehydrogenase-reductase B (TAIR:AT3G12800.1); Has 109 Blast hits to 109 proteins in 14 species: Archae - 0; Bacteria - 0; Metazoa - 0; Fungi - 0; Plants - 107; Viruses - 0; Other Eukaryotes - 2 (source: NCBI BLink). | ns | ns | ns | **0.87** | **0.84** |
| CATMA1C72346 | AT1G36622 | unknown protein | ns | ns | ns | ns | **1.12** |
| CATMA1B35155 | AT1G37130 | ATNR2_B29_CHL3_NIA2_NIA2-1_NR_NR2__nitrate reductase 2 | ns | ns | ns | **1.17** | ns |
| CATMA1A36330 | AT1G42990 | ATBZIP60_BZIP60_BZIP60__basic region/leucine zipper motif 60 | ns | ns | ns | ns | **1.34** |
| CATMA1A36590 | AT1G43160 | RAP2.6__related to AP2 6 | ns | ns | **-1.57** | **-1.16** | **-0.99** |
| CATMA1A36595 | AT1G43170 | ARP1_emb2207_RP1_RPL3A__ribosomal protein 1 | ns | ns | ns | ns | **-0.75** |
| CATMA1C71613 | AT1G44350 | ILL6__IAA-leucine resistant (ILR)-like gene 6 | ns | ns | ns | **0.79** | ns |
| CATMA1C71618 | AT1G44575 | CP22_NPQ4_PSBS__Chlorophyll A-B binding family protein | ns | ns | ns | ns | **-0.75** |
| CATMA1C71632 | AT1G45201 | ATTLL1_TLL1__triacylglycerol lipase-like 1 | ns | ns | ns | **-0.76** | ns |
| CATMA1A38770 | AT1G47720 | OSB1__Primosome PriB/single-strand DNA-binding | ns | ns | ns | **0.71** | **0.82** |
| CATMA1A38970 | AT1G47890 | AtRLP7_RLP7__receptor like protein 7 | ns | ns | ns | **-0.70** | **-0.92** |
| CATMA1A39400 | AT1G48320 | Thioesterase superfamily protein | ns | **-0.80** | ns | **-0.93** | ns |
| CATMA1A40900 | AT1G49820 | ATMTK_MTK_MTK1__S-methyl-5-thioribose kinase | ns | ns | ns | ns | **0.88** |
| CATMA1A41950 | AT1G50910 | unknown protein | ns | ns | ns | ns | **-0.76** |
| CATMA1A42700 | AT1G51570 | Calcium-dependent lipid-binding (CaLB domain) plant phosphoribosyltransferase family protein | ns | ns | ns | ns | **-0.71** |
| CATMA1A42750 | AT1G51620 | Protein kinase superfamily protein | ns | ns | ns | ns | **0.71** |
| CATMA1A42790 | AT1G51700 | ADOF1_DOF1__DOF zinc finger protein 1 | ns | ns | ns | ns | **0.74** |
| CATMA1A42890 | AT1G51800 | IOS1__Leucine-rich repeat protein kinase family protein | ns | ns | ns | ns | **0.72** |
| CATMA1D00376 | AT1G51820 | Leucine-rich repeat protein kinase family protein | ns | ns | ns | ns | **1.21** |
| CATMA1A43060 | AT1G51940 | protein kinase family protein / peptidoglycan-binding LysM domain-containing protein | ns | ns | ns | **-0.87** | **-1.13** |
| CATMA1A43630 | AT1G52580 | ATRBL5_RBL5__RHOMBOID-like protein 5 | ns | ns | ns | **-1.10** | **-0.66** |
| CATMA1A43790 | AT1G52730 | Transducin/WD40 repeat-like superfamily protein | ns | ns | ns | **1.03** | **1.24** |
| CATMA1A44030 | AT1G53010 | RING/U-box superfamily protein | ns | ns | ns | ns | **-0.78** |
| CATMA1A44350 | AT1G53320 | AtTLP7_TLP7__tubby like protein 7 | ns | ns | ns | **1.19** | ns |
| CATMA1A44596 | AT1G53580 | ETHE1_GLX2-3_GLY3__glyoxalase II 3 | ns | ns | ns | **1.07** | ns |
| CATMA1C71795 | AT1G53625 | unknown protein | ns | ns | ns | ns | **0.72** |

| CATMA identifier | AGI identifier | Gene annotation | 30 min | 2h | 4h | 8h | 24h |
|---|---|---|---|---|---|---|---|
| CATMA1A45100 | AT1G54000 | GLL22__GDSL-like Lipase/Acylhydrolase superfamily protein | ns | ns | ns | ns | **-1.06** |
| CATMA1A45145 | AT1G54040 | ESP_ESR_TASTY__epithiospecifier protein | ns | ns | ns | **0.70** | ns |
| CATMA1A45820 | AT1G54740 | Protein of unknown function (DUF3049) | ns | ns | **-1.12** | ns | ns |
| CATMA1A46090 | AT1G55050 | unknown protein. | ns | ns | **-1.01** | ns | **-0.81** |
| CATMA1A46140 | AT1G55110 | AtIDD7_IDD7__indeterminate(ID)-domain 7 | ns | ns | ns | **-0.71** | ns |
| CATMA1A46180 | AT1G55152 | unknown protein | ns | ns | ns | ns | **-0.71** |
| CATMA1A46400 | AT1G55320 | AAE18__acyl-activating enzyme 18 | ns | ns | ns | **-0.69** | ns |
| CATMA1C71832 | AT1G55330 | AGP21_ATAGP21__arabinogalactan protein 21 | ns | ns | ns | **0.75** | ns |
| CATMA1B46590 | AT1G55490 | CPN60B_Cpn60beta1_LEN1__chaperonin 60 beta | ns | ns | ns | **-0.79** | ns |
| CATMA1A46603 | AT1G55510 | BCDH BETA1__branched-chain alpha-keto acid decarboxylase E1 beta subunit | ns | ns | ns | **0.83** | ns |
| CATMA_GFT_02657 | AT1G55720 | ATCAX6_CAX6__cation exchanger 6 | ns | ns | ns | ns | **0.80** |
| CATMA1A47044 | AT1G55850 | ATCSLE1_CSLE1__cellulose synthase like E1 | ns | ns | ns | **1.17** | ns |
| CATMA1C71857 | AT1G56060 | unknown protein | ns | ns | ns | ns | **0.97** |
| CATMA1A47290 | AT1G56190 | Phosphoglycerate kinase family protein | ns | ns | ns | ns | **-0.69** |
| CATMA1A47320 | AT1G56220 | Dormancy/auxin associated family protein | ns | ns | **-1.32** | **-0.70** | ns |
| CATMA1A47890 | AT1G57590 | Pectinacetylesterase family protein | ns | ns | ns | **0.73** | ns |
| CATMA1A48498 | AT1G58370 | ATXYN1_RXF12__glycosyl hydrolase family 10 protein / carbohydrate-binding domain-containing protein | ns | ns | **1.13** | ns | **-0.86** |
| CATMA1A48650 | AT1G59590 | ZCF37 | ns | ns | ns | ns | **0.77** |
| CATMA1A48850 | AT1G59800 | Cullin family protein | ns | ns | ns | ns | **-0.83** |
| CATMA1A48920 | AT1G59860 | HSP20-like chaperones superfamily protein | ns | ns | ns | ns | **0.91** |
| CATMA1C71892 | AT1G60680 | NAD(P)-linked oxidoreductase superfamily protein | ns | ns | ns | ns | **0.91** |
| CATMA1C71893 | AT1G60690 | NAD(P)-linked oxidoreductase superfamily protein | ns | ns | ns | ns | **1.03** |
| CATMA1A49705 | AT1G60710 | ATB2__NAD(P)-linked oxidoreductase superfamily protein | ns | ns | ns | ns | **0.72** |
| CATMA1A49740 | AT1G60750 | NAD(P)-linked oxidoreductase superfamily protein | ns | ns | ns | **1.15** | **1.21** |
| CATMA1C71897 | AT1G60950 | ATFD2_FED A__2Fe-2S ferredoxin-like superfamily protein | ns | ns | ns | ns | **-0.72** |
| CATMA1A50390 | AT1G61340 | F-box family protein | ns | ns | ns | ns | **0.78** |
| CATMA1A50430 | AT1G61380 | SD1-29__S-domain-1 29 | ns | ns | ns | ns | **0.90** |
| CATMA1A50605 | AT1G61520 | LHCA3__photosystem I light harvesting complex gene 3 | ns | ns | ns | ns | **-0.75** |
| CATMA1A50730 | AT1G61630 | ATENT7_ENT7__equilibrative nucleoside transporter 7 | ns | ns | ns | ns | **0.80** |
| CATMA1A50870 | AT1G61790 | Oligosaccharyltransferase complex/magnesium transporter family protein | ns | ns | ns | **0.74** | ns |
| CATMA1A50880 | AT1G61800 | ATGPT2_GPT2__glucose-6-phosphate/phosphate translocator 2 | ns | ns | ns | ns | **0.83** |
| CATMA1C71919 | AT1G61820 | BGLU46__beta glucosidase 46 | ns | ns | ns | **-0.93** | ns |
| CATMA1A51440 | AT1G62320 | ERD (early-responsive to dehydration stress) family protein | ns | **0.98** | ns | **0.94** | **0.85** |
| CATMA1A51690 | AT1G62570 | FMO GS-OX4__flavin-monooxygenase glucosinolate S-oxygenase 4 | ns | ns | ns | ns | **0.78** |
| CATMA1A52120 | AT1G62960 | ACS10__ACC synthase 10 | ns | ns | ns | ns | **-0.98** |
| CATMA1A53050 | AT1G63830 | PLAC8 family protein | ns | ns | ns | ns | **0.87** |
| CATMA1A53235 | AT1G63980 | D111/G-patch domain-containing protein | ns | ns | ns | ns | **-0.69** |
| CATMA1A53640 | AT1G64355 | unknown protein | ns | ns | ns | ns | **0.97** |
| CATMA1A53660 | AT1G64370 | unknown protein | ns | ns | **-1.01** | **-0.77** | ns |
| CATMA1A53750 | AT1G64450 | Glycine-rich protein family | ns | ns | **-1.05** | **-0.84** | ns |
| CATMA1A54050 | AT1G64740 | TUA1__alpha-1 tubulin | ns | ns | ns | **-0.83** | ns |
| CATMA1A54205 | AT1G64900 | CYP89_CYP89A2__cytochrome P450, family 89, subfamily A, polypeptide 2 | ns | ns | **1.08** | **1.16** | **1.19** |
| CATMA1C71981 | AT1G64930 | CYP89A7__cytochrome P450, family 87, subfamily A, polypeptide 7 | ns | ns | ns | **0.85** | **0.94** |
| CATMA1A54390 | AT1G65110 | Ubiquitin carboxyl-terminal hydrolase-related protein | ns | ns | ns | **0.79** | **1.18** |
| CATMA1A54570 | AT1G65280 | DNAJ heat shock N-terminal domain-containing protein | ns | ns | ns | **0.89** | **1.56** |
| CATMA1A54580 | AT1G65290 | mtACP2__mitochondrial acyl carrier protein 2 | ns | ns | ns | ns | **2.63** |
| CATMA1A54830 | AT1G65490 | unknown protein | ns | ns | ns | ns | **-0.67** |
| CATMA1A54970 | AT1G65690 | Late embryogenesis abundant (LEA) hydroxyproline-rich glycoprotein family | ns | **1.01** | ns | **1.13** | **1.54** |
| CATMA1C72001 | AT1G65845 | unknown protein | ns | ns | ns | ns | **0.81** |
| CATMA1A55220 | AT1G65930 | cICDH__cytosolic NADP+-dependent isocitrate dehydrogenase | ns | ns | **-1.13** | **-0.96** | ns |
| CATMA1A55350 | AT1G66090 | Disease resistance protein (TIR-NBS class) | ns | ns | ns | ns | **1.67** |
| CATMA1A55360 | AT1G66100 | Plant thionin | ns | ns | ns | **0.82** | **-1.11** |
| CATMA1A55410 | AT1G66160 | ATCMPG1_CMPG1__CYS, MET, PRO, and GLY protein 1 | ns | ns | ns | ns | **0.75** |
| CATMA1A55440 | AT1G66180 | Eukaryotic aspartyl protease family protein | ns | ns | **-1.07** | ns | **-0.68** |
| CATMA1A55460 | AT1G66200 | ATGSR2_GLN1;2_GSR2__glutamine synthase clone F11 | ns | ns | ns | **-1.18** | ns |
| CATMA_GFT_02693 | AT1G66570 | ATSUC7_SUC7__sucrose-proton symporter 7 | ns | ns | ns | **0.73** | ns |
| CATMA1A55860 | AT1G66580 | RPL10C_SAG24__senescence associated gene 24 | ns | ns | ns | **1.26** | **1.44** |
| CATMA1A55946 | AT1G66670 | CLPP3_NCLPP3__CLP protease proteolytic subunit 3 | ns | ns | ns | ns | **0.69** |
| CATMA1A56210 | AT1G66920 | Protein kinase superfamily protein | ns | ns | ns | ns | **0.77** |
| CATMA1A56880 | AT1G67530 | ARM repeat superfamily protein | ns | ns | ns | **0.69** | **1.01** |
| CATMA1A56950 | AT1G67600 | Acid phosphatase/vanadium-dependent haloperoxidase-related protein | ns | ns | ns | **1.25** | **1.07** |
| CATMA1C72047 | AT1G67970 | AT-HSFA8_HSFA8__heat shock transcription factor A8 | ns | ns | ns | ns | **0.71** |
| CATMA1A57396_N | AT1G67980 | CCOAMT__caffeoyl-CoA 3-O-methyltransferase | ns | ns | ns | ns | **1.14** |
| CATMA1A57406_N | AT1G68010 | ATHPR1_HPR__hydroxypyruvate reductase | ns | ns | ns | **-0.82** | **-0.71** |
| CATMA1A57530 | AT1G68160 | Protein of unknown function (DUF3755) | ns | ns | ns | **0.70** | ns |
| CATMA1A57790 | AT1G68410 | Protein phosphatase 2C family protein | ns | ns | ns | **0.96** | ns |

| CATMA identifier | AGI identifier | Gene annotation | 30 min | 2h | 4h | 8h | 24h |
|---|---|---|---|---|---|---|---|
| CATMA1A57900 | AT1G68520 | B-box type zinc finger protein with CCT domain | ns | ns | ns | **-0.76** | ns |
| CATMA1A57940 | AT1G68570 | Major facilitator superfamily protein | ns | ns | ns | ns | **1.14** |
| CATMA1A58250 | AT1G68850 | Peroxidase superfamily protein | ns | **0.86** | **1.01** | ns | ns |
| CATMA1A58470 | AT1G69100 | Eukaryotic aspartyl protease family protein | ns | ns | **-1.06** | **-1.21** | **-1.03** |
| CATMA1A58493 | AT1G69170 | Squamosa promoter-binding protein-like (SBP domain) transcription factor family protein | ns | ns | ns | ns | **-0.74** |
| CATMA1A58810 | AT1G69500 | CYP704B1__cytochrome P450, family 704, subfamily B, polypeptide 1 | ns | ns | ns | **-0.71** | **0.71** |
| CATMA1C72074 | AT1G69520 | S-adenosyl-L-methionine-dependent methyltransferases superfamily protein | ns | ns | ns | **-0.69** | ns |
| CATMA1A59020 | AT1G69710 | Regulator of chromosome condensation (RCC1) family with FYVE zinc finger domain | ns | ns | ns | ns | **-0.76** |
| CATMA_GFT_02702 | AT1G69750 | ATCOX19-2_COX19-2__cytochrome c oxidase 19-2 | ns | ns | **1.15** | **1.19** | **0.68** |
| CATMA1A59420 | AT1G70140 | ATFH8_FH8__formin 8 | ns | ns | ns | ns | **0.70** |
| CATMA1A59450 | AT1G70170 | MMP__matrix metalloproteinase | ns | **0.85** | ns | **0.79** | **1.05** |
| CATMA1A59560 | AT1G70280 | NHL domain-containing protein | ns | ns | ns | **-0.90** | ns |
| CATMA1A59760 | AT1G70490 | ARFA1D_ATARFA1D__Ras-related small GTP-binding family protein | ns | ns | ns | ns | **1.04** |
| CATMA1A59940 | AT1G70660 | MMZ2_UEV1B__MMS ZWEI homologue 2 | ns | ns | ns | ns | **-0.87** |
| CATMA1A60040 | AT1G70770 | Protein of unknown function DUF2359, transmembrane | ns | ns | ns | ns | **-0.71** |
| CATMA1A60070 | AT1G70790 | Calcium-dependent lipid-binding (CaLB domain) family protein | ns | ns | ns | **0.72** | ns |
| CATMA1C72092 | AT1G70810 | Calcium-dependent lipid-binding (CaLB domain) family protein | ns | ns | ns | **0.88** | **1.01** |
| CATMA1A60130 | AT1G70850 | MLP34__MLP-like protein 34 | ns | ns | ns | ns | **-0.77** |
| CATMA1A60820 | AT1G71500 | Rieske (2Fe-2S) domain-containing protein | ns | ns | ns | ns | **-0.76** |
| CATMA1A60830 | AT1G71520 | Integrase-type DNA-binding superfamily protein | ns | ns | ns | **1.47** | ns |
| CATMA1A60840 | AT1G71530 | Protein kinase superfamily protein | ns | ns | ns | **0.70** | ns |
| CATMA1A61280 | AT1G72060 | serine-type endopeptidase inhibitors | ns | ns | ns | ns | **-0.67** |
| CATMA1A61300 | AT1G72090 | Methylthiotransferase | ns | ns | ns | **-0.74** | ns |
| CATMA1A61380 | AT1G72150 | PATL1__PATELLIN 1 | ns | ns | **-1.36** | ns | ns |
| CATMA1A61710 | AT1G72490 | unknown protein | ns | ns | ns | **1.25** | **1.10** |
| CATMA1A61835 | AT1G72610 | ATGER1_GER1_GLP1__germin-like protein 1 | ns | ns | ns | **-0.82** | **-1.15** |
| CATMA1A61900 | AT1G72680 | ATCAD1_CAD1__cinnamyl-alcohol dehydrogenase | ns | ns | ns | **0.81** | **1.37** |
| CATMA1C72125 | AT1G72930 | TIR__toll/interleukin-1 receptor-like | ns | ns | ns | **-1.33** | ns |
| CATMA1A62510 | AT1G73220 | AtOCT1_OCT1__organic cation/carnitine transporter1 | ns | ns | ns | ns | **-0.74** |
| CATMA1A62540 | AT1G73260 | ATKTI1_KTI1__kunitz trypsin inhibitor 1 | ns | ns | **-1.74** | ns | ns |
| CATMA1A62800 | AT1G73490 | RNA-binding (RRM/RBD/RNP motifs) family protein | ns | ns | ns | **0.77** | ns |
| CATMA1A63360 | AT1G74010 | Calcium-dependent phosphotriesterase superfamily protein | ns | **1.39** | **1.68** | **1.32** | **2.50** |
| CATMA1A63370 | AT1G74020 | SS2__strictosidine synthase 2 | ns | **1.02** | ns | **1.43** | **1.40** |
| CATMA1A63440 | AT1G74070 | Cyclophilin-like peptidyl-prolyl cis-trans isomerase family protein | ns | ns | ns | ns | **-0.74** |
| CATMA1A63850 | AT1G74450 | Protein of unknown function (DUF793) | ns | **1.09** | **1.16** | **1.06** | **1.10** |
| CATMA1A64075 | AT1G74710 | ATICS1_EDS16_ICS1_SID2__ADC synthase superfamily protein | ns | ns | ns | ns | **1.41** |
| CATMA1C72158 | AT1G75030 | ATLP-3_TLP-3__thaumatin-like protein 3 | ns | ns | **1.13** | **1.45** | **1.35** |
| CATMA1A64376 | AT1G75040 | PR-5_PR5__pathogenesis-related gene 5 | ns | **1.32** | **1.50** | **1.71** | **1.75** |
| CATMA1A64610 | AT1G75270 | DHAR2__dehydroascorbate reductase 2 | ns | ns | **1.09** | **1.60** | **1.49** |
| CATMA1A64615 | AT1G75280 | NmrA-like negative transcriptional regulator family protein | ns | ns | ns | **1.56** | **1.37** |
| CATMA1D02716 | AT1G75290 | NAD(P)-binding Rossmann-fold superfamily protein | ns | ns | ns | **0.92** | **0.86** |
| CATMA1C72164 | AT1G75490 | Integrase-type DNA-binding superfamily protein | ns | ns | ns | ns | **-0.78** |
| CATMA1A64990 | AT1G75690 | LQY1__DnaJ/Hsp40 cysteine-rich domain superfamily protein | ns | ns | ns | ns | **-0.97** |
| CATMA1C72165 | AT1G75750 | GASA1__GAST1 protein homolog 1 | ns | ns | **-1.23** | ns | ns |
| CATMA1A65090 | AT1G75800 | Pathogenesis-related thaumatin superfamily protein | ns | ns | ns | ns | **-0.66** |
| CATMA1A65170 | AT1G75900 | GDSL-like Lipase/Acylhydrolase superfamily protein | ns | **1.31** | **1.60** | **1.36** | **1.02** |
| CATMA1A65300 | AT1G76070 | unknown protein | ns | ns | ns | **0.90** | **0.68** |
| CATMA1A65370 | AT1G76150 | ATECH2_ECH2__enoyl-CoA hydratase 2 | ns | ns | ns | ns | **0.78** |
| CATMA1A65380 | AT1G76160 | sks5__SKU5 similar 5 | ns | ns | ns | **-1.08** | ns |
| CATMA1A65720 | AT1G76520 | Auxin efflux carrier family protein | ns | ns | ns | **0.87** | **0.66** |
| CATMA1A65730 | AT1G76530 | Auxin efflux carrier family protein | ns | ns | ns | **0.90** | **0.88** |
| CATMA1A65800 | AT1G76600 | unknown protein | ns | ns | ns | **1.06** | **0.70** |
| CATMA1C72183 | AT1G76680 | ATOPR1_OPR1__12-oxophytodienoate reductase 1 | ns | ns | ns | **1.22** | **2.04** |
| CATMA1A66220 | AT1G76980 | unknown protein | ns | **1.15** | **1.67** | **1.78** | **1.85** |
| CATMA1A66320 | AT1G77120 | ADH_ADH1_ATADH_ATADH1__alcohol dehydrogenase 1 | ns | ns | ns | **1.30** | **1.02** |
| CATMA1A66420 | AT1G77210 | AtSTP14_STP14__sugar transporter 14 | ns | ns | ns | **-0.72** | **-0.86** |
| CATMA1A66550 | AT1G77330 | 2-oxoglutarate (2OG) and Fe(II)-dependent oxygenase superfamily protein | ns | **-0.80** | ns | ns | ns |
| CATMA1A66600 | AT1G77380 | AAP3_ATAAP3__amino acid permease 3 | ns | ns | ns | **-0.91** | ns |
| CATMA1C72199 | AT1G77510 | ATPDI6_ATPDIL1-2_PDI6_PDIL1-2__PDI-like 1-2 | ns | ns | ns | ns | **0.96** |
| CATMA1A66910 | AT1G77760 | GNR1_NIA1_NR1__nitrate reductase 1 | ns | ns | **-1.38** | ns | ns |
| CATMA1A67090 | AT1G77940 | Ribosomal protein L7Ae/L30e/S12e/Gadd45 family protein | ns | ns | ns | ns | **-0.73** |
| CATMA1A67360 | AT1G78240 | OSU1_QUA2_TSD2__S-adenosyl-L-methionine-dependent methyltransferases superfamily protein | ns | ns | ns | **-0.82** | ns |
| CATMA1A67380 | AT1G78270 | AtUGT85A4_UGT85A4__UDP-glucosyl transferase 85A4 | ns | ns | ns | **-0.79** | ns |
| CATMA1C72216 | AT1G78340 | ATGSTU22_GSTU22__glutathione S-transferase TAU 22 | ns | ns | **1.62** | **1.75** | **1.69** |
| CATMA1A67475 | AT1G78380 | ATGSTU19_GST8_GSTU19__glutathione S-transferase TAU 19 | ns | ns | **1.23** | **1.45** | **1.49** |
| CATMA1A67640 | AT1G78570 | ATRHM1_RHM1_ROL1__rhamnose biosynthesis 1 | ns | ns | ns | ns | **0.76** |
| CATMA1A67730 | AT1G78660 | ATGGH1_GGH1__gamma-glutamyl hydrolase 1 | ns | **1.98** | ns | **1.96** | **1.27** |
| CATMA1A67740 | AT1G78670 | ATGGH3_GGH3__gamma-glutamyl hydrolase 3 | ns | ns | ns | **0.97** | **0.80** |

| CATMA identifier | AGI identifier | Gene annotation | 30 min | 2h | 4h | 8h | 24h |
|---|---|---|---|---|---|---|---|
| CATMA1A67745 | AT1G78680 | ATGGH2_GGH2__gamma-glutamyl hydrolase 2 | ns | **1.24** | ns | **1.53** | **1.00** |
| CATMA1A68110 | AT1G78995 | unknown protein | ns | ns | ns | **-0.88** | **-0.73** |
| CATMA1A68510 | AT1G79410 | AtOCT5_OCT5__organic cation/carnitine transporter5 | ns | ns | ns | **1.49** | **1.35** |
| CATMA1A69225 | AT1G80050 | APT2_ATAPT2_PHT1.1__adenine phosphoribosyl transferase 2 | ns | ns | ns | ns | **-0.70** |
| CATMA1A69240 | AT1G80070 | EMB14_EMB177_EMB33_SUS2__Pre-mRNA-processing-splicing factor | ns | ns | ns | **-0.69** | ns |
| CATMA1A69430 | AT1G80240 | Protein of unknown function, DUF642 | ns | ns | ns | ns | **0.95** |
| CATMA1A69530 | AT1G80330 | ATGA3OX4_GA3OX4__gibberellin 3-oxidase 4 | ns | ns | ns | ns | **0.83** |
| CATMA1A70055 | AT1G80830 | ATNRAMP1_NRAMP1_PMIT1__natural resistance-associated macrophage protein 1 | ns | ns | ns | **-0.99** | **-0.75** |
| CATMA2A00260 | AT2G01180 | ATLPP1_ATPAP1_LPP1_PAP1__phosphatidic acid phosphatase 1 | ns | ns | ns | **1.44** | **1.97** |
| CATMA2A00720 | AT2G01670 | atnudt17_NUDT17__nudix hydrolase homolog 17 | ns | ns | ns | ns | **1.19** |
| CATMA2A00905 | AT2G01850 | ATXTH27_EXGT-A3_XTH27__endoxyloglucan transferase A3 | ns | ns | **-1.26** | ns | ns |
| CATMA2B00960 | AT2G01910 | ATMAP65-6_MAP65-6__Microtubule associated protein (MAP65/ASE1) family protein | ns | ns | ns | **-0.71** | ns |
| CATMA2A01060 | AT2G02000 | GAD3__glutamate decarboxylase 3 | ns | ns | ns | ns | **0.71** |
| CATMA2A01260 | AT2G02180 | TOM3__tobamovirus multiplication protein 3 | ns | ns | ns | **0.78** | ns |
| CATMA2A01645 | AT2G02760 | ATUBC2_UBC2_UBC2__ubiquiting-conjugating enzyme 2 | ns | ns | ns | **0.73** | ns |
| CATMA2A01705 | AT2G02800 | APK2B_Kin2__protein kinase 2B | ns | ns | ns | **0.71** | **0.71** |
| CATMA2A01885 | AT2G02990 | ATRNS1_RNS1__ribonuclease 1 | ns | ns | **1.14** | ns | **1.23** |
| CATMA2A02140 | AT2G03240 | EXS (ERD1/XPR1/SYG1) family protein | ns | ns | ns | **-0.71** | ns |
| CATMA2A02770 | AT2G03890 | ATPI4K GAMMA 7_PI4K GAMMA 7_UBDK GAMMA 7__phosphoinositide 4-kinase gamma 7 | ns | ns | ns | **-0.75** | ns |
| CATMA2A04100 | AT2G05220 | Ribosomal S17 family protein | ns | ns | ns | ns | **-0.86** |
| CATMA2A04160 | AT2G05310 | unknown protein | ns | ns | ns | ns | **-0.69** |
| CATMA2A04205 | AT2G05380 | GRP3S__glycine-rich protein 3 short isoform | ns | ns | ns | **1.00** | **1.85** |
| CATMA2A04295 | AT2G05520 | ATGRP-3_ATGRP3_GRP-3_GRP3__glycine-rich protein 3 | ns | ns | ns | **0.70** | **1.61** |
| CATMA2C47087 | AT2G05530 | Glycine-rich protein family | ns | ns | ns | **0.85** | **1.73** |
| CATMA2A04450 | AT2G05710 | ACO3__aconitase 3 | ns | ns | ns | **0.69** | **0.81** |
| CATMA2A04625 | AT2G05840 | PAA2__20S proteasome subunit PAA2 | ns | ns | ns | ns | **0.77** |
| CATMA2A04765 | AT2G05990 | ENR1_MOD1__NAD(P)-binding Rossmann-fold superfamily protein | ns | ns | ns | ns | **-0.72** |
| CATMA2A05190 | AT2G06520 | PSBX__photosystem II subunit X | ns | ns | ns | ns | **-0.67** |
| CATMA2A05540 | AT2G06850 | EXGT-A1_EXT_XTH4__xyloglucan endotransglucosylase/hydrolase 4 | ns | ns | ns | **-0.84** | ns |
| CATMA2A05825 | AT2G07050 | CAS1__cycloartenol synthase 1 | ns | ns | ns | **-0.96** | ns |
| CATMA2A06390 | AT2G07671 | ATP synthase subunit C family protein | ns | ns | ns | **0.86** | **0.82** |
| CATMA_GFT_02404 | AT2G07699 | unknown protein | ns | ns | ns | ns | **0.81** |
| CATMA2A06650 | AT2G07811 | unknown protein | ns | ns | ns | **1.01** | ns |
| CATMA_GFT_00745 | AT2G12190 | Cytochrome P450 superfamily protein | ns | ns | **1.04** | **0.97** | **0.96** |
| CATMA2A10730 | AT2G12557 | unknown protein | ns | ns | ns | **0.81** | ns |
| CATMA2A13650 | AT2G14920 | ATST4A_ST4A__sulfotransferase 4A | ns | ns | ns | ns | **-0.73** |
| CATMA2A13890 | AT2G15090 | KCS8__3-ketoacyl-CoA synthase 8 | ns | ns | ns | ns | **-0.66** |
| CATMA2C47189 | AT2G15220 | Plant basic secretory protein (BSP) family protein | ns | ns | ns | ns | **0.85** |
| CATMA2D02807 | AT2G15240 | UNC-50 family protein | ns | ns | ns | ns | **1.02** |
| CATMA2C47194 | AT2G15500 | RNA-binding protein | ns | ns | ns | **0.76** | **0.90** |
| CATMA2A14420 | AT2G15530 | RING/U-box superfamily protein | ns | **0.81** | ns | **1.71** | **2.15** |
| CATMA2A15240 | AT2G16430 | ATPAP10_PAP10__purple acid phosphatase 10 | ns | ns | ns | ns | **0.96** |
| CATMA2C47224 | AT2G16500 | ADC1_ARGDC_ARGDC1_SPE1__arginine decarboxylase 1 | ns | ns | ns | **1.85** | **1.23** |
| CATMA2D02819 | AT2G16586 | unknown protein | ns | ns | ns | **0.69** | ns |
| CATMA2A15360 | AT2G16640 | ATTOC132_TOC132__multimeric translocon complex in the outer envelope membrane 132 | ns | ns | ns | **-0.79** | ns |
| CATMA2A16180 | AT2G17500 | Auxin efflux carrier family protein | ns | **0.80** | **1.19** | **1.79** | **1.20** |
| CATMA2A16420 | AT2G17740 | Cysteine/Histidine-rich C1 domain family protein | ns | ns | ns | ns | **1.67** |
| CATMA2A16500 | AT2G17840 | ERD7__Senescence/dehydration-associated protein-related | ns | ns | ns | ns | **0.85** |
| CATMA2A16860 | AT2G18193 | P-loop containing nucleoside triphosphate hydrolases superfamily protein | ns | ns | ns | **0.90** | **0.87** |
| CATMA2A17100 | AT2G18450 | SDH1-2__succinate dehydrogenase 1-2 | ns | ns | ns | ns | **0.78** |
| CATMA2A17330 | AT2G18680 | unknown protein | ns | ns | ns | **0.75** | **1.97** |
| CATMA2A17340_N | AT2G18690 | unknown protein | ns | ns | ns | ns | **1.98** |
| CATMA2A17545 | AT2G18960 | AHA1_HA1_OST2_PMA__H(+)-ATPase 1 | ns | ns | ns | **-0.91** | ns |
| CATMA2A18290 | AT2G19750 | Ribosomal protein S30 family protein | ns | ns | ns | ns | **-0.76** |
| CATMA2C47318 | AT2G20050 | protein serine/threonine phosphatases;protein kinases;catalytics;cAMP-dependent protein kinase regulators;ATP binding;protein serine/threonine phosphatases | ns | ns | ns | **-0.79** | ns |
| CATMA_GFT_00812 | AT2G20142 | Toll-Interleukin-Resistance (TIR) domain family protein | ns | ns | ns | ns | **1.47** |
| CATMA2A19320 | AT2G20760 | Clathrin light chain protein | ns | ns | ns | ns | **0.70** |
| CATMA2A19595 | AT2G20960 | pEARLI4__Arabidopsis phospholipase-like protein (PEARLI 4) family | ns | ns | ns | **0.75** | ns |
| CATMA2A19870 | AT2G21210 | SAUR-like auxin-responsive protein family | ns | ns | ns | ns | **-0.78** |
| CATMA2A20020 | AT2G21330 | FBA1__fructose-bisphosphate aldolase 1 | ns | ns | ns | ns | **-0.89** |
| CATMA2A20280 | AT2G21620 | RD2__Adenine nucleotide alpha hydrolases-like superfamily protein | ns | ns | ns | **1.28** | **1.82** |
| CATMA2A20680 | AT2G22122 | unknown protein | ns | ns | ns | **-1.00** | **-0.96** |
| CATMA2A20690 | AT2G22125 | CSI1_POM2__binding | ns | ns | ns | **-0.76** | ns |

| CATMA identifier | AGI identifier | Gene annotation | 30 min | 2h | 4h | 8h | 24h |
|---|---|---|---|---|---|---|---|
| CATMA2A21020 | AT2G22500 | ATPUMP5_DIC1_UCP5__uncoupling protein 5 | ns | ns | ns | ns | **0.87** |
| CATMA2A21470 | AT2G22980 | SCPL13__serine carboxypeptidase-like 13 | ns | ns | ns | ns | **-0.66** |
| CATMA2A21610 | AT2G23110 | Late embryogenesis abundant protein, group 6 | ns | ns | ns | **1.87** | **2.04** |
| CATMA2A21620 | AT2G23120 | Late embryogenesis abundant protein, group 6 | ns | ns | ns | ns | **1.23** |
| CATMA2A21655 | AT2G23150 | ATNRAMP3_NRAMP3__natural resistance-associated macrophage protein 3 | ns | ns | ns | ns | **1.69** |
| CATMA2C47379 | AT2G23170 | GH3.3__Auxin-responsive GH3 family protein | ns | ns | ns | ns | **0.73** |
| CATMA2A22070 | AT2G23680 | Cold acclimation protein WCOR413 family | ns | ns | ns | **0.88** | **1.12** |
| CATMA2A22170 | AT2G23810 | TET8__tetraspanin8 | ns | ns | ns | ns | **1.15** |
| CATMA2A22600 | AT2G24270 | ALDH11A3__aldehyde dehydrogenase 11A3 | ns | ns | ns | ns | **-0.70** |
| CATMA2A22825 | AT2G24500 | FZF__Zinc finger protein 622 | ns | ns | ns | **1.13** | **0.76** |
| CATMA2A22930 | AT2G24600 | Ankyrin repeat family protein | ns | ns | ns | **-0.92** | ns |
| CATMA2A23310 | AT2G25000 | ATWRKY60_WRKY60__WRKY DNA-binding protein 60 | ns | ns | ns | **-0.93** | ns |
| CATMA2A23850 | AT2G25510 | unknown protein | ns | ns | ns | ns | **-1.52** |
| CATMA2A24710 | AT2G26380 | Leucine-rich repeat (LRR) family protein | ns | ns | ns | **1.69** | **1.59** |
| CATMA2A24760 | AT2G26440 | Plant invertase/pectin methylesterase inhibitor superfamily | ns | ns | ns | **-0.72** | **0.68** |
| CATMA2A24825 | AT2G26500 | cytochrome b6f complex subunit (petM), putative | ns | ns | ns | ns | **-0.68** |
| CATMA2A25790 | AT2G27385 | Pollen Ole e 1 allergen and extensin family protein | ns | ns | **-1.40** | ns | **-1.00** |
| CATMA2C47453 | AT2G27402 | unknown protein | ns | ns | ns | ns | **-1.04** |
| CATMA2B25830 | AT2G27420 | Cysteine proteinases superfamily protein | ns | ns | ns | ns | **-1.47** |
| CATMA2C47455 | AT2G27530 | PGY1__Ribosomal protein L1p/L10e family | ns | ns | ns | ns | **-0.74** |
| CATMA2A26000 | AT2G27580 | A20/AN1-like zinc finger family protein | ns | ns | ns | **0.75** | ns |
| CATMA2C47460 | AT2G27720 | 60S acidic ribosomal protein family | ns | ns | ns | ns | **-0.66** |
| CATMA2A27030 | AT2G28605 | Photosystem II reaction center PsbP family protein | ns | ns | ns | ns | **-0.80** |
| CATMA2A27320 | AT2G28930 | APK1B_PK1B__protein kinase 1B | ns | ns | ns | ns | **0.70** |
| CATMA2B27340 | AT2G28950 | ATEXP6_ATEXPA6_ATHEXP ALPHA 1.8_EXPA6__expansin A6 | ns | ns | ns | ns | **-1.02** |
| CATMA_GFT_02855 | AT2G29310 | NAD(P)-binding Rossmann-fold superfamily protein | ns | ns | **-1.07** | **-0.92** | ns |
| CATMA2A27740 | AT2G29340 | NAD-dependent epimerase/dehydratase family protein | ns | ns | **-1.17** | ns | ns |
| CATMA2A27750 | AT2G29350 | SAG13__senescence-associated gene 13 | ns | ns | ns | ns | **1.55** |
| CATMA2A27810 | AT2G29420 | ATGSTU7_GST25_GSTU7__glutathione S-transferase tau 7 | ns | ns | ns | **1.49** | **1.36** |
| CATMA2A27830 | AT2G29440 | ATGSTU6_GST24_GSTU6__glutathione S-transferase tau 6 | ns | **1.24** | **1.32** | **1.45** | ns |
| CATMA2D02856 | AT2G29460 | ATGSTU4_GST22_GSTU4__glutathione S-transferase tau 4 | ns | ns | ns | **1.37** | **0.95** |
| CATMA2C47487 | AT2G29470 | ATGSTU3_GST21_GSTU3__glutathione S-transferase tau 3 | ns | ns | ns | **1.14** | **0.76** |
| CATMA2C47488 | AT2G29480 | ATGSTU2_GST20_GSTU2__glutathione S-transferase tau 2 | ns | ns | ns | **0.91** | **0.73** |
| CATMA2C47489 | AT2G29490 | ATGSTU1_GST19_GSTU1__glutathione S-transferase TAU 1 | ns | ns | **1.34** | **1.00** | ns |
| CATMA2A27880 | AT2G29500 | HSP20-like chaperones superfamily protein | ns | ns | **1.15** | **1.11** | **1.53** |
| CATMA2A28010 | AT2G29630 | PY_THIC__thiaminC | ns | ns | ns | **-0.71** | ns |
| CATMA2A28280 | AT2G29940 | ABCG31_ATPDR3_PDR3__pleiotropic drug resistance 3 | ns | ns | ns | **0.96** | ns |
| CATMA2A28340 | AT2G30010 | TBL45__TRICHOME BIREFRINGENCE-LIKE 45 | ns | ns | ns | ns | **-0.66** |
| CATMA2A28440 | AT2G30140 | UDP-Glycosyltransferase superfamily protein | ns | ns | ns | ns | **0.67** |
| CATMA2A28685 | AT2G30390 | ATFC-II_FC-II_FC2__ferrochelatase 2 | ns | ns | ns | **-0.80** | ns |
| CATMA2A28715 | AT2G30440 | Plsp2B_TPP__thylakoid processing peptide | ns | ns | ns | ns | **0.73** |
| CATMA2A28746 | AT2G30490 | ATC4H_C4H_CYP73A5_REF3__cinnamate-4-hydroxylase | ns | ns | **-1.19** | **-1.50** | **-1.21** |
| CATMA2A28860 | AT2G30600 | BTB/POZ domain-containing protein | ns | ns | **-1.07** | ns | ns |
| CATMA2C47512 | AT2G30670 | NAD(P)-binding Rossmann-fold superfamily protein | ns | ns | ns | **-0.73** | ns |
| CATMA2C47515 | AT2G30860 | ATGSTF7_ATGSTF9_GLUTTR_GSTF9__glutathione S-transferase PHI 9 | ns | ns | ns | **-1.31** | ns |
| CATMA2A29670 | AT2G31430 | Plant invertase/pectin methylesterase inhibitor superfamily protein | ns | ns | ns | ns | **0.66** |
| CATMA2A29880 | AT2G31660 | EMA1_SAD2_URM9__ARM repeat superfamily protein | ns | ns | ns | ns | **0.68** |
| CATMA2A30110 | AT2G31865 | PARG2__poly(ADP-ribose) glycohydrolase 2 | ns | ns | ns | ns | **1.17** |
| CATMA2A30340 | AT2G32060 | Ribosomal protein L7Ae/L30e/S12e/Gadd45 family protein | ns | ns | ns | ns | **-0.89** |
| CATMA2C47548 | AT2G32190 | unknown protein | ns | ns | ns | ns | **1.33** |
| CATMA2D02863 | AT2G32200 | unknown protein | ns | ns | ns | ns | **0.93** |
| CATMA2A30800 | AT2G32510 | MAPKKK17__mitogen-activated protein kinase kinase kinase 17 | ns | **0.94** | ns | ns | ns |
| CATMA2A30970 | AT2G32720 | ATCB5-B_B5 #4_CB5-B__cytochrome B5 isoform B | ns | ns | ns | **-1.04** | **-1.08** |
| CATMA2A31025 | AT2G32800 | AP4.3A__protein kinase family protein | ns | **0.88** | ns | ns | **1.05** |
| CATMA2A31295 | AT2G33120 | ATVAMP722_SAR1_VAMP722__synaptobrevin-related protein 1 | ns | ns | ns | ns | **0.81** |
| CATMA2A31305 | AT2G33150 | KAT2_PED1_PKT3__peroxisomal 3-ketoacyl-CoA thiolase 3 | ns | ns | ns | **0.84** | **0.68** |
| CATMA2A31540 | AT2G33380 | AtCLO3_CLO-3_CLO3_RD20__Caleosin-related family protein | ns | ns | ns | ns | **0.77** |
| CATMA2A31850 | AT2G33690 | Late embryogenesis abundant protein, group 6 | ns | ns | ns | ns | **0.68** |
| CATMA2A32070 | AT2G33850 | unknown protein | ns | ns | ns | ns | **-0.66** |
| CATMA2A32200 | AT2G34070 | TBL37__TRICHOME BIREFRINGENCE-LIKE 37 | ns | ns | ns | **0.99** | ns |
| CATMA2A32300 | AT2G34180 | ATWL2_CIPK13_SnRK3.7_WL2__CBL-interacting protein kinase 13 | ns | ns | ns | ns | **0.75** |
| CATMA2A32490 | AT2G34355 | Major facilitator superfamily protein | ns | ns | ns | **1.07** | ns |
| CATMA2A32620 | AT2G34480 | Ribosomal protein L18ae/LX family protein | ns | ns | ns | ns | **-0.75** |
| CATMA2A32640 | AT2G34500 | CYP710A1__cytochrome P450, family 710, subfamily A, polypeptide 1 | ns | **1.17** | ns | **1.13** | **1.07** |
| CATMA2A32650 | AT2G34510 | Protein of unknown function, DUF642 | ns | ns | ns | **-0.78** | ns |

| CATMA identifier | AGI identifier | Gene annotation | 30 min | 2h | 4h | 8h | 24h |
|---|---|---|---|---|---|---|---|
| CATMA2A32895 | AT2G34770 | ATFAH1_FAH1__fatty acid hydroxylase 1 | ns | ns | ns | **0.69** | ns |
| CATMA2C47605 | AT2G35620 | FEI2__Leucine-rich repeat protein kinase family protein | ns | ns | ns | **-0.73** | ns |
| CATMA2A33980 | AT2G35800 | SAMTL__mitochondrial substrate carrier family protein | ns | ns | ns | **-0.74** | ns |
| CATMA2A34180 | AT2G35980 | ATNHL10_NHL10_YLS9__Late embryogenesis abundant (LEA) hydroxyproline-rich glycoprotein family | ns | **1.72** | **1.96** | **1.81** | **2.34** |
| CATMA2A34320 | AT2G36120 | DOT1__Glycine-rich protein family | ns | ns | ns | ns | **-0.67** |
| CATMA2A34710 | AT2G36460 | Aldolase superfamily protein | ns | ns | ns | **0.72** | **1.08** |
| CATMA2A34850 | AT2G36620 | RPL24A__ribosomal protein L24 | ns | ns | ns | ns | **-0.81** |
| CATMA2A34860 | AT2G36630 | Sulfite exporter TauE/SafE family protein | ns | ns | ns | ns | **-0.79** |
| CATMA2A34910 | AT2G36690 | 2-oxoglutarate (2OG) and Fe(II)-dependent oxygenase superfamily protein | ns | **-1.13** | ns | ns | ns |
| CATMA2A34980 | AT2G36750 | UGT73C1__UDP-glucosyl transferase 73C1 | ns | ns | ns | **0.99** | ns |
| CATMA_GFT_02874 | AT2G36770 | UDP-Glycosyltransferase superfamily protein | ns | ns | ns | **1.65** | ns |
| CATMA2A35230 | AT2G36950 | Heavy metal transport/detoxification superfamily protein | ns | ns | ns | **1.26** | **1.01** |
| CATMA2A35330 | AT2G37040 | ATPAL1_PAL1__PHE ammonia lyase 1 | ns | **-1.09** | ns | **-0.69** | **-1.21** |
| CATMA2A35400 | AT2G37110 | PLAC8 family protein | ns | ns | ns | ns | **0.94** |
| CATMA2A35430 | AT2G37130 | Peroxidase superfamily protein | ns | ns | **-1.05** | **-1.04** | **-0.67** |
| CATMA2C47630_N | AT2G37170 | PIP2;2_PIP2B__plasma membrane intrinsic protein 2 | ns | ns | ns | **-0.98** | ns |
| CATMA2A35456 | AT2G37180 | PIP2;3_PIP2C_RD28__Aquaporin-like superfamily protein | ns | ns | ns | **-0.87** | **-0.82** |
| CATMA2A35500 | AT2G37220 | RNA-binding (RRM/RBD/RNP motifs) family protein | ns | ns | ns | ns | **-0.85** |
| CATMA2A35880 | AT2G37600 | Ribosomal protein L36e family protein | ns | ns | ns | ns | **-0.82** |
| CATMA2A35920 | AT2G37640 | ATEXP3_ATEXPA3_ATHEXP ALPHA 1.9_EXP3__Barwin-like endoglucanases superfamily protein | ns | ns | ns | **-0.88** | **-0.71** |
| CATMA2A36040 | AT2G37760 | AKR4C8__NAD(P)-linked oxidoreductase superfamily protein | ns | ns | ns | ns | **0.82** |
| CATMA2A36240 | AT2G37940 | AtIPCS2_ERH1__Arabidopsis Inositol phosphorylceramide synthase 2 | ns | ns | ns | ns | **0.79** |
| CATMA2A36270 | AT2G37970 | SOUL-1__SOUL heme-binding family protein | ns | ns | ns | **0.83** | **0.74** |
| CATMA2A36560 | AT2G38250 | Homeodomain-like superfamily protein | ns | ns | ns | **0.71** | ns |
| CATMA2A36760 | AT2G38470 | ATWRKY33_WRKY33__WRKY DNA-binding protein 33 | ns | ns | ns | ns | **0.99** |
| CATMA2A37026 | AT2G38750 | ANNAT4__annexin 4 | ns | ns | **1.11** | ns | ns |
| CATMA2A37130 | AT2G38870 | Serine protease inhibitor, potato inhibitor I-type family protein | ns | ns | ns | ns | **1.18** |
| CATMA2A37430 | AT2G39200 | ATMLO12_MLO12__Seven transmembrane MLO family protein | ns | ns | ns | ns | **1.17** |
| CATMA2A37735 | AT2G39460 | ATRPL23A_RPL23A_RPL23A1_RPL23AA__ribosomal protein L23AA | ns | ns | ns | ns | **-0.86** |
| CATMA2A37780 | AT2G39510 | nodulin MtN21 /EamA-like transporter family protein | ns | **0.84** | ns | ns | ns |
| CATMA2A37790 | AT2G39520 | unknown protein | ns | ns | ns | ns | **0.74** |
| CATMA2A37967 | AT2G39730 | RCA__rubisco activase | ns | ns | ns | **-0.71** | **-0.88** |
| CATMA2A38220 | AT2G40000 | ATHSPRO2_HSPRO2__ortholog of sugar beet HS1 PRO-1 2 | ns | ns | **-1.03** | ns | ns |
| CATMA2A38330 | AT2G40095 | Alpha/beta hydrolase related protein | ns | ns | ns | **0.84** | ns |
| CATMA2A38380 | AT2G40140 | ATSZF2_CZF1_SZF2_ZFAR1__zinc finger (CCCH-type) family protein | ns | ns | ns | ns | **1.06** |
| CATMA2A38620 | AT2G40340 | AtERF48_DREB2C__Integrase-type DNA-binding superfamily protein | ns | ns | ns | **1.10** | **0.85** |
| CATMA2A39220 | AT2G40890 | CYP98A3__cytochrome P450, family 98, subfamily A, polypeptide 3 | ns | ns | ns | ns | **-0.74** |
| CATMA2A39435 | AT2G41090 | Calcium-binding EF-hand family protein | ns | ns | ns | **-0.69** | **0.70** |
| CATMA2C47695 | AT2G41100 | ATCAL4_TCH3__Calcium-binding EF hand family protein | ns | ns | ns | ns | **1.10** |
| CATMA2A39530 | AT2G41180 | SIB2__VQ motif-containing protein | ns | ns | ns | **0.75** | ns |
| CATMA2A39750 | AT2G41380 | S-adenosyl-L-methionine-dependent methyltransferases superfamily protein | ns | ns | ns | **0.87** | **1.99** |
| CATMA2A39780 | AT2G41410 | Calcium-binding EF-hand family protein | ns | ns | ns | ns | **0.84** |
| CATMA2A39960 | AT2G41560 | ACA4__autoinhibited Ca(2+)-ATPase, isoform 4 | ns | ns | ns | **-0.95** | ns |
| CATMA2B40960 | AT2G42530 | COR15B__cold regulated 15b | ns | ns | ns | **0.88** | ns |
| CATMA2C47720 | AT2G42540 | COR15_COR15A__cold-regulated 15a | ns | ns | **1.10** | **0.79** | ns |
| CATMA2A41170 | AT2G42740 | RPL16A__ribosomal protein large subunit 16A | ns | ns | ns | ns | **-0.66** |
| CATMA2A41220 | AT2G42790 | CSY3__citrate synthase 3 | ns | ns | ns | ns | **0.76** |
| CATMA2C47735 | AT2G43290 | MSS3__Calcium-binding EF-hand family protein | ns | ns | ns | ns | **0.71** |
| CATMA2A41775 | AT2G43360 | BIO2_BIOB__Radical SAM superfamily protein | ns | ns | ns | **-0.95** | ns |
| CATMA2C47736 | AT2G43445 | F-box and associated interaction domains-containing protein | ns | ns | ns | **0.73** | ns |
| CATMA2A41920 | AT2G43510 | ATTI1_TI1__trypsin inhibitor protein 1 | ns | ns | ns | ns | **0.77** |
| CATMA2C47737 | AT2G43535 | Scorpion toxin-like knottin superfamily protein | ns | ns | ns | ns | **-0.79** |
| CATMA2B42010 | AT2G43590 | Chitinase family protein | ns | ns | ns | ns | **1.09** |
| CATMA2A42040 | AT2G43620 | Chitinase family protein | ns | ns | ns | ns | **1.46** |
| CATMA2A42575 | AT2G44160 | MTHFR2__methylenetetrahydrofolate reductase 2 | ns | ns | ns | **-1.28** | **-0.95** |
| CATMA2A42660 | AT2G44230 | Plant protein of unknown function (DUF946) | ns | ns | ns | ns | **-1.03** |
| CATMA2C47752 | AT2G44290 | Bifunctional inhibitor/lipid-transfer protein/seed storage 2S albumin superfamily protein | ns | ns | ns | ns | **1.13** |
| CATMA2A42760 | AT2G44350 | ATCS_CSY4__Citrate synthase family protein | ns | ns | ns | ns | **0.91** |
| CATMA2A42780 | AT2G44370 | Cysteine/Histidine-rich C1 domain family protein | ns | ns | ns | ns | **0.79** |
| CATMA2A42890 | AT2G44460 | BGLU28__beta glucosidase 28 | ns | ns | ns | **0.74** | **0.70** |
| CATMA2A43610 | AT2G45220 | Plant invertase/pectin methylesterase inhibitor superfamily | ns | ns | ns | ns | **0.70** |
| CATMA2A43760 | AT2G45360 | Protein of unknown function (DUF1442) | ns | **-0.89** | ns | **-0.93** | **-0.88** |
| CATMA2A43870 | AT2G45470 | AGP8_FLA8__FASCICLIN-like arabinogalactan protein 8 | ns | ns | ns | ns | **-0.77** |

| CATMA identifier | AGI identifier | Gene annotation | 30 min | 2h | 4h | 8h | 24h |
|---|---|---|---|---|---|---|---|
| CATMA2A43960 | AT2G45550 | CYP76C4__cytochrome P450, family 76, subfamily C, polypeptide 4 | ns | ns | ns | **0.91** | **0.89** |
| CATMA2A43970 | AT2G45570 | CYP76C2__cytochrome P450, family 76, subfamily C, polypeptide 2 | ns | ns | ns | ns | **0.90** |
| CATMA2A44365 | AT2G45960 | ATHH2_PIP1;2_PIP1B_TMP-A__plasma membrane intrinsic protein 1B | ns | ns | **-1.14** | **-0.77** | ns |
| CATMA2A44610 | AT2G46220 | Uncharacterized conserved protein (DUF2358) | ns | ns | ns | **0.96** | ns |
| CATMA2C47791 | AT2G46390 | SDH8__unknown protein | ns | ns | ns | ns | **0.73** |
| CATMA2A44770 | AT2G46400 | ATWRKY46_WRKY46__WRKY DNA-binding protein 46 | ns | ns | ns | ns | **0.76** |
| CATMA2A44780 | AT2G46420 | Plant protein 1589 of unknown function | ns | ns | ns | **-0.72** | ns |
| CATMA2A45030 | AT2G46600 | Calcium-binding EF-hand family protein | ns | ns | ns | ns | **0.90** |
| CATMA2A45470 | AT2G47000 | ABCB4_ATPGP4_MDR4_PGP4__ATP binding cassette subfamily B4 | ns | ns | ns | ns | **0.72** |
| CATMA2A45700 | AT2G47240 | CER8_LACS1__AMP-dependent synthetase and ligase family protein | ns | ns | ns | **-0.93** | ns |
| CATMA2A45920 | AT2G47480 | Protein of unknown function (DUF3511) | ns | ns | ns | ns | **0.77** |
| CATMA2A46140 | AT2G47710 | Adenine nucleotide alpha hydrolases-like superfamily protein | ns | ns | ns | ns | **0.78** |
| CATMA2A46160 | AT2G47730 | ATGSTF5_ATGSTF8_GST6_GSTF8__glutathione S-transferase phi 8 | ns | ns | ns | **1.34** | **1.80** |
| CATMA2A46310 | AT2G47890 | B-box type zinc finger protein with CCT domain | ns | ns | ns | **0.98** | ns |
| CATMA2A46380 | AT2G47940 | DEGP2_EMB3117__DEGP protease 2 | ns | ns | ns | **0.73** | ns |
| CATMA2A46540 | AT2G48130 | Bifunctional inhibitor/lipid-transfer protein/seed storage 2S albumin superfamily protein | ns | **0.94** | ns | ns | ns |
| CATMA2A46550 | AT2G48140 | EDA4__Bifunctional inhibitor/lipid-transfer protein/seed storage 2S albumin superfamily protein | ns | ns | **1.20** | **0.73** | ns |
| CATMA3A00185 | AT3G01190 | Peroxidase superfamily protein | ns | **-0.89** | **-1.01** | **-1.66** | **-1.02** |
| CATMA3A00350 | AT3G01370 | ATCFM2_CFM2__CRM family member 2 | ns | ns | ns | **-0.72** | ns |
| CATMA3A00390 | AT3G01420 | ALPHA-DOX1_DIOX1_DOX1_PADOX-1__Peroxidase superfamily protein | ns | ns | ns | ns | **0.77** |
| CATMA3A00470 | AT3G01480 | ATCYP38_CYP38__cyclophilin 38 | ns | ns | ns | ns | **-0.88** |
| CATMA3A00490 | AT3G01500 | ATBCA1_ATSABP3_CA1_SABP3__carbonic anhydrase 1 | ns | ns | ns | ns | **-0.68** |
| CATMA3A00640 | AT3G01640 | ATGLCAK_GLCAK__glucuronokinase G | ns | ns | ns | **0.75** | ns |
| CATMA3A00690 | AT3G01690 | alpha/beta-Hydrolases superfamily protein | ns | ns | ns | ns | **-0.70** |
| CATMA3C57014 | AT3G01930 | Major facilitator superfamily protein | ns | ns | **-1.18** | ns | **-0.71** |
| CATMA3A00955 | AT3G01970 | ATWRKY45_WRKY45__WRKY DNA-binding protein 45 | ns | ns | ns | **0.71** | ns |
| CATMA3A01030 | AT3G02040 | AtGDPD1_GDPD1_SRG3__senescence-related gene 3 | ns | ns | ns | **0.71** | ns |
| CATMA3A01070 | AT3G02080 | Ribosomal protein S19e family protein | ns | ns | ns | ns | **-0.69** |
| CATMA3A01355 | AT3G02380 | ATCOL2_COL2__CONSTANS-like 2 | ns | ns | ns | ns | **-1.15** |
| CATMA3A01530_N | AT3G02560 | Ribosomal protein S7e family protein | ns | ns | ns | ns | **-0.80** |
| CATMA3A01800 | AT3G02875 | ILR1__Peptidase M20/M25/M40 family protein | ns | ns | ns | ns | **0.73** |
| CATMA3C57042 | AT3G03150 | unknown protein | ns | ns | **-1.17** | **-0.82** | ns |
| CATMA3C57935 | AT3G03341 | unknown protein | ns | ns | **1.15** | ns | ns |
| CATMA3A02720 | AT3G03780 | ATMS2_MS2__methionine synthase 2 | ns | ns | ns | **-1.66** | **-2.22** |
| CATMA3A02970 | AT3G04000 | NAD(P)-binding Rossmann-fold superfamily protein | ns | **0.95** | **1.16** | **1.53** | **1.23** |
| CATMA3A02980 | AT3G04010 | O-Glycosyl hydrolases family 17 protein | ns | ns | ns | **0.90** | **0.66** |
| CATMA3A03070 | AT3G04120 | GAPC_GAPC-1_GAPC1__glyceraldehyde-3-phosphate dehydrogenase C subunit 1 | ns | ns | ns | **1.09** | **1.11** |
| CATMA3A03260 | AT3G04290 | ATLTL1_LTL1__Li-tolerant lipase 1 | ns | ns | ns | ns | **-0.81** |
| CATMA3A03265 | AT3G04300 | RmlC-like cupins superfamily protein | ns | **1.25** | **1.73** | **2.08** | **2.25** |
| CATMA3A03370 | AT3G04400 | emb2171__Ribosomal protein L14p/L23e family protein | ns | ns | ns | ns | **-0.67** |
| CATMA3A03743 | AT3G04720 | HEL_PR-4_PR4__pathogenesis-related 4 | ns | ns | ns | ns | **1.00** |
| CATMA3A03860 | AT3G04840 | Ribosomal protein S3Ae | ns | ns | ns | ns | **-0.81** |
| CATMA3A03955 | AT3G04940 | ATCYSD1_CYSD1__cysteine synthase D1 | ns | ns | ns | **-0.70** | ns |
| CATMA3A04215 | AT3G05200 | ATL6__RING/U-box superfamily protein | ns | ns | ns | **0.75** | ns |
| CATMA3A04930 | AT3G05900 | neurofilament protein-related | ns | ns | ns | ns | **-1.15** |
| CATMA3A05430 | AT3G06350 | EMB3004_MEE32__dehydroquinate dehydratase, putative / shikimate dehydrogenase, putative | ns | ns | ns | **-1.03** | **-0.85** |
| CATMA3A05500 | AT3G06420 | ATG8H__Ubiquitin-like superfamily protein | ns | ns | ns | **0.84** | ns |
| CATMA3A05650 | AT3G06510 | ATSFR2_SFR2__Glycosyl hydrolase superfamily protein | ns | ns | ns | **-0.76** | ns |
| CATMA3A05810 | AT3G06650 | ACLB-1__ATP-citrate lyase B-1 | ns | ns | ns | **-0.73** | ns |
| CATMA3C57105 | AT3G06750 | hydroxyproline-rich glycoprotein family protein | ns | ns | ns | ns | **-0.68** |
| CATMA3A05990 | AT3G06770 | Pectin lyase-like superfamily protein | ns | ns | ns | ns | **-0.68** |
| CATMA3A06180 | AT3G06980 | DEA(D/H)-box RNA helicase family protein | ns | ns | ns | **-0.99** | ns |
| CATMA3A06550 | AT3G07310 | Protein of unknown function (DUF760) | ns | ns | **-1.12** | ns | ns |
| CATMA3A07410 | AT3G08590 | iPGAM2__Phosphoglycerate mutase, 2,3-bisphosphoglycerate-independent | ns | ns | ns | ns | **0.94** |
| CATMA3A07510 | AT3G08690 | ATUBC11_UBC11__ubiquitin-conjugating enzyme 11 | ns | ns | ns | **0.69** | ns |
| CATMA3A07540 | AT3G08740 | elongation factor P (EF-P) family protein | ns | ns | ns | ns | **-0.95** |
| CATMA3A08125 | AT3G09260 | BGLU23_LEB_PSR3.1_PYK10__Glycosyl hydrolase superfamily protein | ns | ns | ns | **-0.85** | **-0.81** |
| CATMA3A08130 | AT3G09270 | ATGSTU8_GSTU8__glutathione S-transferase TAU 8 | ns | ns | **1.15** | ns | **1.09** |
| CATMA3A08210 | AT3G09350 | Fes1A | ns | ns | ns | **0.70** | ns |
| CATMA3A08275 | AT3G09390 | ATMT-1_ATMT-K_MT2A__metallothionein 2A | ns | ns | ns | ns | **0.81** |
| CATMA3C57134 | AT3G09440 | Heat shock protein 70 (Hsp 70) family protein | ns | ns | ns | ns | **1.36** |
| CATMA3A08690 | AT3G09820 | ADK1_ATADK1__adenosine kinase 1 | ns | ns | ns | **-0.97** | **-0.75** |
| CATMA3A08820 | AT3G09940 | ATMDAR3_MDAR2_MDAR3_MDHAR__monodehydroascorbate reductase | ns | ns | ns | ns | **0.98** |
| CATMA3A09500 | AT3G10500 | anac053_NAC053__NAC domain containing protein 53 | ns | ns | ns | **1.48** | **1.16** |
| CATMA3A09650 | AT3G10610 | Ribosomal S17 family protein | ns | ns | ns | ns | **-0.67** |

| CATMA identifier | AGI identifier | Gene annotation | 30 min | 2h | 4h | 8h | 24h |
|---|---|---|---|---|---|---|---|
| CATMA3A10050 | AT3G10985 | ATWI-12_SAG20_WI12__senescence associated gene 20 | ns | ns | **-1.07** | ns | **0.74** |
| CATMA3A10205 | AT3G11170 | AtFAD7_FAD7_FADD__fatty acid desaturase 7 | ns | ns | ns | ns | **-0.87** |
| CATMA3A10360 | AT3G11340 | UGT76B1__UDP-Glycosyltransferase superfamily protein | ns | ns | ns | ns | **0.73** |
| CATMA3A10470 | AT3G11510 | Ribosomal protein S11 family protein | ns | ns | ns | ns | **-0.83** |
| CATMA3A10755 | AT3G11820 | AT-SYR1_ATSYP121_ATSYR1_PEN1_SYP121_SYR1__syntaxin of plants 121 | ns | ns | ns | ns | **0.77** |
| CATMA3A11535 | AT3G12580 | ATHSP70_HSP70__heat shock protein 70 | ns | ns | ns | **0.77** | **1.42** |
| CATMA3A11910 | AT3G12930 | Lojap-related protein | ns | ns | ns | ns | **-0.67** |
| CATMA3C57188 | AT3G13320 | atcax2_CAX2__cation exchanger 2 | ns | **0.87** | ns | ns | **0.89** |
| CATMA3A12620 | AT3G13470 | Cpn60beta2__TCP-1/cpn60 chaperonin family protein | ns | ns | ns | **-0.74** | ns |
| CATMA3A12660 | AT3G13520 | AGP12_ATAGP12__arabinogalactan protein 12 | ns | ns | **1.08** | **1.39** | **0.88** |
| CATMA3C57193 | AT3G13620 | Amino acid permease family protein | ns | ns | ns | ns | **0.81** |
| CATMA3A13170 | AT3G13950 | unknown protein | ns | ns | ns | ns | **1.12** |
| CATMA3A13230 | AT3G14000 | ATBRXL2_BRX-LIKE2__DZC (Disease resistance/zinc finger/chromosome condensation-like region) domain containing protein | ns | ns | ns | **0.91** | ns |
| CATMA3A13460 | AT3G14200 | Chaperone DnaJ-domain superfamily protein | ns | ns | ns | **0.77** | ns |
| CATMA3A13520 | AT3G14240 | Subtilase family protein | ns | ns | ns | **-0.83** | ns |
| CATMA3A13690 | AT3G14415 | Aldolase-type TIM barrel family protein | ns | ns | ns | **-0.74** | ns |
| CATMA3A13940 | AT3G14620 | CYP72A8__cytochrome P450, family 72, subfamily A, polypeptide 8 | ns | ns | ns | **0.86** | **1.40** |
| CATMA3C57211 | AT3G14690 | CYP72A15__cytochrome P450, family 72, subfamily A, polypeptide 15 | ns | ns | ns | **0.70** | **0.66** |
| CATMA3A14120 | AT3G14770 | AtSWEET2_SWEET2__Nodulin MtN3 family protein | ns | ns | ns | **1.02** | ns |
| CATMA3A14930 | AT3G15518 | unknown protein | ns | ns | ns | ns | **0.83** |
| CATMA3A14940 | AT3G15520 | Cyclophilin-like peptidyl-prolyl cis-trans isomerase family protein | ns | ns | ns | ns | **-0.70** |
| CATMA3A15240 | AT3G15850 | ADS3_FAD5_FADB_JB67__fatty acid desaturase 5 | ns | ns | ns | ns | **-0.91** |
| CATMA3A15360 | AT3G15950 | NAI2__DNA topoisomerase-related | ns | ns | ns | **-0.94** | **-1.30** |
| CATMA3A15500 | AT3G16080 | Zinc-binding ribosomal protein family protein | ns | ns | ns | ns | **-0.69** |
| CATMA3A15560 | AT3G16150 | ASPGB1__N-terminal nucleophile aminohydrolases (Ntn hydrolases) superfamily protein | ns | ns | **-1.48** | ns | ns |
| CATMA_GFT_02931 | AT3G16390 | NSP3__nitrile specifier protein 3 | ns | ns | ns | **-1.03** | **-1.02** |
| CATMA3C57236 | AT3G16400 | ATMLP-470_ATNSP1_NSP1__nitrile specifier protein 1 | ns | ns | ns | ns | **-1.11** |
| CATMA3C57238 | AT3G16420 | JAL30_PBP1__PYK10-binding protein 1 | ns | ns | ns | ns | **-1.02** |
| CATMA3C57239 | AT3G16430 | JAL31__jacalin-related lectin 31 | ns | ns | ns | ns | **-0.87** |
| CATMA3A15865 | AT3G16440 | ATMLP-300B_MEE36_MLP-300B__myrosinase-binding protein-like protein-300B | ns | ns | ns | ns | **-0.91** |
| CATMA3A15870 | AT3G16450 | JAL33__Mannose-binding lectin superfamily protein | ns | ns | ns | ns | **-1.30** |
| CATMA3A15880 | AT3G16460 | JAL34__Mannose-binding lectin superfamily protein | ns | ns | ns | **-0.89** | **-1.53** |
| CATMA3C57243 | AT3G16690 | AtSWEET16_SWEET16__Nodulin MtN3 family protein | ns | ns | ns | ns | **-0.81** |
| CATMA3A16175 | AT3G16770 | ATEBP_EBP_ERF72_RAP2.3__ethylene-responsive element binding protein | ns | ns | **-1.16** | **-0.76** | **-0.71** |
| CATMA3A16580 | AT3G17170 | RFC3__Translation elongation factor EF1B/ribosomal protein S6 family protein | ns | ns | ns | **-0.72** | **-0.79** |
| CATMA3A16820 | AT3G17390 | MAT4_MTO3_SAMS3__S-adenosylmethionine synthetase family protein | ns | ns | ns | **-0.85** | ns |
| CATMA3A16940 | AT3G17510 | CIPK1_SnRK3.16__CBL-interacting protein kinase 1 | ns | ns | ns | ns | **-0.76** |
| CATMA3A17290 | AT3G17790 | ATACP5_ATPAP17_PAP17__purple acid phosphatase 17 | ns | ns | ns | ns | **0.86** |
| CATMA3A17310 | AT3G17810 | PYD1__pyrimidine 1 | ns | ns | ns | ns | **0.72** |
| CATMA3A17790 | AT3G18250 | Putative membrane lipoprotein | ns | ns | ns | ns | **0.71** |
| CATMA3A17960 | AT3G18390 | EMB1865__CRS1 / YhbY (CRM) domain-containing protein | ns | ns | ns | **-0.83** | **-0.76** |
| CATMA3A18350 | AT3G18740 | RLK902__Ribosomal protein L7Ae/L30e/S12e/Gadd45 family protein | ns | ns | ns | ns | **-0.67** |
| CATMA3A19045 | AT3G19450 | ATCAD4_CAD_CAD-C_CAD4__GroES-like zinc-binding alcohol dehydrogenase family protein | ns | **-0.82** | **-1.22** | **-1.74** | **-1.74** |
| CATMA3A19070 | AT3G19480 | D-3-phosphoglycerate dehydrogenase | ns | ns | ns | ns | **-0.77** |
| CATMA3A19415 | AT3G19820 | CBB1_DIM_DIM1_DWF1_EVE1__cell elongation protein / DWARF1 / DIMINUTO (DIM) | ns | ns | ns | **-1.27** | **-1.15** |
| CATMA3A19545 | AT3G19930 | ATSTP4_STP4__sugar transporter 4 | ns | ns | **-1.18** | ns | ns |
| CATMA3A20050 | AT3G20370 | TRAF-like family protein | ns | ns | ns | **-0.94** | **-1.06** |
| CATMA3A20070 | AT3G20390 | endoribonuclease L-PSP family protein | ns | ns | ns | ns | **-0.78** |
| CATMA3A20080 | AT3G20395 | RING/U-box superfamily protein | ns | ns | ns | ns | **-0.71** |
| CATMA3A20210 | AT3G20500 | ATPAP18_PAP18__purple acid phosphatase 18 | ns | ns | ns | ns | **0.68** |
| CATMA3A20220 | AT3G20510 | Transmembrane proteins 14C | ns | ns | ns | ns | **0.96** |
| CATMA3A20560 | AT3G20820 | Leucine-rich repeat (LRR) family protein | ns | ns | ns | ns | **-0.86** |
| CATMA3A20880 | AT3G21055 | PSBTN__photosystem II subunit T | ns | ns | ns | **-1.01** | ns |
| CATMA3A20920 | AT3G21080 | ABC transporter-related | ns | ns | ns | ns | **0.87** |
| CATMA3A21390 | AT3G21520 | AtDMP1_DMP1__DUF679 domain membrane protein 1 | ns | **1.10** | ns | **0.92** | **0.97** |
| CATMA3A21430 | AT3G21560 | UGT84A2__UDP-Glycosyltransferase superfamily protein | ns | **1.48** | **2.21** | **1.60** | **1.93** |
| CATMA3A21590 | AT3G21720 | ICL__isocitrate lyase | ns | ns | ns | **0.72** | ns |
| CATMA3C57319 | AT3G22210 | unknown protein | ns | ns | ns | ns | **-0.74** |
| CATMA3A22365 | AT3G22370 | AOX1A_ATAOX1A_AtHSR3_HSR3__alternative oxidase 1A | ns | ns | ns | **0.99** | **1.18** |
| CATMA3A22410 | AT3G22420 | ATWNK2_WNK2_ZIK3__with no lysine (K) kinase 2 | ns | ns | ns | **-0.70** | **-1.04** |
| CATMA3A22520 | AT3G22530 | unknown protein | ns | ns | ns | **0.72** | ns |
| CATMA3C57326 | AT3G22600 | Bifunctional inhibitor/lipid-transfer protein/seed storage 2S albumin superfamily protein | ns | **1.68** | **1.96** | **1.36** | **1.96** |

| CATMA identifier | AGI identifier | Gene annotation | 30 min | 2h | 4h | 8h | 24h |
|---|---|---|---|---|---|---|---|
| CATMA3A22590 | AT3G22620 | Bifunctional inhibitor/lipid-transfer protein/seed storage 2S albumin superfamily protein | ns | **1.35** | ns | **0.82** | **1.00** |
| CATMA3A22910 | AT3G22960 | PKP-ALPHA_PKP1__Pyruvate kinase family protein | ns | ns | ns | **-0.70** | ns |
| CATMA3A23300 | AT3G23300 | S-adenosyl-L-methionine-dependent methyltransferases superfamily protein | ns | ns | ns | **-0.72** | ns |
| CATMA3A23320 | AT3G23390 | Zinc-binding ribosomal protein family protein | ns | ns | ns | ns | **-0.77** |
| CATMA3A23470 | AT3G23560 | ALF5__MATE efflux family protein | ns | ns | ns | ns | **0.82** |
| CATMA3A23830 | AT3G23880 | F-box and associated interaction domains-containing protein | ns | **-0.81** | ns | ns | ns |
| CATMA3A23850 | AT3G23920 | BAM1_BMY7_TR-BAMY__beta-amylase 1 | ns | ns | ns | ns | **0.77** |
| CATMA3A23870 | AT3G23940 | dehydratase family | ns | ns | ns | **-0.87** | ns |
| CATMA3A24096 | AT3G24170 | ATGR1_GR1__glutathione-disulfide reductase | ns | ns | ns | ns | **0.73** |
| CATMA3A24390 | AT3G24500 | ATMBF1C_MBF1C__multiprotein bridging factor 1C | ns | ns | ns | **0.77** | ns |
| CATMA3A24400 | AT3G24503 | ALDH1A_ALDH2C4_REF1__aldehyde dehydrogenase 2C4 | ns | ns | ns | ns | **1.13** |
| CATMA3A24500 | AT3G24540 | AtPERK3_PERK3__Protein kinase superfamily protein | ns | ns | ns | ns | **0.81** |
| CATMA3C57381 | AT3G25610 | ATPase E1-E2 type family protein / haloacid dehalogenase-like hydrolase family protein | ns | ns | ns | **1.02** | **1.78** |
| CATMA3A25470 | AT3G25690 | AtCHUP1_CHUP1__Hydroxyproline-rich glycoprotein family protein | ns | ns | **-1.05** | ns | ns |
| CATMA_GFT_01090 | AT3G25830 | ATTPS-CIN_TPS-CIN_TPS-CIN__terpene synthase-like sequence-1,8-cineole | ns | ns | **1.19** | ns | ns |
| CATMA3A25860 | AT3G26060 | ATPRX Q_PRXQ__Thioredoxin superfamily protein | ns | ns | ns | **-0.79** | **-0.67** |
| CATMA3A26050 | AT3G26200 | CYP71B22__cytochrome P450, family 71, subfamily B, polypeptide 22 | ns | ns | ns | **1.07** | **1.07** |
| CATMA3A26060 | AT3G26210 | CYP71B23__cytochrome P450, family 71, subfamily B, polypeptide 23 | ns | ns | ns | ns | **1.01** |
| CATMA3C57399 | AT3G26220 | CYP71B3__cytochrome P450, family 71, subfamily B, polypeptide 3 | ns | ns | ns | ns | **0.70** |
| CATMA_GFT_01102 | AT3G26450 | Polyketide cyclase/dehydrase and lipid transport superfamily protein | ns | ns | **1.04** | ns | ns |
| CATMA3A26310 | AT3G26470 | Powdery mildew resistance protein, RPW8 domain | ns | ns | ns | **0.73** | **1.26** |
| CATMA3A26416 | AT3G26650 | GAPA_GAPA-1__glyceraldehyde 3-phosphate dehydrogenase A subunit | ns | ns | ns | **-0.77** | **-0.69** |
| CATMA3A26630 | AT3G26890 | unknown protein | ns | ns | ns | **-0.70** | ns |
| CATMA3A27240 | AT3G27380 | SDH2-1__succinate dehydrogenase 2-1 | ns | ns | ns | **0.99** | **0.95** |
| CATMA3C57427 | AT3G27690 | LHCB2_LHCB2.3_LHCB2.4__photosystem II light harvesting complex gene 2.3 | ns | ns | ns | ns | **-1.00** |
| CATMA3A27615 | AT3G27770 | unknown protein | ns | ns | ns | **0.78** | ns |
| CATMA3A27690 | AT3G27880 | Protein of unknown function (DUF1645) | ns | **0.94** | ns | **0.71** | ns |
| CATMA3A27830 | AT3G28040 | Leucine-rich receptor-like protein kinase family protein | ns | ns | ns | ns | **-0.80** |
| CATMA3A28035 | AT3G28210 | PMZ_SAP12__zinc finger (AN1-like) family protein | ns | ns | ns | **1.60** | **2.09** |
| CATMA3A28050 | AT3G28220 | TRAF-like family protein | ns | ns | ns | ns | **-0.91** |
| CATMA3A28100 | AT3G28270 | Protein of unknown function (DUF677) | ns | ns | ns | ns | **-1.26** |
| CATMA3A28190 | AT3G28340 | GATL10_GolS8__galacturonosyltransferase-like 10 | ns | ns | ns | **0.92** | **0.67** |
| CATMA3C57443 | AT3G28740 | CYP81D11__Cytochrome P450 superfamily protein | ns | ns | ns | **0.88** | **0.92** |
| CATMA3A28845 | AT3G28910 | ATMYB30_MYB30__myb domain protein 30 | ns | ns | ns | **0.89** | ns |
| CATMA3A29010 | AT3G29000 | Calcium-binding EF-hand family protein | ns | ns | ns | ns | **0.69** |
| CATMA3A29325_N | AT3G29200 | ATCM1_CM1__chorismate mutase 1 | ns | ns | ns | **-0.95** | **-0.96** |
| CATMA3A29390 | AT3G29250 | AtSDR4_SDR4__NAD(P)-binding Rossmann-fold superfamily protein | ns | ns | ns | **-1.26** | ns |
| CATMA3C57461 | AT3G29360 | UGD2__UDP-glucose 6-dehydrogenase family protein | ns | ns | ns | ns | **0.87** |
| CATMA3A31275 | AT3G30775 | AT-POX_ATPDH_ATPOX_ERD5_PDH1_PRO1_PRODH__ Methylenetetrahydrofolate reductase family protein | ns | ns | **-1.57** | ns | ns |
| CATMA3A36600 | AT3G43720 | Bifunctional inhibitor/lipid-transfer protein/seed storage 2S albumin superfamily protein | ns | ns | ns | **-0.71** | **-0.86** |
| CATMA3A37080 | AT3G44190 | FAD/NAD(P)-binding oxidoreductase family protein | ns | ns | ns | **2.05** | **2.01** |
| CATMA3A37360 | AT3G44430 | unknown protein | ns | ns | ns | **0.76** | ns |
| CATMA3A37900 | AT3G44880 | ACD1_LLS1_PAO__Pheophorbide a oxygenase family protein with Rieske [2Fe-2S] domain | ns | ns | ns | ns | **0.68** |
| CATMA3A38175 | AT3G45140 | ATLOX2_LOX2__lipoxygenase 2 | ns | ns | ns | ns | **-1.11** |
| CATMA3A38190 | AT3G45160 | Putative membrane lipoprotein | ns | ns | ns | ns | **-0.68** |
| CATMA3C57563 | AT3G45180 | Ubiquitin-like superfamily protein | ns | ns | ns | **0.86** | **0.87** |
| CATMA3C57579 | AT3G45700 | Major facilitator superfamily protein | ns | ns | ns | **-0.91** | **-0.93** |
| CATMA3C57580 | AT3G45710 | Major facilitator superfamily protein | ns | ns | ns | **-0.73** | ns |
| CATMA3C57581 | AT3G45730 | unknown protein | ns | ns | **-1.05** | **-0.71** | **-1.52** |
| CATMA_GFT_01303 | AT3G46070 | C2H2-type zinc finger family protein | ns | ns | ns | **0.88** | **1.29** |
| CATMA_GFT_01304 | AT3G46080 | C2H2-type zinc finger family protein | ns | **1.03** | ns | **1.39** | **1.72** |
| CATMA3A39230 | AT3G46230 | ATHSP17.4_HSP17.4__heat shock protein 17.4 | ns | ns | ns | ns | **0.95** |
| CATMA3A39300 | AT3G46280 | protein kinase-related | ns | ns | ns | ns | **0.73** |
| CATMA3A39760 | AT3G46670 | UGT76E11__UDP-glucosyl transferase 76E11 | ns | ns | ns | **0.79** | **0.90** |
| CATMA3A40150 | AT3G47070 | Unknown protein | ns | ns | ns | **-0.76** | ns |
| CATMA3C57618 | AT3G47470 | CAB4_LHCA4__light-harvesting chlorophyll-protein complex I subunit A4 | ns | ns | ns | ns | **-0.71** |
| CATMA3A40490 | AT3G47480 | Calcium-binding EF-hand family protein | ns | ns | ns | ns | **0.93** |
| CATMA3A40980 | AT3G47960 | Major facilitator superfamily protein | ns | ns | ns | **-1.24** | ns |
| CATMA3A41100 | AT3G48070 | RING/U-box superfamily protein | ns | ns | ns | ns | **0.84** |
| CATMA_GFT_01324 | AT3G48320 | CYP71A21__cytochrome P450, family 71, subfamily A, polypeptide 21 | ns | ns | ns | **0.88** | ns |
| CATMA3A41720 | AT3G48730 | GSA2__glutamate-1-semialdehyde 2,1-aminomutase 2 | ns | ns | ns | **-0.72** | ns |
| CATMA3A41875 | AT3G48870 | ATCLPC_ATHSP93-III_ClpC2_HSP93-III__Clp ATPase | ns | ns | ns | **-0.85** | ns |

| CATMA identifier | AGI identifier | Gene annotation | 30 min | 2h | 4h | 8h | 24h |
|---|---|---|---|---|---|---|---|
| CATMA3A41910 | AT3G48930 | EMB1080__Nucleic acid-binding, OB-fold-like protein | ns | ns | ns | ns | **-0.68** |
| CATMA3A41980 | AT3G48990 | AMP-dependent synthetase and ligase family protein | ns | ns | ns | **0.70** | ns |
| CATMA3A42560 | AT3G49530 | ANAC062_NAC062_NTL6__NAC domain containing protein 62 | ns | ns | ns | ns | **1.28** |
| CATMA3C57667 | AT3G49570 | LSU3__response to low sulfur 3 | ns | ns | **1.04** | ns | ns |
| CATMA3A42710 | AT3G49670 | BAM2__Leucine-rich receptor-like protein kinase family protein | ns | ns | ns | **-0.93** | **-0.76** |
| CATMA3A42990 | AT3G49940 | LBD38__LOB domain-containing protein 38 | ns | ns | ns | ns | **-0.69** |
| CATMA3A43500 | AT3G50440 | ATMES10_MES10__methyl esterase 10 | ns | **0.96** | ns | ns | **1.12** |
| CATMA3A43600 | AT3G50560 | NAD(P)-binding Rossmann-fold superfamily protein | ns | **1.05** | ns | ns | ns |
| CATMA3A43687 | AT3G50685 | unknown protein | ns | ns | ns | ns | **-0.66** |
| CATMA3A43750 | AT3G50740 | UGT72E1__UDP-glucosyl transferase 72E1 | ns | ns | ns | **-0.88** | ns |
| CATMA3C57691 | AT3G50770 | CML41__calmodulin-like 41 | ns | ns | ns | **-0.72** | **1.10** |
| CATMA3A43920 | AT3G50910 | unknown protein | ns | ns | ns | **0.86** | **0.66** |
| CATMA3A43940 | AT3G50930 | BCS1__cytochrome BC1 synthesis | ns | ns | ns | ns | **0.76** |
| CATMA3A43980 | AT3G50970 | LTI30_XERO2__dehydrin family protein | ns | **0.92** | ns | **1.16** | ns |
| CATMA3A44140 | AT3G51130 | unknown protein | ns | ns | ns | **0.83** | **0.67** |
| CATMA3A44230 | AT3G51240 | F3'H_F3H_TT6__flavanone 3-hydroxylase | ns | ns | **1.09** | ns | ns |
| CATMA3A44245 | AT3G51260 | PAD1__20S proteasome alpha subunit PAD1 | ns | ns | ns | ns | **0.71** |
| CATMA3A44640 | AT3G51660 | Tautomerase/MIF superfamily protein | ns | ns | **1.47** | **1.80** | **2.27** |
| CATMA3A44650 | AT3G51670 | SEC14 cytosolic factor family protein / phosphoglyceride transfer family protein | ns | ns | ns | ns | **1.15** |
| CATMA3A44970 | AT3G52060 | Core-2/I-branching beta-1,6-N-acetylglucosaminyltransferase family protein | ns | ns | ns | **0.70** | ns |
| CATMA3A45070 | AT3G52150 | RNA-binding (RRM/RBD/RNP motifs) family protein | ns | ns | ns | ns | **-0.82** |
| CATMA3A45345 | AT3G52430 | ATPAD4_PAD4__alpha/beta-Hydrolases superfamily protein | ns | ns | ns | ns | **0.79** |
| CATMA3A45773 | AT3G52840 | BGAL2__beta-galactosidase 2 | ns | ns | ns | **-0.78** | ns |
| CATMA3A45870 | AT3G52930 | Aldolase superfamily protein | ns | ns | ns | ns | **0.81** |
| CATMA3A46180_N | AT3G53260 | ATPAL2_PAL2__phenylalanine ammonia-lyase 2 | ns | **-0.99** | ns | ns | **-0.97** |
| CATMA3A46410_N | AT3G53460 | CP29__chloroplast RNA-binding protein 29 | ns | ns | **-1.04** | ns | ns |
| CATMA3A46760 | AT3G53810 | Concanavalin A-like lectin protein kinase family protein | ns | ns | ns | ns | **0.94** |
| CATMA3A46865 | AT3G53920 | SIG3_SIGC__RNApolymerase sigma-subunit C | ns | ns | ns | **-0.69** | ns |
| CATMA3A46990 | AT3G54040 | PAR1 protein | ns | ns | **-1.20** | ns | ns |
| CATMA3A47000 | AT3G54050 | HCEF1__high cyclic electron flow 1 | ns | ns | ns | ns | **-0.72** |
| CATMA3A47350 | AT3G54420 | ATCHITIV_ATEP3_CHIV_EP3__homolog of carrot EP3-3 chitinase | ns | ns | ns | **0.98** | **2.05** |
| CATMA3A47520 | AT3G54580 | Proline-rich extensin-like family protein | ns | ns | ns | **-0.91** | **-0.82** |
| CATMA3C57794 | AT3G54590 | ATHRGP1_HRGP1__hydroxyproline-rich glycoprotein | ns | ns | ns | **-0.91** | **-0.74** |
| CATMA3A47540 | AT3G54600 | Class I glutamine amidotransferase-like superfamily protein | ns | ns | ns | **-0.77** | ns |
| CATMA3A47730 | AT3G54810 | BME3_BME3-ZF_GATA8__Plant-specific GATA-type zinc finger transcription factor family protein | ns | ns | ns | ns | **0.76** |
| CATMA3A47740 | AT3G54820 | PIP2;5_PIP2D__plasma membrane intrinsic protein 2;5 | ns | **0.98** | ns | **0.77** | **1.01** |
| CATMA3A47840 | AT3G54880 | unknown protein | ns | ns | ns | ns | **-0.81** |
| CATMA3A48130 | AT3G55120 | A11_CFI_TT5__Chalcone-flavanone isomerase family protein | ns | ns | ns | ns | **-0.69** |
| CATMA3A48330 | AT3G55330 | PPL1__PsbP-like protein 1 | ns | ns | ns | ns | **-0.88** |
| CATMA3A48400 | AT3G55430 | O-Glycosyl hydrolases family 17 protein | ns | ns | ns | **0.73** | ns |
| CATMA3B48595 | AT3G55610 | P5CS2__delta 1-pyrroline-5-carboxylate synthase 2 | ns | ns | ns | ns | **-0.66** |
| CATMA3A48610 | AT3G55630 | ATDFD_DFD_FPGS3__DHFS-FPGS homolog D | ns | ns | ns | **-0.86** | **-1.06** |
| CATMA3A48860 | AT3G55880 | SUE4__Alpha/beta hydrolase related protein | ns | ns | ns | **0.82** | **0.94** |
| CATMA3A48940 | AT3G55970 | ATJRG21_JRG21__jasmonate-regulated gene 21 | ns | ns | ns | **1.12** | **1.21** |
| CATMA3A48950 | AT3G55980 | ATSZF1_SZF1__salt-inducible zinc finger 1 | ns | ns | ns | ns | **0.98** |
| CATMA3A49200 | AT3G56260 | unknown protein | ns | ns | ns | ns | **0.88** |
| CATMA3A49380 | AT3G56400 | ATWRKY70_WRKY70__WRKY DNA-binding protein 70 | ns | ns | ns | ns | **0.70** |
| CATMA3A49680 | AT3G56710 | SIB1__sigma factor binding protein 1 | ns | ns | ns | **0.75** | ns |
| CATMA3A49900 | AT3G56910 | PSRP5__plastid-specific 50S ribosomal protein 5 | ns | ns | ns | ns | **-0.75** |
| CATMA3A50026 | AT3G57050 | CBL__cystathionine beta-lyase | ns | ns | ns | **-0.77** | ns |
| CATMA3A50400 | AT3G57400 | unknown protein | ns | ns | ns | **0.82** | ns |
| CATMA3A50520 | AT3G57520 | AtSIP2_RS2_SIP2__seed imbibition 2 | ns | ns | ns | ns | **-0.78** |
| CATMA3A50680 | AT3G57670 | NTT_WIP2__C2H2-type zinc finger family protein | ns | ns | ns | ns | **0.85** |
| CATMA3A51750 | AT3G58750 | CSY2__citrate synthase 2 | ns | ns | ns | ns | **0.76** |
| CATMA3A52190 | AT3G59140 | ABCC10_ATMRP14_MRP14__multidrug resistance-associated protein 14 | ns | ns | ns | **0.76** | **0.67** |
| CATMA3A52725 | AT3G59700 | ATHLECRK_HLECRK_LECRK1__lectin-receptor kinase | ns | ns | ns | ns | **0.99** |
| CATMA3A52975 | AT3G59970 | MTHFR1__methylenetetrahydrofolate reductase 1 | ns | ns | ns | **-1.30** | **-1.06** |
| CATMA3A53225 | AT3G60190 | ADL1E_ADL4_ADLP2_DL1E_DRP1E_EDR3__DYNAMIN-like 1E | ns | **0.82** | ns | ns | **1.11** |
| CATMA3A53335 | AT3G60320 | Protein of unknown function (DUF630 and DUF632) | ns | ns | ns | **-1.10** | **-0.77** |
| CATMA3A53430 | AT3G60420 | Phosphoglycerate mutase family protein | ns | ns | ns | ns | **1.16** |
| CATMA3A53460 | AT3G60450 | Phosphoglycerate mutase family protein | ns | ns | ns | ns | **0.95** |
| CATMA3A54593 | AT3G61430 | ATPIP1_PIP1_PIP1;1_PIP1A__plasma membrane intrinsic protein 1A | ns | ns | **-1.16** | **-0.94** | ns |
| CATMA3A54980 | AT3G61820 | Eukaryotic aspartyl protease family protein | ns | **1.06** | **1.35** | ns | **1.30** |
| CATMA3A55250 | AT3G62110 | Pectin lyase-like superfamily protein | ns | ns | ns | **-0.88** | ns |
| CATMA3A55290 | AT3G62150 | ABCB21_PGP21__P-glycoprotein 21 | ns | ns | ns | **1.00** | **0.71** |

| CATMA identifier | AGI identifier | Gene annotation | 30 min | 2h | 4h | 8h | 24h |
|---|---|---|---|---|---|---|---|
| CATMA3A55410 | AT3G62260 | Protein phosphatase 2C family protein | ns | ns | ns | ns | **0.81** |
| CATMA3A55700 | AT3G62530 | ARM repeat superfamily protein | ns | ns | ns | ns | **-0.81** |
| CATMA3A55770 | AT3G62600 | ATERDJ3B_ERDJ3B__DNAJ heat shock family protein | ns | ns | ns | ns | **0.79** |
| CATMA3A56350 | AT3G63160 | Unknown protein | ns | ns | ns | **-0.92** | ns |
| CATMA4C42011 | AT4G00550 | DGD2__digalactosyl diacylglycerol deficient 2 | ns | ns | ns | ns | **0.66** |
| CATMA4A00800 | AT4G00750 | S-adenosyl-L-methionine-dependent methyltransferases superfamily protein | ns | ns | ns | **0.95** | ns |
| CATMA4A01250 | AT4G01070 | GT72B1_UGT72B1__UDP-Glycosyltransferase superfamily protein | ns | **0.84** | ns | **1.03** | **0.86** |
| CATMA4A01430 | AT4G01250 | AtWRKY22_WRKY22__WRKY family transcription factor | ns | ns | ns | ns | **0.77** |
| CATMA4C42026 | AT4G01265 | Unknown protein | ns | ns | **-1.34** | ns | ns |
| CATMA_GFT_01425 | AT4G01770 | RGXT1__rhamnogalacturonan xylosyltransferase 1 | ns | ns | ns | ns | **0.95** |
| CATMA4C42043 | AT4G01800 | AGY1_AtcpSecA_SECA1__Albino or Glassy Yellow 1 | ns | ns | ns | **-0.81** | ns |
| CATMA4A02680 | AT4G02380 | AtLEA5_SAG21__senescence-associated gene 21 | ns | ns | ns | ns | **1.17** |
| CATMA4A03280 | AT4G02940 | oxidoreductase, 2OG-Fe(II) oxygenase family protein | ns | ns | **1.00** | **1.30** | **0.87** |
| CATMA4A03586_N | AT4G03280 | PETC_PGR1__photosynthetic electron transfer C | ns | ns | ns | ns | **-0.69** |
| CATMA4C42083 | AT4G03320 | AtTic20-IV_Tic20-IV__translocon at the inner envelope membrane of chloroplasts 20-IV | ns | ns | ns | **1.00** | **0.82** |
| CATMA4A03800 | AT4G03450 | Ankyrin repeat family protein | ns | ns | ns | ns | **0.76** |
| CATMA4C42092 | AT4G03540 | Uncharacterised protein family (UPF0497) | ns | ns | **1.09** | ns | ns |
| CATMA4A05135 | AT4G04610 | APR_APR1_ATAPR1_PRH19__APS reductase 1 | ns | ns | ns | **1.09** | **0.98** |
| CATMA4C42113 | AT4G04745 | unknown protein | ns | ns | **1.01** | ns | ns |
| CATMA4A05940 | AT4G05310 | Ubiquitin-like superfamily protein | ns | ns | ns | ns | **-0.71** |
| CATMA4C42144 | AT4G06744 | Leucine-rich repeat (LRR) family protein | ns | ns | ns | **-0.73** | ns |
| CATMA4A09810 | AT4G09750 | NAD(P)-binding Rossmann-fold superfamily protein | ns | ns | ns | ns | **0.71** |
| CATMA4A10160 | AT4G10110 | RNA-binding (RRM/RBD/RNP motifs) family protein | ns | ns | ns | ns | **0.95** |
| CATMA4A10410 | AT4G10380 | AtNIP5;1_NIP5;1_NLM6_NLM8__NOD26-like intrinsic protein 5;1 | ns | ns | ns | ns | **0.85** |
| CATMA4A10490 | AT4G10450 | Ribosomal protein L6 family | ns | ns | ns | **-0.71** | ns |
| CATMA4C42222 | AT4G11310 | Papain family cysteine protease | ns | ns | ns | **-0.75** | ns |
| CATMA4A11720 | AT4G11570 | Haloacid dehalogenase-like hydrolase (HAD) superfamily protein | ns | ns | ns | **0.78** | ns |
| CATMA4A11745 | AT4G11600 | ATGPX6_GPX6_LSC803_PHGPX__glutathione peroxidase 6 | ns | ns | ns | **1.03** | **1.95** |
| CATMA4A11780_N | AT4G11650 | ATOSM34_OSM34__osmotin 34 | ns | **0.93** | ns | ns | **1.31** |
| CATMA4A12000 | AT4G11890 | Protein kinase superfamily protein | ns | ns | ns | ns | **1.38** |
| CATMA_GFT_01594 | AT4G12310 | CYP706A5__cytochrome P450, family 706, subfamily A, polypeptide 5 | ns | ns | ns | **-0.88** | ns |
| CATMA4A12530 | AT4G12420 | SKU5__Cupredoxin superfamily protein | ns | ns | ns | **-1.07** | ns |
| CATMA4C42251 | AT4G12480 | EARLI1_pEARLI 1__Bifunctional inhibitor/lipid-transfer protein/seed storage 2S albumin superfamily protein | ns | ns | ns | ns | **1.19** |
| CATMA4C42252 | AT4G12490 | Bifunctional inhibitor/lipid-transfer protein/seed storage 2S albumin superfamily protein | ns | ns | ns | ns | **1.90** |
| CATMA4C42253 | AT4G12500 | Bifunctional inhibitor/lipid-transfer protein/seed storage 2S albumin superfamily protein | ns | ns | ns | ns | **1.32** |
| CATMA4D03132 | AT4G12545 | Bifunctional inhibitor/lipid-transfer protein/seed storage 2S albumin superfamily protein | ns | ns | ns | **-1.20** | **-1.66** |
| CATMA4A12760 | AT4G12600 | Ribosomal protein L7Ae/L30e/S12e/Gadd45 family protein | ns | ns | ns | ns | **-0.92** |
| CATMA4A12860 | AT4G12720 | AtNUDT7_GFG1_NUDT7__MutT/nudix family protein | ns | ns | ns | ns | **1.07** |
| CATMA4A13280 | AT4G13180 | NAD(P)-binding Rossmann-fold superfamily protein | ns | ns | **1.03** | **1.07** | **1.39** |
| CATMA4A13370 | AT4G13250 | NYC1__NAD(P)-binding Rossmann-fold superfamily protein | ns | ns | ns | ns | **1.08** |
| CATMA4C42276 | AT4G13410 | ATCSLA15_CSLA15__Nucleotide-diphospho-sugar transferases superfamily protein | ns | ns | ns | ns | **-0.77** |
| CATMA4A14010 | AT4G13840 | HXXXD-type acyl-transferase family protein | ns | ns | ns | ns | **-0.79** |
| CATMA4A14040 | AT4G13870 | ATWEX_ATWRNEXO_WEX_WRNEXO__Werner syndrome-like exonuclease | ns | ns | ns | ns | **-1.19** |
| CATMA4A14135 | AT4G13940 | ATSAHH1_EMB1395_HOG1_MEE58_SAHH1__S-adenosyl-L-homocysteine hydrolase | ns | ns | ns | **-0.82** | ns |
| CATMA4A14250 | AT4G14040 | EDA38_SBP2__selenium-binding protein 2 | ns | ns | **-1.01** | **-0.70** | ns |
| CATMA4A14375 | AT4G14130 | XTH15_XTR7__xyloglucan endotransglucosylase/hydrolase 15 | ns | ns | ns | ns | **-0.67** |
| CATMA4A14640 | AT4G14320 | Zinc-binding ribosomal protein family protein | ns | ns | ns | ns | **-0.70** |
| CATMA4A14700 | AT4G14365 | XBAT34__XB3 ortholog 4 in Arabidopsis thaliana | ns | ns | ns | ns | **1.36** |
| CATMA4A15020 | AT4G14630 | GLP9__germin-like protein 9 | ns | ns | ns | ns | **1.09** |
| CATMA4A15350 | AT4G14890 | FdC2__2Fe-2S ferredoxin-like superfamily protein | ns | ns | ns | **-0.97** | **-1.01** |
| CATMA4A15480 | AT4G15000 | Ribosomal L27e protein family | ns | ns | ns | ns | **-0.70** |
| CATMA4A15700 | AT4G15160 | Bifunctional inhibitor/lipid-transfer protein/seed storage 2S albumin superfamily protein | ns | ns | ns | ns | **-0.75** |
| CATMA4A15970 | AT4G15340 | 04C11_ATPEN1_PEN1__pentacyclic triterpene synthase 1 | ns | ns | ns | **-0.80** | ns |
| CATMA4D03142 | AT4G15390 | HXXXD-type acyl-transferase family protein | ns | ns | ns | **-1.39** | **-1.54** |
| CATMA4A16210 | AT4G15480 | UGT84A1__UDP-Glycosyltransferase superfamily protein | ns | ns | **1.27** | **1.02** | **1.40** |
| CATMA4A16293 | AT4G15550 | IAGLU__indole-3-acetate beta-D-glucosyltransferase | ns | ns | ns | **0.91** | ns |
| CATMA4D03144 | AT4G15630 | Uncharacterised protein family (UPF0497) | ns | ns | ns | ns | **-0.79** |
| CATMA4A16545 | AT4G15760 | MO1__monooxygenase 1 | ns | ns | ns | ns | **0.75** |
| CATMA4C42335 | AT4G16146 | cAMP-regulated phosphoprotein 19-related protein | ns | ns | ns | **-0.80** | ns |
| CATMA4A16980 | AT4G16190 | Papain family cysteine protease | ns | ns | ns | **0.91** | **0.66** |
| CATMA4A17500 | AT4G16563 | Eukaryotic aspartyl protease family protein | ns | ns | **-1.06** | **-0.73** | ns |
| CATMA4A17600 | AT4G16660 | heat shock protein 70 (Hsp 70) family protein | ns | ns | ns | ns | **0.72** |
| CATMA4A17800 | AT4G16830 | Hyaluronan / mRNA binding family | ns | ns | ns | **-0.82** | ns |

| CATMA identifier | AGI identifier | Gene annotation | 30 min | 2h | 4h | 8h | 24h |
|---|---|---|---|---|---|---|---|
| CATMA4C42351 | AT4G16860 | RPP4__Disease resistance protein (TIR-NBS-LRR class) family | ns | ns | ns | ns | **0.74** |
| CATMA_GFT_01632 | AT4G16920 | Disease resistance protein (TIR-NBS-LRR class) family | ns | ns | ns | **0.76** | **0.68** |
| CATMA4A18000 | AT4G16980 | arabinogalactan-protein family | ns | ns | ns | ns | **-1.14** |
| CATMA4A18330 | AT4G17280 | Auxin-responsive family protein | ns | **0.89** | ns | ns | ns |
| CATMA4A18370 | AT4G17340 | DELTA-TIP2_TIP2;2__tonoplast intrinsic protein 2;2 | ns | ns | ns | ns | **0.94** |
| CATMA4A18440 | AT4G17390 | Ribosomal protein L23/L15e family protein | ns | ns | ns | ns | **-0.70** |
| CATMA4A18485 | AT4G17460 | HAT1__Homeobox-leucine zipper protein 4 (HB-4) / HD-ZIP protein | ns | ns | ns | ns | **-0.83** |
| CATMA4A18580 | AT4G17560 | Ribosomal protein L19 family protein | ns | ns | ns | ns | **-0.66** |
| CATMA4A18645 | AT4G17615 | ATCBL1_CBL1_SCABP5__calcineurin B-like protein 1 | ns | ns | ns | **1.10** | **0.73** |
| CATMA4A18850 | AT4G17810 | C2H2 and C2HC zinc fingers superfamily protein | ns | ns | ns | **-0.78** | **-1.03** |
| CATMA4A18870 | AT4G17840 | unknown protein | ns | ns | ns | **0.99** | ns |
| CATMA4A19280 | AT4G18240 | ATSS4_SS4_SSIV__starch synthase 4 | ns | ns | ns | **-0.77** | ns |
| CATMA4A19570 | AT4G18480 | CH-42_CH42_CHL11_CHLI-1_CHLI1__P-loop containing nucleoside triphosphate hydrolases superfamily protein | ns | ns | ns | **-0.73** | ns |
| CATMA4A19590 | AT4G18510 | CLE2__CLAVATA3/ESR-related 2 | ns | ns | ns | **-0.92** | ns |
| CATMA4A20400 | AT4G19200 | proline-rich family protein | ns | ns | ns | **0.69** | **1.10** |
| CATMA4C42396 | AT4G19420 | Pectinacetylesterase family protein | ns | ns | ns | **-0.71** | ns |
| CATMA4C42406 | AT4G19880 | Glutathione S-transferase family protein | ns | ns | ns | ns | **0.98** |
| CATMA4A22340 | AT4G20830 | FAD-binding Berberine family protein | ns | ns | ns | **0.87** | **1.20** |
| CATMA4A22370 | AT4G20860 | FAD-binding Berberine family protein | ns | **0.91** | ns | **1.45** | **1.79** |
| CATMA4A22690 | AT4G21120 | AAT1_CAT1__amino acid transporter 1 | ns | ns | ns | ns | **0.76** |
| CATMA4A23540 | AT4G21870 | HSP20-like chaperones superfamily protein | ns | ns | ns | ns | **-0.88** |
| CATMA4A23655 | AT4G21960 | PRXR1__Peroxidase superfamily protein | ns | ns | ns | **-0.76** | ns |
| CATMA4C42448 | AT4G22210 | LCR85__low-molecular-weight cysteine-rich 85 | ns | ns | ns | **-1.56** | **-1.27** |
| CATMA4A24100 | AT4G22380 | Ribosomal protein L7Ae/L30e/S12e/Gadd45 family protein | ns | ns | ns | ns | **-0.69** |
| CATMA4A24750 | AT4G23010 | ATUTR2_UTR2__UDP-galactose transporter 2 | ns | ns | ns | ns | **0.72** |
| CATMA4A24800 | AT4G23050 | PAS domain-containing protein tyrosine kinase family protein | ns | ns | ns | **0.81** | ns |
| CATMA4A24945 | AT4G23190 | AT-RLK3_CRK11__cysteine-rich RLK (RECEPTOR-like protein kinase) 11 | ns | ns | ns | **0.80** | **1.38** |
| CATMA4A25210 | AT4G23400 | PIP1;5_PIP1D__plasma membrane intrinsic protein 1;5 | ns | ns | **-1.06** | **-0.99** | **-1.50** |
| CATMA4A25290 | AT4G23470 | PLAC8 family protein | ns | ns | ns | ns | **1.14** |
| CATMA4A25390 | AT4G23550 | ATWRKY29_WRKY29__WRKY family transcription factor | ns | ns | ns | **-0.76** | **-1.01** |
| CATMA4C42473 | AT4G23680 | Polyketide cyclase/dehydrase and lipid transport superfamily protein | ns | ns | ns | ns | **0.76** |
| CATMA4A25530 | AT4G23700 | ATCHX17_CHX17__cation/H+ exchanger 17 | ns | ns | ns | ns | **0.97** |
| CATMA4A25590 | AT4G23770 | unknown protein | ns | ns | ns | ns | **0.75** |
| CATMA4A25640 | AT4G23820 | Pectin lyase-like superfamily protein | ns | ns | ns | **-0.74** | **-0.76** |
| CATMA4A25880 | AT4G24160 | alpha/beta-Hydrolases superfamily protein | ns | ns | ns | **1.52** | **1.25** |
| CATMA4A25970 | AT4G24230 | ACBP3__acyl-CoA-binding domain 3 | ns | ns | **-1.22** | ns | ns |
| CATMA4A26240 | AT4G24510 | CER2_VC-2_VC2__HXXXD-type acyl-transferase family protein | ns | ns | ns | ns | **-0.76** |
| CATMA4A26400 | AT4G24690 | AtNBR1_NBR1__ubiquitin-associated (UBA)/TS-N domain-containing protein / octicosapeptide/Phox/Bemp1 (PB1) domain-containing protein | ns | ns | ns | ns | **0.93** |
| CATMA4A26430 | AT4G24730 | Calcineurin-like metallo-phosphoesterase superfamily protein | ns | ns | ns | **0.69** | ns |
| CATMA4A26465 | AT4G24770 | ATRBP31_ATRBP33_CP31_RBP31__31-kDa RNA binding protein | ns | ns | ns | ns | **-0.70** |
| CATMA4A26470 | AT4G24780 | Pectin lyase-like superfamily protein | ns | ns | ns | **-1.20** | **-1.15** |
| CATMA4A26620 | AT4G24930 | thylakoid lumenal 17.9 kDa protein, chloroplast | ns | ns | ns | ns | **-0.78** |
| CATMA4A26750 | AT4G25050 | ACP4__acyl carrier protein 4 | ns | ns | ns | ns | **-0.84** |
| CATMA4A26770 | AT4G25080 | CHLM__magnesium-protoporphyrin IX methyltransferase | ns | ns | **-1.06** | **-0.76** | **-0.68** |
| CATMA4A26790 | AT4G25100 | ATFSD1_FSD1__Fe superoxide dismutase 1 | ns | ns | ns | ns | **-0.89** |
| CATMA4A26860 | AT4G25170 | Uncharacterised conserved protein (UCP012943) | ns | ns | **-1.13** | ns | ns |
| CATMA4A27330 | AT4G25640 | ATDTX35_DTX35_FFT__detoxifying efflux carrier 35 | ns | **1.66** | **1.40** | **1.98** | **2.11** |
| CATMA4A27360 | AT4G25672 | CPuORF12__conserved peptide upstream open reading frame 12 | ns | ns | ns | ns | **0.84** |
| CATMA4A27430 | AT4G25740 | RNA binding Plectin/S10 domain-containing protein | ns | ns | ns | ns | **-0.86** |
| CATMA4A27590 | AT4G25890 | 60S acidic ribosomal protein family | ns | ns | ns | ns | **-0.72** |
| CATMA4A27600 | AT4G25900 | Galactose mutarotase-like superfamily protein | ns | ns | ns | ns | **0.82** |
| CATMA4A27720 | AT4G26200 | ACS7_ATACS7__1-amino-cyclopropane-1-carboxylate synthase 7 | ns | ns | ns | ns | **1.44** |
| CATMA4A28100 | AT4G26530 | Aldolase superfamily protein | ns | ns | **-1.32** | **-1.03** | **-1.31** |
| CATMA4A28430 | AT4G26850 | VTC2__mannose-1-phosphate guanylyltransferase (GDP)s | ns | ns | ns | ns | **0.84** |
| CATMA4C42516 | AT4G27090 | Ribosomal protein L14 | ns | ns | ns | ns | **-0.71** |
| CATMA4C42519 | AT4G27270 | Quinone reductase family protein | ns | **0.98** | **1.20** | **1.69** | **1.56** |
| CATMA4C42532 | AT4G28080 | Tetratricopeptide repeat (TPR)-like superfamily protein | ns | ns | ns | **-0.78** | ns |
| CATMA4A29880 | AT4G28240 | Wound-responsive family protein | ns | ns | **-1.01** | ns | ns |
| CATMA4A29890 | AT4G28250 | ATEXPB3_ATHEXP BETA 1.6_EXPB3__expansin B3 | ns | ns | ns | **-0.77** | **-0.87** |
| CATMA4A30310 | AT4G28660 | PSB28__photosystem II reaction center PSB28 protein | ns | ns | ns | ns | **-0.71** |
| CATMA4A30705 | AT4G29040 | RPT2a__regulatory particle AAA-ATPase 2A | ns | ns | ns | ns | **0.79** |
| CATMA4A30720 | AT4G29060 | emb2726__elongation factor Ts family protein | ns | ns | ns | **-1.07** | ns |
| CATMA4A31300 | AT4G29670 | ACHT2__atypical CYS HIS rich thioredoxin 2 | ns | ns | ns | **0.80** | ns |
| CATMA4A31560 | AT4G29905 | unknown protein | ns | ns | **-1.16** | **-0.76** | **-1.83** |
| CATMA4A31820 | AT4G30190 | AHA2_HA2_PMA2__H(+)-ATPase 2 | ns | ns | ns | **-1.12** | **0.68** |

| CATMA identifier | AGI identifier | Gene annotation | 30 min | 2h | 4h | 8h | 24h |
|---|---|---|---|---|---|---|---|
| CATMA_GFT_01747 | AT4G30280 | ATXTH18_XTH18__xyloglucan endotransglucosylase/hydrolase 18 | ns | ns | ns | ns | **1.86** |
| CATMA4A32100 | AT4G30480 | AtTPR1_TPR1__Tetratricopeptide repeat (TPR)-like superfamily protein | ns | ns | ns | **1.01** | **0.87** |
| CATMA4A32140 | AT4G30530 | GGP1__Class I glutamine amidotransferase-like superfamily protein | ns | ns | ns | **-0.69** | ns |
| CATMA4C42566 | AT4G30670 | Putative membrane lipoprotein | ns | ns | ns | ns | **-0.71** |
| CATMA4A32330 | AT4G30720 | PDE327__FAD/NAD(P)-binding oxidoreductase family protein | ns | ns | ns | **-0.74** | ns |
| CATMA4A33066 | AT4G31380 | FLP1__FPF1-like protein 1 | ns | ns | ns | **0.70** | ns |
| CATMA4A33145 | AT4G31500 | ATR4_CYP83B1_RED1_RNT1_SUR2__cytochrome P450, family 83, subfamily B, polypeptide 1 | ns | ns | ns | **-1.51** | ns |
| CATMA4A33440 | AT4G31800 | ATWRKY18_WRKY18__WRKY DNA-binding protein 18 | ns | ns | ns | ns | **0.90** |
| CATMA4A33510 | AT4G31850 | PGR3__proton gradient regulation 3 | ns | ns | ns | **1.09** | **0.79** |
| CATMA4C42596 | AT4G32410 | AtCESA1_CESA1_RSW1__cellulose synthase 1 | ns | ns | ns | **-0.75** | ns |
| CATMA4A34760 | AT4G33010 | AtGLDP1_GLDP1__glycine decarboxylase P-protein 1 | ns | ns | ns | **-0.97** | **-0.83** |
| CATMA4A34830 | AT4G33090 | APM1_ATAPM1__aminopeptidase M1 | ns | ns | ns | **-0.75** | ns |
| CATMA4A35030 | AT4G33300 | ADR1-L1__ADR1-like 1 | ns | ns | ns | ns | **0.82** |
| CATMA4A35140 | AT4G33420 | Peroxidase superfamily protein | ns | ns | ns | **0.74** | **0.85** |
| CATMA4A35270 | AT4G33540 | metallo-beta-lactamase family protein | ns | ns | ns | ns | **0.77** |
| CATMA_GFT_01764 | AT4G33610 | glycine-rich protein | ns | **1.24** | **1.49** | **0.69** | **0.80** |
| CATMA4A35720 | AT4G33920 | Protein phosphatase 2C family protein | ns | **0.81** | ns | **0.76** | **1.06** |
| CATMA4A35845 | AT4G34050 | CCoAOMT1__S-adenosyl-L-methionine-dependent methyltransferases superfamily protein | ns | ns | ns | **-1.80** | **-1.30** |
| CATMA4A35910 | AT4G34120 | CBSX2_CDCP1_LEJ1__Cystathionine beta-synthase (CBS) family protein | ns | ns | ns | **0.77** | **0.86** |
| CATMA4A35920 | AT4G34131 | UGT73B3__UDP-glucosyl transferase 73B3 | ns | ns | ns | **1.31** | **1.38** |
| CATMA4A35950 | AT4G34138 | UGT73B1__UDP-glucosyl transferase 73B1 | ns | ns | ns | **1.00** | **0.87** |
| CATMA4A35980 | AT4G34150 | Calcium-dependent lipid-binding (CaLB domain) family protein | ns | ns | ns | ns | **0.78** |
| CATMA4A36070 | AT4G34250 | KCS16__3-ketoacyl-CoA synthase 16 | ns | ns | ns | **0.70** | ns |
| CATMA4A36120 | AT4G34290 | SWIB/MDM2 domain superfamily protein | ns | ns | ns | ns | **-0.74** |
| CATMA4A36210 | AT4G34380 | Transducin/WD40 repeat-like superfamily protein | ns | ns | ns | ns | **0.69** |
| CATMA4A36220 | AT4G34390 | XLG2__extra-large GTP-binding protein 2 | ns | ns | ns | ns | **0.71** |
| CATMA4A36460 | AT4G34620 | SSR16__small subunit ribosomal protein 16 | ns | ns | ns | ns | **-0.85** |
| CATMA4A36493 | AT4G34670 | Ribosomal protein S3Ae | ns | ns | ns | ns | **-0.76** |
| CATMA4A36503 | AT4G34710 | ADC2_ATADC2_SPE2__arginine decarboxylase 2 | ns | ns | ns | **0.93** | **1.40** |
| CATMA4A36600 | AT4G34830 | MRL1_PDE346__Pentatricopeptide repeat (PPR) superfamily protein | ns | ns | ns | **-0.78** | ns |
| CATMA4A36827 | AT4G35100 | PIP2;7_PIP3_PIP3A_SIMIP__plasma membrane intrinsic protein 3 | ns | ns | ns | ns | **-1.26** |
| CATMA4A37120 | AT4G35430 | unknown protein | ns | ns | ns | **-0.83** | ns |
| CATMA4A37660 | AT4G36010 | Pathogenesis-related thaumatin superfamily protein | ns | ns | **1.26** | **1.24** | **0.95** |
| CATMA4A37700 | AT4G36050 | endonuclease/exonuclease/phosphatase family protein | ns | ns | ns | **0.77** | ns |
| CATMA4A38150 | AT4G36610 | alpha/beta-Hydrolases superfamily protein | ns | **1.43** | ns | ns | ns |
| CATMA4A38190 | AT4G36640 | Sec14p-like phosphatidylinositol transfer family protein | ns | ns | ns | ns | **0.75** |
| CATMA4A38320 | AT4G36760 | APP1_ATAPP1__aminopeptidase P1 | ns | ns | ns | ns | **0.74** |
| CATMA4A38440 | AT4G36850 | PQ-loop repeat family protein / transmembrane family protein | ns | ns | **-1.17** | ns | **-0.95** |
| CATMA4A38575 | AT4G36990 | AT-HSFB1_ATHSF4_HSF4_HSFB1__heat shock factor 4 | ns | **1.32** | ns | **1.81** | **1.72** |
| CATMA4A38880 | AT4G37300 | MEE59__maternal effect embryo arrest 59 | ns | ns | ns | **-0.94** | ns |
| CATMA4C42674 | AT4G37370 | CYP81D8__cytochrome P450, family 81, subfamily D, polypeptide 8 | ns | ns | ns | **0.86** | **1.07** |
| CATMA4A39300 | AT4G37800 | XTH7__xyloglucan endotransglucosylase/hydrolase 7 | ns | ns | ns | **-0.69** | ns |
| CATMA4A39440 | AT4G37925 | NDH-M_NdhM__subunit NDH-M of NAD(P)H:plastoquinone dehydrogenase complex | ns | ns | ns | **-0.83** | **-1.07** |
| CATMA4A39445 | AT4G37930 | SHM1_SHMT1_STM__serine transhydroxymethyltransferase 1 | ns | ns | ns | ns | **-0.81** |
| CATMA4C42686 | AT4G37990 | ATCAD8_CAD-B2_ELI3_ELI3-2__elicitor-activated gene 3-2 | ns | ns | ns | ns | **2.43** |
| CATMA4A39600 | AT4G38080 | hydroxyproline-rich glycoprotein family protein | ns | **0.83** | ns | ns | ns |
| CATMA4A39680 | AT4G38160 | pde191__Mitochondrial transcription termination factor family protein | ns | ns | ns | **-0.92** | **-0.79** |
| CATMA4A40030 | AT4G38520 | Protein phosphatase 2C family protein | ns | ns | ns | **-0.80** | ns |
| CATMA4A40036 | AT4G38540 | FAD/NAD(P)-binding oxidoreductase family protein | ns | ns | ns | ns | **0.81** |
| CATMA4A40040 | AT4G38550 | Arabidopsis phospholipase-like protein (PEARLI 4) family | ns | ns | ns | ns | **0.68** |
| CATMA4A40140 | AT4G38690 | PLC-like phosphodiesterases superfamily protein | ns | ns | ns | ns | **-0.71** |
| CATMA4A40230 | AT4G38810 | Calcium-binding EF-hand family protein | ns | ns | ns | **0.88** | ns |
| CATMA4C42695 | AT4G38840 | SAUR-like auxin-responsive protein family | ns | ns | ns | **-0.84** | **-1.31** |
| CATMA4A40290 | AT4G38860 | SAUR-like auxin-responsive protein family | ns | ns | ns | ns | **-0.70** |
| CATMA4A40580 | AT4G39090 | RD19_RD19A__Papain family cysteine protease | ns | ns | ns | ns | **0.72** |
| CATMA4C42701 | AT4G39330 | ATCAD9_CAD9__cinnamyl alcohol dehydrogenase 9 | ns | ns | ns | **-0.82** | ns |
| CATMA4A40743 | AT4G39350 | ATCESA2_ATH-A_CESA2__cellulose synthase A2 | ns | ns | ns | **-1.10** | ns |
| CATMA4A41030 | AT4G39675 | unknown protein | ns | ns | **-1.04** | ns | ns |
| CATMA4A41393 | AT4G39980 | DHS1__3-deoxy-D-arabino-heptulosonate 7-phosphate synthase 1 | ns | **-0.98** | **-1.02** | **-1.76** | **-1.19** |
| CATMA5A00030 | AT5G01015 | unknown protein | ns | ns | ns | **-0.78** | **-1.03** |
| CATMA5A00240 | AT5G01210 | HXXXD-type acyl-transferase family protein | ns | ns | **-1.65** | **-1.37** | ns |
| CATMA5A00600 | AT5G01540 | LECRKA4.1__lectin receptor kinase a4.1 | ns | ns | ns | ns | **1.17** |
| CATMA5A00790 | AT5G01740 | Nuclear transport factor 2 (NTF2) family protein | ns | ns | ns | **0.72** | ns |
| CATMA5A00800 | AT5G01750 | Protein of unknown function (DUF567) | ns | ns | ns | ns | **0.72** |

| CATMA identifier | AGI identifier | Gene annotation | 30 min | 2h | 4h | 8h | 24h |
|---|---|---|---|---|---|---|---|
| CATMA5A00870 | AT5G01820 | ATCIPK14_ATSR1_CIPK14_PKS24_SnRK3.15_SR1__serine/threonine protein kinase 1 | ns | ns | ns | ns | **0.69** |
| CATMA5A01340 | AT5G02260 | ATEXP9_ATEXPA9_ATHEXP ALPHA 1.10_EXP9_EXPA9__expansin A9 | ns | ns | ns | ns | **-0.93** |
| CATMA5A01530 | AT5G02450 | Ribosomal protein L36e family protein | ns | ns | ns | ns | **-0.90** |
| CATMA5A01570 | AT5G02490 | AtHsp70-2_Hsp70-2__Heat shock protein 70 (Hsp 70) family protein | ns | ns | ns | ns | **1.16** |
| CATMA5A01910 | AT5G02820 | BIN5_RHL2__Spo11/DNA topoisomerase VI, subunit A protein | ns | ns | ns | **-0.73** | ns |
| CATMA5A02060 | AT5G02960 | Ribosomal protein S12/S23 family protein | ns | ns | ns | ns | **-0.67** |
| CATMA5A02260 | AT5G03150 | JKD__C2H2-like zinc finger protein | ns | ns | ns | ns | **0.82** |
| CATMA5A02400 | AT5G03290 | IDH-V__isocitrate dehydrogenase V | ns | ns | ns | ns | **0.71** |
| CATMA5A02410 | AT5G03300 | ADK2__adenosine kinase 2 | ns | ns | ns | **-0.99** | **-0.94** |
| CATMA5A02790 | AT5G03610 | GDSL-like Lipase/Acylhydrolase superfamily protein | ns | ns | ns | ns | **1.15** |
| CATMA5A02810 | AT5G03630 | ATMDAR2__Pyridine nucleotide-disulphide oxidoreductase family protein | ns | ns | ns | **0.75** | **1.80** |
| CATMA5A03320 | AT5G04140 | FD-GOGAT_GLS1_GLU1_GLUS__glutamate synthase 1 | ns | ns | ns | ns | **-0.70** |
| CATMA5A03420 | AT5G04230 | ATPAL3_PAL3__phenyl alanine ammonia-lyase 3 | ns | ns | ns | **-0.88** | **-0.81** |
| CATMA5A03450 | AT5G04250 | Cysteine proteinases superfamily protein | ns | ns | ns | **0.73** | ns |
| CATMA5A03550 | AT5G04340 | C2H2_CZF2_ZAT6__zinc finger of Arabidopsis thaliana 6 | ns | **0.96** | ns | ns | ns |
| CATMA5C64056 | AT5G04410 | anac078_NAC2__NAC domain containing protein 2 | ns | ns | ns | ns | **0.75** |
| CATMA5A03660 | AT5G04430 | BTR1_BTR1L_BTR1S__binding to TOMV RNA 1L (long form) | ns | ns | ns | ns | **-0.72** |
| CATMA5A03750 | AT5G04530 | KCS19__3-ketoacyl-CoA synthase 19 | ns | ns | ns | ns | **-0.66** |
| CATMA5A04460 | AT5G05270 | Chalcone-flavanone isomerase family protein | ns | ns | ns | ns | **-1.10** |
| CATMA5A04585 | AT5G05410 | DREB2_DREB2A__DRE-binding protein 2A | ns | ns | ns | **1.64** | **1.26** |
| CATMA5A05530 | AT5G06320 | NHL3__NDR1/HIN1-like 3 | ns | ns | ns | ns | **1.60** |
| CATMA5C64099 | AT5G06860 | ATPGIP1_PGIP1__polygalacturonase inhibiting protein 1 | ns | ns | ns | ns | **0.90** |
| CATMA5A06270 | AT5G07090 | Ribosomal protein S4 (RPS4A) family protein | ns | ns | ns | ns | **-0.80** |
| CATMA5A06560 | AT5G07340 | Calreticulin family protein | ns | ns | ns | **-0.96** | ns |
| CATMA5A07120 | AT5G07870 | HXXXD-type acyl-transferase family protein | ns | ns | ns | **1.20** | ns |
| CATMA_GFT_01848 | AT5G09590 | HSC70-5_MTHSC70-2__mitochondrial HSO70 2 | ns | ns | ns | **0.71** | **0.96** |
| CATMA5A08637 | AT5G09870 | CESA5__cellulose synthase 5 | ns | ns | ns | **-0.76** | ns |
| CATMA5A09290 | AT5G10560 | Glycosyl hydrolase family protein | ns | ns | ns | **-1.00** | ns |
| CATMA5A09510 | AT5G10770 | Eukaryotic aspartyl protease family protein | ns | ns | ns | ns | **0.67** |
| CATMA5A09830 | AT5G11070 | unknown protein | ns | ns | ns | **-1.05** | ns |
| CATMA5A09870 | AT5G11110 | ATSPS2F_KNS2_SPS1_SPS2F_SPSA2__sucrose phosphate synthase 2F | ns | **1.20** | ns | ns | **0.84** |
| CATMA5A10190 | AT5G11420 | Protein of unknown function, DUF642 | ns | ns | ns | **-0.79** | **-0.71** |
| CATMA5A10285 | AT5G11520 | ASP3_YLS4__aspartate aminotransferase 3 | ns | ns | ns | **0.72** | ns |
| CATMA5A10440 | AT5G11670 | ATNADP-ME2_NADP-ME2__NADP-malic enzyme 2 | ns | ns | ns | ns | **1.06** |
| CATMA5A11120 | AT5G12890 | UDP-Glycosyltransferase superfamily protein | ns | ns | ns | ns | **0.67** |
| CATMA_GFT_03239 | AT5G12960 | Putative glycosyl hydrolase of unknown function (DUF1680) | ns | **1.12** | ns | ns | ns |
| CATMA5A11290 | AT5G13080 | ATWRKY75_WRKY75__WRKY DNA-binding protein 75 | ns | ns | ns | **1.14** | ns |
| CATMA5A11330 | AT5G13120 | ATCYP20-2_CYP20-2_Pnsl5__cyclophilin 20-2 | ns | ns | ns | ns | **-0.67** |
| CATMA5A11350 | AT5G13140 | Pollen Ole e 1 allergen and extensin family protein | ns | ns | ns | ns | **-0.78** |
| CATMA5C64213 | AT5G13190 | AtGILP_GILP__CONTAINS InterPro DOMAIN/s: LPS-induced tumor necrosis factor alpha factor | ns | **0.80** | ns | **0.69** | **1.22** |
| CATMA5A11410 | AT5G13200 | GRAM domain family protein | ns | **0.80** | ns | ns | **0.69** |
| CATMA5C64215 | AT5G13320 | GDG1_GH3.12_PBS3_WIN3__Auxin-responsive GH3 family protein | ns | ns | ns | ns | **1.54** |
| CATMA5A11620 | AT5G13420 | Aldolase-type TIM barrel family protein | ns | ns | ns | **-0.89** | ns |
| CATMA5A11720 | AT5G13490 | AAC2__ADP/ATP carrier 2 | ns | ns | ns | **0.69** | **1.00** |
| CATMA5A11860 | AT5G13630 | ABAR_CCH_CCH1_CHLH_GUN5__magnesium-chelatase subunit chlH, chloroplast, putative / Mg-protoporphyrin IX chelatase, putative (CHLH) | ns | ns | ns | **-0.79** | ns |
| CATMA5A11990 | AT5G13750 | ZIFL1__zinc induced facilitator-like 1 | ns | ns | ns | **1.40** | **0.91** |
| CATMA5A12150 | AT5G13930 | ATCHS_CHS_TT4__Chalcone and stilbene synthase family protein | ns | ns | ns | ns | **-0.90** |
| CATMA5A12210 | AT5G13980 | Glycosyl hydrolase family 38 protein | ns | ns | ns | **-0.88** | ns |
| CATMA5A12350 | AT5G14120 | Major facilitator superfamily protein | ns | ns | **-2.20** | ns | **-0.90** |
| CATMA5A12650 | AT5G14410 | unknown protein | ns | ns | ns | **-0.98** | **-1.15** |
| CATMA5A12710 | AT5G14470 | GHMP kinase family protein | ns | ns | ns | **0.98** | ns |
| CATMA5A12950 | AT5G14730 | Unknown protein | ns | ns | ns | **0.77** | ns |
| CATMA5C64237 | AT5G14740 | BETA CA2_CA18_CA2__carbonic anhydrase 2 | ns | ns | ns | ns | **-0.95** |
| CATMA5A13000 | AT5G14780 | FDH__formate dehydrogenase | ns | ns | ns | ns | **1.33** |
| CATMA5A13200 | AT5G14930 | SAG101__senescence-associated gene 101 | ns | ns | ns | ns | **0.98** |
| CATMA5A13675 | AT5G15410 | ATCNGC2_CNGC2_DND1__Cyclic nucleotide-regulated ion channel family protein | ns | ns | ns | **-0.78** | ns |
| CATMA5A13890 | AT5G15640 | Mitochondrial substrate carrier family protein | ns | ns | ns | **1.19** | ns |
| CATMA5C64254 | AT5G15970 | AtCor6.6_COR6.6_KIN2__stress-responsive protein (KIN2) / stress-induced protein (KIN2) / cold-responsive protein (COR6.6) / cold-regulated protein (COR6.6) | ns | ns | ns | ns | **0.78** |
| CATMA5A14290 | AT5G16010 | 3-oxo-5-alpha-steroid 4-dehydrogenase family protein | ns | ns | ns | ns | **1.01** |
| CATMA5A14420 | AT5G16130 | Ribosomal protein S7e family protein | ns | ns | ns | ns | **-0.97** |
| CATMA_GFT_01871 | AT5G16970 | AER_AT-AER__alkenal reductase | ns | ns | ns | **1.15** | **1.28** |
| CATMA5C64275 | AT5G17000 | Zinc-binding dehydrogenase family protein | ns | ns | ns | **1.02** | **1.09** |
| CATMA5A15505 | AT5G17230 | PSY__PHYTOENE SYNTHASE | ns | ns | ns | **-0.86** | ns |
| CATMA5A15570 | AT5G17300 | RVE1__Homeodomain-like superfamily protein | ns | ns | ns | ns | **-0.88** |
| CATMA5A15640 | AT5G17380 | Thiamine pyrophosphate dependent pyruvate decarboxylase family protein | ns | ns | ns | ns | **1.48** |

| CATMA identifier | AGI identifier | Gene annotation | 30 min | 2h | 4h | 8h | 24h |
|---|---|---|---|---|---|---|---|
| CATMA5A15960 | AT5G17670 | alpha/beta-Hydrolases superfamily protein | ns | ns | ns | ns | **-0.66** |
| CATMA5A16060 | AT5G17760 | P-loop containing nucleoside triphosphate hydrolases superfamily protein | ns | ns | ns | ns | **0.91** |
| CATMA5A16140 | AT5G17860 | CAX7__calcium exchanger 7 | ns | ns | ns | ns | **0.66** |
| CATMA5A16195 | AT5G17920 | ATCIMS_ATMETS_ATMS1__Cobalamin-independent synthase family protein | ns | ns | ns | **-1.06** | **-0.99** |
| CATMA5A16780 | AT5G18480 | PGSIP6__plant glycogenin-like starch initiation protein 6 | ns | ns | ns | ns | **1.05** |
| CATMA5A17020 | AT5G18670 | BAM9_BMY3__beta-amylase 3 | ns | ns | ns | ns | **-1.17** |
| CATMA5A17550 | AT5G19140 | AILP1_ATAILP1__Aluminium induced protein with YGL and LRDR motifs | ns | ns | **-1.03** | ns | ns |
| CATMA5A17870 | AT5G19440 | NAD(P)-binding Rossmann-fold superfamily protein | ns | ns | ns | ns | **1.28** |
| CATMA5A17990 | AT5G19550 | AAT2_ASP2__aspartate aminotransferase 2 | ns | ns | ns | ns | **1.26** |
| CATMA5C64314 | AT5G19800 | hydroxyproline-rich glycoprotein family protein | ns | ns | ns | ns | **0.67** |
| CATMA5A18280 | AT5G19855 | AtRbcX2_RbcX2__Chaperonin-like RbcX protein | ns | ns | ns | **0.73** | ns |
| CATMA5A18380 | AT5G19940 | Plastid-lipid associated protein PAP / fibrillin family protein | ns | ns | ns | ns | **-0.74** |
| CATMA5A18440 | AT5G20000 | AAA-type ATPase family protein | ns | ns | ns | ns | **0.79** |
| CATMA5A18670 | AT5G20230 | ATBCB_BCB_BCB_SAG14__blue-copper-binding protein | ns | ns | ns | ns | **0.72** |
| CATMA5A18720 | AT5G20280 | ATSPS1F_SPS1F_SPSA1__sucrose phosphate synthase 1F | ns | ns | ns | **-0.72** | ns |
| CATMA5C64324 | AT5G20400 | 2-oxoglutarate (2OG) and Fe(II)-dependent oxygenase superfamily protein | ns | ns | ns | ns | **1.03** |
| CATMA5A19130 | AT5G20630 | ATGER3_GER3_GLP3_GLP3A_GLP3B__germin 3 | ns | ns | ns | **-0.84** | ns |
| CATMA5C64371 | AT5G22140 | FAD/NAD(P)-binding oxidoreductase family protein | ns | ns | ns | **2.15** | **1.97** |
| CATMA5A19778 | AT5G22350 | ELM1__Protein of unknown function (DUF1022) | ns | ns | ns | ns | **0.73** |
| CATMA5A19900 | AT5G22440 | Ribosomal protein L1p/L10e family | ns | ns | ns | ns | **-0.80** |
| CATMA5A20120 | AT5G22640 | emb1211__MORN (Membrane Occupation and Recognition Nexus) repeat-containing protein | ns | ns | ns | **-0.90** | ns |
| CATMA5A20350 | AT5G22850 | Eukaryotic aspartyl protease family protein | ns | ns | ns | ns | **0.69** |
| CATMA5A20510 | AT5G23020 | IMS2_MAM-L_MAM3__2-isopropylmalate synthase 2 | ns | ns | ns | **-0.86** | ns |
| CATMA5A21060 | AT5G23540 | Mov34/MPN/PAD-1 family protein | ns | ns | ns | ns | **0.68** |
| CATMA5A21225 | AT5G23740 | RPS11-BETA__ribosomal protein S11-beta | ns | ns | ns | ns | **-0.87** |
| CATMA5A21620 | AT5G24090 | ATCHIA_CHIA__chitinase A | ns | **1.01** | ns | **1.50** | **1.48** |
| CATMA5A21750 | AT5G24200 | alpha/beta-Hydrolases superfamily protein | ns | ns | ns | ns | **1.03** |
| CATMA5A21760 | AT5G24210 | alpha/beta-Hydrolases superfamily protein | ns | ns | ns | ns | **1.32** |
| CATMA5A21890 | AT5G24314 | PDE225_PTAC7__plastid transcriptionally active7 | ns | ns | ns | **-0.72** | ns |
| CATMA5A22030 | AT5G24420 | PGL5__6-phosphogluconolactonase 5 | ns | ns | ns | ns | **-1.20** |
| CATMA5A22430 | AT5G24760 | GroES-like zinc-binding dehydrogenase family protein | ns | ns | ns | **-1.08** | **-1.19** |
| CATMA5A22960 | AT5G25250 | SPFH/Band 7/PHB domain-containing membrane-associated protein family | ns | ns | ns | ns | **1.38** |
| CATMA5C64427 | AT5G25260 | SPFH/Band 7/PHB domain-containing membrane-associated protein family | ns | ns | ns | ns | **2.07** |
| CATMA5C64436 | AT5G25460 | Protein of unknown function, DUF642 | ns | ns | **-1.30** | **-1.72** | **-1.41** |
| CATMA5A23590 | AT5G25930 | Protein kinase family protein with leucine-rich repeat domain | ns | ns | ns | **1.18** | **1.06** |
| CATMA5A23675 | AT5G26030 | ATFC-I_FC-I_FC1__ferrochelatase 1 | ns | ns | ns | ns | **0.69** |
| CATMA5C64456 | AT5G26260 | TRAF-like family protein | ns | ns | ns | **-0.78** | **-0.99** |
| CATMA_GFT_01923 | AT5G26280 | TRAF-like family protein | ns | ns | **-1.02** | ns | **-0.86** |
| CATMA5C64457 | AT5G26290 | TRAF-like family protein | ns | **-0.87** | ns | **-1.50** | **-1.36** |
| CATMA5A24060 | AT5G26570 | ATGWD3_OK1_PWD__catalytics;carbohydrate kinases;phosphoglucan, water dikinases | ns | ns | ns | **-0.75** | ns |
| CATMA5A24080 | AT5G26740 | Protein of unknown function (DUF300) | ns | ns | ns | ns | **-0.66** |
| CATMA5A24850 | AT5G27420 | ATL31_CNI1__carbon/nitrogen insensitive 1 | ns | **0.91** | ns | **1.50** | **1.39** |
| CATMA5A24910 | AT5G27520 | AtPNC2_PNC2__peroxisomal adenine nucleotide carrier 2 | ns | ns | ns | **0.72** | ns |
| CATMA5A25170 | AT5G27760 | Hypoxia-responsive family protein | ns | ns | ns | **1.19** | **1.43** |
| CATMA5A25280 | AT5G27850 | Ribosomal protein L18e/L15 superfamily protein | ns | ns | ns | ns | **-0.92** |
| CATMA5A26920 | AT5G28840 | GME__GDP-D-mannose 3',5'-epimerase | ns | ns | **-1.01** | ns | ns |
| CATMA5C64535 | AT5G33320 | ARAPPT_CUE1_PPT__Glucose-6-phosphate/phosphate translocator-related | ns | ns | ns | **-0.87** | ns |
| CATMA5C64549 | AT5G35480 | unknown protein | ns | ns | ns | ns | **-0.68** |
| CATMA5A30990 | AT5G35690 | unknown protein | ns | ns | ns | **0.83** | **0.86** |
| CATMA5A31080 | AT5G35735 | Auxin-responsive family protein | ns | **1.01** | **1.09** | **1.15** | **1.12** |
| CATMA5A31830 | AT5G36270 | Unknown protein | ns | ns | **1.38** | **1.56** | **1.74** |
| CATMA5A32135 | AT5G36910 | THI2.2__thionin 2.2 | ns | ns | ns | ns | **-1.73** |
| CATMA5A32230 | AT5G36960 | unknown protein | ns | ns | ns | ns | **0.68** |
| CATMA5A32930 | AT5G37600 | ATGLN1;1_ATGSR1_GLN1;1_GSR 1__glutamine synthase clone R1 | ns | ns | ns | ns | **1.29** |
| CATMA5C64593 | AT5G37920 | Family of unknown function (DUF577) | ns | ns | ns | **0.80** | **0.79** |
| CATMA5C64595 | AT5G38020 | S-adenosyl-L-methionine-dependent methyltransferases superfamily protein | ns | ns | **1.15** | ns | ns |
| CATMA5A33960 | AT5G38410 | Ribulose bisphosphate carboxylase (small chain) family protein | ns | ns | ns | ns | **-0.81** |
| CATMA5C64608 | AT5G38430 | Ribulose bisphosphate carboxylase (small chain) family protein | ns | ns | ns | **-0.74** | **-0.98** |
| CATMA5A34050 | AT5G38520 | alpha/beta-Hydrolases superfamily protein | ns | ns | ns | ns | **-0.69** |
| CATMA5A34060 | AT5G38530 | TSBtype2__tryptophan synthase beta type 2 | ns | ns | ns | ns | **0.68** |
| CATMA5A34590 | AT5G38980 | unknown protein | ns | ns | ns | **-0.96** | **-1.09** |
| CATMA5A34660 | AT5G39050 | PMAT1__HXXXD-type acyl-transferase family protein | ns | **0.86** | ns | **0.86** | **1.57** |
| CATMA5A34710 | AT5G39090 | HXXXD-type acyl-transferase family protein | ns | ns | ns | **0.82** | **1.05** |
| CATMA5A34820 | AT5G39210 | CRR7__chlororespiratory reduction 7 | ns | ns | ns | **-1.27** | **-0.89** |
| CATMA5A35160 | AT5G39580 | Peroxidase superfamily protein | ns | ns | **-1.78** | ns | **1.01** |

| CATMA identifier | AGI identifier | Gene annotation | 30 min | 2h | 4h | 8h | 24h |
|---|---|---|---|---|---|---|---|
| CATMA5A35200 | AT5G39610 | ANAC092_ATNAC2_ATNAC6_NAC2_NAC6_ORE1__NAC domain containing protein 6 | ns | ns | ns | ns | **0.82** |
| CATMA5A35240 | AT5G39670 | Calcium-binding EF-hand family protein | ns | ns | ns | ns | **1.38** |
| CATMA5A36030 | AT5G40370 | GRXC2__Glutaredoxin family protein | ns | ns | ns | ns | **0.79** |
| CATMA5A36458 | AT5G40780 | LHT1__lysine histidine transporter 1 | ns | ns | ns | **-0.85** | **0.93** |
| CATMA5A36700 | AT5G41040 | HXXXD-type acyl-transferase family protein | ns | **0.91** | ns | ns | ns |
| CATMA5A37020 | AT5G41390 | PLAC8 family protein | ns | ns | ns | ns | **0.79** |
| CATMA5A37030 | AT5G41400 | RING/U-box superfamily protein | ns | **0.91** | **1.04** | **0.85** | **0.91** |
| CATMA5A37770 | AT5G42050 | DCD (Development and Cell Death) domain protein | ns | ns | ns | ns | **1.41** |
| CATMA5A37800 | AT5G42090 | Lung seven transmembrane receptor family protein | ns | ns | ns | ns | **0.69** |
| CATMA5A37820 | AT5G42100 | ATBG_PPAP_BG_PPAP__beta-1,3-glucanase_putative | ns | ns | ns | **-0.77** | ns |
| CATMA5A37830 | AT5G42110 | unknown protein | ns | ns | ns | ns | **-0.76** |
| CATMA5C64706 | AT5G42300 | UBL5__ubiquitin-like protein 5 | ns | ns | ns | **0.81** | **1.23** |
| CATMA5A39130 | AT5G43260 | chaperone protein dnaJ-related | ns | ns | ns | **0.71** | ns |
| CATMA5A39290 | AT5G43430 | ETFBETA__electron transfer flavoprotein beta | ns | ns | ns | **0.86** | ns |
| CATMA5A39530 | AT5G43700 | ATAUX2-11_IAA4__AUX/IAA transcriptional regulator family protein | ns | ns | ns | **-0.89** | **-1.08** |
| CATMA5A40380 | AT5G44580 | unknown protein | ns | ns | ns | **-0.81** | ns |
| CATMA5A40400 | AT5G44585 | unknown protein | ns | ns | **-1.48** | **-0.99** | ns |
| CATMA5A41300 | AT5G45350 | proline-rich family protein | ns | ns | ns | ns | **0.84** |
| CATMA5A41430 | AT5G45490 | P-loop containing nucleoside triphosphate hydrolases superfamily protein | ns | ns | ns | **-0.89** | **-0.68** |
| CATMA5A41930 | AT5G45930 | CHL I2_CHLI-2_CHLI2__magnesium chelatase i2 | ns | ns | ns | **-0.88** | ns |
| CATMA5A42580 | AT5G46580 | pentatricopeptide (PPR) repeat-containing protein | ns | ns | ns | **-0.93** | ns |
| CATMA5A42810 | AT5G46800 | BOU__Mitochondrial substrate carrier family protein | ns | ns | ns | ns | **-0.69** |
| CATMA5C64809 | AT5G47120 | ATBI-1_ATBI1_BI-1_BI1__BAX inhibitor 1 | ns | ns | ns | ns | **1.21** |
| CATMA5A43120 | AT5G47130 | Bax inhibitor-1 family protein | ns | ns | ns | ns | **1.16** |
| CATMA5A43190 | AT5G47200 | ATRAB1A_ATRABD2B_RAB1A__RAB GTPase homolog 1A | ns | ns | ns | ns | **0.76** |
| CATMA5A43205 | AT5G47220 | ATERF-2_ATERF2_ERF2__ethylene responsive element binding factor 2 | ns | ns | ns | ns | **0.80** |
| CATMA5A43920 | AT5G47950 | HXXXD-type acyl-transferase family protein | ns | ns | ns | **-0.96** | **-1.11** |
| CATMA5C64822 | AT5G47990 | CYP705A5_THAD_THAD1__cytochrome P450, family 705, subfamily A, polypeptide 5 | ns | ns | ns | **-0.75** | ns |
| CATMA5A44340 | AT5G48380 | BIR1__BAK1-interacting receptor-like kinase 1 | ns | ns | ns | ns | **0.74** |
| CATMA_GFT_02191 | AT5G48400 | ATGLR1.2_GLR1.2__Glutamate receptor family protein | ns | ns | ns | **0.77** | **1.54** |
| CATMA5A44410 | AT5G48430 | Eukaryotic aspartyl protease family protein | ns | ns | **-1.12** | ns | **1.47** |
| CATMA5A44460 | AT5G48485 | DIR1__Bifunctional inhibitor/lipid-transfer protein/seed storage 2S albumin superfamily protein | ns | ns | ns | ns | **-0.74** |
| CATMA5A44530 | AT5G48545 | HINT3__histidine triad nucleotide-binding 3 | ns | ns | ns | ns | **-0.68** |
| CATMA5A44660 | AT5G48657 | defense protein-related | ns | ns | ns | ns | **0.80** |
| CATMA5C64839 | AT5G48810 | ATB5-B_ATCB5-D_B5 #3_CB5-D__cytochrome B5 isoform D | ns | ns | ns | **-0.71** | ns |
| CATMA5A44840 | AT5G48930 | HCT__hydroxycinnamoyl-CoA shikimate/quinate hydroxycinnamoyl transferase | ns | **-1.17** | **-1.11** | **-1.50** | **-1.18** |
| CATMA5A44970 | AT5G49030 | OVA2__tRNA synthetase class I (I, L, M and V) family protein | ns | ns | ns | **-0.77** | ns |
| CATMA5A45465 | AT5G49480 | ATCP1_CP1__Ca2+-binding protein 1 | ns | ns | ns | **0.96** | ns |
| CATMA5A45500 | AT5G49520 | ATWRKY48_WRKY48__WRKY DNA-binding protein 48 | ns | ns | ns | **0.74** | **1.05** |
| CATMA5A45660 | AT5G49730 | ATFRO6_FRO6_FRO6__ferric reduction oxidase 6 | ns | ns | **-1.35** | **-0.79** | **-1.46** |
| CATMA5A45825 | AT5G49910 | cpHsc70-2_HSC70-7__chloroplast heat shock protein 70-2 | ns | ns | ns | **-0.71** | ns |
| CATMA5A46160 | AT5G50200 | ATNRT3.1_NRT3.1_WR3__nitrate transmembrane transporters | ns | ns | ns | **0.92** | **1.17** |
| CATMA5A46170 | AT5G50210 | OLD5_QS_SUFE3__quinolinate synthase | ns | ns | ns | **0.75** | **1.02** |
| CATMA5A46355 | AT5G50375 | CPI1__cyclopropyl isomerase | ns | ns | ns | **-0.76** | ns |
| CATMA5A46860 | AT5G50920 | ATHSP93-V_CLPC1_DCA1_HSP93-V__CLPC homologue 1 | ns | ns | ns | **-0.86** | ns |
| CATMA5A46970 | AT5G51040 | unknown protein | ns | ns | ns | ns | **0.83** |
| CATMA5A46995 | AT5G51070 | CLPD_ERD1_SAG15__Clp ATPase | ns | ns | ns | ns | **0.72** |
| CATMA5A47350 | AT5G51440 | HSP20-like chaperones superfamily protein | ns | ns | ns | **0.90** | ns |
| CATMA5A47480 | AT5G51550 | EXL3__EXORDIUM like 3 | ns | ns | ns | **-0.94** | **-0.90** |
| CATMA5A47660 | AT5G51720 | 2 iron, 2 sulfur cluster binding | ns | ns | ns | ns | **-1.24** |
| CATMA5A47700 | AT5G51770 | Protein kinase superfamily protein | ns | ns | ns | ns | **1.00** |
| CATMA5A47760 | AT5G51830 | pfkB-like carbohydrate kinase family protein | ns | ns | ns | **1.07** | **1.10** |
| CATMA5A48130 | AT5G52190 | Sugar isomerase (SIS) family protein | ns | ns | ns | ns | **-0.73** |
| CATMA5A48515 | AT5G52640 | ATHS83_AtHsp90-1_ATHSP90.1_HSP81-1_HSP81.1_HSP83_HSP90.1__heat shock protein 90.1 | ns | ns | ns | ns | **1.13** |
| CATMA5A48640 | AT5G52780 | Protein of unknown function (DUF3464) | ns | ns | ns | **-0.88** | ns |
| CATMA5A48670 | AT5G52810 | NAD(P)-binding Rossmann-fold superfamily protein | ns | ns | ns | ns | **1.00** |
| CATMA5A49030 | AT5G53120 | ATSPDS3_SPDS3_SPMS__spermidine synthase 3 | ns | ns | ns | ns | **0.88** |
| CATMA5A49070 | AT5G53160 | PYL8_RCAR3__regulatory components of ABA receptor 3 | ns | ns | ns | ns | **-0.76** |
| CATMA5A49080 | AT5G53170 | FTSH11__FTSH protease 11 | ns | ns | ns | **-0.69** | ns |
| CATMA5A49360 | AT5G53460 | GLT1__NADH-dependent glutamate synthase 1 | ns | ns | ns | **-1.16** | ns |
| CATMA5A49390 | AT5G53490 | Tetratricopeptide repeat (TPR)-like superfamily protein | ns | ns | ns | ns | **-0.83** |
| CATMA5A49490 | AT5G53590 | SAUR-like auxin-responsive protein family | ns | ns | ns | **0.73** | **0.83** |
| CATMA5A49880 | AT5G53970 | TAT7__Tyrosine transaminase family protein | ns | ns | ns | **0.84** | ns |
| CATMA5A50126 | AT5G54206 | 0 | ns | ns | ns | **1.41** | **2.04** |
| CATMA5C64941 | AT5G54500 | FQR1__flavodoxin-like quinone reductase 1 | ns | **1.12** | **1.14** | **1.50** | **1.79** |

| CATMA identifier | AGI identifier | Gene annotation | 30 min | 2h | 4h | 8h | 24h |
|---|---|---|---|---|---|---|---|
| CATMA5C64943 | AT5G54640 | ATHTA1_HTA1_RAT5__Histone superfamily protein | ns | ns | ns | **0.94** | ns |
| CATMA5C64946 | AT5G54710 | Ankyrin repeat family protein | ns | ns | ns | ns | **1.15** |
| CATMA5A50595 | AT5G54770 | THI1_THI4_TZ__thiazole biosynthetic enzyme, chloroplast (ARA6) (THI1) (THI4) | ns | ns | ns | **-0.75** | **-0.89** |
| CATMA5A50760 | AT5G54960 | PDC2__pyruvate decarboxylase-2 | ns | ns | ns | ns | **0.90** |
| CATMA5A50820 | AT5G55050 | GDSL-like Lipase/Acylhydrolase superfamily protein | ns | ns | ns | ns | **0.69** |
| CATMA5A50990 | AT5G55230 | ATMAP65-1_MAP65-1_MAP65-1__microtubule-associated proteins 65-1 | ns | ns | ns | **-1.06** | ns |
| CATMA5A51370 | AT5G55620 | unknown protein | ns | ns | ns | ns | **-1.11** |
| CATMA5C64969 | AT5G55750 | hydroxyproline-rich glycoprotein family protein | ns | ns | ns | **0.95** | **1.62** |
| CATMA5A51710 | AT5G55930 | ATOPT1_OPT1__oligopeptide transporter 1 | ns | ns | ns | **-1.07** | ns |
| CATMA5A51750 | AT5G55970 | RING/U-box superfamily protein | ns | ns | ns | **0.82** | ns |
| CATMA5C64978 | AT5G56030 | AtHsp90.2_ERD8_HSP81-2_HSP81.2_HSP90.2__heat shock protein 81-2 | ns | ns | ns | ns | **0.70** |
| CATMA5A51870 | AT5G56100 | glycine-rich protein / oleosin | ns | ns | ns | ns | **-0.98** |
| CATMA5A52490 | AT5G56710 | Ribosomal protein L31e family protein | ns | ns | ns | ns | **-0.70** |
| CATMA5A53440 | AT5G57710 | Double Clp-N motif-containing P-loop nucleoside triphosphate hydrolases superfamily protein | ns | ns | ns | ns | **0.91** |
| CATMA5C65014 | AT5G57887 | unknown protein | ns | ns | **-1.02** | ns | ns |
| CATMA5A54020 | AT5G58260 | NdhN__oxidoreductases, acting on NADH or NADPH, quinone or similar compound as acceptor | ns | ns | ns | ns | **-1.05** |
| CATMA5A54045 | AT5G58290 | RPT3__regulatory particle triple-A ATPase 3 | ns | ns | ns | ns | **0.69** |
| CATMA_GFT_03391 | AT5G58570 | unknown protein | ns | ns | ns | ns | **0.70** |
| CATMA5A54650 | AT5G58900 | Homeodomain-like transcriptional regulator | ns | ns | ns | **-0.72** | ns |
| CATMA5A54840 | AT5G59090 | ATSBT4.12_SBT4.12__subtilase 4.12 | ns | ns | ns | **-0.73** | ns |
| CATMA5A55310 | AT5G59570 | BOA__Homeodomain-like superfamily protein | ns | ns | ns | **1.32** | ns |
| CATMA5A55565 | AT5G59780 | ATMYB59_ATMYB59-1_ATMYB59-2_ATMYB59-3_MYB59__myb domain protein 59 | ns | ns | ns | ns | **-0.67** |
| CATMA5A55640 | AT5G59870 | HTA6__histone H2A 6 | ns | ns | ns | ns | **-0.78** |
| CATMA5A55646 | AT5G59890 | ADF4_ATADF4__actin depolymerizing factor 4 | ns | ns | ns | ns | **0.70** |
| CATMA5A56030 | AT5G60270 | Concanavalin A-like lectin protein kinase family protein | ns | ns | ns | ns | **0.80** |
| CATMA5A56105 | AT5G60360 | AALP_ALP_SAG2__aleurain-like protease | ns | ns | ns | ns | **0.77** |
| CATMA5A56140 | AT5G60400 | unknown protein | ns | ns | ns | **-0.84** | **-0.93** |
| CATMA5A56360 | AT5G60640 | ATPDI2_ATPDIL1-4_PDI2_PDIL1-4__PDI-like 1-4 | ns | ns | ns | **-0.73** | ns |
| CATMA5A56650 | AT5G61010 | ATEXO70E2_EXO70E2__exocyst subunit exo70 family protein E2 | ns | ns | ns | ns | **0.70** |
| CATMA5A57025 | AT5G61380 | APRR1_AtTOC1_PRR1_TOC1__CCT motif -containing response regulator protein | ns | ns | ns | **-0.71** | ns |
| CATMA5A57390 | AT5G61790 | ATCNX1_CNX1__calnexin 1 | ns | ns | ns | ns | **0.72** |
| CATMA5A57420 | AT5G61820 | unknown protein | ns | ns | ns | **0.96** | **1.25** |
| CATMA5A57490 | AT5G61900 | BON_BON1_CPN1__Calcium-dependent phospholipid-binding Copine family protein | ns | ns | ns | ns | **0.68** |
| CATMA5A57623 | AT5G62020 | AT-HSFB2A_HSFB2A__heat shock transcription factor B2A | ns | **0.96** | ns | **1.07** | **0.95** |
| CATMA5C65085 | AT5G62480 | ATGSTU9_GST14_GST14B_GSTU9__glutathione S-transferase tau 9 | ns | ns | ns | ns | **0.70** |
| CATMA5A58220 | AT5G62630 | HIPL2__hipl2 protein precursor | ns | ns | ns | ns | **1.21** |
| CATMA5A58260 | AT5G62670 | AHA11_HA11__H(+)-ATPase 11 | ns | ns | ns | ns | **-0.77** |
| CATMA5A58310 | AT5G62720 | Integral membrane HPP family protein | ns | ns | ns | **0.91** | ns |
| CATMA5A58590 | AT5G63030 | GRXC1__Thioredoxin superfamily protein | ns | ns | ns | ns | **0.87** |
| CATMA5A58780 | AT5G63180 | Pectin lyase-like superfamily protein | ns | ns | ns | ns | **-0.79** |
| CATMA5A58950 | AT5G63420 | emb2746__RNA-metabolising metallo-beta-lactamase family protein | ns | ns | ns | **-0.74** | ns |
| CATMA5A59230 | AT5G63680 | Pyruvate kinase family protein | ns | ns | ns | ns | **0.79** |
| CATMA5A59330 | AT5G63790 | ANAC102_NAC102__NAC domain containing protein 102 | ns | ns | ns | ns | **0.90** |
| CATMA5A59535 | AT5G64040 | PSAN__photosystem I reaction center subunit PSI-N, chloroplast, putative / PSI-N, putative (PSAN) | ns | ns | ns | ns | **-0.86** |
| CATMA5A59575_N | AT5G64100 | Peroxidase superfamily protein | ns | **-0.84** | **-1.70** | **-0.69** | ns |
| CATMA5A59660 | AT5G64200 | At-SC35_ATSC35_SC35__ortholog of human splicing factor SC35 | ns | ns | ns | **-0.84** | ns |
| CATMA5C65119 | AT5G64250 | Aldolase-type TIM barrel family protein | ns | ns | ns | **1.62** | **1.55** |
| CATMA5A59763 | AT5G64310 | AGP1_ATAGP1__arabinogalactan protein 1 | ns | ns | ns | **0.72** | ns |
| CATMA5A60320 | AT5G64890 | PROPEP2__elicitor peptide 2 precursor | ns | ns | ns | **1.07** | ns |
| CATMA5A60423 | AT5G65010 | ASN2__asparagine synthetase 2 | ns | ns | ns | **-0.97** | **-0.84** |
| CATMA_GFT_03400 | AT5G66052 | unknown protein | ns | ns | ns | **0.75** | ns |
| CATMA5A61460 | AT5G66070 | RING/U-box superfamily protein | ns | ns | ns | ns | **0.68** |
| CATMA5A61750 | AT5G66420 | unknown protein | ns | **-0.83** | **-1.22** | ns | **0.89** |
| CATMA5A61900 | AT5G66540 | Unknown protein | ns | ns | **-1.00** | ns | ns |
| CATMA5A62120 | AT5G66720 | Protein phosphatase 2C family protein | ns | ns | ns | ns | **-0.88** |
| CATMA5A62765 | AT5G67300 | ATMYB44_ATMYBR1_MYB44_MYBR1__myb domain protein r1 | ns | ns | ns | **0.76** | **0.71** |
| CATMA5A62800 | AT5G67350 | unknown protein | ns | ns | ns | **0.96** | ns |
| CATMA5A62810 | AT5G67360 | ARA12__Subtilase family protein | ns | ns | ns | **-0.85** | ns |
| CATMA5C65166 | AT5G67600 | WIH1__unknown protein; LOCATED IN: plasma membrane | ns | ns | ns | **0.96** | ns |

**Supplemental Table III:** Genes found to be differentially expressed in all the comparisons between phenanthrene-treated and control plants (hybridizations 5-9), selected after ANOVA analysis. Among the 467 differentially expressed genes, 14, 47, 77, 275 and 360 genes were expressed at 30 min, 2 h, 4 h, 8 h and 24 h, respectively. *Arabidopsis* annotation from TAIR, called TAIR10 (most recent versions as of 21 September 2012). Expression changes are given as log2. Expression changes in bolt correspond to genes differentially expressed at the significant threshold of Bonferroni p-value<0.05. AGI and gene annotation in bold face correspond to gene involved in the "xenome".

| AGI identifier | Gene annotation | 30 min | 2h | 4h | 8h | 24h |
|---|---|---|---|---|---|---|
| AT4G38620 | ATMYB4_MYB4__myb domain protein 4 | **3.51** | **2.19** | **2.30** | **2.18** | **1.94** |
| AT2G47950 | unknown protein | **1.49** | **2.27** | **2.27** | **2.65** | **1.91** |
| AT5G48540 | receptor-like protein kinase-related family protein | **1.42** | **2.44** | **3.27** | **3.48** | **3.51** |
| AT4G15248 | B-box type zinc finger family protein | **1.39** | **1.75** | **1.04** | 0.35 | **1.63** |
| AT5G59820 | RHL41_ZAT12__C2H2-type zinc finger family protein | **1.19** | **1.63** | **2.14** | **2.70** | **2.50** |
| AT2G16900 | *Arabidopsis* phospholipase-like protein (PEARLI 4) family | **0.98** | **1.68** | **1.67** | **1.61** | **2.16** |
| AT1G68620 | alpha/beta-Hydrolases superfamily protein | **0.93** | **2.18** | **1.68** | **2.77** | **2.70** |
| AT5G56630 | PFK7__phosphofructokinase 7 | **0.91** | **1.59** | **2.41** | **1.54** | **2.53** |
| AT3G22840 | ELIP_ELIP1__Chlorophyll A-B binding family protein | **0.89** | **1.40** | **2.19** | **1.70** | **2.38** |
| AT1G63840 | RING/U-box superfamily protein | **0.83** | **1.80** | **1.64** | **2.10** | **2.16** |
| AT2G36590 | ATPROT3_ProT3__proline transporter 3 | **0.79** | **1.42** | **1.93** | **1.80** | **2.24** |
| AT4G39670 | Glycolipid transfer protein (GLTP) family protein | **0.73** | **1.26** | **1.01** | **1.42** | **2.13** |
| AT4G27657 | unknown protein | **0.70** | **1.26** | **1.10** | **1.75** | **0.74** |
| AT1G70800 | EHB1__Calcium-dependent lipid-binding (CaLB domain) family protein | **0.64** | **1.23** | **1.91** | **1.97** | **1.19** |
| **AT3G21560** | **UGT84A2__UDP-Glycosyltransferase superfamily protein** | 0.52 | **1.48** | **2.21** | **1.60** | **1.93** |
| **AT1G27120** | **Galactosyltransferase family protein** | 0.00 | **0.91** | **2.00** | **2.30** | **2.45** |
| AT3G22600 | Bifunctional inhibitor/lipid-transfer protein/seed storage 2S albumin superfamily protein | 0.16 | **1.68** | **1.96** | **1.36** | **1.96** |
| AT2G35980 | ATNHL10_NHL10_YLS9__Late embryogenesis abundant (LEA) hydroxyproline-rich glycoprotein family | 0.56 | **1.72** | **1.96** | **1.81** | **2.34** |
| AT3G04300 | RmlC-like cupins superfamily protein | 0.37 | **1.25** | **1.73** | **2.08** | **2.25** |
| AT1G74010 | Calcium-dependent phosphotriesterase superfamily protein | 0.46 | **1.39** | **1.68** | **1.32** | **2.50** |
| AT1G76980 | unknown protein | 0.51 | **1.15** | **1.67** | **1.78** | **1.85** |
| AT1G18980 | RmlC-like cupins superfamily protein | 0.20 | **1.16** | **1.55** | **1.57** | **1.59** |
| AT1G75040 | PR-5_PR5__pathogenesis-related gene 5 | 0.21 | **1.32** | **1.50** | **1.71** | **1.75** |

| AGI identifier | Gene annotation | 30 min | 2h | 4h | 8h | 24h |
|---|---|---|---|---|---|---|
| AT4G25640 | ATDTX35_DTX35_FFT_detoxifying efflux carrier 35 | 0.27 | **1.66** | **1.40** | **1.98** | **2.11** |
| AT2G17500 | Auxin efflux carrier family protein | -0.20 | **0.80** | **1.19** | **1.79** | **1.20** |
| AT1G74450 | Protein of unknown function (DUF793) | 0.41 | **1.09** | **1.16** | **1.06** | **1.10** |
| AT3G04000 | NAD(P)-binding Rossmann-fold superfamily protein | 0.06 | **0.95** | **1.16** | **1.53** | **1.23** |
| AT5G54500 | FQR1__flavodoxin-like quinone reductase 1 | 0.47 | **1.12** | **1.14** | **1.50** | **1.79** |
| AT1G30700 | FAD-binding Berberine family protein | 0.48 | **1.26** | **1.06** | **1.56** | **2.28** |
| AT1G78660 | ATGGH1_GGH1__gamma-glutamyl hydrolase 1 | 0.36 | **1.98** | 0.95 | **1.96** | **1.27** |
| AT2G15530 | RING/U-box superfamily protein | 0.56 | **0.81** | 0.89 | **1.71** | **2.15** |
| AT1G78680 | ATGGH2_GGH2__gamma-glutamyl hydrolase 2 | -0.03 | **1.24** | 0.77 | **1.53** | **1.00** |
| AT4G20860 | FAD-binding Berberine family protein | 0.51 | **0.91** | 0.61 | **1.45** | **1.79** |
| AT3G46080 | C2H2-type zinc finger family protein | 0.27 | **1.03** | 0.95 | **1.39** | **1.72** |
| AT1G21670 | unknown protein. | 0.16 | **0.97** | 0.12 | **1.20** | **1.79** |
| AT1G62320 | ERD (early-responsive to dehydration stress) family protein | 0.50 | **0.98** | 0.90 | **0.94** | **0.85** |
| AT3G21520 | AtDMP1_DMP1__DUF679 domain membrane protein 1 | 0.07 | **1.10** | 0.70 | **0.92** | **0.97** |
| AT3G50440 | ATMES10_MES10__methyl esterase 10 | 0.04 | **0.96** | 0.82 | 0.18 | **1.12** |
| AT5G12960 | Putative glycosyl hydrolase of unknown function (DUF1680) | 0.01 | **1.12** | 0.88 | 0.66 | 0.53 |
| AT1G34630 | FUNCTIONS IN: molecular_function unknown; INVOLVED IN: biological_process unknown; LOCATED IN: cellular_component unknown; EXPRESSED IN: 25 plant structures; EXPRESSED DURING: 15 growth stages; BEST *Arabidopsis thaliana* protein match is: Mitochondrial import inner membrane translocase subunit Tim17/Tim22/Tim23 family protein (TAIR:AT5G51150.1) | -0.19 | **1.06** | 0.52 | 0.42 | 0.36 |
| AT4G17280 | Auxin-responsive family protein | 0.00 | **0.89** | 0.49 | 0.05 | 0.11 |
| **AT1G78340** | **ATGSTU22_GSTU22__glutathione S-transferase TAU 22** | 0.04 | 0.56 | **1.62** | **1.75** | **1.69** |
| **AT1G17170** | **ATGSTU24_GST_GSTU24__glutathione S-transferase TAU 24** | 0.06 | 0.39 | **1.57** | **2.00** | **2.05** |
| AT3G51660 | Tautomerase/MIF superfamily protein | 0.10 | 0.75 | **1.47** | **1.80** | **2.27** |
| **AT5G36270** | **pseudogene of dehydroascorbate reductase** | 0.00 | 0.55 | **1.38** | **1.56** | **1.74** |
| **AT4G15480** | **UGT84A1__UDP-Glycosyltransferase superfamily protein** | 0.18 | 0.47 | **1.27** | **1.02** | **1.40** |
| **AT1G78380** | **ATGSTU19_GST8_GSTU19__glutathione S-transferase TAU 19** | 0.10 | 0.69 | **1.23** | **1.45** | **1.49** |
| **AT1G05680** | **UGT74E2__Uridine diphosphate glycosyltransferase 74E2** | 0.14 | -0.05 | **1.01** | **1.80** | **0.83** |
| **AT1G75270** | **DHAR2__dehydroascorbate reductase 2** | 0.36 | 0.78 | **1.09** | **1.60** | **1.49** |
| AT1G75030 | ATLP-3_TLP-3__thaumatin-like protein 3 | 0.19 | 0.59 | **1.13** | **1.45** | **1.35** |

| AGI identifier | Gene annotation | 30 min | 2h | 4h | 8h | 24h |
|---|---|---|---|---|---|---|
| AT3G13520 | AGP12_ATAGP12__arabinogalactan protein 12 | 0.17 | 0.57 | **1.08** | **1.39** | **0.88** |
| **AT1G64900** | **CYP89_CYP89A2__cytochrome P450, family 89, subfamily A, polypeptide 2** | -0.03 | 0.33 | **1.08** | **1.16** | **1.19** |
| AT2G29500 | HSP20-like chaperones superfamily protein | 0.16 | 0.29 | **1.15** | **1.11** | **1.53** |
| AT4G13180 | NAD(P)-binding Rossmann-fold superfamily protein | 0.28 | 0.29 | **1.03** | **1.07** | **1.39** |
| **AT2G12190** | **Cytochrome P450 superfamily protein** | -0.04 | 0.43 | **1.04** | **0.97** | **0.96** |
| AT2G48140 | EDA4__Bifunctional inhibitor/lipid-transfer protein/seed storage 2S albumin superfamily protein | 0.02 | 0.74 | **1.20** | **0.73** | 0.40 |
| AT1G23490 | ARF1_ATARF_ATARF1_ATARFA1A__ADP-ribosylation factor 1 | 0.48 | 0.76 | **1.04** | 0.64 | **1.32** |
| **AT3G09270** | **ATGSTU8_GSTU8__glutathione S-transferase TAU 8** | -0.12 | 0.41 | **1.15** | 0.26 | **1.09** |
| AT3G49570 | LSU3__response to low sulfur 3 | 0.17 | 0.24 | **1.04** | 0.68 | 0.65 |
| AT5G38020 | S-adenosyl-L-methionine-dependent methyltransferases superfamily protein | 0.13 | 0.06 | **1.15** | -0.35 | -0.11 |
| AT1G14120 | 2-oxoglutarate (2OG) and Fe(II)-dependent oxygenase superfamily protein | 0.08 | 0.22 | **1.08** | -0.05 | -0.21 |
| AT3G25830 | ATTPS-CIN_TPS-CIN_TPS-CIN__terpene synthase-like sequence-1,8-cineole | -0.04 | 0.45 | **1.19** | 0.06 | -0.22 |
| **AT1G58370** | **ATXYN1_RXF12__glycosyl hydrolase family 10 protein / carbohydrate-binding domain-containing protein** | 0.17 | 0.64 | **1.13** | 0.08 | **-0.86** |
| AT3G28210 | PMZ_SAP12__zinc finger (AN1-like) family protein | 0.36 | 0.52 | 0.98 | **1.60** | **2.09** |
| AT3G54420 | ATCHITIV_ATEP3_CHIV_EP3__homolog of carrot EP3-3 chitinase | -0.06 | 0.24 | 0.52 | **0.98** | **2.05** |
| AT2G23110 | Late embryogenesis abundant protein, group 6 | 0.45 | 0.78 | 0.51 | **1.87** | **2.04** |
| AT5G54206 | 0 | 0.17 | 0.15 | 0.29 | **1.41** | **2.04** |
| AT3G44190 | FAD/NAD(P)-binding oxidoreductase family protein | 0.03 | 0.21 | 0.95 | **2.05** | **2.01** |
| AT2G41380 | S-adenosyl-L-methionine-dependent methyltransferases superfamily protein | -0.07 | 0.04 | 0.47 | **0.87** | **1.99** |
| AT2G01180 | ATLPP1_ATPAP1_LPP1_PAP1__phosphatidic acid phosphatase 1 | 0.20 | 0.33 | 0.95 | **1.44** | **1.97** |
| AT2G18680 | unknown protein | 0.19 | 0.78 | 0.19 | **0.75** | **1.97** |
| AT5G22140 | FAD/NAD(P)-binding oxidoreductase family protein | 0.30 | 0.02 | 0.76 | **2.15** | **1.97** |
| AT4G11600 | ATGPX6_GPX6_LSC803_PHGPX__glutathione peroxidase 6 | 0.12 | 0.34 | 0.69 | **1.03** | **1.95** |
| AT2G05380 | GRP3S__glycine-rich protein 3 short isoform | 0.25 | 0.23 | -0.09 | **1.00** | **1.85** |
| AT2G21620 | RD2__Adenine nucleotide alpha hydrolases-like superfamily protein | -0.01 | 0.75 | 0.94 | **1.28** | **1.82** |
| AT5G03630 | ATMDAR2__Pyridine nucleotide-disulphide oxidoreductase family protein | 0.03 | -0.05 | 0.96 | **0.75** | **1.80** |
| AT2G05530 | Glycine-rich protein family | -0.04 | -0.19 | 0.22 | **0.85** | **1.73** |

| AGI identifier | Gene annotation | 30 min | 2h | 4h | 8h | 24h |
|---|---|---|---|---|---|---|
| AT5G55750 | hydroxyproline-rich glycoprotein family protein | 0.01 | -0.24 | 0.29 | **0.95** | **1.62** |
| AT1G65280 | DNAJ heat shock N-terminal domain-containing protein | 0.02 | -0.02 | 0.30 | **0.89** | **1.56** |
| AT5G64250 | Aldolase-type TIM barrel family protein | -0.01 | 0.35 | 0.59 | **1.62** | **1.55** |
| AT5G48400 | ATGLR1.2_GLR1.2__Glutamate receptor family protein | -0.07 | 0.29 | 0.52 | **0.77** | **1.54** |
| AT1G66580 | RPL10C_SAG24__senescence associated gene 24 | 0.32 | 0.45 | 0.63 | **1.26** | **1.44** |
| AT1G33590 | Leucine-rich repeat (LRR) family protein | 0.06 | 0.38 | 0.48 | **0.73** | **1.43** |
| AT5G27760 | Hypoxia-responsive family protein | 0.14 | 0.47 | 0.83 | **1.19** | **1.43** |
| **AT3G14620** | **CYP72A8__cytochrome P450, family 72, subfamily A, polypeptide 8** | -0.05 | 0.41 | -0.13 | **0.86** | **1.40** |
| **AT4G34131** | **UGT73B3__UDP-glucosyl transferase 73B3** | 0.33 | 0.38 | 0.89 | **1.31** | **1.38** |
| AT4G23190 | AT-RLK3_CRK11__cysteine-rich RLK (RECEPTOR-like protein kinase) 11 | 0.21 | 0.07 | 0.14 | **0.80** | **1.38** |
| AT1G75280 | NmrA-like negative transcriptional regulator family protein | 0.15 | 0.62 | 0.86 | **1.56** | **1.37** |
| AT5G16970 | AER_AT-AER__alkenal reductase | -0.22 | 0.02 | 0.18 | **1.15** | **1.28** |
| AT1G22710 | ATSUC2_SUC2_SUT1__sucrose-proton symporter 2 | -0.25 | 0.71 | 0.30 | **0.87** | **1.27** |
| AT4G24160 | alpha/beta-Hydrolases superfamily protein | -0.01 | 0.40 | 0.59 | **1.52** | **1.25** |
| AT5G61820 | unknown protein | 0.11 | 0.05 | 0.72 | **0.96** | **1.25** |
| AT5G42300 | UBL5__ubiquitin-like protein 5 | 0.08 | 0.21 | 0.64 | **0.81** | **1.23** |
| AT4G20830 | FAD-binding Berberine family protein | 0.14 | 0.55 | 0.52 | **0.87** | **1.20** |
| AT3G22370 | AOX1A_ATAOX1A_AtHSR3_HSR3__alternative oxidase 1A | -0.03 | 0.32 | 0.59 | **0.99** | **1.18** |
| AT3G10500 | anac053_NAC053__NAC domain containing protein 53 | 0.12 | 0.77 | 0.66 | **1.48** | **1.16** |
| AT2G23680 | Cold acclimation protein WCOR413 family | 0.10 | 0.21 | 0.77 | **0.88** | **1.12** |
| AT3G04120 | GAPC_GAPC-1_GAPC1__glyceraldehyde-3-phosphate dehydrogenase C subunit 1 | 0.25 | 0.60 | 0.86 | **1.09** | **1.11** |
| AT5G51830 | pfkB-like carbohydrate kinase family protein | 0.03 | -0.13 | 0.42 | **1.07** | **1.10** |
| AT1G72490 | unknown protein | -0.09 | 0.20 | 0.02 | **1.25** | **1.10** |
| AT5G17000 | Zinc-binding dehydrogenase family protein | 0.09 | 0.03 | 0.69 | **1.02** | **1.09** |
| AT1G09400 | FMN-linked oxidoreductases superfamily protein | -0.08 | 0.04 | 0.34 | **0.74** | **1.08** |
| AT2G36460 | Aldolase superfamily protein | 0.12 | 0.45 | 0.48 | **0.72** | **1.08** |
| AT1G67600 | Acid phosphatase/vanadium-dependent haloperoxidase-related protein | 0.01 | 0.45 | 0.50 | **1.25** | **1.07** |
| **AT3G26200** | **CYP71B22__cytochrome P450, family 71, subfamily B, polypeptide 22** | 0.19 | 0.72 | 0.66 | **1.07** | **1.07** |
| **AT5G39090** | **HXXXD-type acyl-transferase family protein** | 0.16 | 0.55 | 0.45 | **0.82** | **1.05** |
| AT5G50210 | OLD5_QS_SUFE3__quinolinate synthase | 0.00 | -0.12 | 0.26 | **0.75** | **1.02** |
| AT1G77120 | ADH_ADH1_ATADH_ATADH1__alcohol dehydrogenase 1 | -0.18 | 0.54 | 0.25 | **1.30** | **1.02** |
| AT2G36950 | Heavy metal transport/detoxification superfamily protein | 0.21 | 0.45 | -0.10 | **1.26** | **1.01** |
| AT3G27380 | SDH2-1__succinate dehydrogenase 2-1 | 0.09 | 0.35 | 0.33 | **0.99** | **0.95** |

| AGI identifier | Gene annotation | 30 min | 2h | 4h | 8h | 24h |
|---|---|---|---|---|---|---|
| **AT2G29460** | **ATGSTU4_GST22_GSTU4__glutathione S-transferase tau 4** | 0.12 | 0.52 | 1.00 | **1.37** | **0.95** |
| **AT1G64930** | **CYP89A7__cytochrome P450, family 87, subfamily A, polypeptide 7** | 0.20 | 0.36 | 0.92 | **0.85** | **0.94** |
| **AT2G45550** | **CYP76C4__cytochrome P450, family 76, subfamily C, polypeptide 4** | -0.01 | 0.11 | -0.15 | **0.91** | **0.89** |
| AT1G76530 | Auxin efflux carrier family protein | 0.06 | 0.13 | 0.30 | **0.90** | **0.88** |
| AT3G45180 | Ubiquitin-like superfamily protein | 0.06 | 0.30 | 0.45 | **0.86** | **0.87** |
| AT1G14130 | 2-oxoglutarate (2OG) and Fe(II)-dependent oxygenase superfamily protein | -0.04 | 0.07 | 0.60 | **1.04** | **0.86** |
| AT4G34120 | CBSX2_CDCP1_LEJ1__Cystathionine beta-synthase (CBS) family protein | 0.11 | 0.43 | 0.46 | **0.77** | **0.86** |
| AT4G33420 | Peroxidase superfamily protein | 0.14 | 0.55 | -0.20 | **0.74** | **0.85** |
| AT4G03320 | AtTic20-IV_Tic20-IV__translocon at the inner envelope membrane of chloroplasts 20-IV | 0.15 | 0.22 | 0.69 | **1.00** | **0.82** |
| AT2G07671 | ATP synthase subunit C family protein | -0.03 | 0.32 | 0.30 | **0.86** | **0.82** |
| AT2G24500 | FZF__Zinc finger protein 622 | 0.11 | 0.45 | 0.35 | **1.13** | **0.76** |
| **AT2G29470** | **ATGSTU3_GST21_GSTU3__glutathione S-transferase tau 3** | 0.12 | 0.40 | 0.77 | **1.14** | **0.76** |
| AT2G44460 | BGLU28__beta glucosidase 28 | -0.15 | -0.03 | 0.11 | **0.74** | **0.70** |
| **AT1G05670** | **Pentatricopeptide repeat (PPR-like) superfamily protein** | 0.20 | 0.02 | 0.71 | **1.30** | **0.69** |
| AT2G33150 | KAT2_PED1_PKT3__peroxisomal 3-ketoacyl-CoA thiolase 3 | -0.25 | 0.67 | -0.42 | **0.84** | **0.68** |
| AT1G76070 | unknown protein | 0.06 | 0.19 | 0.24 | **0.90** | **0.68** |
| AT3G51130 | unknown protein | -0.16 | -0.14 | -0.10 | **0.83** | **0.67** |
| **AT3G59140** | **ABCC10_ATMRP14_MRP14__multidrug resistance-associated protein 14** | -0.15 | 0.01 | 0.19 | **0.76** | **0.67** |
| AT1G76520 | Auxin efflux carrier family protein | -0.04 | 0.11 | 0.35 | **0.87** | **0.66** |
| AT5G07870 | HXXXD-type acyl-transferase family protein | 0.17 | -0.04 | 0.28 | **1.20** | 0.65 |
| **AT2G36770** | **UDP-Glycosyltransferase superfamily protein** | -0.02 | 0.19 | 0.11 | **1.65** | 0.64 |
| AT1G61790 | Oligosaccharyltransferase complex/magnesium transporter family protein | -0.21 | -0.01 | -0.13 | **0.74** | 0.64 |
| AT1G71520 | Integrase-type DNA-binding superfamily protein | 0.11 | 0.57 | 0.73 | **1.47** | 0.62 |
| AT2G07811 | 0 | -0.03 | 0.18 | 0.01 | **1.01** | 0.60 |
| AT3G28910 | ATMYB30_MYB30__myb domain protein 30 | -0.26 | -0.03 | -0.16 | **0.89** | 0.59 |
| AT2G12557 | unknown protein | 0.04 | 0.20 | 0.40 | **0.81** | 0.59 |
| **AT2G29940** | **ABCG31_ATPDR3_PDR3__pleiotropic drug resistance 3** | -0.06 | 0.30 | 0.22 | **0.96** | 0.58 |
| AT1G27190 | Leucine-rich repeat protein kinase family protein | 0.14 | 0.07 | 0.41 | **1.96** | 0.57 |
| AT1G18510 | TET16__tetraspanin 16 | 0.15 | 0.42 | 0.41 | **1.26** | 0.56 |
| AT1G22500 | AtATL15_ATL15__RING/U-box superfamily protein | 0.03 | 0.03 | -0.56 | **0.88** | 0.55 |
| AT2G38250 | Homeodomain-like superfamily protein | -0.17 | 0.44 | 0.40 | **0.71** | 0.54 |

| AGI identifier | Gene annotation | 30 min | 2h | 4h | 8h | 24h |
|---|---|---|---|---|---|---|
| AT4G17840 | unknown protein | -0.28 | 0.10 | -0.62 | **0.99** | 0.52 |
| AT5G15640 | Mitochondrial substrate carrier family protein | -0.11 | 0.29 | 0.29 | **1.19** | 0.49 |
| AT2G34355 | Major facilitator superfamily protein | 0.04 | 0.26 | 0.24 | **1.07** | 0.48 |
| AT1G66570 | ATSUC7_SUC7__sucrose-proton symporter 7 | -0.16 | 0.28 | 0.08 | **0.73** | 0.46 |
| AT5G62720 | Integral membrane HPP family protein | 0.14 | 0.42 | -0.34 | **0.91** | 0.46 |
| AT1G68410 | Protein phosphatase 2C family protein | -0.15 | 0.50 | -0.32 | **0.96** | 0.40 |
| AT1G23890 | NHL domain-containing protein | -0.08 | 0.35 | 0.61 | **1.26** | 0.40 |
| **AT1G55850** | **ATCSLE1_CSLE1__cellulose synthase like E1** | -0.09 | 0.17 | -0.25 | **1.17** | 0.36 |
| AT5G54640 | ATHTA1_HTA1_RAT5__Histone superfamily protein | 0.11 | 0.42 | 0.42 | **0.94** | 0.36 |
| AT1G15415 | The protein encoded by this gene was identified as a part of pollen proteome by mass spec analysis. It has weak homology to LEA (late embryo abundant) proteins. | 0.00 | 0.03 | 0.28 | **0.74** | 0.32 |
| AT1G05100 | Encodes protein phosphatase 2A (PP2A) B'gamma subunit. Targeted to nucleus and cytosol. MAPKKK18__mitogen-activated protein kinase kinase kinase 18 | 0.14 | 0.70 | 0.26 | **0.99** | 0.32 |
| AT4G29670 | ACHT2__atypical CYS HIS rich thioredoxin 2 | -0.21 | 0.17 | 0.03 | **0.80** | 0.30 |
| AT1G53580 | ETHE1_GLX2-3_GLY3__glyoxalase II 3 | -0.14 | 0.39 | -0.06 | **1.07** | 0.29 |
| AT1G71530 | Protein kinase superfamily protein | 0.06 | 0.31 | 0.34 | **0.70** | 0.27 |
| AT5G64890 | PROPEP2__elicitor peptide 2 precursor | 0.31 | 0.04 | 0.21 | **1.07** | 0.27 |
| AT1G05575 | unknown protein | 0.09 | 0.45 | 0.57 | **1.21** | 0.26 |
| AT5G59570 | BOA__Homeodomain-like superfamily protein | 0.00 | 0.40 | 0.24 | **1.32** | 0.16 |
| AT3G14000 | ATBRXL2_BRX-LIKE2__DZC (Disease resistance/zinc finger/chromosome condensation-like region) domain containing protein | -0.05 | 0.13 | -0.01 | **0.91** | 0.12 |
| AT3G22530 | unknown protein | -0.01 | 0.09 | 0.05 | **0.72** | 0.09 |
| AT2G34070 | TBL37__TRICHOME BIREFRINGENCE-LIKE 37 | -0.19 | 0.09 | 0.13 | **0.99** | 0.03 |
| AT4G00750 | S-adenosyl-L-methionine-dependent methyltransferases superfamily protein | 0.08 | 0.02 | -0.08 | **0.95** | 0.00 |
| AT3G14770 | AtSWEET2_SWEET2__Nodulin MtN3 family protein | 0.05 | 0.47 | -0.48 | **1.02** | -0.15 |
| AT2G43445 | F-box and associated interaction domains-containing protein | -0.05 | 0.07 | 0.19 | **0.73** | -0.39 |
| AT1G66100 | Plant thionin | -0.20 | -0.03 | 0.44 | **0.82** | **-1.11** |
| AT1G65290 | mtACP2__mitochondrial acyl carrier protein 2 | 0.13 | 0.06 | 0.13 | 0.34 | **2.63** |
| AT4G37990 | ATCAD8_CAD-B2_ELI3_ELI3-2__elicitor-activated gene 3-2 | 0.07 | 0.30 | 0.34 | 0.00 | **2.43** |
| AT5G25260 | SPFH/Band 7/PHB domain-containing membrane-associated protein family | -0.10 | -0.06 | 0.30 | 0.04 | **2.07** |
| AT2G18690 | unknown protein | 0.11 | 0.70 | 0.54 | 0.66 | **1.98** |

| AGI identifier | Gene annotation | 30 min | 2h | 4h | 8h | 24h |
|---|---|---|---|---|---|---|
| AT4G12490 | Bifunctional inhibitor/lipid-transfer protein/seed storage 2S albumin superfamily protein | 0.22 | 0.07 | 0.66 | 0.28 | **1.90** |
| AT1G14870 | AtPCR2_PCR2__PLANT CADMIUM RESISTANCE 2 | -0.03 | 0.51 | 0.03 | 0.48 | **1.76** |
| AT2G23150 | ATNRAMP3_NRAMP3__natural resistance-associated macrophage protein 3 | -0.17 | -0.16 | 0.01 | 0.59 | **1.69** |
| AT2G17740 | Cysteine/Histidine-rich C1 domain family protein | -0.03 | -0.15 | 0.66 | 0.20 | **1.67** |
| AT1G66090 | Disease resistance protein (TIR-NBS class) | 0.36 | 0.29 | 0.66 | 0.55 | **1.67** |
| AT5G06320 | NHL3__NDR1/HIN1-like 3 | -0.28 | 0.11 | -0.08 | 0.31 | **1.60** |
| AT2G29350 | SAG13__senescence-associated gene 13 | -0.17 | 0.17 | 0.82 | 0.59 | **1.55** |
| AT1G13330 | AHP2__*Arabidopsis* Hop2 homolog | 0.00 | -0.09 | 0.69 | 0.36 | **1.55** |
| AT5G13320 | GDG1_GH3.12_PBS3_WIN3__Auxin-responsive GH3 family protein | -0.10 | -0.25 | 0.11 | -0.07 | **1.54** |
| AT5G17380 | Thiamine pyrophosphate dependent pyruvate decarboxylase family protein | 0.04 | 0.03 | 0.35 | 0.65 | **1.48** |
| AT2G20142 | Toll-Interleukin-Resistance (TIR) domain family protein | 0.06 | 0.05 | 0.21 | 0.23 | **1.47** |
| AT4G26200 | ACS7_ATACS7__1-amino-cyclopropane-1-carboxylate synthase 7 | 0.22 | -0.01 | 0.18 | 0.26 | **1.44** |
| AT1G74710 | ATICS1_EDS16_ICS1_SID2__ADC synthase superfamily protein | 0.05 | -0.19 | 0.14 | -0.09 | **1.41** |
| AT4G11890 | Protein kinase superfamily protein | 0.10 | 0.19 | -0.04 | 0.56 | **1.38** |
| AT5G25250 | SPFH/Band 7/PHB domain-containing membrane-associated protein family | 0.07 | 0.00 | 0.28 | 0.40 | **1.38** |
| AT1G26380 | FAD-binding Berberine family protein | 0.24 | 0.24 | 0.34 | 0.43 | **1.38** |
| AT5G39670 | Calcium-binding EF-hand family protein | -0.17 | -0.07 | 0.12 | 0.05 | **1.38** |
| AT4G14365 | XBAT34__XB3 ortholog 4 in *Arabidopsis thaliana* | -0.10 | -0.35 | 0.17 | -0.05 | **1.36** |
| AT1G26630 | ATELF5A-2_ELF5A-2_FBR12__Eukaryotic translation initiation factor 5A-1 (eIF-5A 1) protein | 0.04 | -0.12 | 0.51 | 0.26 | **1.36** |
| AT5G14780 | FDH__formate dehydrogenase | -0.17 | -0.60 | -0.79 | 0.05 | **1.33** |
| AT2G32190 | unknown protein | 0.11 | 0.18 | 0.45 | 0.53 | **1.33** |
| AT5G19440 | NAD(P)-binding Rossmann-fold superfamily protein | -0.11 | -0.07 | 0.33 | 0.66 | **1.28** |
| AT3G49530 | ANAC062_NAC062_NTL6__NAC domain containing protein 62 | 0.09 | 0.35 | 0.29 | 0.48 | **1.28** |
| AT1G32960 | ATSBT3.3_SBT3.3__Subtilase family protein | 0.11 | 0.06 | 0.20 | 0.47 | **1.27** |
| AT5G19550 | AAT2_ASP2__aspartate aminotransferase 2 | 0.04 | 0.09 | 0.16 | 0.19 | **1.26** |
| AT5G47120 | ATBI-1_ATBI1_BI-1_BI1__BAX inhibitor 1 | 0.09 | 0.37 | 0.44 | 0.20 | **1.21** |
| AT5G62630 | HIPL2__hipl2 protein precursor | 0.14 | 0.07 | 0.43 | 0.52 | **1.21** |
| AT4G12480 | EARLI1_pEARLI 1__Bifunctional inhibitor/lipid-transfer protein/seed storage 2S albumin superfamily protein | -0.03 | 0.13 | 0.02 | -0.15 | **1.19** |
| AT4G02380 | AtLEA5_SAG21__senescence-associated gene 21 | 0.19 | 0.22 | -0.18 | 0.59 | **1.17** |
| AT2G31865 | PARG2__poly(ADP-ribose) glycohydrolase 2 | -0.04 | -0.22 | 0.33 | 0.31 | **1.17** |

| AGI identifier | Gene annotation | 30 min | 2h | 4h | 8h | 24h |
|---|---|---|---|---|---|---|
| AT2G39200 | ATMLO12_MLO12__Seven transmembrane MLO family protein | -0.16 | -0.44 | -0.20 | -0.18 | **1.17** |
| AT5G01540 | LECRKA4.1__lectin receptor kinase a4.1 | -0.05 | -0.19 | 0.19 | -0.16 | **1.17** |
| AT5G47130 | Bax inhibitor-1 family protein | -0.12 | 0.19 | 0.21 | 0.26 | **1.16** |
| AT5G02490 | AtHsp70-2_Hsp70-2__Heat shock protein 70 (Hsp 70) family protein | 0.00 | -0.23 | 0.19 | -0.11 | **1.16** |
| AT5G54710 | Ankyrin repeat family protein | -0.11 | -0.16 | 0.51 | -0.10 | **1.15** |
| AT2G23810 | TET8__tetraspanin8 | -0.22 | 0.08 | -0.11 | 0.45 | **1.15** |
| AT3G51670 | SEC14 cytosolic factor family protein / phosphoglyceride transfer family protein | -0.05 | 0.32 | 0.64 | 0.18 | **1.15** |
| AT1G68570 | Major facilitator superfamily protein | 0.19 | 0.61 | 0.54 | 0.48 | **1.14** |
| AT5G52640 | ATHS83_AtHsp90-1_ATHSP90.1_HSP81-1_HSP81.1_HSP83_HSP90.1__heat shock protein 90.1 | -0.06 | 0.01 | 0.53 | 0.50 | **1.13** |
| **AT1G11610** | **CYP71A18__cytochrome P450, family 71, subfamily A, polypeptide 18** | 0.03 | 0.09 | 0.43 | 0.47 | **1.12** |
| AT1G36622 | unknown protein | -0.11 | 0.07 | 0.65 | 0.62 | **1.12** |
| AT3G13950 | unknown protein | 0.01 | -0.03 | -0.01 | 0.37 | **1.12** |
| AT2G41100 | ATCAL4_TCH3__Calcium-binding EF hand family protein | -0.06 | -0.48 | -0.93 | -0.42 | **1.10** |
| AT2G43590 | Chitinase family protein | 0.14 | -0.01 | 0.24 | 0.48 | **1.09** |
| AT4G14630 | GLP9__germin-like protein 9 | -0.19 | 0.07 | -0.39 | 0.06 | **1.09** |
| AT4G12720 | AtNUDT7_GFG1_NUDT7__MutT/nudix family protein | -0.10 | -0.16 | -0.18 | 0.16 | **1.07** |
| AT1G32940 | ATSBT3.5_SBT3.5__Subtilase family protein | -0.02 | 0.03 | 0.51 | 0.35 | **1.06** |
| AT5G18480 | PGSIP6__plant glycogenin-like starch initiation protein 6 | -0.17 | 0.21 | -0.15 | 0.53 | **1.05** |
| AT1G70490 | ARFA1D_ATARFA1D__Ras-related small GTP-binding family protein | 0.14 | 0.22 | 0.18 | 0.11 | **1.04** |
| AT5G20400 | 2-oxoglutarate (2OG) and Fe(II)-dependent oxygenase superfamily protein | -0.12 | -0.08 | 0.19 | 0.22 | **1.03** |
| AT2G15240 | UNC-50 family protein | 0.00 | -0.02 | 0.03 | 0.11 | **1.02** |
| **AT3G26210** | **CYP71B23__cytochrome P450, family 71, subfamily B, polypeptide 23** | 0.24 | 0.03 | 0.37 | 0.21 | **1.01** |
| AT5G51770 | Protein kinase superfamily protein | 0.17 | 0.45 | 0.27 | 0.27 | **1.00** |
| AT5G52810 | NAD(P)-binding Rossmann-fold superfamily protein | 0.04 | 0.00 | 0.80 | 0.33 | **1.00** |
| AT3G59700 | ATHLECRK_HLECRK_LECRK1__lectin-receptor kinase | 0.01 | -0.12 | 0.33 | 0.34 | **0.99** |
| AT5G14930 | SAG101__senescence-associated gene 101 | 0.00 | -0.14 | -0.21 | -0.15 | **0.98** |
| AT4G23700 | ATCHX17_CHX17__cation/H+ exchanger 17 | 0.14 | 0.40 | 0.28 | 0.38 | **0.97** |
| AT1G77510 | ATPDI6_ATPDIL1-2_PDI6_PDIL1-2__PDI-like 1-2 | 0.17 | 0.06 | 0.43 | -0.45 | **0.96** |
| AT3G20510 | Transmembrane proteins 14C | 0.00 | 0.38 | 0.59 | 0.20 | **0.96** |
| AT2G16430 | ATPAP10_PAP10__purple acid phosphatase 10 | 0.13 | -0.11 | 0.31 | -0.20 | **0.96** |
| AT4G01770 | RGXT1_rhamnogalacturonan xylosyltransferase 1 | 0.06 | 0.23 | 0.60 | 0.07 | **0.95** |
| AT2G37110 | PLAC8 family protein | 0.01 | -0.03 | -0.27 | 0.26 | **0.94** |

| AGI identifier | Gene annotation | 30 min | 2h | 4h | 8h | 24h |
|---|---|---|---|---|---|---|
| AT1G21750 | ATPDI5_ATPDIL1-1_PDI5_PDIL1-1__PDI-like 1-1 | 0.12 | -0.12 | 0.21 | -0.50 | **0.93** |
| AT3G47480 | Calcium-binding EF-hand family protein | -0.04 | -0.08 | 0.11 | -0.08 | **0.93** |
| AT2G44350 | ATCS_CSY4__Citrate synthase family protein | 0.18 | 0.02 | 0.30 | -0.14 | **0.91** |
| AT5G57710 | Double Clp-N motif-containing P-loop nucleoside triphosphate hydrolases superfamily protein | 0.01 | -0.02 | 0.49 | 0.52 | **0.91** |
| AT1G59860 | HSP20-like chaperones superfamily protein | 0.40 | 0.54 | 0.79 | 0.67 | **0.91** |
| AT1G60680 | NAD(P)-linked oxidoreductase superfamily protein | -0.15 | -0.02 | 0.06 | 0.57 | **0.91** |
| AT5G54960 | PDC2__pyruvate decarboxylase-2 | 0.05 | 0.19 | 0.33 | 0.32 | **0.90** |
| AT5G06860 | ATPGIP1_PGIP1__polygalacturonase inhibiting protein 1 | -0.11 | -0.11 | -0.58 | 0.21 | **0.90** |
| AT1G27080 | NRT1.6__nitrate transporter 1.6 | -0.02 | -0.20 | -0.38 | -0.13 | **0.88** |
| AT3G56260 | unknown protein | 0.08 | 0.23 | 0.62 | 0.47 | **0.88** |
| AT3G29360 | UGD2__UDP-glucose 6-dehydrogenase family protein | -0.07 | 0.07 | 0.38 | -0.16 | **0.87** |
| AT3G57670 | NTT_WIP2__C2H2-type zinc finger family protein | 0.10 | -0.06 | 0.03 | 0.46 | **0.85** |
| AT1G11910 | APA1_ATAPA1__aspartic proteinase A1 | -0.08 | -0.07 | -0.06 | -0.21 | **0.84** |
| AT5G45350 | proline-rich family protein | -0.23 | -0.30 | -0.24 | 0.15 | **0.84** |
| AT1G80330 | ATGA3OX4_GA3OX4__gibberellin 3-oxidase 4 | -0.02 | -0.09 | 0.35 | 0.48 | **0.83** |
| AT5G51040 | unknown protein | -0.04 | -0.09 | 0.31 | 0.33 | **0.83** |
| AT1G61800 | ATGPT2_GPT2__glucose-6-phosphate/phosphate translocator 2 | -0.24 | 0.09 | -0.34 | 0.50 | **0.83** |
| AT2G37760 | AKR4C8__NAD(P)-linked oxidoreductase superfamily protein | -0.08 | 0.05 | 0.58 | 0.63 | **0.82** |
| AT1G19220 | ARF11_ARF19_IAA22__auxin response factor 19 | 0.09 | 0.19 | 0.63 | 0.18 | **0.82** |
| AT4G25900 | Galactose mutarotase-like superfamily protein | -0.05 | 0.07 | -0.01 | 0.11 | **0.82** |
| AT1G65845 | unknown protein | -0.18 | -0.51 | 0.00 | -0.27 | **0.81** |
| AT3G62260 | Protein phosphatase 2C family protein | -0.14 | 0.27 | 0.32 | 0.40 | **0.81** |
| AT4G29040 | RPT2a__regulatory particle AAA-ATPase 2A | 0.11 | -0.08 | 0.17 | 0.51 | **0.79** |
| AT3G62600 | ATERDJ3B_ERDJ3B__DNAJ heat shock family protein | 0.03 | -0.16 | 0.54 | -0.13 | **0.79** |
| AT3G52430 | ATPAD4_PAD4__alpha/beta-Hydrolases superfamily protein | -0.17 | -0.61 | -0.33 | -0.21 | **0.79** |
| AT5G63680 | Pyruvate kinase family protein | 0.20 | 0.36 | 0.64 | 0.15 | **0.79** |
| AT2G37940 | AtIPCS2_ERH1__*Arabidopsis* Inositol phosphorylceramide synthase 2 | 0.00 | 0.29 | 0.38 | 0.52 | **0.79** |
| AT1G62570 | FMO GS-OX4__flavin-monooxygenase glucosinolate S-oxygenase 4 | 0.05 | 0.69 | 0.97 | 0.68 | **0.78** |
| AT1G23880 | NHL domain-containing protein | -0.33 | 0.11 | 0.11 | 0.66 | **0.78** |
| AT2G33380 | AtCLO3_CLO-3_CLO3_RD20__Caleosin-related family protein | -0.31 | -0.01 | 0.03 | 0.09 | **0.77** |
| AT2G05840 | PAA2__20S proteasome subunit PAA2 | 0.07 | 0.06 | 0.47 | 0.44 | **0.77** |

| AGI identifier | Gene annotation | 30 min | 2h | 4h | 8h | 24h |
|---|---|---|---|---|---|---|
| AT2G46400 | ATWRKY46_WRKY46__WRKY DNA-binding protein 46 | -0.19 | -0.20 | 0.27 | 0.15 | **0.76** |
| AT3G50930 | BCS1__cytochrome BC1 synthesis | 0.06 | -0.14 | 0.34 | -0.08 | **0.76** |
| AT4G21120 | AAT1_CAT1__amino acid transporter 1 | -0.13 | -0.13 | -0.21 | 0.45 | **0.76** |
| AT4G36640 | Sec14p-like phosphatidylinositol transfer family protein | 0.02 | -0.01 | 0.85 | 0.56 | **0.75** |
| AT1G14540 | Peroxidase superfamily protein | 0.06 | 0.10 | -0.15 | 0.17 | **0.75** |
| AT1G66160 | ATCMPG1_CMPG1__CYS, MET, PRO, and GLY protein 1 | 0.04 | 0.21 | 0.29 | 0.58 | **0.75** |
| AT4G15760 | MO1__monooxygenase 1 | -0.19 | 0.27 | -0.31 | 0.67 | **0.75** |
| AT2G46390 | SDH8__unknown protein | 0.07 | 0.22 | 0.60 | 0.20 | **0.73** |
| AT3G24170 | ATGR1_GR1__glutathione-disulfide reductase | -0.15 | 0.19 | 0.62 | 0.50 | **0.73** |
| AT5G01750 | Protein of unknown function (DUF567) | 0.16 | 0.06 | -0.56 | 0.20 | **0.72** |
| AT5G61790 | ATCNX1_CNX1__calnexin 1 | 0.20 | -0.02 | 0.42 | -0.34 | **0.72** |
| AT1G60710 | ATB2__NAD(P)-linked oxidoreductase superfamily protein | -0.03 | 0.04 | 0.19 | 0.58 | **0.72** |
| AT3G51260 | PAD1__20S proteasome alpha subunit PAD1 | 0.03 | -0.01 | 0.21 | 0.30 | **0.71** |
| AT4G09750 | NAD(P)-binding Rossmann-fold superfamily protein | -0.12 | 0.08 | 0.58 | 0.37 | **0.71** |
| AT3G18250 | Putative membrane lipoprotein | 0.13 | -0.12 | -0.12 | 0.13 | **0.71** |
| AT5G56030 | AtHsp90.2_ERD8_HSP81-2_HSP81.2_HSP90.2__heat shock protein 81-2 | 0.07 | 0.08 | 0.42 | -0.14 | **0.70** |
| AT3G56400 | ATWRKY70_WRKY70__WRKY DNA-binding protein 70 | -0.18 | -0.08 | 0.23 | -0.10 | **0.70** |
| AT2G28930 | APK1B_PK1B__protein kinase 1B | -0.06 | 0.36 | 0.24 | 0.13 | **0.70** |
| AT5G26030 | ATFC-I_FC-I_FC1__ferrochelatase 1 | -0.40 | 0.05 | 0.26 | 0.64 | **0.69** |
| AT1G29310 | SecY protein transport family protein | 0.04 | 0.12 | 0.22 | 0.06 | **0.68** |
| AT2G31660 | EMA1_SAD2_URM9__ARM repeat superfamily protein | 0.00 | 0.74 | -0.40 | 0.55 | **0.68** |
| AT5G38530 | TSBtype2__tryptophan synthase beta type 2 | 0.08 | 0.09 | 0.50 | 0.18 | **0.68** |
| AT5G36960 | unknown protein | 0.18 | -0.11 | 0.22 | 0.56 | **0.68** |
| AT5G23540 | Mov34/MPN/PAD-1 family protein | 0.04 | -0.04 | 0.25 | 0.60 | **0.68** |
| AT1G07135 | glycine-rich protein | -0.27 | -0.07 | 0.07 | 0.26 | **0.66** |
| AT3G50685 | unknown protein | -0.06 | 0.18 | -0.28 | -0.31 | **-0.66** |
| AT5G13120 | ATCYP20-2_CYP20-2_PnsI5__cyclophilin 20-2 | 0.11 | -0.14 | -0.08 | -0.34 | **-0.67** |
| AT4G14130 | XTH15_XTR7__xyloglucan endotransglucosylase/hydrolase 15 | 0.10 | -0.14 | -0.83 | -0.34 | **-0.67** |
| AT3G48930 | EMB1080__Nucleic acid-binding, OB-fold-like protein | 0.09 | 0.03 | -0.23 | -0.34 | **-0.68** |
| AT1G80050 | APT2_ATAPT2_PHT1.1__adenine phosphoribosyl transferase 2 | 0.03 | -0.26 | -0.54 | -0.58 | **-0.70** |
| AT4G24770 | ATRBP31_ATRBP33_CP31_RBP31__31-kDa RNA binding protein | 0.20 | 0.05 | -0.36 | -0.17 | **-0.70** |
| AT4G14320 | Zinc-binding ribosomal protein family protein | 0.33 | 0.09 | -0.33 | -0.29 | **-0.70** |

| AGI identifier | Gene annotation | 30 min | 2h | 4h | 8h | 24h |
|---|---|---|---|---|---|---|
| AT4G38690 | PLC-like phosphodiesterases superfamily protein | -0.14 | 0.12 | -0.54 | -0.39 | **-0.71** |
| AT4G27090 | Ribosomal protein L14 | -0.03 | 0.02 | -0.06 | -0.28 | **-0.71** |
| AT2G05990 | ENR1_MOD1__NAD(P)-binding Rossmann-fold superfamily protein | 0.25 | 0.12 | -0.18 | -0.46 | **-0.72** |
| AT5G04430 | BTR1_BTR1L_BTR1S__binding to TOMV RNA 1L (long form) | 0.07 | -0.15 | -0.09 | -0.19 | **-0.72** |
| AT1G60950 | ATFD2_FED A__2Fe-2S ferredoxin-like superfamily protein | -0.07 | -0.12 | -0.24 | -0.65 | **-0.72** |
| **AT2G40890** | **CYP98A3__cytochrome P450, family 98, subfamily A, polypeptide 3** | 0.05 | -0.66 | -0.92 | -0.44 | **-0.74** |
| AT4G34290 | SWIB/MDM2 domain superfamily protein | 0.18 | 0.04 | -0.25 | -0.57 | **-0.74** |
| AT3G56910 | PSRP5__plastid-specific 50S ribosomal protein 5 | 0.13 | 0.14 | -0.13 | -0.32 | **-0.75** |
| AT4G34670 | Ribosomal protein S3Ae | 0.22 | 0.12 | -0.14 | -0.40 | **-0.76** |
| AT3G23390 | Zinc-binding ribosomal protein family protein | 0.03 | 0.06 | -0.18 | -0.26 | **-0.77** |
| AT5G62670 | AHA11_HA11__H(+)-ATPase 11 | 0.05 | -0.07 | -0.08 | -0.52 | **-0.77** |
| AT2G45470 | AGP8_FLA8__FASCICLIN-like arabinogalactan protein 8 | -0.06 | 0.08 | -0.48 | -0.55 | **-0.77** |
| AT4G24930 | thylakoid lumenal 17.9 kDa protein, chloroplast | 0.10 | -0.02 | 0.00 | -0.50 | **-0.78** |
| AT3G02560 | Ribosomal protein S7e family protein | 0.06 | -0.05 | 0.23 | -0.31 | **-0.80** |
| AT3G62530 | ARM repeat superfamily protein | 0.03 | 0.07 | 0.04 | -0.32 | **-0.81** |
| AT3G16690 | AtSWEET16_SWEET16__Nodulin MtN3 family protein | -0.20 | 0.08 | 0.14 | -0.18 | **-0.81** |
| AT1G22640 | ATMYB3_MYB3__myb domain protein 3 | 0.20 | -0.47 | -0.67 | -0.58 | **-0.83** |
| AT1G18290 | unknown protein | -0.03 | -0.28 | -0.82 | -0.09 | **-0.83** |
| AT4G34620 | SSR16__small subunit ribosomal protein 16 | 0.07 | 0.10 | -0.26 | -0.33 | **-0.85** |
| AT3G20820 | Leucine-rich repeat (LRR) family protein | 0.01 | -0.07 | -0.80 | -0.60 | **-0.86** |
| AT3G11170 | AtFAD7_FAD7_FADD__fatty acid desaturase 7 | 0.03 | -0.12 | -0.30 | -0.63 | **-0.87** |
| AT3G01480 | ATCYP38_CYP38__cyclophilin 38 | 0.07 | 0.01 | -0.76 | -0.54 | **-0.88** |
| AT3G15850 | ADS3_FAD5_FADB_JB67_fatty acid desaturase 5 | -0.21 | -0.01 | -0.68 | -0.06 | **-0.91** |
| AT3G16440 | ATMLP-300B_MEE36_MLP-300B__myrosinase-binding protein-like protein-300B | -0.24 | 0.21 | -0.37 | -0.38 | **-0.91** |
| AT3G16420 | JAL30_PBP1__PYK10-binding protein 1 | -0.04 | 0.07 | 0.01 | -0.64 | **-1.02** |
| AT5G58260 | NdhN__oxidoreductases, acting on NADH or NADPH, quinone or similar compound as acceptor | 0.04 | -0.01 | -0.14 | -0.58 | **-1.05** |
| AT1G54000 | GLL22__GDSL-like Lipase/Acylhydrolase superfamily protein | 0.03 | -0.28 | -0.77 | -0.55 | **-1.06** |
| AT1G12090 | ELP__extensin-like protein | -0.06 | -0.04 | -0.52 | -0.33 | **-1.08** |
| AT3G45140 | ATLOX2_LOX2__lipoxygenase 2 | -0.12 | 0.51 | 0.51 | -0.24 | **-1.11** |
| AT4G16980 | arabinogalactan-protein family | 0.07 | -0.10 | -0.84 | -0.54 | **-1.14** |
| AT3G02380 | ATCOL2_COL2__CONSTANS-like 2 | -0.11 | -0.60 | -0.41 | 0.04 | **-1.15** |

| AGI identifier | Gene annotation | 30 min | 2h | 4h | 8h | 24h |
|---|---|---|---|---|---|---|
| AT4G13870 | ATWEX_ATWRNEXO_WEX_WRNEXO__Werner syndrome-like exonuclease | -0.02 | 0.10 | 0.61 | -0.34 | **-1.19** |
| AT5G24420 | PGL5__6-phosphogluconolactonase 5 | 0.00 | 0.05 | -0.32 | -0.02 | **-1.20** |
| AT5G51720 | 2 iron, 2 sulfur cluster binding | -0.06 | -0.25 | -0.17 | -0.38 | **-1.24** |
| AT3G28270 | Protein of unknown function (DUF677) | -0.26 | 0.46 | 0.25 | -0.57 | **-1.26** |
| AT4G35100 | PIP2;7_PIP3_PIP3A_SIMIP__plasma membrane intrinsic protein 3 | 0.01 | 0.10 | -0.81 | -0.67 | **-1.26** |
| AT3G16450 | JAL33__Mannose-binding lectin superfamily protein | 0.00 | 0.28 | -0.51 | -0.67 | **-1.30** |
| **AT1G17190** | **ATGSTU26_GSTU26__glutathione S-transferase tau 26** | -0.01 | -0.19 | 0.32 | -0.31 | **-1.41** |
| AT2G25510 | unknown protein | -0.09 | 0.23 | 0.11 | -0.40 | **-1.52** |
| AT5G36910 | THI2.2__thionin 2.2 | -0.16 | 0.04 | -0.38 | 0.21 | **-1.73** |
| **AT1G69500** | **CYP704B1__cytochrome P450, family 704, subfamily B, polypeptide 1** | -0.14 | -0.53 | -0.28 | **-0.71** | **0.71** |
| AT5G26570 | ATGWD3_OK1_PWD__catalytics;carbohydrate kinases;phosphoglucan, water dikinases | 0.17 | 0.05 | -0.06 | **-0.75** | 0.34 |
| AT5G07340 | Calreticulin family protein | 0.08 | -0.18 | -0.16 | **-0.96** | 0.26 |
| AT1G69520 | S-adenosyl-L-methionine-dependent methyltransferases superfamily protein | -0.06 | 0.13 | 0.12 | **-0.69** | 0.13 |
| AT1G19100 | Histidine kinase-, DNA gyrase B-, and HSP90-like ATPase family protein | -0.02 | -0.25 | -0.38 | **-0.69** | 0.12 |
| AT5G58900 | Homeodomain-like transcriptional regulator | -0.06 | -0.40 | -0.22 | **-0.72** | 0.11 |
| AT1G01960 | EDA10__SEC7-like guanine nucleotide exchange family protein | 0.23 | 0.05 | -0.37 | **-0.96** | 0.06 |
| AT3G23300 | S-adenosyl-L-methionine-dependent methyltransferases superfamily protein | 0.05 | -0.23 | -0.14 | **-0.72** | 0.05 |
| AT1G66200 | ATGSR2_GLN1;2_GSR2__glutamine synthase clone F11 | 0.02 | -0.41 | -0.26 | **-1.18** | -0.04 |
| AT2G07050 | CAS1__cycloartenol synthase 1 | 0.28 | 0.05 | -0.39 | **-0.96** | -0.08 |
| AT3G13470 | Cpn60beta2__TCP-1/cpn60 chaperonin family protein | 0.16 | -0.06 | 0.36 | **-0.74** | -0.08 |
| AT5G55930 | ATOPT1_OPT1__oligopeptide transporter 1 | 0.08 | -0.61 | -0.72 | **-1.07** | -0.09 |
| AT5G63420 | emb2746__RNA-metabolising metallo-beta-lactamase family protein | 0.12 | -0.13 | -0.15 | **-0.74** | -0.11 |
| **AT3G50740** | **UGT72E1__UDP-glucosyl transferase 72E1** | 0.00 | -0.38 | -0.02 | **-0.88** | -0.18 |
| AT1G04430 | S-adenosyl-L-methionine-dependent methyltransferases superfamily protein | -0.02 | -0.25 | -0.13 | **-0.78** | -0.21 |
| AT5G49910 | cpHsc70-2_HSC70-7__chloroplast heat shock protein 70-2 | 0.10 | -0.13 | 0.09 | **-0.71** | -0.24 |
| AT5G17230 | PSY__PHYTOENE SYNTHASE | 0.11 | -0.16 | -0.08 | **-0.86** | -0.27 |
| AT1G72090 | Methylthiotransferase | 0.03 | 0.05 | 0.00 | **-0.74** | -0.27 |
| AT3G54600 | Class I glutamine amidotransferase-like superfamily protein | 0.18 | -0.12 | 0.04 | **-0.77** | -0.27 |
| AT1G18810 | phytochrome kinase substrate-related | 0.05 | -0.64 | -0.89 | **-1.27** | -0.29 |
| AT5G55230 | ATMAP65-1_MAP65-1_MAP65-1__microtubule-associated proteins 65-1 | 0.11 | -0.16 | -0.25 | **-1.06** | -0.30 |
| AT2G25000 | ATWRKY60_WRKY60__WRKY DNA-binding protein 60 | -0.04 | -0.29 | -0.13 | **-0.93** | -0.32 |

| AGI identifier | Gene annotation | 30 min | 2h | 4h | 8h | 24h |
|---|---|---|---|---|---|---|
| AT1G55490 | CPN60B_Cpn60beta1_LEN1__chaperonin 60 beta | 0.03 | 0.03 | -0.10 | **-0.79** | -0.38 |
| **AT5G09870** | **CESA5__cellulose synthase 5** | 0.11 | -0.09 | 0.08 | **-0.76** | -0.39 |
| **AT4G12310** | **CYP706A5__cytochrome P450, family 706, subfamily A, polypeptide 5** | -0.33 | -0.08 | -0.33 | **-0.88** | -0.39 |
| AT5G33320 | ARAPPT_CUE1_PPT__Glucose-6-phosphate/phosphate translocator-related | 0.10 | -0.15 | 0.05 | **-0.87** | -0.39 |
| AT1G70280 | NHL domain-containing protein | 0.04 | 0.00 | -0.32 | **-0.90** | -0.39 |
| AT3G57050 | CBL__cystathionine beta-lyase | 0.11 | -0.07 | -0.24 | **-0.77** | -0.41 |
| AT5G44580 | unknown protein | 0.01 | -0.32 | -0.33 | **-0.81** | -0.44 |
| AT1G29050 | TBL38__TRICHOME BIREFRINGENCE-LIKE 38 | -0.04 | -0.06 | -0.03 | **-0.77** | -0.44 |
| AT5G45930 | CHL I2_CHLI-2_CHLI2__magnesium chelatase i2 | -0.06 | -0.13 | -0.15 | **-0.88** | -0.46 |
| AT1G76160 | sks5__SKU5 similar 5 | 0.09 | -0.26 | -0.75 | **-1.08** | -0.46 |
| AT3G04940 | ATCYSD1_CYSD1__cysteine synthase D1 | 0.00 | -0.05 | -0.50 | **-0.70** | -0.48 |
| AT1G29280 | ATWRKY65_WRKY65__WRKY DNA-binding protein 65 | 0.02 | 0.07 | -0.09 | **-0.95** | -0.51 |
| AT4G18480 | CH-42_CH42_CHL11_CHLI-1_CHLI1__P-loop containing nucleoside triphosphate hydrolases superfamily protein | 0.15 | -0.16 | 0.00 | **-0.73** | -0.54 |
| **AT4G39350** | **ATCESA2_ATH-A_CESA2__cellulose synthase A2** | 0.12 | -0.19 | -0.25 | **-1.10** | -0.54 |
| AT4G16830 | Hyaluronan / mRNA binding family | 0.01 | -0.02 | -0.42 | **-0.82** | -0.54 |
| AT1G21570 | Unknown protein | -0.07 | -0.70 | -0.14 | **-1.57** | -0.55 |
| AT3G23940 | dehydratase family | 0.02 | 0.07 | -0.12 | **-0.87** | -0.55 |
| AT5G50375 | CPI1__cyclopropyl isomerase | 0.03 | -0.35 | -0.19 | **-0.76** | -0.55 |
| AT4G37800 | XTH7__xyloglucan endotransglucosylase/hydrolase 7 | 0.07 | 0.07 | -0.35 | **-0.69** | -0.56 |
| AT5G22640 | emb1211__MORN (Membrane Occupation and Recognition Nexus) repeat-containing protein | 0.24 | 0.03 | -0.37 | **-0.90** | -0.56 |
| AT5G10560 | Glycosyl hydrolase family protein | 0.03 | -0.22 | -0.53 | **-1.00** | -0.56 |
| AT1G72930 | TIR__toll/interleukin-1 receptor-like | -0.12 | -0.33 | -0.10 | **-1.33** | -0.57 |
| AT1G07280 | Tetratricopeptide repeat (TPR)-like superfamily protein | -0.09 | -0.35 | -0.59 | **-0.92** | -0.58 |
| AT3G06650 | ACLB-1__ATP-citrate lyase B-1 | 0.26 | -0.09 | -0.24 | **-0.73** | -0.59 |
| AT4G12420 | SKU5__Cupredoxin superfamily protein | 0.10 | -0.11 | -0.93 | **-1.07** | -0.60 |
| AT4G29060 | emb2726__elongation factor Ts family protein | -0.03 | 0.04 | -0.24 | **-1.07** | -0.60 |
| AT1G64740 | TUA1__alpha-1 tubulin | 0.09 | -0.15 | -0.06 | **-0.83** | -0.61 |
| AT1G16350 | Aldolase-type TIM barrel family protein | 0.07 | -0.31 | -0.33 | **-0.74** | -0.61 |
| AT3G47070 | LOCATED IN: thylakoid, chloroplast thylakoid membrane, chloroplast, chloroplast envelope; EXPRESSED IN: 22 plant structures; EXPRESSED DURING: 13 growth stages; CONTAINS InterPro DOMAIN/s: Thylakoid soluble phosphoprotein TSP9 (InterPro:IPR021584 (source: NCBI BLink). | 0.09 | -0.05 | -0.46 | **-0.76** | -0.62 |

| AGI identifier | Gene annotation | 30 min | 2h | 4h | 8h | 24h |
|---|---|---|---|---|---|---|
| AT1G06550 | ATP-dependent caseinolytic (Clp) protease/crotonase family protein | 0.17 | -0.16 | 0.19 | **-0.77** | -0.62 |
| AT5G15410 | ATCNGC2_CNGC2_DND1__Cyclic nucleotide-regulated ion channel family protein | 0.08 | -0.16 | -0.63 | **-0.78** | -0.63 |
| AT5G46580 | pentatricopeptide (PPR) repeat-containing protein | -0.10 | -0.01 | -0.02 | **-0.93** | -0.64 |
| AT3G26060 | ATPRX Q_PRXQ__Thioredoxin superfamily protein | 0.16 | -0.07 | -0.16 | **-0.79** | **-0.67** |
| AT5G45490 | P-loop containing nucleoside triphosphate hydrolases superfamily protein | 0.04 | -0.24 | -0.42 | **-0.89** | **-0.68** |
| AT5G11420 | Protein of unknown function, DUF642 | -0.08 | -0.31 | -0.89 | **-0.79** | **-0.71** |
| AT1G80830 | ATNRAMP1_NRAMP1_PMIT1__natural resistance-associated macrophage protein 1 | -0.02 | -0.46 | -0.93 | **-0.99** | **-0.75** |
| AT4G23820 | Pectin lyase-like superfamily protein | 0.25 | -0.11 | -0.74 | **-0.74** | **-0.76** |
| AT3G49670 | BAM2__Leucine-rich receptor-like protein kinase family protein | 0.01 | 0.02 | -0.33 | **-0.93** | **-0.76** |
| AT3G60320 | Protein of unknown function (DUF630 and DUF632) | 0.03 | -0.18 | -0.72 | **-1.10** | **-0.77** |
| AT4G38160 | pde191__Mitochondrial transcription termination factor family protein | 0.27 | -0.10 | -0.90 | **-0.92** | **-0.79** |
| AT3G17170 | RFC3__Translation elongation factor EF1B/ribosomal protein S6 family protein | 0.02 | 0.23 | -0.31 | **-0.72** | **-0.79** |
| AT3G09260 | BGLU23_LEB_PSR3.1_PYK10__Glycosyl hydrolase superfamily protein | 0.08 | 0.24 | 0.27 | **-0.85** | **-0.81** |
| AT5G04230 | ATPAL3_PAL3__phenyl alanine ammonia-lyase 3 | -0.05 | -0.48 | -0.59 | **-0.88** | **-0.81** |
| AT2G37180 | PIP2;3_PIP2C_RD28__Aquaporin-like superfamily protein | -0.16 | -0.10 | -0.82 | **-0.87** | **-0.82** |
| AT3G54580 | Proline-rich extensin-like family protein | -0.15 | 0.35 | -0.61 | **-0.91** | **-0.82** |
| AT4G33010 | AtGLDP1_GLDP1__glycine decarboxylase P-protein 1 | 0.11 | 0.03 | -0.54 | **-0.97** | **-0.83** |
| AT5G65010 | ASN2__asparagine synthetase 2 | -0.03 | 0.07 | -0.15 | **-0.97** | **-0.84** |
| AT3G06350 | EMB3004_MEE32__dehydroquinate dehydratase, putative / shikimate dehydrogenase, putative | -0.11 | -0.25 | -0.62 | **-1.03** | **-0.85** |
| AT2G39730 | RCA__rubisco activase | 0.13 | -0.01 | -0.78 | **-0.71** | **-0.88** |
| AT5G54770 | THI1_THI4_TZ__thiazole biosynthetic enzyme, chloroplast (ARA6) (THI1) (THI4) | 0.09 | -0.07 | -0.11 | **-0.75** | **-0.89** |
| AT5G39210 | CRR7__chlororespiratory reduction 7 | -0.09 | 0.14 | -0.58 | **-1.27** | **-0.89** |
| AT5G51550 | EXL3__EXORDIUM like 3 | 0.08 | -0.27 | -0.91 | **-0.94** | **-0.90** |
| AT1G47890 | AtRLP7_RLP7__receptor like protein 7 | -0.15 | -0.41 | -0.59 | **-0.70** | **-0.92** |
| AT3G45700 | Major facilitator superfamily protein | -0.28 | -0.42 | 0.27 | **-0.91** | **-0.93** |
| AT1G29560 | Zinc finger C-x8-C-x5-C-x3-H type family protein | 0.15 | -0.38 | -0.45 | **-1.00** | **-0.93** |
| AT5G03300 | ADK2__adenosine kinase 2 | 0.16 | -0.30 | 0.03 | **-0.99** | **-0.94** |
| AT2G44160 | MTHFR2_methylenetetrahydrofolate reductase 2 | 0.20 | -0.28 | -0.52 | **-1.28** | **-0.95** |
| AT3G29200 | ATCM1_CM1__chorismate mutase 1 | -0.11 | -0.42 | -0.39 | **-0.95** | **-0.96** |

| AGI identifier | Gene annotation | 30 min | 2h | 4h | 8h | 24h |
|---|---|---|---|---|---|---|
| AT5G38430 | Ribulose bisphosphate carboxylase (small chain) family protein | 0.05 | -0.15 | -0.30 | **-0.74** | **-0.98** |
| AT5G26260 | TRAF-like family protein | 0.04 | -0.18 | 0.14 | **-0.78** | **-0.99** |
| AT5G17920 | ATCIMS_ATMETS_ATMS1__Cobalamin-independent synthase family protein | 0.13 | -0.26 | -0.41 | **-1.06** | **-0.99** |
| AT4G23550 | ATWRKY29_WRKY29__WRKY family transcription factor | -0.19 | -0.38 | -0.73 | **-0.76** | **-1.01** |
| AT4G14890 | FdC2__2Fe-2S ferredoxin-like superfamily protein | -0.10 | -0.19 | -0.48 | **-0.97** | **-1.01** |
| AT1G29600 | Zinc finger C-x8-C-x5-C-x3-H type family protein | -0.10 | -0.15 | -0.19 | **-1.22** | **-1.02** |
| AT3G16390 | NSP3__nitrile specifier protein 3 | 0.06 | 0.20 | 0.30 | **-1.03** | **-1.02** |
| AT4G17810 | C2H2 and C2HC zinc fingers superfamily protein | 0.11 | -0.18 | -0.89 | **-0.78** | **-1.03** |
| AT5G01015 | unknown protein | 0.00 | -0.36 | -0.60 | **-0.78** | **-1.03** |
| AT3G59970 | MTHFR1_methylenetetrahydrofolate reductase 1 | 0.02 | -0.54 | -0.40 | **-1.30** | **-1.06** |
| AT3G20370 | TRAF-like family protein | 0.07 | -0.20 | 0.35 | **-0.94** | **-1.06** |
| AT3G55630 | ATDFD_DFD_FPGS3__DHFS-FPGS homolog D | -0.05 | -0.19 | -0.23 | **-0.86** | **-1.06** |
| AT5G38980 | unknown protein | -0.15 | -0.03 | -0.30 | **-0.96** | **-1.09** |
| AT5G47950 | HXXXD-type acyl-transferase family protein | -0.17 | -0.54 | -0.15 | **-0.96** | **-1.11** |
| AT1G51940 | protein kinase family protein / peptidoglycan-binding LysM domain-containing protein | -0.32 | -0.08 | 0.11 | **-0.87** | **-1.13** |
| AT1G11860 | Glycine cleavage T-protein family | 0.00 | -0.16 | -0.32 | **-1.17** | **-1.14** |
| AT3G19820 | CBB1_DIM_DIM1_DWF1_EVE1__cell elongation protein / DWARF1 / DIMINUTO (DIM) | 0.07 | -0.11 | -0.45 | **-1.27** | **-1.15** |
| AT5G24760 | GroES-like zinc-binding dehydrogenase family protein | -0.04 | -0.50 | -0.34 | **-1.08** | **-1.19** |
| AT4G22210 | LCR85__low-molecular-weight cysteine-rich 85 | -0.16 | -0.27 | -0.69 | **-1.56** | **-1.27** |
| AT4G38840 | SAUR-like auxin-responsive protein family | -0.04 | -0.42 | -0.57 | **-0.84** | **-1.31** |
| AT3G16460 | JAL34__Mannose-binding lectin superfamily protein | -0.11 | 0.14 | -0.51 | **-0.89** | **-1.53** |
| AT4G15390 | HXXXD-type acyl-transferase family protein | 0.08 | -0.44 | -0.70 | **-1.39** | **-1.54** |
| AT4G12545 | Bifunctional inhibitor/lipid-transfer protein/seed storage 2S albumin superfamily protein | -0.03 | 0.28 | -0.70 | **-1.20** | **-1.66** |
| AT3G03780 | ATMS2_MS2__methionine synthase 2 | 0.15 | -0.55 | -0.50 | **-1.66** | **-2.22** |
| AT5G48430 | Eukaryotic aspartyl protease family protein | -0.21 | -0.77 | **-1.12** | 0.67 | **1.47** |
| AT3G10985 | ATWI-12_SAG20_WI12__senescence associated gene 20 | 0.12 | 0.04 | **-1.07** | -0.17 | **0.74** |
| AT1G73260 | ATKTI1_KTI1__kunitz trypsin inhibitor 1 | -0.05 | 0.20 | **-1.74** | -0.39 | 0.23 |
| AT1G12780 | ATUGE1_UGE1__UDP-D-glucose/UDP-D-galactose 4-epimerase 1 | -0.25 | -0.10 | **-1.06** | 0.46 | -0.09 |

| AGI identifier | Gene annotation | 30 min | 2h | 4h | 8h | 24h |
|---|---|---|---|---|---|---|
| AT3G16150 | ASPGB1__N-terminal nucleophile aminohydrolases (Ntn hydrolases) superfamily protein | -0.04 | -0.57 | **-1.48** | 0.23 | -0.36 |
| AT3G53460 | CP29__chloroplast RNA-binding protein 29 | -0.19 | -0.27 | **-1.04** | -0.50 | -0.56 |
| AT1G66180 | Eukaryotic aspartyl protease family protein | -0.33 | -0.48 | **-1.07** | -0.40 | **-0.68** |
| AT5G26280 | TRAF-like family protein | 0.17 | -0.29 | **-1.02** | -0.16 | **-0.86** |
| AT4G36850 | PQ-loop repeat family protein / transmembrane family protein | -0.13 | -0.17 | **-1.17** | 0.30 | **-0.95** |
| AT2G27385 | Pollen Ole e 1 allergen and extensin family protein | -0.01 | -0.10 | **-1.40** | -0.57 | **-1.00** |
| AT1G64370 | unknown protein | -0.15 | -0.22 | **-1.01** | **-0.77** | -0.16 |
| AT2G45960 | ATHH2_PIP1;2_PIP1B_TMP-A__plasma membrane intrinsic protein 1B | -0.17 | -0.11 | **-1.14** | **-0.77** | -0.37 |
| AT5G01210 | HXXXD-type acyl-transferase family protein | 0.05 | -0.78 | **-1.65** | **-1.37** | -0.38 |
| AT1G65930 | cICDH__cytosolic NADP+-dependent isocitrate dehydrogenase | -0.03 | -0.29 | **-1.13** | **-0.96** | -0.56 |
| AT4G14040 | EDA38_SBP2__selenium-binding protein 2 | 0.21 | -0.31 | **-1.01** | **-0.70** | -0.60 |
| AT1G05240 | Peroxidase superfamily protein | 0.08 | 0.19 | **-1.07** | **-1.48** | **-0.91** |
| AT1G43160 | RAP2.6__related to AP2 6 | 0.02 | -0.57 | **-1.57** | **-1.16** | **-0.99** |
| AT1G69100 | Eukaryotic aspartyl protease family protein | 0.13 | -0.04 | **-1.06** | **-1.21** | **-1.03** |
| AT5G25460 | Protein of unknown function, DUF642 | -0.03 | -0.55 | **-1.30** | **-1.72** | **-1.41** |
| AT5G49730 | ATFRO6_FRO6_FRO6_ferric reduction oxidase 6 | -0.05 | -0.27 | **-1.35** | **-0.79** | **-1.46** |
| AT4G23400 | PIP1;5_PIP1D__plasma membrane intrinsic protein 1;5 | -0.29 | -0.16 | **-1.06** | **-0.99** | **-1.50** |
| AT1G08630 | THA1__threonine aldolase 1 | 0.06 | -0.54 | **-1.81** | **-0.92** | **-1.62** |
| AT4G29905 | unknown protein | 0.00 | 0.29 | **-1.16** | **-0.76** | **-1.83** |
| AT2G36690 | 2-oxoglutarate (2OG) and Fe(II)-dependent oxygenase superfamily protein | 0.09 | **-1.13** | -0.18 | -0.61 | 0.31 |
| AT1G48320 | Thioesterase superfamily protein | -0.16 | **-0.80** | -0.78 | **-0.93** | -0.52 |
| AT5G26290 | TRAF-like family protein | -0.15 | **-0.87** | -0.71 | **-1.50** | **-1.36** |
| AT5G48930 | HCT__hydroxycinnamoyl-CoA shikimate/quinate hydroxycinnamoyl transferase | -0.20 | **-1.17** | **-1.11** | **-1.50** | **-1.18** |
| AT3G19450 | ATCAD4_CAD_CAD-C_CAD4__GroES-like zinc-binding alcohol dehydrogenase family protein | 0.03 | **-0.82** | **-1.22** | **-1.74** | **-1.74** |
| **AT1G26810** | **GALT1__galactosyltransferase1** | -0.13 | **-1.16** | **-1.71** | **-1.65** | **-1.79** |

**Supplemental Table IV:** Biological pathways with significant genes over-represented (P-values < 0.05), indicated in bold face. Genes lists for each time point used correspond to diffentially expressed genes selected after ANOVA analysis.
Normed Frequency is calculated as follows: (Number_in_Classinput_set/Number_Classifiedinput_set)/(Number_in_Classreference_set (25k)/Number_Classifiedreference_set). DEG: Differentially expressed gene.
The 3rd column of the normalized value table represents the p-value of the hypergeometric distribution, which was calculated as follows: p = BC(M,x) * BC(N-M, n-x) / BC(N,n). BC is the binomial coefficient, calculated as follows: BC(n,k) = n! / (k! * [n-k]!). In the above equations, x is the number of input genes with the selected classification, n is the total number of input genes, M is the number of genes with the selected classification in the database (GO/MapMan), and N is the total number of genes in this database. The MapMan data used by Classification SuperViewer is updated to Ath_AGI_LOCUS_TAIR10_Aug2012.txt. [most recent version as of 4 June 2013].

| MAPMAN based classification | DEG 2 h down | | | DEG 4 h down | | | DEG 8 h down | | | DEG 24 h down | | |
|---|---|---|---|---|---|---|---|---|---|---|---|---|
| | Normed frequency | ± bootstrap StdDev | p-value | Normed frequency | ± bootstrap StdDev | p-value | Normed frequency | ± bootstrap StdDev | p-value | Normed frequency | ± bootstrap StdDev | p-value |
| amino acid metabolism (Input set freq.: 0.06; 0) | - | - | - | **9.94** | ***6.496*** | **0.016** | **11.74** | ***3.492*** | **2.71E-09** | **7.86** | ***3.05*** | **2.96E-05** |
| C1-metabolism (Input set freq.: 0.03; 0) | - | - | - | - | - | - | **27.77** | ***13.538*** | **1.29E-05** | **29.21** | ***14.576*** | **1.06E-05** |
| cell wall (Input set freq.: 0.04; 0.01) | - | - | - | 2.35 | *1.58* | 0.281 | **2.53** | ***0.856*** | **0.034** | **2.66** | ***1.191*** | **0.029** |
| Co-factor and vitamine metabolism (Input set freq.: 0; 0) | - | - | - | - | - | - | **6.85** | ***4.24*** | **0.031** | 3.6 | *3.168* | 0.211 |
| DNA (Input set freq.: 0; 0.09) | - | - | - | - | - | - | **0.08** | ***0.074*** | **9.14E-05** | **0.09** | ***0.086*** | **1.56E-04** |
| hormone metabolism (Input set freq.: 0.06; 0.01) | - | - | - | - | - | - | **3.07** | ***1.191*** | **0.01** | **3.78** | ***1.295*** | **2.09E-03** |
| lipid metabolism (Input set freq.: 0.03; 0.01) | 13.05 | - | 0.072 | - | - | - | 1.94 | *1.062* | 0.132 | **2.72** | ***1.415*** | **0.044** |
| metal handling (Input set freq.: 0; 0) | - | - | - | **31.14** | ***17.149*** | **1.85E-03** | **6.69** | ***4.07*** | **0.033** | 3.52 | *2.31* | 0.215 |
| misc (Input set freq.: 0.07; 0.04) | 3.52 | *3.184* | 0.223 | 0.81 | *0.687* | 0.366 | 1.04 | *0.375* | 0.164 | **1.65** | ***0.551*** | **0.049** |
| not assigned (Input set freq.: 0.22; 0.35) | 0.47 | *0.399* | 0.242 | 0.76 | *0.265* | 0.117 | **0.56** | ***0.104*** | **9.78E-05** | **0.64** | ***0.111*** | **1.26E-03** |
| protein (Input set freq.: 0.11; 0.14) | 1.15 | *0.911* | 0.397 | 0.8 | *0.457* | 0.217 | **0.28** | ***0.125*** | **1.78E-04** | 0.78 | *0.19* | 0.072 |
| PS (Input set freq.: 0.05; 0) | - | - | - | - | - | - | **6.74** | ***2.684*** | **8.17E-04** | **8.51** | ***3.302*** | **7.24E-05** |
| secondary metabolism (Input set freq.: 0.05; 0.01) | **25.22** | ***14.944*** | **2.48E-03** | **8.73** | ***4.084*** | **4.40E-03** | **5.62** | ***1.7*** | **2.97E-05** | **3.94** | ***1.665*** | **3.46E-03** |
| signalling (Input set freq.: 0; 0.04) | - | - | - | - | - | - | 0.81 | *0.395* | 0.181 | **0.21** | ***0.175*** | **0.041** |
| TCA / org transformation (Input set freq.: 0.01; 0) | - | - | - | 16.35 | *11.594* | 0.058 | **7.03** | ***5.297*** | **0.03** | - | - | - |
| tetrapyrrole synthesis (Input set freq.: 0.01; 0) | - | - | - | - | - | - | **11.57** | ***6.227*** | **0.012** | - | - | - |
| transport (Input set freq.: 0.05; 0.03) | - | - | - | 2.53 | *1.763* | 0.143 | **2.17** | ***0.805*** | **0.02** | 1.71 | *0.676* | 0.077 |

| MAPMAN based classification | DEG 30 min up | | | DEG 2 h up | | | DEG 4 h up | | | DEG 8 h up | | | DEG 24 h up | | |
|---|---|---|---|---|---|---|---|---|---|---|---|---|---|---|---|
| | Normed frequency | ± bootstrap StdDev | p-value | Normed frequency | ± bootstrap StdDev | p-value | Normed frequency | ± bootstrap StdDev | p-value | Normed frequency | ± bootstrap StdDev | p-value | Normed frequency | ± bootstrap StdDev | p-value |
| DNA (Input set freq.: 0; 0.09) | 0.76 | *0.557* | 0.366 | 0.26 | *0.207* | 0.077 | **0.21** | ***0.143*** | **0.036** | **0.07** | ***0.052*** | **5.04E-06** | **0.04** | ***0.028*** | **9.72E-10** |
| fermentation (Input set freq.: 0.01; 0) | - | - | - | - | - | - | - | - | - | 15.68 | *12.201* | 0.06 | **29.38** | ***15.091*** | **1.29E-04** |
| glycolysis (Input set freq.: 0.01; 0) | **30.38** | ***31.597*** | **0.032** | 10.37 | *12.411* | 0.088 | 8.34 | *6.131* | 0.107 | **8.34** | ***4.696*** | **5.21E-03** | **6.94** | ***3.017*** | **2.41E-03** |
| hormone metabolism (Input set freq.: 0.04; 0.01) | - | - | - | 1.51 | *1.272* | 0.345 | 2.43 | *1.516* | 0.149 | 2.02 | *0.937* | 0.064 | **2.78** | ***0.781*** | **1.55E-03** |
| misc (Input set freq.: 0.17; 0.04) | - | - | - | **3.09** | ***1.262*** | **9.19E-03** | **6.21** | ***1.269*** | **7.03E-09** | **4.14** | ***0.62*** | **2.39E-11** | **3.62** | ***0.531*** | **3.29E-13** |
| not assigned (Input set freq.: 0.21; 0.35) | 1.22 | *0.423* | 0.177 | 0.97 | *0.225* | 0.129 | **0.61** | ***0.148*** | **0.015** | **0.68** | ***0.112*** | **1.04E-03** | **0.6** | ***0.072*** | **7.37E-07** |
| protein (Input set freq.: 0.11; 0.14) | 0.49 | *0.368* | 0.267 | 0.67 | *0.325* | 0.138 | **0.27** | ***0.17*** | **0.013** | **0.54** | ***0.144*** | **5.24E-03** | **0.79** | ***0.143*** | **0.031** |
| redox (Input set freq.: 0.02; 0) | - | - | - | - | - | - | **6.27** | ***3.542*** | **0.037** | **5.22** | ***2.279*** | **2.40E-03** | **4.57** | ***1.606*** | **7.64E-04** |
| RNA (Input set freq.: 0.04; 0.09) | 1.57 | *0.64* | 0.239 | 0.8 | *0.428* | 0.215 | 0.43 | *0.295* | 0.099 | **0.64** | ***0.212*** | **0.047** | **0.45** | ***0.134*** | **1.31E-03** |
| stress (Input set freq.: 0.09; 0.03) | - | - | - | 2 | *1.059* | 0.126 | 2.14 | *1.023* | 0.077 | **2.32** | ***0.597*** | **2.66E-03** | **2.68** | ***0.552*** | **8.68E-06** |
| transport (Input set freq.: 0.06; 0.03) | 2.35 | *2.307* | 0.285 | 2.4 | *1.324* | 0.093 | 1.93 | *1.027* | 0.133 | **2.79** | ***0.814*** | **5.82E-04** | **2.14** | ***0.515*** | **2.14E-03** |

**Supplemental Table V:** The 467 genes found to be differentially expressed in all the comparisons between phenanthrene-treated and control plants (hybridizations 5-9), selected after ANOVA analysis. Expression changes in bolt correspond to genes differentially expressed at the significant threshold of Bonferroni p-value<0.05. AGI and gene annotation in bold face correspond to gene involved in the "xenome". Our list of genes was compare to diffentially expressed genes identified in the plant response aluminum (60), atrazine (33), BOA (benzoxazolin-2(3H)-one) (61), cadmium (62), PCB (Polychlorinated biphenyl) (63), phenol (64) selenium (65) and TNT (trinitrotoluene) (66). Our list was also compare to genes differentially regulated by anoxia, hypoxia, and O2 deprivation in the seedlings/shoots of *Arabidopsis* microarray datasets (Picciariello et al., 2012). *: log2 ratios

| AGI identifier | Bincode identifier | MAPMAN classification | Gene annotation | Our study | | | | | DEG in common with other xenobiotic transcriptomes | Weisman et al., 2010 | Jin *et al.*, 2011 | Van Hoewyk *et al.*, 2008 | | Ramel *et al.*, 2007 | | Baerson *et al.*, 2005 | Goodwin and Sutter, 2009 | Xu *et al.*, 2012 | Landa *et al.*, 2010 | | Herbette *et al.*, 2006 | | Pucciariello et al., 2012 |
|---|---|---|---|---|---|---|---|---|---|---|---|---|---|---|---|---|---|---|---|---|---|---|---|
| | | | | Phenanthrene Seedlings | | | | | | Phenanthrene Seedlings | PCB ? | Selenium | | Atrazine Mannitol | Atrazine Sucrose | BOA | Aluminium | Phénol | Trinitrotoluene | | Cadmium | | Anoxia-hypoxia |
| | | | | 30 min* | 2h* | 4h* | 8h* | 24h* | Number in common | 109 | 146 | Leaves 32 | Roots 52 | Seedlings 113 | 119 | 45 | 14 | 16 | Leaves 15 | Roots 2 | Leaves 134 | Roots 182 | 3 |
| **AT1G05670** | **17.8.1** | **hormone metabolism.salicylic acid.synthesis-degradation** | **Pentatricopeptide repeat (PPR-like) superfamily protein** | ns | ns | ns | **1.30** | **0.69** | | | | | | | X | | | | | | | | |
| **AT1G05680** | **17.8.1** | **hormone metabolism.salicylic acid.synthesis-degradation** | **UGT74E2__UDP-glycosyltransferase 74E2** | ns | ns | **1.01** | **1.80** | **0.83** | X | | X | X | X | | | X | | | | | | | |
| **AT1G11610** | **26.10** | **misc.cytochrome P450** | **CYP71A18__cytochrome P450, family 71, subfamily A, polypeptide 18** | ns | ns | ns | ns | **1.12** | | | | | | | | | | | | | | | |
| **AT1G17170** | **26.9** | **misc.glutathione S transferases** | **ATGSTU24_GST_GSTU24__glutathione S-transferase TAU 24** | ns | ns | **1.57** | **2.00** | **2.05** | X | up | | X | | | | X | | | | | | | |
| **AT1G17190** | **26.9** | **misc.glutathione S transferases** | **ATGSTU26_GSTU26__glutathione S-transferase tau 26** | ns | ns | ns | ns | **-1.41** | X | | | | | | | | | | | | | X | |
| **AT1G26810** | **29.7.12** | **protein.glycosylation.beta-1,3-galactosyltransferase(beta-1,3-GalT)** | **GALACTOSYLTRANSFERASE1** | ns | **-1.16** | **-1.71** | **-1.65** | **-1.79** | | | | | | | | | | | | | | | |
| **AT1G27120** | **26.2** | **misc.UDP glucosyl and glucoronyl transferases** | **Galactosyltransferase family protein** | ns | **0.91** | **2.00** | **2.30** | **2.45** | | | | | | | | | | | | | | | |
| **AT1G55850** | **10.2.1** | **cell wall.cellulose synthesis.cellulose synthase** | **ATCSLE1_CSLE1__cellulose synthase like E1** | ns | ns | ns | **1.17** | ns | X | | | X | | | | X | | | | | | | |
| **AT1G58370** | **10.6.2** | **cell wall.degradation.mannan-xylose-arabinose-fucose** | **ATXYN1_RXF12__glycosyl hydrolase family 10 protein / carbohydrate-binding domain-containing protein** | ns | ns | **1.13** | ns | **-0.86** | X | | X | X | | | | | | | | | | | |
| **AT1G64900** | **26.10** | **misc.cytochrome P450** | **CYP89_CYP89A2__cytochrome P450, family 89, subfamily A, polypeptide 2** | ns | ns | **1.08** | **1.16** | **1.19** | X | | X | X | | | | | | | | | | | |
| **AT1G64930** | **26.10** | **misc.cytochrome P450** | **CYP89A7__cytochrome P450, family 87, subfamily A, polypeptide 7** | ns | ns | ns | **0.85** | **0.94** | | | | | | | | | | | | | | | |
| **AT1G69500** | **26.10** | **misc.cytochrome P450** | **CYP704B1__cytochrome P450, family 704, subfamily B, polypeptide 1** | ns | ns | ns | **-0.71** | **0.71** | | | | | | | | | | | | | | | |
| **AT1G75270** | **21.2.1** | **redox.ascorbate and glutathione.ascorbate** | **DHAR2__dehydroascorbate reductase 2** | ns | ns | **1.09** | **1.60** | **1.49** | X | up | | | | X | | | | | | | | X | |
| **AT1G78340** | **26.9** | **misc.glutathione S transferases** | **ATGSTU22_GSTU22__glutathione S-transferase TAU 22** | ns | ns | **1.62** | **1.75** | **1.69** | X | up | X | | | | | X | | X | | | | | |
| **AT1G78380** | **26.9** | **misc.glutathione S transferases** | **ATGSTU19_GST8_GSTU19__glutathione S-transferase TAU 19** | ns | ns | **1.23** | **1.45** | **1.49** | X | up | | | | | | | | | | | | X | |
| **AT2G12190** | **26.10** | **misc.cytochrome P450** | **Cytochrome P450 superfamily protein** | ns | ns | **1.04** | **0.97** | **0.96** | X | | X | | | | | | | | | | | | |
| **AT2G29460** | **26.9** | **misc.glutathione S transferases** | **ATGSTU4_GST22_GSTU4__glutathione S-transferase tau 4** | ns | ns | ns | **1.37** | **0.95** | X | up | | X | X | | | | | | | | | | |
| **AT2G29470** | **26.9** | **misc.glutathione S transferases** | **ATGSTU3_GST21_GSTU3__glutathione S-transferase tau 3** | ns | ns | ns | **1.14** | **0.76** | | | | | | | | | | | | | | | |
| **AT2G29940** | **34.16** | **transport.ABC transporters and multidrug resistance systems** | **ATPDR3_PDR3__pleiotropic drug resistance 3** | ns | ns | ns | **0.96** | ns | X | | | | | | X | | | | | | | X | |
| **AT2G36770** | **26.2** | **misc.UDP glucosyl and glucoronyl transferases** | **UDP-Glycosyltransferase superfamily protein** | ns | ns | ns | **1.65** | ns | | | | | | | | | | | | | | | |
| **AT2G40890** | **26.10** | **misc.cytochrome P450** | **CYP98A3__cytochrome P450, family 98, subfamily A, polypeptide 3** | ns | ns | ns | ns | **-0.74** | X | | | | | X | | | | | | | | X | |
| **AT2G45550** | **26.10** | **misc.cytochrome P450** | **CYP76C4__cytochrome P450, family 76, subfamily C, polypeptide 4** | ns | ns | ns | **0.91** | **0.89** | X | | | | | X | X | | | | | | | X | |
| **AT3G09270** | **26.9** | **misc.glutathione S transferases** | **ATGSTU8_GSTU8__glutathione S-transferase TAU 8** | ns | ns | **1.15** | ns | **1.09** | X | up | X | | | X | | X | | | | | | X | |
| **AT3G14620** | **26.10** | **misc.cytochrome P450** | **CYP72A8__cytochrome P450, family 72, subfamily A, polypeptide 8** | ns | ns | ns | **0.86** | **1.40** | X | up | | X | | | | X | | | | | | | |
| **AT3G21560** | **26.2** | **misc.UDP glucosyl and glucoronyl transferases** | **UGT84A2__UDP-Glycosyltransferase superfamily protein** | ns | **1.48** | **2.21** | **1.60** | **1.93** | X | up | X | | | | | | | | | | X | | |
| **AT3G26200** | **26.10** | **misc.cytochrome P450** | **CYP71B22__cytochrome P450, family 71, subfamily B, polypeptide 22** | ns | ns | ns | **1.07** | **1.07** | X | | X | | | | | | | | | | X | X | |
| **AT3G26210** | **26.10** | **misc.cytochrome P450** | **CYP71B23__cytochrome P450, family 71, subfamily B, polypeptide 23** | ns | ns | ns | ns | **1.01** | X | up | | | | | | X | | | | | X | | |
| **AT3G50740** | **16.2.1** | **secondary metabolism.phenylpropanoids.lignin biosynthesis** | **UGT72E1__UDP-glucosyl transferase 72E1** | ns | ns | ns | **-0.88** | ns | X | up | | | | X | X | | | | | | | X | |
| **AT3G59140** | **34.16** | **transport.ABC transporters and multidrug resistance systems** | **ATMRP14_MRP14__multidrug resistance-associated protein 14** | ns | ns | ns | **0.76** | **0.67** | X | | X | X | | | | X | | | | | | | |
| **AT4G12310** | **16.8.3** | **secondary metabolism.flavonoids.dihydroflavonols** | **CYP706A5__cytochrome P450, family 706, subfamily A, polypeptide 5** | ns | ns | ns | **-0.88** | ns | X | | X | | | | | | | | | | | | |
| **AT4G15480** | **26.2** | **misc.UDP glucosyl and glucoronyl transferases** | **UGT84A1__UDP-Glycosyltransferase superfamily protein** | ns | ns | **1.27** | **1.02** | **1.40** | X | | X | | | | | | | | | | | | |
| **AT4G34131** | **26.2** | **misc.UDP glucosyl and glucoronyl transferases** | **UGT73B3__UDP-glucosyl transferase 73B3** | ns | ns | ns | **1.31** | **1.38** | | | | | | | | | | | | | | | |
| **AT4G39350** | **10.2.1** | **cell wall.cellulose synthesis.cellulose synthase** | **ATCESA2_ATH-A_CESA2__cellulose synthase A2** | ns | ns | ns | **-1.10** | ns | | | | | | | | | | | | | | | |
| **AT5G09870** | **10.2.1** | **cell wall.cellulose synthesis.cellulose synthase** | **CESA5__cellulose synthase 5** | ns | ns | ns | **-0.76** | ns | X | | | | | | X | | | | | | | X | |
| **AT5G36270** | **21.2.1** | **redox.ascorbate and glutathione.ascorbate** | **pseudogene of dehydroascorbate reductase** | ns | ns | **1.38** | **1.56** | **1.74** | X | | | | X | | | | | | | | | | |

| AGI identifier | Bincode identifier | MAPMAN classification | Gene annotation | Our study | | | | | DEG in common with other xenobiotic transcriptomes | Weisman et al., 2010 | Jin *et al.*, 2011 | Van Hoewyk *et al.*, 2008 | | Ramel *et al.*, 2007 | | Baerson *et al.*, 2005 | Goodwin and Sutter, 2009 | Xu *et al.*, 2012 | Landa *et al.*, 2010 | | Herbette *et al.*, 2006 | | Pucciariello et al., 2012 |
|---|---|---|---|---|---|---|---|---|---|---|---|---|---|---|---|---|---|---|---|---|---|---|---|
| | | | | Phenanthrene | | | | | | Phenanthrene | PCB | Selenium | | Atrazine Mannitol | Atrazine Sucrose | BOA | Aluminium | Phénol | Trinitrotoluene | | Cadmium | | Anoxia-hypoxia |
| | | | | Seedlings | | | | | | Seedlings | ? | Leaves | Roots | Seedlings | | | | | Leaves | Roots | Leaves | Roots | |
| | | | | 30 min* | 2h* | 4h* | 8h* | 24h* | Number in commmon | 109 | 146 | 32 | 52 | 113 | 119 | 45 | 14 | 16 | 15 | 2 | 134 | 182 | 3 |
| **AT5G39090** | **16.8.1.21** | **secondary metabolism.flavonoids.anthocyanins.anthocyanin 5-aromatic acyltransferase** | **HXXXD-type acyl-transferase family protein** | ns | ns | ns | **0.82** | **1.05** | X | | | X | | | | | | | | | X | X | |
| AT1G60950 | 1.1.5.2 | PS.lightreaction.other electron carrier (ox/red).ferredoxin | ATFD2_FED A__2Fe-2S ferredoxin-like superfamily protein | ns | ns | ns | ns | **-0.72** | X | down | X | | | | | | | | | | X | X | |
| AT5G58260 | 1.1.6 | PS.lightreaction.NADH DH | oxidoreductases, acting on NADH or NADPH, quinone or similar compound as acceptor | ns | ns | ns | ns | **-1.05** | X | down | X | | | | | | | | | | X | | |
| AT4G33010 | 1.2.4.1 | PS.photorespiration.glycine cleavage.P subunit | AtGLDP1_GLDP1__glycine decarboxylase P-protein 1 | ns | ns | ns | **-0.97** | **-0.83** | X | down | X | | | | | | | | | | | | |
| AT1G11860 | 1.2.4.2 | PS.photorespiration.glycine cleavage.T subunit | Glycine cleavage T-protein family | ns | ns | ns | **-1.17** | **-1.14** | X | down | X | | | | | | | | | | X | X | |
| AT2G39730 | 1.3.13 | PS.calvin cyle.rubisco interacting | RCA__rubisco activase | ns | ns | ns | **-0.71** | **-0.88** | X | down | X | | | X | X | | | | | | X | X | |
| AT4G16980 | 10.5.1 | cell wall.cell wall proteins.AGPs | arabinogalactan-protein family | ns | ns | ns | ns | **-1.14** | X | down | X | | | | | | | X | | | X | X | |
| AT2G45470 | 10.5.1 | cell wall.cell wall proteins.AGPs | AGP8_FLA8__FASCICLIN-like arabinogalactan protein 8 | ns | ns | ns | ns | **-0.77** | X | down | | | | X | X | | | | | | X | X | |
| AT4G23820 | 10.6.3 | cell wall.degradation.pectate lyases and polygalacturonases | Pectin lyase-like superfamily protein | ns | ns | ns | **-0.74** | **-0.76** | X | down | X | | | X | | | | | | | X | | |
| AT5G06860 | 10.6.3 | cell wall.degradation.pectate lyases and polygalacturonases | ATPGIP1_PGIP1__polygalacturonase inhibiting protein 1 | ns | ns | ns | ns | **0.90** | X | up | | | | X | | X | | | X | | X | X | |
| AT4G37800 | 10.7 | cell wall.modification | XTH7__xyloglucan endotransglucosylase/hydrolase 7 | ns | ns | ns | **-0.69** | ns | X | down | | | X | X | X | | | | | | | X | |
| AT3G15850 | 11.2.1 | lipid metabolism.FA desaturation.desaturase | ADS3_FAD5_FADB_JB67__fatty acid desaturase 5 | ns | ns | ns | ns | **-0.91** | X | down | | | | X | X | | | | | | | | |
| AT5G54500 | 11.8 | lipid metabolism."exotics" (steroids, squalene etc) | FQR1__flavodoxin-like quinone reductase 1 | ns | **1.12** | **1.14** | **1.50** | **1.79** | X | up | | | | | | X | | | | | | | |
| AT4G38690 | 11.9.3 | lipid metabolism.lipid degradation.lysophospholipases | PLC-like phosphodiesterases superfamily protein | ns | ns | ns | ns | **-0.71** | X | down | X | | X | | | | | | | | | | |
| AT1G68620 | 11.9.3.2 | lipid metabolism.lipid degradation.lysophospholipases.carboxylesterase | alpha/beta-Hydrolases superfamily protein | **0.93** | **2.18** | **1.68** | **2.77** | **2.70** | X | up | X | | X | X | X | X | | | X | | | X | |
| AT5G19550 | 13.1.1.2.1 | amino acid metabolism.synthesis.central amino acid metabolism.aspartate.aspartate aminotransferase | AAT2_ASP2__aspartate aminotransferase 2 | ns | ns | ns | ns | **1.26** | X | up | | | | X | X | | X | | | | X | X |
| AT5G65010 | 13.1.3.1.1 | amino acid metabolism.synthesis.aspartate family.asparagine.asparagine synthetase | ASN2__asparagine synthetase 2 | ns | ns | ns | **-0.97** | **-0.84** | X | down | X | | | X | X | | | | | | | | |
| AT2G33150 | 13.2.4.1 | amino acid metabolism.degradation.branched-chain group.shared | KAT2_PED1_PKT3__peroxisomal 3-ketoacyl-CoA thiolase 3 | ns | ns | ns | **0.84** | **0.68** | X | up | X | | | X | X | | | | | | | | |
| AT1G62570 | 16.5.1.1.1.10 | secondary metabolism.sulfur-containing.glucosinolates.synthesis.aliphatic.flavin-containing monooxygenase | FMO GS-OX4__flavin-monooxygenase glucosinolate S-oxygenase 4 | ns | ns | ns | ns | **0.78** | X | up | | | | | X | | | | | | X | |
| AT3G45140 | 17.7.1.2 | hormone metabolism.jasmonate.synthesis-degradation.lipoxygenase | ATLOX2_LOX2__lipoxygenase 2 | ns | ns | ns | ns | **-1.11** | X | up | X | | | X | X | | | | | | | | |
| AT5G45930 | 19.10 | tetrapyrrole synthesis.magnesium chelatase | CHL I2_CHLI-2_CHLI2__magnesium chelatase i2 | ns | ns | ns | **-0.88** | ns | X | down | | | | X | X | | | | | | | X | |
| AT1G66100 | 20.1 | stress.biotic | Plant thionin | ns | ns | ns | **0.82** | **-1.11** | X | down | | | | | X | | | | | | X | | |
| AT2G43590 | 20.1 | stress.biotic | Chitinase family protein | ns | ns | ns | ns | **1.09** | X | up | X | | | | | X | | | | | | | |
| AT1G75040 | 20.1 | stress.biotic | PR-5_PR5__pathogenesis-related gene 5 | ns | **1.32** | **1.50** | **1.71** | **1.75** | X | up | X | X | | | | | | | | | X | X | |
| AT1G73260 | 20.1.7.6.1 | stress.biotic.PR-proteins.proteinase inhibitors.trypsin inhibitor | ATKTI1_KTI1__kunitz trypsin inhibitor 1 | ns | ns | **-1.74** | ns | ns | X | up | | | | | X | | | | | | X | X | |
| AT3G62600 | 20.2.1 | stress.abiotic.heat | ATERDJ3B_ERDJ3B__DNAJ heat shock family protein | ns | ns | ns | ns | **0.79** | X | up | | | | X | X | | | | | | X | X | |
| AT1G18980 | 20.2.99 | stress.abiotic.unspecified | RmlC-like cupins superfamily protein | ns | **1.16** | **1.55** | **1.57** | **1.59** | X | up | | | | | | | | | | | | X | |
| AT2G21620 | 20.2.99 | stress.abiotic.unspecified | RD2__Adenine nucleotide alpha hydrolases-like superfamily protein | ns | ns | ns | **1.28** | **1.82** | X | up | | | | | X | | X | | | | X | | |
| AT1G21750 | 21.1 | redox.thioredoxin | ATPDI5_ATPDIL1-1_PDI5_PDIL1-1__PDI-like 1-1 | ns | ns | ns | ns | **0.93** | X | up | | | | X | X | | | | | | X | | |
| AT1G77510 | 21.1 | redox.thioredoxin | ATPDI6_ATPDIL1-2_PDI6_PDIL1-2__PDI-like 1-2 | ns | ns | ns | ns | **0.96** | X | up | X | | | | | | | | | | | | |
| AT3G24170 | 21.2.2 | redox.ascorbate and glutathione.glutathione | ATGR1_GR1__glutathione-disulfide reductase | ns | ns | ns | ns | **0.73** | X | up | X | | | | | | X | | | | | X | |
| AT3G55630 | 25.8 | C1-metabolism.tetrahydrofolate synthase | ATDFD_DFD__DHFS-FPGS homolog D | ns | ns | ns | **-0.86** | **-1.06** | X | down | X | | | X | X | | | | | | X | | |
| AT5G64250 | 26.1 | misc.misc2 | Aldolase-type TIM barrel family protein | ns | ns | ns | **1.62** | **1.55** | X | up | | | | | | X | | | | | | | |
| AT5G19440 | 26.11.1 | misc.alcohol dehydrogenases | NAD(P)-binding Rossmann-fold superfamily protein | ns | ns | ns | ns | **1.28** | X | up | | | | | | | | | | | | X | |
| AT1G12090 | 26.21 | misc.protease inhibitor/seed storage/lipid transfer protein (LTP) family protein | ELP__extensin-like protein | ns | ns | ns | ns | **-1.08** | X | down | | | | | | | X | | | | X | X | |
| AT4G12480 | 26.21 | misc.protease inhibitor/seed storage/lipid transfer protein (LTP) family protein | pEARLI 1__Bifunctional inhibitor/lipid-transfer protein/seed storage 2S albumin superfamily protein | ns | ns | ns | ns | **1.19** | X | up | | X | | | | X | | | | | | | |
| AT4G12490 | 26.21 | misc.protease inhibitor/seed storage/lipid transfer protein (LTP) family protein | Bifunctional inhibitor/lipid-transfer protein/seed storage 2S albumin superfamily protein | ns | ns | ns | ns | **1.90** | X | up | X | | | | | X | X | | | | | | |
| AT3G22600 | 26.21 | misc.protease inhibitor/seed storage/lipid transfer protein (LTP) family protein | Bifunctional inhibitor/lipid-transfer protein/seed storage 2S albumin superfamily protein | ns | **1.68** | **1.96** | **1.36** | **1.96** | X | up | X | | | | | | | | | | | | |
| AT2G48140 | 26.21 | misc.protease inhibitor/seed storage/lipid transfer protein (LTP) family protein | EDA4__Bifunctional inhibitor/lipid-transfer protein/seed storage 2S albumin superfamily protein | ns | ns | **1.20** | **0.73** | ns | X | up | | | | | | | | | | | | X | |
| AT3G04000 | 26.22 | misc.short chain dehydrogenase/reductase (SDR) | NAD(P)-binding Rossmann-fold superfamily protein | ns | **0.95** | **1.16** | **1.53** | **1.23** | X | up | | X | | | | X | | | | | | | |
| AT4G13180 | 26.22 | misc.short chain dehydrogenase/reductase (SDR) | NAD(P)-binding Rossmann-fold superfamily protein | ns | ns | **1.03** | **1.07** | **1.39** | X | up | | | | | X | X | | | | | X | X | |
| AT4G14890 | 26.30 | misc. other Ferredoxins and Rieske domain | 2Fe-2S ferredoxin-like superfamily protein | ns | ns | ns | **-0.97** | **-1.01** | X | down | | | | | | | | | | | | X | |
| AT5G16970 | 26.7 | misc.oxidases - copper, flavone etc. | AER_AT-AER__alkenal reductase | ns | ns | ns | **1.15** | **1.28** | X | up | X | X | | | | X | | | | | | | |
| AT2G29350 | 26.8 | misc.nitrilases, *nitrile lyases, berberine bridge enzymes, reticuline oxidases, troponine reductases | SAG13__senescence-associated gene 13 | ns | ns | ns | ns | **1.55** | X | up | X | | | X | X | X | | | | | X | | |
| AT4G20860 | 26.8 | misc.nitrilases, *nitrile lyases, berberine bridge enzymes, reticuline oxidases, troponine reductases | FAD-binding Berberine family protein | ns | **0.91** | ns | **1.45** | **1.79** | X | up | X | | X | X | | X | | | | | | | |
| AT1G30700 | 26.8 | misc.nitrilases, *nitrile lyases, berberine bridge enzymes, reticuline oxidases, troponine reductases | FAD-binding Berberine family protein | ns | **1.26** | **1.06** | **1.56** | **2.28** | X | up | | | | X | X | X | | | | | | X | |
| AT5G59820 | 27.3.11 | RNA.regulation of transcription.C2H2 zinc finger family | RHL41_ZAT12__C2H2-type zinc finger family protein | **1.19** | **1.63** | **2.14** | **2.70** | **2.50** | X | up | | | X | | X | | | | | | | X | |
| AT1G22640 | 27.3.25 | RNA.regulation of transcription.MYB domain transcription factor family | ATMYB3_MYB3__myb domain protein 3 | ns | ns | ns | ns | **-0.83** | X | down | | | | | | | | | | | | X | |
| AT4G38620 | 27.3.25 | RNA.regulation of transcription.MYB domain transcription factor family | ATMYB4_MYB4__myb domain protein 4 | **3.51** | **2.19** | **2.30** | **2.18** | **1.94** | X | up | | | | | | X | | | | | | | |
| AT4G24770 | 27.4 | RNA.RNA binding | ATRBP31_ATRBP33_CP31_RBP31__31-kDa RNA binding protein | ns | ns | ns | ns | **-0.70** | X | down | | | | | | | | | | | X | | |

| AGI identifier | Bincode identifier | MAPMAN classification | Gene annotation | Our study | | | | | DEG in common with other xenobiotic transcriptomes | Weisman et al., 2010 | Jin *et al.*, 2011 | Van Hoewyk *et al.*, 2008 | | Ramel *et al.*, 2007 | | Baerson *et al.*, 2005 | Goodwin and Sutter, 2009 | Xu *et al.*, 2012 | Landa *et al.*, 2010 | | Herbette *et al.*, 2006 | | Pucciariello et al., 2012 |
|---|---|---|---|---|---|---|---|---|---|---|---|---|---|---|---|---|---|---|---|---|---|---|---|
| | | | | Phenanthrene | | | | | | Phenanthrene | PCB | Selenium | | Atrazine Mannitol | Atrazine Sucrose | BOA | Aluminium | Phénol | Trinitrotoluene | | Cadmium | | Anoxia-hypoxia |
| | | | | Seedlings | | | | | | Seedlings | ? | Leaves | Roots | Seedlings | | | | | Leaves | Roots | Leaves | Roots | |
| | | | | 30 min* | 2h* | 4h* | 8h* | 24h* | Number in commmon | 109 | 146 | 32 | 52 | 113 | 119 | 45 | 14 | 16 | 15 | 2 | 134 | 182 | 3 |
| AT3G56910 | 29.2.1.1.1.2.85 | protein.synthesis.ribosomal protein.prokaryotic.chloroplast.50S subunit.PSRP5 | PSRP5__plastid-specific 50S ribosomal protein 5 | ns | ns | ns | ns | **-0.75** | X | down | | | | | | | | | | | X | | |
| AT1G66580 | 29.2.1.2.2.10 | protein.synthesis.ribosomal protein.eukaryotic.60S subunit.L10 | RPL10C_SAG24__senescence associated gene 24 | ns | ns | ns | **1.26** | **1.44** | X | up | | | | | X | | | | | | X | X | |
| AT4G29060 | 29.2.4 | protein.synthesis.elongation | emb2726__elongation factor Ts family protein | ns | ns | ns | **-1.07** | ns | X | down | X | | | | | | | | | | X | | |
| AT1G78660 | 29.5 | protein.degradation | ATGGH1_GGH1__gamma-glutamyl hydrolase 1 | ns | **1.98** | ns | **1.96** | **1.27** | X | up | | | | X | | | | | | | | X | |
| AT1G32960 | 29.5.1 | protein.degradation.subtilases | ATSBT3.3_SBT3.3__Subtilase family protein | ns | ns | ns | ns | **1.27** | X | up | | | | | | X | | | | | | | |
| AT5G42300 | 29.5.11.1 | protein.degradation.ubiquitin.ubiquitin | UBL5__ubiquitin-like protein 5 | ns | ns | ns | **0.81** | **1.23** | X | up | | | | | | | | | | | | | |
| AT1G63840 | 29.5.11.4.2 | protein.degradation.ubiquitin.E3.RING | RING/U-box superfamily protein | **0.83** | **1.80** | **1.64** | **2.10** | **2.16** | X | up | | | | | | | | | | | | | |
| AT3G01480 | 29.6 | protein.folding | ATCYP38_CYP38__cyclophilin 38 | ns | ns | ns | ns | **-0.88** | X | down | | | | | | | | | | | X | | |
| AT4G25900 | 3.5 | minor CHO metabolism.others | Galactose mutarotase-like superfamily protein | ns | ns | ns | ns | **0.82** | X | up | | | | | | | | | | | X | X | |
| AT2G37760 | 3.5 | minor CHO metabolism.others | NAD(P)-linked oxidoreductase superfamily protein | ns | ns | ns | ns | **0.82** | X | up | | X | | | | X | | | | | | | |
| AT3G22840 | 30.11 | signalling.light | ELIP_ELIP1__Chlorophyll A-B binding family protein | **0.89** | **1.40** | **2.19** | **1.70** | **2.38** | X | up | X | | X | | | | X | | | | X | X | |
| AT1G51940 | 30.2.21 | signalling.receptor kinases.lysine motif | protein kinase family protein / peptidoglycan-binding LysM domain-containing protein | ns | ns | ns | **-0.87** | **-1.13** | X | down | X | | | X | X | | | | X | | | X | |
| AT5G61790 | 30.3 | signalling.calcium | ATCNX1_CNX1__calnexin 1 | ns | ns | ns | ns | **0.72** | X | up | | | | X | X | | | | | | X | X | |
| AT2G33380 | 30.3 | signalling.calcium | CLO-3_RD20__Caleosin-related family protein | ns | ns | ns | ns | **0.77** | X | up | X | X | | | | | | | | | X | | |
| AT2G41100 | 30.3 | signalling.calcium | ATCAL4_TCH3__Calcium-binding EF hand family protein | ns | ns | ns | ns | **1.10** | X | down | | | X | | | | | | X | | | | |
| AT4G14365 | 31.1 | cell.organisation | XBAT34__XB3 ortholog 4 in Arabidopsis thaliana | ns | ns | ns | ns | **1.36** | X | up | | | X | | | X | | | | | X | X | |
| AT4G02380 | 33.2 | development.late embryogenesis abundant | AtLEA5_SAG21__senescence-associated gene 21 | ns | ns | ns | ns | **1.17** | X | up | X | | | X | X | | | | | | X | | |
| AT3G10500 | 33.99 | development.unspecified | anac053_NAC053__NAC domain containing protein 53 | ns | ns | ns | **1.48** | **1.16** | X | up | | | | | | X | | | | | X | | |
| AT2G41380 | 33.99 | development.unspecified | S-adenosyl-L-methionine-dependent methyltransferases superfamily protein | ns | ns | ns | **0.87** | **1.99** | X | up | | | | | | X | | | | | X | X | |
| AT5G22640 | 33.99 | development.unspecified | emb1211__MORN (Membrane Occupation and Recognition Nexus) repeat-containing protein | ns | ns | ns | **-0.90** | ns | X | down | | | | | | | | | | | | | |
| AT4G23700 | 34.12 | transport.metal | ATCHX17_CHX17__cation/H+ exchanger 17 | ns | ns | ns | ns | **0.97** | X | up | | | X | | | X | | | | | | X | |
| AT1G68570 | 34.13 | transport.peptides and oligopeptides | Major facilitator superfamily protein | ns | ns | ns | ns | **1.14** | X | up | X | X | | X | X | X | | | | | | X | |
| AT4G23400 | 34.19.1 | transport.Major Intrinsic Proteins.PIP | PIP1;5_PIP1D__plasma membrane intrinsic protein 1;5 | ns | ns | **-1.06** | **-0.99** | **-1.50** | X | down | X | | | | | | | | | | X | X | |
| AT2G36950 | 34.99 | transport.misc | Heavy metal transport/detoxification superfamily protein | ns | ns | ns | **1.26** | **1.01** | X | up | | | | X | | | | | | X | | X | |
| AT4G25640 | 34.99 | transport.misc | ATDTX35_DTX35_FFT__detoxifying efflux carrier 35 | ns | **1.66** | **1.40** | **1.98** | **2.11** | X | up | X | | | X | X | | | | | | | | |
| AT3G20820 | 35.1 | not assigned.no ontology | Leucine-rich repeat (LRR) family protein | ns | ns | ns | ns | **-0.86** | X | down | | | | | | | X | | | | X | | |
| AT3G50440 | 35.1 | not assigned.no ontology | ATMES10_MES10__methyl esterase 10 | ns | **0.96** | ns | ns | **1.12** | X | up | X | | | | | | | | | | | | |
| AT5G27760 | 35.1 | not assigned.no ontology | Hypoxia-responsive family protein | ns | ns | ns | **1.19** | **1.43** | X | up | X | | | | | | | | | | X | X | |
| AT1G21670 | 35.1 | not assigned.no ontology | unknown protein | ns | **0.97** | ns | **1.20** | **1.79** | X | up | | | | | | X | | | | | | | |
| AT2G05380 | 35.1.40 | not assigned.no ontology.glycine rich proteins | GRP3S__glycine-rich protein 3 short isoform | ns | ns | ns | **1.00** | **1.85** | X | up | | | | | | | | | | | | | |
| AT2G25510 | 35.2 | not assigned.unknown | unknown protein | ns | ns | ns | ns | **-1.52** | X | up | | | | X | X | | | | X | | X | X | |
| AT5G51720 | 35.2 | not assigned.unknown | 2 iron, 2 sulfur cluster binding | ns | ns | ns | ns | **-1.24** | X | down | | | | X | X | | | | | | X | | |
| AT5G39210 | 35.2 | not assigned.unknown | CRR7__chlororespiratory reduction 7 | ns | ns | ns | **-1.27** | **-0.89** | X | down | X | | | | | | | | | | X | | |
| AT5G11420 | 35.2 | not assigned.unknown | Protein of unknown function, DUF642 | ns | ns | ns | **-0.79** | **-0.71** | X | down | X | | | X | | | | | | | X | X | |
| AT3G50685 | 35.2 | not assigned.unknown | unknown protein | ns | ns | ns | ns | **-0.66** | X | down | | | | | | | | | | | X | | |
| AT3G18250 | 35.2 | not assigned.unknown | Putative membrane lipoprotein | ns | ns | ns | ns | **0.71** | X | up | | | | | X | X | | | | | X | X | |
| AT5G51040 | 35.2 | not assigned.unknown | unknown protein | ns | ns | ns | ns | **0.83** | X | up | | | | | | | | | | | | | |
| AT5G62630 | 35.2 | not assigned.unknown | HIPL2__hipl2 protein precursor | ns | ns | ns | ns | **1.21** | X | up | | | | | | X | | | | | | X | |
| AT5G61820 | 35.2 | not assigned.unknown | unknown protein | ns | ns | ns | **0.96** | **1.25** | X | up | X | X | | X | X | X | | | | | | | |
| AT2G18690 | 35.2 | not assigned.unknown | unknown protein | ns | ns | ns | ns | **1.98** | X | up | | | X | | | X | | | | | | X | |
| AT2G16900 | 35.2 | not assigned.unknown | Arabidopsis phospholipase-like protein (PEARLI 4) family | **0.98** | **1.68** | **1.67** | **1.61** | **2.16** | X | up | | | | | X | | | | | | X | X | |
| AT5G48540 | 35.2 | not assigned.unknown | receptor-like protein kinase-related family protein | **1.42** | **2.44** | **3.27** | **3.48** | **3.51** | X | up | | | | | | X | | | | | X | | |
| AT1G07280 | 35.2 | not assigned.unknown | Tetratricopeptide repeat (TPR)-like superfamily protein | ns | ns | ns | **-0.92** | ns | X | down | X | | | | | | | | | | | | |
| AT3G47070 | 35.2 | not assigned.unknown | unknown protein | ns | ns | ns | **-0.76** | ns | X | down | | | | | X | | | | | | X | X | |
| AT5G63680 | 4.1.15 | glycolysis.cytosolic branch.pyruvate kinase (PK) | Pyruvate kinase family protein | ns | ns | ns | ns | **0.79** | X | up | | | | | | | | | | | X | X | |
| AT3G04120 | 4.1.9 | glycolysis.cytosolic branch.glyceraldehyde 3-phosphate dehydrogenase (GAP-DH) | GAPC_GAPC-1_GAPC1__glyceraldehyde-3-phosphate dehydrogenase C subunit 1 | ns | ns | ns | ns | **1.09** | **1.11** | X | up | | | | X | | | | | | | | |
| AT5G56630 | 4.3.5 | glycolysis.unclear/dually targeted.phosphofructokinase (PFK) | PFK7__phosphofructokinase 7 | **0.91** | **1.59** | **2.41** | **1.54** | **2.53** | X | up | X | | | | X | | X | | | | X | | |
| AT5G17380 | 5.2 | fermentation.PDC | Thiamine pyrophosphate dependent pyruvate decarboxylase family protein | ns | ns | ns | ns | **1.48** | X | up | | | | | | | | | | | X | X | |
| AT1G77120 | 5.3 | fermentation.ADH | ADH_ADH1_ATADH_ATADH1__alcohol dehydrogenase 1 | ns | ns | ns | **1.30** | **1.02** | X | up | X | X | X | X | | | X | | | | | X | X |
| AT2G44350 | 8.1.2 | TCA / org. transformation.TCA.CS | ATCS_CSY4__Citrate synthase family protein | ns | ns | ns | ns | **0.91** | X | up | | | | X | | | | | | | | | |

| AGI identifier | Bincode identifier | MAPMAN classification | Gene annotation | Our study | | | | | DEG in common with other xenobiotic transcriptpomes | Weisman et al., 2010 | Jin *et al.*, 2011 | Van Hoewyk *et al.*, 2008 | | Ramel *et al.*, 2007 | | Baerson *et al.*, 2005 | Goodwin and Sutter, 2009 | Xu *et al.*, 2012 | Landa *et al.*, 2010 | | Herbette *et al.*, 2006 | | Pucciariello et al., 2012 |
|---|---|---|---|---|---|---|---|---|---|---|---|---|---|---|---|---|---|---|---|---|---|---|---|
| | | | | Phenanthrene Seedlings | | | | | | Phenanthrene Seedlings | PCB ? | Selenium | | Atrazine Mannitol Seedlings | Atrazine Sucrose Seedlings | BOA | Aluminium | Phénol | Trinitrotoluene | | Cadmium | | Anoxia-hypoxia |
| | | | | 30 min* | 2h* | 4h* | 8h* | 24h* | Number in commmon | 109 | 146 | Leaves 32 | Roots 52 | 113 | 119 | 45 | 14 | 16 | Leaves 15 | Roots 2 | Leaves 134 | Roots 182 | 3 |
| AT4G14040 | 15 | metal handling | EDA38_SBP2__selenium-binding protein 2 | ns | ns | **-1.01** | **-0.70** | ns | X | | | | X | | | | | | | | X | | |
| AT1G55490 | 1.3.13 | PS.calvin cyle.rubisco interacting | CPN60B_LEN1__chaperonin 60 beta | ns | ns | ns | **-0.79** | ns | X | | | | | X | X | | | | | | X | | |
| AT5G38430 | 1.3.2 | PS.calvin cyle.rubisco small subunit | Ribulose bisphosphate carboxylase (small chain) family protein | ns | ns | ns | **-0.74** | **-0.98** | X | | | | | | | | | | X | | | | |
| AT1G12780 | 10.1.2 | cell wall.precursor synthesis.UGE | ATUGE1_UGE1__UDP-D-glucose/UDP-D-galactose 4-epimerase 1 | ns | ns | **-1.06** | ns | ns | X | | X | | | X | X | | | | X | | | | |
| AT3G29360 | 10.1.4 | cell wall.precursor synthesis.UGD | UDP-glucose 6-dehydrogenase family protein | ns | ns | ns | ns | **0.87** | | | | | | | | | | | | | | | |
| AT4G01770 | 10.4.3.6 | cell wall.pectin synthesis.rhamnogalacturonan II.Xylose Transferase with Fucose Acceptor | RGXT1__rhamnogalacturonan xylosyltransferase 1 | ns | ns | ns | ns | **0.95** | | | | | | | | | | | | | | | |
| AT3G13520 | 10.5.1 | cell wall.cell wall proteins.AGPs | AGP12_ATAGP12__arabinogalactan protein 12 | ns | ns | **1.08** | **1.39** | **0.88** | X | | X | | | | | | | | X | | X | | |
| AT5G10560 | 10.6.2 | cell wall.degradation.mannan-xylose-arabinose-fucose | Glycosyl hydrolase family protein | ns | ns | ns | **-1.00** | ns | X | | | | | X | X | | | | | | | X | |
| AT4G14130 | 10.7 | cell wall.modification | XTH15_XTR7__xyloglucan endotransglucosylase/hydrolase 15 | ns | ns | ns | ns | **-0.67** | X | | X | | | | | | X | | | | | | |
| AT1G65290 | 11.1.12 | lipid metabolism.FA synthesis and FA elongation.ACP | mtACP2__mitochondrial acyl carrier protein 2 | ns | ns | ns | ns | **2.63** | X | | | | | X | X | | | | | | | | |
| AT2G05990 | 11.1.6 | lipid metabolism.FA synthesis and FA elongation.enoyl ACP reductase | ENR1_MOD1__NAD(P)-binding Rossmann-fold superfamily protein | ns | ns | ns | ns | **-0.72** | X | | | | | X | X | | | | | | | X | |
| AT3G11170 | 11.2.3 | lipid metabolism.FA desaturation.omega 3 desaturase | FAD7_FADD__fatty acid desaturase 7 | ns | ns | ns | ns | **-0.87** | X | | | | X | | | | | | | | | | |
| AT1G06550 | 11.9.4.3 | lipid metabolism.lipid degradation.beta-oxidation.enoyl CoA hydratase | ATP-dependent caseinolytic (Clp) protease/crotonase family protein | ns | ns | ns | **-0.77** | ns | X | | | | | X | X | | | | | | | X | |
| AT1G48320 | 11.9.4.5 | lipid metabolism.lipid degradation.beta-oxidation.acyl-CoA thioesterase | Thioesterase superfamily protein | ns | ns | ns | **-0.93** | ns | X | | | | | | | | | | | | X | | |
| AT1G66200 | 12.2.2 | N-metabolism.ammonia metabolism.glutamine synthase | ATGSR2_GSR2__glutamine synthase clone F11 | ns | ns | ns | **-1.18** | ns | | | | | | | | | | | | | | | |
| AT5G17920 | 13.1.3.4 | amino acid metabolism.synthesis.aspartate family.methionine | ATCIMS_ATMETS_ATMS1__Cobalamin-independent synthase family protein | ns | ns | ns | **-1.06** | **-0.99** | X | | | | | X | X | | | | | | | | |
| AT1G69520 | 13.1.3.4.12 | amino acid metabolism.synthesis.aspartate family.methionine.homocysteine S-methyltransferase | S-adenosyl-L-methionine-dependent methyltransferases superfamily protein | ns | ns | ns | **-0.69** | ns | X | | X | | | | | | | | | | | | |
| AT3G57050 | 13.1.3.4.2 | amino acid metabolism.synthesis.aspartate family.methionine.cystathionine beta-lyase | CBL__cystathionine beta-lyase | ns | ns | ns | **-0.77** | ns | | | | | | | | | | | | | | | |
| AT3G03780 | 13.1.3.4.3 | amino acid metabolism.synthesis.aspartate family.methionine.methionine synthase | ATMS2_MS2__methionine synthase 2 | ns | ns | ns | **-1.66** | **-2.22** | X | | X | | | X | X | | | | | | X | X | |
| AT3G04940 | 13.1.5.3.1 | amino acid metabolism.synthesis.serine-glycine-cysteine group.cysteine.OASTL | ATCYSD1_CYSD1__cysteine synthase D1 | ns | ns | ns | **-0.70** | ns | | | | | | | | | | | | | | | |
| AT3G06350 | 13.1.6.1.10 | amino acid metabolism.synthesis.aromatic aa.chorismate.dehydroquinate/shikimate dehydrogenase | EMB3004_MEE32__dehydroquinate dehydratase, putative / shikimate dehydrogenase, putative | ns | ns | ns | **-1.03** | **-0.85** | | | | | | | | | | | | | | | |
| AT3G29200 | 13.1.6.2.1 | amino acid metabolism.synthesis.aromatic aa.phenylalanine and tyrosine.chorismate mutase | ATCM1_CM1__chorismate mutase 1 | ns | ns | ns | **-0.95** | **-0.96** | | | | | | | | | | | | | | | |
| AT5G38530 | 13.1.6.5.5 | amino acid metabolism.synthesis.aromatic aa.tryptophan.tryptophan synthase | TSBtype2__tryptophan synthase beta type 2 | ns | ns | ns | ns | **0.68** | X | | | X | | X | | | | | | | | | |
| AT3G16150 | 13.2.3.1.1 | amino acid metabolism.degradation.aspartate family.asparagine.L-asparaginase | N-terminal nucleophile aminohydrolases (Ntn hydrolases) superfamily protein | ns | ns | **-1.48** | ns | ns | X | | | X | | X | X | | | | | | | X | |
| AT1G08630 | 13.2.5.2 | amino acid metabolism.degradation.serine-glycine-cysteine group.glycine | THA1__threonine aldolase 1 | ns | ns | **-1.81** | **-0.92** | **-1.62** | X | | X | | | X | X | | | | | | | | |
| AT5G49730 | 15.1 | metal handling.acquisition | ATFRO6_FRO6_FRO6__ferric reduction oxidase 6 | ns | ns | **-1.35** | **-0.79** | **-1.46** | X | | X | | | | X | | | | | | X | | |
| AT5G17230 | 16.1.4.1 | secondary metabolism.isoprenoids.carotenoids.phytoene synthase | PSY__PHYTOENE SYNTHASE | ns | ns | ns | **-0.86** | ns | X | | X | | | | | | | | | | | | |
| AT3G25830 | 16.1.5 | secondary metabolism.isoprenoids.terpenoids | ATTPS-CIN_TPS-CIN_TPS-CIN__terpene synthase-like sequence-1,8-cineole | ns | ns | **1.19** | ns | ns | | | | | | | | | | | | | | | |
| AT5G01210 | 16.2 | secondary metabolism.phenylpropanoids | HXXXD-type acyl-transferase family protein | ns | ns | **-1.65** | **-1.37** | ns | X | | X | | | | | | | | | | X | X | |
| AT5G47950 | 16.2 | secondary metabolism.phenylpropanoids | HXXXD-type acyl-transferase family protein | ns | ns | ns | **-0.96** | **-1.11** | X | | | | | | | | | | | | | X | |
| AT5G07870 | 16.2 | secondary metabolism.phenylpropanoids | HXXXD-type acyl-transferase family protein | ns | ns | ns | **1.20** | ns | | | | | | | | | | | | | | | |
| AT5G04230 | 16.2.1.1 | secondary metabolism.phenylpropanoids.lignin biosynthesis.PAL | ATPAL3_PAL3__phenyl alanine ammonia-lyase 3 | ns | ns | ns | **-0.88** | **-0.81** | | | | | | X | | | | | | | | | |
| AT3G19450 | 16.2.1.10 | secondary metabolism.phenylpropanoids.lignin biosynthesis.CAD | ATCAD4_CAD_CAD-C_CAD4__GroES-like zinc-binding alcohol dehydrogenase family protein | ns | ns | **-1.22** | **-1.74** | **-1.74** | X | | X | | | | | | | | | | | X | |
| AT4G37990 | 16.2.1.10 | secondary metabolism.phenylpropanoids.lignin biosynthesis.CAD | ATCAD8_CAD-B2_ELI3_ELI3-2__elicitor-activated gene 3-2 | ns | ns | ns | ns | **2.43** | | | | | | | | | | | | | | | |
| AT5G48930 | 16.2.1.4 | secondary metabolism.phenylpropanoids.lignin biosynthesis.HCT | HCT__hydroxycinnamoyl-CoA shikimate/quinate hydroxycinnamoyl transferase | ns | **-1.17** | **-1.11** | **-1.50** | **-1.18** | X | | | | | X | | | | | | | | X | |
| AT1G74010 | 16.4.1 | secondary metabolism.N misc.alkaloid-like | Calcium-dependent phosphotriesterase superfamily protein | ns | **1.39** | **1.68** | **1.32** | **2.50** | X | | | | | | | | | | | | X | X | |
| AT3G16390 | 16.5.1.3.2 | secondary metabolism.sulfur-containing.glucosinolates.degradation.nitrilespecifier protein | NSP3__nitrile specifier protein 3 | ns | ns | ns | **-1.03** | **-1.02** | | | | | | | | | | | | | | | |
| AT1G75280 | 16.8.5 | secondary metabolism.flavonoids.isoflavonols | NmrA-like negative transcriptional regulator family protein | ns | ns | ns | **1.56** | **1.37** | X | | | | X | X | X | | | | | | | X | |
| AT5G52810 | 16.99 | secondary metabolism.unspecified | NAD(P)-binding Rossmann-fold superfamily protein | ns | ns | ns | ns | **1.00** | X | | X | | | X | | | | | | | X | X | |
| AT4G17280 | 17.2.3 | hormone metabolism.auxin.induced-regulated-responsive-activated | Auxin-responsive family protein | ns | **0.89** | ns | ns | ns | X | | | | | | | | | X | | | | X | |
| AT4G38840 | 17.2.3 | hormone metabolism.auxin.induced-regulated-responsive-activated | SAUR-like auxin-responsive protein family | ns | ns | ns | **-0.84** | **-1.31** | X | | | | | | X | | | X | | | X | | |
| AT1G60710 | 17.2.3 | hormone metabolism.auxin.induced-regulated-responsive-activated | ATB2__NAD(P)-linked oxidoreductase superfamily protein | ns | ns | ns | ns | **0.72** | X | | | | | | | | | | | | | X | |
| AT1G60680 | 17.2.3 | hormone metabolism.auxin.induced-regulated-responsive-activated | NAD(P)-linked oxidoreductase superfamily protein | ns | ns | ns | ns | **0.91** | X | | | | | | | | | | | | | X | |
| AT5G13320 | 17.2.3 | hormone metabolism.auxin.induced-regulated-responsive-activated | GDG1_GH3.12_PBS3_WIN3__Auxin-responsive GH3 family protein | ns | ns | ns | ns | **1.54** | X | | X | | | | | | | | | | X | X | |
| AT3G19820 | 17.3.1.2.8 | hormone metabolism.brassinosteroid.synthesis-degradation.sterols.DWF1 | CBB1_DIM_DIM1_DWF1_EVE1__cell elongation protein / DWARF1 / DIMINUTO (DIM) | ns | ns | ns | **-1.27** | **-1.15** | X | | X | | | | | | | | | | | X | |
| AT2G07050 | 17.3.1.2.99 | hormone metabolism.brassinosteroid.synthesis-degradation.sterols.other | CAS1__cycloartenol synthase 1 | ns | ns | ns | **-0.96** | ns | | | | | | | | | | | | | | | |
| AT5G50375 | 17.3.1.2.99 | hormone metabolism.brassinosteroid.synthesis-degradation.sterols.other | CPI1__cyclopropyl isomerase | ns | ns | ns | **-0.76** | ns | X | | | | | X | X | | | | | | | X | |
| AT5G20400 | 17.5.1 | hormone metabolism.ethylene.synthesis-degradation | 2-oxoglutarate (2OG) and Fe(II)-dependent oxygenase superfamily protein | ns | ns | ns | ns | **1.03** | X | | | X | | | | | | | | | | | |

| AGI identifier | Bincode identifier | MAPMAN classification | Gene annotation | Our study | | | | | DEG in common with other xenobiotic transcriptomes | Weisman et al., 2010 | Jin *et al.*, 2011 | Van Hoewyk *et al.*, 2008 | | Ramel *et al.*, 2007 | | Baerson *et al.*, 2005 | Goodwin and Sutter, 2009 | Xu *et al.*, 2012 | Landa *et al.*, 2010 | | Herbette *et al.*, 2006 | | Pucciariello et al., 2012 |
|---|---|---|---|---|---|---|---|---|---|---|---|---|---|---|---|---|---|---|---|---|---|---|---|
| | | | | Phenanthrene | | | | | | Phenanthrene | PCB | Selenium | | Atrazine Mannitol | Atrazine Sucrose | BOA | Aluminium | Phénol | Trinitrotoluene | | Cadmium | | Anoxia-hypoxia |
| | | | | Seedlings | | | | | | Seedlings | ? | Leaves | Roots | Seedlings | | | | | Leaves | Roots | Leaves | Roots | |
| | | | | 30 min* | 2h* | 4h* | 8h* | 24h* | Number in commmon | 109 | 146 | 32 | 52 | 113 | 119 | 45 | 14 | 16 | 15 | 2 | 134 | 182 | 3 |
| AT4G26200 | 17.5.1.1 | hormone metabolism.ethylene.synthesis-degradation.1-aminocyclopropane-1-carboxylate synthase | ACS7_ATACS7__1-amino-cyclopropane-1-carboxylate synthase 7 | ns | ns | ns | ns | **1.44** | X | | X | X | | | | | | | | | | X | |
| AT1G80330 | 17.6.1.12 | hormone metabolism.gibberelin.synthesis-degradation.GA3 oxidase | ATGA3OX4_GA3OX4__gibberellin 3-oxidase 4 | ns | ns | ns | ns | **0.83** | | | | | | | | | | | | | | | | |
| AT1G09400 | 17.7.1.5 | hormone metabolism.jasmonate.synthesis-degradation.12-Oxo-PDA-reductase | FMN-linked oxidoreductases superfamily protein | ns | ns | ns | **0.74** | **1.08** | X | | X | | | | | | | | | | | | | |
| AT5G54206 | 17.7.1.5 | hormone metabolism.jasmonate.synthesis-degradation.12-Oxo-PDA-reductase | pseudogene | ns | ns | ns | **1.41** | **2.04** | X | | | | | | X | | | | | | | | X | |
| AT3G16460 | 17.7.3 | hormone metabolism.jasmonate.induced-regulated-responsive-activated | Mannose-binding lectin superfamily protein | ns | ns | ns | **-0.89** | **-1.53** | X | | | | | X | | | | | | | | | X | |
| AT3G16450 | 17.7.3 | hormone metabolism.jasmonate.induced-regulated-responsive-activated | Mannose-binding lectin superfamily protein | ns | ns | ns | ns | **-1.30** | X | | X | | | X | | | | | | | | | X | |
| AT3G16440 | 17.7.3 | hormone metabolism.jasmonate.induced-regulated-responsive-activated | ATMLP-300B_MEE36_MLP-300B__myrosinase-binding protein-like protein-300B | ns | ns | ns | ns | **-0.91** | X | | | | | | | | | | | | | | X | |
| AT5G38020 | 17.8.1 | hormone metabolism.salicylic acid.synthesis-degradation | S-adenosyl-L-methionine-dependent methyltransferases superfamily protein | ns | ns | **1.15** | ns | ns | X | | | X | | | | | | | | | | | | |
| AT5G54770 | 18.2 | Co-factor and vitamine metabolism.thiamine | THI1_THI4_TZ__thiazole biosynthetic enzyme, chloroplast (ARA6) (THI1) (THI4) | ns | ns | ns | **-0.75** | **-0.89** | X | | | | | | | | X | | | | | | | |
| AT1G74710 | 18.5.2.1 | Co-factor and vitamine metabolism.folate & vitamine K.vitamine K.isochorismate synthase | ATICS1_EDS16_ICS1_SID2__ADC synthase superfamily protein | ns | ns | ns | ns | **1.41** | X | | X | | | | | | X | | | | X | X | | |
| AT1G72090 | 18.7 | Co-factor and vitamine metabolism.iron-sulphur clusters | Methylthiotransferase | ns | ns | ns | **-0.74** | ns | | | | | | | | | | | | | | | | |
| AT5G50210 | 18.7 | Co-factor and vitamine metabolism.iron-sulphur clusters | OLD5_QS_SUFE3__quinolinate synthase | ns | ns | ns | **0.75** | **1.02** | | | | | | | X | | | | | | | | | |
| AT4G18480 | 19.10 | tetrapyrrole synthesis.magnesium chelatase | CH-42_CH42_CHL11_CHLI-1_CHLI1__P-loop containing nucleoside triphosphate hydrolases superfamily protein | ns | ns | ns | **-0.73** | ns | X | | | | | X | X | | | | | | X | | | |
| AT5G26030 | 19.20 | tetrapyrrole synthesis.ferrochelatase | ATFC-I_FC-I_FC1__ferrochelatase 1 | ns | ns | ns | ns | **0.69** | X | | | | X | | | | | | | | | | X | |
| AT5G51830 | 2.2.1.1 | major CHO metabolism.degradation.sucrose.fructokinase | pfkB-like carbohydrate kinase family protein | ns | ns | ns | **1.07** | **1.10** | X | | | | | | X | | | | | | X | | X | |
| AT5G26570 | 2.2.2.3 | major CHO metabolism.degradation.starch.glucan water dikinase | ATGWD3_OK1_PWD__catalytics;carbohydrate kinases;phosphoglucan, water dikinases | ns | ns | ns | **-0.75** | ns | | | | | | | | | | | | | | | | |
| AT1G75030 | 20.1 | stress.biotic | ATLP-3_TLP-3__thaumatin-like protein 3 | ns | ns | **1.13** | **1.45** | **1.35** | | | | | | | | | | | | | | | | |
| AT3G54420 | 20.1 | stress.biotic | ATCHITIV_ATEP3_CHIV_EP3__homolog of carrot EP3-3 chitinase | ns | ns | ns | **0.98** | **2.05** | X | | | | | | | | | | | | | | X | |
| AT3G52430 | 20.1 | stress.biotic | ATPAD4_PAD4__alpha/beta-Hydrolases superfamily protein | ns | ns | ns | ns | **0.79** | X | | X | | | | | | | | | | | | X | |
| AT5G47130 | 20.1 | stress.biotic | Bax inhibitor-1 family protein | ns | ns | ns | ns | **1.16** | X | | X | | | | | | | | | | | | X | |
| AT5G47120 | 20.1 | stress.biotic | ATBI-1_ATBI1_BI-1_BI1__BAX inhibitor 1 | ns | ns | ns | ns | **1.21** | X | | | | | | | | | | | | | | X | |
| AT5G06320 | 20.1 | stress.biotic | NHL3__NDR1/HIN1-like 3 | ns | ns | ns | ns | **1.60** | X | | | | X | | | | | | X | | X | X | | |
| AT1G72930 | 20.1.2 | stress.biotic.receptors | TIR__toll/interleukin-1 receptor-like | ns | ns | ns | **-1.33** | ns | X | | | | X | | | | | | | | X | X | | |
| AT5G36910 | 20.1.2 | stress.biotic.receptors | THI2.2__thionin 2.2 | ns | ns | ns | ns | **-1.73** | X | | X | | | | | | | | | | | | X | |
| AT2G20142 | 20.1.2 | stress.biotic.receptors | Toll-Interleukin-Resistance (TIR) domain family protein | ns | ns | ns | ns | **1.47** | X | | X | | | | | | | | | | | | X | |
| AT5G64890 | 20.1.3 | stress.biotic.signalling | PROPEP2__elicitor peptide 2 precursor | ns | ns | ns | **1.07** | ns | X | | X | | | | | | | | | | | | | |
| AT2G39200 | 20.1.3.1 | stress.biotic.signalling.MLO-like | ATMLO12_MLO12__Seven transmembrane MLO family protein | ns | ns | ns | ns | **1.17** | X | | | | | | | X | | | | | | | | |
| AT4G22210 | 20.1.7 | stress.biotic.PR-proteins | LCR85 (Low-molecular-weight cysteine-rich 85) | ns | ns | ns | **-1.56** | **-1.27** | | | | | | | | | | | | | | | | |
| AT5G45490 | 20.1.7 | stress.biotic.PR-proteins | P-loop containing nucleoside triphosphate hydrolases superfamily protein | ns | ns | ns | **-0.89** | **-0.68** | X | | | | | | | | | | | | X | X | | |
| AT1G47890 | 20.1.7 | stress.biotic.PR-proteins | AtRLP7_RLP7__receptor like protein 7 | ns | ns | ns | **-0.70** | **-0.92** | X | | X | | | | | | | | | | | | | |
| AT1G33590 | 20.1.7 | stress.biotic.PR-proteins | Leucine-rich repeat (LRR) family protein | ns | ns | ns | **0.73** | **1.43** | X | | X | | X | | | | | | | | | | | |
| AT1G66090 | 20.1.7 | stress.biotic.PR-proteins | Disease resistance protein (TIR-NBS class) | ns | ns | ns | ns | **1.67** | X | | | | | | X | | | X | X | | | | X | |
| AT2G29500 | 20.2.1 | stress.abiotic.heat | HSP20-like chaperones superfamily protein | ns | ns | **1.15** | **1.11** | **1.53** | X | | | | X | | | | | | | | | | X | |
| AT5G49910 | 20.2.1 | stress.abiotic.heat | cpHsc70-2_CPHSC70-2EAT SHOCK PROTEIN 70-2_HSC70-7__chloroplast heat shock protein 70-2 | ns | ns | ns | **-0.71** | ns | X | | X | | | | X | | | | | | X | | | |
| AT3G22530 | 20.2.1 | stress.abiotic.heat | unknown protein | ns | ns | ns | **0.72** | ns | | | | | | | | | | | | | | | | |
| AT1G65280 | 20.2.1 | stress.abiotic.heat | DNAJ heat shock N-terminal domain-containing protein | ns | ns | ns | **0.89** | **1.56** | | | | | | | | | | | | | | | | |
| AT5G56030 | 20.2.1 | stress.abiotic.heat | AtHsp90.2_ERD8_HSP81-2_HSP90.2__heat shock protein 81-2 | ns | ns | ns | ns | **0.70** | X | | X | | | X | | | | | | | | | | |
| AT1G59860 | 20.2.1 | stress.abiotic.heat | HSP20-like chaperones superfamily protein | ns | ns | ns | ns | **0.91** | X | | X | | X | X | X | | X | | | | | | X | |
| AT5G57710 | 20.2.1 | stress.abiotic.heat | Double Clp-N motif-containing P-loop nucleoside triphosphate hydrolases superfamily protein | ns | ns | ns | ns | **0.91** | X | | | | | | | | | | | | X | X | | |
| AT5G52640 | 20.2.1 | stress.abiotic.heat | ATHS83_AtHsp90-1_ATHSP90.1_HSP81-1_HSP81.1_HSP83_HSP90.1__heat shock protein 90.1 | ns | ns | ns | ns | **1.13** | X | | | | X | X | X | | | | | | X | X | | |
| AT1G62320 | 20.2.3 | stress.abiotic.drought/salt | ERD (early-responsive to dehydration stress) family protein | ns | **0.98** | ns | **0.94** | **0.85** | | | | | | | | | | | | | | | | |
| AT1G04430 | 20.2.3 | stress.abiotic.drought/salt | S-adenosyl-L-methionine-dependent methyltransferases superfamily protein | ns | ns | ns | **-0.78** | ns | X | | X | | | X | X | | | | | | | | | |
| AT3G23300 | 20.2.3 | stress.abiotic.drought/salt | S-adenosyl-L-methionine-dependent methyltransferases superfamily protein | ns | ns | ns | **-0.72** | ns | X | | | | | X | X | | | | | | | | | |
| AT4G00750 | 20.2.3 | stress.abiotic.drought/salt | S-adenosyl-L-methionine-dependent methyltransferases superfamily protein | ns | ns | ns | **0.95** | ns | | | | | | X | | | | | | | | | | |
| AT3G10985 | 20.2.4 | stress.abiotic.touch/wounding | ATWI-12_SAG20_WI12__senescence associated gene 20 | ns | ns | **-1.07** | ns | **0.74** | X | | | | | | X | | | | | | X | X | | |
| AT4G14630 | 20.2.99 | stress.abiotic.unspecified | GLP9__germin-like protein 9 | ns | ns | ns | ns | **1.09** | X | | X | | | | | | | | | | | | | |
| AT4G29670 | 21.1 | redox.thioredoxin | ACHT2__atypical CYS HIS rich thioredoxin 2 | ns | ns | ns | **0.80** | ns | X | | | | X | | | | | | | | | | | |
| **AT5G03630** | **21.2.1** | **redox.ascorbate and glutathione.ascorbate** | **ATMDAR2__Pyridine nucleotide-disulphide oxidoreductase family protein** | ns | ns | ns | **0.75** | **1.80** | X | | | | | X | | | | | | | X | | | |
| **AT4G11600** | **21.2.2** | **redox.ascorbate and glutathione.glutathione** | **ATGPX6_GPX6_LSC803_PHGPX__glutathione peroxidase 6** | ns | ns | ns | **1.03** | **1.95** | | | | | | | | | | | | | | | | |

| AGI identifier | Bincode identifier | MAPMAN classification | Gene annotation | Our study | | | | | DEG in common with other xenobiotic transcriptomes | Weisman et al., 2010 | Jin *et al.*, 2011 | Van Hoewyk *et al.*, 2008 | | Ramel *et al.*, 2007 | | Baerson *et al.*, 2005 | Goodwin and Sutter, 2009 | Xu *et al.*, 2012 | Landa *et al.*, 2010 | | Herbette *et al.*, 2006 | | Pucciariello et al., 2012 |
|---|---|---|---|---|---|---|---|---|---|---|---|---|---|---|---|---|---|---|---|---|---|---|---|
| | | | | Phenanthrene | | | | | | Phenanthrene | PCB | Selenium | | Atrazine Mannitol | Atrazine Sucrose | BOA | Aluminium | Phénol | Trinitrotoluene | | Cadmium | | Anoxia-hypoxia |
| | | | | Seedlings | | | | | | Seedlings | ? | Leaves | Roots | Seedlings | | | | | Leaves | Roots | Leaves | Roots | |
| | | | | 30 min* | 2h* | 4h* | 8h* | 24h* | Number in common | 109 | 146 | 32 | 52 | 113 | 119 | 45 | 14 | 16 | 15 | 2 | 134 | 182 | 3 |
| AT3G26060 | 21.5 | redox.peroxiredoxin | ATPRX Q__Thioredoxin superfamily protein | ns | ns | ns | **-0.79** | **-0.67** | X | | | | | | | | | | | | X | | |
| AT1G16350 | 23.1.2.30 | nucleotide metabolism.synthesis.purine.IMP dehydrogenase | Aldolase-type TIM barrel family protein | ns | ns | ns | **-0.74** | ns | X | | | | | X | X | | | | | | | X | |
| AT1G80050 | 23.3.1.1 | nucleotide metabolism.salvage.phosphoribosyltransferases.aprt | APT2_ATAPT2_PHT1.1__adenine phosphoribosyl transferase 2 | ns | ns | ns | ns | **-0.70** | X | | | | | | | | | | | | X | X | |
| AT5G03300 | 23.3.2.1 | nucleotide metabolism.salvage.nucleoside kinases.adenosine kinase | ADK2__adenosine kinase 2 | ns | ns | ns | **-0.99** | **-0.94** | X | | | | | X | X | | | | | | | X | |
| AT4G12720 | 23.3.3 | nucleotide metabolism.salvage.NUDIX hydrolases | AtNUDT7_ATNUDX7_GFG1_NUDT7__MutT/nudix family protein | ns | ns | ns | ns | **1.07** | X | | | | X | | X | | | | | | X | X | |
| AT1G53580 | 24.1 | Biodegradation of Xenobiotics.hydroxyacylglutathione hydrolase | ETHE1_GLX2-3_GLY3__glyoxalase II 3 | ns | ns | ns | **1.07** | ns | X | | | | | X | X | | | | | | | | |
| AT5G14780 | 25.10 | C1-metabolism.formate dehydrogenase | FDH__formate dehydrogenase | ns | ns | ns | ns | **1.33** | X | | | | | | | | | | | | | X | |
| AT3G59970 | 25.6 | C1-metabolism.methylenetetrahydrofolate reductase | MTHFR1__methylenetetrahydrofolate reductase 1 | ns | ns | ns | **-1.30** | **-1.06** | X | | | | | X | X | | | | | | X | X | |
| AT2G44160 | 25.6 | C1-metabolism.methylenetetrahydrofolate reductase | MTHFR2__methylenetetrahydrofolate reductase 2 | ns | ns | ns | **-1.28** | **-0.95** | | | | | | | | | | | | | | | |
| AT5G24760 | 26.11.1 | misc.alcohol dehydrogenases | GroES-like zinc-binding dehydrogenase family protein | ns | ns | ns | **-1.08** | **-1.19** | X | | | | | X | | | | | | | | X | |
| AT1G05240 | 26.12 | misc.peroxidases | Peroxidase superfamily protein | ns | ns | **-1.07** | **-1.48** | **-0.91** | X | | | | | | | | | | | | | X | |
| AT4G33420 | 26.12 | misc.peroxidases | Peroxidase superfamily protein | ns | ns | ns | **0.74** | **0.85** | | | | | | | | | | | | | | | |
| AT2G01180 | 26.13 | misc.acid and other phosphatases | ATLPP1_ATPAP1_LPP1_PAP1__phosphatidic acid phosphatase 1 | ns | ns | ns | **1.44** | **1.97** | X | | | | | | | | | | X | | | | |
| AT2G16430 | 26.13 | misc.acid and other phosphatases | ATPAP10_PAP10__purple acid phosphatase 10 | ns | ns | ns | ns | **0.96** | X | | X | | | X | X | | | | | | | X | |
| AT1G54000 | 26.16 | misc.myrosinases-lectin-jacalin | GDSL-like Lipase/Acylhydrolase superfamily protein | ns | ns | ns | ns | **-1.06** | X | | X | | | X | | | | | | | | | |
| AT3G16420 | 26.16 | misc.myrosinases-lectin-jacalin | JAL30_PBP1__PYK10-binding protein 1 | ns | ns | ns | ns | **-1.02** | X | | X | | | | | | | | | | | | |
| AT4G12545 | 26.21 | misc.protease inhibitor/seed storage/lipid transfer protein (LTP) family protein | Bifunctional inhibitor/lipid-transfer protein/seed storage 2S albumin superfamily protein | ns | ns | ns | **-1.20** | **-1.66** | | | | | | | | | | | | | | | |
| AT4G09750 | 26.22 | misc.short chain dehydrogenase/reductase (SDR) | NAD(P)-binding Rossmann-fold superfamily protein | ns | ns | ns | ns | **0.71** | X | | X | | | | | | | | | | X | | |
| AT3G09260 | 26.3 | misc.gluco-, galacto- and mannosidases | BGLU23_LEB_PSR3.1_PYK10__Glycosyl hydrolase superfamily protein | ns | ns | ns | **-0.85** | **-0.81** | X | | X | | | | | | | | | | | | |
| AT2G44460 | 26.3 | misc.gluco-, galacto- and mannosidases | BGLU28__beta glucosidase 28 | ns | ns | ns | **0.74** | **0.70** | X | | X | X | X | | X | | | | | | | | |
| AT2G36690 | 26.7 | misc.oxidases - copper, flavone etc. | 2-oxoglutarate (2OG) and Fe(II)-dependent oxygenase superfamily protein | ns | **-1.13** | ns | ns | ns | X | | X | | | | | | | | | | | X | X |
| AT1G14120 | 26.7 | misc.oxidases - copper, flavone etc. | 2-oxoglutarate (2OG) and Fe(II)-dependent oxygenase superfamily protein | ns | ns | **1.08** | ns | ns | X | | X | | | X | | | | X | | | | | |
| AT5G17000 | 26.7 | misc.oxidases - copper, flavone etc. | Zinc-binding dehydrogenase family | ns | ns | ns | **1.02** | **1.09** | X | | X | | | | | | | | | | | | |
| AT1G14130 | 26.7 | misc.oxidases - copper, flavone etc. | 2-oxoglutarate (2OG) and Fe(II)-dependent oxygenase superfamily protein | ns | ns | ns | **1.04** | **0.86** | X | | | | | | | X | | | | | | | |
| AT4G15760 | 26.7 | misc.oxidases - copper, flavone etc. | Encodes a protein with similarity to monooxygenases that are known to degrade salicylic acid (SA). | ns | ns | ns | ns | **0.75** | X | | X | | | X | X | | | | | | | | |
| AT4G20830 | 26.8 | misc.nitrilases, *nitrile lyases, berberine bridge enzymes, reticuline oxidases, troponine reductases | FAD-binding Berberine family protein | ns | ns | ns | **0.87** | **1.20** | X | | | | | | X | X | | | | | | X | |
| AT1G26380 | 26.8 | misc.nitrilases, *nitrile lyases, berberine bridge enzymes, reticuline oxidases, troponine reductases | FAD-binding Berberine family protein | ns | ns | ns | ns | **1.38** | X | | X | X | | | | | | | | | | | |
| **AT1G14540** | **26.9** | **misc.glutathione S transferases** | **Peroxidase superfamily protein** | ns | ns | ns | ns | **0.75** | X | | | | | | | | | | | | | X | |
| AT1G29600 | 27.3.11 | RNA.regulation of transcription.C2H2 zinc finger family | Zinc finger C-x8-C-x5-C-x3-H type family protein | ns | ns | ns | **-1.22** | **-1.02** | | | | | | | | | | | | | | | |
| AT4G17810 | 27.3.11 | RNA.regulation of transcription.C2H2 zinc finger family | C2H2 and C2HC zinc fingers superfamily protein | ns | ns | ns | **-0.78** | **-1.03** | | | | | | | | | | | | | | | |
| AT2G24500 | 27.3.11 | RNA.regulation of transcription.C2H2 zinc finger family | FZF__Zinc finger protein 622 | ns | ns | ns | **1.13** | **0.76** | | | | | | | | | | | | | | | |
| AT3G28210 | 27.3.11 | RNA.regulation of transcription.C2H2 zinc finger family | PMZ_SAP12__zinc finger (AN1-like) family protein | ns | ns | ns | **1.60** | **2.09** | X | | | | X | | X | | | | | | X | X | |
| AT3G57670 | 27.3.11 | RNA.regulation of transcription.C2H2 zinc finger family | NTT_WIP2__C2H2-type zinc finger family protein | ns | ns | ns | ns | **0.85** | | | | | | | | | | | | | | | |
| AT3G46080 | 27.3.11 | RNA.regulation of transcription.C2H2 zinc finger family | C2H2-type zinc finger family protein | ns | **1.03** | ns | **1.39** | **1.72** | | | | | | | | | | | | | | | |
| AT5G59570 | 27.3.20 | RNA.regulation of transcription.G2-like transcription factor family, GARP | Homeodomain-like superfamily protein | ns | ns | ns | **1.32** | ns | X | | X | | | | | | | | | | | | |
| AT3G28910 | 27.3.25 | RNA.regulation of transcription.MYB domain transcription factor family | ATMYB30_MYB30__myb domain protein 30 | ns | ns | ns | **0.89** | ns | X | | | | | | | | | | | | | X | |
| AT5G58900 | 27.3.26 | RNA.regulation of transcription.MYB-related transcription factor family | Homeodomain-like transcriptional regulator | ns | ns | ns | **-0.72** | ns | X | | | | | | X | | | | | | | X | |
| AT1G71520 | 27.3.3 | RNA.regulation of transcription.AP2/EREBP, APETALA2/Ethylene-responsive element binding protein family | encodes a member of the DREB subfamily A-5 of ERF/AP2 transcription factor family | ns | ns | ns | **1.47** | ns | | | | | | | | | | | | | | | |
| AT1G43160 | 27.3.3 | RNA.regulation of transcription.AP2/EREBP, APETALA2/Ethylene-responsive element binding protein family | RAP2.6__related to AP2 6 | ns | ns | **-1.57** | **-1.16** | **-0.99** | X | | X | | | | | | | | | | | | |
| AT2G38250 | 27.3.30 | RNA.regulation of transcription.Trihelix, Triple-Helix transcription factor family | Homeodomain-like superfamily protein | ns | ns | ns | **0.71** | ns | X | | | | | | | | | X | | | | | |
| AT1G29280 | 27.3.32 | RNA.regulation of transcription.WRKY domain transcription factor family | ATWRKY65_WRKY65__WRKY DNA-binding protein 65 | ns | ns | ns | **-0.95** | ns | | | | | | | | | | | | | | | |
| AT2G25000 | 27.3.32 | RNA.regulation of transcription.WRKY domain transcription factor family | ATWRKY60_WRKY60__WRKY DNA-binding protein 60 | ns | ns | ns | **-0.93** | ns | X | | X | | | X | X | | | | | | | | |
| AT4G23550 | 27.3.32 | RNA.regulation of transcription.WRKY domain transcription factor family | WRKY29 (WRKY DNA-binding protein 29); transcription factor | ns | ns | ns | **-0.76** | **-1.01** | X | | | | | | | | | | | | X | X | |
| AT3G56400 | 27.3.32 | RNA.regulation of transcription.WRKY domain transcription factor family | ATWRKY70_WRKY70__WRKY DNA-binding protein 70 | ns | ns | ns | ns | **0.70** | X | | | | | | | | | | | | | X | |
| AT2G46400 | 27.3.32 | RNA.regulation of transcription.WRKY domain transcription factor family | ATWRKY46_WRKY46__WRKY DNA-binding protein 46 | ns | ns | ns | ns | **0.76** | X | | | | X | | | | | | | | | X | |
| AT1G19220 | 27.3.4 | RNA.regulation of transcription.ARF, Auxin Response Factor family | ARF11_ARF19_IAA22__auxin response factor 19 | ns | ns | ns | ns | **0.82** | | | | | | | | | | | | | | | |
| AT1G66160 | 27.3.64 | RNA.regulation of transcription.PHOR1 | ATCMPG1_CMPG1__CYS, MET, PRO, and GLY protein 1 | ns | ns | ns | ns | **0.75** | X | | | | X | | | | | | X | | | | |
| AT1G21570 | 27.3.99 | RNA.regulation of transcription.unclassified | zinc finger (CCCH-type) family protein | ns | ns | ns | **-1.57** | ns | | | | | | | | | | | | | | | |
| AT4G38160 | 27.3.99 | RNA.regulation of transcription.unclassified | pde191__Mitochondrial transcription termination factor family protein | ns | ns | ns | **-0.92** | **-0.79** | X | | | | | | | | | | | | X | X | |
| AT3G53460 | 27.3.99 | RNA.regulation of transcription.unclassified | CP29__chloroplast RNA-binding protein 29 | ns | ns | **-1.04** | ns | ns | X | | X | | | | | | | | | | | | |
| AT4G16830 | 27.4 | RNA.RNA binding | Hyaluronan / mRNA binding family | ns | ns | ns | **-0.82** | ns | X | | X | | | | | | | | | | | | |
| AT5G04430 | 27.4 | RNA.RNA binding | BTR1_BTR1L_BTR1S__binding to TOMV RNA 1L (long form) | ns | ns | ns | ns | **-0.72** | | | | | | | | | | | | | | | |

| AGI identifier | Bincode identifier | MAPMAN classification | Gene annotation | Our study | | | | | DEG in common with other xenobiotic transcriptomes | Weisman et al., 2010 | Jin *et al.*, 2011 | Van Hoewyk *et al.*, 2008 | | Ramel *et al.*, 2007 | | Baerson *et al.*, 2005 | Goodwin and Sutter, 2009 | Xu *et al.*, 2012 | Landa *et al.*, 2010 | | Herbette *et al.*, 2006 | | Pucciariello et al., 2012 |
|---|---|---|---|---|---|---|---|---|---|---|---|---|---|---|---|---|---|---|---|---|---|---|---|
| | | | | Phenanthrene Seedlings | | | | | | Phenanthrene Seedlings | PCB ? | Selenium | | Atrazine Mannitol | Atrazine Sucrose | BOA | Aluminium | Phénol | Trinitrotoluene | | Cadmium | | Anoxia-hypoxia |
| | | | | 30 min* | 2h* | 4h* | 8h* | 24h* | Number in commmon | 109 | 146 | Leaves 32 | Roots 52 | Seedlings 113 | 119 | 45 | 14 | 16 | Leaves 15 | Roots 2 | Leaves 134 | Roots 182 | 3 |
| AT5G46580 | 28.1 | DNA.synthesis/chromatin structure | pentatricopeptide (PPR) repeat-containing protein | ns | ns | ns | **-0.93** | ns | X | | | | | | X | | | | | | X | | |
| AT5G54640 | 28.1.3 | DNA.synthesis/chromatin structure.histone | ATHTA1_HTA1_RAT5__Histone superfamily protein | ns | ns | ns | **0.94** | ns | | | | | | | | | | | | | | | |
| AT4G15248 | 28.99 | DNA.unspecified | B-box type zinc finger family protein | **1.39** | **1.75** | **1.04** | ns | **1.63** | X | | X | | | | | | | | | | | | |
| AT4G13870 | 28.99 | DNA.unspecified | WRNEXO (WERNER SYNDROME-LIKE EXONUCLEASE); 3p-5p exonuclease/ nucleic acid binding, glycine-rich RNA-binding protein, putative | ns | ns | ns | ns | **-1.19** | | | | | | | | | | | | | | | |
| AT2G07811 | 29.2.1.1.2.1.3 | protein.synthesis.ribosomal protein.prokaryotic.mitochondrion.30S subunit.S3 | unknown protein | ns | ns | ns | **1.01** | ns | | | | | | | | | | | | | | | |
| AT4G34620 | 29.2.1.1.3.1.16 | protein.synthesis.ribosomal protein.prokaryotic.unknown organellar.30S subunit.S16 | SSR16__small subunit ribosomal protein 16 | ns | ns | ns | ns | **-0.85** | X | | | | | | | | | | | | | X | |
| AT3G17170 | 29.2.1.1.3.1.6 | protein.synthesis.ribosomal protein.prokaryotic.unknown organellar.30S subunit.S6 | RFC3__Translation elongation factor EF1B/ribosomal protein S6 family protein | ns | ns | ns | **-0.72** | **-0.79** | X | | X | | | X | X | | | | | | X | X | |
| AT3G48930 | 29.2.1.2.1.11 | protein.synthesis.ribosomal protein.eukaryotic.40S subunit.S11 | EMB1080__Nucleic acid-binding, OB-fold-like protein | ns | ns | ns | ns | **-0.68** | X | | | | | X | X | | | | | | X | | |
| AT4G34670 | 29.2.1.2.1.53 | protein.synthesis.ribosomal protein.eukaryotic.40S subunit.S3A | Ribosomal protein S3Ae | ns | ns | ns | ns | **-0.76** | X | | | | | | | | | | | | | X | |
| AT3G02560 | 29.2.1.2.1.7 | protein.synthesis.ribosomal protein.eukaryotic.40S subunit.S7 | Ribosomal protein S7e family protein | ns | ns | ns | ns | **-0.80** | | | | | | | | | | | | | | | |
| AT4G27090 | 29.2.1.2.2.14 | protein.synthesis.ribosomal protein.eukaryotic.60S subunit.L14 | Ribosomal protein L14 | ns | ns | ns | ns | **-0.71** | | | | | | | | | | | | | | | |
| AT3G23390 | 29.2.1.2.2.536 | protein.synthesis.ribosomal protein.eukaryotic.60S subunit.L36A | Zinc-binding ribosomal protein family protein | ns | ns | ns | ns | **-0.77** | X | | X | | | X | X | | | | | | | X | |
| AT4G14320 | 29.2.1.2.2.536 | protein.synthesis.ribosomal protein.eukaryotic.60S subunit.L36A | Zinc-binding ribosomal protein family protein | ns | ns | ns | ns | **-0.70** | X | | | | | | | | | | | | | X | |
| AT1G26630 | 29.2.3 | protein.synthesis.initiation | ATELF5A-2_ELF5A-2_FBR12__Eukaryotic translation initiation factor 5A-1 (eIF-5A 1) protein | ns | ns | ns | ns | **1.36** | | | | | | X | | | | | | | | | |
| AT2G31660 | 29.3.1 | protein.targeting.nucleus | SAD2_URM9__ARM repeat superfamily protein | ns | ns | ns | ns | **0.68** | | | | | | | | | | | | | | | |
| AT4G03320 | 29.3.3 | protein.targeting.chloroplast | tic20-IV__translocon at the inner envelope membrane of chloroplasts 20-IV | ns | ns | ns | **1.00** | **0.82** | | | | | | | | | | | | | | | |
| AT1G23490 | 29.3.4.99 | protein.targeting.secretory pathway.unspecified | ARF1_ATARF_ATARF1_ATARFA1A__ADP-ribosylation factor 1 | ns | ns | **1.04** | ns | **1.32** | | | | | | | | | | | | | | | |
| AT1G71530 | 29.4 | protein.postranslational modification | Protein kinase superfamily protein | ns | ns | ns | **0.70** | ns | X | | | | | | X | | | | | | | X | |
| AT1G68410 | 29.4 | protein.postranslational modification | Protein phosphatase 2C family protein | ns | ns | ns | **0.96** | ns | | | | | | | X | | | | | | | | |
| AT3G62260 | 29.4 | protein.postranslational modification | Protein phosphatase 2C family protein | ns | ns | ns | ns | **0.81** | X | | | | X | | X | | | X | X | | | X | |
| AT1G70490 | 29.4 | protein.postranslational modification | ARFA1D_ATARFA1D__Ras-related small GTP-binding family protein | ns | ns | ns | ns | **1.04** | | | | | | X | | | | | | | | | |
| AT4G11890 | 29.4.1 | protein.postranslational modification.kinase | Protein kinase superfamily protein | ns | ns | ns | ns | **1.38** | X | | | X | | | X | | | | | | X | X | |
| AT2G28930 | 29.4.1.57 | protein.postranslational modification.kinase.receptor like cytoplasmatic kinase VII | APK1B_PK1B__protein kinase 1B | ns | ns | ns | ns | **0.70** | X | | X | | | | | | | | | | | | |
| AT5G51770 | 29.4.1.61 | protein.postranslational modification.kinase.receptor like cytoplasmatic kinase X | Protein kinase superfamily protein | ns | ns | ns | ns | **1.00** | X | | | | | | | | | | | | X | | |
| AT1G78680 | 29.5 | protein.degradation | ATGGH2_GGH2__gamma-glutamyl hydrolase 2 | ns | **1.24** | ns | **1.53** | **1.00** | X | | X | | | | X | | | | | | | X | |
| AT3G51260 | 29.5 | protein.degradation | PAD1__20S proteasome alpha subunit PAD1 | ns | ns | ns | ns | **0.71** | | | | | | X | | | | | | | | | |
| AT2G31865 | 29.5 | protein.degradation | poly(ADP-ribose) glycohydrolase 2 (PARG2) | ns | ns | ns | ns | **1.17** | X | | | | | | X | | | | | | X | X | |
| AT1G32940 | 29.5.1 | protein.degradation.subtilases | ATSBT3.5_SBT3.5__Subtilase family protein | ns | ns | ns | ns | **1.06** | X | | | | | | | X | | | | | | | |
| AT3G45180 | 29.5.11.1 | protein.degradation.ubiquitin.ubiquitin | ubiquitin family protein | ns | ns | ns | **0.86** | **0.87** | | | | | | | | | | | | | | | |
| AT5G23540 | 29.5.11.20 | protein.degradation.ubiquitin.proteasom | Mov34/MPN/PAD-1 family protein | ns | ns | ns | ns | **0.68** | | | | | | | | | | | | | | | |
| AT2G05840 | 29.5.11.20 | protein.degradation.ubiquitin.proteasom | PAA2__20S proteasome subunit PAA2 | ns | ns | ns | ns | **0.77** | | | | | | X | | | | | | | | | |
| AT4G29040 | 29.5.11.20 | protein.degradation.ubiquitin.proteasom | RPT2a__regulatory particle AAA-ATPase 2A | ns | ns | ns | ns | **0.79** | | | | | | X | | | | | | | | | |
| AT2G15530 | 29.5.11.4.2 | protein.degradation.ubiquitin.E3.RING | RING/U-box superfamily protein | ns | **0.81** | ns | **1.71** | **2.15** | | | | | | | | | | | | | | | |
| AT1G22500 | 29.5.11.4.2 | protein.degradation.ubiquitin.E3.RING | RING/U-box superfamily protein | ns | ns | ns | **0.88** | ns | X | | X | | | | | | | | | | | | |
| AT1G66180 | 29.5.4 | protein.degradation.aspartate protease | Eukaryotic aspartyl protease family protein | ns | ns | **-1.07** | ns | **-0.68** | | | | | | | | | | | | | | | |
| AT1G69100 | 29.5.4 | protein.degradation.aspartate protease | Eukaryotic aspartyl protease family protein | ns | ns | **-1.06** | **-1.21** | **-1.03** | X | | | | | | | | | | | | X | | |
| AT1G11910 | 29.5.4 | protein.degradation.aspartate protease | APA1_ATAPA1__aspartic proteinase A1 | ns | ns | ns | ns | **0.84** | | | | | | | | | | | | | | | |
| AT3G50930 | 29.5.9 | protein.degradation.AAA type | BCS1__cytochrome BC1 synthesis | ns | ns | ns | ns | **0.76** | X | | | | X | X | | | | | | | X | X | |
| AT3G13470 | 29.6 | protein.folding | TCP-1/cpn60 chaperonin family protein | ns | ns | ns | **-0.74** | ns | X | | | | | X | X | | | | | | X | | |
| AT5G02490 | 29.6 | protein.folding | Heat shock protein 70 (Hsp 70) family protein | ns | ns | ns | ns | **1.16** | X | | | | X | | | | | X | | | X | X | |
| AT5G48400 | 30.1.1 | signalling.in sugar and nutrient physiology | ATGLR1.2_GLR1.2__Glutamate receptor family protein | ns | ns | ns | **0.77** | **1.54** | X | | X | | | | | | | | | | | | |
| AT1G18810 | 30.11 | signalling.light | phytochrome kinase substrate-related | ns | ns | ns | **-1.27** | ns | X | | X | | | | | | | | | | | | |
| AT1G27190 | 30.2.10 | signalling.receptor kinases.leucine rich repeat X | Leucine-rich repeat protein kinase family protein | ns | ns | ns | **1.96** | ns | | | | | | | | | | | | | | | |
| AT4G23190 | 30.2.17 | signalling.receptor kinases.DUF 26 | AT-RLK3_CRK11__cysteine-rich RLK (RECEPTOR-like protein kinase) 11 | ns | ns | ns | **0.80** | **1.38** | X | | X | | | | | | | | | | | X | X |
| AT3G59700 | 30.2.19 | signalling.receptor kinases.legume-lectin | ATHLECRK_HLECRK_LECRK1__lectin-receptor kinase | ns | ns | ns | ns | **0.99** | X | | | | | | | | | | | | X | X | |
| AT5G01540 | 30.2.99 | signalling.receptor kinases.misc | LECRKA4.1__lectin receptor kinase a4.1 | ns | ns | ns | ns | **1.17** | | | | | | | | | | | | | | | |
| AT5G07340 | 30.3 | signalling.calcium | Calreticulin family protein | ns | ns | ns | **-0.96** | ns | X | | X | | | X | X | | | | | | | | |
| AT3G47480 | 30.3 | signalling.calcium | Calcium-binding EF-hand family protein | ns | ns | ns | ns | **0.93** | X | | X | X | X | | X | | | | | | X | X | |
| AT5G39670 | 30.3 | signalling.calcium | Calcium-binding EF-hand family protein | ns | ns | ns | ns | **1.38** | X | | | | X | | | | | | | | X | X | |
| AT1G01960 | 30.5 | signalling.G-proteins | EDA10__SEC7-like guanine nucleotide exchange family protein | ns | ns | ns | **-0.96** | ns | | | | | | | | | | | | | | | |

| AGI identifier | Bincode identifier | MAPMAN classification | Gene annotation | Our study | | | | | DEG in common with other xenobiotic transcriptpomes | Weisman et al., 2010 | Jin *et al.*, 2011 | Van Hoewyk *et al.*, 2008 | | Ramel *et al.*, 2007 | | Baerson *et al.*, 2005 | Goodwin and Sutter, 2009 | Xu *et al.*, 2012 | Landa *et al.*, 2010 | | Herbette *et al.*, 2006 | | Pucciariello et al., 2012 |
|---|---|---|---|---|---|---|---|---|---|---|---|---|---|---|---|---|---|---|---|---|---|---|---|
| | | | | Phenanthrene Seedlings | | | | | | Phenanthrene Seedlings | PCB ? | Selenium Seedlings | | Atrazine Mannitol Seedlings | Atrazine Sucrose Seedlings | BOA | Aluminium | Phénol | Trinitrotoluene | | Cadmium | | Anoxia-hypoxia |
| | | | | 30 min* | 2h* | 4h* | 8h* | 24h* | Number in commmon | 109 | 146 | Leaves 32 | Roots 52 | 113 | 119 | 45 | 14 | 16 | Leaves 15 | Roots 2 | Leaves 134 | Roots 182 | 3 |
| AT1G05100 | 30.6 | signalling.MAP kinases | MAPKKK18__mitogen-activated protein kinase kinase kinase 18 | ns | ns | ns | **0.99** | ns | X | | X | | | | | | | | | | | | |
| AT5G55230 | 31.1 | cell.organisation | ATMAP65-1_MAP65-1_MAP65-1__microtubule-associated proteins 65-1 | ns | ns | ns | **-1.06** | ns | X | | | | | X | X | | | | | | | X | |
| AT1G64740 | 31.1 | cell.organisation | TUA1__alpha-1 tubulin | ns | ns | ns | **-0.83** | ns | X | | | | | X | X | | | | | | | X | |
| AT5G54710 | 31.1 | cell.organisation | Ankyrin repeat family protein | ns | ns | ns | ns | **1.15** | | | | | | | | | | | | | | | |
| AT1G13330 | 31.1 | cell.organisation | AHP2__Arabidopsis Hop2 homolog | ns | ns | ns | ns | **1.55** | X | | | | | | X | | | | | | X | X | |
| AT5G13120 | 31.3.1 | cell.cycle.peptidylprolyl isomerase | ATCYP20-2_CYP20-2__cyclophilin 20-2 | ns | ns | ns | ns | **-0.67** | X | | | | | X | X | | | | | | | X | |
| AT3G49670 | 33.99 | development.unspecified | BAM2__Leucine-rich receptor-like protein kinase family protein | ns | ns | ns | **-0.93** | **-0.76** | X | | | X | | X | | | | | | | X | X | |
| AT2G35980 | 33.99 | development.unspecified | ATNHL10_NHL10_YLS9__Late embryogenesis abundant (LEA) hydroxyproline-rich glycoprotein family | ns | **1.72** | **1.96** | **1.81** | **2.34** | X | | | | | | | X | X | | | | X | X | |
| AT4G12420 | 33.99 | development.unspecified | SKU5__Cupredoxin superfamily protein | ns | ns | ns | **-1.07** | ns | X | | X | | | | | | | | | | X | X | |
| AT5G63420 | 33.99 | development.unspecified | emb2746__RNA-metabolising metallo-beta-lactamase family protein | ns | ns | ns | **-0.74** | ns | X | | | | | | | | | | | | X | | |
| AT3G14770 | 33.99 | development.unspecified | Nodulin MtN3 family protein | ns | ns | ns | **1.02** | ns | X | | | | | X | X | | | | | | | | |
| AT2G34355 | 33.99 | development.unspecified | nodulin-related | ns | ns | ns | **1.07** | ns | X | | X | | | | | | | | | | | | |
| AT3G02380 | 33.99 | development.unspecified | ATCOL2_COL2__CONSTANS-like 2 | ns | ns | ns | ns | **-1.15** | X | | X | | | | | | | | | X | | | |
| AT3G16690 | 33.99 | development.unspecified | Nodulin MtN3 family protein | ns | ns | ns | ns | **-0.81** | | | | | | | | | | | | | | | |
| AT5G14930 | 33.99 | development.unspecified | SAG101__senescence-associated gene 101 | ns | ns | ns | ns | **0.98** | X | | | | | | | | | | | | | X | |
| AT2G23810 | 33.99 | development.unspecified | TET8__tetraspanin8 | ns | ns | ns | ns | **1.15** | X | | | | | | | | | | | | X | X | |
| AT3G49530 | 33.99 | development.unspecified | ANAC062_NAC062_NTL6__NAC domain containing protein 62 | ns | ns | ns | ns | **1.28** | X | | | | X | | | | | | | | X | X | |
| AT5G62670 | 34.1 | transport.p- and v-ATPases | AHA11_HA11__H(+)-ATPase 11 | ns | ns | ns | ns | **-0.77** | X | | | | | | | | | | | | | X | |
| AT2G07671 | 34.1.1.2 | transport.p- and v-ATPases.H+-transporting two-sector ATPase.subunit C | ATP synthase subunit C family protein | ns | ns | ns | **0.86** | **0.82** | X | | X | | | | X | | | | | | | X | |
| AT1G80830 | 34.12 | transport.metal | ATNRAMP1_NRAMP1_PMIT1__natural resistance-associated macrophage protein 1 | ns | ns | ns | **-0.99** | **-0.75** | X | | X | | | | | | | | | | | | |
| AT2G23150 | 34.12 | transport.metal | ATNRAMP3_NRAMP3__natural resistance-associated macrophage protein 3 | ns | ns | ns | ns | **1.69** | X | | | | | | | | | | | | X | X | |
| AT5G55930 | 34.13 | transport.peptides and oligopeptides | ATOPT1_OPT1__oligopeptide transporter 1 | ns | ns | ns | **-1.07** | ns | X | | X | | | X | | | | | | | X | | |
| AT3G45700 | 34.13 | transport.peptides and oligopeptides | Major facilitator superfamily protein | ns | ns | ns | **-0.91** | **-0.93** | X | | | | X | | | | | | | | | | |
| AT1G27080 | 34.13 | transport.peptides and oligopeptides | NRT1.6__nitrate transporter 1.6 | ns | ns | ns | ns | **0.88** | | | | | | | | | | | | | | | |
| AT2G45960 | 34.19.1 | transport.Major Intrinsic Proteins.PIP | ATHH2_PIP1;2_PIP1B_TMP-A__plasma membrane intrinsic protein 1B | ns | ns | **-1.14** | **-0.77** | ns | X | | X | | | | | | | | | | X | X | |
| AT2G37180 | 34.19.1 | transport.Major Intrinsic Proteins.PIP | PIP2;3_PIP2C_RD28__Aquaporin-like superfamily protein | ns | ns | ns | **-0.87** | **-0.82** | X | | X | | | | | | X | | | | | X | |
| AT4G35100 | 34.19.1 | transport.Major Intrinsic Proteins.PIP | PIP2;7_PIP3_PIP3A_SIMIP__plasma membrane intrinsic protein 3 | ns | ns | ns | ns | **-1.26** | X | | X | | | | | | | | | | X | X | |
| AT1G66570 | 34.2.1 | transporter.sugars.sucrose | ATSUC7_SUC7__sucrose-proton symporter 7 | ns | ns | ns | **0.73** | ns | X | | X | | | | | | | | | | | | |
| AT1G22710 | 34.2.1 | transporter.sugars.sucrose | ATSUC2_SUC2_SUT1__sucrose-proton symporter 2 | ns | ns | ns | **0.87** | **1.27** | | | | | | | | | | | | | | | |
| AT5G15410 | 34.22 | transport.cyclic nucleotide or calcium regulated channels | ATCNGC2_CNGC2_DND1__Cyclic nucleotide-regulated ion channel family protein | ns | ns | ns | **-0.78** | ns | | | | | | | | | | | | | | | |
| AT2G36590 | 34.3 | transport.amino acids | ATPROT3_ProT3__proline transporter 3 | **0.79** | **1.42** | **1.93** | **1.80** | **2.24** | X | | | | | | | | | | | X | | | |
| AT1G61790 | 34.3 | transport.amino acids | Oligosaccharyltransferase complex/magnesium transporter family protein | ns | ns | ns | **0.74** | ns | X | | | | | | | | | | | | | X | |
| AT4G21120 | 34.3 | transport.amino acids | AAT1_CAT1__amino acid transporter 1 | ns | ns | ns | ns | **0.76** | | | | | | | | | | | | | | | |
| AT5G33320 | 34.8 | transport.metabolite transporters at the envelope membrane | ARAPPT_CUE1_PPT__Glucose-6-phosphate/phosphate translocator-related | ns | ns | ns | **-0.87** | ns | | | | | | | | | | | | | | | |
| AT1G61800 | 34.8 | transport.metabolite transporters at the envelope membrane | ATGPT2_GPT2__glucose-6-phosphate/phosphate translocator 2 | ns | ns | ns | ns | **0.83** | | | | | | | | | | | | | | | |
| AT5G15640 | 34.9 | transport.metabolite transporters at the mitochondrial membrane | Mitochondrial substrate carrier family protein | ns | ns | ns | **1.19** | ns | X | | | | | | | | | | | | | X | |
| AT2G17500 | 34.99 | transport.misc | Auxin efflux carrier family protein | ns | **0.80** | **1.19** | **1.79** | **1.20** | X | | | | | X | X | | | | | | | | |
| AT1G76520 | 34.99 | transport.misc | Auxin efflux carrier family protein | ns | ns | ns | **0.87** | **0.66** | X | | | | | | | X | | | | | | | |
| AT1G76530 | 34.99 | transport.misc | Auxin efflux carrier family protein | ns | ns | ns | **0.90** | **0.88** | X | | X | X | | | | | | | | | | | X | |
| AT1G29310 | 34.99 | transport.misc | SecY protein transport family protein | ns | ns | ns | ns | **0.68** | | | | | | | | | | | | | | | |
| AT4G36640 | 34.99 | transport.misc | Sec14p-like phosphatidylinositol transfer family protein | ns | ns | ns | ns | **0.75** | X | | | | | | | | | | | | X | | |
| AT3G51670 | 34.99 | transport.misc | SEC14 cytosolic factor family protein / phosphoglyceride transfer family protein | ns | ns | ns | ns | **1.15** | X | | | | | X | X | | | | | | X | | |
| AT1G19100 | 35.1 | not assigned.no ontology | Histidine kinase-, DNA gyrase B-, and HSP90-like ATPase family protein | ns | ns | ns | **-0.69** | ns | | | | | | | | | | | | | | | |
| AT5G26290 | 35.1 | not assigned.no ontology | TRAF-like family protein | ns | **-0.87** | ns | **-1.50** | **-1.36** | | | | | | | | | | | | | | | |
| AT4G36850 | 35.1 | not assigned.no ontology | PQ-loop repeat family protein / transmembrane family protein | ns | ns | **-1.17** | ns | **-0.95** | X | | X | | | X | X | | | | | | | | |
| AT5G48430 | 35.1 | not assigned.no ontology | Eukaryotic aspartyl protease family protein | ns | ns | **-1.12** | ns | **1.47** | X | | | | | X | | | | | | | | X | |
| AT5G26280 | 35.1 | not assigned.no ontology | TRAF-like family protein | ns | ns | **-1.02** | ns | **-0.86** | | | | | | | | | | | | | | | |
| AT3G51660 | 35.1 | not assigned.no ontology | Tautomerase/MIF superfamily protein | ns | ns | **1.47** | **1.80** | **2.27** | X | | | | | X | | | | | X | | X | X | |
| AT4G15390 | 35.1 | not assigned.no ontology | HXXXD-type acyl-transferase family protein | ns | ns | ns | **-1.39** | **-1.54** | X | | X | | | | | X | | | | | | | |
| AT1G76160 | 35.1 | not assigned.no ontology | sks5__SKU5 similar 5 | ns | ns | ns | **-1.08** | ns | X | | X | | | X | X | | | | | | | | |

| AGI identifier | Bincode identifier | MAPMAN classification | Gene annotation | Our study | | | | | DEG in common with other xenobiotic transcritpomes | Weisman et al., 2010 | Jin *et al.*, 2011 | Van Hoewyk *et al.*, 2008 | | Ramel *et al.*, 2007 | | Baerson *et al.*, 2005 | Goodwin and Sutter, 2009 | Xu *et al.*, 2012 | Landa *et al.*, 2010 | | Herbette *et al.*, 2006 | | Pucciariello et al., 2012 |
|---|---|---|---|---|---|---|---|---|---|---|---|---|---|---|---|---|---|---|---|---|---|---|---|
| | | | | Phenanthrene Seedlings | | | | | | Phenanthrene Seedlings | PCB ? | Selenium | | Atrazine Mannitol | Atrazine Sucrose | BOA | Aluminium | Phénol | Trinitrotoluene | | Cadmium | | Anoxia-hypoxia |
| | | | | | | | | | | | | Leaves | Roots | Seedlings | | | | | Leaves | Roots | Leaves | Roots | |
| | | | | 30 min* | 2h* | 4h* | 8h* | 24h* | Number in commmon | 109 | 146 | 32 | 52 | 113 | 119 | 45 | 14 | 16 | 15 | 2 | 134 | 182 | 3 |
| AT5G51550 | 35.1 | not assigned.no ontology | EXL3__EXORDIUM like 3 | ns | ns | ns | **-0.94** | **-0.90** | X | | X | | | | | | | | | | | X | |
| AT3G20370 | 35.1 | not assigned.no ontology | TRAF-like family protein | ns | ns | ns | **-0.94** | **-1.06** | X | | | | | X | X | | | X | | | | X | |
| AT1G70280 | 35.1 | not assigned.no ontology | NHL domain-containing protein | ns | ns | ns | **-0.90** | ns | X | | | | | X | X | | | | | | X | | |
| AT3G23940 | 35.1 | not assigned.no ontology | dehydratase family | ns | ns | ns | **-0.87** | ns | X | | | | | X | X | | | | | | X | | |
| AT5G26260 | 35.1 | not assigned.no ontology | TRAF-like family protein | ns | ns | ns | **-0.78** | **-0.99** | | | | | | | | | | | | | | | |
| AT3G54600 | 35.1 | not assigned.no ontology | Class I glutamine amidotransferase-like superfamily protein | ns | ns | ns | **-0.77** | ns | X | | X | | | X | X | | | | | | | | |
| AT2G43445 | 35.1 | not assigned.no ontology | unknown protein | ns | ns | ns | **0.73** | ns | X | | X | | | | | | | | | | | | |
| AT4G34120 | 35.1 | not assigned.no ontology | CDCP1_LEJ1__Cystathionine beta-synthase (CBS) family protein | ns | ns | ns | **0.77** | **0.86** | | | | | | | | | | | | | | | |
| AT2G23680 | 35.1 | not assigned.no ontology | Cold acclimation protein WCOR413 family | ns | ns | ns | **0.88** | **1.12** | X | | X | | | | | | | | | | X | X | |
| AT5G62720 | 35.1 | not assigned.no ontology | Integral membrane HPP family protein | ns | ns | ns | **0.91** | ns | X | | | | X | | | | | X | | | X | | |
| AT1G23890 | 35.1 | not assigned.no ontology | NHL domain-containing protein | ns | ns | ns | **1.26** | ns | | | | | | | | | | | | | | | |
| AT4G24160 | 35.1 | not assigned.no ontology | alpha/beta-Hydrolases superfamily protein | ns | ns | ns | **1.52** | **1.25** | X | | | | | | X | X | | | | | | | |
| AT3G44190 | 35.1 | not assigned.no ontology | FAD/NAD(P)-binding oxidoreductase family protein | ns | ns | ns | **2.05** | **2.01** | X | | | | | | X | | | X | | | | X | |
| AT5G22140 | 35.1 | not assigned.no ontology | FAD/NAD(P)-binding oxidoreductase family protein | ns | ns | ns | **2.15** | **1.97** | X | | X | | | | | | | | | | | | |
| AT3G28270 | 35.1 | not assigned.no ontology | Protein of unknown function (DUF677) | ns | ns | ns | ns | **-1.26** | X | | X | X | | | | | | X | | | X | | |
| AT4G24930 | 35.1 | not assigned.no ontology | thylakoid lumenal 17.9 kDa protein, chloroplast | ns | ns | ns | ns | **-0.78** | X | | | | | | | | | | | | X | | |
| AT4G34290 | 35.1 | not assigned.no ontology | SWIB/MDM2 domain superfamily protein | ns | ns | ns | ns | **-0.74** | X | | | | | X | | | | | | | X | X | |
| AT1G23880 | 35.1 | not assigned.no ontology | NHL domain-containing protein | ns | ns | ns | ns | **0.78** | | | | | | | | | | | | | | | |
| AT2G15240 | 35.1 | not assigned.no ontology | UNC-50 family protein | ns | ns | ns | ns | **1.02** | | | | | | | | | | | | | | | |
| AT5G18480 | 35.1 | not assigned.no ontology | plant glycogenin-like starch initiation protein 6 (PGSIP6) | ns | ns | ns | ns | **1.05** | X | | | | | | | | | | | | | X | |
| AT1G36622 | 35.1 | not assigned.no ontology | unknown protein | ns | ns | ns | ns | **1.12** | X | | X | | | | | | | | | | X | | |
| AT1G14870 | 35.1 | not assigned.no ontology | PCR2__PLANT CADMIUM RESISTANCE 2 | ns | ns | ns | ns | **1.76** | | | | | | | | | | | | | | | |
| AT1G70800 | 35.1.19 | not assigned.no ontology.C2 domain-containing protein | ENHANCED BENDING 1 | **0.64** | **1.23** | **1.91** | **1.97** | **1.19** | | | | | | | | | | | | | | | |
| AT2G17740 | 35.1.26 | not assigned.no ontology.DC1 domain containing protein | Cysteine/Histidine-rich C1 domain family protein | ns | ns | ns | ns | **1.67** | X | | X | | | | | X | | X | | | | | |
| AT3G62530 | 35.1.3 | not assigned.no ontology.armadillo/beta-catenin repeat family protein | ARM repeat superfamily protein | ns | ns | ns | ns | **-0.81** | X | | | | | X | X | | | | | | X | | |
| AT2G05530 | 35.1.40 | not assigned.no ontology.glycine rich proteins | Glycine-rich protein family | ns | ns | ns | **0.85** | **1.73** | | | | | | | | | | | | | | | |
| AT1G07135 | 35.1.40 | not assigned.no ontology.glycine rich proteins | glycine-rich protein | ns | ns | ns | ns | **0.66** | X | | | | X | | X | | | | | | | X | |
| AT5G55750 | 35.1.41 | not assigned.no ontology.hydroxyproline rich proteins | hydroxyproline-rich glycoprotein family protein | ns | ns | ns | **0.95** | **1.62** | | | | | | | | | | | | | | | |
| AT3G54580 | 35.1.42 | not assigned.no ontology.proline rich family | Proline-rich extensin-like family protein | ns | ns | ns | **-0.91** | **-0.82** | X | | | | X | | | | | | | | | X | |
| AT5G45350 | 35.1.42 | not assigned.no ontology.proline rich family | proline-rich family protein | ns | ns | ns | ns | **0.84** | X | | X | | X | | | | | | | | | X | |
| AT1G67600 | 35.2 | not assigned.unknown | Acid phosphatase/vanadium-dependent haloperoxidase-related protein | ns | ns | ns | **1.25** | **1.07** | X | | X | | | | | | | | | | | | |
| AT4G27657 | 35.2 | not assigned.unknown | unknown protein | **0.70** | **1.26** | **1.10** | **1.75** | **0.74** | X | | | | X | X | | | | | | | | | |
| AT4G39670 | 35.2 | not assigned.unknown | Glycolipid transfer protein (GLTP) family protein | **0.73** | **1.26** | **1.01** | **1.42** | **2.13** | X | | | | X | | X | | | X | | | | X | |
| AT2G47950 | 35.2 | not assigned.unknown | unknown protein | **1.49** | **2.27** | **2.27** | **2.65** | **1.91** | X | | X | | X | | | | | X | | | X | X | |
| AT1G34630 | 35.2 | not assigned.unknown | unknown protein | ns | **1.06** | ns | ns | ns | X | | X | | | X | X | | | | | | | | |
| AT1G74450 | 35.2 | not assigned.unknown | Protein of unknown function (DUF793) | ns | **1.09** | **1.16** | **1.06** | **1.10** | X | | X | | X | | | | | | | | X | X | |
| AT3G21520 | 35.2 | not assigned.unknown | AtDMP1_DMP1__DUF679 domain membrane protein 1 | ns | **1.10** | ns | **0.92** | **0.97** | X | | X | | X | | | | | | | | X | X | |
| AT5G12960 | 35.2 | not assigned.unknown | Putative glycosyl hydrolase of unknown function (DUF1680) | ns | **1.12** | ns | ns | ns | | | | | | | | | | | | | | | |
| AT1G76980 | 35.2 | not assigned.unknown | unknown protein | ns | **1.15** | **1.67** | **1.78** | **1.85** | X | | X | | | | | | | | | | X | X | |
| AT3G04300 | 35.2 | not assigned.unknown | RmlC-like cupins superfamily protein; | ns | **1.25** | **1.73** | **2.08** | **2.25** | | | | | | | | | | | | | | | |
| AT2G27385 | 35.2 | not assigned.unknown | Pollen Ole e 1 allergen and extensin family protein | ns | ns | **-1.40** | ns | **-1.00** | X | | | | | | X | | | | | | X | | |
| AT5G25460 | 35.2 | not assigned.unknown | Protein of unknown function, DUF642 | ns | ns | **-1.30** | **-1.72** | **-1.41** | X | | X | | | | | | | | | | X | X | |
| AT4G29905 | 35.2 | not assigned.unknown | unknown protein | ns | ns | **-1.16** | **-0.76** | **-1.83** | X | | | | | | X | | | | | | X | X | |
| AT1G64370 | 35.2 | not assigned.unknown | unknown protein | ns | ns | **-1.01** | **-0.77** | ns | X | | | | X | | | | | | | | | | |
| AT3G49570 | 35.2 | not assigned.unknown | unknown protein | ns | ns | **1.04** | ns | ns | X | | X | | | | | | | | | | | | |
| AT3G60320 | 35.2 | not assigned.unknown | Protein of unknown function (DUF630 and DUF632) | ns | ns | ns | **-1.10** | **-0.77** | X | | X | | | | | | | | | | | | |
| AT1G29560 | 35.2 | not assigned.unknown | Zinc finger C-x8-C-x5-C-x3-H type family protein | ns | ns | ns | **-1.00** | **-0.93** | | | | | | | | | | | | | | | |
| AT5G38980 | 35.2 | not assigned.unknown | unknown protein | ns | ns | ns | **-0.96** | **-1.09** | X | | | | | | | | | | | | | X | |
| AT5G44580 | 35.2 | not assigned.unknown | unknown protein | ns | ns | ns | **-0.81** | ns | X | | | | | | | | | | | | | X | |
| AT5G01015 | 35.2 | not assigned.unknown | unknown protein | ns | ns | ns | **-0.78** | **-1.03** | X | | | | | | | | | | | | X | | |

| AGI identifier | Bincode identifier | MAPMAN classification | Gene annotation | Our study | | | | | DEG in common with other xenobiotic transcritpomes | Weisman et al., 2010 | Jin *et al.*, 2011 | Van Hoewyk *et al.*, 2008 | | Ramel *et al.*, 2007 | | Baerson *et al.*, 2005 | Goodwin and Sutter, 2009 | Xu *et al.*, 2012 | Landa *et al.*, 2010 | | Herbette *et al.*, 2006 | | Pucciariello et al., 2012 |
|---|---|---|---|---|---|---|---|---|---|---|---|---|---|---|---|---|---|---|---|---|---|---|---|
| | | | | Phenanthrene Seedlings | | | | | | Phenanthrene | PCB | Selenium | | Atrazine Mannitol | Atrazine Sucrose | BOA | Aluminium | Phénol | Trinitrotoluene | | Cadmium | | Anoxia-hypoxia |
| | | | | 30 min* | 2h* | 4h* | 8h* | 24h* | Number in commmon | Seedlings 109 | ? 146 | Leaves 32 | Roots 52 | Seedlings 113 | 119 | 45 | 14 | 16 | Leaves 15 | Roots 2 | Leaves 134 | Roots 182 | 3 |
| AT1G29050 | 35.2 | not assigned.unknown | TBL38__TRICHOME BIREFRINGENCE-LIKE 38 | ns | ns | ns | **-0.77** | ns | X | | | | | | | | | | | | | X | |
| AT1G15415 | 35.2 | not assigned.unknown | part of pollen proteome | ns | ns | ns | **0.74** | ns | X | | X | | | | X | | | | | | | | |
| AT2G18680 | 35.2 | not assigned.unknown | unknown protein | ns | ns | ns | **0.75** | **1.97** | | | | | | | | | | | | | | | |
| AT2G12557 | 35.2 | not assigned.unknown | unknown protein | ns | ns | ns | **0.81** | ns | | | | | | | | | | | | | | | |
| AT3G51130 | 35.2 | not assigned.unknown | unknown protein | ns | ns | ns | **0.83** | **0.67** | X | | | | | X | X | | | | | | | | |
| AT1G76070 | 35.2 | not assigned.unknown | unknown protein | ns | ns | ns | **0.90** | **0.68** | X | | | | | | X | | | | | | X | X | |
| AT3G14000 | 35.2 | not assigned.unknown | ATBRXL2_BRX-LIKE2__DZC (Disease resistance/zinc finger/chromosome condensation-like region) domain containing protein | ns | ns | ns | **0.91** | ns | | | | | | | X | | | | | | | | |
| AT4G17840 | 35.2 | not assigned.unknown | unknown protein | ns | ns | ns | **0.99** | ns | X | | X | | | X | X | | | | | | | | |
| AT2G34070 | 35.2 | not assigned.unknown | TBL37__TRICHOME BIREFRINGENCE-LIKE 37 | ns | ns | ns | **0.99** | ns | X | | X | | | X | | | | | | | | | |
| AT1G05575 | 35.2 | not assigned.unknown | unknown protein | ns | ns | ns | **1.21** | ns | X | | | | X | | | | | | | | | | |
| AT1G72490 | 35.2 | not assigned.unknown | unknown protein | ns | ns | ns | **1.25** | **1.10** | | | | | | | | | | | | | | | |
| AT1G18510 | 35.2 | not assigned.unknown | TET16 _ tetraspanin 16 | ns | ns | ns | **1.26** | ns | | | | | | | | | | | | | | | |
| AT2G23110 | 35.2 | not assigned.unknown | Late embryogenesis abundant protein, group 6 | ns | ns | ns | **1.87** | **2.04** | | | | | | X | | | | | | | | | |
| AT1G18290 | 35.2 | not assigned.unknown | unknown protein | ns | ns | ns | ns | **-0.83** | X | | | | X | X | X | | | | | | X | | |
| AT5G36960 | 35.2 | not assigned.unknown | unknown protein | ns | ns | ns | ns | **0.68** | | | | | | | | | | | | | | | |
| AT5G01750 | 35.2 | not assigned.unknown | Protein of unknown function (DUF567) | ns | ns | ns | ns | **0.72** | X | | | | | | | | | | | | | X | |
| AT2G46390 | 35.2 | not assigned.unknown | unknown protein | ns | ns | ns | ns | **0.73** | | | | | | | | | | | | | | | |
| AT2G37940 | 35.2 | not assigned.unknown | AtIPCS2__Arabidopsis Inositol phosphorylceramide synthase 2 | ns | ns | ns | ns | **0.79** | X | | | | | | | | | | | | X | | |
| AT1G65845 | 35.2 | not assigned.unknown | unknown protein | ns | ns | ns | ns | **0.81** | | | | | | | | | | | | | | | |
| AT3G56260 | 35.2 | not assigned.unknown | unknown protein | ns | ns | ns | ns | **0.88** | X | | X | | | X | X | | | | | | | | |
| AT2G37110 | 35.2 | not assigned.unknown | PLAC8 family protein | ns | ns | ns | ns | **0.94** | X | | | | | | | | | | | | X | X | |
| AT3G20510 | 35.2 | not assigned.unknown | Transmembrane proteins 14C | ns | ns | ns | ns | **0.96** | X | | | | | X | | | | | | | X | X | |
| AT3G13950 | 35.2 | not assigned.unknown | unknown protein | ns | ns | ns | ns | **1.12** | X | | X | | | | X | | | | | | X | X | |
| AT2G32190 | 35.2 | not assigned.unknown | unknown protein | ns | ns | ns | ns | **1.33** | X | | | | X | | | | | | | | | | |
| AT5G25250 | 35.2 | not assigned.unknown | SPFH/Band 7/PHB domain-containing membrane-associated protein family | ns | ns | ns | ns | **1.38** | X | | | | | X | X | | | | | | X | X | |
| AT5G25260 | 35.2 | not assigned.unknown | SPFH/Band 7/PHB domain-containing membrane-associated protein family | ns | ns | ns | ns | **2.07** | X | | X | | | | | | | | | | | | |
| AT2G36460 | 4.1.11 | glycolysis.cytosolic branch.aldolase | Aldolase superfamily protein | ns | ns | ns | **0.72** | **1.08** | X | | | | | | | | | | | | | X | |
| AT5G54960 | 5.2 | fermentation.PDC | PDC2__pyruvate decarboxylase-2 | ns | ns | ns | ns | **0.90** | X | | X | | X | | | | | | | | X | | |
| AT5G24420 | 7.1.2 | OPP.oxidative PP.6-phosphogluconolactonase | PGL5__6-phosphogluconolactonase 5 | ns | ns | ns | ns | **-1.20** | X | | X | X | | | | | | | | | X | X | |
| AT1G65930 | 8.1.4 | TCA / org. transformation.TCA.IDH | cICDH__cytosolic NADP+-dependent isocitrate dehydrogenase | ns | ns | **-1.13** | **-0.96** | ns | | | | | | | | | | | | | | | |
| AT3G27380 | 8.1.7 | TCA / org. transformation.TCA.succinate dehydrogenase | SDH2-1__succinate dehydrogenase 2-1 | ns | ns | ns | **0.99** | **0.95** | X | | | | | | | | | | | | X | | |
| AT3G06650 | 8.2.11 | TCA / org. transformation.other organic acid transformaitons.atp-citrate lyase | ACLB-1__ATP-citrate lyase B-1 | ns | ns | ns | **-0.73** | ns | | | | | | | | | | | | | | | |
| AT3G22370 | 9.4 | mitochondrial electron transport / ATP synthesis.alternative oxidase | AOX1A_ATAOX1A__alternative oxidase 1A | ns | ns | ns | **0.99** | **1.18** | X | | | X | | | | | | | | | | | |

**Supplemental Table VI:** Primers used for quantitative RT-PCR.

| Primer name | Sequence (5' → 3') | Targets |
|---|---|---|
| 3G16390_L1 | GACCCACTCCTCGTAGTTTCC | AT3G16390 |
| 3G16390_R1 | CGAACAATGAAACCACGTCTT | |
| 3G24170_L2 | CCCACAAACCCAAACCTAAGA | AT3G24170 |
| 3G24170_R2 | CAAATCCTTTATTGGGACACG | |
| 3G48990_L1 | TCTCCGTTTCTGGAAAATTCA | AT3G48990 |
| 3G48990_R1 | GGTGTTAGGGAAGGTGAGAGC | |
| 4G13615_L2 | AGAAAGCGGCTAAGAAAGCTG | |
| 4G13615_R2 | TGCTCAAAAGACAAACCAAATG | AT4G13615 |
| 4G37930_L1 | AAGGATTTCGTGTCAGCAATG | AT4G37930 |
| 4G37930_R1 | CCAATTGTTGGGAACTGCTTA | |
| 4G38970_L2 | CAAAGAAACCAAAGGCAGAGA | AT4G38970 |
| 4G38970_R2 | AGAAGGCTGACGGAAGAGAAC | |
| 5G11670_L2 | AGTTTGCAGAGAGCAGCATGT | AT5G11670 |
| 5G11670_R2 | CAAACAACAAACAAACAAACAAAA | |
| 5G17380_L1 | ATATTGTGGAAACACCCGATG | AT5G17380 |
| 5G17380_R1 | GCACCAGCAAAAGGATCAATA | |
| 5G21090_L2 | GAGAACAACCCGAGATTGGA | |
| 5G21090_R2 | CCCCCAATTCTTCATTTTCAG | AT5G21090 |
| 5G24490_L2 | GTGCTGAGGAAGATGCTGAGA | AT5G24490 |
| 5G24490_R2 | TGAAACCTTTCATGTGCCTTC | |
| 5G43700_L2 | AAAGGTTTAGGTTGTGGTGGTC | AT5G43700 |
| 5G43700_R2 | AAACATCTCTCCCCAAGAACC | |
| 5G47990_L1 | CCAGTGGTAAGGACGTTCAAA | AT5G47990 |
| 5G47990_R1 | CTCAGGGTCTTCCCAGAAATC | |
| 5G48000_L1 | AGACGTTCATGGTGTTTGGAG | AT5G48000 |
| 5G48000_R1 | ATTCTTGGGCCAATGAGAAAT | |
| 5G48010_L1 | CATGAGAACTGTGATGCTCCA | AT5G48010 |
| 5G48010_R1 | TGTGACATGGTTAAGGGAGGA | |
| 5G56630_L2 | GGAGCTGTCGATATTCCTCCT | AT5G56630 |
| 5G56630_R2 | GCATCGGTTACAGAACCCTCT | |

**Acknoledgments**

This work was supported in part by Axson-Coatings (France) firm and the French government (CIFRE n°1017/2009). The authors thank Marie Laure Martin Magniette for statistical analysis performed on microarray data, Marie-Noëlle Soler for help with microscopy, Nathalie Marnet for making target analysis of metabolites.

**Authors' contributions**

The grant was written and obtained by AE. RB and AE conceived the study and designed experiments. ASD, EB and DB performed the experiments. RB coordinated the microarray analysis at the Unité de Recherche en Génomique Végétale (URGV) using the Complete *Arabidopsis* Transcriptome MicroArray (CATMA), ASD and LT performed microarray experiments. MLMM carried out statistical analysis for microarray data and GR ANOVA analysis. ASD and RB carried out analysis and interpretation of experimental data including bioinformatics analyses. The manuscript was written by RB, AE and ASD and read and revised by all other authors.

**Literature cited**

**Abramoff MD, Magalhães PJ, Ram SJ** (2004) Image processing with ImageJ. Biophotonics Int **11**: 36–42

**Alena Torres Netto EC** (2005) Photosynthetic pigments, nitrogen, chlorophyll a fluorescence and SPAD-502 readings in coffee leaves. Sci Hortic 199–209

**Alkio M, Tabuchi TM, Wang X, Colón-Carmona A** (2005) Stress responses to polycyclic aromatic hydrocarbons in Arabidopsis include growth inhibition and hypersensitive response-like symptoms. J Exp Bot **56**: 2983–2994

**Alkorta I, Garbisu C** (2001) Phytoremediation of organic contaminants in soils. Bioresour Technol **79**: 273–276

**Andersson BE, Henrysson T** (1996) Accumulation and degradation of dead-end metabolites during treatment of soil contaminated with polycyclic aromatic hydrocarbons with five strains of white-rot fungi. Appl Microbiol Biotechnol **46**: 647–652

**Andersson BE, Lundstedt S, Tornberg K, Schnürer Y, Öberg LG, Mattiasson B** (2003) Incomplete degradation of polycyclic aromatic hydrocarbons in soil inoculated with wood-rotting fungi and their effect on the indigenous soil bacteria. Environ Toxicol Chem **22**: 1238–1243

**Armstrong B, Hutchinson E, Unwin J, Fletcher T** (2004) Lung Cancer Risk after Exposure to Polycyclic Aromatic Hydrocarbons: A Review and Meta-Analysis. Environ Health Perspect **112**: 970–978

**Ashraf M, Foolad MR** (2007) Roles of glycine betaine and proline in improving plant abiotic stress resistance. Environ Exp Bot **59**: 206–216

**Atagana HI** (2004) Bioremediation of creosote-contaminated soil in South Africa by landfarming. J Appl Microbiol **96**: 510–520

**Bae J-W, Park Y-H** (2006) Homogeneous versus heterogeneous probes for microbial ecological microarrays. Trends Biotechnol **24**: 318–323

**Baerson SR, Sánchez-Moreiras A, Pedrol-Bonjoch N, Schulz M, Kagan IA, Agarwal AK, Reigosa MJ, Duke SO** (2005) Detoxification and Transcriptome Response in Arabidopsis Seedlings Exposed to the Allelochemical Benzoxazolin-2(3H)-one. J Biol Chem **280**: 21867–21881

**Bak S, Beisson F, Bishop G, Hamberger B, Höfer R, Paquette S, Werck-Reichhart D** (2011) Cytochromes P450. Arab Book e0144

**Balabanič D, Rupnik M, Klemenčič AK** (2011) Negative impact of endocrine-disrupting compounds on human reproductive health. Reprod Fertil Dev **23**: 403–416

**Bhargava A, Carmona FF, Bhargava M, Srivastava S** (2012) Approaches for enhanced phytoextraction of heavy metals. J Environ Manage **105**: 103–120

**Bilgin DD, Zavala JA, Zhu J, Clough SJ, Ort DR, DeLUCIA EH** (2010) Biotic stress globally down regulates photosynthesis genes. Plant Cell Environ **33**: 1597–1613

**Bizub D, Wood AW, Skalka AM** (1986) Mutagenesis of the Ha-ras oncogene in mouse skin tumors induced by polycyclic aromatic hydrocarbons. Proc Natl Acad Sci **83**: 6048–6052

**Boyes DC, Zayed AM, Ascenzi R, McCaskill AJ, Hoffman NE, Davis KR, Görlach J** (2001) Growth stage-based phenotypic analysis of Arabidopsis: a model for high throughput functional genomics in plants. Plant Cell **13**: 1499–1510

**Callén MS, López JM, Iturmendi A, Mastral AM** (2012) Nature and sources of particle associated polycyclic aromatic hydrocarbons (PAH) in the atmospheric environment of an urban area. Environ Pollut Barking Essex 1987. doi: 10.1016/j.envpol.2012.11.009

**Carillo P, Grazia M, Pontecorvo G, Fuggi A, Woodrow P** (2011) Salinity Stress and Salt Tolerance. Abiotic Stress Plants - Mech. Adapt.

**Cheema SA, Imran Khan M, Shen C, Tang X, Farooq M, Chen L, Zhang C, Chen Y** (2010) Degradation of phenanthrene and pyrene in spiked soils by single and combined plants cultivation. J Hazard Mater **177**: 384–389

**Chitwood DH, Guo M, Nogueira FTS, Timmermans MCP** (2007) Establishing leaf polarity: the role of small RNAs and positional signals in the shoot apex. Dev Camb Engl **134**: 813–823

**Choi YE, Harada E, Wada M, Tsuboi H, Morita Y, Kusano T, Sano H** (2001) Detoxification of cadmium in tobacco plants: formation and active excretion of crystals containing cadmium and calcium through trichomes. Planta **213**: 45–50

**Couée I, Sulmon C, Gouesbet G, Amrani AE** (2006) Involvement of soluble sugars in reactive oxygen species balance and responses to oxidative stress in plants. J Exp Bot **57**: 449–459

**Crowe ML, Serizet C, Thareau V, Aubourg S, Rouze P, Hilson P, Beynon J, Weisbeek P, van Hummelen P, Reymond P, et al** (2003) CATMA: a complete Arabidopsis GST database. Nucleic Acids Res **31**: 156–158

**Deng WL, Preston G, Collmer A, Chang CJ, Huang HC** (1998) Characterization of the hrpC and hrpRS operons of Pseudomonas syringae pathovars syringae, tomato, and glycinea and analysis of the ability of hrpF, hrpG, hrcC, hrpT, and hrpV mutants to elicit the hypersensitive response and disease in plants. J Bacteriol **180**: 4523–4531

**Domínguez-Solís JR, López-Martín MC, Ager FJ, Ynsa MD, Romero LC, Gotor C** (2004) Increased cysteine availability is essential for cadmium tolerance and accumulation in Arabidopsis thaliana. Plant Biotechnol J **2**: 469–476

**Edwards R, BrazieHicks M, Dixon DP, Cummins I** (2005) Chemical Manipulation of Antioxidant Defences in Plants. *In* J. A. Callow, ed, Adv. Bot. Res. Academic Press, pp 1–32

**Ellis MH, Dennis ES, Peacock WJ** (1999) Arabidopsis roots and shoots have different mechanisms for hypoxic stress tolerance. Plant Physiol **119**: 57–64

**Furuno S, Foss S, Wild E, Jones KC, Semple KT, Harms H, Wick LY** (2012) Mycelia Promote Active Transport and Spatial Dispersion of Polycyclic Aromatic Hydrocarbons. Environ Sci Technol **46**: 5463–5470

**Furuno S, Päzolt K, Rabe C, Neu TR, Harms H, Wick LY** (2010) Fungal mycelia allow chemotactic dispersal of polycyclic aromatic hydrocarbon-degrading bacteria in water-unsaturated systems. Environ Microbiol **12**: 1391–1398

**Gagnot S, Tamby J-P, Martin-Magniette M-L, Bitton F, Taconnat L, Balzergue S, Aubourg S, Renou J-P, Lecharny A, Brunaud V** (2008) CATdb: a public access to Arabidopsis transcriptome data from the URGV-CATMA platform. Nucleic Acids Res **36**: D986–D990

**Galili G** (1995) Regulation of Lysine and Threonine Synthesis. Plant Cell **7**: 899–906

**Gammon MD, Santella RM** (2008) PAH, genetic susceptibility and breast cancer risk: an update from the Long Island Breast Cancer Study Project. Eur J Cancer Oxf Engl 1990 **44**: 636–640

**Gan S, Lau EV, Ng HK** (2009) Remediation of soils contaminated with polycyclic aromatic hydrocarbons (PAHs). J Hazard Mater **172**: 532–549

**Ge Y, Dudoit S, Speed TP** (2003) Resampling-based multiple testing for microarray data analysis. Test **12**: 1–77

**Göhre V, Jones AME, Sklenář J, Robatzek S, Weber APM** (2012) Molecular crosstalk between PAMP-triggered immunity and photosynthesis. Mol Plant-Microbe Interactions MPMI **25**: 1083–1092

**Guo W-J, Bundithya W, Goldsbrough PB** (2003) Characterization of the Arabidopsis metallothionein gene family: tissue-specific expression and induction during senescence and in response to copper. New Phytol **159**: 369–381

**Gutiérrez-Alcalá G, Gotor C, Meyer AJ, Fricker M, Vega JM, Romero LC** (2000) Glutathione biosynthesis in Arabidopsis trichome cells. Proc Natl Acad Sci **97**: 11108–11113

**Haritash AK, Kaushik CP** (2009) Biodegradation aspects of Polycyclic Aromatic Hydrocarbons (PAHs): A review. J Hazard Mater **169**: 1–15

**Herbette S, Taconnat L, Hugouvieux V, Piette L, Magniette M-LM, Cuine S, Auroy P, Richaud P, Forestier C, Bourguignon J, et al** (2006) Genome-wide transcriptome profiling of the early cadmium response of Arabidopsis roots and shoots. Biochimie **88**: 1751–1765

**Hilson P, Allemeersch J, Altmann T, Aubourg S, Avon A, Beynon J, Bhalerao RP, Bitton F, Caboche M, Cannoot B, et al** (2004) Versatile Gene-Specific Sequence Tags for Arabidopsis Functional Genomics: Transcript Profiling and Reverse Genetics Applications. Genome Res **14**: 2176–2189

**Van Hoewyk D, Takahashi H, Inoue E, Hess A, Tamaoki M, Pilon-Smits EAH** (2008) Transcriptome analyses give insights into selenium-stress responses and selenium tolerance mechanisms in Arabidopsis. Physiol Plant **132**: 236–253

**Jin X-F, Shuai J-J, Peng R-H, Zhu B, Fu X-Y, Tian Y-S, Zhao W, Han H-J, Chen C, Xu J, et al** (2011) Identification of candidate genes involved in responses of Arabidopsis to polychlorinated biphenyls based on microarray analysis. Plant Growth Regul **65**: 127–135

**Katsoyiannis A, Sweetman AJ, Jones KC** (2011) PAH molecular diagnostic ratios applied to atmospheric sources: a critical evaluation using two decades of source inventory and air concentration data from the UK. Environ Sci Technol **45**: 8897–8906

**Keunen E, Peshev D, Vangronsveld J, VAN DEN Ende W, Cuypers A** (2013) Plant sugars are crucial players in the oxidative challenge during abiotic stress: extending the traditional concept. Plant Cell Environ. doi: 10.1111/pce.12061

**Kim MG, Geng X, Lee SY, Mackey D** (2009a) The Pseudomonas syringae type III effector AvrRpm1 induces significant defenses by activating the Arabidopsis nucleotide-binding leucine-rich repeat protein RPS2. Plant J Cell Mol Biol **57**: 645–653

**Kolb M, Harms H** (2000) Metabolism of fluoranthene in different plant cell cultures and intact plants. Environ Toxicol Chem **19**: 1304–1310

**Kvesitadze E, Sadunishvili T, Kvesitadze G** (2009) Mechanisms of Organic Contaminants Uptake and Degradation in Plants. World Acad Sci Eng Technol **55**: 458

**Landa P, Storchova H, Hodek J, Vankova R, Podlipna R, Marsik P, Ovesna J, Vanek T** (2010) Transferases and transporters mediate the detoxification and capacity to tolerate trinitrotoluene in Arabidopsis. Funct Integr Genomics **10**: 547–559

**Larcher W** (2003) Physiological Plant Ecology: Ecophysiology and Stress Physiology of Functional Groups. Springer

**Lichtenthaler H, Wellburn A** (1983) Determinations of total carotenoids and chlorophylls a and b of leaf extracts indifferent solvents. Biochem Soc Trans **603**: 591–592

**Liu H, Weisman D, Ye Y, Cui B, Huang Y, Colón-Carmona A, Wang Z** (2009) An oxidative stress response to polycyclic aromatic hydrocarbon exposure is rapid and complex in Arabidopsis thaliana. Plant Sci **176**: 375 – 382

**Luch A** (2005) The carcinogenic effects of polycyclic aromatic hydrocarbons. Imperial College Press, Hackensack, NJ

**Lurin C, Andrés C, Aubourg S, Bellaoui M, Bitton F, Bruyère C, Caboche M, Debast C, Gualberto J, Hoffmann B, et al** (2004) Genome-wide analysis of Arabidopsis pentatricopeptide repeat proteins reveals their essential role in organelle biogenesis. Plant Cell **16**: 2089–2103

**Mitsch WJ** (2012) What is ecological engineering? Ecol Eng **45**: 5–12

**Panz K, Miksch K** (2012) Phytoremediation of explosives (TNT, RDX, HMX) by wild-type and transgenic plants. J Environ Manage **113**: 85–92

**Paul MJ, Pellny TK** (2003) Carbon metabolite feedback regulation of leaf photosynthesis and development. J Exp Bot **54**: 539–547

**Provart T. and Z** (2003) A Browser-based Functional Classification SuperViewer for Arabidopsis Genomics. Curr Comput Mol Biol 271–272

**Pucciariello C, Parlanti S, Banti V, Novi G, Perata P** (2012) Reactive oxygen species-driven transcription in Arabidopsis under oxygen deprivation. Plant Physiol **159**: 184–196

**Ramel F, Sulmon C, Bogard M, Couée I, Gouesbet G** (2009) Differential patterns of reactive oxygen species and antioxidative mechanisms during atrazine injury and sucrose-induced tolerance in Arabidopsis thaliana plantlets. BMC Plant Biol **9**: 28

**Ramel F, Sulmon C, Cabello-Hurtado F, Taconnat L, Martin-Magniette M-L, Renou J-P, Amrani AE, Couée I, Gouesbet G** (2007) Genome-wide interacting effects of sucrose and herbicide-mediated stress in Arabidopsis thaliana: novel insights into atrazine toxicity and sucrose-induced tolerance. BMC Genomics **8**: 450

**Ramel F, Sulmon C, Serra A-A, Gouesbet G, Couée I** (2012) Xenobiotic sensing and signalling in higher plants. J Exp Bot **63**: 3999–4014

**Rozen S, Skaletsky H** (2000) Primer3 on the WWW for general users and for biologist programmers. Methods Mol Biol Clifton NJ **132**: 365–386

**Rylott EL, Budarina MV, Barker A, Lorenz A, Strand SE, Bruce NC** (2011) Engineering plants for the phytoremediation of RDX in the presence of the co-contaminating explosive TNT. New Phytol **192**: 405–413

**Sandermann Jr. H** (1992) Plant metabolism of xenobiotics. Trends Biochem Sci **17**: 82–84

**Sandermann Jr. H, Scheel D, Trenck T v. d.** (1984) Use of plant cell cultures to study the metabolism of environmental chemicals. Ecotoxicol Environ Saf **8**: 167–182

**Sarret G, Harada E, Choi Y-E, Isaure M-P, Geoffroy N, Fakra S, Marcus MA, Birschwilks M, Clemens S, Manceau A** (2006) Trichomes of Tobacco Excrete Zinc as Zinc-Substituted Calcium Carbonate and Other Zinc-Containing Compounds. Plant Physiol **141**: 1021–1034

**Sattler SE, Mene-Saffrane L, Farmer EE, Krischke M, Mueller MJ, DellaPenna D** (2006) Nonenzymatic Lipid Peroxidation Reprograms Gene Expression and Activates Defense Markers in Arabidopsis Tocopherol-Deficient Mutants. Plant Cell **18**: 3706–3720

**Schamfuß S, Neu TR, van der Meer JR, Tecon R, Harms H, Wick LY** (2013b) Impact of Mycelia on the Accessibility of Fluorene to PAH-Degrading Bacteria. Environ Sci Technol **47**: 6908–6915

**Schreiber R, Altenburger R, Paschke A, Küster E** (2008) How to deal with lipophilic and volatile organic substances in microtiter plate assays. Environ Toxicol Chem SETAC **27**: 1676–1682

**Shim D, Kim S, Choi Y-I, Song W-Y, Park J, Youk ES, Jeong S-C, Martinoia E, Noh E-W, Lee Y** (2013) Transgenic poplar trees expressing yeast cadmium factor 1 exhibit the characteristics necessary for the phytoremediation of mine tailing soil. Chemosphere **90**: 1478–1486

**Sitaras IE, Bakeas EB, Siskos PA** (2004) Gas/particle partitioning of seven volatile polycyclic aromatic hydrocarbons in a heavy traffic urban area. Sci Total Environ **327**: 249–264

**Skipsey M, Knight KM, Brazier-Hicks M, Dixon DP, Steel PG, Edwards R** (2011) Xenobiotic Responsiveness of Arabidopsis thaliana to a Chemical Series Derived from a Herbicide Safener. J Biol Chem **286**: 32268–32276

**Ana Sofia Duque AMDA** (2013) Abiotic Stress Responses in Plants: Unraveling the Complexity of Genes and Networks to Survive. doi: 10.5772/52779

**Sulmon C, Gouesbet G, Binet F, Martin-Laurent F, El Amrani A, Couée I** (2007a) Sucrose amendment enhances phytoaccumulation of the herbicide atrazine in Arabidopsis thaliana. Environ Pollut **145**: 507–515

**Sulmon C, Gouesbet G, Couée I, Amrani AE** (2004) Sugar-induced tolerance to atrazine in Arabidopsis seedlings: interacting effects of atrazine and soluble sugars on psbA mRNA and D1 protein levels. Plant Sci **167**: 913–923

**Sulmon C, Gouesbet G, El Amrani A, Couee I** (2007b) Involvement of the ethylene-signalling pathway in sugar-induced tolerance to the herbicide atrazine in Arabidopsis thaliana seedlings. J Plant Physiol **164**: 1083–1092

**team RDC** (2013) R: a language and environment for statistical computing. R foundation for statistical computing, Vienna, Austria

**Verslues PE, Zhu J-K** (2005) Before and beyond ABA: upstream sensing and internal signals that determine ABA accumulation and response under abiotic stress. Biochem Soc Trans **33**: 375–379

**Wang P, Song C-P** (2008) Guard-cell signalling for hydrogen peroxide and abscisic acid. New Phytol **178**: 703–718

**Weisman D, Alkio M, Colón-Carmona A** (2010b) Transcriptional responses to polycyclic aromatic hydrocarbon-induced stress in Arabidopsis thaliana reveal the involvement of hormone and defense signaling pathways. BMC Plant Biol **10**: 59

**Wu J, Omokawa H, Hatzios KK** (1996) GlutathioneS-Transferase Activity in Unsafened and Fenclorim-Safened Rice (Oryza sativa). Pestic Biochem Physiol **54**: 220–229

**Xu J, Su Z-H, Chen C, Han H-J, Zhu B, Fu X-Y, Zhao W, Jin X-F, Wu A-Z, Yao Q-H** (2012) Stress responses to phenol in Arabidopsis and transcriptional changes revealed by microarray analysis. Planta **235**: 399–410

**Zhan X-H, Ma H-L, Zhou L-X, Liang J-R, Jiang T-H, Xu G-H** (2010) Accumulation of phenanthrene by roots of intact wheat (Triticum acstivnm L.) seedlings: passive or active uptake? BMC Plant Biol **10**: 52

**Zrenner R, Stitt M, Sonnewald U, Boldt R** (2006) Pyrimidine and purine biosynthesis and degradation in plants. Annu Rev Plant Biol **57**: 805–836

**Zurbriggen MD, Carrillo N, Hajirezaei M-R** (2010) ROS signaling in the hypersensitive response. Plant Signal Behav **5**: 393–396

# Chapitre 3 : **Etude des mécanismes moléculaires et métabolique de protection de saccharose en condition de stress provoqué par le phénanthrène**

**Préambule**

Dans le chapitre précédant, nous avons vu que le phénanthrène causait rapidement des dommages sévères aux cellules, ce qui se traduit par des modifications transcriptionnelles et métaboliques.

Dans cette partie du manuscrit, nous avons utilisé les propriétés du saccharose, qui est une molécule aux fonctions multiples. Il est à la fois un métabolite important, une molécule signal et il a aussi des fonctions de protection face aux stress abiotiques. L'objectif de cette partie de mon travail a été de voir si le saccharose a un effet protecteur face à l'effet nocif du phénanthrène, et quelles sont éventuellement les processus cellulaires qui sont à l'origine de cette tolérance induite.

Dans un premier temps, une étude à long terme sur l'impact du saccharose sur le développement d'*Arabidopsis thaliana* en présence de phénanthrène a permis de montrer l'effet protecteur du saccharose. Une étude de l'effet du saccharose au niveau du métabolome et du transcriptome a montré que, même en condition de stress abiotique, les plantes, ici Arabidopsis, sont capables de prélever le sucre de leur milieu de culture et de le métaboliser rapidement après quelques heures, compensant ainsi les effets du phénanthrène sur leur métabolisme primaire.

D'autre part, de nombreuses études, notamment celles de Ramel et al. (2004 et 2006), ont mis en évidence le rôle protecteur du saccharose face aux dérivés actifs de l'oxygène (ROS). Il est donc intéressant de voir comment le saccharose régule le système antioxydant en condition de stress causé par le phénanthrène. De plus, afin de mieux cerner cet effet protecteur, une étude des gènes liés à la réponse à un stress est importante.

Enfin, le modèle de détoxification dit du « green-liver » semble pouvoir se transposer pour la détoxification des HAPs. Il est donc important d'étudier l'action du saccharose sur ces gènes de détoxification.

**Title:** Sucrose mitigated phenanthrene-induced stress and reconfigured wide genes transcription and metabolome profiles in *Arabidopsis thaliana*

**Authors:**

Anne-Sophie Dumas[1]

Richard Berthomé[2]

Emilie Jardet[3]

Abdelhak El Amrani[1]

**Institutions:**

[1]Université de Rennes1, CNRS UMR 6553, Ecosystèmes-Biodiversité-Evolution, 35042 Rennes cedex, France.

[2]INRA, UMR 1165, Unité de Recherche en Génomique Végétale (URGV), CNRS, ERL 8196, UEVE, 91057, Evry cedex, France.

[3]Université de Rennes 1, Géosciences Rennes, UMR6118, Campus de Beaulieu, 35042 Rennes cedex

**Key words:** transcriptomic, Arabidopsis, stress, phenanthrene, sucrose

Corresponding author**:** Abdelhak El Amrani (abdelhak.elamrani@uni-rennes1.fr)

**Abstract:**

Plants have developed strategies to adapt quickly to environmental changes. However, the regulation of these adaptive responses and coordination of signals involved remains poorly understood for many abiotic stresses. Indeed, signalling molecules play a central role in the perception of environmental stimuli and may participate in adaption of the plants behaviour to environmental cues. Sucrose is the major transport carbohydrate in higher plants, in addition to its metabolic role, recent investigations suggested that sucrose impact the plasticity of plant development by controlling gene expression. It was also suggested to play a role as scavenger and signalling molecule. In this paper we showed that sucrose mitigate phenanthrene-induced plant response. Indeed, sucrose allowed growth and chlorophyll accumulation in the presence of high phenanthrene concentrations, whereas *Arabidopsis* development was blocked and seedlings were unable to accumulate chlorophyll without sucrose. To decipher the earlier molecular changes that seem to be involved in sucrose tolerance to phenanthrene, wide transcriptional genes analysis and targeted metabolic profiling were carried out. We showed that sucrose induced plant response was associated with a deep reconfiguration of both genes expression and metabolites accumulation. Results suggest that sucrose, through its different functions, allowed the plant to sustain the primary metabolism and to overcome the phenanthrene-induced injuries.

## 1. Introduction

Higher plants are sessile organisms; they have to regulate their physiology and genes expression to adapt to biotic and abiotic stresses. Environmental pollution constitutes a new world wide ecological problem and may affect plant development.

Among the main pollutants, Polycyclic Aromatic Hydrocarbons (PAHs) are ubiquitous organic pollutant found in all the compartments of the environment. They are mainly considered as byproducts of anthropogenic activities with the incomplete combustion of petroleum products for example. This pollutant represents a great hazard for human health, creating the necessity to remediate contaminated environment.

Traditional clean-up techniques like incineration or physical-chemical processes represent a high cost and could also impact the environment. Indeed, development of green technologies using natural capacity of leaving organisms to store and degrade pollutants led to the creation of biological remediation techniques such as bioremediation and phytoremediation. A model of plant detoxification system, inspired by the detoxification system of the mammalian liver, was proposed by Sandermann (1992) and named the “green liver model”. In other hand, Edwards et al. (2005) defined the xenome as the whole expressed genome involved in the detection, signaling, transformation and transport of xenobiotics. While little is known about the sensing and transport mechanisms, the “green liver” is a molecular model of the transformation and transport. Several multigenic enzymes families are involved in these processes: cytochrome P450 (CYP) for the activation step, Glutathione-S-transferase (GST) and UDP-glucuronosyltransferase(UGT) for the conjugation step and ATP-binding cassette transporter (ABC transporter) for the compartmentalization step.

Phytoremediation is the utilization of plants and their associated micro-organisms to decontaminate a polluted environment. It is of high interest to get a better understanding on how plants cope with the presence of organic pollutants s in their environment. In-vitro studies, using the model plant *Arabidopsis thaliana*, revealed that phenanthrene, used as a model molecule of PAHs, cause several damages in plants. After a long-term (14 to 30 days) phenanthrene treatment, *Arabidopsis* presents a decrease in shoots development, roots length, chlorophyll content in a dose dependent way (Alkio et al., 2005; Liu et al., 2009).

Phenanthrene induced, like several abiotic stresses, an accumulation of reactive oxygen species (ROS). It also increased the activity of several anti-oxidant enzymes like the superoxide dismutase (SOD), the peroxide dismutase (POD) and the ascorbate peroxidase (APX) (Liu et al., 2009). These biochemical data corroborated with a transcriptomic analysis carried out in phenanthrene containing medium (Weisman et al., 2010a) which revealed that phenanthrene induced significant change in genes expression involved ROS scavenging pathways.

Sucrose is considered as the major form of transport and the main product of photosynthesis. It plays a pivotal role in plants responses to abiotic stresses, and acts not only as a metabolite, but has also signaling properties (Koch, 2004; Rosa et al., 2009; Wind et al., 2010). Several studies (Price et al., 2004; Thum et al., 2004) showed that sugars modulate a broad range of genes involved in central cellular processes: carbohydrate and nitrogen metabolism, signal transduction, metabolites transport and stress responses. In addition disaccharides such as sucrose, raffinose family polysaccharides (RFO) and fructans are water-soluble carbohydrates known to be involved in plant stress response (Valluru and Ende, 2008; Rosa et al., 2009).

It has been shown that under different abiotic stresses, soluble sugars accumulate in response to the oxidative stress. They are potentially involved in the modulation of oxidative stress and might interact with ROS signaling pathway (Bolouri-Moghaddam et al., 2010). Soluble sugars have a central position in the cellular redox balance system: they are at the junction of photosynthesis, mitochondrial respiration and the beta-oxidation of fatty acids, pathways that lead to ROS production (Couée et al., 2006).

An emerging concept suggested that sugars act as antioxidants (Ende and Valluru, 2009; Keunen et al., 2013). In vitro studies have shown that the *in-vivo* antioxidant capacity of soluble sugars have been underestimated: among other sugars, sucrose have been suggested to function as an antioxidant (Ende and Valluru, 2009; Bolouri-Moghaddam et al., 2010; Keunen et al., 2013).

Sucrose has been shown to increase tolerance to a variety of abiotic stress such anoxia (Loreti et al., 2005), herbice induced stress. Indeed, plants grown on sucrose showed increased tolerance to the herbicide (Sulmon et al., 2006; Ramel et al., 2007; Ramel et al.,

2009). Hence, Sucrose enhances protection against reactive oxygen species (ROS) through the activation of specific ROS scavenging systems.

The aim of this work was to examine if sucrose play a protective effect when *Arabidopsis* was challenged with phenanthrene stressed condition, and to elucidate the early molecular events involved in the presence of exogenous sucrose. Transcriptional profiling and targeted metabolomic approaches were used to decipher the main signaling and metabolic pathways involved in sucrose induced tolerance to phenanthrene injury.

## 2. Material and methods

### 2.1. Plant material and growth conditions

Seeds of *Arabidopsis thaliana,* ecotype Columbia-0 (Col-0) were used in all experiments. Seeds were surface sterilized and sown on Petri dishes containing half-strength Murashige and Skoog (1962) medium, supplemented with sugar (sucrose, glucose or mannitol), phenanthrene and dimethylsulfoxide (DMSO).

As phenanthrene solubility in water is low, a stock solution of phenanthrene in DMSO was prepared at the concentration of 700mM and used to adapt the final concentration in the culture medium. DMSO was added in the same amount in all the conditions of each experiment. So that phenanthrene dose was the only parameter changing.

Petri dishes were placed at 4°C during 48h in order to break dormancy and to homogenize germination. Plants were grown at 22°C under a 16h-light period at approximately 5000lux.

### 2.2. Measurement of plant growth and development

For root measurement and determination of the fresh weight, plants were grown on MS/2 solid medium supplemented with 88mM of sugar (mannitol, sucrose or glucose), phenanthrene and DMSO. Phenanthrene was added from a 700mM stock solution of phenanthrene in DMSO (as a solvent). DMSO was added in order to have the same amount of the solvent in all conditions.

Fresh weight was determined after 22 days of growth for plants grown on MS/ supplemented with mannitol or sucrose at 88mM and with 0, 50, 100, 200 and 500µM of phenanthrene or with DMSO alone. Plantlets were grown on circle dishes horizontally for a better development and aerial parts were separated and harvested. For the two biological replicates, for each condition, 6 samples with 3 plantlets were harvested.

For a better observation of the primary root, plants were cultivated on Petri dishes vertically. Roots were measured after 14 days of growth on digital photographs using ImageJ v 1.45s software (Abramoff et al., 2004). For each condition, 30 independent plants were measured.

Results represent the mean with the standard error (SE). Statistical analyses were carried on using the Wilcoxon test by R software (team RDC, 2013).

### 2.3. Fluorescence microscopy

Microscopic observations were performed at the Imagif platform, in the Cellular Biology Pole (CNRS, Gif-sur-Yvette, France).

*Arabidopsis* plantlets used in this experiment were grown on half-strength MS medium for 15 days, then transferred on half-strength MS medium supplemented with sucrose at 88mM containing 200µM of phenanthrene (prepared from a 700mM solution of phenanthrene in DMSO) or the same volume of DMSO. In order to facilitate the transfer, plants were grown vertically. A sterile and transparent plastic film was added to protect the shoot, so only roots are in contact with the contaminated medium.

After 5 days of phenanthrene treatment, leaves and roots were observed with a Zeiss LSM510 META microscope under UV-light (excitation 364nm and acquisition with 32

channels between 362nm and 704nm). Data were acquired using Zen2008 software developed by Zeiss (Germany).

### 2.4. Phenanthrene quantification

Plants used for phenanthrene quantification were grown for 15 days on MS/2 then transferred in liquid medium supplemented with 0mM or 88mM of sucrose and containing 200µM of phenanthrene.

After 24h of incubation, plants were harvested and rinsed with water, absolute ethanol and then water. 3 samples of 20 plantlets pooled were taken. Plants samples were dried then pounded and weighted.

Phenanthrene was extracted from plants tissues by an accelerated solvent extractor (ASE 200, Dionex) with dichloromethane at 100°C and under a pressure of 100bar. Extracts were dried under a gentle flux of nitrogen, and finally weight for quantification using internal standard. One microliter of the extract was injected onto a Shimadzu QP2010+MS gas chromatograph/mass spectrometer (Shimadzu, Tokyo, Japan). The injector used was in splitless mode and maintained at a temperature of 310°C. The chromatographic separation was performed on a fused silica SLB-5 ms capillary column (from Supelco, length = 60 m, diameter = 0.25 mm, film thickness = 0.25µm) under the following temperature program: 70°C (held for 1 min) to 130 at 15°C/min, then 130 to 300°C (held for 15 min) at 3°C/min. The helium flow was maintained at 1mL/min. The chromatograph was coupled to the mass spectrometer by a transfer line heated to 250°C. The analyses were performed in SIM mode (selective ion monitoring). Quantification was based on the internal standard phenanthrene-d10, which was added to the sample post-extraction and prior to the analysis by GC-MS.

### 2.5. Targeted analysis of metabolites

Analysis of metabolites levels were performed by the CORSAIRE platform (Biogenouest, INRA UMR 1359, Le Rheu, France).

*Arabidopsis* plants used for this analysis were grown on half-strength MS medium for 15 days, then transferred on liquid half-strength MS medium supplemented with 0 or 88mM of sucrose and containing 200µM of phenanthrene (prepared from a 700mM solution of phenanthrene in DMSO) or the same volume of DMSO.

After 24 hours of incubation, plants were harvested, frost in liquid nitrogen, lyophilized and ground. A total of 10mg of dry plant material was extracted in 500µL of extraction solvent and 250µL of chloroform. The extraction solvent is composed of 5% of methanol and 95% of beta amino benzoic acid (10mM) – adonitol (20mM) concentrated solution. Samples were shaken 10 min at room temperature then 500µL of ultra pure water were added. All samples were vortexed for 30s then centrifugated for 5 min at 12000g at 15°C. The entire liquid phase is transferred to a new tube. For amino acids analysis, 50µL of the extract was dried under vacuum and 50µL of water were added. Samples are derivated using the AccQTag method (Waters) and analyzed by Ultra Performance Liquid Chromatography (UPLC, Waters). For sugars, organic acids, alcohol and ammonium quantification, 50µL of the extract supplemented with 50µL of internal standard are dried under vacuum. 50µL of methoxamine in pyridine (concentration 20mg/mL) were added to the dried samples which are incubated 90min at 30°C. 50µL of MSTFA (N-Methyl-N-(trimethylsilyl)trifluoroacetamide) are added to each sample which are incubated for 30min at 37°C and than analyzed by GC-MS.

### 2.6. Transcriptome studies

Transcriptome analysis was carried out at the Research Unit in Plant Genomics (INRA, Evry, France), using the CATMA version 5 microarrayscontaining 31776 specific gene tags corresponding to 22,089 genes from *Arabidopsis* (Crowe et al., 2003; Hilson et al., 2004).

*Arabidopsis thaliana* ecotype Columbia (Col 0) was grown *in-vitro* for 15 days on solid half-strength Murashige and Skoog (MS) medium. Plantlets at stage 1.04 (Boyes et al., 2001)

were then transferred on liquid half-strength MS medium containing 0.2mM of phenanthrene (prepared from a 700mM solution of phenanthrene in DMSO) or the same amount of phenanthrene and 3% sucrose. Total RNA extractions of two independent replicates were performed using the Qiagen RNAeasy plant minikit according to the manufacturer's instructions. Each biological replicates content phenanthrene-treated and phenanthrene plus sucrose treated plants. Each sample corresponding to 30 plants pooled were harvested after 30 min, 2h and 8h of incubation. For all comparisons performed, the experiment was done using the dye-switch technique. Lurin et al. (2004) described the protocol used for the labelling of antisense amplified mRNA with Cy3-dUTP and Cy5-dUTP (Perkins-Elmer-NEN Life science products), the hybridization to the slides and the scanning.

### 2.7. Statistical Analysis of microarray data

The Bioinformatic and Predictive Genomics group at the Research Unit in Plants Genomics (Evry, France), with whom the experiments were designed, developed specific statistics to analyse CATMA hybridations. For each array, the raw data include the logarithm of median feature pixel intensity (in log base 2) at wavelengths of 635 nm (red) and 532 nm (green). No background was subtracted. The normalization method used was described by (Lurin et al., 2004). Differentially expressed genes were determined by performing a paired t-test on the log ratios averaged on the dye switch. A trimmed variance was calculated from spots that did not display extreme variance. The raw P values were adjusted by the Bonferroni method, which controls the family-wise error rate (with a type I error equal to 5%). We also adjusted the raw P values to control a false discovery rate using Benjamini-Yetkutieli at a level of 1%. Nonetheless, in the CATMA analysis pipeline, family-wise error rate proved to be the best solution to balance the estimated number of false positives and false negatives (Ge et al., 2003). As described by Gagnot et al. (2008), when the Bonferroni P value was lower than 0.05, the gene was declared differentially expressed.

### 2.8. Biological pathways enrichment

Biological pathways significantly over-represented in the list of differentially expressed genes were identified with the classification superviewer tool of the university of Toronto website (http://bar.utoronto.ca/ntools/cgi-bin/ntools_classification_superviewer.cgi) using MAPMAN classification (Provart T., 2003a) as a source.

### 2.9. Microarrays data validation by quantitative Real-Time PCR (qRT-PCR)

The qRT-PCR validation was carried on 15 genes being found differentially expressed in the microarrays experiments.

Primers were designed using the online software Primers3 ((Rozen and Skaletsky, 2000), http://frodo.wi.mit.edu/, optimal temperature 60°C, Supplemental Table I).

The primer pairs were first tested on a dilution series of genomic DNA (5, 0.5, 0.05, and 0.005ng) to generate a standard curve and assess their PCR efficiency, which ranged between 90% and 110%. RT was performed on 1µg of total RNA with oligo(dT) primer (18-mer) and the SuperScript II RNase H- reverse transcriptase according to the manufacturer's instructions (Invitrogen). In every run, at least three replicates PCRs were done for each cDNAs. For each gene investigated using qPCR, a dilution series covering 3 orders of magnitude (1, 1/10 and 1/100) of the cDNA stock solution was prepared. Three replicates of each of the three standards were used in qPCR experiment together with three no-template controls. qPCR was performed in 5□L, with 0.5 □L of RT reaction (1/100 dilution), 900 nM final concentration of each primer pair, and 2,5µL of MESA GREEN qPCR MasterMix Plus for SYBR® Assay (Eurogentec) ). Corresponding minus-RT controls were performed with each primer pair. All reactions were performed with the CFX384 Touch™ Real-Time PCR Detection System (Bio-Rad) as follows: 95°C for 5 min; 40x95°C for 10 s and 60°C for 30 s ; and a dissociation step to discriminate primer dimers from the PCR product. Using CFX Manager™ Software version 3.0 provided by the manufacturer, the optimal cycle threshold (Ct) was determined from the dilution series, with the raw expression data derived. Six housekeeping genes were assessed in this experiment, and the two best control genes, consistently expressed, were selected to calculate the average normalization factor: AT4G13615 and

AT5G21090 for each sample pair. Normalized (Norm) ΔCt for each differentially expressed gene was calculated as following: Norm ΔCt = - (rawΔCt - Norm factor). Microarray data from this article were deposited at Gene Expression Omnibus (http://www.ncbi.nlm.nih.gov/geo/), accession no. GSE48181) and at CATdb (http://urgv.evry.inra.fr/CATdb/; Project: AU10-04_phytoremediation) according to the "Minimum Information About a Microarray Experiment" standards.

## 3. Results and discussion

### 3.1. Sucrose induced tolerance to phenanthrene injury

Sucrose was shown to protect the plant against abiotic stresses such anoxia and herbice injury (Sulmon et al., 2004; Loreti et al., 2005). However no data were available about its effect on stresses induced by organic pollutants such as PAHs. In this work, we studied the incidence of sucrose implementation on plant response to phenanthrene exposition.

*Arabidopsis* plants were grown on media containing 3% w/v of sucrose (=88mM), then compared to control plants grown in the same culture medium supplemented with 88mM of mannitol, used as previously described as an osmoticum (Borsani et al., 2001; Sulmon et al., 2004). In these conditions, plants were submitted to a phenanthrene treatment at different concentrations ranging from 0µM to 400µM. Shoots fresh weight was measured as marker of development to assess sucrose effects. Control plants, grown on mannitol supplemented medium, showed a significant reduction of growth development even at low phenanthrene concentration (50 µm) (Fig.1 and Fig.2), and reduction of the number and leaves surface. 70% of plants failed to accumulate chlorophyll (Fig.1). In parallel, when phenanthrene increased up to 100 µm, 100% of plants showed high toxicity symptoms (chlorosis) and are unable to initiate first leaves are unable to initiate first leaves development and chlorophyll synthesis. On the contrary, plants growing on sucrose supplemented media showed a significantly highest fresh weight compared to plants grown on mannitol-supplemented media whatever the phenanthrene concentration applied, and even at high phenanthrene

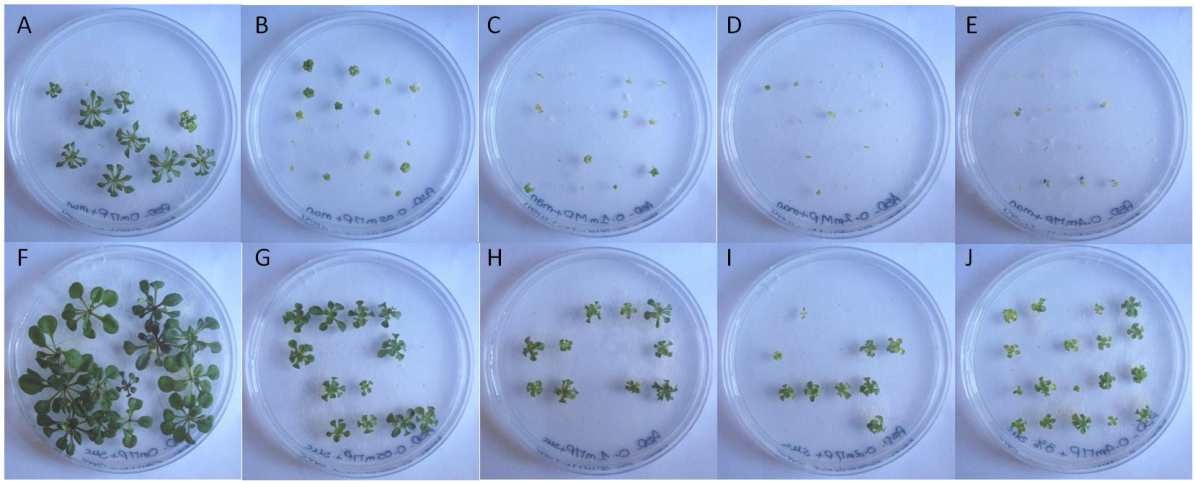


**Figure 1: Sucrose mitigated phenanthrene induced stress.**
22 days old plantlets were grown on half MS medium. Phenanthrene was supplemented at 0µM (A, F), 50µM (B, G), 100µM (C, H), 200µM (D, I) and 400µM (E, J). Control plants (A to E) were grown on medium supplemented with mannitol as an osmoticum, plants from pictures F to J grown on sucrose supplemented media.

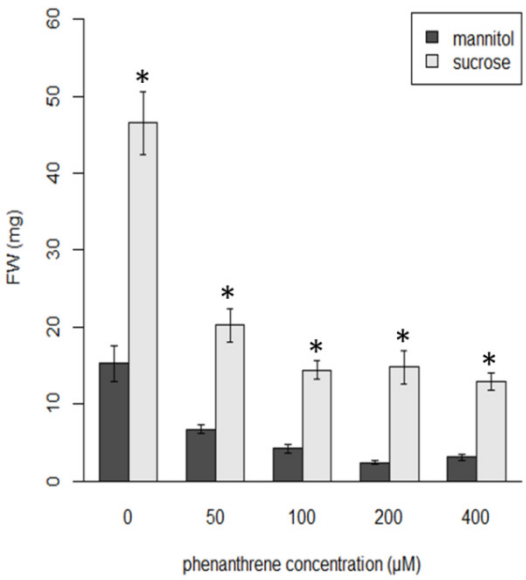


**Figure 2: Fresh weight of 22-day-old plants following a phenanthrene treatment** (0µM, 50µM, 100µM, 200µM and 400µM) in a growth medium supplemented with sucrose or mannitol (used as osmoticum). * statistical difference between sucrose and mannitol treatments (p-value≤0.05).

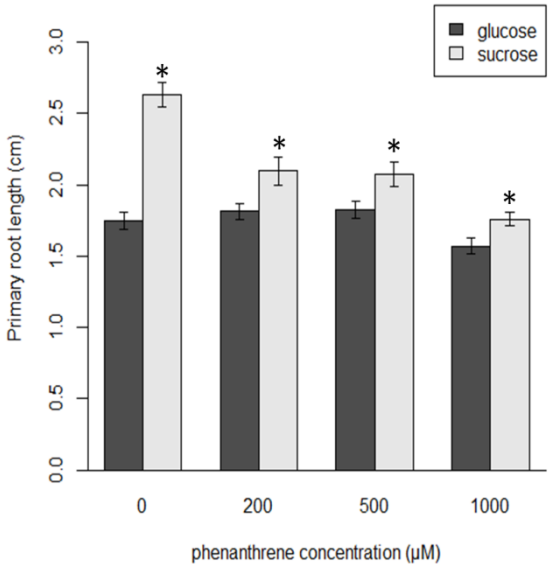


**Figure 3: Primary root length of 14-day-old plantlets after a phenanthrene treatment** (grown on 0µM, 200µM, 500µM and 1000µM respectively) in a growth-medium supplemented with 88mM of sucrose or glucose. * statistical difference between sucrose and glucose treatments (p-value≤0.05).

concentration (400 µm) plants maintained growth and developed leaves and chlorophyll biosynthesis.

In order to assess the specific sucrose effect, to evaluate to what extend sucrose protects plants against high doses of phenanthrene and to better understand the role of sucrose in plant development under a phenanthrene-induced stress, a comparison has been carried out with plants grown on media supplement with glucose. Both molecules were exogenously added to the growing medium at identical concentration (88mM) under high content of phenanthrene ranging from 200µM to 1000µM. In this experiment, we used primary root elongation as marker, since this later was highly sensitive to abiotic stresses (Fig. 3) (Pasternak et al., 2005). Statistical analysis of results obtained revealed that sucrose showed a pronounced effect in high phenanthrene supplemented medium, even if glucose mitigated the phenanthrene inhibition of the primary roots this protection was at a lesser extent. This observation corroborates with several already published data about the specific effect of sucrose. Moreover, figure 2 showed that in the presence of exogenous sucrose, no significant differences were observed in the fresh weigh between 200µM and 400µM doses. These results suggested that, even for lethal doses of phenanthrene, sucrose protected plants against the toxic effects of this molecule.

Solfanelli *et al*, (2006) carried out transcriptome analysis and showed that sucrose exhibited specific induction of the anthocyanin biosynthetic pathway. In other hand, emerging ideas suggested that sucrose impacts also plant tolerance to environmental stress. Loreti et al (2010) showed exogenous sucrose greatly enhances anoxia tolerance of *Arabidopsis* seedlings but glucose did not substitute for sucrose in this process. Sucrose exhibited similar effect when *Arabidopsis* was challenged with atrazine. In these conditions sucrose induced the ROS scavenging system and allowed plant development and growth (Sulmon et al., 2006; Ramel et al., 2007).

Hence, Barker et al. (2000) proposed that sucrose transporter SUT2 act as a sucrose sensor, but this assumption, has not been demonstrated yet. Since the elucidation of sucrose-specific signaling pathway is difficult to study as sucrose is readily hydrolyzed into hexoses. However, functional genomics and omics approaches should give new insight to

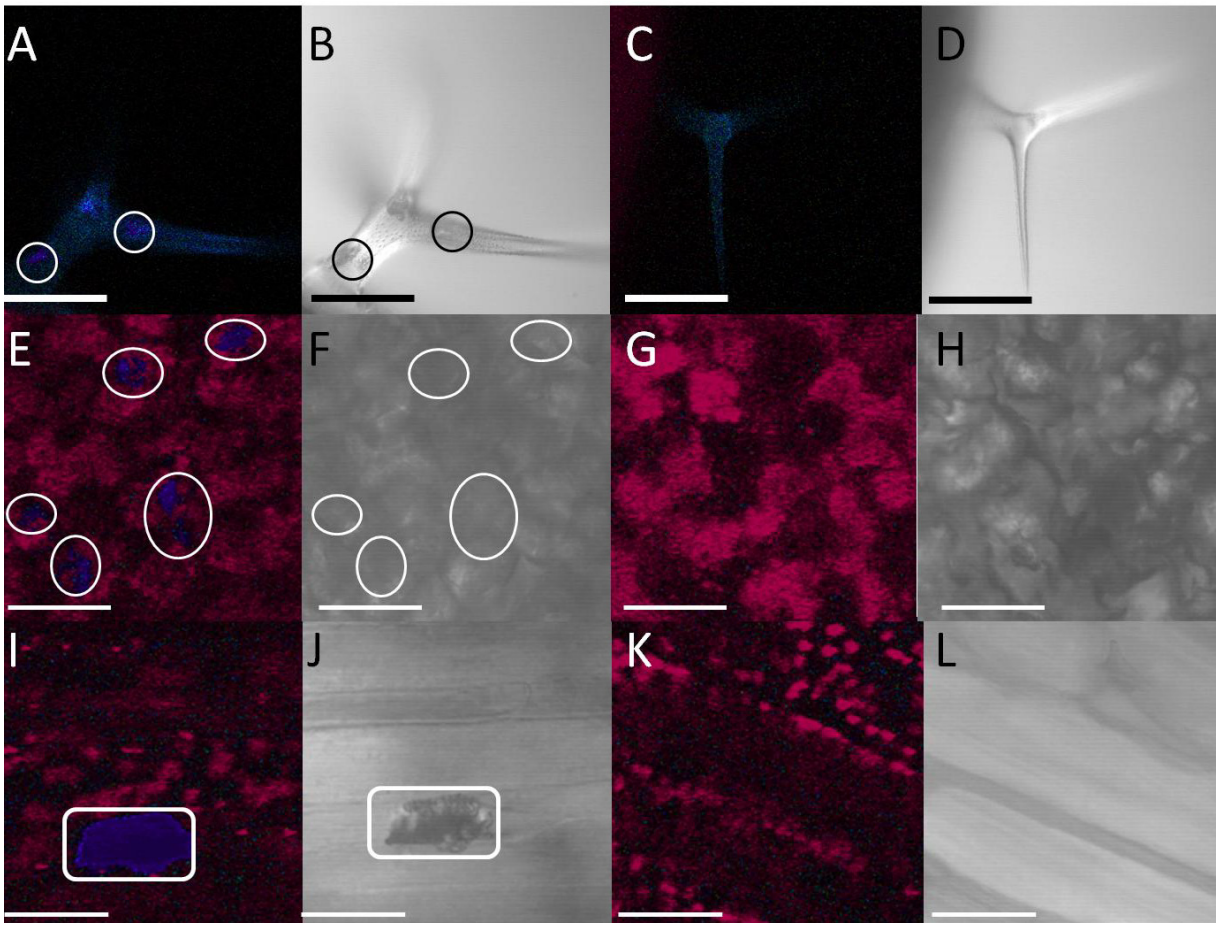


**<u>Figure 4</u>: Cellular and histological localization of free phenanthrene**.
Plants were treated for 6 days with 0.2mM of phenanthrene + sucrose (A, B, E, F, I, J and M) or DMSO + sucrose as control (C, D, G, H, K and L). Pictures A to D are an observation of the trichomes, E to H of the underside of the leaves and I to L of the vein from the underside of the leaf. 2 consecutives photos (A-B, C-D …) represent the same area. A, C, E, G, I, K and M are observations made under UV light and B, D, F, H, J and L with transmission. Circles show the localization of phenanthrene. Bar scales represent 100µm for pictures A to D and 50µM for pictures E to L.

understand how this important molecule controls plant development and tolerance to environmental constraints.

### 3.2. Cellular and histological localization of phenanthrene under protective sucrose condition

It is of high interest to understand how sucrose modulates the phenanthrene accumulation in plant cells and tissues. In this paper, we used fluorescence properties of free phenanthrene under UV light (Dabestani and Ivanov, 1999) for *in-planta* histological localization. Indeed, after an excitation at 564nm, a specific signal was emitted between 450-500nm, corresponding to phenanthrene fluorescence.

In sucrose supplemented medium, confocal microscopy analysis showed accumulation of free phenanthrene in the trichome (Fig.4A) and in the abaxial leaf surface (Fig.4E). In addition, sucrose allows the accumulation in vascular tissues (Fig. 4I). This last result was different from those published in Dumas et *al*. (paper in preparation, 2013). Which showed that when plants were grown on sucrose free medium the phenanthrene accumulated only in trichome and abaxial cells of *Arabidopsis* leaves.

These results corroborates data published by Alkio et al. (2005), where plant treated with phenanthrene during 21 days on a sucrose containing medium showed local necrosis similar to hypersensitive responses. Authors also found that the frequency and size of these lesions were dose-dependent on the phenanthrene concentration in the medium.

These results suggested that sucrose triggered discrete changes in the cellular and tissular transport and/or accumulation of the free phenanthrene, as this later was also localized in vascular tissues.

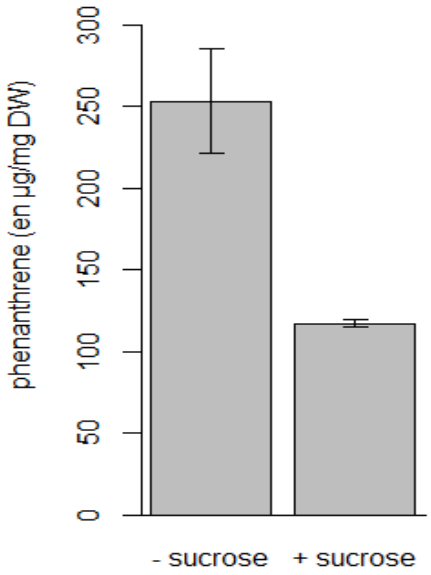


**<u>Figure 5:</u> Phenanthrene concentration of 16-day-old plantlets** incubated for 24h with 200µM of phenanthrene, supplemented with or without sucrose in the growth medium.

In order to quantify phenanthrene accumulation in plant tissues, 16 days old plantlets were transferred to liquid medium containing phenanthrene alone (control) or phenanthrene plus sucrose. After 24h of incubation, phenanthrene quantification was carried out. Surprisingly, plants grown on sucrose supplemented medium accumulated 50% less phenanthrene compared to plants grown on a sugar free medium (Fig. 5). This observation suggested that sucrose induced either new gene-network involved in phenanthrene metabolization, transport or likely a complete degradation, which were silenced when phenanthrene was present alone.

All these data taken together suggested that sucrose reconfigure cellular and molecular processes involved in storage, metabolization and/or tolerance strategy in phenanthrene-induced stress condition.

In several other organisms such bacteria and fungus, genes such as P-450 have been demonstrated to be involved in complete phenanthrene degradation (Bezalel et al., 1997; Syed et al., 2010). However, until today, data demonstrating that plants are able to degrade phenanthrene are still missing. Meanwhile, genome sequencing programs revealed a myriad of genes coding for proteins that could be involved in detoxification of xenobiotics, such phenanthrene. These processes involved several genes family known to be involved in the xenome, described firstly in animals and suggested to function similarly in plants (Sandermann Jr., 1992). In this work, in order to understand molecular and metabolic changes involved in sucrose induced tolerance, “-omics” approaches were used.

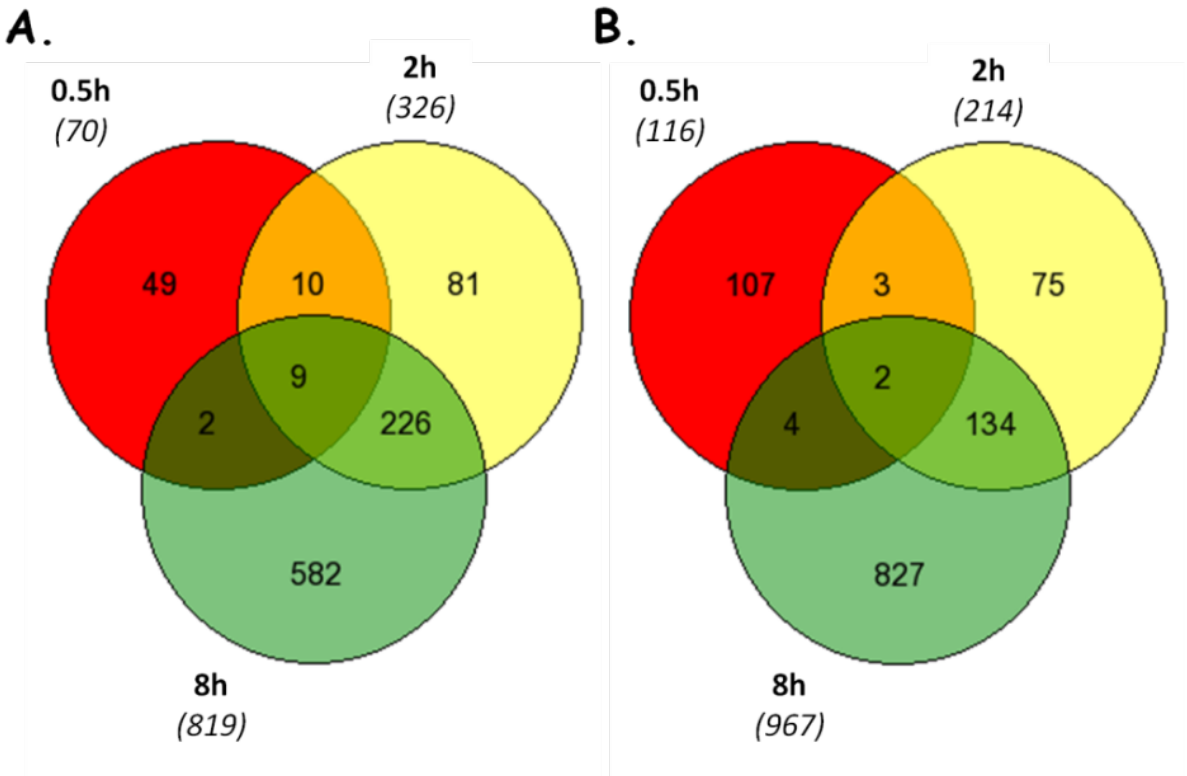


**<u>Figure 6</u>: Number of down- (A.) and up-(B.) regulated genes at 0.5h, 2h and 8h**
Venn diagrams were generated using the online application Gene List Venn Diagram (http://simbioinf.com/mcbc/applications/genevenn/genevenn.htm, (Pirooznia et al., 2007))

## 3.3. Sucrose reconfigured transcriptomic and metabolomic profile under phenanthrene-induced stress

### *3.3.1. Early Arabidopsis transcriptional responses to sucrose under phenanthrene-induced stress*

Transcriptional analysis was carried out at the 2.04 developmental stage (Boyes et al., 2001). Plantlets were grown on solid medium for 15 days, and then were transferred respectively into liquid medium supplemented with 200µM of phenanthrene or with 200µM of phenanthrene in protective condition (88mM of sucrose). During the incubation, liquid medium was agitated in order to avoid any oxygen deprivation.

Transcriptional analysis was performed using CATMA microarrays (version 5) and two independent biological replicates were carried out. The experimental design was performed to study sucrose effect on transcriptional response of plants incubated with phenanthrene- during 0.5h, 2h and 8h, respectively. We will refer this experiment as the “sucrose experiment” (Supplemental table II). In other hand, the microarray experiment previously performed to study the plant response to phenanthrene alone (Dumas et al., 2014, in preparation) will be referred as the “phenanthrene experiment”.

Overall, 2088 differentially expressed genes (DEG) were found in all the kinetic points of the experiment (Supplemental table III).

Hence, list of DEG at each kinetic point were compared with Venn diagrams (Fig. 6 A and B). Indeed, 186, 540 and 1786 DEG were found at 0.5h, 2h and 8h respectively. While at 0.5h and 8h, most of DEG were up regulated (respectively 70 down/116 up and 819 down /967 up), DEG found at 2h treatment, where mainly down-regulated (326 down/214 up). It might be argued that 2h constitute a transition point where a change of transcriptional regulation occurred. Meanwhile, few genes were found to be common, 7 genes (*AT1G31817*, *AT1G54740*, *AT1G70290*, *AT2G20670*, *AT2G31810*, *AT4G21870* and

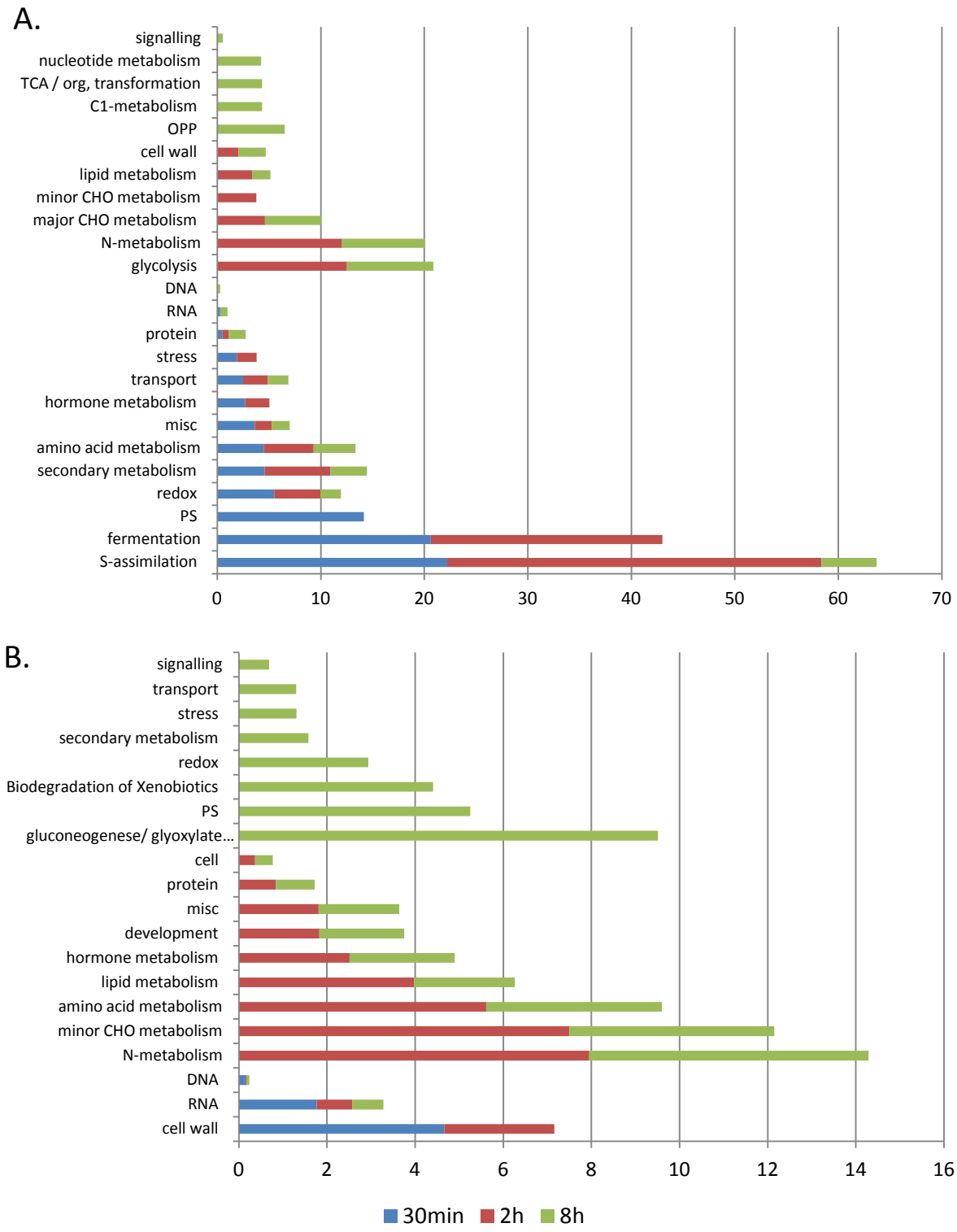


**Figure 7: Biological pathways with significant over-representation of up- (A) and down-regulated (B) genes** (P-values<0.05) after 0.5h, 2h and 8h of treatment with sucrose unde phenanthrene-induced stress. Functional enrichment is shown for differentially expressed genes analyzed using the classification superviewer tool from the Bio-Array Resource for Plant Biology (Provart T., 2003b) (http://www.bar.utoronto.ca/ntools/cgi-bin/ntools_classification_superviewer.cgi) using the MapMan classification as the source. PS, Photosynthesis. Misc, miscellaneous.

*AT5G61590*) are down-regulated at each point of the kinetic. The ascorbate peroxidase 1 (APX1, *AT1G07890*) and the cytochrome P450 83A1 (CYP83A1, *AT4G13770*) are up-regulated at all kinetic points of the experiment.

In parallel, the classification superviewer tool from the Bio-Array Resource for Plant Biology (Provart T., 2003a) using the MapMan classification (Thimm et al., 2004) (Fig. 7) were used to identify the most affected pathways by sucrose under phenanthrene-induced stress. We found that as early as 0.5h, sucrose induced up regulation of 50% of the analyzed pathways, and most of them are involved in the energy production (fermentation, photosynthesis) and stress tolerance (redox, stress, misc) . However, only few pathways (12.5%) involved in cell development (cell wall, RNA and DNA) were significantly down regulated. These data strongly suggested that, in phenanthrene-induced stress conditions, sucrose induced rapid transcriptional changes to maintain high energy production in order to face phenanthrene deleterious effects. These evidences suggested that sucrose or its derivates (glucose, fructose…) act very rapidly as a signaling molecule to induce very rapid changes to adapt transcriptional activity to unbalance phenanthrene-induced stress. Surprisingly, photosynthesis was found to be induced also very early in these conditions. This observation showed a discrepancy with published data since available carbon source induce inhibition of photosynthesis as shown by Roitsch (1999) and Paul and Foyer (2001). It is interesting to notice that these changes were obtained under long sucrose treatment, as we found, after 8 hours of sucrose treatment, that the transcriptional activity of genes involved in photosynthesis was down regulated. This repression of photosynthesis after 8 hours of treatment is characteristic of the late sucrose effect as previously described (Roitsch, 1999; Rolland et al., 2002). All these data taken together indicated that sucrose might trigger directly or indirectly different responses, rapid response (as a signaling molecule) and late response (as metabolic molecule).

In other hand, pathways significantly induced during late stages of sucrose treatment (8h) involves a strong regulation of primary metabolism with the activation of the oxidative pentose phosphate pathway (OPP), the tricarboxilic acid (TCA) pathway and the C1-metabolism and the inhibition of gluconeogenese/glyoxylate cycle pathway and

photosynthesis. Most of these pathways are known to be regulated by sucrose (Coruzzi and Zhou, 2001; Price et al., 2004; Thum et al., 2004; Rosa et al., 2009). Meanwhile, sucrose was also described to play an important role in the antioxidant system (Couée et al., 2006; Ende and Peshev, 2013). This action of sucrose is observable through the strong regulation of the redox system at 8h.

Strikingly, fermentation was up-regulated after at 0.5h and 2 hours of the kinetic points. This phenomenon was also observed after 24h treatment of phenanthrene alone (see Dumas et *al*., 2014). We argued that fermentation do not seems to be associated to our experimental condition as plants during incubation were shaken to avoid any oxygen deprivation. In other hand, to exclude this possibility, we compared our gene lists to genes differentially regulated by anoxia, hypoxia, and $O_2$ deprivation in the seedlings/shoots of *Arabidopsis* microarray datasets (55) and showed that only 3 genes are found in common (see Dumas et *al*. (2014), in preparation).

### *3.3.2. Targeted metabolomic changes under phenanthrene in unprotected and protected conditions*

During higher plants evolution, sucrose was selected as the major form of transport of carbohydrates. It has been shown that its variation induced a close regulation of many cell processes including the primary metabolism (Roitsch, 1999; Farrar et al., 2000; Rosa et al., 2009; Wind et al., 2010). Indeed, our transcriptional analysis showed that primary metabolism was affected by sucrose since 2h of treatment. Indeed, glycolysis and TCA were found to be induced contrary to gluconeogenese/glyoxylate cycle pathways were inhibited after 8h of treatment. In order to get insight into these transcriptional changed, we carried out a targeted metabolomic analysis. Targeted metabolomic analysis was performed on plants at the stage 2.04 (Boyes et al., 2001). 15 days old plantlets were grown on solid basal medium, and then transferred into liquid medium. Comparison was carried out on plants incubated during 24h in the presence of either 200µM of phenanthrene or 200µm of phenanthrene and 3% of sucrose. This comparison allowed the analysis of the effect of sucrose under phenanthrene-induced stress at the metabolomic level.

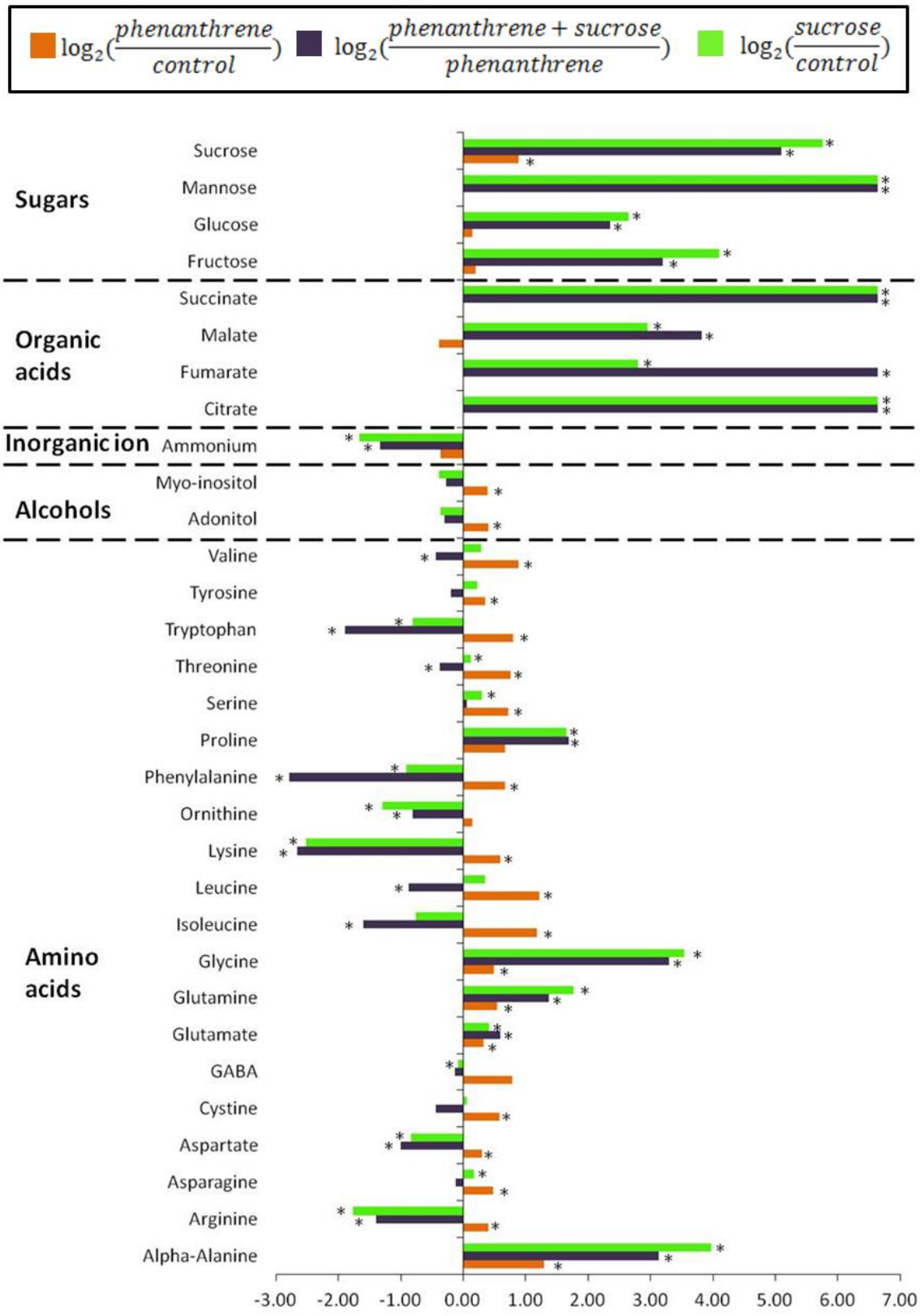


**<u>Figure 8</u>: Logarithmic ratios of average metabolites content in whole plants according to the treatment applied.**

Selected metabolites (with *) are statistically different between both conditions of the ratio (t-Test, p-value≤0.05). Complete data are available in supplemental table IV.

Figure 8 showed sucrose effects on metabolites ratio in control (green) and stressed condition (purple). Sucrose induced deep reconfiguration of several metabolites levels in both conditions. 20 metabolites levels were affected by sucrose in non-stressed conditions and 24 in phenanthrene-induced stress conditions. 8 metabolites are affected in only one condition (stressed or control). Sucrose strongly induced the accumulation of sugars and organic acids after 24h of incubation, which are intermediates of the TCA cycle. All together, these results revealed a strong regulation of the primary metabolism. Metabolomic and transcriptomic changes induced by sucrose under phenanthrene-induced-stress revealed a strong activation of primary metabolism suggesting that plants absorb and metabolize through glycolysis and TCA the exogenous sucrose (Fig 8). In parallel, exogenous sucrose induced a reduction of ammonium levels in both condition. Amino acids content is also strongly regulated by sucrose. These changes of nitrogen compounds revealed the impact of the addition of a carbon source on nitrogen metabolism and showed the importance of the balance between nitrogen and carbon (Coruzzi and Zhou, 2001).

Additionally, figure 8 showed comparison of metabolites ratios of plants grown in unprotected condition, ($\log_2 \frac{phenanthrene}{control}$), where phenanthrene induced significant changes of 20 metabolites levels, while 24 metabolites were impacted by sucrose under phenanthrene induced stress, ($\log_2 \frac{sucrose+phenanthrene}{phenanthrene}$). As it was previously observed, phenanthrene alone induced a slight accumulation of sucrose. However, in protective conditions, we observed accumulation of not only sucrose but also several other sugars (mannose, maltose, glucose, gentiobiose and fructose). In protective conditions, the accumulation of soluble sugars was highly increased. This result corroborates with the protective effect of the soluble sugars observed in our precedent results and showed in different abiotic stress conditions, such as anoxia (Loreti et al., 2005) and atrazine (Sulmon et al., 2004). Similarly, several studies revealed that abiotic stresses induced the accumulation of sugars (Dubey and Singh, 1999; Gill et al., 2003; Lloyd and Zakhleniuk, 2004). Recently, it was suggested by several authors that sugars, like sucrose, fructans and raffinose family oligosaccharides (RFOs), may contribute directly or indirectly to antioxidative mechanisms (Valluru and Ende, 2008; Bolouri-Moghaddam et al., 2010; Ende and Peshev, 2013; Keunen et al., 2013; Peshev et al., 2013). In other hand, after 24h of incubation in phenanthrene-

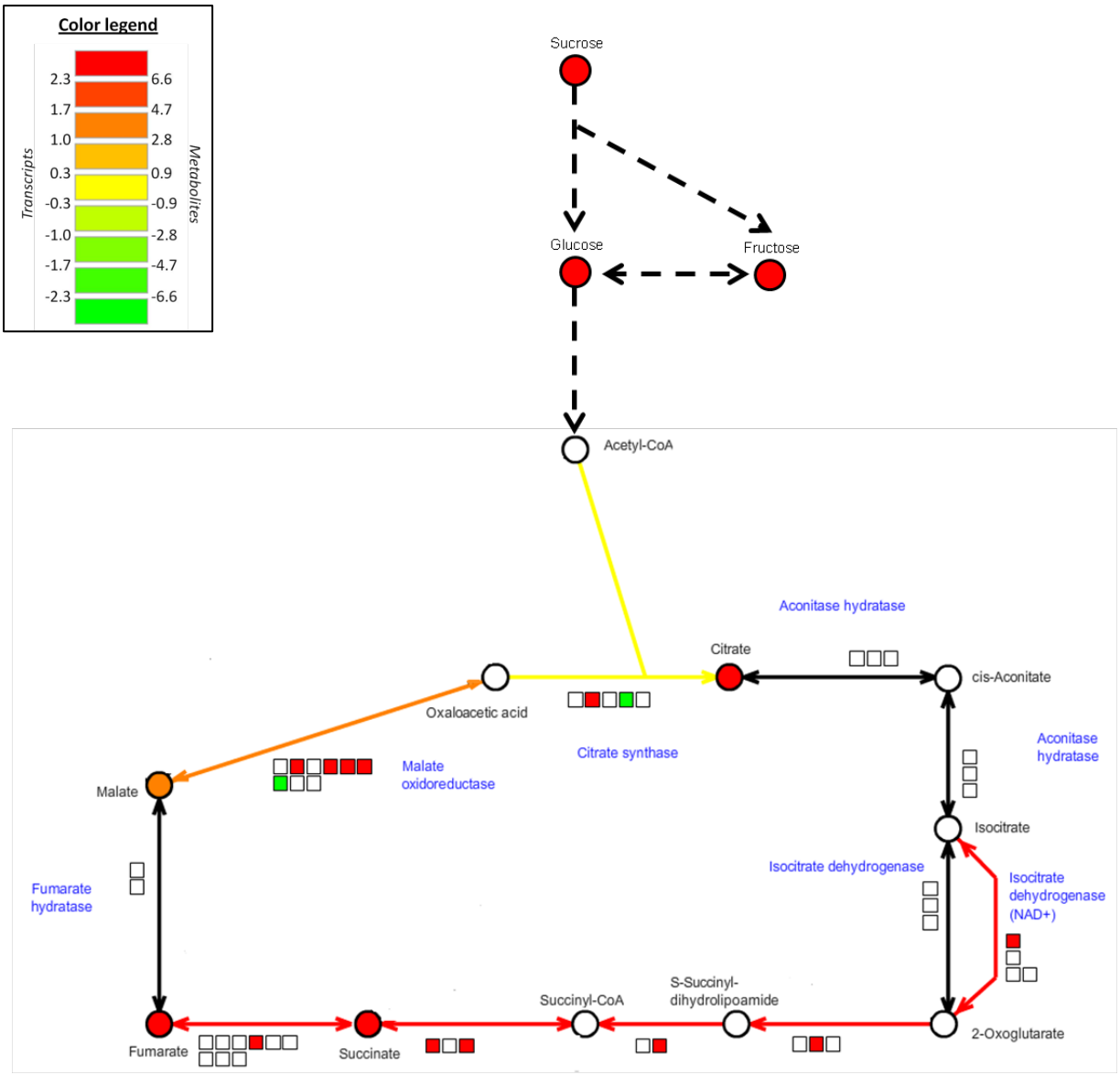


**Figure 9: Citric acid cycle and glycolysis representation.**

Circles showed the metabolomic data from the experiment phenanthrene vs phenanthrene+sucrose (Raw data are in table 1). Squares represented differentially expressed genes from the transcriptomic experiment for an incubation time of 8h. Modified from diagrams acquired with the online software KaPPaView 4 (Tokimatsu et al., 2005)

induced stress condition, sucrose allowed the accumulation of organic acid such succinate, malate, fumarate and citrate. These data corroborate with the transcriptional activity observed at late stage of treatment; as major carbohydrate pathways were strongly up-regulated such glycolysis and TCA. Genes, involved in sucrose and starch degradation, were also shown to be significantly induced, possibly leading to the accumulation of glucose and fructose observed in the metabolomic analysis (Fig. 8). Figure 9 summarizes and links transcriptomic and metabolomic data, showing a strong regulation of sugar metabolization and the formation of organic acids.

Most of amino acids monitored in our experiment (18 among 25) increased significantly in non-protective conditions ($\log_2 \frac{phenanthrene}{control}$)). Rai (2002) stated that plants subjected to stress (water, heavy metals, cold, salt…) tended to accumulate amino acids. This author discussed the roles of amino acids that are not only precursors for protein synthesis but also act at different levels (enzyme synthesis and activity regulation, gene expression, redox homeostasis, osmolyte…). This observation may also explain a proteolytic activity related to stressed conditions. Contrary, the comparison of phenanthrene effect in protective against stressed conditions ($\log_2 \frac{sucrose+phenanthrene}{phenanthrene}$) revealed that sucrose induced a deep reconfiguration of metabolites levels as among the 25 amino acids analyzed, 5 amino acids increased (proline, glycine, glutamine, glutamate and alpha-alanine) while 14 amino acids showed significant reduction (Fig. 8).

Transcription activity of genes involved in nitrogen metabolism is strongly affected by sucrose after 2h and 8h of treatment. Moreover, amino acid and protein metabolism are also strongly regulated at these kinetic pints (Fig. 7). Through these pathways, glutamate and glutamine synthesis is stimulated which is consistent with the accumulation of alpha-alanine, glutamine, glutamate and proline (Fig. 8). Proline is known to be accumulated in numerous stress response such as water, heavy metals, cold, salt (Rai, 2002; Szabados and Savouré, 2010). Proline like sucrose is known to be a multi-functional metabolite involved not only in primary metabolism but also in signaling and in the redox balance (Szabados and Savouré, 2010). It was also found that external application of proline had a protective effect under abiotic stress (salt and drought) (Ashraf and Foolad, 2007). Sucrose induced a more

important accumulation of glutamate and glutamine that are precursors of proline synthesis. While most amino acids analyzed (Fig. 8) are accumulated in response to a phenanthrene-induced stress, amino acids contain seems to decrease when sucrose is added, suggesting that through the sucrose protective effects, plants are less impacted by the phenanthrene in their environment and their stress response is quite limited.

In conclusion, data obtained from the "phenanthrene experiment" revealed that phenanthrene strongly affected primary metabolism, as photosynthesis and respiration were dramatically down regulated. Meanwhile, soluble sugars and amino acids levels increased. This physiological unbalance revealed a carbohydrate starvation as cell metabolism was unable to face energetic demand. These metabolic unbalance was associated with chlorotic phenotype and inhibition of plant development. However, in protective conditions, sucrose allowed to maintain metabolic pathways involved in cell building structures (cell wall, amino acids and nucleotide synthesis, S assimilation) and energy production (fermentation, glycolysis and TCA cycle) (Fig. 7). It may be argued that sucrose, at the later stage, compensates the negative effect of phenanthrene as it is used as metabolic molecule to face energy demand.

### *3.3.3. Transcriptional profile of genes involved in stress was reconfigured by exogenous sucrose*

Several published data showed that phenanthrene induced oxidative stress (Alkio et al., 2005; Liu et al., 2009; Weisman et al., 2010a). In parallel it might also induce a myriad of other genes involved in stress. It is of high interest to study how these specific genes family are regulated in the presence of sucrose.

Results obtained from pathways enrichment analysis in "sucrose experiment" (Fig. 7) revealed that up-regulated genes belonging to the stress response pathways were over-represented only in the early stages. In contrast, at the late stage, they were down regulated (Fig. 7B). A close analysis of the DEG involved in these two stages revealed that they constitute two distinct clusters, suggesting the involvement of different control mechanisms.

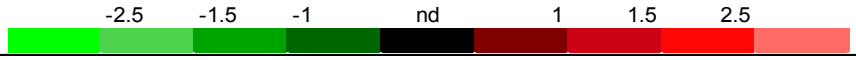


| AGI | GO | "Sucrose experiment" (Suc+ phen /phen) 30min | 2h | 8h | "Phenanthrene experiment" (phenanthrene / control) 30 min | 2h | 8h |
|---|---|---|---|---|---|---|---|
| AT3G05890 | RCI2B__Low temperature and salt responsive protein family | -1.01 | | -0.99 | | | |
| AT4G21870 | HSP20-like chaperones superfamily protein | -0.74 | -1.31 | -1.75 | | | |
| AT1G80920 | J8__Chaperone DnaJ-domain superfamily protein | | -2.95 | -1.98 | | | |
| AT1G75380 | ATBBD1_BBD1__bifunctional nuclease in basal defense response 1 | | -1.88 | -1.14 | | | |
| AT2G24550 | unknown protein | | -1.61 | -0.96 | | | |
| AT3G50480 | HR4 (HOMOLOG OF RPW8 4) | | -1.21 | -1.25 | | 1.80 | 2.35 |
| AT2G41430 | CID1_ERD15_LSR1__dehydration-induced protein (ERD15) | | -1.18 | -0.99 | | | |
| AT3G59930 | Encodes a defensin-like (DEFL) family protein. | | -1.16 | -2.13 | | 1.79 | 2.04 |
| AT1G58190 | AtRLP9_RLP9__receptor like protein 9 | | -1.10 | -1.38 | | | |
| AT4G28240 | Wound-responsive family protein | | -1.03 | -1.00 | | | -0.63 |
| AT1G19660 | Wound-responsive family protein | | -0.81 | -1.86 | | | |
| AT1G04430 | S-adenosyl-L-methionine-dependent methyltransferases superfamily protein | | -0.77 | 0.93 | | | -0.78 |
| AT5G43570 | PR (pathogenesis-related) peptide that belongs to the PR-6 proteinase inhibitor family. | | | -1.88 | | | |
| AT2G38870 | Serine protease inhibitor, potato inhibitor I-type family protein | | x | -1.75 | | | |
| AT4G11650 | ATOSM34_OSM34__osmotin 34 | | | -1.55 | | 0.93 | |
| AT4G36040 | Chaperone DnaJ-domain superfamily protein | | | -1.55 | | 0.69 | |
| AT3G50970 | LTI30_XERO2__dehydrin family protein | | | -1.42 | | 0.92 | 1.16 |
| AT2G02180 | TOM3__tobamovirus multiplication protein 3 | | | -1.36 | | | 0.78 |
| AT1G56280 | ATDI19_DI19__drought-induced 19 | | | -1.29 | | | |
| AT1G01170 | Protein of unknown function (DUF1138) | | | -1.25 | | | |
| AT2G21970 | SEP2__stress enhanced protein 2 | | | -1.09 | | | |
| AT2G43510 | ATTI1_TI1__trypsin inhibitor protein 1 | | | -1.07 | | | |
| AT5G44420 | LCR77_PDF1.2_PDF1.2A__plant defensin 1.2 | | | -1.06 | | | |
| AT1G75830 | LCR67_PDF1.1__low-molecular-weight cysteine-rich 67 | | | -1.06 | | | |
| AT5G18140 | Chaperone DnaJ-domain superfamily protein | | | -1.05 | 1.13 | 1.12 | 1.27 |
| AT3G10985 | ATWI-12_SAG20_WI12__senescence associated gene 20 | | | -1.00 | | | |
| AT4G00750 | S-adenosyl-L-methionine-dependent methyltransferases superfamily protein | | | -0.98 | | | 0.95 |
| AT1G34047 | Encodes a defensin-like (DEFL) family protein. | | | -0.93 | | | 0.82 |
| AT2G43520 | ATTI2_TI2__trypsin inhibitor protein 2 | | | -0.91 | | | |
| AT3G05880 | RCI2A__Low temperature and salt responsive protein family | | | -0.86 | | | |
| AT1G17860 | Kunitz family trypsin and protease inhibitor protein | | | -0.86 | | | 1.10 |
| AT3G22530 | unknown protein | | | -0.84 | | | 0.72 |
| AT3G62190 | Chaperone DnaJ-domain superfamily protein | x | | -0.83 | | | |
| AT3G01520 | Adenine nucleotide alpha hydrolases-like superfamily protein | | | -0.82 | | | |
| AT1G24020 | MLP423__MLP-like protein 423 | | | -0.78 | | | |
| AT3G25760 | AOC1_ERD12__allene oxide cyclase 1 | | | -0.78 | | | |
| AT5G64890 | PROPEP2__elicitor peptide 2 precursor | | | -0.75 | | | 1.07 |
| AT3G06340 | DNAJ heat shock N-terminal domain-containing protein | | | -0.75 | | | |
| AT4G21320 | HSA32 (HEAT-STRESS-ASSOCIATED 32) | | | -0.74 | | | |
| AT5G56010 | AtHsp90-3_AtHsp90.3_HSP81-3_Hsp81.3__heat shock protein 81-3 | | 0.76 | | | | |
| AT5G51440 | HSP20-like chaperones superfamily protein | | 0.79 | | | | 0.90 |
| AT4G36020 | CSDP1__cold shock domain protein 1 | | 0.79 | 0.97 | | | |
| AT3G54420 | ATCHITIV_ATEP3_CHIV_EP3__homolog of carrot EP3-3 chitinase | | 0.85 | | | | 0.98 |
| AT5G53760 | ATMLO11_MLO11__Seven transmembrane MLO family protein | | 0.88 | | | | |
| AT2G42540 | COR15_COR15A__cold-regulated 15a | | 0.90 | 0.90 | | | 0.79 |
| AT1G07400 | HSP20-like chaperones superfamily protein | | 0.92 | | | | 1.18 |
| AT5G56030 | AtHsp90.2_ERD8_HSP81-2_HSP90.2__heat shock protein 81-2 | | 0.98 | 0.98 | | | |
| AT3G14200 | Chaperone DnaJ-domain superfamily protein | | 1.01 | | | | 0.77 |
| AT3G09440 | Heat shock protein 70 (Hsp 70) family protein | | 1.06 | x | | | |
| AT3G12580 | ATHSP70_HSP70__heat shock protein 70 | | 1.11 | | | | 0.77 |
| AT5G25610 | ATRD22_RD22__BURP domain-containing protein | | 1.12 | 1.25 | | | |
| AT4G36010 | Pathogenesis-related thaumatin superfamily protein | | 1.34 | 0.81 | | | 1.24 |
| AT2G43620 | Chitinase family protein | | 1.45 | 1.86 | | | |
| AT5G36910 | THI2.2__thionin 2.2 | 0.68 | | | | | |
| AT3G01420 | ALPHA-DOX1_DIOX1_DOX1_PADOX-1__Peroxidase superfamily protein | 0.68 | | | | | |
| AT3G50950 | ZAR1__HOPZ-ACTIVATED RESISTANCE 1 | 0.71 | | | | | |
| AT1G18700 | DNAJ heat shock N-terminal domain-containing protein | 0.79 | | | | | 0.77 |
| AT3G26450 | Polyketide cyclase/dehydrase and lipid transport superfamily protein | 0.80 | | | | | |
| AT5G42020 | BIP_BIP2__Heat shock protein 70 (Hsp 70) family protein | 0.93 | x | | | | |
| AT1G76180 | ERD14__Dehydrin family protein | 0.97 | | -1.27 | | | |
| AT1G13930 | Involved in response to salt stress. Knockout mutants are hypersensitive to salt stress. | 0.98 | | | | | |

**Figure 10: List of differentially expressed genes belonging to the stress response pathway in the "sucrose experiment". In parallel, data extracted from the "phenanthrene experiment" were also shown (right) (Dumas et al (2014) in preparation).** A negative ratio indicates that the gene is decreased and a positive ratio indicates that the gene is increased in expression in the indicative point of the kinetic, respectively. Ratios in black boxes were not found to be statistically significant after Bonferroni correction (P >0.05)

It is interesting to notice that, in the presence of sucrose, genes involved in stress responses are mostly down-regulated (68%) after 8h of treatment in comparison to phenanthrene-induced stress condition (Fig. 10). These results suggested that sucrose mitigated phenanthrene-induced stress at the transcriptional level, particularly at the late stage. Indeed, more analysis are needed to investigate if these transcriptional regulations are sucrose specific responses or might be induced by other metabolic molecules such glucose or fructose. Additionally, sucrose is also known to induce changes in the redox scavenging system (Ramel et al., 2007; Bolouri-Moghaddam et al., 2010; Ende and Peshev, 2013).

Published data obtained trough long phenanthrene exposition in sucrose supplemented medium revealed strong activity of antioxidant enzymes such as ascorbate peroxidases (APX) and catalases (CAT) (Liu et al., 2009). In other hand, transcriptomic analysis of 21-day-old plantlets grown phenanthrene and sucrose supplemented medium also revealed a strong stimulation of the redox scavenging system (Weisman et al., 2010a). In our experiment ("sucrose experiment"), the redox pathway is significantly over-represented over the whole experiment (Fig 7A). Redox genes up-regulated in the early stages (0.5h) are all involved in the ascorbate and glutathione redox system. Liu et al. (2009) showed that phenanthrene-induced an increase in the activity of ascorbate peroxidase and that *APX1* (*AT1G07890*) mRNA levels which increased after 48h of treatment. In our experiment, this gene is up-regulated all over the kinetic while, in the "phenanthrene experiment", it was up-regulated only after 24h of treatment (Fig. 11). This antioxidant enzyme seems to play a key role in the abiotic stress tolerance. In other hand, among the 26 genes of the redox pathway differentially expressed at 8h, 11 are up-regulated and 15 are down-regulated. They are mainly belonging to the ascorbate and glutathione redox system (8/26) and to the thioredoxin system (11/26). Indeed, both systems are described as major antioxidant systems in plants (Vieira Dos Santos and Rey, 2006; Foyer and Noctor, 2011). These observations suggested a strong regulation of oxidative scavenging system occurred at the late stage in the presence of exogenous sucrose.

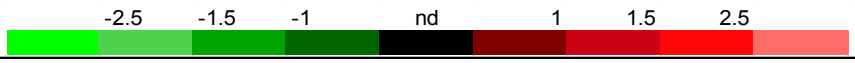


| AGI identifier | GO | "Sucrose experiment" suc+phen/phen 30min | 2h | 8h | "Phenanthrene experiment" phen/control 30 min | 2h | 8h |
|---|---|---|---|---|---|---|---|
| AT1G03850 | Glutaredoxin family protein | | -1.83 | -1.53 | | | |
| AT5G06690 | WCRKC1__WCRKC thioredoxin 1 | | -1.24 | -1.51 | | | |
| AT1G11530 | ATCXXS1_CXXS1__C-terminal cysteine residue is changed to a serine 1 | | -0.86 | -1.46 | | | |
| AT5G63030 | Thioredoxin superfamily protein | | | -1.07 | | | |
| AT3G62930 | Thioredoxin superfamily protein | | | -1.06 | | | |
| AT1G76080 | ATCDSP32_CDSP32__chloroplastic drought-induced stress protein of 32 kD | | | -1.03 | | | |
| AT4G35090 | CAT2__catalase 2 | | | -0.98 | | | |
| AT5G28840 | GME__GDP-D-mannose 3',5'-epimerase | | | -0.95 | | | -0.68 |
| AT4G25570 | ACYB-2__Cytochrome b561/ferric reductase transmembrane protein family | | | -0.94 | | | |
| AT5G16400 | ATF2_TRXF2__thioredoxin F2 | | | -0.92 | | | |
| AT5G51010 | Rubredoxin-like superfamily protein | | | -0.88 | | | |
| AT4G31870 | ATGPX7_GPX7__glutathione peroxidase 7 | | | -0.81 | | | |
| AT1G07700 | Thioredoxin superfamily protein | | | -0.77 | | | |
| AT5G61440 | ACHT5__atypical CYS HIS rich thioredoxin 5 | | | -0.75 | | | |
| AT1G12520 | ATCCS_CCS__copper chaperone for SOD1 | | | -0.72 | | | |
| AT3G54960 | ATPDI1_ATPDIL1-3_PDI1_PDIL1-3__PDI-like 1-3 | | | 0.81 | | | |
| AT5G60640 | ATPDI2_ATPDIL1-4_PDI2_PDIL1-4__PDI-like 1-4 | | | 0.85 | | | -0.73 |
| AT1G06830 | Glutaredoxin family protein | | | 0.90 | | | |
| AT2G32720 | ATCB5-B_B5 #4_CB5-B__cytochrome B5 isoform B | | | 0.93 | | | -1.04 |
| AT3G10520 | AHB2_ARATH GLB2 ATGLB2_GLB2_HB2_NSHB2__haemoglobin 2 | | | 0.94 | | | |
| AT1G77510 | ATPDI6_ATPDIL1-2_PDI6_PDIL1-2__PDI-like 1-2 | | | 1.08 | | | |
| AT1G21750 | ATPDI5_ATPDIL1-1_PDI5_PDIL1-1__PDI-like 1-1 | | | 1.13 | | | |
| AT2G46650 | ATCB5-C_B5 #1_CB5-C__cytochrome B5 isoform C | | 0.74 | 0.99 | | | |
| AT5G03630 | ATMDAR2__Pyridine nucleotide-disulphide oxidoreductase family protein | | 0.77 | 0.76 | | | 0.75 |
| AT1G19570 | ATDHAR1_DHAR1_DHAR5__dehydroascorbate reductase | | 0.79 | 1.06 | | | |
| AT1G19550 | Glutathione S-transferase family protein | | 0.82 | | | | 1.05 |
| AT4G26850 | VTC2__mannose-1-phosphate guanylyltransferase (GDP)s | | 1.15 | | | | |
| AT4G23100 | ATECS1_CAD2_GSH1_GSHA_PAD2_RML1__glutamate-cysteine ligase | 0.67 | | | | | |
| AT2G25080 | ATGPX1_GPX1__glutathione peroxidase 1 | 0.67 | | | | | |
| AT4G11600 | ATGPX6_GPX6_LSC803_PHGPX__glutathione peroxidase 6 | 0.82 | x | | | | 1.03 |
| AT1G07890 | APX1_ATAPX01_ATAPX1_CS1_MEE6 _ascorbate peroxidase 1 | 1.18 | 1.10 | 0.90 | | | |

**Figure 11: List of differentially expressed genes of the redox pathway in the "sucrose experiment".In parallel, data extracted from the "phenanthrene experiment" were also shown (right) (Dumas et al (2013) submitted paper).** A negative ratio indicates that the gene is decreased and a positive ratio indicates that the gene is increased in expression in the indicative point of the kinetic, respectively. Ratios in black boxes were not found to be statistically significant after Bonferroni correction (P >0.05)

### 3.3.4. *The xenome expression was reconfigured by exogenous sucrose*

Transport and detoxification encoding genes of the xenome are belonging to several multigenic enzymes families involved in a three-step process: the first step is an activation of the xenobiotic performed by the cytochrome P450 (CYP), the second step is a conjugation of the xenobiotic with a glutathione performed by glutathione-S-transferases (GST) or a conjugation of the activated xenobiotic with UDP-glucose catalyzed by the UDP-glucuronosyltransferase (UGT), additional malonylation may occurred using a malonyltransferases. Finally, the last step consist in the compartmentalization through the transport of the conjugated xenobiotic by the ATP-binding cassette transporters (ABC transporters) (Edwards et al., 2005; Edwards et al., 2011b). Hence, we hypothesized that sucrose might induce also xenome transcription changes to reduce phenanthrene toxicity or even metabolization. In order to understand how sucrose mitigates phenanthrene-induced stress at the transcriptional xenome expression, all differentially expressed genes family belonging to the xenome were identified and compared with phenanthrene-induced stress condition. This approach might bring new insight into sucrose role in plant tolerance to phenanthrene-induced stress.

The complete set of differentially expressed xenome genes in the presence of sucrose is listed in figure 12. This list was confronted to results previously obtained in the “phenanthrene experiment”.

50 genes belonging to the xenome set are differentially expressed in the “sucrose experiment”. The most noticeable modifications of the xenome genes, induced by sucrose, occurred at the late stage, as 46 genes among the 50 xenome DEG are differentially expressed after 8h of treatment, while only 3 are up-regulated after 0.5h of treatment. All xenome genes differentially expressed in the “sucrose experiment” also appeared to be differentially expressed in at least one other “xenobiotic experiment” and, by consequences, are in the xenome list established in our previous work on phenanthrene effect.

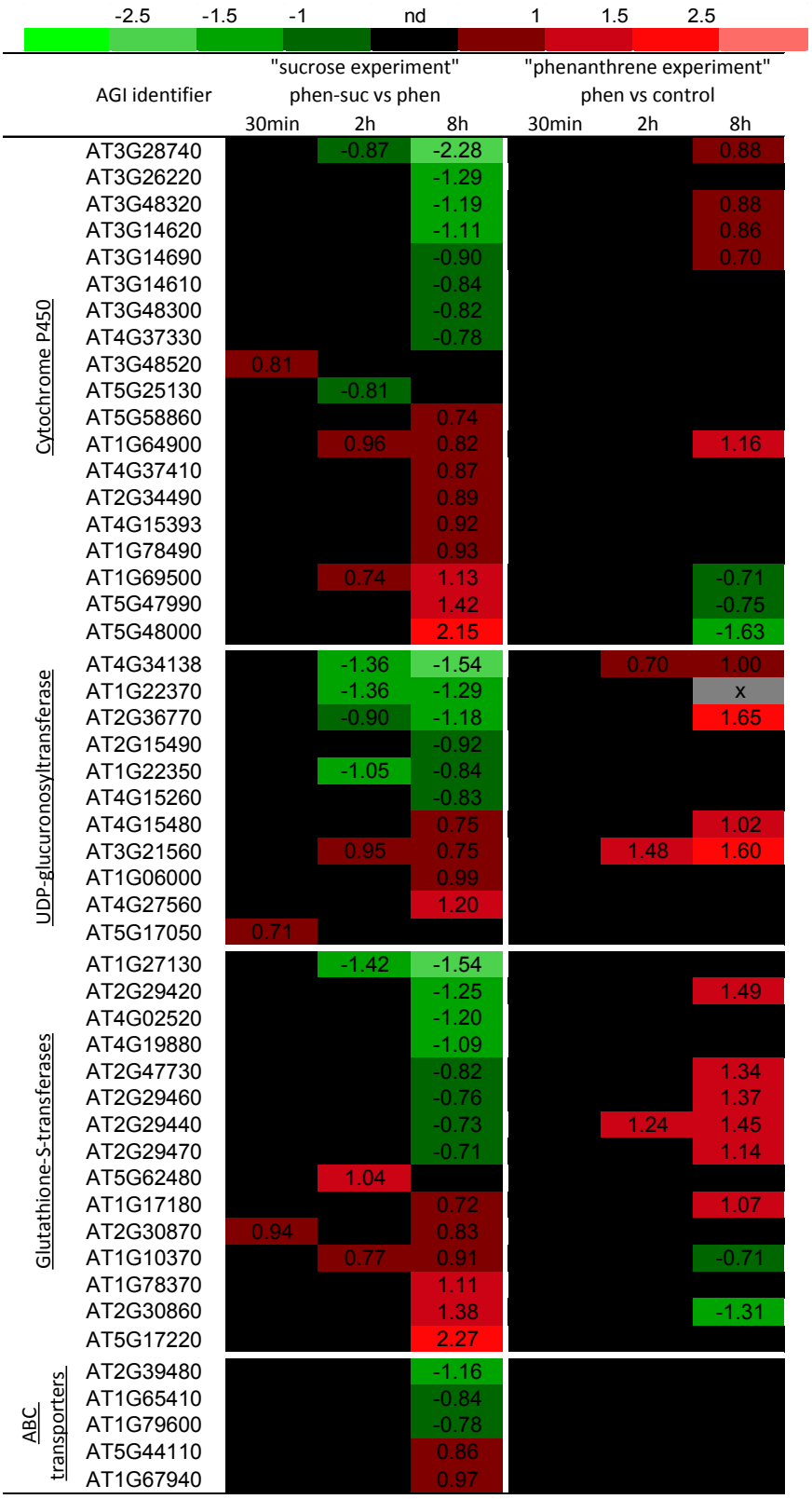


**Figure 12: List of differentially expressed xenome genes in the "sucrose experiment".In parallel, data extracted from the "phenanthrene experiment" were also shown (right) (Dumas et al (2014) in preparation).** A negative ratio indicates that the gene is decreased and a positive ratio indicates that the gene is increased in expression in the indicative point of the kinetic, respectively. Ratios in black boxes were not found to be statistically significant after Bonferroni correction (P >0.05).

The transcriptional reconfiguration of the xenome, in the presence of sucrose suggests significant changes in the potential phenanthrene conjugation or metabolization. These observations were corroborated by fluorescence microscopy and GC-MS quantification. Since plants accumulated less free phenanthrene in the presence of exogenous sucrose. The signaling and metabolic mechanisms involved in sucrose induced tolerance is still unknown, however, our results and accumulated data suggested that sucrose play a pivotal role in environmental adaptation.

## 4. Conclusion

In this work, we showed that, whereas phenanthrene alone induced a sever inhibition of plant growth and chlorophyll accumulation, exogenous sucrose allowed to maintain plant development even at high phenanthrene concentration. This protective effect was associated with discrete changes in tissues accumulation of this pollutant. In parallel, quantification by GC-MS showed that treated plants with exogenous sucrose reduced plant phenanthrene content; this observation was associated with tolerant phenotype. Indicating either the induction of cellular processes involved in phenanthrene tolerance or the occurrence of biochemical changes this molecule, such as conjugation or association with cell wall polymers as it was suggested for phenolic xenobiotics (Taguchi et al., 2010; Matsui et al., 2011). Thus we hypothesized that sucrose, induced either new gene-network involved in phenanthrene tolerance such oxidative stress scavenging system, metabolization, transport or likely a complete degradation. In order to verify this hypothesis wide-genome transcriptional and targeted metabolomic approaches were used to decipher early molecular processes involved in sucrose induce tolerance. 2088 genes were found to be differentially expressed in the presence of exogenous sucrose during the first 8h which allowed the identification of significant over represented metabolic pathways.

Indeed, as early as 0.5 h, at the transcriptional level, sucrose allowed maintaining the activity of photosynthesis, energy supply and biosyntheses of protein genes. In contrary to

phenanthrene-induced injury where cellular homeostasis was unbalanced as respiration and photosynthesis were inhibited, whereas amino acids and soluble sugars increased which indicated the incapacity of cells to overcame phenanthrene toxicity and likely a sugar starvation symptoms. Surprisingly fermentation was also significantly induced. However, the metabolic switch from respiration to fermentation is dictated by oxygen availability. Pyruvate decarboxylase and alcohol dehydrogenase are dedicated to ethanolic fermentation and are induced under oxygen deprivation. Tadege and Kuhlemeier (1997) showed that similar situation have been occurred in rapid developing pollen tube, and a flux through ethanolic fermentation pathway could already be detected very early in pollen development. This flux was primarily controlled not by oxygen availability, but rather by sugar supply. It was suggested that at a high rate of sugar metabolism, respiration and fermentation took place concurrently. These authors proposed that aerobic fermentation provides a shunt from pyruvate to acetyl-CoA to accommodate the increased demand for energy and biosynthetic intermediates. Additionally, aerobic fermentation was discussed in the context of stress-signal transduction; as this metabolic pathway was induce under abiotic stress such as cold, deshydratation and ozone exposure, produce considerable amounts of acetaldehyde and ethanol at ambient or even at elevated oxygen concentration(Tadege et al., 1999). Our results give additional data indicating that aerobic fermentation may play a pivotal role in sugar metabolism under abiotic stress conditions. But the functional significance is still to be elucidated.

Tolerance and metabolization of organic pollutants in higher plants alter a myriad of genes family. We showed in this word that exogenous sucrose reconfigured most genes involved in oxidative stress and the xenome. Thus, the P-450 which are involved in the metabolization of organic pollutants in fungus and animal, showed in the presence of sucrose many transcriptional changes, as 19 genes have been differentially regulated. The identification of mutants corresponding to the induced genes have been isolated and their characterization is under investigation. In other hand, metabolization of organic pollutant involves a variety of biochemical pathways. The family 1 Glycosyltransferase (UGT) has emerged as an important group of bio-conjugating enzymes that are involved in the detoxification of xenobiotic (Cole and Edwards, 2000), as they catalyze the O-, S- and N-glyco-conjugation of a range of pollutants using NDP-activated sugar donors (Schröder *et al*.,

2001). In Arabidopsis, a UGT termed UGT72B1 catalyse the conjugation 3,4-dichloroaniline (DCA) with glucose, was identified by Loutre et al. 2003. *UGT72B1* knockout *Arabidopsis* mutant where the UGT72B1 was selectively disrupted by transposon mutagenesis, and over-expression approaches (Brazier-Hicks et al.2007) revealed the identification of competing patways (i) the N-glucosylation produced soluble conjugates which are addressed to extrea celullar space and (ii) insoluble and bound residue mainly attached to cell wall. Thus, when N-glycolsylation activity was suppressed *in planta*, the DCA was directed into lignin fraction. Meanwhile, Matsui et al. (2011) showed that peroxidase have been involved in the removal of organic pollutants, such phenolic compounds, by the cross-linking them to cell wall polysaccharides or proteins at the expense of reduction of hydrogen peroxide. According to these data, we may hypothesize that metabolic pathways involved in pollutants detoxification may be unbalanced depending of environment, nutritional status or signaling stimuli. Our analyses showed that sucrose induced seven genes coding UDP-Glycosil-transferases and nine peroxidases respectively (Supplemental table V). Functional analysis of these genes such knockout strategy, protein expression, will give new insight to understand how sucrose induces tolerance to abiotic stresses.

**Supplemental Table I:** Primers used for quantitative RT-PCR

| Primers name | Sequence (5' → 3') | Targets |
|---|---|---|
| 1G07890_L1 | CTCTGCTGGAACTTTCGATTG | AT1G07890 |
| 1G07890_R1 | ATGGGGTCCAACAACCTAAGA | |
| 1G07890_L2 | TTCGGAACAATGAGGTTTGAC | |
| 1G07890_R2 | TCAGCAAAAGAGATGGTAGGG | |
| 1G15380_L1 | GAAGAAGGAGGGATCCAAGTG | AT1G15380 |
| 1G15380_R1 | TTTCTCCTACGAGGGGGACTA | |
| 1G15380_L2 | AGAAGAAGCTGGAGGAAATGG | |
| 1G15380_R2 | GCTATCGCAGTTGCAAATCTC | |
| 1G30530_L1 | GAAGGTTGGAGTGATGATGGA | AT1G30530 |
| 1G30530_R1 | AGCTTCTTGGCATTAGCCTTC | |
| 1G30530_L2 | TCAGTGTTGGAGAGTGTGTCG | |
| 1G30530_R2 | TCCATCATCACTCCAACCTTC | |
| 1G44750_L1 | TCGCTCTTCTCAAACGTCATT | AT1G44750 |
| 1G44750_R1 | CGATCAGCATTGCCATAATCT | |
| 1G44750_L2 | CATCGACGTATTCGCTCATTT | |
| 1G44750_R2 | CGGAGTTGAGAATCAAAGCAG | |
| 1G53310_L1 | GCGACCACACATTTCTAAGGA | AT1G53310 |
| 1G53310_R1 | TGTAGACCAGCAGCAATACCC | |
| 1G53310_L2 | CAAAACACCGGTTAAGCTACAA | |
| 1G53310_R2 | AATCAACATTTTGACGGTGGA | |
| 2G30870_L1 | CTGAGTATCTCGCGATTCAGG | AT2G30870 |
| 2G30870_R1 | GACTGGGATTTTACCGAAAGG | |
| 2G30870_L2 | TGTTGTGACATTGGTGGAGAA | |
| 2G30870_R2 | AAAGAGGGAAAATCGGAACCT | |
| 3G03250_L1 | TGCTCTTTGAATTTTCCCAAA | AT3G03250 |
| 3G03250_R1 | CCATCAGTTTCCAAGCAAAGA | |
| 3G03250_L2 | AAAGATCACAAGTGGCACAGC | |
| 3G03250_R2 | TGGGAAAATTCAAAGAGCAAA | |
| 3G13450_L1 | GGATGCAATCAGATCCACTGT | AT3G13450 |
| 3G13450_R1 | GTCTGAACCACCAGCATCAAT | |
| 3G13450_L2 | GCATTGTACACATGATTCTCTGTC | |
| 3G13450_R2 | CAAAGATGGAGAGTTTCAAGATCA | |
| 3G52930_L1 | CTAAGCTTGGTGATGGAGCAG | AT3G52930 |
| 3G52930_R1 | TCCAGGAAGATGACAAACGTC | |
| 3G52930_L2 | GAGTTCTTCCCGGTATCAAGG | |
| 3G52930_R2 | ACGAGCACCAGCTTCGTAGTA | |
| 3G54470_L1 | ATTACACGGAGGGAGGAGAAA | AT3G54470 |
| 3G54470_R1 | CCAAACAAAAGAATCATCAACG | |
| 3G54470_L2 | CGTTTTATTGAAATCGCCAAG | |
| 3G54470_R2 | TGTTGTTAGTAAATGAACGATGAGG | |
| 4G03950_L1 | TTGCCTCAATCATCATCTTCC | AT4G03950 |
| 4G03950_R1 | GCATTCCTAGACAAAGAACAAGC | |
| 4G03950_L2 | CCAAACCCTCTTAAACATGTCA | |

| | | |
|---|---|---|
| 4G03950_R2 | AGGTTCAAGCATTCCTAGACAAA | |
| Primers name | Sequence (5' → 3') | Targets |
| 4G13770_L1 | GTGGCCACCTTTAAGCATGTA | AT4G13770 |
| 4G13770_R1 | CGAGTTCGTGAAGGTCAACAT | |
| 4G13770_L2 | TCCCATATTGTGGCTTTCTTG | |
| 4G13770_R2 | CGGGCTTGACTCTCTTAGGAT | |
| 4G33030_L1 | TGATGGAACTTGGACTTGAGC | AT4G33030 |
| 4G33030_R1 | AGGCATGATTTGTTTCGTGTC | |
| 4G33030_L2 | TTGGGCTAGACGTGAAAAAGA | |
| 4G33030_R2 | AGGCTCAAGTCCAAGTTCCAT | |
| 4G39940_L1 | AACACACAGGAGACGACGAGT | AT4G39940 |
| 4G39940_R1 | ATTGGGTTGATTTTTCCGACT | |
| 4G39940_L2 | ACGTCAGATGGCTGAGAACAT | |
| 4G39940_R2 | ACCGAATCAGGGAGAACAATC | |
| 5G03300_L1 | GCATTTGTGGGAGGATTTATG | AT5G03300 |
| 5G03300_R1 | GTTAAAGTCGGGCTTCTCAGG | |
| 5G03300_L2 | GATTGAGGAATGCGTGAAGG | |
| 5G03300_R2 | AAACTGAGGGTAACCCAATTGTT | |
| 5G08570_L1 | CTCGAGAGTCTTGCATCATCC | AT5G08570 |
| 5G08570_R1 | AGCCACGAGATTAGCAGTTGA | |
| 5G08570_L2 | GCAAATGCTGTTCTTGATGGT | |
| 5G08570_R2 | CGGCTTCAATGCAGATCTTAG | |
| 5G14180_L1 | AGATAGCCTGGCTGATGTGAA | AT5G14180 |
| 5G14180_R1 | TTTGGCAGTAACACCCATGAT | |
| 5G14180_L2 | CATACAACATATCGGCGATCC | |
| 5G14180_R2 | TGGTCAAGGAGAAACTCAACG | |

**Supplemental Table II:** Transcriptome data obtained for each kinetic point (30min, 2h and 8h) performed. Differentially regulated genes, in bold face, were selected by statistical analysis based on the Bonferroni method using a P value cut-off of 0.05.
*(cf. electronic data)*

**Supplemental Table III:** Genes found to be differentially expressed in all the comparisons between phenanthrene-treated and phenanthrene+sucrose treated plants. *Arabidopsis* annotation from TAIR, called TAIR10 (most recent versions as of 21 September 2012). Expression changes are given as log2. Expression changes in bolt correspond to genes differentially expressed at the significant threshold of Bonferroni p-value<0.05.

| AGI identifier | Gene annotation | 30 min | 2h | 8h |
|---|---|---|---|---|
| AT1E11140 | EUGENE prediction | -0.03 | -0.02 | **-0.88** |
| AT1E21870 | EUGENE prediction | -0.17 | 0.74 | **0.99** |
| AT1E29130 | EUGENE prediction | -0.06 | **-1.66** | **-1.99** |
| AT1E61070 | EUGENE prediction | -0.28 | **-1.65** | **-2.02** |
| AT1E70680 | EUGENE prediction | -0.04 | 0.23 | **0.86** |
| AT1G01140 | CIPK9_PKS6_SnRK3.12__CBL-interacting protein kinase 9 | **0.89** | -0.16 | x |
| AT1G01170 | Protein of unknown function (DUF1138) | -0.11 | -0.40 | **-1.25** |
| AT1G01470 | LEA14_LSR3__Late embryogenesis abundant protein | 0.44 | x | **-0.83** |
| AT1G01490 | Heavy metal transport/detoxification superfamily protein | 0.00 | -0.51 | **-0.84** |
| AT1G01640 | BTB/POZ domain-containing protein | 0.45 | 0.09 | **0.80** |
| AT1G02080 | transcription regulators | **-0.68** | -0.04 | 0.19 |
| AT1G02305 | Cysteine proteinases superfamily protein | -0.01 | -0.18 | **-0.96** |
| AT1G02400 | ATGA2OX4_ATGA2OX6_DTA1_GA2OX6__gibberellin 2-oxidase 6 | **0.81** | 0.07 | -0.03 |
| AT1G02660 | alpha/beta-Hydrolases superfamily protein | -0.01 | **-0.96** | **-1.36** |
| AT1G02816 | Protein of unknown function, DUF538 | x | -0.56 | **-1.06** |
| AT1G03090 | MCCA__methylcrotonyl-CoA carboxylase alpha chain, mitochondrial / 3-methylcrotonyl-CoA carboxylase 1 (MCCA) | -0.14 | **-1.01** | **-1.61** |
| AT1G03220 | Eukaryotic aspartyl protease family protein | 0.26 | -0.70 | **-1.33** |
| AT1G03230 | Eukaryotic aspartyl protease family protein | 0.14 | -0.44 | **-0.80** |
| AT1G03610 | Protein of unknown function (DUF789) | -0.03 | **-1.05** | -0.68 |
| AT1G03850 | Glutaredoxin family protein | -0.20 | **-1.83** | **-1.53** |
| AT1G03870 | FLA9__FASCICLIN-like arabinoogalactan 9 | -0.51 | **-1.10** | 0.52 |
| AT1G04170 | EIF2 GAMMA__eukaryotic translation initiation factor 2 gamma subunit | -0.45 | 0.45 | **1.28** |
| AT1G04190 | Tetratricopeptide repeat (TPR)-like superfamily protein | -0.20 | 0.34 | **0.95** |
| AT1G04270 | RPS15__cytosolic ribosomal protein S15 | -0.09 | 0.38 | **0.95** |
| AT1G04350 | 2-oxoglutarate (2OG) and Fe(II)-dependent oxygenase superfamily protein | -0.15 | -0.08 | **-0.93** |
| AT1G04400 | AT-PHH1_ATCRY2_CRY2_FHA_PHH1 _cryptochrome 2 | -0.06 | **-1.02** | **-0.85** |
| AT1G04430 | S-adenosyl-L-methionine-dependent methyltransferases superfamily protein | -0.44 | **-0.77** | **0.93** |
| AT1G04680 | Pectin lyase-like superfamily protein | -0.16 | -0.12 | **1.08** |
| AT1G04710 | KAT1_PKT4__peroxisomal 3-ketoacyl-CoA thiolase 4 | -0.01 | -0.32 | **-0.88** |
| AT1G04820 | TOR2_TUA4__tubulin alpha-4 chain | -0.35 | -0.16 | **1.21** |
| AT1G05010 | ACO4_EAT1_EFE__ethylene-forming enzyme | **1.54** | 0.23 | 0.40 |
| AT1G05170 | Galactosyltransferase family protein | -0.04 | **1.10** | 0.23 |
| AT1G05240 | Peroxidase superfamily protein | 0.31 | -0.08 | **1.68** |
| AT1G05250 | Peroxidase superfamily protein | 0.30 | 0.06 | **0.82** |
| AT1G05300 | ZIP5__zinc transporter 5 precursor | 0.06 | 0.34 | **0.87** |
| AT1G05340 | unknown protein | -0.05 | -0.70 | **-1.66** |

| AGI identifier | Gene annotation | 30 min | 2h | 8h |
|---|---|---|---|---|
| AT1G05560 | UGT1_UGT75B1__UDP-glucosyltransferase 75B1 | -0.05 | -0.55 | **-0.93** |
| AT1G05575 | unknown protein | 0.48 | 0.18 | **-1.41** |
| AT1G05670 | Pentatricopeptide repeat (PPR-like) superfamily protein | 0.25 | -0.01 | **-0.72** |
| AT1G05680 | UGT74E2__UDP-glycosyltransferase 74E2 | 0.01 | -0.24 | **-0.93** |
| AT1G05890 | ARI5_ATARI5__RING/U-box superfamily protein | -0.36 | -0.46 | **-0.74** |
| AT1G06000 | UDP-Glycosyltransferase superfamily protein | 0.15 | 0.71 | **0.99** |
| AT1G06400 | ARA-2_ARA2_ATRAB11E_ATRABA1A__Ras-related small GTP-binding family protein | -0.26 | **-0.90** | x |
| AT1G06550 | ATP-dependent caseinolytic (Clp) protease/crotonase family protein | -0.21 | 0.07 | **0.91** |
| AT1G06570 | HPD_PDS1__phytoene desaturation 1 | 0.40 | -0.59 | **-1.89** |
| AT1G06700 | Protein kinase superfamily protein | 0.35 | -0.70 | **-1.52** |
| AT1G06720 | P-loop containing nucleoside triphosphate hydrolases superfamily protein | x | 0.14 | **0.79** |
| AT1G06830 | Glutaredoxin family protein | -0.20 | -0.19 | **0.90** |
| AT1G07040 | unknown protein | -0.32 | -0.19 | **-1.17** |
| AT1G07070 | Ribosomal protein L35Ae family protein | -0.16 | 0.67 | **1.01** |
| AT1G07135 | glycine-rich protein | -0.58 | -0.35 | **-0.83** |
| AT1G07370 | ATPCNA1_PCNA1__proliferating cellular nuclear antigen 1 | -0.28 | 0.48 | **0.95** |
| AT1G07400 | HSP20-like chaperones superfamily protein | 0.20 | **0.92** | -0.29 |
| AT1G07700 | Thioredoxin superfamily protein | 0.02 | -0.04 | **-0.77** |
| AT1G07890 | APX1_ATAPX01_ATAPX1_CS1_MEE6__ascorbate peroxidase 1 | **1.18** | **1.10** | **0.90** |
| AT1G07930 | GTP binding Elongation factor Tu family protein | -0.23 | 0.28 | **0.85** |
| AT1G08090 | ACH1_ATNRT2.1_ATNRT2:1_LIN1_NRT2_NRT2.1_NRT2:1_NRT2;1AT__nitrate transporter 2:1 | 0.18 | 0.03 | **1.05** |
| AT1G08360 | Ribosomal protein L1p/L10e family | -0.15 | 0.41 | **0.83** |
| AT1G08550 | AVDE1_NPQ1__non-photochemical quenching 1 | -0.02 | -0.66 | **-0.85** |
| AT1G08630 | THA1__threonine aldolase 1 | 0.29 | **-0.78** | **-2.09** |
| AT1G08650 | ATPPCK1_PPCK1__phosphoenolpyruvate carboxylase kinase 1 | 0.03 | **1.28** | **0.95** |
| AT1G08920 | ESL1__ERD (early response to dehydration) six-like 1 | -0.37 | 0.08 | **-0.94** |
| AT1G08980 | AMI1_ATAMI1_ATTOC64-I_TOC64-I__amidase 1 | 0.30 | -0.31 | **-0.77** |
| AT1G09070 | (AT)SRC2_SRC2__soybean gene regulated by cold-2 | 0.37 | -0.63 | **-1.32** |
| AT1G09310 | Protein of unknown function, DUF538 | 0.55 | **0.86** | **0.95** |
| AT1G09340 | CRB_CSP41B__chloroplast RNA binding | -0.02 | -0.09 | **-0.72** |
| AT1G09400 | FMN-linked oxidoreductases superfamily protein | 0.18 | -0.32 | **-0.79** |
| AT1G09430 | ACLA-3__ATP-citrate lyase A-3 | 0.09 | -0.31 | **-0.87** |
| AT1G09480 | NAD(P)-binding Rossmann-fold superfamily protein | 0.29 | 0.01 | **-1.02** |
| AT1G09500 | NAD(P)-binding Rossmann-fold superfamily protein | -0.06 | -0.44 | **-1.56** |
| AT1G09590 | Translation protein SH3-like family protein | -0.02 | 0.50 | **0.97** |
| AT1G09690 | Translation protein SH3-like family protein | -0.03 | 0.38 | **0.92** |
| AT1G09830 | Glycinamide ribonucleotide (GAR) synthetase | -0.19 | 0.43 | **0.87** |
| AT1G10020 | Protein of unknown function (DUF1005) | **-0.78** | **-0.95** | -0.41 |
| AT1G10070 | ATBCAT-2_BCAT-2__branched-chain amino acid transaminase 2 | 0.16 | **-1.26** | **-2.69** |
| AT1G10140 | Uncharacterised conserved protein UCP031279 | -0.19 | **-0.87** | **-1.16** |

| AGI identifier | Gene annotation | 30 min | 2h | 8h |
|---|---|---|---|---|
| AT1G10150 | Carbohydrate-binding protein | -0.46 | **-1.75** | **-1.21** |
| AT1G10370 | ATGSTU17_ERD9_GST30_GST30B__Glutathione S-transferase family protein | 0.14 | **0.77** | **0.91** |
| AT1G11530 | ATCXXS1_CXXS1__C-terminal cysteine residue is changed to a serine 1 | 0.21 | **-0.86** | **-1.46** |
| AT1G11700 | Protein of unknown function, DUF584 | **0.68** | -0.13 | 0.13 |
| AT1G11840 | ATGLX1_GLX1__glyoxalase I homolog | x | 0.32 | **1.37** |
| AT1G12110 | ATNRT1_B-1_CHL1_CHL1-1_NRT1_NRT1.1__nitrate transporter 1.1 | 0.56 | **0.94** | x |
| AT1G12250 | Pentapeptide repeat-containing protein | 0.01 | -0.48 | **-1.40** |
| AT1G12440 | A20/AN1-like zinc finger family protein | -0.15 | **-1.03** | **-1.27** |
| AT1G12520 | ATCCS_CCS__copper chaperone for SOD1 | -0.03 | -0.27 | **-0.72** |
| AT1G12560 | ATEXP7_ATEXPA7_ATHEXP ALPHA 1.26_EXP7_EXPA7__expansin A7 | 0.29 | 0.26 | **0.96** |
| AT1G12780 | ATUGE1_UGE1__UDP-D-glucose/UDP-D-galactose 4-epimerase 1 | 0.36 | **-0.84** | **-1.85** |
| AT1G12900 | GAPA-2__glyceraldehyde 3-phosphate dehydrogenase A subunit 2 | -0.06 | -0.07 | **-0.72** |
| AT1G13245 | ROTUNDIFOLIA like 17 (RTFL17) | -0.39 | **-1.06** | **-0.90** |
| AT1G13260 | EDF4_RAV1__related to ABI3/VP1 1 | -0.15 | **-1.09** | **-0.91** |
| AT1G13440 | GAPC-2_GAPC2__glyceraldehyde-3-phosphate dehydrogenase C2 | -0.07 | 0.47 | **0.87** |
| AT1G13930 | Involved in response to salt stress. Knockout mutants are hypersensitive to salt stress. | **0.98** | 0.20 | 0.00 |
| AT1G14120 | 2-oxoglutarate (2OG) and Fe(II)-dependent oxygenase superfamily protein | -0.10 | 0.24 | **0.76** |
| AT1G14200 | RING/U-box superfamily protein | 0.01 | -0.37 | **-0.79** |
| AT1G14290 | SBH2__sphingoid base hydroxylase 2 | -0.32 | **-0.91** | -0.43 |
| AT1G14610 | TWN2_VALRS__valyl-tRNA synthetase / valine--tRNA ligase (VALRS) | -0.28 | 0.18 | **0.82** |
| AT1G14620 | DECOY__decoy | -0.28 | 0.30 | **1.08** |
| AT1G14870 | PCR2__PLANT CADMIUM RESISTANCE 2 | 0.08 | -0.54 | **-1.00** |
| AT1G14880 | PCR1__PLANT CADMIUM RESISTANCE 1 | -0.07 | -0.28 | **-0.78** |
| AT1G14980 | CPN10__chaperonin 10 | -0.21 | 0.54 | **1.07** |
| AT1G15040 | Class I glutamine amidotransferase-like superfamily protein | -0.07 | **-1.17** | **-2.01** |
| AT1G15250 | Zinc-binding ribosomal protein family protein | -0.22 | 0.64 | **0.94** |
| AT1G15380 | Lactoylglutathione lyase / glyoxalase I family protein | -0.26 | **-1.38** | **-2.30** |
| AT1G15440 | ATPWP2_PWP2__periodic tryptophan protein 2 | -0.11 | 0.61 | **0.73** |
| AT1G15670 | Galactose oxidase/kelch repeat superfamily protein | 0.18 | **-0.87** | -0.69 |
| AT1G15740 | Leucine-rich repeat family protein | -0.14 | **-1.00** | **-1.06** |
| AT1G15820 | CP24_LHCB6__light harvesting complex photosystem II subunit 6 | **0.79** | 0.31 | -0.36 |
| AT1G15980 | NDF1_NDH48__NDH-dependent cyclic electron flow 1 | 0.21 | -0.32 | **-1.18** |
| AT1G16240 | ATSYP51_SYP51__syntaxin of plants 51 | -0.22 | **-0.75** | -0.69 |
| AT1G16390 | ATOCT3__organic cation/carnitine transporter 3 | -0.28 | **-0.80** | -0.06 |
| AT1G16410 | BUS1_CYP79F1_SPS1__cytochrome p450 79f1 | -0.05 | 0.46 | **1.24** |
| AT1G16530 | ASL9_LBD3__ASYMMETRIC LEAVES 2-like 9 | 0.13 | 0.26 | **0.92** |
| AT1G16720 | HCF173__high chlorophyll fluorescence phenotype 173 | 0.47 | **-0.82** | **-1.30** |

| AGI identifier | Gene annotation | 30 min | 2h | 8h |
|---|---|---|---|---|
| AT1G16880 | uridylyltransferase-related | 0.51 | 0.15 | **-0.97** |
| AT1G17100 | SOUL heme-binding family protein | 0.20 | 0.65 | **-0.74** |
| AT1G17147 | VQ motif-containing protein | 0.21 | -0.66 | **-1.71** |
| AT1G17180 | ATGSTU25_GSTU25__glutathione S-transferase TAU 25 | 0.15 | 0.59 | **0.72** |
| AT1G17420 | LOX3__lipoxygenase 3 | 0.04 | **0.79** | 0.38 |
| AT1G17560 | HLL__Ribosomal protein L14p/L23e family protein | x | 0.01 | **1.06** |
| AT1G17720 | ATB BETA__Protein phosphatase 2A, regulatory subunit PR55 | **-0.68** | -0.01 | x |
| AT1G17860 | Kunitz family trypsin and protease inhibitor protein | 0.39 | 0.04 | **-0.86** |
| AT1G17880 | ATBTF3_BTF3__basic transcription factor 3 | -0.14 | 0.44 | **0.96** |
| AT1G18020 | FMN-linked oxidoreductases superfamily protein | -0.62 | **-0.90** | **-1.37** |
| AT1G18060 | unknown protein | 0.03 | -0.02 | **-0.78** |
| AT1G18080 | ATARCA_RACK1A_RACK1A_AT__Transducin/WD40 repeat-like superfamily protein | 0.17 | 0.63 | **0.89** |
| AT1G18290 | unknown protein | -0.14 | -0.63 | **-0.78** |
| AT1G18320 | Mitochondrial import inner membrane translocase subunit Tim17/Tim22/Tim23 family protein | -0.06 | 0.36 | **1.14** |
| AT1G18510 | TET16__tetraspanin 16 | -0.14 | -0.26 | **-0.76** |
| AT1G18540 | Ribosomal protein L6 family protein | 0.32 | 0.68 | **1.04** |
| AT1G18700 | DNAJ heat shock N-terminal domain-containing protein | **0.79** | -0.12 | -0.63 |
| AT1G18800 | NRP2__NAP1-related protein 2 | -0.16 | 0.25 | **0.83** |
| AT1G19400 | Erythronate-4-phosphate dehydrogenase family protein | -0.27 | **-0.77** | **-1.10** |
| AT1G19450 | Major facilitator superfamily protein | -0.41 | 0.09 | **1.08** |
| AT1G19520 | NFD5__pentatricopeptide (PPR) repeat-containing protein | -0.46 | 0.27 | **1.08** |
| AT1G19530 | unknown protein | -0.29 | **-2.21** | **-2.48** |
| AT1G19550 | Glutathione S-transferase family protein | 0.38 | **0.82** | 0.53 |
| AT1G19570 | ATDHAR1_DHAR1_DHAR5__dehydroascorbate reductase | 0.35 | **0.79** | **1.06** |
| AT1G19660 | Wound-responsive family protein | -0.01 | **-0.81** | **-1.86** |
| AT1G19770 | ATPUP14_PUP14__purine permease 14 | -0.29 | **-1.29** | **-1.25** |
| AT1G19800 | TGD1__trigalactosyldiacylglycerol 1 | -0.17 | 0.16 | **0.72** |
| AT1G20340 | DRT112_PETE2__Cupredoxin superfamily protein | 0.29 | 0.11 | **-0.74** |
| AT1G20530 | Protein of unknown function (DUF630 and DUF632) | 0.11 | 0.71 | **1.91** |
| AT1G20650 | Protein kinase superfamily protein | **0.73** | -0.70 | -0.68 |
| AT1G20720 | RAD3-like DNA-binding helicase protein | -0.32 | 0.25 | **0.96** |
| AT1G20860 | PHT1;8__phosphate transporter 1;8 | 0.38 | 0.10 | **1.17** |
| AT1G20870 | HSP20-like chaperones superfamily protein | 0.00 | -0.67 | **-2.15** |
| AT1G20925 | Auxin efflux carrier family protein | -0.14 | **-1.73** | **-2.05** |
| AT1G20940 | F-box family protein | x | **-1.75** | **-3.27** |
| AT1G20950 | Phosphofructokinase family protein | 0.21 | -0.36 | **-0.77** |
| AT1G21000 | PLATZ transcription factor family protein | 0.12 | -0.61 | **-0.88** |
| AT1G21080 | DNAJ heat shock N-terminal domain-containing protein | 0.17 | 0.07 | **0.90** |
| AT1G21090 | Cupredoxin superfamily protein | -0.32 | 0.32 | **1.24** |
| AT1G21190 | Small nuclear ribonucleoprotein family protein | -0.14 | -0.06 | **0.91** |
| AT1G21320 | nucleotide binding;nucleic acid binding | 0.12 | 0.46 | **1.11** |
| AT1G21480 | Exostosin family protein | -0.04 | -0.41 | **-1.17** |
| AT1G21525 | unknown protein | -0.05 | 0.45 | **0.93** |
| AT1G21570 | zinc finger (CCCH-type) family protein | -0.01 | 0.07 | **0.71** |

| AGI identifier | Gene annotation | 30 min | 2h | 8h |
|---|---|---|---|---|
| AT1G21680 | DPP6 N-terminal domain-like protein | 0.08 | -0.62 | **-1.46** |
| AT1G21750 | ATPDI5_ATPDIL1-1_PDI5_PDIL1-1__PDI-like 1-1 | 0.16 | 0.28 | **1.13** |
| AT1G21780 | BTB/POZ domain-containing protein | 0.18 | 0.03 | **-0.76** |
| AT1G21910 | Integrase-type DNA-binding superfamily protein | **-1.16** | **-1.04** | -0.19 |
| AT1G21920 | Histone H3 K4-specific methyltransferase SET7/9 family protein | -0.08 | **-0.79** | -0.63 |
| AT1G22070 | TGA3__TGA1A-related gene 3 | 0.02 | **1.05** | **1.16** |
| AT1G22190 | Integrase-type DNA-binding superfamily protein | **-0.74** | **-0.85** | -0.39 |
| AT1G22270 | Trm112p-like protein | 0.03 | **0.74** | **0.75** |
| AT1G22350 | putative UDP-glucose glucosyltransferase | -0.03 | **-1.05** | **-0.84** |
| AT1G22370 | AtUGT85A5_UGT85A5__UDP-glucosyl transferase 85A5 | 0.14 | **-1.36** | **-1.29** |
| AT1G22400 | ATUGT85A1_UGT85A1__UDP-Glycosyltransferase superfamily protein | -0.39 | **-0.97** | **-0.74** |
| AT1G22500 | RING/U-box superfamily protein | 0.20 | -0.34 | **-1.13** |
| AT1G22530 | PATL2__PATELLIN 2 | 0.39 | **-1.09** | -0.45 |
| AT1G22630 | unknown protein | -0.34 | **-0.96** | **-1.22** |
| AT1G22950 | 2-oxoglutarate (2OG) and Fe(II)-dependent oxygenase superfamily protein | -0.14 | -0.03 | **0.74** |
| AT1G23200 | Plant invertase/pectin methylesterase inhibitor superfamily | 0.65 | **1.63** | **1.99** |
| AT1G23280 | MAK16 protein-related | -0.08 | 0.42 | **0.99** |
| AT1G23350 | Plant invertase/pectin methylesterase inhibitor superfamily protein | -0.06 | **-1.14** | **-1.29** |
| AT1G23750 | Nucleic acid-binding, OB-fold-like protein | 0.29 | -0.25 | **-0.82** |
| AT1G23790 | Plant protein of unknown function (DUF936) | **0.88** | x | -0.08 |
| AT1G24020 | MLP423__MLP-like protein 423 | 0.06 | -0.04 | **-0.78** |
| AT1G24290 | AAA-type ATPase family protein | -0.09 | **1.07** | **1.32** |
| AT1G24440 | RING/U-box superfamily protein | 0.02 | -0.64 | **-0.88** |
| AT1G24510 | TCP-1/cpn60 chaperonin family protein | x | 0.01 | **0.78** |
| AT1G25097 | unknown protein | **-0.97** | -0.36 | -0.39 |
| AT1G25260 | Ribosomal protein L10 family protein | -0.10 | 0.43 | **0.71** |
| AT1G25275 | unknown protein | 0.38 | **-0.96** | **-1.03** |
| AT1G25400 | unknown protein | -0.45 | **-1.61** | **-1.32** |
| AT1G26500 | Pentatricopeptide repeat (PPR) superfamily protein | -0.20 | **0.85** | 0.62 |
| AT1G26630 | ATELF5A-2_ELF5A-2_FBR12__Eukaryotic translation initiation factor 5A-1 (eIF-5A 1) protein | 0.60 | 0.37 | **0.77** |
| AT1G26761 | Arabinanase/levansucrase/invertase | -0.11 | **-1.00** | **-1.37** |
| AT1G27030 | unknown protein | -0.04 | -0.05 | **0.92** |
| AT1G27130 | ATGSTU13_GST12_GSTU13__glutathione S-transferase tau 13 | -0.03 | **-1.42** | **-1.54** |
| AT1G27190 | Leucine-rich repeat protein kinase family protein | -0.12 | -0.21 | **-1.63** |
| AT1G27470 | Transducin family protein / WD-40 repeat family protein | -0.12 | 0.45 | **0.73** |
| AT1G27760 | ATSAT32_SAT32__interferon-related developmental regulator family protein / IFRD protein family | 0.27 | **0.91** | 0.67 |
| AT1G27950 | LTPG1__glycosylphosphatidylinositol-anchored lipid protein transfer 1 | 0.58 | 0.50 | **1.12** |
| AT1G28100 | unknown protein | -0.03 | -0.73 | **-0.76** |
| AT1G28110 | SCPL45__serine carboxypeptidase-like 45 | -0.15 | **-0.85** | -0.57 |

| AGI identifier | Gene annotation | 30 min | 2h | 8h |
|---|---|---|---|---|
| AT1G28150 | unknown protein | -0.15 | -0.40 | **-0.82** |
| AT1G28290 | AGP31__arabinogalactan protein 31 | -0.30 | -0.04 | **1.01** |
| AT1G28330 | DRM1_DYL1__dormancy-associated protein-like 1 | -0.26 | **-2.53** | **-2.19** |
| AT1G28340 | AtRLP4_RLP4__receptor like protein 4 | -0.21 | 0.09 | **0.87** |
| AT1G28400 | unknown protein | -0.06 | 0.16 | **0.90** |
| AT1G29070 | Ribosomal protein L34 | 0.03 | 0.58 | **0.96** |
| AT1G29280 | ATWRKY65_WRKY65__WRKY DNA-binding protein 65 | -0.13 | 0.26 | **1.13** |
| AT1G29400 | AML5_ML5__MEI2-like protein 5 | -0.34 | **-0.80** | **-0.80** |
| AT1G29630 | 5'-3' exonuclease family protein | -0.15 | 0.58 | **1.19** |
| AT1G29670 | GDSL-like Lipase/Acylhydrolase superfamily protein | **1.17** | -0.07 | 0.28 |
| AT1G29724 | protein binding | -0.03 | 0.02 | **0.90** |
| AT1G29970 | RPL18AA__60S ribosomal protein L18A-1 | -0.04 | -0.11 | **0.96** |
| AT1G29980 | Protein of unknown function, DUF642 | 0.24 | -0.08 | **-1.01** |
| AT1G30280 | Chaperone DnaJ-domain superfamily protein | -0.59 | **-0.83** | -0.01 |
| AT1G30510 | ATRFNR2_RFNR2__root FNR 2 | 0.50 | 0.60 | **1.09** |
| AT1G30530 | UGT78D1__UDP-glucosyl transferase 78D1 | -0.08 | **0.75** | **1.48** |
| AT1G30580 | GTP binding | -0.33 | 0.21 | **0.87** |
| AT1G30700 | FAD-binding Berberine family protein | 0.41 | -0.18 | **-0.91** |
| AT1G30720 | FAD-binding Berberine family protein | 0.28 | -0.39 | **-0.90** |
| AT1G30730 | FAD-binding Berberine family protein | 0.23 | **-0.93** | **-1.01** |
| AT1G30820 | CTP synthase family protein | -0.25 | **-1.95** | **-1.12** |
| AT1G30870 | Peroxidase superfamily protein | 0.34 | -0.06 | **0.79** |
| AT1G31180 | ATIMD3_IMD3_IPMDH1_isopropylmalate dehydrogenase 3 | **0.88** | 0.57 | **1.24** |
| AT1G31817 | NFD3__Ribosomal L18p/L5e family protein | **-0.68** | **-1.22** | **-0.98** |
| AT1G31930 | XLG3__extra-large GTP-binding protein 3 | -0.28 | 0.37 | **1.86** |
| AT1G31940 | unknown protein | -0.33 | 0.07 | **1.15** |
| AT1G32100 | ATPRR1_PRR1__pinoresinol reductase 1 | **0.74** | 0.10 | -0.17 |
| AT1G32320 | ATMKK10_MKK10__MAP kinase kinase 10 | 0.30 | 0.04 | **-0.86** |
| AT1G32375 | F-box/RNI-like/FBD-like domains-containing protein | 0.10 | 0.59 | **1.06** |
| AT1G32400 | TOM2A__tobamovirus multiplication 2A | 0.12 | 0.46 | **0.91** |
| AT1G32860 | Glycosyl hydrolase superfamily protein | 0.05 | 0.22 | **0.92** |
| AT1G32900 | UDP-Glycosyltransferase superfamily protein | -0.07 | **1.75** | **2.36** |
| AT1G32928 | unknown protein | 0.07 | -0.64 | **-0.97** |
| AT1G33050 | unknown protein | 0.06 | -0.71 | **-0.95** |
| AT1G33110 | MATE efflux family protein | -0.25 | 0.15 | **-0.79** |
| AT1G33140 | PGY2__Ribosomal protein L6 family | -0.02 | 0.21 | **0.74** |
| AT1G33760 | Integrase-type DNA-binding superfamily protein | **-0.79** | -0.04 | -0.07 |
| AT1G33800 | Protein of unknown function (DUF579) | 0.09 | 0.63 | **0.74** |
| AT1G34000 | OHP2__one-helix protein 2 | -0.02 | -0.47 | **-0.97** |
| AT1G34042 | unknown protein | **-0.74** | 0.05 | -0.18 |
| AT1G34047 | Encodes a defensin-like (DEFL) family protein. | 0.12 | -0.31 | **-0.93** |
| AT1G34130 | STT3B__staurosporin and temperature sensitive 3-like b | -0.29 | 0.36 | **0.79** |
| AT1G34355 | ATPS1_PS1__forkhead-associated (FHA) domain-containing protein | 0.06 | -0.34 | **-0.73** |
| AT1G34440 | unknown protein | -0.34 | -0.08 | **-0.92** |
| AT1G34460 | CYC3_CYCB1;5__CYCLIN B1;5 | -0.01 | -0.16 | **-0.90** |
| AT1G34630 | unknown protein | -0.10 | **0.97** | 0.20 |

| AGI identifier | Gene annotation | 30 min | 2h | 8h |
|---|---|---|---|---|
| AT1G34680 | pseudogene, ribosomal maturase | **-0.89** | 0.17 | 0.03 |
| AT1G35140 | EXL7_PHI-1__Phosphate-responsive 1 family protein | -0.21 | **-1.89** | **-2.18** |
| AT1G35160 | 14-3-3PHI_GF14 PHI_GRF4__GF14 protein phi chain | -0.19 | -0.29 | **-1.10** |
| AT1G35350 | EXS (ERD1/XPR1/SYG1) family protein | -0.51 | **-0.75** | -0.46 |
| AT1G35490 | bZIP family transcription factor | 0.39 | 0.27 | **0.93** |
| AT1G35510 | O-fucosyltransferase family protein | 0.15 | **-0.79** | **-1.22** |
| AT1G35550 | elongation factor Tu C-terminal domain-containing protein | x | 0.18 | **0.86** |
| AT1G36230 | unknown protein | -0.33 | 0.10 | **0.98** |
| AT1G37130 | ATNR2_B29_CHL3_NIA2_NIA2-1_NR_NR2__nitrate reductase 2 | 0.16 | -0.62 | **-1.25** |
| AT1G41830 | SKS6_SKS6__SKU5-similar 6 | -0.05 | 0.17 | **1.18** |
| AT1G42440 | unknown protein | -0.04 | 0.58 | **1.28** |
| AT1G43160 | RAP2.6__related to AP2 6 | -0.02 | -0.70 | **-0.94** |
| AT1G43170 | ARP1_emb2207_RP1_RPL3A__ribosomal protein 1 | -0.58 | 0.20 | **1.17** |
| AT1G43670 | Inositol monophosphatase family protein | 0.46 | -0.14 | **-1.11** |
| AT1G43710 | emb1075__Pyridoxal phosphate (PLP)-dependent transferases superfamily protein | -0.10 | 0.68 | **0.83** |
| AT1G43790 | TED6__tracheary element differentiation-related 6 | **0.99** | 0.15 | 0.12 |
| AT1G44350 | ILL6__IAA-leucine resistant (ILR)-like gene 6 | -0.02 | 0.27 | **-0.95** |
| AT1G44750 | ATPUP11_PUP11__purine permease 11 | 0.13 | **1.13** | **1.49** |
| AT1G44960 | SNARE associated Golgi protein family | 0.07 | **-1.03** | -0.59 |
| AT1G45063 | copper ion binding;electron carriers | -0.17 | 0.65 | **1.11** |
| AT1G45201 | TRIACYLGLYCEROL LIPASE-LIKE 1 | 0.09 | 0.61 | **1.74** |
| AT1G45688 | unknown protein | 0.12 | 0.02 | **0.83** |
| AT1G47128 | RD21_RD21A__Granulin repeat cysteine protease family protein | 0.05 | -0.38 | **-0.75** |
| AT1G47240 | ATNRAMP2_NRAMP2__NRAMP metal ion transporter 2 | 0.20 | **-0.81** | **-1.08** |
| AT1G47490 | ATRBP47C_RBP47C__RNA-binding protein 47C | -0.14 | 0.34 | **0.81** |
| AT1G47720 | OSB1__Primosome PriB/single-strand DNA-binding | 0.29 | 0.15 | **-0.82** |
| AT1G47750 | PEX11A__peroxin 11A | -0.05 | -0.31 | **-0.96** |
| AT1G48300 | unknown protein | -0.04 | -0.39 | **-0.97** |
| AT1G48570 | zinc finger (Ran-binding) family protein | 0.03 | 0.34 | **0.89** |
| AT1G48600 | AtPMEAMT_PMEAMT__S-adenosyl-L-methionine-dependent methyltransferases superfamily protein | 0.03 | 0.32 | **1.33** |
| AT1G48760 | delta-ADR__delta-adaptin | 0.26 | 0.32 | **0.95** |
| AT1G48830 | Ribosomal protein S7e family protein | 0.13 | 0.24 | **0.82** |
| AT1G48850 | EMB1144__chorismate synthase, putative / 5-enolpyruvylshikimate-3-phosphate phospholyase, putative | -0.06 | 0.51 | **0.79** |
| AT1G48920 | ATNUC-L1_NUC-L1_PARL1__nucleolin like 1 | -0.15 | 0.69 | **1.00** |
| AT1G49360 | F-box family protein | -0.18 | 0.25 | **0.84** |
| AT1G49570 | Peroxidase superfamily protein | -0.38 | 0.45 | **0.83** |
| AT1G49630 | ATPREP2_PREP2__presequence protease 2 | **0.72** | -0.34 | -0.30 |
| AT1G49780 | PUB26__plant U-box 26 | 0.41 | -0.09 | **1.05** |
| AT1G49880 | Erv1/Alr family protein | -0.03 | -0.54 | **-0.86** |
| AT1G49980 | DNA/RNA polymerases superfamily protein | -0.37 | 0.38 | **0.79** |
| AT1G50280 | Phototropic-responsive NPH3 family protein | 0.14 | -0.34 | **-0.71** |

| AGI identifier | Gene annotation | 30 min | 2h | 8h |
|---|---|---|---|---|
| AT1G50640 | ATERF3_ERF3_ethylene responsive element binding factor 3 | -0.08 | -0.06 | **-0.83** |
| AT1G50920 | Nucleolar GTP-binding protein | -0.21 | 0.30 | **0.76** |
| AT1G51402 | unknown protein | 0.25 | -0.40 | **-0.98** |
| AT1G51630 | O-fucosyltransferase family protein | -0.03 | 0.21 | **0.78** |
| AT1G51980 | Insulinase (Peptidase family M16) protein | 0.19 | 0.69 | **0.94** |
| AT1G52060 | Mannose-binding lectin superfamily protein | **0.98** | -0.04 | **0.90** |
| AT1G52220 | unknown protein | **0.74** | -0.34 | -0.40 |
| AT1G52380 | NUP50 (Nucleoporin 50 kDa) protein | -0.20 | 0.14 | **1.01** |
| AT1G52580 | ATRBL5_RBL5__RHOMBOID-like protein 5 | 0.31 | -0.10 | **-1.10** |
| AT1G52620 | Pentatricopeptide repeat (PPR) superfamily protein | **0.84** | 0.15 | 0.38 |
| AT1G52730 | Transducin family protein / WD-40 repeat family protein | -0.15 | **-0.89** | **-1.33** |
| AT1G52970 | DD11__downregulated in DIF1 11 | -0.27 | 0.43 | **0.80** |
| AT1G53010 | RING/U-box superfamily protein | -0.02 | 0.46 | **0.74** |
| AT1G53040 | Protein of unknown function (DUF616) | 0.03 | **-1.08** | **-1.15** |
| AT1G53240 | mMDH1__Lactate/malate dehydrogenase family protein | -0.23 | 0.56 | **0.85** |
| AT1G53310 | ATPEPC1_ATPPC1_PEPC1_PPC1__phosphoenolpyruvate carboxylase 1 | 0.15 | **0.75** | **1.45** |
| AT1G53320 | AtTLP7_TLP7__tubby like protein 7 | 0.18 | -0.07 | **-0.72** |
| AT1G53380 | Plant protein of unknown function (DUF641) | -0.26 | -0.04 | **0.75** |
| AT1G53480 | MTO 1 RESPONDING DOWN 1 | -0.11 | 0.13 | **0.74** |
| AT1G53500 | ATMUM4_ATRHM2_MUM4_RHM2__NAD-dependent epimerase/dehydratase family protein | -0.08 | 0.31 | **0.87** |
| AT1G53560 | Ribosomal protein L18ae family | 0.35 | -0.16 | **-0.97** |
| AT1G53580 | ETHE1_GLX2-3_GLY3__glyoxalase II 3 | 0.42 | -0.19 | **-1.17** |
| AT1G53645 | hydroxyproline-rich glycoprotein family protein | -0.36 | 0.17 | **0.96** |
| AT1G53670 | ATMSRB1_MSRB1__methionine sulfoxide reductase B 1 | 0.13 | 0.05 | **-0.87** |
| AT1G53890 | Protein of unknown function (DUF567) | -0.08 | **-0.82** | x |
| AT1G54000 | GDSL-like Lipase/Acylhydrolase superfamily protein | 0.27 | 0.27 | **1.07** |
| AT1G54010 | GDSL-like Lipase/Acylhydrolase superfamily protein | 0.09 | 0.41 | **0.91** |
| AT1G54030 | MVP1__GDSL-like Lipase/Acylhydrolase superfamily protein | 0.03 | 0.29 | **1.11** |
| AT1G54100 | ALDH7B4__aldehyde dehydrogenase 7B4 | 0.48 | -0.31 | **-1.24** |
| AT1G54210 | APG12_ATATG12_ATG12A__Ubiquitin-like superfamily protein | -0.09 | **-0.75** | **-1.19** |
| AT1G54270 | EIF4A-2__eif4a-2 | **0.66** | 0.71 | 0.39 |
| AT1G54630 | ACP3__acyl carrier protein 3 | -0.28 | 0.15 | **0.89** |
| AT1G54740 | Protein of unknown function (DUF3049) | **-0.76** | **-2.16** | **-0.87** |
| AT1G54780 | TLP18.3__thylakoid lumen 18.3 kDa protein | 0.01 | -0.03 | **-1.14** |
| AT1G55050 | unknown protein | -0.07 | **-1.12** | **-1.19** |
| AT1G55090 | carbon-nitrogen hydrolase family protein | **-0.68** | -0.13 | -0.50 |
| AT1G55180 | PLDALPHA4_PLDEPSILON__phospholipase D alpha 4 | x | 0.40 | **1.28** |
| AT1G55190 | PRA1.F2_PRA7__PRA1 (Prenylated rab acceptor) family protein | 0.03 | 0.31 | **0.76** |
| AT1G55210 | Disease resistance-responsive (dirigent-like protein) family protein | 0.19 | 0.72 | **0.94** |
| AT1G55510 | BCDH BETA1__branched-chain alpha-keto acid decarboxylase E1 beta subunit | 0.30 | **-0.79** | **-1.95** |

| AGI identifier | Gene annotation | 30 min | 2h | 8h |
|---|---|---|---|---|
| AT1G55850 | ATCSLE1_CSLE1__cellulose synthase like E1 | 0.09 | -0.29 | **-1.09** |
| AT1G55890 | Tetratricopeptide repeat (TPR)-like superfamily protein | -0.24 | 0.44 | **0.80** |
| AT1G55900 | emb1860_TIM50__Haloacid dehalogenase-like hydrolase (HAD) superfamily protein | 0.16 | 0.48 | **0.83** |
| AT1G55910 | ZIP11__zinc transporter 11 precursor | 0.51 | **0.86** | 0.11 |
| AT1G56000 | FAD/NAD(P)-binding oxidoreductase family protein | -0.07 | -0.54 | **-0.96** |
| AT1G56010 | anac021_ANAC022_NAC1_NAC domain containing protein 1 | -0.05 | -0.26 | **-0.80** |
| AT1G56070 | LOS1__Ribosomal protein S5/Elongation factor G/III/V family protein | -0.30 | 0.45 | **0.81** |
| AT1G56110 | NOP56__homolog of nucleolar protein NOP56 | -0.43 | 0.65 | **1.32** |
| AT1G56200 | emb1303__embryo defective 1303 | -0.24 | -0.56 | **-0.90** |
| AT1G56220 | Dormancy/auxin associated family protein | 0.31 | **-1.08** | **-1.54** |
| AT1G56280 | ATDI19_DI19__drought-induced 19 | 0.20 | -0.37 | **-1.29** |
| AT1G56330 | ATSAR1_ATSAR1B_ATSARA1B_SAR1_SAR1B__secretion-associated RAS 1B | 0.13 | 0.12 | **0.93** |
| AT1G56580 | SVB__Protein of unknown function, DUF538 | -0.02 | 0.62 | **0.96** |
| AT1G56650 | ATMYB75_MYB75_PAP1_SIAA1__production of anthocyanin pigment 1 | -0.03 | 0.62 | **1.27** |
| AT1G56700 | Peptidase C15, pyroglutamyl peptidase I-like | -0.25 | -0.57 | **-1.27** |
| AT1G57590 | Pectinacetylesterase family protein | -0.05 | **0.86** | **0.75** |
| AT1G57770 | FAD/NAD(P)-binding oxidoreductase family protein | 0.05 | -0.46 | **-0.80** |
| AT1G57990 | ATPUP18_PUP18__purine permease 18 | 0.27 | **-0.90** | -0.67 |
| AT1G58180 | ATBCA6_BCA6__beta carbonic anhydrase 6 | -0.53 | **-1.53** | **-1.68** |
| AT1G58190 | AtRLP9_RLP9__receptor like protein 9 | 0.18 | **-1.10** | **-1.38** |
| AT1G58210 | EMB1674__kinase interacting family protein | 0.20 | 0.19 | **1.79** |
| AT1G58235 | unknown protein | 0.00 | 0.09 | **-0.83** |
| AT1G58430 | RXF26__GDSL-like Lipase/Acylhydrolase family protein | -0.08 | 0.11 | **0.87** |
| AT1G59840 | CCB4__cofactor assembly of complex C | -0.19 | -0.08 | **0.97** |
| AT1G60140 | ATTPS10_TPS10_TPS10__trehalose phosphate synthase | -0.12 | **-1.08** | **-0.88** |
| AT1G60750 | NAD(P)-linked oxidoreductase superfamily protein | -0.02 | 0.06 | **-0.74** |
| AT1G60770 | Tetratricopeptide repeat (TPR)-like superfamily protein | 0.06 | 0.42 | **1.00** |
| AT1G60940 | SNRK2-10_SNRK2.10_SRK2B__SNF1-related protein kinase 2.10 | 0.08 | -0.42 | **-0.71** |
| AT1G61580 | ARP2_RPL3B__R-protein L3 B | -0.43 | 0.30 | **1.36** |
| AT1G61630 | ATENT7_ENT7__equilibrative nucleoside transporter 7 | 0.49 | 0.26 | **-0.77** |
| AT1G61670 | Lung seven transmembrane receptor family protein | -0.35 | -0.30 | **-0.75** |
| AT1G61820 | BGLU46__beta glucosidase 46 | -0.12 | -0.64 | **-0.76** |
| AT1G61900 | unknown protein | -0.12 | **-0.88** | -0.67 |
| AT1G62130 | AAA-type ATPase family protein | -0.08 | **0.77** | **1.16** |
| AT1G62310 | transcription factor jumonji (jmjC) domain-containing protein | x | -0.17 | **-0.73** |
| AT1G62422 | unknown protein | 0.02 | **0.90** | **1.03** |
| AT1G62660 | Glycosyl hydrolases family 32 protein | 0.39 | -0.65 | **-0.73** |
| AT1G62690 | unknown protein | **0.83** | -0.08 | **-0.75** |

| AGI identifier | Gene annotation | 30 min | 2h | 8h |
|---|---|---|---|---|
| AT1G62960 | ACS10__ACC synthase 10 | -0.06 | -0.11 | **-0.98** |
| AT1G63660 | GMP synthase (glutamine-hydrolyzing), putative / glutamine amidotransferase, putative | -0.15 | 0.31 | **0.93** |
| AT1G64090 | RTNLB3__Reticulan like protein B3 | -0.02 | 0.23 | **0.73** |
| AT1G64170 | ATCHX16_CHX16__cation/H+ exchanger 16 | 0.11 | 0.33 | **0.75** |
| AT1G64190 | 6-phosphogluconate dehydrogenase family protein | -0.13 | 0.52 | **0.85** |
| AT1G64230 | UBC28__ubiquitin-conjugating enzyme 28 | 0.17 | -0.61 | **-1.08** |
| AT1G64350 | SEH1H__Transducin/WD40 repeat-like superfamily protein | -0.03 | 0.28 | **0.77** |
| AT1G64355 | unknown protein | 0.59 | -0.03 | **-1.25** |
| AT1G64385 | unknown protein | 0.02 | **1.08** | **0.87** |
| AT1G64640 | AtENODL8_ENODL8__early nodulin-like protein 8 | **0.90** | 0.35 | 0.49 |
| AT1G64740 | TUA1__alpha-1 tubulin | -0.07 | 0.28 | **1.02** |
| AT1G64760 | O-Glycosyl hydrolases family 17 protein | -0.22 | 0.00 | **0.78** |
| AT1G64900 | CYP89_CYP89A2__cytochrome P450, family 89, subfamily A, polypeptide 2 | 0.33 | **0.96** | **0.82** |
| AT1G65040 | HOMOLOG OF YEAST HRD1 | 0.04 | **0.95** | **1.31** |
| AT1G65130 | Ubiquitin carboxyl-terminal hydrolase-related protein | 0.08 | **-1.04** | **-1.81** |
| AT1G65250 | Protein kinase superfamily protein | 0.20 | -0.12 | **-0.71** |
| AT1G65260 | PTAC4_VIPP1__plastid transcriptionally active 4 | -0.05 | -0.42 | **-0.72** |
| AT1G65410 | ATNAP11_NAP11_TGD3__non-intrinsic ABC protein 11 | 0.23 | -0.52 | **-0.84** |
| AT1G65510 | unknown protein | 0.51 | -0.32 | **-0.95** |
| AT1G65840 | ATPAO4_PAO4__polyamine oxidase 4 | -0.03 | **0.76** | **1.54** |
| AT1G65845 | unknown protein | 0.15 | -0.28 | **-0.91** |
| AT1G65960 | GAD2__glutamate decarboxylase 2 | **0.75** | 0.07 | 0.39 |
| AT1G66150 | TMK1__transmembrane kinase 1 | -0.08 | **-0.90** | -0.34 |
| AT1G66180 | Eukaryotic aspartyl protease family protein | -0.26 | -0.50 | **-0.76** |
| AT1G66200 | ATGSR2_GSR2__glutamine synthase clone F11 | -0.01 | -0.18 | **1.59** |
| AT1G66330 | senescence-associated family protein | **0.71** | -0.61 | **-0.79** |
| AT1G66390 | ATMYB90_MYB90_PAP2__myb domain protein 90 | 0.15 | 0.74 | **1.48** |
| AT1G66430 | pfkB-like carbohydrate kinase family protein | -0.26 | 0.15 | **0.81** |
| AT1G66530 | Arginyl-tRNA synthetase, class Ic | -0.30 | -0.66 | **-0.81** |
| AT1G66670 | CLPP3_NCLPP3__CLP protease proteolytic subunit 3 | -0.15 | -0.06 | **-0.83** |
| AT1G66760 | MATE efflux family protein | 0.29 | 0.02 | **-1.36** |
| AT1G66940 | protein kinase-related | -0.54 | 0.15 | **0.77** |
| AT1G67020 | unknown protein | -0.06 | 0.28 | **-0.72** |
| AT1G67070 | DIN9_PMI2__Mannose-6-phosphate isomerase, type I | 0.27 | -0.52 | **-0.95** |
| AT1G67300 | Major facilitator superfamily protein | 0.09 | **0.98** | 0.38 |
| AT1G67350 | unknown protein | 0.16 | 0.39 | **0.93** |
| AT1G67440 | emb1688__Minichromosome maintenance (MCM2/3/5) family protein | 0.06 | -0.19 | **-1.28** |
| AT1G67500 | ATREV3_REV3__recovery protein 3 | -0.51 | x | **-1.76** |
| AT1G67530 | ARM repeat superfamily protein | 0.09 | -0.56 | **-1.10** |
| AT1G67570 | Protein of unknown function (DUF3537) | 0.00 | **-0.99** | 0.02 |

| AGI identifier | Gene annotation | 30 min | 2h | 8h |
|---|---|---|---|---|
| AT1G67800 | Copine (Calcium-dependent phospholipid-binding protein) family | -0.21 | **-1.24** | **-1.21** |
| AT1G67860 | unknown protein | -0.03 | **0.82** | **1.92** |
| AT1G67870 | glycine-rich protein | 0.10 | -0.64 | **-1.13** |
| AT1G67920 | unknown protein | 0.10 | **0.76** | 0.66 |
| AT1G67940 | ATNAP3_AtSTAR1_NAP3_NAP3_non-intrinsic ABC protein 3 | 0.12 | 0.21 | **0.97** |
| AT1G67980 | CCOAMT__caffeoyl-CoA 3-O-methyltransferase | -0.20 | -0.10 | **-1.40** |
| AT1G68010 | ATHPR1_HPR__hydroxypyruvate reductase | 0.13 | -0.28 | **-1.25** |
| AT1G68420 | Class II aaRS and biotin synthetases superfamily protein | 0.06 | 0.05 | **0.72** |
| AT1G68440 | unknown protein | -0.32 | **-1.19** | **-1.16** |
| AT1G68550 | Integrase-type DNA-binding superfamily protein | x | 0.71 | **0.81** |
| AT1G68560 | ATXYL1_TRG1_XYL1__alpha-xylosidase 1 | -0.10 | 0.24 | **0.84** |
| AT1G68620 | alpha/beta-Hydrolases superfamily protein | x | 0.13 | **-1.29** |
| AT1G69070 | unknown protein | **-0.68** | 0.35 | 0.59 |
| AT1G69170 | Squamosa promoter-binding protein-like (SBP domain) transcription factor family protein | -0.61 | -0.31 | **-1.00** |
| AT1G69430 | unknown protein | -0.09 | -0.22 | **-0.77** |
| AT1G69440 | AGO7_ZIP__Argonaute family protein | 0.12 | -0.54 | **-0.99** |
| AT1G69500 | CYP704B1__cytochrome P450, family 704, subfamily B, polypeptide 1 | 0.12 | **0.74** | **1.13** |
| AT1G69526 | S-adenosyl-L-methionine-dependent methyltransferases superfamily protein | 0.03 | **-0.91** | **-1.40** |
| AT1G69570 | Dof-type zinc finger DNA-binding family protein | -0.19 | 0.14 | **0.73** |
| AT1G69600 | ATHB29_ZFHD1__zinc finger homeodomain 1 | 0.00 | 0.53 | **1.03** |
| AT1G69620 | RPL34__ribosomal protein L34 | -0.29 | 0.08 | **0.78** |
| AT1G69740 | HEMB1__Aldolase superfamily protein | **0.70** | -0.02 | x |
| AT1G69860 | Major facilitator superfamily protein | -0.09 | **-0.85** | -0.58 |
| AT1G69890 | Protein of unknown function (DUF569) | 0.21 | 0.25 | **0.72** |
| AT1G70130 | Concanavalin A-like lectin protein kinase family protein | -0.18 | -0.06 | **0.79** |
| AT1G70230 | TBL27__TRICHOME BIREFRINGENCE-LIKE 27 | -0.16 | **0.86** | **0.86** |
| AT1G70290 | ATTPS8_ATTPSC_TPS8__trehalose-6-phosphatase synthase S8 | **-0.72** | **-1.96** | **-1.28** |
| AT1G70420 | Protein of unknown function (DUF1645) | 0.16 | -0.56 | **-0.77** |
| AT1G70490 | ARFA1D_ATARFA1D__Ras-related small GTP-binding family protein | -0.11 | 0.18 | **0.77** |
| AT1G70530 | CRK3__cysteine-rich RLK (RECEPTOR-like protein kinase) 3 | 0.05 | -0.70 | **-0.81** |
| AT1G70660 | MMZ2_UEV1B__MMS ZWEI homologue 2 | x | -0.50 | **-0.97** |
| AT1G70700 | JAZ9_TIFY7__TIFY domain/Divergent CCT motif family protein | x | 0.24 | **-1.38** |
| AT1G70770 | Protein of unknown function DUF2359, transmembrane | 0.17 | 0.30 | **0.94** |
| AT1G70820 | phosphoglucomutase, putative / glucose phosphomutase, putative | x | **-0.85** | **-1.09** |
| AT1G70900 | unknown protein | 0.03 | 0.55 | **0.85** |
| AT1G70980 | SYNC3__Class II aminoacyl-tRNA and biotin synthetases superfamily protein | -0.30 | 0.31 | **0.80** |
| AT1G71030 | ATMYBL2_MYBL2__MYB-like 2 | -0.39 | **-2.33** | **-1.91** |
| AT1G71500 | Rieske (2Fe-2S) domain-containing protein | -0.18 | -0.30 | **-1.19** |

| AGI identifier | Gene annotation | 30 min | 2h | 8h |
|---|---|---|---|---|
| AT1G71520 | encodes a member of the DREB subfamily A-5 of ERF/AP2 transcription factor family | 0.29 | 0.00 | **-1.28** |
| AT1G71695 | Peroxidase superfamily protein | **0.87** | 0.07 | 0.04 |
| AT1G71980 | Protease-associated (PA) RING/U-box zinc finger family protein | -0.11 | -0.68 | **-0.81** |
| AT1G72040 | P-loop containing nucleoside triphosphate hydrolases superfamily protein | -0.15 | 0.36 | **0.90** |
| AT1G72060 | serine-type endopeptidase inhibitors | 0.10 | -0.64 | **-1.76** |
| AT1G72090 | Methylthiotransferase | -0.41 | 0.27 | **0.84** |
| AT1G72150 | PATL1__PATELLIN 1 | **0.73** | **-1.11** | **-1.44** |
| AT1G72340 | NagB/RpiA/CoA transferase-like superfamily protein | 0.24 | 0.06 | **0.75** |
| AT1G72450 | JAZ6_TIFY11B__jasmonate-zim-domain protein 6 | -0.36 | **0.76** | 0.23 |
| AT1G72490 | unknown protein | 0.02 | -0.16 | **-0.84** |
| AT1G72520 | PLAT/LH2 domain-containing lipoxygenase family protein | 0.01 | **0.81** | 0.18 |
| AT1G72680 | ATCAD1_CAD1__cinnamyl-alcohol dehydrogenase | 0.22 | **-0.97** | **-1.33** |
| AT1G72730 | DEA(D/H)-box RNA helicase family protein | -0.22 | 0.28 | **0.97** |
| AT1G72800 | RNA-binding (RRM/RBD/RNP motifs) family protein | -0.22 | **0.94** | 0.17 |
| AT1G73010 | ATPS2_PS2__phosphate starvation-induced gene 2 | 0.08 | **1.15** | 0.70 |
| AT1G73120 | unknown protein | 0.13 | -0.38 | **-0.87** |
| AT1G73220 | 1-Oct_AtOCT1__organic cation/carnitine transporter1 | -0.38 | 0.44 | **0.80** |
| AT1G73490 | RNA-binding (RRM/RBD/RNP motifs) family protein | **-0.68** | 0.39 | 0.38 |
| AT1G73500 | ATMKK9_MKK9__MAP kinase kinase 9 | -0.32 | -0.51 | **-0.96** |
| AT1G73600 | S-adenosyl-L-methionine-dependent methyltransferases superfamily protein | -0.21 | **0.78** | **1.36** |
| AT1G73620 | Pathogenesis-related thaumatin superfamily protein | 0.08 | 0.30 | **0.79** |
| AT1G73650 | Protein of unknown function (DUF1295) | 0.03 | -0.19 | **-0.72** |
| AT1G73655 | FKBP-like peptidyl-prolyl cis-trans isomerase family protein | 0.20 | -0.36 | **-0.78** |
| AT1G73885 | unknown protein | 0.07 | 0.03 | **-1.01** |
| AT1G73920 | alpha/beta-Hydrolases superfamily protein | -0.27 | **-1.10** | **-1.29** |
| AT1G73940 | unknown protein | -0.11 | 0.32 | **0.88** |
| AT1G74010 | Calcium-dependent phosphotriesterase superfamily protein | 0.13 | 0.51 | **0.98** |
| AT1G74030 | ENO1__enolase 1 | -0.12 | 0.18 | **1.56** |
| AT1G74100 | ATSOT16_ATST5A_CORI-7_SOT16__sulfotransferase 16 | 0.08 | **1.11** | **0.86** |
| AT1G74260 | PUR4__purine biosynthesis 4 | -0.44 | 0.38 | **0.95** |
| AT1G74270 | Ribosomal protein L35Ae family protein | 0.00 | 0.40 | **0.90** |
| AT1G74460 | GDSL-like Lipase/Acylhydrolase superfamily protein | 0.20 | 0.38 | **1.13** |
| AT1G74560 | NRP1__NAP1-related protein 1 | -0.06 | 0.26 | **1.00** |
| AT1G74840 | Homeodomain-like superfamily protein | 0.09 | **-0.91** | -0.42 |
| AT1G74900 | OTP43__Pentatricopeptide repeat (PPR) superfamily protein | -0.14 | **-0.87** | **-0.79** |
| AT1G75040 | PR-5_PR5__pathogenesis-related gene 5 | 0.08 | **0.80** | **0.83** |
| AT1G75220 | Major facilitator superfamily protein | -0.31 | **-1.30** | **-1.38** |
| AT1G75290 | NAD(P)-binding Rossmann-fold superfamily protein | -0.04 | 0.16 | **-0.72** |
| AT1G75380 | ATBBD1_BBD1__bifunctional nuclease in basal defense response 1 | -0.26 | **-1.88** | **-1.14** |
| AT1G75500 | WAT1__Walls Are Thin 1 | 0.12 | 0.11 | **0.76** |
| AT1G75670 | DNA-directed RNA polymerases | 0.09 | **0.75** | **0.83** |

| AGI identifier | Gene annotation | 30 min | 2h | 8h |
|---|---|---|---|---|
| AT1G75690 | DnaJ/Hsp40 cysteine-rich domain superfamily protein | -0.10 | -0.15 | **-1.13** |
| AT1G75750 | GASA1__GAST1 protein homolog 1 | 0.24 | **-0.93** | **-1.58** |
| AT1G75830 | LCR67_PDF1.1__low-molecular-weight cysteine-rich 67 | -0.26 | -0.29 | **-1.06** |
| AT1G76070 | unknown protein | 0.19 | -0.14 | **-0.83** |
| AT1G76080 | ATCDSP32_CDSP32__chloroplastic drought-induced stress protein of 32 kD | 0.07 | -0.41 | **-1.03** |
| AT1G76150 | ATECH2_ECH2__enoyl-CoA hydratase 2 | 0.27 | -0.38 | **-0.74** |
| AT1G76160 | sks5__SKU5 similar 5 | -0.28 | **-0.85** | 0.56 |
| AT1G76180 | ERD14__Dehydrin family protein | **0.97** | -0.05 | **-1.27** |
| AT1G76400 | Ribophorin I | -0.01 | 0.54 | **0.74** |
| AT1G76490 | HMG1_HMGR1__hydroxy methylglutaryl CoA reductase 1 | -0.13 | -0.48 | **-0.79** |
| AT1G76590 | PLATZ transcription factor family protein | -0.14 | **-1.06** | **-1.09** |
| AT1G76600 | unknown protein | -0.21 | **-0.98** | **-1.37** |
| AT1G76670 | Nucleotide-sugar transporter family protein | -0.02 | -0.10 | **0.90** |
| AT1G76680 | ATOPR1_OPR1__12-oxophytodienoate reductase 1 | 0.03 | -0.57 | **-0.97** |
| AT1G76720 | eukaryotic translation initiation factor 2 (eIF-2) family protein | **-0.68** | 0.10 | -0.04 |
| AT1G76790 | O-methyltransferase family protein | -0.13 | 0.38 | **1.57** |
| AT1G76825 | obsolete and replaced by AT1G76820 on 2009-04-27 | **-1.44** | 0.33 | -0.19 |
| AT1G76960 | unknown protein | 0.40 | **0.82** | **1.17** |
| AT1G76980 | unknown protein | 0.43 | **0.74** | -0.36 |
| AT1G77210 | AtSTP14_STP14__sugar transporter 14 | -0.15 | **-1.36** | **-1.46** |
| AT1G77510 | ATPDI6_ATPDIL1-2_PDI6_PDIL1-2__PDI-like 1-2 | -0.02 | 0.42 | **1.08** |
| AT1G77750 | Ribosomal protein S13/S18 family | 0.08 | 0.22 | **0.83** |
| AT1G77760 | GNR1_NIA1_NR1__nitrate reductase 1 | -0.29 | -0.14 | **-1.30** |
| AT1G77940 | Ribosomal protein L7Ae/L30e/S12e/Gadd45 family protein | -0.14 | 0.49 | **0.72** |
| AT1G78290 | SNRK2-8_SNRK2.8_SRK2C__Protein kinase superfamily protein | -0.08 | **-0.76** | -0.26 |
| AT1G78370 | ATGSTU20_GSTU20__glutathione S-transferase TAU 20 | 0.05 | 0.53 | **1.11** |
| AT1G78460 | SOUL heme-binding family protein | 0.18 | -0.63 | **-1.23** |
| AT1G78490 | CYP708A3__cytochrome P450, family 708, subfamily A, polypeptide 3 | -0.36 | 0.26 | **0.93** |
| AT1G78570 | ATRHM1_RHM1_ROL1__rhamnose biosynthesis 1 | 0.13 | 0.69 | **1.61** |
| AT1G78680 | ATGGH2_GGH2__gamma-glutamyl hydrolase 2 | 0.21 | **0.96** | 0.42 |
| AT1G78820 | D-mannose binding lectin protein with Apple-like carbohydrate-binding domain | 0.08 | **-1.19** | **-1.47** |
| AT1G78830 | Curculin-like (mannose-binding) lectin family protein | 0.02 | **-1.60** | **-1.59** |
| AT1G79040 | PSBR__photosystem II subunit R | 0.08 | -0.05 | **-0.79** |
| AT1G79150 | binding | -0.05 | 0.36 | **1.23** |
| AT1G79245 | pseudogene | **-1.04** | 0.14 | -0.03 |
| AT1G79390 | unknown protein | 0.25 | 0.31 | **1.02** |
| AT1G79470 | Aldolase-type TIM barrel family protein | -0.22 | 0.50 | **1.33** |
| AT1G79530 | GAPCP-1__glyceraldehyde-3-phosphate dehydrogenase of plastid 1 | -0.07 | 0.24 | **1.52** |
| AT1G79550 | PGK__phosphoglycerate kinase | 0.06 | 0.59 | **1.05** |
| AT1G79600 | Protein kinase superfamily protein | 0.31 | -0.20 | **-0.78** |
| AT1G79920 | Heat shock protein 70 (Hsp 70) family protein | -0.46 | 0.47 | **0.81** |
| AT1G79930 | HSP91__heat shock protein 91 | -0.11 | 0.21 | **0.78** |

| AGI identifier | Gene annotation | 30 min | 2h | 8h |
|---|---|---|---|---|
| AT1G80070 | EMB14_EMB177_EMB33_SUS2__Pre-mRNA-processing-splicing factor | **-0.84** | 0.07 | 0.46 |
| AT1G80130 | Tetratricopeptide repeat (TPR)-like superfamily protein | -0.02 | 0.47 | **1.06** |
| AT1G80160 | Lactoylglutathione lyase / glyoxalase I family protein | -0.06 | -0.45 | **-1.57** |
| AT1G80180 | unknown protein | 0.49 | -0.71 | **-1.22** |
| AT1G80280 | alpha/beta-Hydrolases superfamily protein | **-0.70** | 0.20 | 0.05 |
| AT1G80380 | P-loop containing nucleoside triphosphate hydrolases superfamily protein | **0.70** | **-0.78** | **-1.59** |
| AT1G80440 | Galactose oxidase/kelch repeat superfamily protein | -0.14 | **-2.70** | **-2.51** |
| AT1G80460 | GLI1_NHO1__Actin-like ATPase superfamily protein | 0.19 | -0.58 | **-0.75** |
| AT1G80530 | Major facilitator superfamily protein | 0.10 | 0.69 | **1.24** |
| AT1G80560 | ATIMD2_IMD2__isopropylmalate dehydrogenase 2 | -0.11 | 0.22 | **0.72** |
| AT1G80750 | Ribosomal protein L30/L7 family protein | 0.11 | **0.83** | **1.00** |
| AT1G80800 | pseudogene | **-0.72** | -0.10 | -0.25 |
| AT1G80920 | J8__Chaperone DnaJ-domain superfamily protein | -0.60 | **-2.95** | **-1.98** |
| AT2E04300 | EUGENE prediction | -0.08 | 0.62 | **1.01** |
| AT2E05040 | EUGENE prediction | **-1.14** | 0.47 | -0.37 |
| AT2E07670 | EUGENE prediction | -0.17 | -0.15 | **-0.98** |
| AT2E07770 | EUGENE prediction | 0.05 | -0.10 | **-0.77** |
| AT2G01140 | Aldolase superfamily protein | 0.15 | 0.35 | **1.07** |
| AT2G01250 | Ribosomal protein L30/L7 family protein | -0.18 | 0.30 | **0.90** |
| AT2G01490 | phytanoyl-CoA dioxygenase (PhyH) family protein | 0.16 | -0.15 | **-0.74** |
| AT2G01540 | Calcium-dependent lipid-binding (CaLB domain) family protein | -0.02 | -0.14 | **-0.77** |
| AT2G01620 | MEE11__RNI-like superfamily protein | 0.16 | 0.11 | **-0.77** |
| AT2G01850 | ATXTH27_EXGT-A3_XTH27__endoxyloglucan transferase A3 | -0.47 | **-1.38** | -0.49 |
| AT2G01860 | EMB975__Tetratricopeptide repeat (TPR)-like superfamily protein | 0.11 | -0.62 | **-0.83** |
| AT2G02010 | GAD4__glutamate decarboxylase 4 | **0.67** | 0.16 | 0.58 |
| AT2G02180 | TOM3__tobamovirus multiplication protein 3 | 0.25 | -0.73 | **-1.36** |
| AT2G02710 | PLP_PLPA_PLPB_PLPC__PAS/LOV protein B | 0.09 | **-1.93** | **-1.67** |
| AT2G02750 | Pentatricopeptide repeat (PPR) superfamily protein | -0.09 | 0.32 | **0.92** |
| AT2G02800 | APK2B__protein kinase 2B | -0.24 | -0.13 | **-0.76** |
| AT2G02950 | PKS1__phytochrome kinase substrate 1 | -0.04 | **-0.77** | -0.42 |
| AT2G02990 | ATRNS1_RNS1__ribonuclease 1 | -0.13 | **1.00** | **1.43** |
| AT2G03090 | ATEXP15_ATEXPA15_ATHEXP ALPHA 1.3_EXP15_EXPA15__expansin A15 | -0.34 | 0.56 | **2.23** |
| AT2G03480 | QUL2__QUASIMODO2 LIKE 2 | -0.21 | 0.19 | **0.82** |
| AT2G03505 | glycosyl hydrolase family protein 17 | 0.12 | 0.11 | **0.71** |
| AT2G03730 | ACR5__ACT domain repeat 5 | -0.12 | **-0.81** | -0.25 |
| AT2G03760 | AtSOT1_AtSOT12_ATST1_RAR047_SOT12_ST_ST1__sulphotransferase 12 | 0.03 | 0.28 | **1.06** |
| AT2G04030 | AtHsp90.5_CR88_EMB1956_Hsp88.1_HSP90.5__Chaperone protein htpG family protein | -0.60 | 0.30 | **0.79** |
| AT2G04050 | MATE efflux family protein | -0.02 | 0.20 | **0.89** |
| AT2G04160 | AIR3__Subtilisin-like serine endopeptidase family protein | 0.05 | 0.43 | **1.13** |

| AGI identifier | Gene annotation | 30 min | 2h | 8h |
|---|---|---|---|---|
| AT2G04390 | Ribosomal S17 family protein | 0.13 | 0.61 | **0.92** |
| AT2G04690 | Pyridoxamine 5'-phosphate oxidase family protein | 0.11 | -0.55 | **-0.72** |
| AT2G04780 | FLA7__FASCICLIN-like arabinoogalactan 7 | 0.11 | 0.23 | **1.12** |
| AT2G04795 | unknown protein | -0.04 | **-0.98** | x |
| AT2G05140 | phosphoribosylaminoimidazole carboxylase family protein / AIR carboxylase family protein | 0.05 | 0.14 | **1.07** |
| AT2G05220 | Ribosomal S17 family protein | -0.27 | 0.54 | **0.81** |
| AT2G05380 | GRP3S__glycine-rich protein 3 short isoform | 0.36 | -0.42 | **-1.09** |
| AT2G05510 | Glycine-rich protein family | -0.12 | -0.37 | **-0.73** |
| AT2G05520 | ATGRP-3_ATGRP3_GRP-3_GRP3__glycine-rich protein 3 | **1.22** | -0.72 | **-1.26** |
| AT2G05530 | Glycine-rich protein family | **0.68** | -0.67 | **-1.14** |
| AT2G05540 | Glycine-rich protein family | 0.16 | **-1.96** | **-2.66** |
| AT2G05620 | PGR5__proton gradient regulation 5 | 0.25 | 0.09 | **-0.96** |
| AT2G05920 | Subtilase family protein | -0.56 | 0.17 | **1.33** |
| AT2G05990 | ENR1_MOD1__NAD(P)-binding Rossmann-fold superfamily protein | -0.33 | 0.35 | **0.90** |
| AT2G06025 | GCN5-related N-acetyltransferase (GNAT) family protein | -0.12 | **-0.96** | **-0.96** |
| AT2G06050 | DDE1_OPR3__oxophytodienoate-reductase 3 | **0.72** | 0.61 | x |
| AT2G06850 | EXGT-A1_EXT_XTH4__xyloglucan endotransglucosylase/hydrolase 4 | -0.40 | **-1.32** | -0.20 |
| AT2G07600 | pseudogene | x | x | **-1.82** |
| AT2G07688 | pseudogene | -0.17 | x | **-0.73** |
| AT2G07689 | NADH-ubiquinone oxidoreductase, putative | **-1.28** | -0.11 | -0.05 |
| AT2G07732 | Ribulose bisphosphate carboxylase large chain, catalytic domain | **-0.67** | x | -0.28 |
| AT2G12462 | unknown protein | 0.13 | -0.02 | **0.76** |
| AT2G13360 | AGT_AGT1_SGAT__alanine:glyoxylate aminotransferase | -0.36 | -0.47 | **-2.17** |
| AT2G13820 | Bifunctional inhibitor/lipid-transfer protein/seed storage 2S albumin superfamily protein | 0.14 | 0.51 | **1.30** |
| AT2G14080 | Disease resistance protein (TIR-NBS-LRR class) family | **-0.73** | **-0.77** | -0.52 |
| AT2G14750 | AKN1_APK_APK1_ATAKN1__APS kinase | -0.30 | **0.82** | **0.79** |
| AT2G14820 | NAKED PINS IN YUC MUTANTS 2, NPY2 | 0.64 | -0.18 | **-0.77** |
| AT2G14860 | Peroxisomal membrane 22 kDa (Mpv17/PMP22) family protein | 0.07 | **0.86** | 0.69 |
| AT2G14890 | AGP9__arabinogalactan protein 9 | -0.10 | 0.04 | **1.25** |
| AT2G14910 | unknown protein | 0.18 | -0.12 | **-0.89** |
| AT2G15020 | unknown protein | **0.69** | -0.29 | -0.12 |
| AT2G15050 | LTP_LTP7__lipid transfer protein | 0.42 | **0.77** | 0.55 |
| AT2G15090 | KCS8__3-ketoacyl-CoA synthase 8 | -0.21 | **-0.75** | 0.24 |
| AT2G15490 | UGT73B4__UDP-glycosyltransferase 73B4 | 0.22 | -0.17 | **-0.92** |
| AT2G15620 | ATHNIR_NIR_NIR1__nitrite reductase 1 | -0.08 | **1.01** | **1.34** |
| AT2G15695 | Protein of unknown function DUF829, transmembrane 53 | -0.03 | -0.36 | **-1.05** |
| AT2G15890 | MEE14__maternal effect embryo arrest 14 | 0.29 | **-1.74** | **-1.51** |
| AT2G15960 | unknown protein | -0.37 | **-2.69** | **-2.44** |
| AT2G16280 | KCS9__3-ketoacyl-CoA synthase 9 | 0.45 | **-0.80** | -0.12 |
| AT2G16340 | unknown protein | 0.29 | 0.07 | **0.71** |
| AT2G16430 | ATPAP10_PAP10__purple acid phosphatase 10 | 0.10 | **0.78** | **1.24** |
| AT2G16586 | unknown protein | -0.35 | -0.28 | **-0.73** |

| AGI identifier | Gene annotation | 30 min | 2h | 8h |
|---|---|---|---|---|
| AT2G16600 | ROC3__rotamase CYP 3 | -0.01 | 0.23 | **0.77** |
| AT2G16660 | Major facilitator superfamily protein | 0.31 | **0.77** | **1.54** |
| AT2G17033 | pentatricopeptide (PPR) repeat-containing protein | -0.01 | -0.52 | **-0.83** |
| AT2G17230 | EXL5__EXORDIUM like 5 | **-0.83** | -0.15 | x |
| AT2G17250 | EMB2762__CCAAT-binding factor | 0.03 | 0.32 | **0.71** |
| AT2G17350 | unknown protein | 0.23 | -0.15 | **-0.72** |
| AT2G17360 | Ribosomal protein S4 (RPS4A) family protein | 0.03 | 0.46 | **1.07** |
| AT2G17450 | RHA3A__RING-H2 finger A3A | 0.22 | -0.51 | **-0.88** |
| AT2G17500 | Auxin efflux carrier family protein | 0.29 | 0.18 | **-0.85** |
| AT2G17630 | Pyridoxal phosphate (PLP)-dependent transferases superfamily protein | -0.02 | 0.37 | **1.27** |
| AT2G17670 | Tetratricopeptide repeat (TPR)-like superfamily protein | 0.05 | 0.37 | **0.84** |
| AT2G17720 | 2-oxoglutarate (2OG) and Fe(II)-dependent oxygenase superfamily protein | 0.38 | 0.34 | **0.72** |
| AT2G17880 | Chaperone DnaJ-domain superfamily protein | -0.25 | **-1.10** | x |
| AT2G18110 | Translation elongation factor EF1B/ribosomal protein S6 family protein | -0.01 | 0.40 | **0.76** |
| AT2G18290 | APC10__anaphase promoting complex 10 | 0.12 | -0.45 | **-0.94** |
| AT2G18420 | Gibberellin-regulated family protein | 0.18 | -0.59 | **-1.74** |
| AT2G18690 | unknown protein | 0.25 | -0.04 | **-0.71** |
| AT2G18700 | ATTPS11_ATTPSB_TPS11_TPS11__trehalose phosphatase/synthase 11 | -0.54 | **-2.44** | **-1.75** |
| AT2G18900 | Transducin family protein / WD-40 repeat family protein | -0.39 | 0.63 | **1.42** |
| AT2G18960 | AHA1_HA1_OST2_PMA__H(+)-ATPase 1 | -0.22 | 0.37 | **0.92** |
| AT2G19350 | Eukaryotic protein of unknown function (DUF872) | 0.07 | -0.35 | **-0.78** |
| AT2G19385 | zinc ion binding | -0.07 | 0.27 | **0.79** |
| AT2G19480 | NAP1;2_NFA02_NFA2__nucleosome assembly protein 1;2 | 0.14 | 0.24 | **0.87** |
| AT2G19520 | ACG1_ATMSI4_FVE_MSI4_NFC04_NFC4__Transducin family protein / WD-40 repeat family protein | -0.38 | 0.17 | **0.72** |
| AT2G19540 | Transducin family protein / WD-40 repeat family protein | 0.08 | 0.53 | **1.12** |
| AT2G19620 | N-MYC downregulated-like 3 (NDL3) | **-0.73** | -0.34 | 0.35 |
| AT2G19670 | *ARABIDOPSIS THALIANA* PROTEIN ARGININE METHYLTRANSFERASE 1A | -0.13 | 0.35 | **0.77** |
| AT2G19730 | Ribosomal L28e protein family | -0.06 | 0.33 | **0.71** |
| AT2G19750 | Ribosomal protein S30 family protein | 0.18 | 0.72 | **1.10** |
| AT2G19800 | MIOX2__myo-inositol oxygenase 2 | -0.10 | **-2.51** | **-1.33** |
| AT2G19860 | ATHXK2 (HEXOKINASE 2) | 0.14 | 0.45 | **0.93** |
| AT2G20060 | Ribosomal protein L4/L1 family | -0.12 | 0.10 | **0.75** |
| AT2G20230 | Tetraspanin family protein | 0.06 | -0.35 | **-0.76** |
| AT2G20260 | PSAE-2__photosystem I subunit E-2 | **0.93** | 0.14 | -0.28 |
| AT2G20420 | ATP citrate lyase (ACL) family protein | -0.13 | 0.15 | **0.78** |
| AT2G20450 | Ribosomal protein L14 | -0.28 | 0.61 | **1.15** |
| AT2G20490 | NOP10 | -0.22 | 0.57 | **1.17** |
| AT2G20610 | ALF1_HLS3_RTY_RTY1_SUR1__Tyrosine transaminase family protein | -0.13 | 0.61 | **0.71** |
| AT2G20670 | Protein of unknown function (DUF506) | **-0.89** | **-1.86** | **-1.65** |
| AT2G20740 | Tetraspanin family protein | 0.03 | -0.22 | **-0.97** |

| AGI identifier | Gene annotation | 30 min | 2h | 8h |
|---|---|---|---|---|
| AT2G20920 | Protein of unknown function (DUF3353) | -0.10 | -0.25 | **-1.00** |
| AT2G21045 | Rhodanese/Cell cycle control phosphatase superfamily protein | 0.38 | -0.19 | **0.72** |
| AT2G21050 | LAX2__like AUXIN RESISTANT 2 | 0.42 | 0.47 | **1.00** |
| AT2G21300 | ATP binding microtubule motor family protein | -0.26 | 0.17 | **0.72** |
| AT2G21320 | B-box zinc finger family protein | 0.13 | **0.75** | -0.08 |
| AT2G21390 | Coatomer, alpha subunit | -0.26 | 0.00 | **0.74** |
| AT2G21580 | Ribosomal protein S25 family protein | -0.21 | 0.67 | **1.03** |
| AT2G21640 | Encodes a protein of unknown function that is a marker for oxidative stress response. | -0.15 | 0.02 | **1.30** |
| AT2G21660 | ATGRP7_CCR2_GR-RBP7_GRP7__cold, circadian rhythm, and rna binding 2 | -0.04 | 0.40 | **0.93** |
| AT2G21960 | unknown protein | 0.06 | -0.05 | **-1.01** |
| AT2G21970 | SEP2__stress enhanced protein 2 | 0.35 | -0.46 | **-1.09** |
| AT2G22170 | Lipase/lipooxygenase, PLAT/LH2 family protein | 0.00 | -0.24 | **0.92** |
| AT2G22400 | S-adenosyl-L-methionine-dependent methyltransferases superfamily protein | -0.31 | 0.39 | **0.81** |
| AT2G22500 | ATPUMP5_DIC1_UCP5__uncoupling protein 5 | **0.69** | **0.93** | 0.46 |
| AT2G22510 | hydroxyproline-rich glycoprotein family protein | 0.04 | 0.37 | **0.83** |
| AT2G22900 | Galactosyl transferase GMA12/MNN10 family protein | 0.09 | 0.20 | **0.80** |
| AT2G23110 | Late embryogenesis abundant protein, group 6 | -0.03 | -0.70 | **-1.53** |
| AT2G23120 | Late embryogenesis abundant protein, group 6 | 0.59 | -0.38 | **-0.96** |
| AT2G23810 | TET8__tetraspanin8 | -0.56 | **-0.76** | -0.65 |
| AT2G24100 | unknown protein | -0.07 | -0.49 | **-0.78** |
| AT2G24170 | Endomembrane protein 70 protein family | -0.14 | 0.23 | **1.03** |
| AT2G24550 | unknown protein | -0.13 | **-1.61** | **-0.96** |
| AT2G24590 | RNA recognition motif and CCHC-type zinc finger domains containing protein | -0.09 | 0.42 | **0.87** |
| AT2G24730 | 60S ribosomal protein L4/L1 (RPL4C), pseudogene | 0.10 | 0.48 | **1.25** |
| AT2G24762 | AtGDU4_GDU4__glutamine dumper 4 | -0.03 | 0.26 | **0.94** |
| AT2G25080 | ATGPX1_GPX1__glutathione peroxidase 1 | **0.67** | -0.07 | -0.61 |
| AT2G25090 | CIPK16_SnRK3.18__CBL-interacting protein kinase 16 | -0.01 | -0.42 | **-0.80** |
| AT2G25200 | Plant protein of unknown function (DUF868) | -0.47 | -0.69 | **-0.74** |
| AT2G25210 | Ribosomal protein L39 family protein | -0.02 | 0.37 | **0.96** |
| AT2G25450 | 2-oxoglutarate (2OG) and Fe(II)-dependent oxygenase superfamily protein | -0.17 | **-1.25** | x |
| AT2G25540 | CESA10__cellulose synthase 10 | -0.33 | -0.20 | **0.74** |
| AT2G25625 | unknown protein | 0.33 | 0.49 | **1.17** |
| AT2G25735 | unknown protein | 0.09 | -0.48 | **-0.82** |
| AT2G25900 | ATCTH_ATTZF1__Zinc finger C-x8-C-x5-C-x3-H type family protein | -0.17 | **-1.21** | **-0.93** |
| AT2G26250 | FDH_KCS10__3-ketoacyl-CoA synthase 10 | **0.73** | 0.20 | 0.07 |
| AT2G26340 | unknown protein | -0.33 | -0.20 | **-0.74** |
| AT2G26500 | cytochrome b6f complex subunit (petM), putative | 0.09 | -0.10 | **-1.01** |
| AT2G26530 | AR781__Protein of unknown function (DUF1645) | 0.27 | 0.04 | **-0.78** |
| AT2G26560 | PLA IIA_PLA2A_PLP2_PLP2__phospholipase A 2A | 0.25 | -0.63 | **-0.78** |
| AT2G26670 | ATHO1_GUN2_HO1_HY1_HY6_TED4__Plant haem oxygenase (decyclizing) family protein | 0.19 | -0.30 | **-0.85** |

| AGI identifier | Gene annotation | 30 min | 2h | 8h |
|---|---|---|---|---|
| AT2G26740 | ATSEH_SEH__soluble epoxide hydrolase | -0.13 | 0.05 | **-0.83** |
| AT2G26975 | unknown protein | 0.28 | -0.20 | **-0.96** |
| AT2G27040 | AGO4_OCP11__Argonaute family protein | -0.40 | 0.31 | **0.72** |
| AT2G27050 | AtEIL1_EIL1__ETHYLENE-INSENSITIVE3-like 1 | 0.59 | -0.58 | **-0.77** |
| AT2G27290 | Protein of unknown function (DUF1279) | -0.13 | -0.18 | **-0.78** |
| AT2G27402 | unknown protein | 0.29 | 0.05 | **1.43** |
| AT2G27420 | Cysteine proteinases superfamily protein | 0.36 | **0.76** | 0.00 |
| AT2G27510 | ATFD3_FD3__ferredoxin 3 | -0.03 | 0.74 | **1.11** |
| AT2G27530 | PGY1__Ribosomal protein L1p/L10e family | 0.36 | 0.55 | **1.18** |
| AT2G27550 | ATC__centroradialis | 0.04 | 0.66 | **1.67** |
| AT2G27710 | 60S acidic ribosomal protein family | -0.37 | 0.32 | **0.87** |
| AT2G27830 | unknown protein | -0.26 | **-1.26** | **-1.52** |
| AT2G27840 | HDA13_HDT04_HDT4__histone deacetylase-related / HD-related | -0.10 | **0.96** | **1.28** |
| AT2G28000 | CH-CPN60A_CPN60A_SLP__chaperonin-60alpha | 0.30 | 0.63 | **0.80** |
| AT2G28110 | FRA8_IRX7__Exostosin family protein | 0.03 | -0.37 | **-0.86** |
| AT2G28120 | Major facilitator superfamily protein | 0.08 | **-1.03** | **-1.12** |
| AT2G28315 | Nucleotide/sugar transporter family protein | 0.04 | -0.06 | **0.76** |
| AT2G28460 | Cysteine/Histidine-rich C1 domain family protein | **-0.66** | -0.41 | 0.09 |
| AT2G28510 | Dof-type zinc finger DNA-binding family protein | 0.09 | 0.58 | **1.02** |
| AT2G28600 | P-loop containing nucleoside triphosphate hydrolases superfamily protein | 0.08 | 0.37 | **0.80** |
| AT2G28820 | pseudogene | **-1.30** | 0.28 | -0.44 |
| AT2G28900 | ATOEP16-1_ATOEP16-L_OEP16_OEP16-1__outer plastid envelope protein 16-1 | -0.02 | **1.12** | **2.09** |
| AT2G28950 | ATEXP6_ATEXPA6_ATHEXP ALPHA 1.8_EXPA6__expansin A6 | 0.15 | 0.19 | **0.99** |
| AT2G29310 | NAD(P)-binding Rossmann-fold superfamily protein | 0.20 | **-0.90** | **-1.18** |
| AT2G29340 | NAD-dependent epimerase/dehydratase family protein | 0.51 | -0.37 | **-1.37** |
| AT2G29420 | ATGSTU7_GST25_GSTU7__glutathione S-transferase tau 7 | 0.33 | -0.21 | **-1.25** |
| AT2G29440 | ATGSTU6_GST24_GSTU6__glutathione S-transferase tau 6 | 0.02 | 0.18 | **-0.73** |
| AT2G29460 | ATGSTU4_GST22_GSTU4__glutathione S-transferase tau 4 | 0.05 | 0.10 | **-0.76** |
| AT2G29470 | ATGSTU3_GST21_GSTU3__glutathione S-transferase tau 3 | 0.09 | 0.08 | **-0.71** |
| AT2G29530 | TIM10__Tim10/DDP family zinc finger protein | -0.52 | 0.45 | **1.03** |
| AT2G29670 | Tetratricopeptide repeat (TPR)-like superfamily protein | 0.29 | **0.82** | **1.42** |
| AT2G29720 | CTF2B__FAD/NAD(P)-binding oxidoreductase family protein | 0.29 | 0.06 | **-0.98** |
| AT2G30040 | MAPKKK14__mitogen-activated protein kinase kinase kinase 14 | -0.02 | **-0.78** | **-0.74** |
| AT2G30490 | ATC4H_C4H_CYP73A5_REF3__cinnamate-4-hydroxylase | 0.03 | 0.17 | **0.96** |
| AT2G30520 | RPT2__Phototropic-responsive NPH3 family protein | 0.37 | **-0.90** | **-1.09** |
| AT2G30600 | BTB/POZ domain-containing protein | -0.16 | **-0.88** | **-1.08** |
| AT2G30790 | PSBP-2__photosystem II subunit P-2 | -0.32 | 0.30 | **0.89** |
| AT2G30830 | 2-oxoglutarate (2OG) and Fe(II)-dependent oxygenase superfamily protein | -0.47 | 0.20 | **1.20** |
| AT2G30860 | ATGSTF7_ATGSTF9_GLUTTR_GSTF9__glutathione S-transferase PHI 9 | -0.10 | 0.46 | **1.38** |

| AGI identifier | Gene annotation | 30 min | 2h | 8h |
|---|---|---|---|---|
| AT2G30870 | ATGSTF10_ATGSTF4_ERD13_GSTF10__glutathione S-transferase PHI 10 | **0.94** | 0.60 | **0.83** |
| AT2G31010 | Protein kinase superfamily protein | 0.04 | -0.12 | **-0.85** |
| AT2G31140 | unknown protein | -0.03 | 0.28 | **0.73** |
| AT2G31370 | Basic-leucine zipper (bZIP) transcription factor family protein | -0.02 | 0.30 | **1.16** |
| AT2G31430 | Plant invertase/pectin methylesterase inhibitor superfamily protein | 0.40 | 0.24 | **0.73** |
| AT2G31460 | Domain of unknown function (DUF313) | 0.61 | x | **-1.04** |
| AT2G31560 | unknown protein | -0.09 | 0.30 | **0.76** |
| AT2G31610 | Ribosomal protein S3 family protein | 0.21 | **0.75** | **1.55** |
| AT2G31660 | SAD2_URM9__ARM repeat superfamily protein | -0.05 | **-1.00** | **-1.50** |
| AT2G31780 | ARI11_ATARI11__RING/U-box superfamily protein | **0.66** | 0.34 | **-0.86** |
| AT2G31810 | ACT domain-containing small subunit of acetolactate synthase protein | **-0.83** | **-1.55** | **-1.17** |
| AT2G31860 | pseudogene | 0.21 | -0.22 | **-1.02** |
| AT2G31945 | unknown protein | 0.04 | **-1.02** | **-1.88** |
| AT2G32060 | Ribosomal protein L7Ae/L30e/S12e/Gadd45 family protein | -0.25 | 0.63 | **1.17** |
| AT2G32150 | Haloacid dehalogenase-like hydrolase (HAD) superfamily protein | -0.24 | **-1.69** | **-1.26** |
| AT2G32220 | Ribosomal L27e protein family | 0.02 | 0.66 | **1.01** |
| AT2G32690 | ATGRP23_GRP23__glycine-rich protein 23 | **0.90** | -0.55 | 0.30 |
| AT2G32720 | ATCB5-B_B5 #4_CB5-B__cytochrome B5 isoform B | -0.09 | 0.25 | **0.93** |
| AT2G32800 | AP4.3A__protein kinase family protein | 0.06 | **-0.82** | **-0.71** |
| AT2G32990 | AtGH9B8_GH9B8__glycosyl hydrolase 9B8 | 0.20 | 0.33 | **0.85** |
| AT2G33150 | KAT2_PED1_PKT3__peroxisomal 3-ketoacyl-CoA thiolase 3 | 0.45 | -0.22 | **-0.94** |
| AT2G33210 | HSP60-2__heat shock protein 60-2 | -0.19 | 0.21 | **1.43** |
| AT2G33250 | unknown protein | -0.30 | -0.35 | **-0.87** |
| AT2G33830 | Dormancy/auxin associated family protein | 0.24 | **-2.39** | **-2.08** |
| AT2G33840 | Tyrosyl-tRNA synthetase, class Ib, bacterial/mitochondrial | 0.11 | 0.25 | **0.78** |
| AT2G33850 | unknown protein | 0.12 | -0.01 | **0.83** |
| AT2G34357 | ARM repeat superfamily protein | -0.21 | 0.27 | **0.77** |
| AT2G34410 | REDUCED WALL ACETYLATION 3 | 0.01 | -0.26 | **-0.97** |
| AT2G34430 | LHB1B1_LHCB1.4__light-harvesting chlorophyll-protein complex II subunit B1 | 0.23 | -0.38 | **-1.07** |
| AT2G34480 | Ribosomal protein L18ae/LX family protein | -0.37 | 0.32 | **1.02** |
| AT2G34490 | CYP710A2__cytochrome P450, family 710, subfamily A, polypeptide 2 | -0.05 | 0.72 | **0.89** |
| AT2G34570 | MEE21__PIN domain-like family protein | -0.14 | 0.51 | **0.71** |
| AT2G34750 | RNA polymerase I specific transcription initiation factor RRN3 protein | -0.35 | 0.14 | **0.80** |
| AT2G34770 | ATFAH1_FAH1__fatty acid hydroxylase 1 | -0.21 | **-0.87** | -0.16 |
| AT2G34890 | CTP synthase family protein | 0.06 | **-1.22** | -0.54 |
| AT2G35040 | AICARFT/IMPCHase bienzyme family protein | 0.12 | 0.28 | **1.06** |
| AT2G35120 | Single hybrid motif superfamily protein | -0.09 | 0.23 | **0.72** |
| AT2G35190 | ATNPSN11_NPSN11_NSPN11__novel plant snare 11 | -0.12 | -0.15 | **0.76** |
| AT2G35860 | FLA16__FASCICLIN-like arabinogalactan protein 16 precursor | -0.19 | 0.40 | **1.37** |

| AGI identifier | Gene annotation | 30 min | 2h | 8h |
|---|---|---|---|---|
| AT2G36070 | ATTIM44-2_TIM44-2__translocase inner membrane subunit 44-2 | -0.06 | 0.32 | **0.93** |
| AT2G36170 | Ubiquitin supergroup;Ribosomal protein L40e | -0.04 | 0.50 | **0.72** |
| AT2G36230 | APG10_HISN3__Aldolase-type TIM barrel family protein | x | 0.16 | **0.71** |
| AT2G36310 | URH1__uridine-ribohydrolase 1 | -0.09 | **-1.27** | **-0.81** |
| AT2G36320 | A20/AN1-like zinc finger family protein | 0.10 | **-1.39** | **-1.43** |
| AT2G36390 | BE3_SBE2.1__starch branching enzyme 2.1 | -0.38 | 0.48 | **0.81** |
| AT2G36530 | ENO2_LOS2__Enolase | -0.15 | 0.73 | **1.50** |
| AT2G36570 | Leucine-rich repeat protein kinase family protein | -0.11 | 0.28 | **0.78** |
| AT2G36590 | ATPROT3_ProT3__proline transporter 3 | -0.05 | **1.60** | **1.41** |
| AT2G36620 | RPL24A__ribosomal protein L24 | -0.19 | 0.38 | **1.15** |
| AT2G36770 | UDP-Glycosyltransferase superfamily protein | 0.18 | **-0.90** | **-1.18** |
| AT2G36830 | GAMMA-TIP_GAMMA-TIP1_TIP1;1__gamma tonoplast intrinsic protein | **0.82** | 0.24 | -0.55 |
| AT2G36835 | unknown protein | -0.11 | -0.15 | **-0.94** |
| AT2G36870 | XTH32__xyloglucan endotransglucosylase/hydrolase 32 | 0.40 | 0.67 | **1.10** |
| AT2G36880 | MAT3__methionine adenosyltransferase 3 | 0.18 | **0.92** | **1.32** |
| AT2G36895 | unknown protein | -0.09 | -0.42 | **-0.96** |
| AT2G36950 | Heavy metal transport/detoxification superfamily protein | 0.16 | -0.58 | **-1.40** |
| AT2G37040 | ATPAL1_PAL1__PHE ammonia lyase 1 | **0.91** | 0.38 | 0.59 |
| AT2G37130 | Peroxidase superfamily protein | x | -0.09 | **-0.93** |
| AT2G37190 | Ribosomal protein L11 family protein | 0.46 | 0.39 | **1.00** |
| AT2G37250 | ADK_ATPADK1__adenosine kinase | x | 0.59 | **1.14** |
| AT2G37270 | ATRPS5B_RPS5B__ribosomal protein 5B | -0.02 | 0.60 | **0.91** |
| AT2G37400 | Tetratricopeptide repeat (TPR)-like superfamily protein | -0.01 | 0.28 | **0.73** |
| AT2G37540 | NAD(P)-binding Rossmann-fold superfamily protein | -0.01 | -0.55 | **-0.77** |
| AT2G37550 | AGD7_ASP1__ARF-GAP domain 7 | 0.12 | -0.15 | **0.71** |
| AT2G37600 | Ribosomal protein L36e family protein | -0.08 | 0.29 | **0.74** |
| AT2G37710 | RLK__receptor lectin kinase | 0.31 | **0.80** | **0.95** |
| AT2G37750 | unknown protein | 0.07 | **-0.98** | **-1.91** |
| AT2G37770 | NAD(P)-linked oxidoreductase superfamily protein | 0.00 | **1.10** | 0.64 |
| AT2G37830 | pseudogene | **0.66** | -0.03 | x |
| AT2G37970 | SOUL-1__SOUL heme-binding family protein | 0.47 | -0.26 | **-1.20** |
| AT2G37990 | ribosome biogenesis regulatory protein (RRS1) family protein | 0.08 | 0.49 | **0.86** |
| AT2G38170 | ATCAX1_CAX1_RCI4__cation exchanger 1 | -0.09 | **1.44** | **1.12** |
| AT2G38210 | PDX1L4__putative PDX1-like protein 4 | 0.05 | 0.20 | **-0.85** |
| AT2G38240 | 2-oxoglutarate (2OG) and Fe(II)-dependent oxygenase superfamily protein | -0.16 | **-0.90** | x |
| AT2G38360 | PRA1.B4__prenylated RAB acceptor 1.B4 | -0.17 | 0.50 | **0.84** |
| AT2G38400 | AGT3__alanine:glyoxylate aminotransferase 3 | -0.22 | **-1.11** | **-1.78** |
| AT2G38540 | ATLTP1_LP1_LTP1__lipid transfer protein 1 | 0.41 | **1.08** | **1.29** |
| AT2G38550 | Transmembrane proteins 14C | -0.23 | 0.26 | **0.92** |
| AT2G38700 | ATMVD1_MVD1_mevalonate diphosphate decarboxylase 1 | -0.01 | 0.11 | **1.07** |
| AT2G38740 | Haloacid dehalogenase-like hydrolase (HAD) superfamily protein | 0.03 | 0.47 | **0.71** |
| AT2G38750 | ANNAT4__annexin 4 | 0.14 | **1.04** | **1.12** |

| AGI identifier | Gene annotation | 30 min | 2h | 8h |
|---|---|---|---|---|
| AT2G38820 | Protein of unknown function (DUF506) | -0.07 | **-1.00** | x |
| AT2G38870 | Serine protease inhibitor, potato inhibitor I-type family protein | 0.41 | x | **-1.75** |
| AT2G38940 | ATPT2_PHT1;4__phosphate transporter 1;4 | 0.14 | **1.64** | **1.95** |
| AT2G39000 | Acyl-CoA N-acyltransferases (NAT) superfamily protein | 0.01 | -0.63 | **-1.27** |
| AT2G39130 | Transmembrane amino acid transporter family protein | 0.13 | 0.40 | **0.82** |
| AT2G39310 | JAL22__jacalin-related lectin 22 | 0.17 | -0.20 | **0.90** |
| AT2G39390 | Ribosomal L29 family protein | -0.10 | 0.57 | **0.87** |
| AT2G39400 | alpha/beta-Hydrolases superfamily protein | 0.28 | **-1.71** | **-1.77** |
| AT2G39450 | ATMTP11_MTP11__Cation efflux family protein | 0.03 | 0.06 | **-0.76** |
| AT2G39460 | ATRPL23A_RPL23A_RPL23AA__ribosomal protein L23AA | 0.42 | 0.66 | **1.17** |
| AT2G39480 | PGP6__P-glycoprotein 6 | -0.18 | -0.26 | **-1.16** |
| AT2G39570 | ACT domain-containing protein | -0.48 | **-2.66** | **-2.01** |
| AT2G39580 | unknown protein | **-0.90** | -0.47 | -0.24 |
| AT2G39700 | ATEXPA4 (*ARABIDOPSIS THALIANA* EXPANSIN A4) | 0.12 | 0.32 | **1.11** |
| AT2G39730 | RCA__rubisco activase | 0.10 | 0.20 | **-1.14** |
| AT2G39795 | Mitochondrial glycoprotein family protein | -0.01 | 0.33 | **0.74** |
| AT2G39820 | Translation initiation factor IF6 | -0.02 | 0.42 | **0.78** |
| AT2G39870 | unknown protein | **-0.67** | -0.05 | 0.13 |
| AT2G39900 | GATA type zinc finger transcription factor family protein | -0.24 | 0.30 | **0.85** |
| AT2G40000 | ATHSPRO2_HSPRO2__ortholog of sugar beet HS1 PRO-1 2 | **0.74** | **-2.11** | **-1.12** |
| AT2G40010 | Ribosomal protein L10 family protein | 0.43 | 0.45 | **0.80** |
| AT2G40360 | Transducin family protein / WD-40 repeat family protein | -0.05 | 0.57 | **1.07** |
| AT2G40420 | Transmembrane amino acid transporter family protein | -0.04 | -0.28 | **-1.35** |
| AT2G40475 | unknown protein | 0.20 | 0.72 | **1.04** |
| AT2G40590 | Ribosomal protein S26e family protein | 0.08 | 0.56 | **0.93** |
| AT2G40840 | DPE2__disproportionating enzyme 2 | 0.06 | 0.71 | **1.53** |
| AT2G41090 | Calcium-binding EF-hand family protein | -0.16 | 0.40 | **0.98** |
| AT2G41100 | ATCAL4_TCH3__Calcium-binding EF hand family protein | 0.03 | -0.63 | **-0.81** |
| AT2G41220 | GLU2__glutamate synthase 2 | -0.35 | 0.25 | **1.27** |
| AT2G41250 | Haloacid dehalogenase-like hydrolase (HAD) superfamily protein | 0.03 | **-1.41** | -0.52 |
| AT2G41420 | proline-rich family protein | -0.29 | **-0.77** | -0.62 |
| AT2G41430 | CID1_ERD15_LSR1__dehydration-induced protein (ERD15) | -0.25 | **-1.18** | **-0.99** |
| AT2G41475 | unknown protein | 0.25 | 0.07 | **0.94** |
| AT2G41650 | unknown protein | -0.51 | 0.47 | **1.23** |
| AT2G41800 | Protein of unknown function, DUF642 | -0.09 | 0.60 | **1.22** |
| AT2G41840 | Ribosomal protein S5 family protein | -0.09 | 0.47 | **1.00** |
| AT2G42170 | actin, putative | 0.44 | -0.47 | **-0.89** |
| AT2G42395 | unknown protein | 0.11 | 0.06 | **0.80** |
| AT2G42540 | COR15_COR15A__cold-regulated 15a | 0.14 | **0.90** | **0.90** |
| AT2G42590 | GF14 MU_GRF9__general regulatory factor 9 | 0.02 | -0.29 | **-0.89** |
| AT2G42600 | ATPPC2_PPC2__phosphoenolpyruvate carboxylase 2 | 0.17 | 0.62 | **0.81** |
| AT2G42740 | RPL16A__ribosomal protein large subunit 16A | -0.24 | 0.44 | **1.03** |
| AT2G42890 | AML2_ML2__MEI2-like 2 | -0.14 | -0.36 | **-0.96** |
| AT2G43020 | ATPAO2_PAO2__polyamine oxidase 2 | -0.13 | 0.53 | **0.81** |
| AT2G43290 | calmodulin-like MSS3. | 0.63 | 0.47 | **0.75** |

| AGI identifier | Gene annotation | 30 min | 2h | 8h |
|---|---|---|---|---|
| AT2G43330 | ATINT1_INT1__inositol transporter 1 | -0.15 | **-0.79** | -0.31 |
| AT2G43360 | BIO2_BIOB__Radical SAM superfamily protein | 0.18 | 0.37 | **0.93** |
| AT2G43460 | Ribosomal L38e protein family | 0.01 | 0.52 | **0.96** |
| AT2G43510 | ATTI1_TI1__trypsin inhibitor protein 1 | -0.30 | -0.22 | **-1.07** |
| AT2G43520 | ATTI2_TI2__trypsin inhibitor protein 2 | -0.07 | -0.29 | **-0.91** |
| AT2G43620 | Chitinase family protein | 0.23 | **1.45** | **1.86** |
| AT2G43650 | EMB2777__Sas10/U3 ribonucleoprotein (Utp) family protein | -0.21 | 0.45 | **0.77** |
| AT2G43820 | ATSAGT1_GT_SAGT1_SGT1_UGT74F2__UDP-glucosyltransferase 74F2 | 0.14 | **-0.92** | x |
| AT2G44060 | Late embryogenesis abundant protein, group 2 | **0.71** | -0.05 | 0.09 |
| AT2G44140 | Peptidase family C54 protein | 0.05 | -0.56 | **-0.95** |
| AT2G44160 | MTHFR2__methylenetetrahydrofolate reductase 2 | -0.18 | -0.04 | **0.87** |
| AT2G44350 | ATCS_CSY4__Citrate synthase family protein | x | 0.19 | **0.74** |
| AT2G44380 | Cysteine/Histidine-rich C1 domain family protein | 0.17 | **-0.97** | **-0.86** |
| AT2G44500 | O-fucosyltransferase family protein | **-0.89** | -0.56 | 0.03 |
| AT2G44670 | Protein of unknown function (DUF581) | 0.01 | **0.94** | x |
| AT2G44790 | UCC2__uclacyanin 2 | **0.68** | -0.19 | **-1.35** |
| AT2G44860 | Ribosomal protein L24e family protein | -0.03 | 0.59 | **0.74** |
| AT2G44920 | Tetratricopeptide repeat (TPR)-like superfamily protein | 0.09 | x | **-0.79** |
| AT2G44940 | Integrase-type DNA-binding superfamily protein | -0.16 | **0.81** | 0.32 |
| AT2G45170 | ATATG8E_ATG8E__AUTOPHAGY 8E | -0.21 | **-1.58** | **-1.06** |
| AT2G45470 | AGP8_FLA8__FASCICLIN-like arabinogalactan protein 8 | 0.00 | 0.08 | **0.71** |
| AT2G45710 | Zinc-binding ribosomal protein family protein | x | 0.59 | **0.82** |
| AT2G45820 | Remorin family protein | **0.88** | -0.33 | x |
| AT2G45960 | ATHH2_PIP1;2_PIP1B_TMP-A__plasma membrane intrinsic protein 1B | 0.32 | -0.21 | **-1.16** |
| AT2G46220 | Uncharacterized conserved protein (DUF2358) | 0.30 | -0.64 | **-2.04** |
| AT2G46420 | Plant protein 1589 of unknown function | -0.06 | **0.80** | **1.17** |
| AT2G46600 | Calcium-binding EF-hand family protein | 0.03 | **0.80** | -0.01 |
| AT2G46650 | ATCB5-C_B5 #1_CB5-C__cytochrome B5 isoform C | 0.10 | **0.74** | **0.99** |
| AT2G46740 | D-arabinono-1,4-lactone oxidase family protein | 0.15 | -0.34 | **-0.75** |
| AT2G46750 | D-arabinono-1,4-lactone oxidase family protein | 0.12 | -0.24 | **-0.99** |
| AT2G47110 | UBQ6__ubiquitin 6 | -0.09 | 0.46 | **0.99** |
| AT2G47270 | sequence-specific DNA binding transcription factors;transcription regulators | -0.27 | **-0.95** | **-1.50** |
| AT2G47400 | CP12-1__CP12 domain-containing protein 1 | 0.05 | -0.12 | **-0.86** |
| AT2G47440 | Tetratricopeptide repeat (TPR)-like superfamily protein | **-0.73** | 0.04 | x |
| AT2G47450 | CAO_CPSRP43__chloroplast signal recognition particle component (CAO) | 0.09 | -0.44 | **-0.93** |
| AT2G47480 | Protein of unknown function (DUF3511) | -0.10 | 0.26 | **0.97** |
| AT2G47610 | Ribosomal protein L7Ae/L30e/S12e/Gadd45 family protein | -0.37 | 0.34 | **1.03** |
| AT2G47650 | UXS4__UDP-xylose synthase 4 | -0.03 | 0.10 | **0.75** |
| AT2G47730 | ATGSTF5_ATGSTF8_GST6_GSTF8__glutathione S-transferase phi 8 | 0.23 | 0.05 | **-0.82** |
| AT2G48020 | Major facilitator superfamily protein | -0.31 | -0.61 | **-1.19** |
| AT3E56080 | EUGENE prediction | 0.01 | -0.05 | **-0.83** |

| AGI identifier | Gene annotation | 30 min | 2h | 8h |
|---|---|---|---|---|
| AT3G01190 | Peroxidase superfamily protein | **0.69** | -0.11 | **1.12** |
| AT3G01280 | ATVDAC1_VDAC1__voltage dependent anion channel 1 | -0.01 | 0.31 | **0.86** |
| AT3G01290 | SPFH/Band 7/PHB domain-containing membrane-associated protein family | **0.77** | **-0.93** | **-1.96** |
| AT3G01420 | ALPHA-DOX1_DIOX1_DOX1_PADOX-1__Peroxidase superfamily protein | **0.68** | 0.35 | -0.31 |
| AT3G01520 | Adenine nucleotide alpha hydrolases-like superfamily protein | 0.01 | -0.38 | **-0.82** |
| AT3G01770 | ATBET10_BET10__bromodomain and extraterminal domain protein 10 | -0.21 | -0.42 | **-0.80** |
| AT3G01820 | P-loop containing nucleoside triphosphate hydrolases superfamily protein | -0.01 | **0.89** | 0.66 |
| AT3G01850 | Aldolase-type TIM barrel family protein | 0.01 | -0.19 | **-1.02** |
| AT3G01930 | Major facilitator superfamily protein | 0.38 | -0.35 | **-1.14** |
| AT3G01970 | ATWRKY45_WRKY45__WRKY DNA-binding protein 45 | -0.08 | 0.01 | **-1.21** |
| AT3G02020 | AK3__aspartate kinase 3 | -0.02 | 0.31 | **0.78** |
| AT3G02040 | SRG3__senescence-related gene 3 | 0.19 | **1.24** | 0.58 |
| AT3G02140 | AFP4_TMAC2__AFP2 (ABI five-binding protein 2) family protein | -0.23 | -0.37 | **-0.76** |
| AT3G02230 | ATRGP1_RGP1__reversibly glycosylated polypeptide 1 | 0.06 | **0.85** | **2.27** |
| AT3G02340 | RING/U-box superfamily protein | -0.03 | -0.37 | **-0.74** |
| AT3G02390 | unknown protein | -0.15 | **-1.17** | **-0.82** |
| AT3G02470 | SAMDC__S-adenosylmethionine decarboxylase | **0.80** | -0.35 | x |
| AT3G02530 | TCP-1/cpn60 chaperonin family protein | -0.31 | 0.20 | **1.00** |
| AT3G02630 | Plant stearoyl-acyl-carrier-protein desaturase family protein | 0.03 | 0.30 | **0.79** |
| AT3G02650 | Tetratricopeptide repeat (TPR)-like superfamily protein | 0.30 | 0.10 | **0.93** |
| AT3G02700 | NC domain-containing protein-related | -0.13 | -0.57 | **-0.85** |
| AT3G02870 | VTC4__Inositol monophosphatase family protein | -0.05 | 0.55 | **0.97** |
| AT3G02885 | GASA5__GAST1 protein homolog 5 | 0.03 | -0.19 | **0.80** |
| AT3G02910 | AIG2-like (avirulence induced gene) family protein | -0.17 | **1.10** | **1.46** |
| AT3G03060 | P-loop containing nucleoside triphosphate hydrolases superfamily protein | -0.17 | 0.55 | **1.51** |
| AT3G03150 | unknown protein | 0.35 | -0.39 | **-1.41** |
| AT3G03250 | AtUGP1_UGP_UGP1__UDP-GLUCOSE PYROPHOSPHORYLASE 1 | 0.06 | **0.81** | **1.89** |
| AT3G03780 | ATMS2_MS2__methionine synthase 2 | -0.01 | **0.92** | **2.30** |
| AT3G03920 | H/ACA ribonucleoprotein complex, subunit Gar1/Naf1 protein | -0.21 | 0.38 | **1.14** |
| AT3G03960 | TCP-1/cpn60 chaperonin family protein | -0.14 | 0.46 | **1.13** |
| AT3G03990 | alpha/beta-Hydrolases superfamily protein | 0.00 | **-1.21** | **-1.88** |
| AT3G04290 | ATLTL1_LTL1__Li-tolerant lipase 1 | -0.19 | 0.25 | **1.32** |
| AT3G04400 | emb2171__Ribosomal protein L14p/L23e family protein | -0.15 | 0.19 | **0.79** |
| AT3G04730 | IAA16__indoleacetic acid-induced protein 16 | 0.54 | -0.59 | **-0.81** |
| AT3G04770 | RPSAb__40s ribosomal protein SA B | -0.35 | **0.85** | **1.12** |
| AT3G04840 | Ribosomal protein S3Ae | -0.18 | 0.44 | **1.42** |
| AT3G04920 | Ribosomal protein S24e family protein | -0.39 | 0.20 | **0.84** |
| AT3G05060 | NOP56-like pre RNA processing ribonucleoprotein | 0.08 | 0.66 | **1.24** |

| AGI identifier | Gene annotation | 30 min | 2h | 8h |
|---|---|---|---|---|
| AT3G05590 | RPL18__ribosomal protein L18 | -0.50 | 0.39 | **0.94** |
| AT3G05880 | RCI2A__Low temperature and salt responsive protein family | -0.41 | -0.53 | **-0.86** |
| AT3G05890 | RCI2B__Low temperature and salt responsive protein family | **-1.01** | 0.03 | **-0.99** |
| AT3G05910 | Pectinacetylesterase family protein | -0.08 | -0.04 | **1.45** |
| AT3G06070 | unknown protein | -0.37 | **-0.96** | -0.41 |
| AT3G06080 | TBL10__Plant protein of unknown function (DUF828) | 0.05 | **-0.89** | -0.66 |
| AT3G06340 | DNAJ heat shock N-terminal domain-containing protein | 0.00 | -0.36 | **-0.75** |
| AT3G06380 | ATTLP9_TLP9__tubby-like protein 9 | -0.14 | **-1.04** | **-1.32** |
| AT3G06420 | ATG8H__Ubiquitin-like superfamily protein | -0.01 | **-0.85** | **-1.47** |
| AT3G06483 | ATPDHK_PDK__pyruvate dehydrogenase kinase | -0.13 | -0.52 | **-0.94** |
| AT3G06530 | ARM repeat superfamily protein | -0.53 | 0.41 | **0.97** |
| AT3G06550 | unknown protein | 0.37 | 0.16 | **1.01** |
| AT3G06700 | Ribosomal L29e protein family | -0.10 | 0.44 | **0.87** |
| AT3G06850 | BCE2_DIN3_LTA1__2-oxoacid dehydrogenases acyltransferase family protein | 0.00 | **-1.56** | **-1.81** |
| AT3G06890 | unknown protein | -0.02 | 0.43 | **0.98** |
| AT3G06930 | ATPRMT4B_PRMT4B__protein arginine methyltransferase 4B | -0.20 | 0.30 | **0.79** |
| AT3G07030 | pseudogene | 0.19 | 0.17 | **0.72** |
| AT3G07050 | GTP-binding family protein | -0.06 | 0.32 | **0.78** |
| AT3G07110 | Ribosomal protein L13 family protein | -0.17 | 0.57 | **0.82** |
| AT3G07310 | Protein of unknown function (DUF760) | -0.03 | **-1.33** | -0.64 |
| AT3G07320 | O-Glycosyl hydrolases family 17 protein | -0.07 | 0.23 | **0.73** |
| AT3G07350 | Protein of unknown function (DUF506) | -0.06 | -0.64 | **-1.05** |
| AT3G07370 | ATCHIP_CHIP__carboxyl terminus of HSC70-interacting protein | -0.37 | -0.48 | **-0.81** |
| AT3G07380 | Domain of unknown function (DUF23) | 0.15 | 0.25 | **1.10** |
| AT3G07390 | AIR12__auxin-responsive family protein | 0.19 | **1.26** | **1.74** |
| AT3G07560 | APM2_PEX13__peroxin 13 | -0.47 | -0.32 | **-1.17** |
| AT3G07650 | COL9__CONSTANS-like 9 | -0.16 | -0.13 | **-1.07** |
| AT3G07770 | AtHsp90-6_AtHsp90.6_Hsp89.1__HEAT SHOCK PROTEIN 89.1 | -0.35 | 0.54 | **1.57** |
| AT3G08020 | PHD finger family protein | -0.27 | -0.18 | **-1.02** |
| AT3G08580 | AAC1__ADP/ATP carrier 1 | -0.15 | 0.61 | **1.35** |
| AT3G08590 | Phosphoglycerate mutase, 2,3-bisphosphoglycerate-independent | -0.08 | 0.61 | **1.45** |
| AT3G08630 | Protein of unknown function (DUF3411) | -0.14 | 0.32 | **1.29** |
| AT3G08640 | Protein of unknown function (DUF3411) | 0.01 | **0.98** | **1.23** |
| AT3G08770 | LTP6__lipid transfer protein 6 | -0.22 | 0.35 | **1.32** |
| AT3G08850 | ATRAPTOR1B_RAPTOR1_RAPTOR1B__HEAT repeat ;WD domain, G-beta repeat protein protein | **-0.74** | -0.18 | x |
| AT3G09200 | Ribosomal protein L10 family protein | -0.22 | 0.25 | **0.85** |
| AT3G09260 | BGLU23_LEB_PSR3.1_PYK10__Glycosyl hydrolase superfamily protein | 0.43 | 0.07 | **1.29** |
| AT3G09350 | Fes1A | -0.11 | **0.91** | -0.31 |

| AGI identifier | Gene annotation | 30 min | 2h | 8h |
|---|---|---|---|---|
| AT3G09440 | Heat shock protein 70 (Hsp 70) family protein | 0.19 | **1.06** | x |
| AT3G09500 | Ribosomal L29 family protein | 0.14 | 0.33 | **0.85** |
| AT3G09630 | Ribosomal protein L4/L1 family | -0.33 | 0.35 | **0.95** |
| AT3G09820 | ADK1_ATADK1__adenosine kinase 1 | -0.11 | 0.23 | **1.60** |
| AT3G09860 | unknown protein | 0.08 | -0.17 | **-0.74** |
| AT3G10020 | unknown protein | 0.10 | **-2.14** | **-2.40** |
| AT3G10113 | myb family transcription factor | -0.47 | **-1.36** | **-1.53** |
| AT3G10120 | unknown protein | -0.10 | -0.34 | **-0.81** |
| AT3G10230 | LYC__lycopene cyclase | 0.47 | -0.23 | **-0.90** |
| AT3G10250 | Plant protein 1589 of unknown function | 0.00 | -0.05 | **-0.71** |
| AT3G10450 | SCPL7__serine carboxypeptidase-like 7 | -0.13 | -0.17 | **-0.94** |
| AT3G10520 | AHB2_ARATH GLB2_ATGLB2_GLB2_HB2_NSHB2_ haemoglobin 2 | -0.10 | 0.43 | **0.94** |
| AT3G10610 | Ribosomal S17 family protein | -0.33 | 0.48 | **1.00** |
| AT3G10690 | GYRA__DNA GYRASE A | -0.22 | 0.12 | **0.87** |
| AT3G10770 | Single-stranded nucleic acid binding R3H protein | -0.09 | -0.24 | **-0.86** |
| AT3G10985 | ATWI-12_SAG20_WI12__senescence associated gene 20 | 0.18 | -0.47 | **-1.00** |
| AT3G11230 | Yippee family putative zinc-binding protein | -0.39 | -0.31 | **-0.79** |
| AT3G11250 | Ribosomal protein L10 family protein | -0.04 | 0.27 | **0.81** |
| AT3G11510 | Ribosomal protein S11 family protein | -0.22 | 0.39 | **0.85** |
| AT3G11560 | LETM1-like protein | -0.03 | -0.10 | **-0.89** |
| AT3G12150 | unknown protein | -0.28 | **-1.31** | **-1.02** |
| AT3G12240 | SCPL15__serine carboxypeptidase-like 15 | x | -0.23 | **-0.80** |
| AT3G12345 | unknown protein | 0.00 | -0.34 | **-1.23** |
| AT3G12370 | Ribosomal protein L10 family protein | 0.12 | 0.41 | **0.74** |
| AT3G12390 | Nascent polypeptide-associated complex (NAC), alpha subunit family protein | -0.08 | 0.32 | **0.86** |
| AT3G12580 | ATHSP70_HSP70__heat shock protein 70 | -0.03 | **1.11** | 0.58 |
| AT3G12610 | DRT100__Leucine-rich repeat (LRR) family protein | 0.01 | 0.35 | **0.73** |
| AT3G12780 | PGK1__phosphoglycerate kinase 1 | **0.86** | 0.24 | 0.06 |
| AT3G13110 | ATSERAT2;2_SAT-1_SAT-A_SAT-M_SAT3_SERAT2;2__serine acetyltransferase 2;2 | 0.22 | **0.98** | 0.66 |
| AT3G13230 | RNA-binding KH domain-containing protein | 0.22 | **0.93** | **1.06** |
| AT3G13450 | DIN4__Transketolase family protein | -0.09 | **-1.09** | **-2.34** |
| AT3G13470 | TCP-1/cpn60 chaperonin family protein | -0.27 | 0.51 | **0.95** |
| AT3G13610 | 2-oxoglutarate (2OG) and Fe(II)-dependent oxygenase superfamily protein | 0.51 | 0.18 | **0.83** |
| AT3G13750 | BGAL1_BGAL1__beta galactosidase 1 | 0.61 | **-1.15** | **-0.83** |
| AT3G13940 | DNA binding;DNA-directed RNA polymerases | 0.20 | 0.65 | **1.22** |
| AT3G14100 | RNA-binding (RRM/RBD/RNP motifs) family protein | **0.67** | -0.02 | -0.05 |
| AT3G14200 | Chaperone DnaJ-domain superfamily protein | 0.04 | **1.01** | 0.51 |
| AT3G14210 | ESM1__epithiospecifier modifier 1 | -0.05 | **1.62** | **1.49** |
| AT3G14415 | Aldolase-type TIM barrel family protein | -0.14 | -0.19 | **-1.42** |
| AT3G14420 | Aldolase-type TIM barrel family protein | -0.04 | -0.06 | **-1.01** |
| AT3G14610 | CYP72A7__cytochrome P450, family 72, subfamily A, polypeptide 7 | -0.05 | -0.12 | **-0.84** |
| AT3G14620 | CYP72A8__cytochrome P450, family 72, subfamily A, polypeptide 8 | 0.07 | -0.25 | **-1.11** |

| AGI identifier | Gene annotation | 30 min | 2h | 8h |
|---|---|---|---|---|
| AT3G14690 | CYP72A15__cytochrome P450, family 72, subfamily A, polypeptide 15 | -0.08 | -0.08 | **-0.90** |
| AT3G14770 | Nodulin MtN3 family protein | -0.07 | **-1.14** | **-1.59** |
| AT3G14870 | unknown protein | 0.26 | **-0.77** | -0.01 |
| AT3G14940 | ATPPC3_PPC3__phosphoenolpyruvate carboxylase 3 | 0.13 | 0.30 | **2.25** |
| AT3G14990 | Class I glutamine amidotransferase-like superfamily protein | -0.01 | **-0.74** | **-1.43** |
| AT3G15000 | cobalt ion binding | -0.18 | 0.25 | **0.90** |
| AT3G15020 | mMDH2__Lactate/malate dehydrogenase family protein | -0.10 | 0.36 | **0.97** |
| AT3G15350 | Core-2/I-branching beta-1,6-N-acetylglucosaminyltransferase family protein | -0.19 | 0.53 | **0.82** |
| AT3G15353 | ATMT3_MT3__metallothionein 3 | -0.15 | x | **-1.03** |
| AT3G15356 | Legume lectin family protein | 0.33 | -0.72 | **-1.02** |
| AT3G15450 | Aluminium induced protein with YGL and LRDR motifs | -0.16 | **-3.69** | **-2.61** |
| AT3G15500 | ANAC055_ATNAC3_NAC055_NAC3__NAC domain containing protein 3 | 0.06 | **-0.83** | **-1.46** |
| AT3G15580 | APG8H_ATG8I__Ubiquitin-like superfamily protein | 0.12 | -0.22 | **-0.78** |
| AT3G15630 | unknown protein | -0.23 | **-2.51** | **-1.80** |
| AT3G15650 | alpha/beta-Hydrolases superfamily protein | -0.35 | **0.82** | x |
| AT3G15770 | unknown protein | -0.10 | **-1.09** | **-1.18** |
| AT3G15840 | PIFI__post-illumination chlorophyll fluorescence increase | 0.10 | -0.39 | **-0.87** |
| AT3G15950 | NAI2__DNA topoisomerase-related | 0.48 | -0.04 | **1.13** |
| AT3G15990 | SULTR3;4__sulfate transporter 3;4 | -0.09 | **0.98** | **0.71** |
| AT3G16050 | A37_ATPDX1.2_PDX1.2__pyridoxine biosynthesis 1.2 | -0.08 | **0.77** | **0.72** |
| AT3G16080 | Zinc-binding ribosomal protein family protein | -0.36 | 0.47 | **0.95** |
| AT3G16190 | Isochorismatase family protein | 0.04 | -0.05 | **-0.84** |
| AT3G16240 | AQP1_ATTIP2;1_DELTA-TIP_DELTA-TIP1_TIP2;1__delta tonoplast integral protein | **0.72** | -0.16 | x |
| AT3G16400 | ATMLP-470_ATNSP1_NSP1__nitrile specifier protein 1 | **0.86** | -0.37 | 0.46 |
| AT3G16410 | NSP4__nitrile specifier protein 4 | x | 0.10 | **0.72** |
| AT3G16470 | JR1__Mannose-binding lectin superfamily protein | -0.04 | 0.18 | **0.94** |
| AT3G16770 | ATEBP_EBP_ERF72_RAP2.3__ethylene-responsive element binding protein | 0.08 | -0.46 | **-1.50** |
| AT3G16780 | Ribosomal protein L19e family protein | -0.26 | 0.43 | **0.99** |
| AT3G16810 | APUM24_PUM24__pumilio 24 | -0.11 | 0.59 | **1.14** |
| AT3G17040 | HCF107__high chlorophyll fluorescent 107 | -0.01 | -0.08 | **-0.73** |
| AT3G17390 | MAT4_MTO3_SAMS3__S-adenosylmethionine synthetase family protein | -0.15 | 0.15 | **1.53** |
| AT3G17430 | Nucleotide-sugar transporter family protein | -0.18 | 0.05 | **0.79** |
| AT3G17440 | ATNPSN13_NPSN13__novel plant snare 13 | -0.49 | **-0.93** | **-0.71** |
| AT3G17465 | RPL3P__ribosomal protein L3 plastid | -0.19 | 0.19 | **0.90** |
| AT3G17510 | CIPK1_SnRK3.16__CBL-interacting protein kinase 1 | -0.14 | -0.69 | **-1.10** |
| AT3G17770 | Dihydroxyacetone kinase | -0.33 | -0.59 | **-1.02** |
| AT3G17790 | ATACP5_ATPAP17_PAP17__purple acid phosphatase 17 | 0.46 | **1.76** | **1.16** |
| AT3G17800 | Protein of unknown function (DUF760) | **1.04** | 0.34 | -0.30 |
| AT3G17810 | PYD1__pyrimidine 1 | 0.07 | -0.13 | **-0.80** |
| AT3G18000 | NMT1_PEAMT_XPL1__S-adenosyl-L-methionine-dependent methyltransferases superfamily protein | -0.33 | 0.29 | **0.97** |

| AGI identifier | Gene annotation | 30 min | 2h | 8h |
|---|---|---|---|---|
| AT3G18130 | RACK1C_AT__receptor for activated C kinase 1C | -0.35 | **0.84** | **1.46** |
| AT3G18190 | TCP-1/cpn60 chaperonin family protein | -0.20 | 0.39 | **1.35** |
| AT3G18600 | P-loop containing nucleoside triphosphate hydrolases superfamily protein | -0.16 | 0.64 | **1.47** |
| AT3G18760 | Translation elongation factor EF1B/ribosomal protein S6 family protein | -0.03 | 0.11 | **0.79** |
| AT3G18773 | zinc finger (C3HC4-type RING finger) family protein | -0.02 | **-0.81** | **-0.73** |
| AT3G18780 | ACT2_DER1_ENL2_LSR2__actin 2 | -0.24 | -0.65 | **-0.74** |
| AT3G18830 | ATPLT5_ATPMT5_PMT5__polyol/monosaccharide transporter 5 | 0.20 | **0.84** | 0.40 |
| AT3G19030 | unknown protein | -0.06 | -0.44 | **-1.27** |
| AT3G19160 | ATIPT8_IPT8_IPT8_PGA22__ATP/ADP isopentenyltransferases | -0.43 | 0.37 | **1.07** |
| AT3G19290 | ABF4_AREB2__ABRE binding factor 4 | -0.02 | -0.67 | **-0.74** |
| AT3G19390 | Granulin repeat cysteine protease family protein | 0.17 | **-0.97** | **-1.20** |
| AT3G19615 | unknown protein | -0.16 | -0.05 | **-0.84** |
| AT3G19680 | Protein of unknown function (DUF1005) | **-1.11** | **-0.81** | -0.10 |
| AT3G19710 | BCAT4__branched-chain aminotransferase4 | 0.21 | 0.07 | **1.35** |
| AT3G19720 | ARC5_DRP5B__P-loop containing nucleoside triphosphate hydrolases superfamily protein | 0.03 | 0.21 | **1.08** |
| AT3G19800 | Protein of unknown function (DUF177) | 0.13 | -0.14 | **-0.71** |
| AT3G19820 | CBB1_DIM_DIM1_DWF1_EVE1__cell elongation protein / DWARF1 / DIMINUTO (DIM) | 0.00 | -0.17 | **1.04** |
| AT3G19930 | ATSTP4_STP4__sugar transporter 4 | 0.20 | **-0.87** | **-1.05** |
| AT3G20000 | TOM40__translocase of the outer mitochondrial membrane 40 | -0.21 | 0.43 | **0.95** |
| AT3G20050 | ATTCP-1_TCP-1__T-complex protein 1 alpha subunit | -0.28 | 0.27 | **1.39** |
| AT3G20060 | UBC19__ubiquitin-conjugating enzyme19 | 0.31 | -0.49 | **-0.87** |
| AT3G20200 | Protein kinase protein with adenine nucleotide alpha hydrolases-like domain | -0.14 | -0.11 | **0.77** |
| AT3G20330 | PYRB__PYRIMIDINE B | -0.11 | 0.44 | **0.90** |
| AT3G20340 | unknown protein | -0.12 | **-0.94** | **-1.80** |
| AT3G20370 | TRAF-like family protein | 0.08 | 0.16 | **1.48** |
| AT3G20390 | endoribonuclease L-PSP family protein | -0.59 | 0.13 | **0.78** |
| AT3G20500 | ATPAP18_PAP18__purple acid phosphatase 18 | **0.87** | 0.21 | -0.02 |
| AT3G20660 | 4-Oct_AtOCT4__organic cation/carnitine transporter4 | 0.06 | -0.44 | **-1.09** |
| AT3G21190 | O-fucosyltransferase family protein | 0.18 | 0.42 | **1.10** |
| AT3G21260 | GLTP3__Glycolipid transfer protein (GLTP) family protein | -0.16 | 0.05 | **-0.99** |
| AT3G21520 | AtDMP1_DMP1__DUF679 domain membrane protein 1 | -0.01 | 0.29 | **-1.07** |
| AT3G21560 | UGT84A2__UDP-Glycosyltransferase superfamily protein | 0.21 | **0.95** | **0.75** |
| AT3G21670 | Major facilitator superfamily protein | 0.50 | **0.95** | -0.30 |
| AT3G21710 | unknown protein | 0.24 | -0.38 | **-0.90** |
| AT3G21770 | Peroxidase superfamily protein | 0.18 | 0.12 | **1.33** |
| AT3G21890 | B-box type zinc finger family protein | 0.49 | **0.76** | -0.01 |
| AT3G22120 | CWLP__cell wall-plasma membrane linker protein | **0.72** | -0.15 | -0.63 |
| AT3G22200 | GABA-T_HER1_POP2__Pyridoxal phosphate (PLP)-dependent transferases superfamily protein | -0.17 | -0.50 | **-0.84** |
| AT3G22210 | unknown protein | 0.00 | -0.40 | **-0.94** |

| AGI identifier | Gene annotation | 30 min | 2h | 8h |
|---|---|---|---|---|
| AT3G22440 | FRIGIDA-like protein | 0.14 | -0.26 | **-0.77** |
| AT3G22460 | OASA2__O-acetylserine (thiol) lyase (OAS-TL) isoform A2 | -0.44 | -0.45 | **-0.92** |
| AT3G22530 | unknown protein | -0.14 | -0.16 | **-0.84** |
| AT3G22660 | rRNA processing protein-related | 0.20 | 0.57 | **0.98** |
| AT3G22850 | Aluminium induced protein with YGL and LRDR motifs | -0.14 | -0.13 | **0.79** |
| AT3G23000 | ATSR2_ATSRPK1_CIPK7_PKS7_SnRK3.10__CBL-interacting protein kinase 7 | 0.35 | 0.65 | **0.81** |
| AT3G23080 | Polyketide cyclase/dehydrase and lipid transport superfamily protein | 0.26 | **-0.77** | **-1.02** |
| AT3G23300 | S-adenosyl-L-methionine-dependent methyltransferases superfamily protein | -0.05 | 0.08 | **0.98** |
| AT3G23450 | unknown protein | **0.70** | -0.29 | x |
| AT3G23550 | MATE efflux family protein | -0.01 | -0.69 | **-0.88** |
| AT3G23620 | Ribosomal RNA processing Brix domain protein | -0.37 | 0.47 | **0.73** |
| AT3G23700 | Nucleic acid-binding proteins superfamily | 0.09 | -0.61 | **-1.12** |
| AT3G23810 | ATSAHH2_SAHH2__S-adenosyl-l-homocysteine (SAH) hydrolase 2 | 0.16 | 0.50 | **1.81** |
| AT3G23830 | GR-RBP4_GRP4__glycine-rich RNA-binding protein 4 | -0.61 | 0.51 | **1.56** |
| AT3G23940 | dehydratase family | -0.40 | 0.33 | **1.21** |
| AT3G23990 | HSP60_HSP60-3B__heat shock protein 60 | -0.18 | 0.47 | **1.29** |
| AT3G24300 | AMT1;3_ATAMT1;3__ammonium transporter 1;3 | 0.24 | 0.41 | **1.25** |
| AT3G24420 | alpha/beta-Hydrolases superfamily protein | 0.44 | -0.30 | **-1.50** |
| AT3G24480 | Leucine-rich repeat (LRR) family protein | -0.06 | -0.32 | **0.76** |
| AT3G24503 | ALDH1A_ALDH2C4_REF1__aldehyde dehydrogenase 2C4 | 0.43 | **0.89** | **0.79** |
| AT3G24600 | unknown protein | 0.22 | 0.28 | **0.76** |
| AT3G24927 | pseudogene | -0.21 | -0.32 | **-0.99** |
| AT3G25110 | AtFaTA_FaTA__fatA acyl-ACP thioesterase | -0.06 | 0.45 | **0.78** |
| AT3G25190 | Vacuolar iron transporter (VIT) family protein | -0.03 | -0.14 | **-1.53** |
| AT3G25700 | Eukaryotic aspartyl protease family protein | 0.08 | 0.43 | **0.77** |
| AT3G25760 | AOC1_ERD12__allene oxide cyclase 1 | 0.30 | 0.62 | **-0.78** |
| AT3G25780 | AOC3__allene oxide cyclase 3 | 0.08 | **0.86** | 0.34 |
| AT3G26030 | ATB' DELTA__serine/threonine protein phosphatase 2A 55 kDa regulatory subunit B prime delta | 0.55 | **-0.90** | **-0.99** |
| AT3G26220 | CYP71B3__cytochrome P450, family 71, subfamily B, polypeptide 3 | 0.05 | -0.52 | **-1.29** |
| AT3G26410 | methyltransferases;nucleic acid binding | -0.05 | 0.24 | **0.73** |
| AT3G26450 | Polyketide cyclase/dehydrase and lipid transport superfamily protein | **0.80** | 0.60 | 0.70 |
| AT3G26520 | GAMMA-TIP2_SITIP_TIP1;2_TIP2__tonoplast intrinsic protein 2 | 0.22 | -0.16 | **-1.06** |
| AT3G26580 | Tetratricopeptide repeat (TPR)-like superfamily protein | -0.15 | -0.41 | **-0.73** |
| AT3G26650 | GAPA_GAPA-1__glyceraldehyde 3-phosphate dehydrogenase A subunit | 0.09 | -0.06 | **-0.80** |
| AT3G26690 | ATNUDT13_ATNUDX13_NUDX13__nudix hydrolase homolog 13 | -0.37 | -0.65 | **-1.01** |
| AT3G26740 | CCL__CCR-like | -0.06 | **-1.67** | **-1.60** |
| AT3G27110 | Peptidase family M48 family protein | 0.16 | -0.16 | **-0.98** |
| AT3G27160 | GHS1__Ribosomal protein S21 family protein | -0.18 | -0.29 | **-0.73** |

| AGI identifier | Gene annotation | 30 min | 2h | 8h |
|---|---|---|---|---|
| AT3G27280 | ATPHB4_PHB4__prohibitin 4 | -0.16 | 0.45 | **1.15** |
| AT3G27570 | Sucrase/ferredoxin-like family protein | -0.10 | **0.86** | **1.32** |
| AT3G27690 | LHCB2_LHCB2.3_LHCB2.4__photosystem II light harvesting complex gene 2.3 | **1.12** | -0.54 | -0.06 |
| AT3G27740 | CARA__carbamoyl phosphate synthetase A | -0.14 | 0.35 | **0.88** |
| AT3G27770 | unknown protein | -0.16 | **-0.96** | **-1.56** |
| AT3G27850 | RPL12-C__ribosomal protein L12-C | **0.77** | 0.48 | 0.01 |
| AT3G28200 | Peroxidase superfamily protein | -0.65 | 0.07 | **0.88** |
| AT3G28740 | CYP81D1__Cytochrome P450 superfamily protein | 0.07 | **-0.87** | **-2.28** |
| AT3G28900 | Ribosomal protein L34e superfamily protein | -0.40 | 0.34 | **0.84** |
| AT3G29035 | ANAC059_ATNAC3_NAC3__NAC domain containing protein 3 | -0.07 | -0.52 | **-0.89** |
| AT3G29240 | Protein of unknown function (DUF179) | 0.16 | **-1.45** | **-1.80** |
| AT3G29250 | NAD(P)-binding Rossmann-fold superfamily protein | 0.45 | -0.18 | **1.13** |
| AT3G29330 | unknown protein | -0.26 | 0.18 | **0.78** |
| AT3G29360 | UDP-glucose 6-dehydrogenase family protein | -0.24 | 0.05 | **1.01** |
| AT3G30390 | Transmembrane amino acid transporter family protein | x | -0.33 | **-0.72** |
| AT3G30775 | AT-POX_ATPDH_ATPOX_ERD5_PRO1_PRODH_ Methylenetetrahydrofolate reductase family protein | 0.55 | **-2.18** | **-2.34** |
| AT3G32990 | pseudogene | **-1.32** | 0.20 | -0.19 |
| AT3G43230 | RING/FYVE/PHD-type zinc finger family protein | -0.08 | -0.44 | **-0.73** |
| AT3G43810 | CAM7__calmodulin 7 | -0.02 | 0.04 | **0.82** |
| AT3G43850 | unknown protein | -0.15 | -0.57 | **-0.74** |
| AT3G43980 | Ribosomal protein S14p/S29e family protein | -0.08 | 0.33 | **0.75** |
| AT3G44190 | FAD/NAD(P)-binding oxidoreductase family protein | 0.33 | -0.04 | **-1.22** |
| AT3G44300 | AtNIT2_NIT2__nitrilase 2 | 0.15 | -0.43 | **-1.63** |
| AT3G44450 | unknown protein | 0.16 | **0.85** | 0.53 |
| AT3G44550 | FAR5__fatty acid reductase 5 | 0.02 | 0.23 | **1.02** |
| AT3G44590 | 60S acidic ribosomal protein family | -0.23 | 0.51 | **0.97** |
| AT3G44750 | ATHD2A_HD2A_HDA3_HDT1__histone deacetylase 3 | -0.04 | 0.60 | **1.69** |
| AT3G44755 | unknown protein | -0.08 | -0.57 | **-1.01** |
| AT3G44860 | FAMT__farnesoic acid carboxyl-O-methyltransferase | 0.07 | **1.06** | x |
| AT3G44870 | S-adenosyl-L-methionine-dependent methyltransferases superfamily protein | 0.42 | **1.36** | -0.13 |
| AT3G44880 | ACD1_LLS1_PAO__Pheophorbide a oxygenase family protein with Rieske [2Fe-2S] domain | 0.39 | -0.04 | **-0.84** |
| AT3G44990 | ATXTR8_XTH31_XTR8__xyloglucan endo-transglycosylase-related 8 | 0.30 | 0.63 | **2.04** |
| AT3G45300 | ATIVD_IVD_IVDH__isovaleryl-CoA-dehydrogenase | 0.56 | **-0.93** | x |
| AT3G45650 | NAXT1__nitrate excretion transporter1 | 0.03 | 0.19 | **0.75** |
| AT3G45700 | Major facilitator superfamily protein | 0.19 | -0.01 | **0.79** |
| AT3G45730 | unknown protein | -0.15 | **-1.44** | **-1.90** |
| AT3G45970 | ATEXLA1_ATEXPL1_ATHEXP BETA 2.1_EXLA1_EXPL1__expansin-like A1 | **-0.68** | **-1.29** | **-0.90** |
| AT3G46080 | C2H2-type zinc finger family protein | -0.16 | -0.72 | **-0.98** |
| AT3G46450 | SEC14 cytosolic factor family protein / phosphoglyceride transfer family protein | -0.02 | 0.37 | **0.74** |

| AGI identifier | Gene annotation | 30 min | 2h | 8h |
|---|---|---|---|---|
| AT3G46540 | ENTH/VHS family protein | 0.14 | 0.65 | **1.01** |
| AT3G46560 | emb2474_TIM9__Tim10/DDP family zinc finger protein | 0.25 | 0.62 | **1.20** |
| AT3G46600 | GRAS family transcription factor | 0.17 | -0.41 | **-0.76** |
| AT3G46970 | ATPHS2_PHS2__alpha-glucan phosphorylase 2 | 0.26 | x | **1.10** |
| AT3G47070 | unknown protein | -0.02 | -0.10 | **-1.25** |
| AT3G47160 | RING/U-box superfamily protein | -0.09 | **-1.37** | x |
| AT3G47340 | ASN1_AT-ASN1_DIN6__glutamine-dependent asparagine synthase 1 | 0.11 | **-2.07** | **-2.59** |
| AT3G47370 | Ribosomal protein S10p/S20e family protein | -0.02 | **0.76** | **1.07** |
| AT3G47420 | ATPS3_PS3__phosphate starvation-induced gene 3 | 0.36 | **0.92** | **0.99** |
| AT3G47470 | CAB4_LHCA4__light-harvesting chlorophyll-protein complex I subunit A4 | -0.20 | -0.41 | **-1.33** |
| AT3G47520 | MDH__malate dehydrogenase | -0.27 | 0.63 | **0.92** |
| AT3G47540 | Chitinase family protein | 0.02 | 0.26 | **0.74** |
| AT3G47800 | Galactose mutarotase-like superfamily protein | 0.31 | **-1.00** | **-2.12** |
| AT3G47960 | Major facilitator superfamily protein | -0.12 | **1.05** | **0.96** |
| AT3G48000 | ALDH2_ALDH2A_ALDH2B4__aldehyde dehydrogenase 2B4 | **0.76** | 0.14 | x |
| AT3G48250 | Pentatricopeptide repeat (PPR) superfamily protein | 0.15 | 0.27 | **0.72** |
| AT3G48300 | CYP71A23 (cytochrome P450, family 71, subfamily A, polypeptide 23); oxygen binding | -0.14 | -0.36 | **-0.82** |
| AT3G48320 | CYP71A21 (cytochrome P450, family 71, subfamily A, polypeptide 21); oxygen binding | 0.25 | -0.60 | **-1.19** |
| AT3G48360 | ATBT2_BT2__BTB and TAZ domain protein 2 | -0.40 | **-2.47** | **-1.66** |
| AT3G48390 | MA3 domain-containing protein | -0.13 | -0.59 | **-0.78** |
| AT3G48520 | CYP94B3__cytochrome P450, family 94, subfamily B, polypeptide 3 | **0.81** | 0.19 | -0.17 |
| AT3G48530 | KING1__SNF1-related protein kinase regulatory subunit gamma 1 | 0.19 | **-0.80** | **-1.33** |
| AT3G48930 | EMB1080__Nucleic acid-binding, OB-fold-like protein | 0.01 | 0.43 | **0.84** |
| AT3G48960 | Ribosomal protein L13e family protein | 0.31 | 0.62 | **1.16** |
| AT3G48990 | AMP-dependent synthetase and ligase family protein | 0.61 | 0.02 | **-1.19** |
| AT3G49010 | ATBBC1_BBC1_RSU2__breast basic conserved 1 | 0.13 | 0.59 | **0.89** |
| AT3G49040 | FBD, F-box and Leucine Rich Repeat domains containing protein | 0.01 | 0.40 | **0.73** |
| AT3G49070 | Protein of unknown function (DUF677) | 0.39 | 0.07 | **-1.10** |
| AT3G49160 | pyruvate kinase family protein | 0.10 | **-0.86** | -0.68 |
| AT3G49220 | Plant invertase/pectin methylesterase inhibitor superfamily | -0.16 | **0.78** | **1.00** |
| AT3G49320 | Metal-dependent protein hydrolase | -0.05 | 0.05 | **0.93** |
| AT3G49590 | Autophagy-related protein 13 | -0.06 | -0.40 | **-0.90** |
| AT3G49620 | DIN11__2-oxoglutarate (2OG) and Fe(II)-dependent oxygenase superfamily protein | -0.21 | -0.10 | **-1.37** |
| AT3G49670 | BAM2__Leucine-rich receptor-like protein kinase family protein | -0.46 | **0.75** | **0.90** |
| AT3G49720 | unknown protein | 0.12 | -0.10 | **0.92** |
| AT3G49780 | ATPSK3 (FORMER SYMBOL)_ATPSK4_PSK4__phytosulfokine 4 precursor | -0.17 | x | **-1.19** |
| AT3G49790 | Carbohydrate-binding protein | 0.00 | **-0.89** | **-1.26** |
| AT3G50130 | Plant protein of unknown function (DUF247) | 0.06 | 0.26 | **0.72** |

| AGI identifier | Gene annotation | 30 min | 2h | 8h |
|---|---|---|---|---|
| AT3G50210 | 2-oxoglutarate (2OG) and Fe(II)-dependent oxygenase superfamily protein | 0.11 | 0.02 | **-0.85** |
| AT3G50260 | ATERF#011_CEJ1_DEAR1__cooperatively regulated by ethylene and jasmonate 1 | x | **-0.84** | **-1.54** |
| AT3G50340 | unknown protein | 0.06 | **0.78** | **0.79** |
| AT3G50480 | HR4 (HOMOLOG OF RPW8 4) | -0.10 | **-1.21** | **-1.25** |
| AT3G50560 | NAD(P)-binding Rossmann-fold superfamily protein | 0.10 | **-1.97** | -0.70 |
| AT3G50610 | unknown protein | -0.09 | 0.12 | **0.77** |
| AT3G50660 | CLM_CYP90B1_DWF4_PSC1_SAV1_SNP2__Cytochrome P450 superfamily protein | 0.05 | 0.05 | **0.74** |
| AT3G50740 | UGT72E1__UDP-glucosyl transferase 72E1 | 0.28 | 0.34 | **1.21** |
| AT3G50820 | OEC33_PSBO-2_PSBO2__photosystem II subunit O-2 | **1.42** | 0.10 | -0.21 |
| AT3G50830 | ATCOR413-PM2_COR413-PM2__cold-regulated 413-plasma membrane 2 | -0.25 | -0.61 | **-0.72** |
| AT3G50950 | ZAR1__HOPZ-ACTIVATED RESISTANCE 1 | **0.71** | -0.33 | -0.40 |
| AT3G50970 | LTI30_XERO2__dehydrin family protein | 0.29 | -0.21 | **-1.42** |
| AT3G51000 | alpha/beta-Hydrolases superfamily protein | x | -0.19 | **-1.07** |
| AT3G51130 | unknown protein | 0.27 | -0.59 | **-1.08** |
| AT3G51240 | F3'H_F3H_TT6__flavanone 3-hydroxylase | 0.19 | **0.97** | **2.11** |
| AT3G51370 | Protein phosphatase 2C family protein | -0.13 | -0.69 | **-0.91** |
| AT3G51600 | LTP5__lipid transfer protein 5 | **0.72** | -0.17 | -0.32 |
| AT3G51730 | saposin B domain-containing protein | 0.36 | -0.61 | **-1.81** |
| AT3G51800 | ATEBP1_ATG2_EBP1__metallopeptidase M24 family protein | -0.15 | 0.45 | **1.09** |
| AT3G51840 | ACX4_ATG6_ATSCX__acyl-CoA oxidase 4 | -0.03 | **-1.01** | **-2.15** |
| AT3G51910 | AT-HSFA7A_HSFA7A__heat shock transcription factor A7A | -0.31 | **-1.63** | **-1.35** |
| AT3G52060 | Core-2/I-branching beta-1,6-N-acetylglucosaminyltransferase family protein | 0.22 | -0.73 | **-0.80** |
| AT3G52105 | unknown protein | 0.00 | -0.48 | **-0.79** |
| AT3G52170 | DNA binding | 0.00 | 0.28 | **0.85** |
| AT3G52180 | ATPTPKIS1_ATSEX4_DSP4_SEX4__dual specificity protein phosphatase (DsPTP1) family protein | -0.15 | 0.57 | **1.74** |
| AT3G52190 | PHF1__phosphate transporter traffic facilitator1 | -0.03 | 0.64 | **1.36** |
| AT3G52340 | ATSPP2_SPP2__sucrose-6F-phosphate phosphohydrolase 2 | -0.19 | 0.69 | **1.34** |
| AT3G52370 | FLA15__FASCICLIN-like arabinogalactan protein 15 precursor | x | 0.56 | **1.46** |
| AT3G52470 | Late embryogenesis abundant (LEA) hydroxyproline-rich glycoprotein family | 0.02 | **0.76** | 0.69 |
| AT3G52600 | AtcwINV2_CWINV2__cell wall invertase 2 | 0.18 | 0.20 | **0.84** |
| AT3G52840 | BGAL2__beta-galactosidase 2 | 0.03 | **-0.83** | -0.59 |
| AT3G52930 | Aldolase superfamily protein | 0.07 | **0.89** | **1.99** |
| AT3G52940 | ELL1_FK_HYD2__Ergosterol biosynthesis ERG4/ERG24 family | -0.04 | -0.10 | **0.86** |
| AT3G52990 | Pyruvate kinase family protein | -0.04 | 0.50 | **0.90** |
| AT3G53020 | RPL24_RPL24B_STV1__Ribosomal protein L24e family protein | -0.50 | 0.37 | **0.71** |
| AT3G53260 | ATPAL2_PAL2__phenylalanine ammonia-lyase 2 | **0.79** | 0.10 | 0.33 |
| AT3G53420 | PIP2_PIP2;1_PIP2A__plasma membrane intrinsic protein 2A | 0.25 | -0.31 | **-0.89** |

| AGI identifier | Gene annotation | 30 min | 2h | 8h |
|---|---|---|---|---|
| AT3G53800 | Fes1B | -0.12 | -0.68 | **-0.74** |
| AT3G53870 | Ribosomal protein S3 family protein | -0.18 | 0.46 | **0.98** |
| AT3G54400 | Eukaryotic aspartyl protease family protein | -0.27 | **1.13** | **1.47** |
| AT3G54420 | ATCHITIV_ATEP3_CHIV_EP3__homolog of carrot EP3-3 chitinase | 0.34 | **0.85** | 0.26 |
| AT3G54470 | uridine 5p-monophosphate synthase / UMP synthase (PYRE-F) (UMPS) | -0.17 | 0.48 | **1.49** |
| AT3G54500 | unknown protein | **-0.93** | -0.56 | -0.65 |
| AT3G54580 | Proline-rich extensin-like family protein | 0.31 | 0.04 | **1.29** |
| AT3G54590 | ATHRGP1_HRGP1__hydroxyproline-rich glycoprotein | 0.23 | -0.09 | **1.39** |
| AT3G54600 | Class I glutamine amidotransferase-like superfamily protein | -0.10 | 0.41 | **0.93** |
| AT3G54640 | TRP3_TSA1__tryptophan synthase alpha chain | 0.05 | 0.67 | **1.27** |
| AT3G54680 | proteophosphoglycan-related | -0.18 | 0.21 | **0.92** |
| AT3G54810 | BME3_BME3-ZF_GATA8__Plant-specific GATA-type zinc finger transcription factor family protein | **-0.66** | 0.34 | 0.67 |
| AT3G54880 | unknown protein | -0.41 | **-1.54** | x |
| AT3G54890 | LHCA1__photosystem I light harvesting complex gene 1 | 0.47 | 0.25 | **-0.80** |
| AT3G54900 | ATGRXCP_CXIP1__CAX interacting protein 1 | **0.66** | 0.27 | 0.00 |
| AT3G54960 | ATPDI1_ATPDIL1-3_PDI1_PDIL1-3__PDI-like 1-3 | -0.06 | 0.31 | **0.81** |
| AT3G55010 | ATPURM_PUR5__phosphoribosylformylglycinamidine cyclo-ligase, chloroplast / phosphoribosyl-aminoimidazole synthetase / AIR synthase (PUR5) | -0.04 | 0.46 | **1.39** |
| AT3G55120 | A11_CFI_TT5__Chalcone-flavanone isomerase family protein | 0.16 | **0.81** | **1.40** |
| AT3G55280 | RPL23AB__ribosomal protein L23AB | -0.35 | 0.69 | **1.07** |
| AT3G55330 | PPL1__PsbP-like protein 1 | -0.50 | -0.38 | **-1.04** |
| AT3G55340 | PHIP1, PHRAGMOPLASTIN INTERACTING PROTEIN 1 | 0.05 | **0.88** | **1.24** |
| AT3G55360 | ATTSC13_CER10_ECR_TSC13__3-oxo-5-alpha-steroid 4-dehydrogenase family protein | 0.21 | **0.75** | **0.75** |
| AT3G55440 | ATCTIMC_CYTOTPI_TPI__triosephosphate isomerase | 0.04 | 0.20 | **0.76** |
| AT3G55605 | Mitochondrial glycoprotein family protein | 0.09 | 0.41 | **0.79** |
| AT3G55610 | P5CS2__delta 1-pyrroline-5-carboxylate synthase 2 | x | -0.59 | **-0.75** |
| AT3G55620 | emb1624__Translation initiation factor IF6 | -0.09 | 0.40 | **0.77** |
| AT3G55760 | unknown protein | 0.03 | 0.61 | **0.79** |
| AT3G55970 | ATJRG21_JRG21__jasmonate-regulated gene 21 | 0.10 | 0.07 | **-0.75** |
| AT3G56070 | ROC2__rotamase cyclophilin 2 | 0.17 | **0.91** | **1.29** |
| AT3G56310 | Melibiase family protein | 0.61 | 0.10 | **-0.79** |
| AT3G56360 | unknown protein | -0.10 | -0.50 | **-1.24** |
| AT3G57010 | Calcium-dependent phosphotriesterase superfamily protein | 0.02 | **1.33** | **1.11** |
| AT3G57150 | AtCBF5_AtNAP57_CBF5_NAP57__homologue of NAP57 | -0.27 | 0.60 | **1.07** |
| AT3G57490 | Ribosomal protein S5 family protein | -0.01 | 0.60 | **1.05** |
| AT3G57520 | AtSIP2_SIP2__seed imbibition 2 | -0.20 | **-1.63** | **-1.48** |
| AT3G57610 | ADSS__adenylosuccinate synthase | -0.37 | 0.37 | **1.04** |
| AT3G57660 | NRPA1__nuclear RNA polymerase A1 | -0.07 | 0.48 | **1.13** |
| AT3G58610 | ketol-acid reductoisomerase | 0.26 | 0.47 | **0.93** |
| AT3G58660 | Ribosomal protein L1p/L10e family | -0.07 | 0.48 | **0.85** |
| AT3G58700 | Ribosomal L5P family protein | 0.00 | 0.54 | **1.00** |

| AGI identifier | Gene annotation | 30 min | 2h | 8h |
|---|---|---|---|---|
| AT3G58750 | CSY2__citrate synthase 2 | 0.00 | -0.46 | **-0.85** |
| AT3G58990 | IPMI1__isopropylmalate isomerase 1 | 0.09 | **1.08** | **1.64** |
| AT3G59220 | ATPIRIN1_PRN_PRN1__pirin | -0.08 | **0.93** | **0.75** |
| AT3G59260 | pirin, putative | 0.29 | **0.91** | **0.79** |
| AT3G59340 | Eukaryotic protein of unknown function (DUF914) | 0.13 | -0.17 | **0.75** |
| AT3G59350 | Protein kinase superfamily protein | -0.49 | **-1.27** | **-0.85** |
| AT3G59540 | Ribosomal L38e protein family | -0.05 | 0.52 | **0.93** |
| AT3G59670 | unknown protein | -0.04 | 0.46 | **0.97** |
| AT3G59890 | Dihydrodipicolinate reductase, bacterial/plant | -0.08 | 0.26 | **0.92** |
| AT3G59930 | Encodes a defensin-like (DEFL) family protein. | 0.45 | **-1.16** | **-2.13** |
| AT3G59940 | Galactose oxidase/kelch repeat superfamily protein | -0.08 | **-1.66** | **-1.77** |
| AT3G59970 | MTHFR1__methylenetetrahydrofolate reductase 1 | 0.03 | -0.01 | **0.89** |
| AT3G60130 | BGLU16__beta glucosidase 16 | -0.01 | **-0.91** | **-1.16** |
| AT3G60140 | BGLU30_DIN2_SRG2__Glycosyl hydrolase superfamily protein | -0.04 | **-0.86** | **-2.02** |
| AT3G60245 | Zinc-binding ribosomal protein family protein | -0.36 | 0.37 | **1.09** |
| AT3G60300 | RWD domain-containing protein | -0.09 | -0.67 | **-1.19** |
| AT3G61010 | Ferritin/ribonucleotide reductase-like family protein | **-0.72** | -0.15 | -0.01 |
| AT3G61060 | AtPP2-A13_PP2-A13__phloem protein 2-A13 | 0.20 | **-2.14** | **-2.13** |
| AT3G61240 | DEA(D/H)-box RNA helicase family protein | -0.45 | 0.29 | **0.76** |
| AT3G61260 | Remorin family protein | 0.45 | **-0.76** | **-0.78** |
| AT3G61470 | LHCA2__photosystem I light harvesting complex gene 2 | 0.46 | 0.20 | **-0.77** |
| AT3G61560 | reticulon family protein (RTNLB6) | -0.02 | 0.47 | **0.71** |
| AT3G61820 | Eukaryotic aspartyl protease family protein | -0.04 | **1.02** | **1.75** |
| AT3G62190 | Chaperone DnaJ-domain superfamily protein | x | -0.15 | **-0.83** |
| AT3G62360 | Carbohydrate-binding-like fold | -0.20 | 0.07 | **0.77** |
| AT3G62410 | CP12-2__CP12 domain-containing protein 2 | 0.45 | -0.28 | **-1.20** |
| AT3G62420 | ATBZIP53_BZIP53__basic region/leucine zipper motif 53 | **-0.80** | **-1.13** | **-0.97** |
| AT3G62460 | Putative endonuclease or glycosyl hydrolase | -0.17 | 0.61 | **1.02** |
| AT3G62550 | Adenine nucleotide alpha hydrolases-like superfamily protein | -0.02 | **-1.20** | **-1.56** |
| AT3G62650 | unknown protein | 0.04 | -0.38 | **-0.93** |
| AT3G62720 | ATXT1_XT1_XXT1__xylosyltransferase 1 | -0.48 | **-0.77** | -0.09 |
| AT3G62870 | Ribosomal protein L7Ae/L30e/S12e/Gadd45 family protein | -0.12 | 0.43 | **1.00** |
| AT3G62930 | Thioredoxin superfamily protein | -0.12 | -0.40 | **-1.06** |
| AT4G00100 | ATRPS13A_PFL2_RPS13_RPS13A__ribosomal protein S13A | -0.17 | 0.50 | **1.00** |
| AT4G00430 | PIP1;4_PIP1E_TMP-C__plasma membrane intrinsic protein 1;4 | 0.37 | **0.87** | **0.82** |
| AT4G00570 | NAD-ME2__NAD-dependent malic enzyme 2 | -0.09 | 0.13 | **0.93** |
| AT4G00600 | Amino acid dehydrogenase family protein | -0.10 | 0.04 | **0.77** |
| AT4G00620 | Amino acid dehydrogenase family protein | -0.12 | 0.18 | **0.76** |
| AT4G00630 | ATKEA2_KEA2__K+ efflux antiporter 2 | -0.18 | 0.40 | **0.85** |
| AT4G00750 | S-adenosyl-L-methionine-dependent methyltransferases superfamily protein | 0.03 | -0.35 | **-0.98** |
| AT4G00752 | UBX domain-containing protein | -0.22 | -0.25 | **-0.87** |
| AT4G00810 | 60S acidic ribosomal protein family | -0.22 | 0.17 | **0.81** |
| AT4G01030 | pentatricopeptide (PPR) repeat-containing protein | 0.05 | **-0.85** | **-0.92** |

| AGI identifier | Gene annotation | 30 min | 2h | 8h |
|---|---|---|---|---|
| AT4G01080 | TBL26__TRICHOME BIREFRINGENCE-LIKE 26 | 0.00 | **1.63** | **1.06** |
| AT4G01100 | ADNT1__adenine nucleotide transporter 1 | -0.32 | -0.21 | **0.81** |
| AT4G01265 | raffinose synthase family protein | 0.16 | **-0.82** | **-0.94** |
| AT4G01770 | RGXT1__rhamnogalacturonan xylosyltransferase 1 | 0.34 | 0.34 | **0.73** |
| AT4G01870 | tolB protein-related | 0.53 | 0.11 | **-0.97** |
| AT4G02220 | zinc finger (MYND type) family protein / programmed cell death 2 C-terminal domain-containing protein | -0.02 | 0.18 | **0.71** |
| AT4G02230 | Ribosomal protein L19e family protein | -0.12 | 0.05 | **0.87** |
| AT4G02405 | unknown protein | 0.05 | 0.38 | **0.82** |
| AT4G02440 | EID1__F-box family protein | -0.32 | -0.62 | **-0.75** |
| AT4G02520 | ATGSTF2_ATPM24_ATPM24.1_GST2_GSTF2__glutathione S-transferase PHI 2 | 0.04 | 0.31 | **-1.20** |
| AT4G02930 | GTP binding Elongation factor Tu family protein | -0.05 | 0.22 | **0.84** |
| AT4G02940 | oxidoreductase, 2OG-Fe(II) oxygenase family protein | 0.17 | **0.97** | 0.38 |
| AT4G03280 | PETC_PGR1__photosynthetic electron transfer C | 0.03 | -0.14 | **-0.87** |
| AT4G03510 | ATRMA1_RMA1__RING membrane-anchor 1 | -0.09 | **-1.29** | x |
| AT4G03540 | Uncharacterised protein family (UPF0497) | 0.05 | **1.04** | 0.27 |
| AT4G03950 | Nucleotide/sugar transporter family protein | 0.17 | **1.00** | **2.21** |
| AT4G04020 | FIB__fibrillin | 0.48 | **0.98** | **0.71** |
| AT4G04330 | Chaperonin-like RbcX protein | -0.06 | -0.39 | **-0.90** |
| AT4G04610 | APR_APR1_ATAPR1_PRH19__APS reductase 1 | **0.68** | **0.85** | 0.09 |
| AT4G04640 | ATPC1__ATPase, F1 complex, gamma subunit protein | **0.78** | 0.28 | -0.43 |
| AT4G04745 | unknown protein | -0.01 | 0.11 | **0.90** |
| AT4G04760 | Major facilitator superfamily protein | 0.12 | 0.06 | **0.86** |
| AT4G04940 | Transducin family protein / WD-40 repeat family protein | -0.22 | 0.26 | **0.71** |
| AT4G04990 | Protein of unknown function (DUF761) | 0.28 | -0.40 | **-0.79** |
| AT4G05310 | Ubiquitin-like superfamily protein | 0.19 | -0.13 | **-1.18** |
| AT4G05420 | DDB1A__damaged DNA binding protein 1A | -0.18 | 0.34 | **0.74** |
| AT4G05450 | ATMFDX1_MFDX1__mitochondrial ferredoxin 1 | -0.09 | 0.67 | **0.99** |
| AT4G06746 | RAP2.9 (related to AP2 9); transcription factor | 0.25 | -0.47 | **-0.99** |
| AT4G08210 | Pentatricopeptide repeat (PPR-like) superfamily protein | 0.17 | 0.66 | **1.44** |
| AT4G08920 | ATCRY1_BLU1_CRY1_HY4_OOP2__cryptochrome 1 | -0.37 | **-1.25** | **-0.87** |
| AT4G08950 | EXO__Phosphate-responsive 1 family protein | **-1.32** | **-1.15** | x |
| AT4G09020 | ATISA3_ISA3__isoamylase 3 | -0.10 | 0.15 | **0.75** |
| AT4G09320 | NDPK1__Nucleoside diphosphate kinase family protein | -0.08 | 0.42 | **1.12** |
| AT4G10110 | RNA-binding (RRM/RBD/RNP motifs) family protein | 0.07 | **1.17** | **1.40** |
| AT4G10160 | RING/U-box superfamily protein | 0.16 | **-0.74** | **-0.93** |
| AT4G10390 | Protein kinase superfamily protein | 0.13 | 0.57 | **0.84** |
| AT4G10480 | Nascent polypeptide-associated complex (NAC), alpha subunit family protein | 0.43 | 0.31 | **0.80** |
| AT4G10770 | ATOPT7_OPT7__oligopeptide transporter 7 | **-0.69** | 0.35 | **0.75** |
| AT4G11130 | RDR2_SMD1__RNA-dependent RNA polymerase 2 | 0.10 | -0.50 | **-0.83** |
| AT4G11175 | Nucleic acid-binding, OB-fold-like protein | **0.69** | 0.18 | x |
| AT4G11360 | RHA1B__RING-H2 finger A1B | 0.03 | -0.46 | **-0.76** |
| AT4G11430 | hydroxyproline-rich glycoprotein family protein | 0.16 | 0.06 | **0.84** |
| AT4G11570 | Haloacid dehalogenase-like hydrolase (HAD) superfamily protein | x | -0.38 | **-0.91** |

| AGI identifier | Gene annotation | 30 min | 2h | 8h |
|---|---|---|---|---|
| AT4G11600 | ATGPX6_GPX6_LSC803_PHGPX__glutathione peroxidase 6 | **0.82** | x | -0.13 |
| AT4G11650 | ATOSM34_OSM34__osmotin 34 | 0.55 | 0.09 | **-1.55** |
| AT4G12030 | BASS5_BAT5__bile acid transporter 5 | -0.13 | 0.61 | **1.22** |
| AT4G12420 | SKU5__Cupredoxin superfamily protein | -0.51 | **-1.14** | 0.15 |
| AT4G12490 | Bifunctional inhibitor/lipid-transfer protein/seed storage 2S albumin superfamily protein | 0.02 | 0.24 | **0.82** |
| AT4G12500 | Bifunctional inhibitor/lipid-transfer protein/seed storage 2S albumin superfamily protein | 0.08 | 0.22 | **0.82** |
| AT4G12560 | PR1 (Constitutive Expresser of PR Genes 1, also known as CPR30) | -0.28 | **-0.80** | **-0.80** |
| AT4G12600 | Ribosomal protein L7Ae/L30e/S12e/Gadd45 family protein | -0.30 | 0.58 | **1.09** |
| AT4G12650 | Endomembrane protein 70 protein family | -0.07 | 0.08 | **1.03** |
| AT4G12730 | FLA2__FASCICLIN-like arabinogalactan 2 | -0.28 | -0.40 | **0.90** |
| AT4G12880 | AtENODL19_ENODL19__early nodulin-like protein 19 | **0.70** | 0.13 | 0.30 |
| AT4G13170 | Ribosomal protein L13 family protein | -0.01 | 0.40 | **1.02** |
| AT4G13180 | NAD(P)-binding Rossmann-fold superfamily protein | **0.80** | 0.64 | -0.05 |
| AT4G13250 | NYC1__NAD(P)-binding Rossmann-fold superfamily protein | 0.10 | -0.16 | **-0.89** |
| AT4G13410 | ATCSLA15_CSLA15__Nucleotide-diphospho-sugar transferases superfamily protein | -0.18 | **0.85** | 0.07 |
| AT4G13430 | ATLEUC1_IIL1__isopropyl malate isomerase large subunit 1 | -0.03 | 0.22 | **1.11** |
| AT4G13530 | unknown protein | 0.39 | -0.47 | **-1.31** |
| AT4G13770 | CYP83A1_REF2__cytochrome P450, family 83, subfamily A, polypeptide 1 | **1.14** | **0.93** | **1.92** |
| AT4G13840 | HXXXD-type acyl-transferase family protein | 0.24 | 0.04 | **0.73** |
| AT4G13940 | ATSAHH1_EMB1395_HOG1_MEE58_SAHH1__S-adenosyl-L-homocysteine hydrolase | -0.27 | 0.24 | **1.20** |
| AT4G14040 | EDA38_SBP2__selenium-binding protein 2 | -0.13 | -0.24 | **-0.78** |
| AT4G14130 | XTH15_XTR7__xyloglucan endotransglucosylase/hydrolase 15 | **-0.75** | **-0.87** | -0.27 |
| AT4G14270 | Protein containing PAM2 motif which mediates interaction with the PABC domain of polyadenyl binding proteins. | -0.37 | **-1.24** | **-0.89** |
| AT4G14320 | Zinc-binding ribosomal protein family protein | -0.34 | 0.23 | **0.80** |
| AT4G14410 | bHLH104__basic helix-loop-helix (bHLH) DNA-binding superfamily protein | 0.08 | -0.10 | **-0.72** |
| AT4G14430 | ATECI2_ECHIB_ECI2_IBR10_PEC12__indole-3-butyric acid response 10 | 0.02 | -0.34 | **-0.79** |
| AT4G14440 | ATECI3_ECI3_HCD1__3-hydroxyacyl-CoA dehydratase 1 | 0.51 | **0.87** | 0.60 |
| AT4G14880 | ATCYS-3A_CYTACS1_OASA1_OLD3__O-acetylserine (thiol) lyase (OAS-TL) isoform A1 | **0.82** | -0.06 | -0.40 |
| AT4G14960 | TUA6__Tubulin/FtsZ family protein | -0.20 | 0.02 | **0.87** |
| AT4G15210 | AT-BETA-AMY_ATBETA-AMY_BAM5_BMY1_RAM1__beta-amylase 5 | 0.09 | 0.55 | **0.73** |
| AT4G15248 | B-box type zinc finger family protein | **0.82** | 0.26 | -0.14 |
| AT4G15260 | UDP-Glycosyltransferase superfamily protein | -0.03 | -0.20 | **-0.83** |
| AT4G15390 | HXXXD-type acyl-transferase family protein | 0.43 | -0.37 | **1.44** |
| AT4G15393 | CYP702A5 (cytochrome P450, family 702, subfamily A, polypeptide 5); heme binding / iron ion binding / monooxygenase | -0.11 | -0.12 | **0.92** |

| AGI identifier | Gene annotation | 30 min | 2h | 8h |
|---|---|---|---|---|
| AT4G15480 | UGT84A1__UDP-Glycosyltransferase superfamily protein | 0.44 | 0.62 | **0.75** |
| AT4G15530 | PPDK__pyruvate orthophosphate dikinase | 0.33 | -0.46 | **-1.94** |
| AT4G15550 | IAGLU__indole-3-acetate beta-D-glucosyltransferase | 0.07 | -0.16 | **-1.18** |
| AT4G15610 | Uncharacterised protein family (UPF0497) | -0.05 | -0.41 | **-1.21** |
| AT4G15640 | unknown protein | -0.10 | 0.36 | **1.25** |
| AT4G15760 | Encodes a protein with similarity to monooxygenases that are known to degrade salicylic acid (SA). | **0.66** | -0.61 | **-0.86** |
| AT4G15765 | FAD/NAD(P)-binding oxidoreductase family protein | -0.10 | -0.34 | **-0.90** |
| AT4G15770 | RNA binding | 0.16 | 0.62 | **0.84** |
| AT4G16141 | unknown protein | **-0.88** | 0.21 | 0.63 |
| AT4G16146 | cAMP-regulated phosphoprotein 19-related protein | -0.12 | 0.28 | **0.95** |
| AT4G16190 | Papain family cysteine protease | 0.57 | 0.21 | **-1.47** |
| AT4G16340 | SPK1__guanyl-nucleotide exchange factors;GTPase binding;GTP binding | -0.53 | -0.01 | **0.74** |
| AT4G16400 | unknown protein | 0.16 | 0.08 | **-0.85** |
| AT4G16520 | ATG8F__Ubiquitin-like superfamily protein | -0.33 | **-1.13** | **-1.75** |
| AT4G16563 | Eukaryotic aspartyl protease family protein | **-1.19** | **-1.25** | -0.46 |
| AT4G16590 | ATCSLA01_ATCSLA1_CSLA01_CSLA01__cellulose synthase-like A01 | 0.08 | **1.26** | **0.74** |
| AT4G16660 | heat shock protein 70 (Hsp 70) family protein | 0.01 | 0.20 | **1.00** |
| AT4G16690 | ATMES16_MES16__methyl esterase 16 | 0.31 | -0.56 | **-0.97** |
| AT4G16720 | Ribosomal protein L23/L15e family protein | -0.14 | 0.49 | **0.95** |
| AT4G16840 | unknown protein | 0.13 | -0.10 | **-0.78** |
| AT4G17090 | BAM3_BMY8_CT-BMY__chloroplast beta-amylase | 0.02 | 0.05 | **1.45** |
| AT4G17245 | RING/U-box superfamily protein | 0.10 | **-0.94** | **-1.26** |
| AT4G17280 | Auxin-responsive family protein | 0.09 | **0.84** | 0.10 |
| AT4G17340 | DELTA-TIP2_TIP2;2__tonoplast intrinsic protein 2;2 | **0.66** | 0.09 | -0.06 |
| AT4G17390 | Ribosomal protein L23/L15e family protein | -0.20 | 0.25 | **0.93** |
| AT4G17460 | HAT1__Homeobox-leucine zipper protein 4 (HB-4) / HD-ZIP protein | **-0.95** | -0.29 | -0.29 |
| AT4G17470 | alpha/beta-Hydrolases superfamily protein | -0.01 | 0.19 | **0.73** |
| AT4G17500 | ATERF-1_ERF-1__ethylene responsive element binding factor 1 | -0.02 | -0.53 | **-1.40** |
| AT4G17520 | Hyaluronan / mRNA binding family | -0.26 | 0.52 | **0.97** |
| AT4G17770 | ATTPS5_TPS5_TPS5__trehalose phosphatase/synthase 5 | -0.02 | 0.51 | **1.35** |
| AT4G17840 | unknown protein | 0.39 | -0.31 | **-1.35** |
| AT4G18010 | 5PTASE2_AT5PTASE2_IP5PII__myo-inositol polyphosphate 5-phosphatase 2 | -0.46 | -0.37 | **-0.90** |
| AT4G18030 | S-adenosyl-L-methionine-dependent methyltransferases superfamily protein | 0.52 | -0.04 | **1.34** |
| AT4G18100 | Ribosomal protein L32e | 0.17 | 0.56 | **0.84** |
| AT4G18230 | unknown protein | -0.17 | -0.70 | **-0.84** |
| AT4G18330 | Translation elongation factor EF1A/initiation factor IF2gamma family protein | 0.16 | 0.38 | **1.03** |
| AT4G18700 | ATWL4_CIPK12_SnRK3.9_WL4__CBL-interacting protein kinase 12 | -0.41 | 0.42 | **1.08** |
| AT4G18730 | RPL16B__ribosomal protein L16B | -0.14 | 0.32 | **0.94** |

| AGI identifier | Gene annotation | 30 min | 2h | 8h |
|---|---|---|---|---|
| AT4G18905 | Transducin family protein / WD-40 repeat family protein | -0.19 | 0.35 | **0.79** |
| AT4G19160 | unknown protein | -0.40 | **-1.48** | **-1.25** |
| AT4G19170 | CCD4_NCED4__nine-cis-epoxycarotenoid dioxygenase 4 | 0.31 | **-0.90** | -0.38 |
| AT4G19200 | proline-rich family protein | 0.36 | -0.31 | **-1.08** |
| AT4G19410 | Pectinacetylesterase family protein | 0.02 | -0.50 | **-1.12** |
| AT4G19530 | disease resistance protein (TIR-NBS-LRR class) family | -0.57 | **-1.19** | -0.25 |
| AT4G19690 | ATIRT1_IRT1__iron-regulated transporter 1 | 0.60 | 0.18 | **1.46** |
| AT4G19860 | alpha/beta-Hydrolases superfamily protein | -0.01 | **-1.01** | **-0.99** |
| AT4G19880 | Glutathione S-transferase family protein | 0.14 | -0.71 | **-1.09** |
| AT4G20070 | AAH_ATAAH__allantoate amidohydrolase | -0.09 | -0.41 | **-0.99** |
| AT4G20380 | LSD1 zinc finger family protein | -0.08 | **-0.80** | -0.70 |
| AT4G20390 | Uncharacterised protein family (UPF0497) | 0.23 | 0.17 | **0.76** |
| AT4G20860 | FAD-binding Berberine family protein | **0.81** | -0.32 | **-1.18** |
| AT4G21150 | HAP6__ribophorin II (RPN2) family protein | -0.12 | 0.16 | **0.73** |
| AT4G21280 | PSBQ_PSBQ-1_PSBQA__photosystem II subunit QA | 0.64 | -0.08 | **-0.84** |
| AT4G21320 | HSA32 (HEAT-STRESS-ASSOCIATED 32) | 0.15 | -0.05 | **-0.74** |
| AT4G21810 | DER2.1__DERLIN-2.1 | 0.40 | -0.55 | **-1.05** |
| AT4G21870 | HSP20-like chaperones superfamily protein | **-0.74** | **-1.31** | **-1.75** |
| AT4G21910 | MATE efflux family protein | -0.32 | 0.41 | **0.91** |
| AT4G21960 | PRXR1__Peroxidase superfamily protein | 0.17 | 0.11 | **1.03** |
| AT4G22210 | LCR85 (Low-molecular-weight cysteine-rich 85) | 0.08 | -0.26 | **0.76** |
| AT4G22220 | ATISU1_ISU1__SufE/NifU family protein | **0.69** | 0.25 | -0.02 |
| AT4G22610 | Bifunctional inhibitor/lipid-transfer protein/seed storage 2S albumin superfamily protein | 0.07 | -0.08 | **0.91** |
| AT4G22750 | DHHC-type zinc finger family protein | 0.04 | -0.16 | **-0.73** |
| AT4G22870 | 2-oxoglutarate (2OG) and Fe(II)-dependent oxygenase superfamily protein | 0.01 | 0.03 | **1.01** |
| AT4G22880 | ANS_LDOX_TDS4_TT18__leucoanthocyanidin dioxygenase | -0.17 | 0.10 | **0.79** |
| AT4G22920 | ATNYE1_NYE1__non-yellowing 1 | 0.14 | -0.29 | **-0.79** |
| AT4G23100 | ATECS1_CAD2_GSH1_GSHA_PAD2_RML1__glutamate-cysteine ligase | **0.67** | 0.09 | -0.33 |
| AT4G23450 | RING/U-box superfamily protein | -0.33 | 0.09 | **-0.77** |
| AT4G23470 | PLAC8 family protein | -0.07 | -0.26 | **-1.00** |
| AT4G23600 | CORI3_JR2__Tyrosine transaminase family protein | -0.08 | **0.87** | **1.12** |
| AT4G23890 | unknown protein | 0.19 | 0.11 | **-0.88** |
| AT4G24120 | ATYSL1_YSL1__YELLOW STRIPE like 1 | -0.05 | 0.14 | **0.75** |
| AT4G24160 | alpha/beta-Hydrolases superfamily protein | 0.17 | -0.31 | **-0.97** |
| AT4G24190 | AtHsp90-7_AtHsp90.7_HSP90.7_SHD__Chaperone protein htpG family protein | 0.05 | 0.00 | **1.04** |
| AT4G24230 | ACBP3 (ACYL-COA-BINDING DOMAIN 3) | 0.19 | **-1.31** | **-1.90** |
| AT4G24620 | PGI_PGI1__phosphoglucose isomerase 1 | 0.03 | 0.29 | **0.96** |
| AT4G24780 | Pectin lyase-like superfamily protein | -0.07 | -0.05 | **1.77** |
| AT4G24830 | arginosuccinate synthase family | 0.17 | **0.78** | **1.41** |
| AT4G25050 | ACP4__acyl carrier protein 4 | -0.30 | -0.24 | **-1.06** |
| AT4G25080 | CHLM__magnesium-protoporphyrin IX methyltransferase | 0.17 | -0.49 | **-1.25** |
| AT4G25170 | Uncharacterised conserved protein (UCP012943) | 0.25 | -0.30 | **-1.75** |
| AT4G25340 | ATFKBP53_FKBP53__FK506 BINDING PROTEIN 53 | -0.46 | 0.48 | **1.10** |

| AGI identifier | Gene annotation | 30 min | 2h | 8h |
|---|---|---|---|---|
| AT4G25480 | ATCBF3_CBF3_DREB1A__dehydration response element B1A | **0.66** | 0.52 | 0.47 |
| AT4G25570 | ACYB-2__Cytochrome b561/ferric reductase transmembrane protein family | 0.05 | 0.00 | **-0.94** |
| AT4G25620 | hydroxyproline-rich glycoprotein family protein | x | **-0.83** | -0.64 |
| AT4G25630 | ATFIB2_FIB2__fibrillarin 2 | -0.39 | **1.15** | **1.97** |
| AT4G25690 | unknown protein | -0.32 | -0.58 | **-1.12** |
| AT4G25730 | FtsJ-like methyltransferase family protein | -0.49 | 0.61 | **1.23** |
| AT4G25810 | XTH23_XTR6_xyloglucan endotransglycosylase 6 | **-0.94** | **-1.38** | -0.46 |
| AT4G25890 | 60S acidic ribosomal protein family | -0.26 | 0.33 | **1.12** |
| AT4G26110 | ATNAP1;1_NAP1;1__nucleosome assembly protein1;1 | -0.35 | 0.17 | **0.76** |
| AT4G26210 | Mitochondrial ATP synthase subunit G protein | -0.22 | 0.40 | **0.84** |
| AT4G26530 | Aldolase superfamily protein | 0.20 | -0.25 | **-1.25** |
| AT4G26850 | VTC2__mannose-1-phosphate guanylyltransferase (GDP)s;GDP-galactose:mannose-1-phosphate guanylyltransferases;GDP-galactose:glucose-1-phosphate guanylyltransferases;GDP-galactose:myoinositol-1-phosphate guanylyltransferases;glucose-1-phosphate guanylyltransferase | 0.18 | **1.15** | 0.14 |
| AT4G26950 | Protein of unknown function, DUF584 | x | **0.76** | 0.60 |
| AT4G27270 | Quinone reductase family protein | 0.15 | 0.06 | **-0.81** |
| AT4G27280 | Calcium-binding EF-hand family protein | **-0.96** | -0.19 | -0.23 |
| AT4G27410 | ANAC072_RD26__NAC (No Apical Meristem) domain transcriptional regulator superfamily protein | 0.12 | **-0.99** | **-1.42** |
| AT4G27450 | Aluminium induced protein with YGL and LRDR motifs | -0.33 | **-2.07** | **-1.88** |
| AT4G27520 | AtENODL2_ENODL2__early nodulin-like protein 2 | 0.42 | **0.95** | 0.63 |
| AT4G27560 | UDP-Glycosyltransferase superfamily protein | -0.13 | 0.67 | **1.20** |
| AT4G27570 | UDP-Glycosyltransferase superfamily protein | 0.09 | 0.53 | **1.30** |
| AT4G27585 | SPFH/Band 7/PHB domain-containing membrane-associated protein family | 0.16 | 0.13 | **0.73** |
| AT4G27600 | NARA5__pfkB-like carbohydrate kinase family protein | -0.33 | -0.49 | **-0.88** |
| AT4G27640 | ARM repeat superfamily protein | x | 0.24 | **0.76** |
| AT4G27745 | unknown protein | -0.02 | **-0.80** | **-1.22** |
| AT4G27900 | CCT motif family protein | -0.13 | **1.14** | 0.62 |
| AT4G27940 | ATMTM1_MTM1__manganese tracking factor for mitochondrial SOD2 | -0.07 | 0.60 | **0.79** |
| AT4G28030 | Acyl-CoA N-acyltransferases (NAT) superfamily protein | -0.06 | -0.06 | **-0.94** |
| AT4G28040 | Nodulin MtN21 /EamA-like transporter family protein | -0.11 | -0.17 | **-1.51** |
| AT4G28240 | Wound-responsive family protein | -0.23 | **-1.03** | **-1.00** |
| AT4G28250 | ATEXPB3_ATHEXP BETA 1.6_EXPB3__expansin B3 | -0.08 | 0.05 | **2.06** |
| AT4G28300 | Protein of unknown function (DUF1421) | 0.00 | -0.42 | **-0.72** |
| AT4G28360 | Ribosomal protein L22p/L17e family protein | -0.13 | 0.28 | **1.06** |
| AT4G28450 | nucleotide binding;protein binding | -0.20 | 0.43 | **0.93** |
| AT4G28510 | ATPHB1_PHB1__prohibitin 1 | -0.15 | -0.03 | **0.95** |
| AT4G29030 | Putative membrane lipoprotein | -0.06 | 0.03 | **0.94** |
| AT4G29230 | anac075_NAC075__NAC domain containing protein 75 | 0.20 | 0.09 | **0.75** |
| AT4G29270 | HAD superfamily, subfamily IIIB acid phosphatase | 0.18 | -0.13 | **0.92** |

| AGI identifier | Gene annotation | 30 min | 2h | 8h |
|---|---|---|---|---|
| AT4G29410 | Ribosomal L28e protein family | -0.25 | 0.54 | **0.90** |
| AT4G29510 | ATPRMT11_ATPRMT1B_PRMT11_PRMT1B__arginine methyltransferase 11 | -0.32 | 0.43 | **0.92** |
| AT4G29680 | Alkaline-phosphatase-like family protein | -0.08 | 0.28 | **0.92** |
| AT4G29700 | Alkaline-phosphatase-like family protein | 0.08 | 0.42 | **0.90** |
| AT4G29905 | unknown protein | -0.35 | **-1.75** | **-1.14** |
| AT4G29930 | basic helix-loop-helix (bHLH) DNA-binding superfamily protein | 0.09 | **0.81** | 0.01 |
| AT4G30150 | unknown protein | -0.10 | 0.21 | **0.73** |
| AT4G30190 | AHA2_HA2_PMA2__H(+)-ATPase 2 | 0.05 | 0.56 | **1.73** |
| AT4G30270 | MERI-5_MERI5B_SEN4_XTH24__xyloglucan endotransglucosylase/hydrolase 24 | -0.07 | **-1.34** | x |
| AT4G30280 | ATXTH18_XTH18__xyloglucan endotransglucosylase/hydrolase 18 | -0.46 | **-1.02** | -0.15 |
| AT4G30530 | Class I glutamine amidotransferase-like superfamily protein | 0.17 | **1.19** | **0.95** |
| AT4G30650 | Low temperature and salt responsive protein family | -0.22 | 0.68 | **1.60** |
| AT4G30660 | Low temperature and salt responsive protein family | -0.09 | 0.55 | **1.06** |
| AT4G30800 | Nucleic acid-binding, OB-fold-like protein | 0.18 | 0.38 | **1.06** |
| AT4G30810 | scpl29__serine carboxypeptidase-like 29 | 0.30 | 0.11 | **0.94** |
| AT4G30930 | NFD1__Ribosomal protein L21 | -0.06 | 0.12 | **0.71** |
| AT4G30993 | Calcineurin-like metallo-phosphoesterase superfamily protein | 0.28 | -0.27 | **-1.08** |
| AT4G31500 | ATR4_CYP83B1_RED1_RNT1_SUR2__cytochrome P450, family 83, subfamily B, polypeptide 1 | 0.04 | **1.13** | **1.40** |
| AT4G31700 | RPS6_RPS6A__ribosomal protein S6 | -0.19 | 0.48 | **1.06** |
| AT4G31790 | Tetrapyrrole (Corrin/Porphyrin) Methylases | 0.25 | 0.48 | **0.82** |
| AT4G31810 | ATP-dependent caseinolytic (Clp) protease/crotonase family protein | -0.15 | 0.39 | **1.19** |
| AT4G31850 | PGR3__proton gradient regulation 3 | -0.29 | -0.12 | **-0.80** |
| AT4G31870 | ATGPX7_GPX7__glutathione peroxidase 7 | 0.28 | -0.27 | **-0.81** |
| AT4G31910 | HXXXD-type acyl-transferase family protein | -0.05 | 0.05 | **0.89** |
| AT4G31985 | Ribosomal protein L39 family protein | -0.08 | 0.32 | **0.95** |
| AT4G32060 | calcium-binding EF hand family protein | -0.50 | **-0.99** | -0.63 |
| AT4G32400 | ATBT1_EMB104_EMB42_SHS1__Mitochondrial substrate carrier family protein | 0.07 | 0.29 | **0.73** |
| AT4G32410 | AtCESA1_CESA1_RSW1__cellulose synthase 1 | -0.56 | -0.33 | **0.88** |
| AT4G32480 | unknown protein | -0.63 | **-1.41** | **-1.20** |
| AT4G32520 | AtSHMT3_SHM3__serine hydroxymethyltransferase 3 | -0.15 | 0.36 | **0.81** |
| AT4G32850 | nPAP_PAP(IV)__nuclear poly(a) polymerase | **-0.68** | -0.19 | -0.17 |
| AT4G32870 | Polyketide cyclase/dehydrase and lipid transport superfamily protein | 0.08 | -0.56 | **-1.60** |
| AT4G32940 | GAMMA-VPE_GAMMAVPE__gamma vacuolar processing enzyme | 0.26 | -0.41 | **-0.98** |
| AT4G33030 | SQD1__sulfoquinovosyldiacylglycerol 1 | 0.14 | **1.02** | **1.61** |
| AT4G33070 | Thiamine pyrophosphate dependent pyruvate decarboxylase family protein | 0.13 | **1.29** | **0.75** |
| AT4G33110 | S-adenosyl-L-methionine-dependent methyltransferases superfamily protein | 0.45 | -0.12 | **-0.80** |

| AGI identifier | Gene annotation | 30 min | 2h | 8h |
|---|---|---|---|---|
| AT4G33420 | Peroxidase superfamily protein | -0.24 | -0.57 | **-0.76** |
| AT4G33540 | metallo-beta-lactamase family protein | -0.10 | 0.21 | **-0.72** |
| AT4G33610 | glycine-rich protein | **0.68** | x | x |
| AT4G33680 | AGD2__Pyridoxal phosphate (PLP)-dependent transferases superfamily protein | 0.36 | 0.24 | **0.93** |
| AT4G33905 | Peroxisomal membrane 22 kDa (Mpv17/PMP22) family protein | -0.04 | **0.89** | 0.56 |
| AT4G33940 | RING/U-box superfamily protein | -0.42 | -0.70 | **-0.96** |
| AT4G33980 | unknown protein | x | 0.01 | **-1.20** |
| AT4G34030 | MCCB__3-methylcrotonyl-CoA carboxylase | 0.36 | **-0.94** | x |
| AT4G34050 | CCoAOMT1__S-adenosyl-L-methionine-dependent methyltransferases superfamily protein | 0.62 | **0.84** | **1.23** |
| AT4G34138 | UGT73B1__UDP-glucosyl transferase 73B1 | -0.03 | **-1.36** | **-1.54** |
| AT4G34250 | KCS16__3-ketoacyl-CoA synthase 16 | -0.17 | **-0.81** | -0.18 |
| AT4G34350 | CLB6_HDR_ISPH__4-hydroxy-3-methylbut-2-enyl diphosphate reductase | -0.08 | -0.08 | **-0.71** |
| AT4G34555 | Ribosomal protein S25 family protein | -0.13 | 0.46 | **0.86** |
| AT4G34588 | CPuORF2__conserved peptide upstream open reading frame 2 | -0.48 | **0.81** | **1.73** |
| AT4G34670 | Ribosomal protein S3Ae | -0.40 | 0.10 | **0.74** |
| AT4G34850 | LAP5__Chalcone and stilbene synthase family protein | -0.09 | 0.14 | **0.78** |
| AT4G34870 | ATCYP1_ROC5__rotamase cyclophilin 5 | -0.21 | 0.51 | **1.05** |
| AT4G34920 | PLC-like phosphodiesterases superfamily protein | x | **-0.96** | **-1.17** |
| AT4G34950 | Major facilitator superfamily protein | 0.04 | **1.57** | **1.83** |
| AT4G35090 | CAT2__catalase 2 | 0.12 | 0.21 | **-0.98** |
| AT4G35160 | O-methyltransferase family protein | -0.10 | 0.41 | **1.00** |
| AT4G35300 | TMT2__tonoplast monosaccharide transporter2 | -0.03 | 0.41 | **0.72** |
| AT4G35630 | PSAT__phosphoserine aminotransferase | 0.65 | **1.12** | **1.58** |
| AT4G35650 | IDH-III__isocitrate dehydrogenase III | 0.40 | 0.39 | **0.75** |
| AT4G35750 | SEC14 cytosolic factor family protein / phosphoglyceride transfer family protein | 0.34 | **-0.83** | **-1.40** |
| AT4G35770 | ATSEN1_DIN1_SEN1_SEN1__Rhodanese/Cell cycle control phosphatase superfamily protein | -0.10 | **-1.64** | **-2.67** |
| AT4G35860 | ATGB2_ATRAB2C_ATRABB1B_GB2__GTP-binding 2 | -0.08 | -0.47 | **-0.90** |
| AT4G36010 | Pathogenesis-related thaumatin superfamily protein | 0.25 | **1.34** | **0.81** |
| AT4G36020 | CSDP1__cold shock domain protein 1 | 0.11 | **0.79** | **0.97** |
| AT4G36040 | Chaperone DnaJ-domain superfamily protein | 0.05 | -0.50 | **-1.55** |
| AT4G36050 | endonuclease/exonuclease/phosphatase family protein | 0.02 | -0.31 | **-0.72** |
| AT4G36130 | Ribosomal protein L2 family | -0.10 | 0.53 | **0.89** |
| AT4G36400 | FAD-linked oxidases family protein | 0.34 | -0.18 | **-0.78** |
| AT4G36410 | UBC17__ubiquitin-conjugating enzyme 17 | x | **-0.85** | -0.17 |
| AT4G36530 | alpha/beta-Hydrolases superfamily protein | -0.10 | -0.22 | **-0.87** |
| AT4G36580 | AAA-type ATPase family protein | 0.11 | 0.48 | **1.17** |
| AT4G36660 | Protein of unknown function (DUF1195) | 0.25 | 0.29 | **0.90** |
| AT4G36670 | Major facilitator superfamily protein | -0.11 | **-2.31** | **-1.61** |
| AT4G36680 | Tetratricopeptide repeat (TPR)-like superfamily protein | -0.17 | 0.32 | **0.82** |
| AT4G36830 | HOS3-1__GNS1/SUR4 membrane protein family | -0.10 | 0.35 | **0.94** |

| AGI identifier | Gene annotation | 30 min | 2h | 8h |
|---|---|---|---|---|
| AT4G36850 | PQ-loop repeat family protein / transmembrane family protein | 0.29 | **-1.27** | **-1.71** |
| AT4G37060 | AtPLAIVB_PLA IVB_PLP5__PATATIN-like protein 5 | 0.12 | -0.19 | **-0.79** |
| AT4G37200 | HCF164__Thioredoxin superfamily protein | x | 0.00 | **-0.76** |
| AT4G37220 | Cold acclimation protein WCOR413 family | x | -0.48 | **-1.75** |
| AT4G37260 | ATMYB73_MYB73__myb domain protein 73 | -0.54 | **-1.09** | -0.34 |
| AT4G37295 | unknown protein | 0.07 | 0.47 | **0.81** |
| AT4G37330 | CYP81D4__cytochrome P450, family 81, subfamily D, polypeptide 4 | 0.32 | -0.16 | **-0.78** |
| AT4G37410 | CYP81F4__cytochrome P450, family 81, subfamily F, polypeptide 4 | 0.26 | 0.35 | **0.87** |
| AT4G37450 | AGP18_ATAGP18__arabinogalactan protein 18 | 0.09 | -0.26 | **0.99** |
| AT4G37520 | Peroxidase superfamily protein | -0.02 | **-1.07** | **-1.63** |
| AT4G37530 | Peroxidase superfamily protein | -0.13 | **-0.74** | **-0.89** |
| AT4G37910 | mtHsc70-1__mitochondrial heat shock protein 70-1 | -0.44 | 0.57 | **1.62** |
| AT4G37925 | NDH-M (SUBUNIT NDH-M OF NAD(P)H:PLASTOQUINONE DEHYDROGENASE COMPLEX) | 0.14 | -0.51 | **-0.79** |
| AT4G38060 | unknown protein | -0.17 | -0.37 | **-0.71** |
| AT4G38080 | hydroxyproline-rich glycoprotein family protein | 0.64 | x | **1.01** |
| AT4G38100 | unknown protein | -0.22 | **0.89** | 0.68 |
| AT4G38400 | ATEXLA2_ATEXPL2_ATHEXP BETA 2.2_EXLA2_EXPL2__expansin-like A2 | **-0.69** | -0.29 | -0.20 |
| AT4G38470 | ACT-like protein tyrosine kinase family protein | -0.60 | **-2.68** | **-2.39** |
| AT4G38510 | ATPase, V1 complex, subunit B protein | -0.04 | 0.13 | **0.86** |
| AT4G38630 | ATMCB1_MBP1_MCB1_RPN10__regulatory particle non-ATPase 10 | 0.49 | 0.47 | **0.76** |
| AT4G38660 | Pathogenesis-related thaumatin superfamily protein | 0.15 | 0.34 | **0.77** |
| AT4G38740 | ROC1__rotamase CYP 1 | -0.15 | 0.62 | **0.98** |
| AT4G38770 | ATPRP4_PRP4__proline-rich protein 4 | **0.91** | 0.12 | x |
| AT4G38810 | Calcium-binding EF-hand family protein | 0.19 | -0.64 | **-1.61** |
| AT4G38970 | FBA2__fructose-bisphosphate aldolase 2 | **1.18** | 0.24 | 0.00 |
| AT4G39070 | B-box zinc finger family protein | 0.07 | -0.31 | **-0.89** |
| AT4G39090 | RD19_RD19A__Papain family cysteine protease | 0.24 | **-0.99** | **-1.38** |
| AT4G39200 | Ribosomal protein S25 family protein | -0.34 | 0.21 | **0.73** |
| AT4G39210 | APL3__Glucose-1-phosphate adenylyltransferase family protein | -0.29 | **0.87** | **2.16** |
| AT4G39260 | ATGRP8_CCR1_GR-RBP8_GRP8__cold, circadian rhythm, and RNA binding 1 | 0.18 | 0.45 | **0.95** |
| AT4G39280 | phenylalanyl-tRNA synthetase, putative / phenylalanine--tRNA ligase, putative | -0.37 | 0.20 | **0.89** |
| AT4G39300 | unknown protein | 0.15 | 0.47 | **0.98** |
| AT4G39330 | ATCAD9_CAD9__cinnamyl alcohol dehydrogenase 9 | -0.05 | **1.04** | 0.55 |
| AT4G39350 | ATCESA2_ATH-A_CESA2__cellulose synthase A2 | -0.47 | -0.02 | **0.88** |
| AT4G39390 | ATNST-KT1_NST-K1__nucleotide sugar transporter-KT 1 | 0.08 | 0.12 | **0.72** |
| AT4G39660 | AGT2__alanine:glyoxylate aminotransferase 2 | -0.10 | -0.42 | **-0.84** |
| AT4G39675 | unknown protein | -0.18 | -0.53 | **-1.15** |
| AT4G39730 | Lipase/lipooxygenase, PLAT/LH2 family protein | 0.25 | 0.74 | **1.12** |
| AT4G39780 | Integrase-type DNA-binding superfamily protein | 0.22 | -0.38 | **-1.09** |

| AGI identifier | Gene annotation | 30 min | 2h | 8h |
|---|---|---|---|---|
| AT4G39800 | ATIPS1_ATMIPS1_MI-1-P SYNTHASE_MIPS1__myo-inositol-1-phosphate synthase 1 | 0.12 | **1.16** | **1.16** |
| AT4G39940 | AKN2_APK2__APS-kinase 2 | 0.11 | **1.43** | **1.92** |
| AT4G39950 | CYP79B2__cytochrome P450, family 79, subfamily B, polypeptide 2 | -0.02 | **1.01** | **1.37** |
| AT4G39980 | DHS1__3-deoxy-D-arabino-heptulosonate 7-phosphate synthase 1 | -0.16 | **0.85** | x |
| AT5G01015 | unknown protein | -0.53 | **-0.80** | -0.39 |
| AT5G01220 | SQD2__sulfoquinovosyldiacylglycerol 2 | 0.37 | **1.18** | **0.88** |
| AT5G01500 | TAAC__thylakoid ATP/ADP carrier | -0.01 | 0.35 | **1.09** |
| AT5G01610 | Protein of unknown function, DUF538 | -0.04 | -0.52 | **-0.92** |
| AT5G01715 | pseudogene | -0.16 | **0.98** | -0.02 |
| AT5G02050 | Mitochondrial glycoprotein family protein | -0.11 | 0.49 | **1.28** |
| AT5G02090 | unknown protein | 0.21 | -0.66 | **-1.17** |
| AT5G02130 | NDP1__Tetratricopeptide repeat (TPR)-like superfamily protein | -0.07 | 0.07 | **-1.06** |
| AT5G02160 | unknown protein | 0.22 | -0.09 | **-0.72** |
| AT5G02240 | NAD(P)-binding Rossmann-fold superfamily protein | -0.25 | 0.18 | **0.75** |
| AT5G02490 | Heat shock protein 70 (Hsp 70) family protein | -0.32 | 0.72 | **0.82** |
| AT5G02500 | AT-HSC70-1_HSC70_HSC70-1_HSP70-1__heat shock cognate protein 70-1 | -0.21 | 0.40 | **0.72** |
| AT5G02610 | Ribosomal L29 family protein | 0.01 | 0.39 | **0.93** |
| AT5G02870 | Ribosomal protein L4/L1 family | -0.08 | 0.44 | **1.08** |
| AT5G02960 | Ribosomal protein S12/S23 family protein | -0.38 | 0.28 | **0.97** |
| AT5G03040 | iqd2__IQ-domain 2 | 0.17 | **-0.78** | 0.06 |
| AT5G03210 | unknown protein | x | **1.23** | **0.80** |
| AT5G03240 | UBQ3__polyubiquitin 3 | 0.01 | -0.33 | **-0.82** |
| AT5G03300 | ADK2__adenosine kinase 2 | -0.17 | 0.35 | **1.53** |
| AT5G03380 | Heavy metal transport/detoxification superfamily protein | **0.90** | -0.20 | 0.18 |
| AT5G03520 | ATRAB-E1D_ATRAB8C_ATRABE1D_RAB-E1D_RAB8C__RAB GTPase homolog 8C | -0.18 | **-0.81** | -0.21 |
| AT5G03610 | GDSL-like Lipase/Acylhydrolase superfamily protein | 0.18 | 0.43 | **0.74** |
| AT5G03630 | ATMDAR2__Pyridine nucleotide-disulphide oxidoreductase family protein | 0.23 | **0.77** | **0.76** |
| AT5G03650 | SBE2.2__starch branching enzyme 2.2 | -0.13 | 0.25 | **1.01** |
| AT5G03740 | HD2C_HDT3__histone deacetylase 2C | -0.14 | 0.64 | **0.76** |
| AT5G04040 | SDP1__Patatin-like phospholipase family protein | -0.22 | -0.59 | **-0.88** |
| AT5G04160 | Nucleotide-sugar transporter family protein | 0.00 | 0.11 | **1.02** |
| AT5G04840 | bZIP protein | -0.04 | 0.25 | **0.71** |
| AT5G04950 | ATNAS1_NAS1__nicotianamine synthase 1 | 0.65 | **1.06** | **1.36** |
| AT5G05010 | clathrin adaptor complexes medium subunit family protein | 0.33 | 0.11 | **0.73** |
| AT5G05100 | Single-stranded nucleic acid binding R3H protein | 0.04 | -0.46 | **-1.07** |
| AT5G05270 | Chalcone-flavanone isomerase family protein | -0.10 | 0.60 | **1.61** |
| AT5G05410 | DREB2_DREB2A__DRE-binding protein 2A | 0.40 | -0.61 | **-1.68** |
| AT5G05440 | PYL5_RCAR8__Polyketide cyclase/dehydrase and lipid transport superfamily protein | -0.05 | **-0.94** | **-0.98** |
| AT5G05500 | Pollen Ole e 1 allergen and extensin family protein | 0.26 | 0.31 | **0.95** |

| AGI identifier | Gene annotation | 30 min | 2h | 8h |
|---|---|---|---|---|
| AT5G05590 | PAI2 (PHOSPHORIBOSYLANTHRANILATE ISOMERASE 2); phosphoribosylanthranilate isomerase, PAI1 (PHOSPHORIBOSYLANTHRANILATE ISOMERASE 1); phosphoribosylanthranilate isomerase | 0.07 | 0.31 | **0.85** |
| AT5G06110 | DnaJ domain ;Myb-like DNA-binding domain | 0.01 | **0.85** | **0.72** |
| AT5G06300 | Putative lysine decarboxylase family protein | -0.39 | -0.62 | **-0.95** |
| AT5G06370 | NC domain-containing protein-related | -0.02 | -0.21 | **-0.78** |
| AT5G06550 | unknown protein | 0.15 | 0.26 | **0.90** |
| AT5G06690 | WCRKC1__WCRKC thioredoxin 1 | 0.02 | **-1.24** | **-1.51** |
| AT5G06760 | LEA4-5__Late Embryogenesis Abundant 4-5 | 0.07 | **0.99** | -0.02 |
| AT5G06860 | ATPGIP1_PGIP1__polygalacturonase inhibiting protein 1 | 0.07 | -0.57 | **-1.02** |
| AT5G06870 | ATPGIP2_PGIP2__polygalacturonase inhibiting protein 2 | -0.02 | -0.42 | **-0.71** |
| AT5G07030 | Eukaryotic aspartyl protease family protein | 0.05 | 0.07 | **0.88** |
| AT5G07080 | HXXXD-type acyl-transferase family protein | 0.27 | **-0.76** | -0.53 |
| AT5G07090 | Ribosomal protein S4 (RPS4A) family protein | -0.16 | 0.18 | **0.94** |
| AT5G07340 | Calreticulin family protein | -0.19 | 0.05 | **0.83** |
| AT5G07440 | GDH2__glutamate dehydrogenase 2 | x | **-2.08** | **-2.09** |
| AT5G07510 | ATGRP-4_ATGRP14_GRP-4_GRP14__glycine-rich protein 14 | **0.71** | -0.71 | -0.67 |
| AT5G07860 | HXXXD-type acyl-transferase family protein | -0.02 | -0.28 | **-0.99** |
| AT5G07870 | HXXXD-type acyl-transferase family protein | -0.10 | -0.31 | **-1.24** |
| AT5G07990 | CYP75B1_D501_TT7__Cytochrome P450 superfamily protein | -0.14 | 0.18 | **1.69** |
| AT5G08180 | Ribosomal protein L7Ae/L30e/S12e/Gadd45 family protein | -0.43 | 0.54 | **0.83** |
| AT5G08260 | scpl35__serine carboxypeptidase-like 35 | -0.02 | 0.10 | **1.24** |
| AT5G08500 | Transmembrane CLPTM1 family protein | **-0.66** | 0.19 | 0.21 |
| AT5G08570 | Pyruvate kinase family protein | 0.08 | **0.94** | **1.25** |
| AT5G08620 | ATRH25_STRS2__DEA(D/H)-box RNA helicase family protein | -0.49 | 0.20 | **0.81** |
| AT5G08640 | ATFLS1_FLS_FLS1__flavonol synthase 1 | -0.10 | **0.76** | **1.50** |
| AT5G09440 | EXL4__EXORDIUM like 4 | -0.19 | **-0.93** | **-0.76** |
| AT5G09510 | Ribosomal protein S19 family protein | -0.18 | 0.25 | **0.84** |
| AT5G09590 | heat shock protein 70 (Hsc70-5); nuclear | 0.10 | 0.72 | **1.13** |
| AT5G09660 | PMDH2__peroxisomal NAD-malate dehydrogenase 2 | 0.19 | -0.11 | **-1.21** |
| AT5G09810 | ACT7__actin 7 | -0.21 | -0.01 | **0.98** |
| AT5G09870 | CESA5__cellulose synthase 5 | -0.49 | 0.17 | **1.20** |
| AT5G09880 | Splicing factor, CC1-like | **-0.85** | -0.16 | 0.01 |
| AT5G10380 | ATRING1_RING1__RING/U-box superfamily protein | 0.22 | **0.76** | -0.30 |
| AT5G10450 | 14-3-3lambda_AFT1_GRF6__G-box regulating factor 6 | 0.17 | -0.51 | **-1.44** |
| AT5G10540 | Zincin-like metalloproteases family protein | **-0.74** | -0.18 | 0.21 |
| AT5G10580 | Protein of unknown function, DUF599 | 0.03 | 0.15 | **0.91** |
| AT5G10695 | unknown protein | -0.07 | **-0.92** | **-0.98** |
| AT5G10830 | S-adenosyl-L-methionine-dependent methyltransferases superfamily protein | 0.06 | 0.00 | **0.74** |
| AT5G10860 | Cystathionine beta-synthase (CBS) family protein | -0.17 | **-0.92** | **-1.54** |
| AT5G10920 | L-Aspartase-like family protein | -0.15 | 0.36 | **1.16** |
| AT5G11110 | ATSPS2F_KNS2_SPS1_SPS2F__sucrose phosphate synthase 2F | -0.22 | **1.50** | **0.72** |

| AGI identifier | Gene annotation | 30 min | 2h | 8h |
|---|---|---|---|---|
| AT5G11170 | DEAD/DEAH box RNA helicase family protein | -0.44 | 0.02 | **0.80** |
| AT5G11240 | Transducin family protein / WD-40 repeat family protein | 0.09 | 0.13 | **0.90** |
| AT5G11520 | ASP3_YLS4__aspartate aminotransferase 3 | 0.17 | -0.31 | **-0.99** |
| AT5G11740 | AGP15_ATAGP15__arabinogalactan protein 15 | -0.24 | 0.21 | **0.95** |
| AT5G11880 | Pyridoxal-dependent decarboxylase family protein | 0.29 | 0.25 | **0.73** |
| AT5G12410 | THUMP domain-containing protein | -0.30 | 0.08 | **0.75** |
| AT5G12470 | Protein of unknown function (DUF3411) | -0.12 | 0.68 | **1.42** |
| AT5G13000 | ATGSL12_gsl12_GSL12__glucan synthase-like 12 | -0.29 | 0.14 | **0.85** |
| AT5G13080 | ATWRKY75_WRKY75__WRKY DNA-binding protein 75 | 0.27 | **-0.76** | **-1.72** |
| AT5G13170 | SAG29__senescence-associated gene 29 | 0.22 | **1.24** | **0.72** |
| AT5G13190 | GSH-INDUCED LITAF DOMAIN PROTEIN | **-0.70** | -0.01 | -0.13 |
| AT5G13200 | GRAM domain family protein | **0.66** | x | 0.24 |
| AT5G13400 | Major facilitator superfamily protein | -0.06 | 0.29 | **1.14** |
| AT5G13420 | Aldolase-type TIM barrel family protein | 0.25 | 0.35 | **1.12** |
| AT5G13490 | AAC2__ADP/ATP carrier 2 | x | 0.66 | **1.05** |
| AT5G13570 | ATDCP2_DCP2_TDT__decapping 2 | -0.17 | -0.40 | **-0.74** |
| AT5G13710 | CPH_SMT1__sterol methyltransferase 1 | -0.19 | **-0.88** | -0.61 |
| AT5G13720 | Uncharacterised protein family (UPF0114) | -0.01 | -0.18 | **-1.10** |
| AT5G13750 | ZIFL1__zinc induced facilitator-like 1 | 0.09 | **0.88** | -0.24 |
| AT5G13770 | Pentatricopeptide repeat (PPR-like) superfamily protein | 0.40 | -0.49 | **-0.87** |
| AT5G13930 | ATCHS_CHS_TT4__Chalcone and stilbene synthase family protein | -0.02 | **0.84** | **1.85** |
| AT5G14040 | PHT3;1__phosphate transporter 3;1 | 0.49 | 0.46 | **0.75** |
| AT5G14120 | Major facilitator superfamily protein | x | **-1.65** | **-2.06** |
| AT5G14180 | MPL1__Myzus persicae-induced lipase 1 | x | **-1.21** | **-2.45** |
| AT5G14200 | ATIMD1_IMD1__isopropylmalate dehydrogenase 1 | 0.06 | 0.44 | **1.70** |
| AT5G14470 | GHMP kinase family protein | -0.05 | -0.46 | **-1.35** |
| AT5G14580 | polyribonucleotide nucleotidyltransferase, putative | -0.23 | 0.11 | **1.30** |
| AT5G14640 | ATSK13_SK13__shaggy-like kinase 13 | 0.03 | 0.60 | **1.24** |
| AT5G14780 | FDH__formate dehydrogenase | **0.67** | -0.02 | **-1.88** |
| AT5G14910 | Heavy metal transport/detoxification superfamily protein | -0.12 | -0.36 | **-1.00** |
| AT5G15090 | ATVDAC3_VDAC3__voltage dependent anion channel 3 | -0.05 | 0.63 | **1.52** |
| AT5G15200 | Ribosomal protein S4 | -0.18 | 0.13 | **0.71** |
| AT5G15350 | AtENODL17_ENODL17__early nodulin-like protein 17 | -0.27 | **-1.26** | -0.01 |
| AT5G15450 | APG6_CLPB-P_CLPB3__casein lytic proteinase B3 | 0.05 | 0.35 | **0.76** |
| AT5G15490 | UDP-glucose 6-dehydrogenase family protein | 0.09 | 0.35 | **1.54** |
| AT5G15550 | Transducin family protein / WD-40 repeat family protein | -0.05 | 0.38 | **0.73** |
| AT5G15650 | ATRGP2_RGP2__reversibly glycosylated polypeptide 2 | -0.03 | 0.01 | **0.81** |
| AT5G15850 | ATCOL1_COL1__CONSTANS-like 1 | 0.42 | -0.23 | **-0.88** |
| AT5G15960 | KIN1__stress-responsive protein (KIN1) / stress-induced protein (KIN1) | -0.18 | 0.25 | **0.87** |
| AT5G16110 | unknown protein | -0.39 | **-1.55** | **-1.37** |
| AT5G16130 | Ribosomal protein S7e family protein | -0.06 | 0.48 | **1.05** |
| AT5G16360 | NC domain-containing protein | x | -0.32 | **-0.72** |
| AT5G16370 | AAE5__acyl activating enzyme 5 | 0.01 | **-1.61** | **-1.58** |
| AT5G16400 | ATF2_TRXF2__thioredoxin F2 | -0.03 | -0.46 | **-0.92** |

| AGI identifier | Gene annotation | 30 min | 2h | 8h |
|---|---|---|---|---|
| AT5G16570 | GLN1;4__glutamine synthetase 1;4 | 0.21 | 0.71 | **1.70** |
| AT5G16660 | unknown protein | 0.11 | -0.28 | **-0.98** |
| AT5G16970 | AER_AT-AER__alkenal reductase | **0.79** | 0.06 | **-1.28** |
| AT5G17010 | Major facilitator superfamily protein | -0.04 | 0.15 | **0.77** |
| AT5G17020 | ATCRM1_ATXPO1_HIT2_XPO1_XPO1A__exportin 1A | **-0.73** | -0.09 | 0.28 |
| AT5G17050 | UGT78D2__UDP-glucosyl transferase 78D2 | **0.71** | 0.37 | 0.01 |
| AT5G17220 | ATGSTF12_GST26_GSTF12_TT19__glutathione S-transferase phi 12 | 0.01 | 0.28 | **2.27** |
| AT5G17280 | unknown protein | 0.41 | -0.42 | **-0.89** |
| AT5G17300 | RVE1__Homeodomain-like superfamily protein | -0.16 | **-1.00** | -0.27 |
| AT5G17310 | AtUGP2_UGP2__UDP-glucose pyrophosphorylase 2 | 0.04 | 0.14 | **0.86** |
| AT5G17400 | ER-ANT1__endoplasmic reticulum-adenine nucleotide transporter 1 | -0.17 | -0.36 | **-0.90** |
| AT5G17920 | ATCIMS_ATMETS_ATMS1__Cobalamin-independent synthase family protein | -0.05 | 0.23 | **1.30** |
| AT5G17990 | pat1_TRP1__tryptophan biosynthesis 1 | 0.49 | 0.14 | **0.72** |
| AT5G18140 | Chaperone DnaJ-domain superfamily protein | 0.08 | -0.65 | **-1.05** |
| AT5G18170 | GDH1__glutamate dehydrogenase 1 | -0.09 | **-1.02** | **-1.48** |
| AT5G18180 | H/ACA ribonucleoprotein complex, subunit Gar1/Naf1 protein | -0.18 | 0.45 | **0.91** |
| AT5G18470 | Curculin-like (mannose-binding) lectin family protein | 0.54 | **1.06** | 0.39 |
| AT5G18490 | Plant protein of unknown function (DUF946) | 0.34 | -0.34 | **-0.78** |
| AT5G18600 | Thioredoxin superfamily protein | -0.49 | **-1.65** | x |
| AT5G18630 | alpha/beta-Hydrolases superfamily protein | -0.30 | **-1.26** | **-1.41** |
| AT5G18650 | CHY-type/CTCHY-type/RING-type Zinc finger protein | -0.17 | **-1.05** | **-1.14** |
| AT5G18670 | BAM9_BMY3__beta-amylase 3 | -0.37 | **-2.19** | **-0.94** |
| AT5G18840 | Major facilitator superfamily protein | 0.09 | -0.28 | **1.00** |
| AT5G19110 | Eukaryotic aspartyl protease family protein | -0.47 | -0.03 | **1.14** |
| AT5G19120 | Eukaryotic aspartyl protease family protein | 0.11 | **-2.31** | **-2.09** |
| AT5G19230 | unknown protein | **0.84** | x | -0.06 |
| AT5G19240 | Glycoprotein membrane precursor GPI-anchored | **0.78** | 0.55 | 0.16 |
| AT5G19510 | Translation elongation factor EF1B/ribosomal protein S6 family protein | -0.10 | 0.40 | **0.97** |
| AT5G19550 | AAT2_ASP2__aspartate aminotransferase 2 | 0.09 | 0.26 | **0.75** |
| AT5G19690 | STT3A__staurosporin and temperature sensitive 3-like A | -0.33 | -0.09 | **0.86** |
| AT5G19855 | Chaperonin-like RbcX protein | 0.18 | -0.20 | **-1.06** |
| AT5G20160 | Ribosomal protein L7Ae/L30e/S12e/Gadd45 family protein | -0.20 | 0.63 | **1.13** |
| AT5G20190 | unknown protein | 0.48 | **1.50** | **1.03** |
| AT5G20230 | ATBCB_BCB_BCB_SAG14__blue-copper-binding protein | 0.08 | **-0.76** | **-1.99** |
| AT5G20250 | DIN10__Raffinose synthase family protein | -0.21 | **-3.14** | **-2.34** |
| AT5G20280 | ATSPS1F_SPS1F__sucrose phosphate synthase 1F | -0.55 | 0.43 | **1.72** |
| AT5G20290 | Ribosomal protein S8e family protein | -0.40 | 0.27 | **0.90** |
| AT5G20320 | ATDCL4_DCL4__dicer-like 4 | -0.05 | -0.56 | **-1.13** |
| AT5G20520 | WAV2__alpha/beta-Hydrolases superfamily protein | 0.24 | -0.42 | **-0.92** |
| AT5G20900 | JAZ12_TIFY3B__jasmonate-zim-domain protein 12 | **0.67** | -0.02 | x |
| AT5G21020 | unknown protein | 0.27 | -0.26 | **-0.99** |
| AT5G21170 | AKINBETA1__5'-AMP-activated protein kinase beta-2 subunit protein | 0.17 | **-0.79** | -0.30 |

| AGI identifier | Gene annotation | 30 min | 2h | 8h |
|---|---|---|---|---|
| AT5G21940 | unknown protein | -0.59 | **-1.80** | x |
| AT5G22100 | RNA cyclase family protein | -0.04 | 0.65 | **0.83** |
| AT5G22140 | FAD/NAD(P)-binding oxidoreductase family protein | 0.19 | 0.26 | **-0.96** |
| AT5G22270 | unknown protein | 0.17 | -0.61 | **-0.78** |
| AT5G22440 | Ribosomal protein L1p/L10e family | -0.29 | 0.63 | **1.20** |
| AT5G22650 | ATHD2_ATHD2B_HD2_HD2B_HDA4_HDT02_HDT2__histone deacetylase 2B | 0.16 | **0.96** | **1.55** |
| AT5G22660 | F-box family protein | -0.11 | **0.75** | **1.28** |
| AT5G22740 | ATCSLA02_ATCSLA2_CSLA02_CSLA2__cellulose synthase-like A02 | -0.27 | 0.34 | **1.23** |
| AT5G22920 | CHY-type/CTCHY-type/RING-type Zinc finger protein | -0.63 | **-2.55** | **-1.82** |
| AT5G23010 | IMS3_MAM1__methylthioalkylmalate synthase 1 | 0.14 | 0.28 | **0.94** |
| AT5G23020 | IMS2_MAM-L_MAM3__2-isopropylmalate synthase 2 | -0.10 | -0.03 | **1.87** |
| AT5G23220 | NIC3__nicotinamidase 3 | 0.30 | **1.63** | **1.00** |
| AT5G23250 | Succinyl-CoA ligase, alpha subunit | -0.03 | 0.31 | **0.83** |
| AT5G23340 | RNI-like superfamily protein | 0.16 | -0.47 | **-1.06** |
| AT5G23530 | AtCXE18_CXE18__carboxyesterase 18 | 0.13 | 0.45 | **0.83** |
| AT5G23660 | MTN3__homolog of Medicago truncatula MTN3 | 0.03 | -0.21 | **-0.97** |
| AT5G23730 | Transducin family protein / WD-40 repeat family protein | **0.73** | -0.47 | **-0.71** |
| AT5G23740 | RPS11-BETA__ribosomal protein S11-beta | -0.10 | 0.42 | **0.97** |
| AT5G23830 | MD-2-related lipid recognition domain-containing protein | -0.06 | -0.12 | **1.59** |
| AT5G23840 | MD-2-related lipid recognition domain-containing protein | 0.08 | 0.04 | **0.78** |
| AT5G23900 | Ribosomal protein L13e family protein | -0.21 | 0.28 | **0.76** |
| AT5G24120 | ATSIG5_SIG5_SIGE__sigma factor E | 0.23 | -0.26 | **-0.84** |
| AT5G24160 | SQE6__squalene monoxygenase 6 | -0.19 | -0.05 | **-1.36** |
| AT5G24165 | unknown protein | 0.05 | -0.40 | **-0.83** |
| AT5G24490 | 30S ribosomal protein, putative | 0.27 | **-1.28** | **-1.82** |
| AT5G24610 | unknown protein | -0.32 | -0.38 | **-0.77** |
| AT5G24655 | LSU4__response to low sulfur 4 | -0.19 | **0.79** | **0.80** |
| AT5G24660 | LSU2__response to low sulfur 2 | -0.03 | **1.42** | **0.93** |
| AT5G24760 | GroES-like zinc-binding dehydrogenase family protein | -0.13 | -0.07 | **1.01** |
| AT5G24810 | ABC1 family protein | -0.15 | x | **-1.08** |
| AT5G25100 | Endomembrane protein 70 protein family | -0.15 | -0.23 | **0.78** |
| AT5G25130 | CYP71B12__cytochrome P450, family 71, subfamily B, polypeptide 12 | -0.22 | **-0.81** | -0.11 |
| AT5G25210 | unknown protein | -0.09 | **-0.82** | -0.42 |
| AT5G25280 | serine-rich protein-related | -0.13 | -0.59 | **-0.73** |
| AT5G25610 | ATRD22_RD22__BURP domain-containing protein | 0.43 | **1.12** | **1.25** |
| AT5G25630 | Tetratricopeptide repeat (TPR)-like superfamily protein | -0.49 | **-0.99** | **-0.75** |
| AT5G25757 | unknown protein | 0.04 | 0.71 | **0.90** |
| AT5G25770 | alpha/beta-Hydrolases superfamily protein | -0.12 | -0.36 | **-0.73** |
| AT5G25780 | ATEIF3B-2_EIF3B_EIF3B-2__eukaryotic translation initiation factor 3B-2 | -0.28 | 0.44 | **0.83** |
| AT5G25900 | ATKO1_CYP701A3_GA3__GA requiring 3 | 0.01 | -0.21 | **-0.78** |
| AT5G26260 | TRAF-like family protein | 0.12 | -0.25 | **1.59** |
| AT5G26667 | uridine 5'-monophosphate (UMP)/cytidine 5'-monophosphate (CMP) kinase. | 0.42 | 0.05 | **0.86** |

| AGI identifier | Gene annotation | 30 min | 2h | 8h |
|---|---|---|---|---|
| AT5G26740 | Protein of unknown function (DUF300) | x | **-1.07** | **-0.73** |
| AT5G26820 | ATIREG3_IREG3_IREG3_MAR1_RTS3__iron-regulated protein 3 | -0.55 | -0.53 | **-0.81** |
| AT5G26830 | Threonyl-tRNA synthetase | -0.38 | 0.20 | **0.80** |
| AT5G26860 | LON1_LON_ARA_ARA__lon protease 1 | -0.01 | 0.07 | **0.77** |
| AT5G27120 | NOP56-like pre RNA processing ribonucleoprotein | -0.08 | 0.50 | **1.43** |
| AT5G27280 | Zim17-type zinc finger protein | x | -0.09 | **-0.98** |
| AT5G27290 | unknown protein | -0.19 | -0.44 | **-0.77** |
| AT5G27330 | Prefoldin chaperone subunit family protein | -0.13 | 0.29 | **1.13** |
| AT5G27350 | SFP1__Major facilitator superfamily protein | -0.05 | -0.69 | **-1.19** |
| AT5G27770 | Ribosomal L22e protein family | 0.02 | 0.13 | **0.83** |
| AT5G27850 | Ribosomal protein L18e/L15 superfamily protein | **-0.70** | 0.36 | **0.88** |
| AT5G27860 | unknown protein | **-0.85** | -0.16 | -0.63 |
| AT5G28050 | Cytidine/deoxycytidylate deaminase family protein | -0.08 | **-1.20** | **-1.79** |
| AT5G28510 | BGLU24__beta glucosidase 24 | **0.94** | 0.07 | 0.47 |
| AT5G28770 | AtbZIP63_BZO2H3__bZIP transcription factor family protein | -0.31 | **-2.38** | **-1.84** |
| AT5G28840 | GME__GDP-D-mannose 3',5'-epimerase | -0.18 | -0.57 | **-0.95** |
| AT5G33290 | XGD1__xylogalacturonan deficient 1 | -0.11 | **0.81** | 0.53 |
| AT5G33320 | ARAPPT_CUE1_PPT__Glucose-6-phosphate/phosphate translocator-related | -0.39 | 0.29 | **1.12** |
| AT5G33370 | GDSL-like Lipase/Acylhydrolase superfamily protein | 0.44 | 0.28 | **1.06** |
| AT5G35525 | unknown protein | x | -0.53 | **-1.17** |
| AT5G35530 | Ribosomal protein S3 family protein | -0.19 | 0.30 | **0.98** |
| AT5G35630 | ATGSL1_GLN2_GS2__glutamine synthetase 2 | **1.18** | 0.32 | 0.03 |
| AT5G36910 | THI2.2__thionin 2.2 | **0.68** | 0.03 | 0.17 |
| AT5G37170 | O-methyltransferase family protein | 0.11 | 0.23 | **0.87** |
| AT5G37260 | CIR1_RVE2__Homeodomain-like superfamily protein | 0.06 | -0.69 | **-1.23** |
| AT5G37600 | ATGLN1;1_ATGSR1_GLN1;1_GSR 1__glutamine synthase clone R1 | 0.17 | **0.91** | **1.51** |
| AT5G37690 | SGNH hydrolase-type esterase superfamily protein | 0.44 | 0.23 | **1.41** |
| AT5G38020 | S-adenosyl-L-methionine-dependent methyltransferases superfamily protein | 0.13 | 0.08 | **1.79** |
| AT5G38060 | unknown protein | -0.13 | -0.25 | **-1.01** |
| AT5G38520 | alpha/beta-Hydrolases superfamily protein | 0.27 | -0.12 | **-0.75** |
| AT5G39080 | HXXXD-type acyl-transferase family protein | -0.38 | **-0.78** | **-0.92** |
| AT5G39320 | UDP-glucose 6-dehydrogenase family protein | 0.17 | 0.11 | **1.24** |
| AT5G39530 | unknown protein | -0.20 | -0.46 | **-0.88** |
| AT5G39580 | Peroxidase superfamily protein | 0.30 | **-1.56** | **-0.95** |
| AT5G39590 | TLD-domain containing nucleolar protein | 0.06 | -0.41 | **-0.75** |
| AT5G39610 | ANAC092_ATNAC2_ATNAC6_NAC2_NAC6_ORE1__NAC domain containing protein 6 | 0.04 | -0.45 | **-0.80** |
| AT5G39690 | ANAC093_NAC093__NAC domain containing protein 93 | 0.35 | -0.24 | **-0.76** |
| AT5G39740 | OLI7_RPL5B__ribosomal protein L5 B | -0.11 | 0.28 | **0.85** |
| AT5G39785 | Protein of unknown function (DUF1666) | -0.63 | **-2.70** | **-2.18** |
| AT5G39850 | Ribosomal protein S4 | -0.08 | 0.44 | **1.25** |
| AT5G40390 | SIP1__Raffinose synthase family protein | 0.21 | **0.78** | 0.66 |
| AT5G40480 | EMB3012__embryo defective 3012 | -0.59 | 0.10 | **1.13** |

| AGI identifier | Gene annotation | 30 min | 2h | 8h |
|---|---|---|---|---|
| AT5G40670 | PQ-loop repeat family protein / transmembrane family protein | 0.10 | -0.07 | **-0.75** |
| AT5G40760 | G6PD6__glucose-6-phosphate dehydrogenase 6 | 0.07 | 0.46 | **1.05** |
| AT5G40770 | ATPHB3_PHB3__prohibitin 3 | 0.14 | 0.59 | **0.90** |
| AT5G40850 | UPM1__urophorphyrin methylase 1 | 0.37 | **1.23** | 0.49 |
| AT5G40890 | ATCLC-A_ATCLCA_CLC-A_CLC-A_CLCA__chloride channel A | -0.08 | **-0.98** | **-1.00** |
| AT5G41080 | PLC-like phosphodiesterases superfamily protein | -0.54 | **-1.91** | **-2.08** |
| AT5G41340 | ATUBC4_UBC4__ubiquitin conjugating enzyme 4 | -0.23 | -0.69 | **-0.76** |
| AT5G41400 | RING/U-box superfamily protein | 0.30 | **0.88** | 0.51 |
| AT5G41600 | BTI3_RTNLB4__VIRB2-interacting protein 3 | -0.20 | 0.08 | **0.72** |
| AT5G41670 | 6-phosphogluconate dehydrogenase family protein | -0.14 | **1.65** | **1.90** |
| AT5G42020 | BIP_BIP2__Heat shock protein 70 (Hsp 70) family protein | **0.93** | x | 0.67 |
| AT5G42060 | DEK, chromatin associated protein | 0.00 | 0.32 | **0.73** |
| AT5G42090 | Lung seven transmembrane receptor family protein | **0.71** | 0.19 | x |
| AT5G42100 | ATBG_PAP_ATBG_PPAP_BG_PPAP__beta-1,3-glucanase_putative | **-0.76** | -0.22 | 0.60 |
| AT5G42110 | unknown protein | -0.43 | 0.15 | **0.73** |
| AT5G42445 | pseudogene | -0.22 | 0.02 | **0.71** |
| AT5G42650 | AOS_CYP74A_DDE2__allene oxide synthase | 0.25 | **1.15** | **1.18** |
| AT5G42800 | DFR_M318_TT3__dihydroflavonol 4-reductase | 0.00 | 0.18 | **0.79** |
| AT5G43060 | Granulin repeat cysteine protease family protein | 0.43 | -0.42 | **-0.79** |
| AT5G43150 | unknown protein | 0.04 | 0.41 | **0.75** |
| AT5G43260 | chaperone protein dnaJ-related | -0.09 | -0.30 | **-0.98** |
| AT5G43370 | APT1_PHT1;2_PHT2__phosphate transporter 2 | 0.43 | 0.21 | **1.01** |
| AT5G43430 | ETFBETA__electron transfer flavoprotein beta | -0.16 | -0.39 | **-0.87** |
| AT5G43520 | Cysteine/Histidine-rich C1 domain family protein | 0.17 | **-0.88** | **-0.80** |
| AT5G43570 | PR (pathogenesis-related) peptide that belongs to the PR-6 proteinase inhibitor family. | -0.37 | -0.72 | **-1.88** |
| AT5G43580 | Serine protease inhibitor, potato inhibitor I-type family protein | -0.18 | -0.62 | **-0.91** |
| AT5G43830 | Aluminium induced protein with YGL and LRDR motifs | -0.13 | **-0.91** | **-0.76** |
| AT5G44020 | HAD superfamily, subfamily IIIB acid phosphatase | 0.49 | **-0.91** | **-0.92** |
| AT5G44110 | ATNAP2_ATPOP1_POP1__P-loop containing nucleoside triphosphate hydrolases superfamily protein | 0.12 | 0.38 | **0.86** |
| AT5G44420 | LCR77_PDF1.2_PDF1.2A__plant defensin 1.2 | -0.15 | -0.34 | **-1.06** |
| AT5G44550 | Uncharacterised protein family (UPF0497) | 0.46 | 0.26 | **1.05** |
| AT5G44585 | unknown protein | 0.11 | -0.19 | **-1.07** |
| AT5G44720 | Molybdenum cofactor sulfurase family protein | -0.13 | 0.46 | **0.91** |
| AT5G45800 | MEE62__Leucine-rich repeat protein kinase family protein | 0.08 | 0.03 | **0.71** |
| AT5G45950 | GDSL-like Lipase/Acylhydrolase superfamily protein | 0.35 | 0.26 | **0.75** |
| AT5G46110 | APE2_TPT__Glucose-6-phosphate/phosphate translocator-related | **0.81** | -0.07 | -0.35 |
| AT5G46180 | DELTA-OAT__ornithine-delta-aminotransferase | 0.27 | -0.43 | **-0.85** |
| AT5G46250 | RNA-binding protein | 0.45 | -0.28 | **-0.74** |
| AT5G46290 | KAS I_KAS1__3-ketoacyl-acyl carrier protein synthase I | 0.06 | 0.37 | **0.75** |
| AT5G47030 | ATPase, F1 complex, delta/epsilon subunit | 0.40 | 0.56 | **0.76** |
| AT5G47060 | Protein of unknown function (DUF581) | 0.09 | **1.24** | 0.62 |

| AGI identifier | Gene annotation | 30 min | 2h | 8h |
|---|---|---|---|---|
| AT5G47220 | ATERF-2_ATERF2_ERF2__ethylene responsive element binding factor 2 | -0.05 | 0.13 | **-0.71** |
| AT5G47500 | Pectin lyase-like superfamily protein | **-0.69** | 0.09 | 0.56 |
| AT5G47550 | Cystatin/monellin superfamily protein | 0.22 | -0.03 | **-0.72** |
| AT5G47560 | ATSDAT_ATTDT_TDT__tonoplast dicarboxylate transporter | 0.28 | -0.50 | **-1.60** |
| AT5G47980 | HXXXD-type acyl-transferase family protein | 0.18 | 0.30 | **0.75** |
| AT5G47990 | CYP705A5_THAD_THAD1__cytochrome P450, family 705, subfamily A, polypeptide 5 | 0.25 | 0.34 | **1.42** |
| AT5G48000 | CYP708 A2_CYP708A2_THAH_THAH1__cytochrome P450, family 708, subfamily A, polypeptide 2 | 0.12 | 0.28 | **2.15** |
| AT5G48010 | THAS_THAS1__thalianol synthase 1 | 0.14 | 0.58 | **2.33** |
| AT5G48030 | GFA2__gametophytic factor 2 | -0.20 | 0.08 | **0.85** |
| AT5G48180 | NSP5__nitrile specifier protein 5 | -0.01 | -0.24 | **-1.04** |
| AT5G48485 | DIR1__Bifunctional inhibitor/lipid-transfer protein/seed storage 2S albumin superfamily protein | -0.22 | -0.61 | **-0.81** |
| AT5G48490 | Bifunctional inhibitor/lipid-transfer protein/seed storage 2S albumin superfamily protein | **-0.67** | **-1.10** | -0.12 |
| AT5G48540 | receptor-like protein kinase-related family protein | **0.74** | **0.80** | -0.13 |
| AT5G48545 | HISTIDINE TRIAD NUCLEOTIDE-BINDING 3 | -0.18 | -0.57 | **-0.72** |
| AT5G48760 | Ribosomal protein L13 family protein | -0.20 | 0.49 | **0.74** |
| AT5G48930 | HCT__hydroxycinnamoyl-CoA shikimate/quinate hydroxycinnamoyl transferase | 0.11 | **0.86** | 0.69 |
| AT5G49330 | ATMYB111_MYB111_PFG3__myb domain protein 111 | 0.07 | 0.10 | **0.92** |
| AT5G49360 | ATBXL1_BXL1__beta-xylosidase 1 | 0.41 | **-2.29** | **-2.77** |
| AT5G49450 | AtbZIP1_bZIP1__basic leucine-zipper 1 | -0.58 | **-2.65** | **-2.36** |
| AT5G49480 | ATCP1_CP1__Ca2+-binding protein 1 | 0.26 | **1.17** | -0.01 |
| AT5G49720 | ATGH9A1_DEC_GH9A1_IRX2_KOR_KOR1_RSW2_TSD1__glycosyl hydrolase 9A1 | **0.67** | -0.58 | -0.16 |
| AT5G49730 | ATFRO6_FRO6_FRO6__ferric reduction oxidase 6 | -0.15 | **-0.95** | -0.14 |
| AT5G49810 | MMT__methionine S-methyltransferase | -0.08 | 0.29 | **0.86** |
| AT5G50370 | Adenylate kinase family protein | 0.08 | 0.65 | **0.84** |
| AT5G50670 | Squamosa promoter-binding protein-like (SBP domain) transcription factor family protein | **-0.77** | -0.09 | -0.02 |
| AT5G51010 | Rubredoxin-like superfamily protein | -0.27 | -0.09 | **-0.88** |
| AT5G51020 | CRL__crumpled leaf | 0.18 | 0.05 | **-0.78** |
| AT5G51070 | CLPD_ERD1_SAG15__Clp ATPase | -0.02 | 0.17 | **-0.71** |
| AT5G51110 | Transcriptional coactivator/pterin dehydratase | -0.13 | 0.04 | **-0.82** |
| AT5G51440 | HSP20-like chaperones superfamily protein | 0.04 | **0.79** | 0.62 |
| AT5G51750 | ATSBT1.3_SBT1.3__subtilase 1.3 | -0.06 | 0.20 | **0.81** |
| AT5G51890 | Peroxidase superfamily protein | **0.72** | 0.35 | 0.65 |
| AT5G51970 | GroES-like zinc-binding alcohol dehydrogenase family protein | 0.06 | **-0.96** | **-1.76** |
| AT5G52190 | Sugar isomerase (SIS) family protein | 0.02 | -0.08 | **-0.83** |
| AT5G52470 | ATFBR1_ATFIB1_FBR1_FIB1_SKIP7__fibrillarin 1 | -0.22 | 0.41 | **1.08** |
| AT5G52780 | Protein of unknown function (DUF3464) | 0.01 | -0.35 | **-1.11** |
| AT5G52820 | WD-40 repeat family protein / notchless protein, putative | 0.00 | 0.49 | **0.72** |
| AT5G52840 | NADH-ubiquinone oxidoreductase-related | -0.10 | 0.10 | **0.85** |
| AT5G53070 | Ribosomal protein L9/RNase H1 | 0.00 | 0.18 | **0.79** |

| AGI identifier | Gene annotation | 30 min | 2h | 8h |
|---|---|---|---|---|
| AT5G53140 | Protein phosphatase 2C family protein | -0.32 | 0.32 | **0.90** |
| AT5G53160 | PYL8_RCAR3__regulatory components of ABA receptor 3 | -0.34 | **-1.07** | **-1.17** |
| AT5G53290 | CRF3__cytokinin response factor 3 | 0.08 | **0.85** | **1.10** |
| AT5G53420 | CCT motif family protein | -0.25 | **1.57** | **0.99** |
| AT5G53460 | GLT1__NADH-dependent glutamate synthase 1 | -0.50 | 0.23 | **0.82** |
| AT5G53490 | Tetratricopeptide repeat (TPR)-like superfamily protein | -0.17 | **-0.78** | **-1.54** |
| AT5G53750 | unknown protein | 0.49 | **1.09** | **1.09** |
| AT5G53760 | ATMLO11_MLO11__Seven transmembrane MLO family protein | -0.21 | **0.88** | 0.47 |
| AT5G53970 | Tyrosine transaminase family protein | 0.34 | -0.50 | **-1.82** |
| AT5G54060 | UF3GT__UDP-glucose:flavonoid 3-o-glucosyltransferase | 0.11 | -0.06 | **0.92** |
| AT5G54080 | HGO__homogentisate 1,2-dioxygenase | 0.07 | **-1.22** | **-2.02** |
| AT5G54090 | DNA mismatch repair protein MutS, type 2 | -0.11 | **-0.91** | -0.29 |
| AT5G54100 | SPFH/Band 7/PHB domain-containing membrane-associated protein family | -0.14 | 0.07 | **1.25** |
| AT5G54160 | ATOMT1_OMT1__O-methyltransferase 1 | **0.82** | 0.20 | x |
| AT5G54170 | Polyketide cyclase/dehydrase and lipid transport superfamily protein | -0.20 | -0.71 | **-1.00** |
| AT5G54206 | pseudogene | 0.43 | -0.38 | **-1.21** |
| AT5G54270 | LHCB3_LHCB3*1__light-harvesting chlorophyll B-binding protein 3 | **1.11** | 0.34 | 0.08 |
| AT5G54370 | Late embryogenesis abundant (LEA) protein-related | 0.63 | 0.20 | **1.16** |
| AT5G54490 | PBP1__pinoid-binding protein 1 | **-0.90** | -0.28 | -0.50 |
| AT5G54540 | Uncharacterised conserved protein (UCP012943) | **0.69** | -0.32 | **-0.92** |
| AT5G54580 | RNA-binding (RRM/RBD/RNP motifs) family protein | -0.13 | 0.35 | **0.72** |
| AT5G54710 | Ankyrin repeat family protein | 0.02 | 0.26 | **1.00** |
| AT5G54800 | ATGPT1_GPT1__glucose 6-phosphate/phosphate translocator 1 | 0.26 | 0.37 | **1.04** |
| AT5G55050 | GDSL-like Lipase/Acylhydrolase superfamily protein | 0.19 | 0.49 | **1.02** |
| AT5G55070 | Dihydrolipoamide succinyltransferase | -0.07 | 0.74 | **1.13** |
| AT5G55230 | ATMAP65-1_MAP65-1_MAP65-1__microtubule-associated proteins 65-1 | -0.10 | -0.36 | **0.76** |
| AT5G55280 | ATFTSZ1-1_CPFTSZ_FTSZ1-1__homolog of bacterial cytokinesis Z-ring protein FTSZ 1-1 | -0.02 | 0.46 | **0.92** |
| AT5G55450 | Bifunctional inhibitor/lipid-transfer protein/seed storage 2S albumin superfamily protein | -0.10 | 0.47 | **1.26** |
| AT5G55480 | SVL1__SHV3-like 1 | -0.10 | -0.05 | **0.88** |
| AT5G55620 | unknown protein | **0.71** | 0.70 | 0.49 |
| AT5G55680 | glycine-rich protein | 0.35 | **0.98** | x |
| AT5G55700 | BAM4_BMY6__beta-amylase 4 | -0.13 | -0.54 | **-0.83** |
| AT5G55750 | hydroxyproline-rich glycoprotein family protein | **0.90** | -0.71 | **-1.13** |
| AT5G55970 | RING/U-box superfamily protein | x | **-1.02** | **-1.32** |
| AT5G56010 | AtHsp90-3_AtHsp90.3_HSP81-3_Hsp81.3__heat shock protein 81-3 | -0.24 | **0.76** | 0.65 |
| AT5G56030 | AtHsp90.2_ERD8_HSP81-2_HSP90.2__heat shock protein 81-2 | -0.07 | **0.98** | **0.98** |
| AT5G56100 | glycine-rich protein / oleosin | -0.30 | -0.63 | **-1.58** |
| AT5G56360 | PSL4__calmodulin-binding protein | -0.26 | -0.10 | **0.71** |

| | | | | |
|---|---|---|---|---|
| AT5G56630 | PFK7__phosphofructokinase 7 | 0.07 | **1.27** | **1.69** |
| AT5G56670 | Ribosomal protein S30 family protein | 0.26 | 0.54 | **1.06** |
| AT5G56680 | EMB2755_SYNC1_SYNC1 ARATH__Class II aminoacyl-tRNA and biotin synthetases superfamily protein | -0.32 | 0.53 | **0.98** |
| AT5G56710 | Ribosomal protein L31e family protein | -0.35 | 0.29 | **0.76** |
| AGI identifier | Gene annotation | 30 min | 2h | 8h |
| AT5G56750 | NDL1__N-MYC downregulated-like 1 | -0.51 | **-1.04** | **-1.50** |
| AT5G56870 | BGAL4__beta-galactosidase 4 | -0.03 | **-1.22** | **-2.04** |
| AT5G57035 | U-box domain-containing protein kinase family protein | 0.14 | -0.01 | **-0.88** |
| AT5G57560 | TCH4_XTH22__Xyloglucan endotransglucosylase/hydrolase family protein | x | **-1.89** | -0.64 |
| AT5G57630 | CIPK21_SnRK3.4__CBL-interacting protein kinase 21 | 0.38 | -0.40 | **-0.71** |
| AT5G57660 | ATCOL5_COL5__CONSTANS-like 5 | 0.20 | -0.49 | **-1.04** |
| AT5G57887 | unknown protein | -0.01 | **-1.24** | **-1.19** |
| AT5G57900 | SKIP1__SKP1 interacting partner 1 | 0.12 | -0.61 | **-0.94** |
| AT5G57910 | unknown protein | -0.05 | -0.26 | **-0.87** |
| AT5G58200 | Calcineurin-like metallo-phosphoesterase superfamily protein | -0.59 | -0.12 | **-0.79** |
| AT5G58350 | WNK4_ZIK2__with no lysine (K) kinase 4 | 0.20 | -0.35 | **-0.87** |
| AT5G58375 | Methyltransferase-related protein | 0.25 | -0.01 | **-0.83** |
| AT5G58420 | Ribosomal protein S4 (RPS4A) family protein | -0.18 | 0.49 | **0.80** |
| AT5G58640 | Selenoprotein, Rdx type | -0.03 | **-1.07** | **-1.81** |
| AT5G58800 | Quinone reductase family protein | 0.13 | 0.00 | **-0.77** |
| AT5G58860 | CYP86A1 (cytochrome P450, family 86, subfamily A, polypeptide 1); oxygen binding | 0.14 | -0.11 | **0.74** |
| AT5G58900 | Homeodomain-like transcriptional regulator | -0.21 | 0.59 | **0.81** |
| AT5G59090 | ATSBT4.12_SBT4.12__subtilase 4.12 | 0.08 | 0.06 | **0.71** |
| AT5G59240 | Ribosomal protein S8e family protein | 0.06 | 0.23 | **0.78** |
| AT5G59330 | Bifunctional inhibitor/lipid-transfer protein/seed storage 2S albumin superfamily protein | 0.06 | **0.90** | 0.43 |
| AT5G59400 | unknown protein | -0.02 | -0.07 | **-0.74** |
| AT5G59570 | Homeodomain-like superfamily protein | -0.09 | -0.38 | **-1.43** |
| AT5G59820 | RHL41_ZAT12__C2H2-type zinc finger family protein | 0.42 | -0.33 | **-1.06** |
| AT5G59850 | Ribosomal protein S8 family protein | -0.34 | 0.51 | **1.00** |
| AT5G59870 | HTA6__histone H2A 6 | -0.37 | 0.24 | **0.86** |
| AT5G59960 | unknown protein | -0.06 | **-0.97** | **-1.23** |
| AT5G60360 | AALP_ALP_SAG2__aleurain-like protease | 0.22 | -0.15 | **-0.83** |
| AT5G60390 | GTP binding Elongation factor Tu family protein | -0.17 | 0.36 | **1.27** |
| AT5G60640 | ATPDI2_ATPDIL1-4_PDI2_PDIL1-4__PDI-like 1-4 | -0.13 | 0.00 | **0.85** |
| AT5G60670 | Ribosomal protein L11 family protein | -0.02 | 0.56 | **0.95** |
| AT5G60680 | Protein of unknown function, DUF584 | -0.18 | **-1.03** | **-0.85** |
| AT5G60780 | ATNRT2.3 (*Arabidopsis thaliana* high affinity nitrate transporter 2.3); nitrate transporter | 0.06 | -0.02 | **1.11** |
| AT5G60890 | ATMYB34_ATR1_MYB34__myb domain protein 34 | 0.02 | **1.21** | **1.32** |
| AT5G61020 | ECT3__evolutionarily conserved C-terminal region 3 | -0.29 | 0.44 | **0.82** |
| AT5G61160 | AACT1__anthocyanin 5-aromatic acyltransferase 1 | -0.03 | 0.12 | **0.86** |
| AT5G61170 | Ribosomal protein S19e family protein | -0.21 | 0.64 | **0.91** |
| AT5G61330 | rRNA processing protein-related | -0.04 | 0.35 | **0.88** |
| AT5G61440 | ACHT5__atypical CYS HIS rich thioredoxin 5 | -0.14 | -0.72 | **-0.75** |

| AGI identifier | Gene annotation | 30 min | 2h | 8h |
|---|---|---|---|---|
| AT5G61520 | Major facilitator superfamily protein | 0.00 | 0.66 | **0.92** |
| AT5G61590 | Integrase-type DNA-binding superfamily protein | **-1.18** | **-2.02** | **-1.68** |
| AT5G61600 | ERF104__ethylene response factor 104 | **-0.83** | -0.61 | **-0.91** |
| AT5G61790 | ATCNX1_CNX1__calnexin 1 | -0.11 | 0.22 | **0.87** |
| AT5G61960 | AML1_ML1__MEI2-like protein 1 | **-0.79** | 0.44 | 0.52 |
| AT5G62020 | AT-HSFB2A_HSFB2A__heat shock transcription factor B2A | -0.33 | -0.14 | **-0.76** |
| AT5G62190 | PRH75__DEAD box RNA helicase (PRH75) | -0.18 | 0.23 | **0.74** |
| AT5G62220 | ATGT18_GT18__glycosyltransferase 18 | 0.06 | **1.04** | **0.85** |
| AT5G62440 | Protein of unknown function (DUF3223) | 0.06 | 0.67 | **0.83** |
| AT5G62480 | ATGSTU9_GST14_GST14B_GSTU9__glutathione S-transferase tau 9 | 0.15 | **1.04** | 0.52 |
| AT5G62540 | UBC3__ubiquitin-conjugating enzyme 3 | -0.16 | -0.22 | **-0.74** |
| AT5G62680 | Major facilitator superfamily protein | **0.83** | 0.34 | 0.20 |
| AT5G63030 | Thioredoxin superfamily protein | -0.08 | -0.26 | **-1.07** |
| AT5G63070 | Ribosomal protein S19 family protein | 0.03 | 0.28 | **0.80** |
| AT5G63085 | unknown protein | -0.24 | 0.29 | **0.79** |
| AT5G63160 | BT1 (BTB and TAZ domain protein 1); protein binding / transcription regulator | -0.09 | **-1.47** | **-1.73** |
| AT5G63190 | MA3 domain-containing protein | 0.31 | -0.53 | **-1.05** |
| AT5G63620 | GroES-like zinc-binding alcohol dehydrogenase family protein | -0.11 | -0.68 | **-1.08** |
| AT5G63680 | Pyruvate kinase family protein | -0.04 | 0.22 | **0.83** |
| AT5G63790 | ANAC102_NAC102__NAC domain containing protein 102 | 0.41 | -0.50 | **-0.97** |
| AT5G63840 | PSL5_RSW3__Glycosyl hydrolases family 31 protein | 0.17 | -0.08 | **-0.84** |
| AT5G63980 | ALX8_ATSAL1_FRY1_HOS2_RON1_SAL1__Inositol monophosphatase family protein | 0.43 | **0.86** | **0.77** |
| AT5G64040 | PSAN__photosystem I reaction center subunit PSI-N, chloroplast, putative / PSI-N, putative (PSAN) | 0.26 | -0.39 | **-1.70** |
| AT5G64100 | Peroxidase superfamily protein | **0.89** | -0.72 | **-1.44** |
| AT5G64120 | Peroxidase superfamily protein | -0.37 | 0.04 | **1.23** |
| AT5G64140 | RPS28__ribosomal protein S28 | -0.20 | 0.43 | **0.75** |
| AT5G64200 | ATSC35_SC35__ortholog of human splicing factor SC35 | 0.43 | -0.23 | **-0.74** |
| AT5G64250 | Aldolase-type TIM barrel family protein | 0.21 | -0.30 | **-1.50** |
| AT5G64560 | ATMGT9_MGT9_MRS2-2__magnesium transporter 9 | 0.11 | 0.12 | **1.05** |
| AT5G64640 | Plant invertase/pectin methylesterase inhibitor superfamily | -0.09 | 0.26 | **1.01** |
| AT5G64820 | unknown protein | **0.81** | -0.23 | **-0.83** |
| AT5G64890 | PROPEP2__elicitor peptide 2 precursor | -0.02 | -0.29 | **-0.75** |
| AT5G65020 | ANNAT2__annexin 2 | 0.42 | 0.06 | **0.78** |
| AT5G65110 | ACX2_ATACX2__acyl-CoA oxidase 2 | 0.11 | **-0.89** | **-1.26** |
| AT5G65300 | unknown protein | **0.88** | 0.19 | -0.05 |
| AT5G65390 | AGP7__arabinogalactan protein 7 | -0.42 | -0.06 | **0.82** |
| AT5G66540 | unknown protein | 0.06 | -0.65 | **-1.23** |
| AT5G66570 | MSP-1_OE33_OEE1_OEE33_PSBO-1_PSBO1__PS II oxygen-evolving complex 1 | **1.34** | 0.08 | -0.50 |
| AT5G66720 | Protein phosphatase 2C family protein | 0.09 | -0.27 | **-0.73** |
| AT5G67210 | Protein of unknown function (DUF579) | 0.00 | 0.57 | **0.77** |
| AT5G67240 | SDN3__small RNA degrading nuclease 3 | -0.03 | 0.57 | **0.76** |

| AGI identifier | Gene annotation | 30 min | 2h | 8h |
|---|---|---|---|---|
| AT5G67300 | ATMYB44_ATMYBR1_MYB44_MYBR1__myb domain protein r1 | 0.27 | **0.77** | 0.25 |
| AT5G67360 | ARA12__Subtilase family protein | 0.23 | **0.79** | **1.33** |
| AT5G67420 | ASL39_LBD37__LOB domain-containing protein 37 | -0.18 | -0.34 | **-0.75** |
| AT5G67480 | ATBT4_BT4_BTB and TAZ domain protein 4 | -0.53 | **-1.00** | -0.17 |

**Supplemental table IV**: Complete data from the metabolomic analysis. Numbers in bold are ratios with a statistical (t-Test, p-value≤0.05) difference between both conditions.

| | $Log_2$ (phenanthrene/ control) | $Log_2$ (sucrose + phenanthrene/ phenanthrene) | $Log_2$ (sucrose/ control) |
|---|---|---|---|
| Adonitol | **0.40** | -0.31 | -0.37 |
| Alpha-Alanine | **1.29** | **3.14** | **3.98** |
| Ammonium | -0.37 | **-1.34** | **-1.66** |
| Arginine | **0.40** | **-1.40** | **-1.76** |
| Asparagine | **0.48** | -0.12 | **0.17** |
| Aspartate | **0.29** | **-1.00** | **-0.83** |
| Beta-Alanine | -3.35 | 0.25 | -3.54 |
| Cellobiose | 0.00 | 0.00 | 0.00 |
| Citrate | 0.00 | **6.64** | **6.64** |
| Cystine | **0.58** | -0.44 | 0.06 |
| Fructose | 0.20 | **3.20** | **4.11** |
| Fumarate | 0.00 | **6.64** | **2.80** |
| GABA | 0.79 | -0.14 | **-0.08** |
| Galactinol | 0.00 | 0.00 | 0.00 |
| Galactose | 0.00 | 0.00 | 0.00 |
| Gentiobiose | 0.00 | 0.00 | 0.00 |
| Glucose | 0.14 | **2.35** | **2.65** |
| Glutamate | **0.33** | **0.60** | **0.41** |
| Glutamine | **0.54** | **1.37** | **1.77** |
| Glycerate | 0.00 | 0.00 | 0.00 |
| Glycine | **0.49** | **3.30** | **3.53** |
| Histidine | 0.28 | 0.07 | 0.39 |
| Hydroxyproline | 0.00 | 0.00 | 0.00 |
| Isoleucine | **1.18** | **-1.60** | -0.76 |
| Leucine | **1.22** | **-0.88** | 0.35 |
| Lysine | **0.59** | **-2.66** | **-2.52** |
| Malate | -0.39 | **3.83** | **2.95** |
| Maltose | 0.00 | 0.00 | 0.00 |
| Mannitol | 0.00 | 0.00 | 0.00 |
| Mannose | 0.00 | **6.64** | **6.64** |
| Melibiose | 0.00 | 0.00 | 0.00 |
| Methionine | 0.52 | -0.17 | -0.77 |
| Methylcysteine | -0.85 | -0.39 | -1.13 |
| Myo-inositol | **0.39** | -0.28 | -0.39 |
| Ornithine | 0.15 | **-0.81** | **-1.29** |
| Phenylalanine | **0.67** | **-2.79** | **-0.91** |
| Proline | 0.67 | **1.68** | **1.66** |
| Quinate | 0.00 | 0.00 | 0.00 |
| Serine | **0.72** | 0.05 | **0.30** |
| Sorbitol | 0.00 | 0.00 | 0.00 |
| Succinate | 0.00 | **6.64** | **6.64** |
| Sucrose | **0.88** | **5.09** | **5.76** |
| Threonine | **0.75** | **-0.38** | **0.12** |
| Trehalose | 0.00 | 0.00 | 0.00 |
| Tryptophan | **0.80** | **-1.89** | **-0.81** |
| Tyrosine | **0.35** | -0.19 | 0.22 |
| Valine | **0.89** | **-0.44** | 0.29 |

**Supplemental table V**: List of UDP-Glycosil-transferases and peroxidases differentially expressed in at leat one condition. Expression changes are given as log2. Expression changes in bolt correspond to genes differentially expressed at the significant threshold of Bonferroni p-value<0.05.

| | AGI identifiers | 30min | 2h | 8h |
|---|---|---|---|---|
| Peroxidases | AT4G37520 | -0.02 | **-1.07** | **-1.63** |
| | AT5G64100 | **0.89** | -0.72 | **-1.44** |
| | AT5G39580 | 0.30 | **-1.56** | **-0.95** |
| | AT2G37130 | x | -0.09 | **-0.93** |
| | AT4G37530 | -0.13 | **-0.74** | **-0.89** |
| | AT4G33420 | -0.24 | -0.57 | **-0.76** |
| | AT1G71695 | **0.87** | 0.07 | 0.04 |
| | AT5G51890 | **0.72** | 0.35 | 0.65 |
| | AT1G30870 | 0.34 | -0.06 | **0.79** |
| | AT1G05250 | 0.30 | 0.06 | **0.82** |
| | AT1G49570 | -0.38 | 0.45 | **0.83** |
| | AT3G28200 | -0.65 | 0.07 | **0.88** |
| | AT4G21960 | 0.17 | 0.11 | **1.03** |
| | AT3G01190 | **0.69** | -0.11 | **1.12** |
| | AT5G64120 | -0.37 | 0.04 | **1.23** |
| | AT3G21770 | 0.18 | 0.12 | **1.33** |
| | AT1G05240 | 0.31 | -0.08 | **1.68** |
| UDP-Glycosil-transferases | AT4G34138 | -0.03 | **-1.36** | **-1.54** |
| | AT1G22370 | 0.14 | **-1.36** | **-1.29** |
| | AT4G15550 | 0.07 | -0.16 | **-1.18** |
| | AT2G36770 | 0.18 | **-0.90** | **-1.18** |
| | AT1G21480 | -0.04 | -0.41 | **-1.17** |
| | AT2G15490 | 0.22 | -0.17 | **-0.92** |
| | AT1G22350 | -0.03 | **-1.05** | **-0.84** |
| | AT4G15260 | -0.03 | -0.20 | **-0.83** |
| | AT3G62720 | -0.48 | **-0.77** | -0.09 |
| | AT5G17050 | **0.71** | 0.37 | 0.01 |
| | AT4G15480 | 0.44 | 0.62 | **0.75** |
| | AT3G21560 | 0.21 | **0.95** | **0.75** |
| | AT2G22900 | 0.09 | 0.20 | **0.80** |
| | AT3G15350 | -0.19 | 0.53 | **0.82** |
| | AT5G62220 | 0.06 | **1.04** | **0.85** |
| | AT1G06000 | 0.15 | 0.71 | **0.99** |
| | AT4G27560 | -0.13 | 0.67 | **1.20** |
| | AT2G43820 | 0.14 | **-0.92** | x |

**Acknowledgment**

This work was funded by the Axson-Coatings firm and the French government (CIFRE n°1017/2009). Authors would like to thank Nathalie Marnet for targeted metabolomic analysis and Marie-Noëlle Soler for observation and imaging of the fluorescence microscopy.

**Bibliography**

**Abramoff MD, Magalhães PJ, Ram SJ** (2004) Image processing with ImageJ. Biophotonics Int **11**: 36–42

**Alkio M, Tabuchi TM, Wang X, Colón-Carmona A** (2005) Stress responses to polycyclic aromatic hydrocarbons in *Arabidopsis* include growth inhibition and hypersensitive response-like symptoms. J Exp Bot **56**: 2983–2994

**Ashraf M, Foolad MR** (2007) Roles of glycine betaine and proline in improving plant abiotic stress resistance. Environ Exp Bot **59**: 206–216

**Barker L, Kühn C, Weise A, Schulz A, Gebhardt C, Hirner B, Hellmann H, Schulze W, Ward JM, Frommer WB** (2000) SUT2, a Putative Sucrose Sensor in Sieve Elements. Plant Cell Online **12**: 1153–1164

**Bezalel L, Hadar Y, Cerniglia CE** (1997) Enzymatic Mechanisms Involved in Phenanthrene Degradation by the White Rot Fungus Pleurotus ostreatus. Appl Environ Microbiol **63**: 2495–2501

**Bolouri-Moghaddam MR, Le Roy K, Xiang L, Rolland F, Van den Ende W** (2010) Sugar signalling and antioxidant network connections in plant cells. FEBS J **277**: 2022–2037

**Borsani O, Valpuesta V, Botella MA** (2001) Evidence for a Role of Salicylic Acid in the Oxidative Damage Generated by NaCl and Osmotic Stress in *Arabidopsis* Seedlings. Plant Physiol **126**: 1024–1030

**Boyes DC, Zayed AM, Ascenzi R, McCaskill AJ, Hoffman NE, Davis KR, Görlach J** (2001) Growth stage-based phenotypic analysis of Arabidopsis: a model for high throughput functional genomics in plants. Plant Cell **13**: 1499–1510

**Coruzzi GM, Zhou L** (2001) Carbon and nitrogen sensing and signaling in plants: emerging "matrix effects."Curr Opin Plant Biol **4**: 247 – 253

**Couée I, Sulmon C, Gouesbet G, Amrani AE** (2006) Involvement of soluble sugars in reactive oxygen species balance and responses to oxidative stress in plants. J Exp Bot **57**: 449–459

**Crowe ML, Serizet C, Thareau V, Aubourg S, Rouze P, Hilson P, Beynon J, Weisbeek P, van Hummelen P, Reymond P, et al** (2003) CATMA: a complete *Arabidopsis* GST database. Nucleic Acids Res **31**: 156–158

**Dabestani R, Ivanov IN** (1999) A Compilation of Physical, Spectroscopic and Photophysical Properties of Polycyclic Aromatic Hydrocarbons. Photochem Photobiol **70**: 10–34

**Dubey RS, Singh AK** (1999) Salinity Induces Accumulation of Soluble Sugars and Alters the Activity of Sugar Metabolising Enzymes in Rice Plants. Biol Plant **42**: 233–239

**Edwards R, Brazier-Hicks M, Dixon DP, Cummins I** (2005) Chemical Manipulation of Antioxidant Defences in Plants. *In* J. A. Callow, ed, Adv. Bot. Res. Academic Press, pp 1–32

**Edwards R, Dixon DP, Cummins I, Brazier-Hicks M, Skipsey M** (2011) New Perspectives on the Metabolism and Detoxification of Synthetic Compounds in Plants. *In* P Schröder, CD Collins, eds, Org. Xenobiotics Plants. Springer Netherlands, pp 125–148

**Ende WV den, Peshev D** (2013) Sugars as Antioxidants in Plants. *In* N Tuteja, SS Gill, eds, Crop Improv. Adverse Cond. Springer New York, pp 285–307

**Ende WV den, Valluru R** (2009) Sucrose, sucrosyl oligosaccharides, and oxidative stress: scavenging and salvaging? J Exp Bot **60**: 9–18

**Farrar J, Pollock C, Gallagher J** (2000) Sucrose and the integration of metabolism in vascular plants. Plant Sci **154**: 1–11

**Foyer CH, Noctor G** (2011) Ascorbate and Glutathione: The Heart of the Redox Hub. Plant Physiol **155**: 2–18

**Gagnot S, Tamby J-P, Martin-Magniette M-L, Bitton F, Taconnat L, Balzergue S, Aubourg S, Renou J-P, Lecharny A, Brunaud V** (2008) CATdb: a public access to *Arabidopsis* transcriptome data from the URGV-CATMA platform. Nucleic Acids Res **36**: D986–D990

**Ge Y, Dudoit S, Speed TP** (2003) Resampling-based multiple testing for microarray data analysis. Test **12**: 1–77

**Gill PK, Sharma AD, Singh P, Bhullar SS** (2003) Changes in germination, growth and soluble sugar contents of Sorghum bicolor (L.) Moench seeds under various abiotic stresses. Plant Growth Regul **40**: 157–162

**Hilson P, Allemeersch J, Altmann T, Aubourg S, Avon A, Beynon J, Bhalerao RP, Bitton F, Caboche M, Cannoot B, et al** (2004) Versatile Gene-Specific Sequence Tags for *Arabidopsis* Functional Genomics: Transcript Profiling and Reverse Genetics Applications. Genome Res **14**: 2176–2189

**Keunen E, Peshev D, Vangronsveld J, VAN DEN Ende W, Cuypers A** (2013) Plant sugars are crucial players in the oxidative challenge during abiotic stress: extending the traditional concept. Plant Cell Environ. doi: 10.1111/pce.12061

**Koch K** (2004) Sucrose metabolism: regulatory mechanisms and pivotal roles in sugar sensing and plant development. Curr Opin Plant Biol **7**: 235 – 246

**Liu H, Weisman D, Ye Y, Cui B, Huang Y, Colón-Carmona A, Wang Z** (2009) An oxidative stress response to polycyclic aromatic hydrocarbon exposure is rapid and complex in *Arabidopsis thaliana*. Plant Sci **176**: 375 – 382

**Lloyd JC, Zakhleniuk OV** (2004) Responses of primary and secondary metabolism to sugar accumulation revealed by microarray expression analysis of the *Arabidopsis* mutant, pho3. J Exp Bot **55**: 1221–1230

**Loreti E, Poggi A, Novi G, Alpi A, Perata P** (2005) A Genome-Wide Analysis of the Effects of Sucrose on Gene Expression in *Arabidopsis* Seedlings under Anoxia. Plant Physiol **137**: 1130–1138

**Lurin C, Andrés C, Aubourg S, Bellaoui M, Bitton F, Bruyère C, Caboche M, Debast C, Gualberto J, Hoffmann B, et al** (2004) Genome-wide analysis of *Arabidopsis* pentatricopeptide repeat proteins reveals their essential role in organelle biogenesis. Plant Cell **16**: 2089–2103

**Matsui T, Nomura Y, Takano M, Imai S, Nakayama H, Miyasaka H, Okuhata H, Tanaka S, Matsuura H, Harada K, et al** (2011) Molecular Cloning and Partial Characterization of a Peroxidase Gene Expressed in the Roots of <I>Portulaca oleracea</I> cv., One Potentially Useful in the Remediation of Phenolic Pollutants. Biosci Biotechnol Biochem **75**: 882–890

**Murashige T, Skoog F** (1962) A Revised Medium for Rapid Growth and Bio Assays with Tobacco Tissue Cultures. Physiol Plant **15**: 473–497

**Pasternak T, Rudas V, Potters G, Jansen MAK** (2005) Morphogenic effects of abiotic stress: reorientation of growth in *Arabidopsis thaliana* seedlings. Environ Exp Bot **53**: 299–314

**Paul MJ, Foyer CH** (2001) Sink regulation of photosynthesis. J Exp Bot **52**: 1383–1400

**Peshev D, Vergauwen R, Moglia A, Hideg É, Ende WV den** (2013) Towards understanding vacuolar antioxidant mechanisms: a role for fructans? J Exp Bot ers377

**Price J, Laxmi A, Martin SKS, Jang J-C** (2004) Global Transcription Profiling Reveals Multiple Sugar Signal Transduction Mechanisms in Arabidopsis. Plant Cell Online **16**: 2128–2150

**Provart T. and Z** (2003) A Browser-based Functional Classification SuperViewer for *Arabidopsis* Genomics. Curr Comput Mol Biol 271–272

**Rai VK** (2002) Role of Amino Acids in Plant Responses to Stresses. Biol Plant **45**: 481–487

**Ramel F, Sulmon C, Bogard M, Couée I, Gouesbet G** (2009) Differential patterns of reactive oxygen species and antioxidative mechanisms during atrazine injury and sucrose-induced tolerance in *Arabidopsis thaliana* plantlets. BMC Plant Biol **9**: 28

**Ramel F, Sulmon C, Cabello-Hurtado F, Taconnat L, Martin-Magniette M-L, Renou J-P, Amrani AE, Couée I, Gouesbet G** (2007) Genome-wide interacting effects of sucrose and herbicide-mediated stress in *Arabidopsis thaliana*: novel insights into atrazine toxicity and sucrose-induced tolerance. BMC Genomics **8**: 450

**Roitsch T** (1999) Source-sink regulation by sugar and stress. Curr Opin Plant Biol **2**: 198–206

**Rolland F, Moore B, Sheen J** (2002) Sugar Sensing and Signaling in Plants. Plant Cell **14**: s185–s205

**Rosa M, Prado C, Podazza G, Interdonato R, Gonzalez JA, Hilal M, Prado FE** (2009) Soluble sugars: Metabolism, sensing and abiotic stress: A complex network in the life of plants. Signal Behav **4**: 288–393

**Rozen S, Skaletsky H** (2000) Primer3 on the WWW for general users and for biologist programmers. Methods Mol Biol Clifton NJ **132**: 365–386

**Sandermann Jr. H** (1992) Plant metabolism of xenobiotics. Trends Biochem Sci **17**: 82–84

**Solfanelli C, Poggi A, Loreti E, Alpi A, Perata P** (2006) Sucrose-Specific Induction of the Anthocyanin Biosynthetic Pathway in Arabidopsis. Plant Physiol **140**: 637–646

**Sulmon C, Gouesbet G, Amrani AE, Couée I** (2006) Sugar-induced tolerance to the herbicide atrazine in *Arabidopsis* seedlings involves activation of oxidative and xenobiotic stress responses. Plant Cell Reports **25**: 489–498

**Sulmon C, Gouesbet G, Couée I, Amrani AE** (2004) Sugar-induced tolerance to atrazine in *Arabidopsis* seedlings: interacting effects of atrazine and soluble sugars on psbA mRNA and D1 protein levels. Plant Sci **167**: 913–923

**Syed K, Doddapaneni H, Subramanian V, Lam YW, Yadav JS** (2010) Genome-to-function characterization of novel fungal P450 monooxygenases oxidizing polycyclic aromatic hydrocarbons (PAHs). Biochem Biophys Res Commun **399**: 492–497

**Szabados L, Savouré A** (2010) Proline: a multifunctional amino acid. Trends Plant Sci **15**: 89–97

**Tadege M, Dupuis I, Kuhlemeier C** (1999) Ethanolic fermentation: new functions for an old pathway. Trends Plant Sci **4**: 320–325

**Taguchi G, Ubukata T, Nozue H, Kobayashi Y, Takahi M, Yamamoto H, Hayashida N** (2010) Malonylation is a key reaction in the metabolism of xenobiotic phenolic glucosides in *Arabidopsis* and tobacco. Plant J **63**: 1031–1041

**team RDC** (2013) R: a language and environment for statistical computing. R foundation for statistical computing, Vienna, Austria

**Thimm O, Bläsing O, Gibon Y, Nagel A, Meyer S, Krüger P, Selbig J, Müller LA, Rhee SY, Stitt M** (2004) MAPMAN: a user-driven tool to display genomics data sets onto diagrams of metabolic pathways and other biological processes. Plant J Cell Mol Biol **37**: 914–939

**Thum KE, Shin MJ, Palenchar PM, Kouranov A, Coruzzi GM** (2004) Genome-wide investigation of light and carbon signaling interactions in Arabidopsis. Genome Biol **5**: R10

**Valluru R, Ende WV den** (2008) Plant fructans in stress environments: emerging concepts and future prospects. J Exp Bot **59**: 2905–2916

**Vieira Dos Santos C, Rey P** (2006) Plant thioredoxins are key actors in the oxidative stress response. Trends Plant Sci **11**: 329–334

**Weisman D, Alkio M, Colón-Carmona A** (2010) Transcriptional responses to polycyclic aromatic hydrocarbon-induced stress in *Arabidopsis thaliana* reveal the involvement of hormone and defense signaling pathways. BMC Plant Biol **10**: 59

**Wind J, Smeekens S, Hanson J** (2010) Sucrose: Metabolite and signaling molecule. Phytochemistry **71**: 1610–1614

# Chapitre 4 : **Approche expérimentale pour l'amélioration de la phytoremédiation naturelle des HAPs: mise en place et conception d'un site pilote.**

## 1. Introduction

L'entreprise Axson-Coatings (anciennement Bs Coatings, membre du groupe Axson) est une entreprise française qui produit des revêtements industriels (protections anticorrosion, isolants thermiques…) qui peuvent être et ont longtemps été synthétisés à partir de produits pétroliers. Au début de son activité, dans les années 1940-1950, dans un contexte d'absence de réglementation, les déchets étaient enfouis dans des trous sur un terrain vague à proximité des bâtiments de production, comme cela était couramment fait à cette époque. Ceci a généré un site fortement contaminé avec un niveau de pollution très hétérogène (Figure supplémentaire S1).

Dans le contexte réglementaire actuel, l'entreprise a pris la décision de remédier à ce problème. Des analyses de sol ont été réalisées au début des années 2000 afin d'évaluer l'ampleur de cette pollution. Elles ont montré que seuls les hydrocarbures aromatiques polycycliques (HAPs) sont retrouvés dans le sol répartis de manière très hétérogène sur l'ensemble du site. Les zones où les déchets ont été enfouis sont fortement contaminées par rapport au reste du site dans lequel les produits ont été diffusés par la suite, créant un effet de pépites (Figure supplémentaire S1).

Des études préliminaires ont été réalisées afin d'évaluer les coûts de dépollution du site avec des méthodes de traitement *ex-situ* « classiques ». En raison du coût important de ces techniques, malgré leur efficacité avérée et leur rapidité, les dirigeants d'Axson-Coatings ont décidé d'étudier, en collaboration avec l'Université de Rennes 1, la faisabilité de l'utilisation d'un système de dépollution naturelle basé sur la capacité des végétaux à décontaminer leur environnement : la phytoremédiation.

Les études préliminaires au laboratoire, *in-vitro*, ont permis de montrer que même si les HAPs affectent le développement des plantes, l'apport de saccharose dans le milieu de culture permet de limiter les effets négatifs des HAPs (inhibition de la croissance des racines et des parties aériennes, chloroses…) et de maintenir le développement des plantes lorsque ces dernières poussent sur des milieux contenant de fortes concentrations de HAPs. De par cette collaboration, un site pilote de phytoremédiation a été mis en place afin de (i) identifier les espèces végétales présentant la meilleure capacité d'adaptation et de décontamination des zones fortement polluées et (ii) voir si un apport de saccharose permet d'améliorer la phytoremédiation des HAPs et la décontamination des sols *in-situ*.

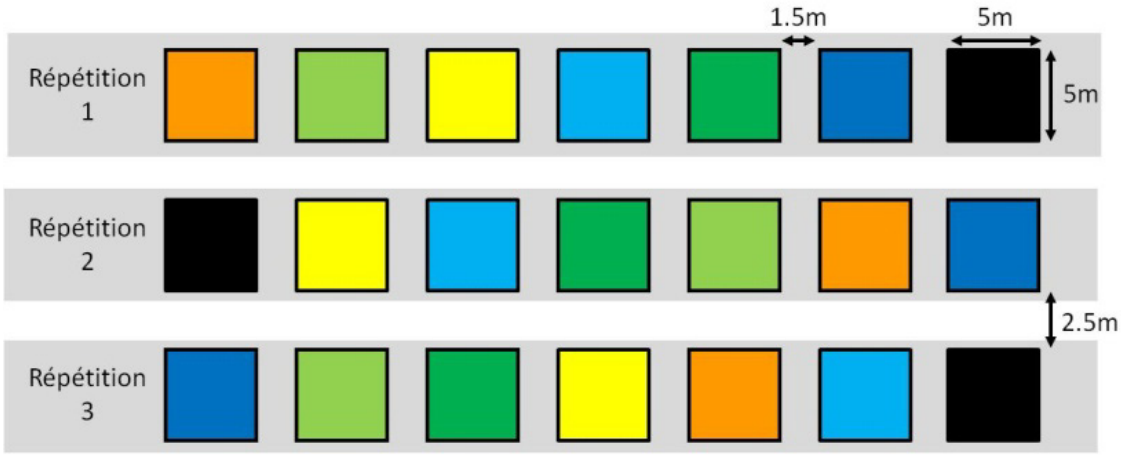


| | Apport de terre végétale | | |
|---|---|---|---|
| | + | | - |
| | Apport de sucrose | | |
| Plantation | + | - | - |
| Aucune | | | |
| Plantes ligneuses | | | |
| Plantes herbacées | | | |

**<u>Figure 1</u> : Plan expérimental du site pilote**

## 2. Matériel et méthodes

### 2.1. Mise en place du système expérimental

#### *2.1.1. Préparation de la parcelle*

Le terrain pollué correspond à une surface totale de plus de 1 hectare. Nous avons choisi, après avoir défini le plan expérimental, de travailler sur une parcelle de 1000m² représentative du site.

Pout obtenir des conclusions objectives et significatives malgré la grande variabilité due à la répartition hétérogène de la pollution, il est nécessaire de faire plusieurs répétitions dans lesquelles les différentes conditions sont réparties aléatoirement. Toutefois, pour des raisons pratiques de circulation avec les engins de terrassement, les parcelles laissées intactes, qui serviront de témoin (en noir sur la figure 1), ont été placées aux extrémités de chaque répétition.

Pour les autres parcelles (en couleur sur la figure 1), la couche superficielle d'environ 20 cm de remblai, constituée de blocs de pierres, apportés après l'enfouissement des déchets, a été enlevée et remplacée par de la terre végétale. Cet apport a deux objectifs : (i) il doit permettre aux plantes de mieux s'installer, et (ii) il apporte de nouveaux consortiums bactériens et fongiques (Huang et al., 2004; Escalante-Espinosa et al., 2005). En effet, de nombreux travaux ont montrés que l'apport de matière organique (compost, terre végétale…) permet de stimuler l'élimination des HAPs du sol (Ghanem et al., 2013; Wang et al., 2012b; Wang et al., 2012a).

#### *2.1.2. Mise en place des plantes*

Plusieurs espèces végétales ont été utilisées. Le choix des espèces végétales s'est effectué selon plusieurs critères. Dans un premier temps, nous avons voulu comparer deux types de plantes différents.

(i) Des plantes ligneuses à enracinement profond : le saule, une plante connue pour sa capacité épuratrice notamment des eaux usées, est également un genre fréquemment utilisé pour la phytoremédiation des sols pollués par les HAPs (Vervaeke et al., 2003; Euliss et al., 2008). De plus, deux espèces de saule étaient déjà présentes sur le site : *Salix fragilis* et *Salix caprea*. *Buddleja davidii* a aussi été choisi comme plante ligneuse à enracinement profond car cette espèce était présente naturellement sur le site et se développait bien et rapidement, ce qui en faisait un bon candidat pour la phytoremédiation des HAPs.

(ii) Une plante herbacée, le miscanthus a été choisi pour d'une part sa capacité à produire une forte biomasse en une saison végétative et d'autre part le potentiel de cette plante pour la phytoremédiation des HAPs (Gawronski and Gawronska, 2007).

Pour chaque parcelle « plantes ligneuses », 6 saules (*Salix fragilis*) et 6 arbres aux papillons (*Buddleja davidii*) ont été plantés. Les parcelles « plantes herbacées » ont reçu des rhizomes de *Miscanthus* × *giganteus*. Les végétaux ont été plantés à la saison adéquate : fin décembre 2010 pour les arbres et fin mars 2011 pour le miscanthus. Un système d'arrosage automatique au goutte-à-goutte a été installé afin d'irriguer de façon continue et la plus homogène possible l'ensemble des parcelles du site pilote.

### 2.2. Apports en saccharose et entretien du site

Les parcelles traitées ont reçu 3kg de saccharose tous les quinze jours. Nous avons choisi d'apporter le saccharose directement sous forme de poudre comme cela est fait pour les apports d'engrais agricoles, après avoir vérifié qu'en deux semaines l'ensemble du saccharose apporté a été bien dissous par l'arrosage et l'humidité naturelle (plus particulièrement en période sèche).

La dose a été établie en se référant aux doses appliquées *in-vitro* et aux besoins en eau d'un arbre. On estime à 8L le besoin en eau moyen d'un arbre à chaque arrosage pour les conditions de sol, précipitations, ensoleillement du site pilote. Sachant que la solution nutritive utilisée *in-vitro* contient 30g/L de saccharose, un arrosage de 8L avec cette solution

apporterait une quantité de 250g de saccharose par arbre soit 3kg pour l'ensemble de la parcelle. La même dose a ensuite été appliquée sur l'ensemble des parcelles ayant reçu un apport de saccharose.

Enfin nous avons pris la décision de ne pas appliquer de désherbant pour éviter toute interférence avec les analyses ultérieures. En effet, même si certains herbicides permettent de cibles les adventices, des études ont montré que les plantes sont capables de les accumuler. D'autre part, le saccharose permet d'augmenter l'accumulation de l'atrazine dans les plantes (Sulmon et al., 2007a), ce qui pourrait avoir un effet croisé avec les HAPs. Les parties aériennes de miscanthus ont été coupées à la fin de la première saison végétative quand les feuilles sont devenues sèches et ont été utilisées comme paillis afin de limiter le développement des adventices, ce qui est couramment fait dans la culture du miscanthus (Chambre d'Agriculture de Picardie, 2010).

### 2.3. Suivi du site pilote

Lors de chaque traitement, l'ensemble des parcelles est photographié successivement au cours des saisons afin de suivre le développement des plantes qui ont été mises en place ainsi que des autres végétaux qui se sont développés naturellement.

Les photographies ont été analysées avec le logiciel 'ImageJ' (Abramoff et al., 2004) afin d'évaluer globalement l'intensité de la chlorophylle, mesure ce qui permet d'évaluer le développement de la végétation au cours du temps (Richardson et al., 2001).

De plus, à la fin de l'expérimentation, un relevé du nombre d'arbres vivants a été effectué pour chacune des parcelles, nous permettant ainsi de calculer un taux de survie pour chaque espèce d'arbres (saules et *Buddleja*) qui est exprimé en pourcentage ($taux = \frac{nombre\ d'arbres\ vivants}{nombre\ d'arbres\ plantés}$). Le taux de survie minimum correspond au taux de survie le plus faible des 3 répétitions d'une condition donnée alors que le taux de survie maximum correspond au taux de survie le plus élevé des 3 répétitions.

### 2.4. Echantillonnage et dosages des HAPs

Les échantillons de sols ont été prélevés sur une profondeur de 30cm sur 5 points de chaque parcelle, mélangés et envoyés à analyser. Les 5 points de prélèvements ont été choisis aléatoirement et regroupés afin d'obtenir un échantillon le plus représentatif de l'état global de la parcelle et de limiter la variabilité qu'il peut y avoir au sein même d'une parcelle. Les échantillons de sols ainsi obtenus ont directement été envoyés au laboratoire d'analyse qui a effectué la préparation (séchage, broyage, tamisage) des échantillons. Le prélèvement des échantillons de sol et de végétaux ont été effectués en fin de saison végétative. L'ensemble des échantillons a été prélevé le même jour.

A la fin de la deuxième saison végétative (début octobre 2012), pour chaque parcelle plantée, l'ensemble de la végétation (saules, miscanthus, *Buddleja*) a été coupé, broyé grossièrement, mélangé avant de prélever 250g de matière fraiche qui sera lyophilisée pour éviter tout risque de moisissures et pourrissements lors de la période de transport.

Afin de déterminer la quantité des HAPs qui a été enlevée des sols et de déterminer la quantité absorbée par les plantes, des dosages des 16 HAPs (Partie 1, Tableau 1) listés comme prioritaires par l'agence de l'environnement américaine (Wilson and Jones, 1993) ont été réalisés par le laboratoire CARSO (Lyon, France). Pour les sols, le dosage est effectué par chromatographie en phase liquide à haute performance (HPLC), après une extraction par des solvants (Accelerated Solvant Extraction, ASE), en suivant le protocole normalisé NF X33-012. Pour les végétaux, le dosage est effectué par chromatographie en phase gazeuse couplée à de la spectrométrie de masse GC-MS.

### 2.5. Analyses statistiques

L'intégralité des analyses statistiques a été réalisé en utilisant le test de Wilcoxon avec le logiciel R (team RDC, 2013). Etant donnée la forte variabilité existant sur le site pilote, les données ont été considérées statistiquement significatives quand la p-value était inférieure à 0,1.

## 3. Résultats-discussion

### 3.1. Suivi du développement de la végétation sur le site pilote

Chaque parcelle a été photographiée tous les mois, entre décembre 2010 et octobre 2012, afin de suivre le développement de la végétation. Ces données montrent que, malgré un sol fortement pollué, où ne poussaient que quelques espèces herbacées clairsemées caractéristiques des friches industrielles (Figure supplémentaire 1), l'ensemble des espèces se sont bien installées. L'apport de terre végétale a probablement aidé les plantes à se développer et a permis d'implanter d'autres espèces (orties et chardons) qui n'étaient pas naturellement présentes sur le site. De plus, on peut noter que des plantes se sont développées sur les parcelles pour lesquelles seul un arrosage a été effectué (parcelles « contrôles ») soulignant ainsi l'importance de l'apport en eau pour favoriser le développement des plantes dans ces conditions sur ce site.

La figure 2 montre l'évolution des différentes conditions testées sur une parcelle représentative au cours des saisons. Nous avons, par ailleurs, cherché à quantifier le développement des plantes en utilisant des marqueurs mesurables et surtout non-destructifs. Une approche très grossière a tout d'abord été utilisée de manière à évaluer l'évolution des plantes à travers la quantification de la chlorophylle par le biais d'analyse d'images numériques. Cette mesure prend en compte aussi bien les espèces que nous avons installées que les espèces qui se sont installées de manière spontanée. L'ensemble des photos a été pris au même moment de la journée, selon le même angle.

A partir des photographies prises tout au long de l'expérimentation (Figure supplémentaire S2), une analyse de l'intensité de la chlorophylle (couleur verte) a été effectuée, grâce au logiciel de traitement d'image 'ImageJ'.

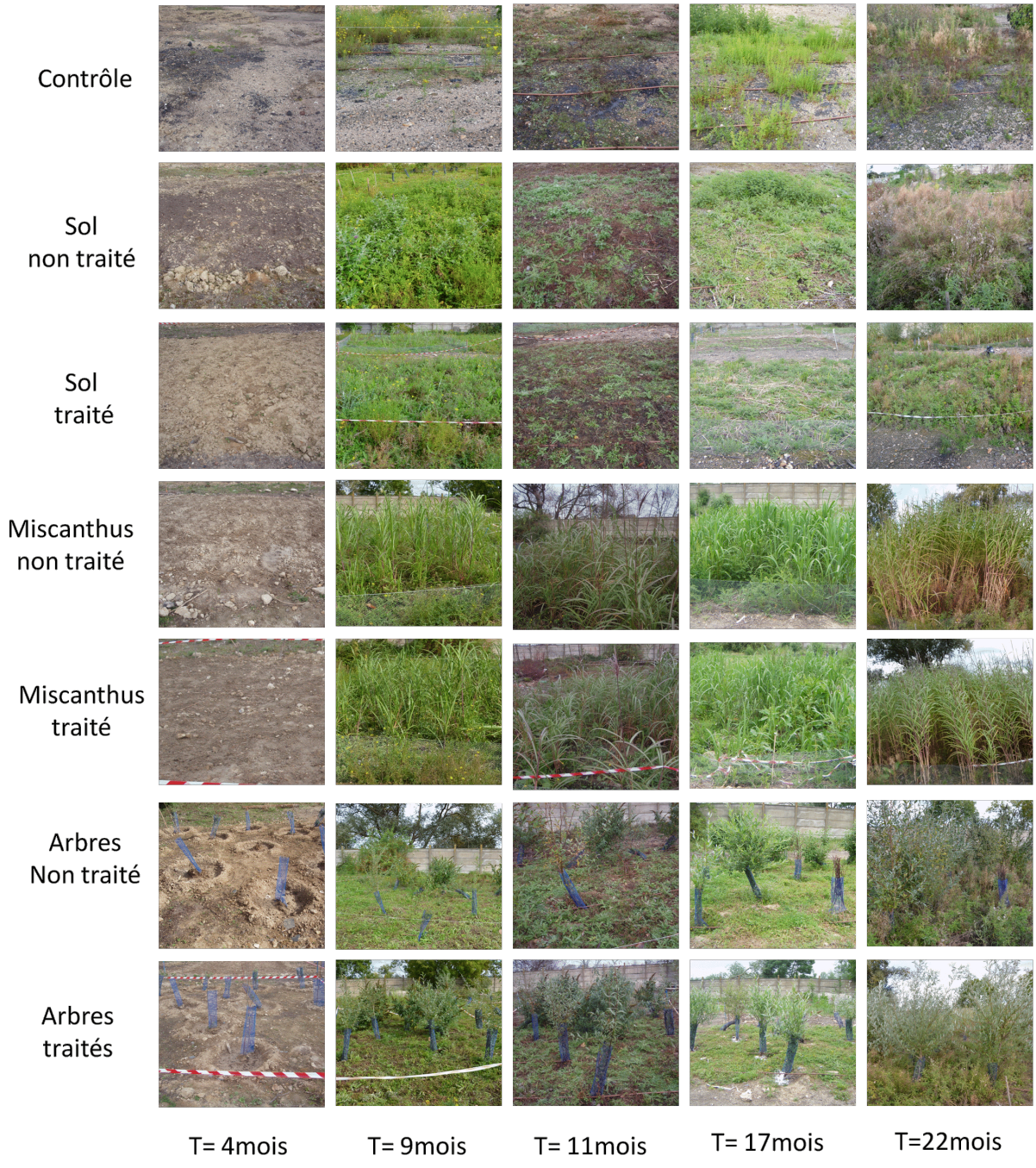


**<u>Figure 2</u> : Suivi du développement de la végétation sur une parcelle représentative de chaque condition**

Les temps indiqués représentent les pics saisonniers pour lesquels le développement de la végétation est à son maximum (en été T=9mois et T=17mois) ou à son minimum (T=4 mois qui est aussi le point de départ de l'ensemble de l'expérimentation et T=11 mois) puis à au moment des prélèvements (T=22mois).

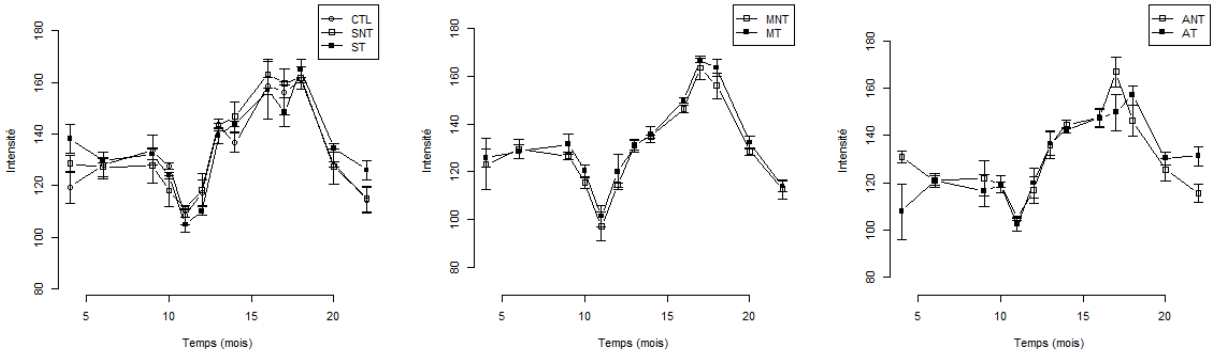


**<u>Figure 3</u> : Evolution de l'intensité du vert des photographies prises au cours de l'expérimentation (en annexe 1) pour les différentes conditions étudiées.**

CTL, contrôle ; SNT, sol nu non traité ; ST, sol nu traité ; MNT, herbacées (miscanthus) non traitées ; MT, herbacées (miscanthus) traitées ; ANT, ligneuses (arbres) non traitées ; AT, ligneuses (arbres) traitées.

La figure 3 retrace l'évolution de ce paramètre au cours du temps. Les pics correspondent aux mois d'été et les creux à ceux d'hiver. En effet, comme on peut l'observer sur la figure S2, la coloration verte due à la chlorophylle des plantes est beaucoup plus intense en été quand la végétation est à son maximum de croissance alors qu'en hiver, les feuilles ont jaunies ou sont tombées d'où la diminution de l'intensité de la couleur verte. La variation saisonnière de ce paramètre montre bien que c'est un indicateur de la variation de la teneur chlorophylle et de développement des parties aériennes (en particuliers des feuilles). De plus, cet indicateur est non destructif et nous permet donc de suivre l'évolution de l'ensemble des plantes au cours du temps. Cette quantification très globale n'a pas permis de dégager des différences significatives entre les différentes conditions de traitement en saccharose. Ce résultat montre que l'apport de saccharose n'a pas rendu les plantes plus « vertes » c'est-à-dire plus riches en chlorophylles. D'autre part, l'absence de différence observée entre les sols plantés et non plantés montrent que le seul apport de terre végétale et surtout l'irrigation ont permis le développement de la végétation sur les parcelles.

Par ailleurs, un taux de survie (Figure 4) a pu être calculé pour les deux espèces ligneuses, étant donné que 6 arbres de chaque espèce ont été plantés dans chaque parcelle. Ce taux est un critère permettant d'évaluer la viabilité des espèces et leur capacité d'adaptation aux conditions aussi bien climatiques et pédologiques du site qu'à la forte

teneur en HAPs. Cependant, aucune différence n'est observable entre les taux moyens de chaque condition, ces résultats pouvant être expliqués par l'hétérogénéité du site.

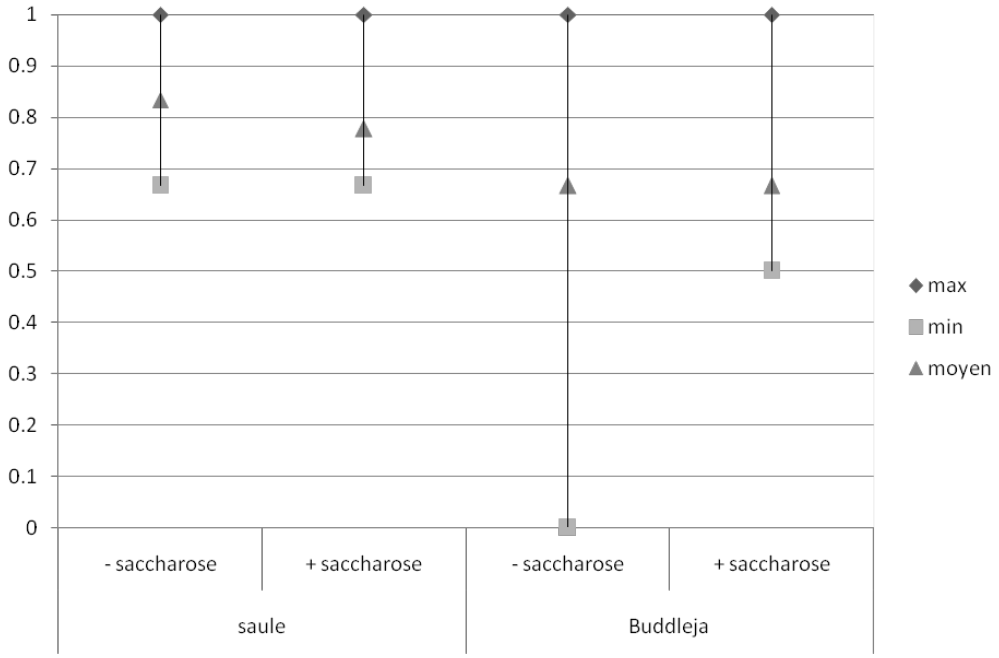


**<u>Figure 4</u> : Taux de survie des plantes ligneuses.**

*Max, représente le taux de survie le plus élevé des 3 répétitions ; min, le taux de survie le plus faible des 3 répétitions ; moyen, le taux de survie moyen des 3 répétitions.*

Cependant, le taux de survie minimal représente le taux de survie pour la parcelle la plus affectée avec le plus d'arbres morts. Les résultats obtenus montrent que *Buddleja* est l'espèce la plus fortement affectée par les HAPs avec un taux de survie nul pour les parcelles non-traitées et de 0,5 pour les traitées alors que pour le saule ce taux est de près de 0,7 sur parcelle traitée, ce qui montrerait l'effet potentiel du saccharose même sur le terrain. De plus, il est important de noter que, dans le cas du *Buddleja*, la parcelle la plus affectée est une parcelle non-traitée alors qu'aucune différence n'est observable pour le saule.

D'autre part, nous avons observé que le miscanthus ne présentait pas une répartition homogène sur certaines parcelles. Ceci serait probablement dû à un manque d'arrosage. L'arrosage par goutte-à-goutte se faisant de la gauche vers la droite du plan expérimental (Figure 1) et les parcelles les plus touchées étant à droite, il se peut que, malgré les précautions prises, ces parcelles-là aient reçu une quantité d'eau insuffisante. De plus, pour les deux espèces ligneuses (*Buddleja* et saule), les parcelles pour lesquelles le taux de survie

(Figure 4) est le plus faible se situent elles aussi vers la droite du site pilote. L'installation d'une irrigation par aspersion serait probablement plus adaptée à la culture du miscanthus (surtout pour de grandes surfaces), étant donné que c'est ce type d'arrosage qui est utilisé pour l'irrigation du maïs. D'autre part, l'utilisation d'un paillis, comme par exemple les résidus de la première coupe de miscanthus, permet de conserver l'humidité dans le sol et d'optimiser au mieux l'arrosage au goutte-à-goutte.

De manière générale, la végétation s'est bien développée et surtout de nouvelles espèces, autres que celles installées, se sont implantées.

De plus, la mise en place des parcelles de phytoremédiation a permis l'introduction d'insectes, arachnides et vers. Un inventaire non-exhaustif effectué au cours de la première saison végétative, après 6 mois d'expérimentation, a permis d'identifier une quarantaine d'espèces végétales qui se développent spontanément sur le site (Figure S2). Parmi ces espèces, on retrouve le saule fragile et *Buddleja* qui ont été utilisés pour l'expérimentation. Certaines espèces telles que le bouillon blanc, le millepertuis ou bien le sureau sont présentes de façon abondante sur le site. La terre végétale a probablement apporté, en plus des micro-organismes et des vers, de nouvelles espèces notamment des chardons qui se développent uniquement dans les zones où se trouve cette terre.

### 3.2. Estimation des capacités de stockage des HAPs par les 3 espèces végétales

La méthode de dosage des HAPs utilisée ne prend en compte que les HAPs libres. Par conséquent, la fraction dosée ne représente probablement pas l'intégralité des HAPs stockés dans la plante. Il est possible que les cellules végétales, comme c'est le cas pour les bactéries, les champignons et les cellules animales, métabolisent les xénobiotiques, ou bien les conjuguent avec des molécules simples comme les sucres ou le glutathion afin de les rendre moins toxiques. Ce processus a été démontré au moins pour les polluants phénoliques chez Arabidopsis. En effet une fois absorbé par les cellules végétales, ces derniers sont glycosylés par une glucosyltransferase (Brazier-Hicks et al., 2007) ou bien associé aux parois via probablement des peroxydases comme l'ont suggéré Matsui et al. 2011.

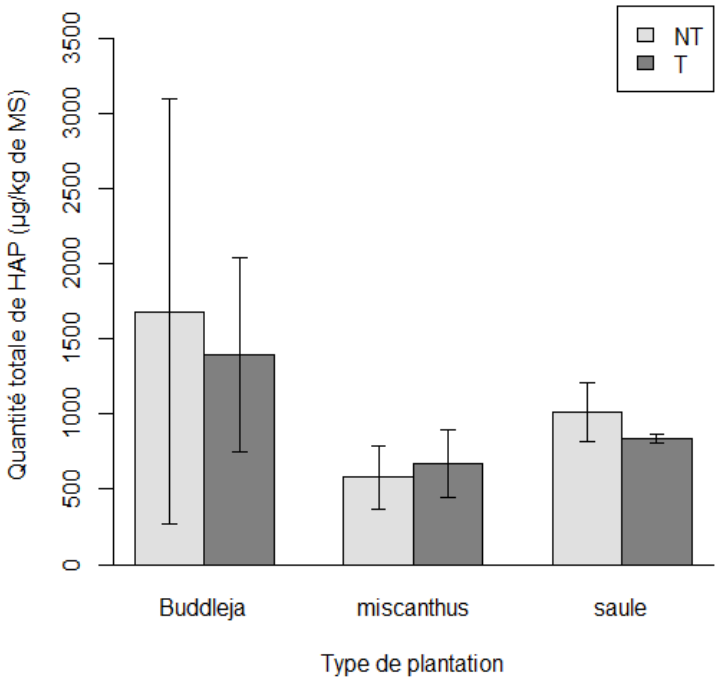


**<u>Figure 5</u>: Quantité totale des 16 HAPs dosés dans les plantes pour l'ensemble des conditions étudiées**.

NT représente les parcelles n'ayant pas reçu un apport de saccharose ; T représente les parcelles ayant reçu un apport de saccharose.

Les HAPs détectés dans les plantes sont donc probablement ceux qui n'ont pas été transformés et pourraient représenter uniquement la partie directement absorbée et accumulée dans la cellule de la plante sans transformation. D'autre part, les HAPs peuvent être retrouvés dans les parties racinaires (racines et rhizomes) mais, généralement, en quantité moins importantes que dans les parties aériennes (Wang et al., 2012c).

Les HAPs ont été dosés uniquement dans les parties aériennes des plantes afin de permettre la repousse des plantes et la poursuite de l'expérimentation sur plusieurs années. Les plantes ont absorbé entre 500 et 1700µg de HAPs totaux par kilogramme de matière sèche analysée. Nos données montrent cependant une grande variabilité de la teneur des HAPs accumulés par les trois espèces, ce qui pourrait refléter l'hétérogénéité de la pollution du site pilote, la présence d'effet pépites mais aussi que les trois espèces n'ont pas la même capacité d'absorption. On peut remarquer que les arbres ont tendance à absorber plus de HAPs que le miscanthus, probablement grâce à leur enracinement beaucoup plus profond qui leur donne une plus grande surface de contact et leur permet d'accéder à des zones plus fortement polluées.

Même si aucune différence statistiquement significative n'est observée entre les trois espèces étudiées, une tendance se dessine montrant que les arbres semblent absorber plus de HAPs que l'espèce herbacée (Figure 5).

Il est intéressant de noter que le *Buddleja,* qui est la plante qui paraît accumuler le plus de HAPs libres, est l'espèce qui présente le plus faible taux de survie. Cette observation semble indiquer que la stratégie de gestion des HAPs par les trois espèces végétales est différente.

Quant à l'effet du saccharose, une tendance se dessine sans être pour autant significative. En effet, le saccharose semble permettre aux miscanthus d'absorber plus de HAPs, mais cette tendance n'apparaît pas pour les deux autres espèces. Le miscanthus a un système racinaire superficiel qui lui permettrait d'absorber le saccharose apporté en surface plus rapidement avant qu'il soit lessivé. De plus, cette espèce est capable de stocker le saccharose dans ses rhizomes directement ou sous forme d'amidon (Lebas, 2012). Malgré ce

résultat très contrasté, on peut noter que les espèces installées sur le site pilote sont capables d'absorber les HAPs et de les stocker.

Toutefois, la fraction de HAPs libres stockée par les plantes ne représente que 1 à 3% de la quantité totale de HAPs enlevée des sols, ce qui montre que la phytoaccumulation des polluants non-transformés n'est pas le processus principal de la phytoremédiation. Dans la part des HAPs enlevés du sol, il y a ceux qui ont été potentiellement transformés voire même complètement dégradés par les plantes. Pour avoir une idée claire sur l'implication des plantes dans les processus de remédiation des HAPs des sols pollués, il serait important de quantifier la partie conjuguée ou métabolisée en procédant à des expérimentations basées sur un marquage au carbone 13, afin d'effectuer un suivi des produits marqués dans la plante. Cette approche compléterait les analyses des HAPs libres dans la biomasse végétale.

Le benzo[b]fluoranthène et le dibenz[a,h]anthracène ne sont pas détectés dans l'ensemble des échantillons. Ce sont deux HMW HAPs, les moins hydrosolubles (Partie 1, Tableau 1) et donc les moins mobiles dans le sol et les moins disponibles pour les plantes. Les valeurs correspondant aux HAPs non détectés ont été majorées au niveau du seuil de détection car, étant donné qu'ils sont présents dans le sol, il est fort possible qu'ils soient dans les plantes en très faibles quantités.

D'autre part, l'acénaphtylène qui n'est pas détecté dans les échantillons de sol est présent dans les plantes, ce qui montre que ce HAP est bien présent dans le sol en très faible quantité. L'acénaphtylène est un HAP à 3 cycles, de faible poids moléculaire et avec une solubilité dans l'eau plutôt élevée pour un HAP (Partie 1, Tableau 1) ce qui le rend facilement disponible pour les plantes. D'autre part, la technique d'analyse utilisée pour les dosages des HAPs dans les végétaux a un seuil de détection beaucoup plus bas que la technique utilisée pour les dosages dans les sols. L'absorption de l'acénaphtylène par les plantes montre que les végétaux sont capables d'éliminer les composés présents de façon résiduelle dans le sol, ce qui peut rendre leur utilisation intéressante pour une « finition » en complément d'autres techniques de dépollution.

En plus des analyses des résultats des HAPs totaux, nous avons réalisé un suivi de chaque molécule séparément. La figure 6 représente la quantité de chaque HAP détecté dans les parties aériennes des trois espèces végétales plantées sur le site pilote.

Malgré le fort écart-type lié à la forte hétérogénéité de la pollution dans le site pilote, on remarque que, globalement la gestion des HAPs, pris un à un, est relativement variable d'une plante à l'autre et d'un traitement à l'autre. Cependant, au moins pour les HAPs les plus fortement accumulés (phénanthrène, fluoranthène et pyrène), les quantités libres dans les espèces ligneuses, à enracinement profond, sont plus importantes dans les plantes contrôles que dans les plantes traitées. Le Buddleja des parcelles non-traitées semblent être la condition pour laquelle la plante stocke le plus de HAPs. Si on met ce résultat en parallèle avec le fait que cette espèce présente une forte mortalité, on peut émettre l'hypothèse que c'est l'absorption des HAPs qui a provoqué la mort de cette espèce. On peut aussi envisager l'idée que le saccharose augmente la tolérance de cette espèce aux HAPs ou bien que le saccharose modifie la population bactérienne au niveau de la rhizosphère, favorisant ainsi la dégradation des polluants et limitant les dégâts qu'ils peuvent causer sur les plantes. Cette hypothèse devrait être validée sur un site pilote pour lequel la pollution est répartie de façon homogène.

Pour une plante à enracinement peu profond comme le miscanthus, cette hypothèse ne semble pas être valide puis qu'elle semble accumuler d'avantage d'HAPs libres dans les plantes traitées que les plantes contrôles, ce qui suggérerait que le miscanthus aurait une gestion cellulaire différente, probablement une compartimentation de ces polluants dans les vacuoles, pour réduire leur toxicité, qui serait liée à une induction de transporteurs non-spécifiques comme c'est la cas pour le blé qui est, comme le miscanthus, une Poacée (Zhan et al., 2010; Zhan et al., 2012). Les résultats d'accumulation des HAPs totaux soutiennent cette hypothèse (Fig. 5). Le miscanthus et les deux espèces d'arbres n'ont pas le même fonctionnement métabolique, en effet, la première espèce est une plante en C4 alors que les deux arbres sont des plantes en C3. Les données bibliographiques disponibles ne montrent pas que les plantes en C4 telles que le miscanthus ont une gestion différente des xénobiotiques de celle des plantes en C3. Vavrek et Campbell (2002) ont essayé de comparer l'efficacité de plantes en C3 et en C4 pour la bioremédiation de produits pétroliers mais ils

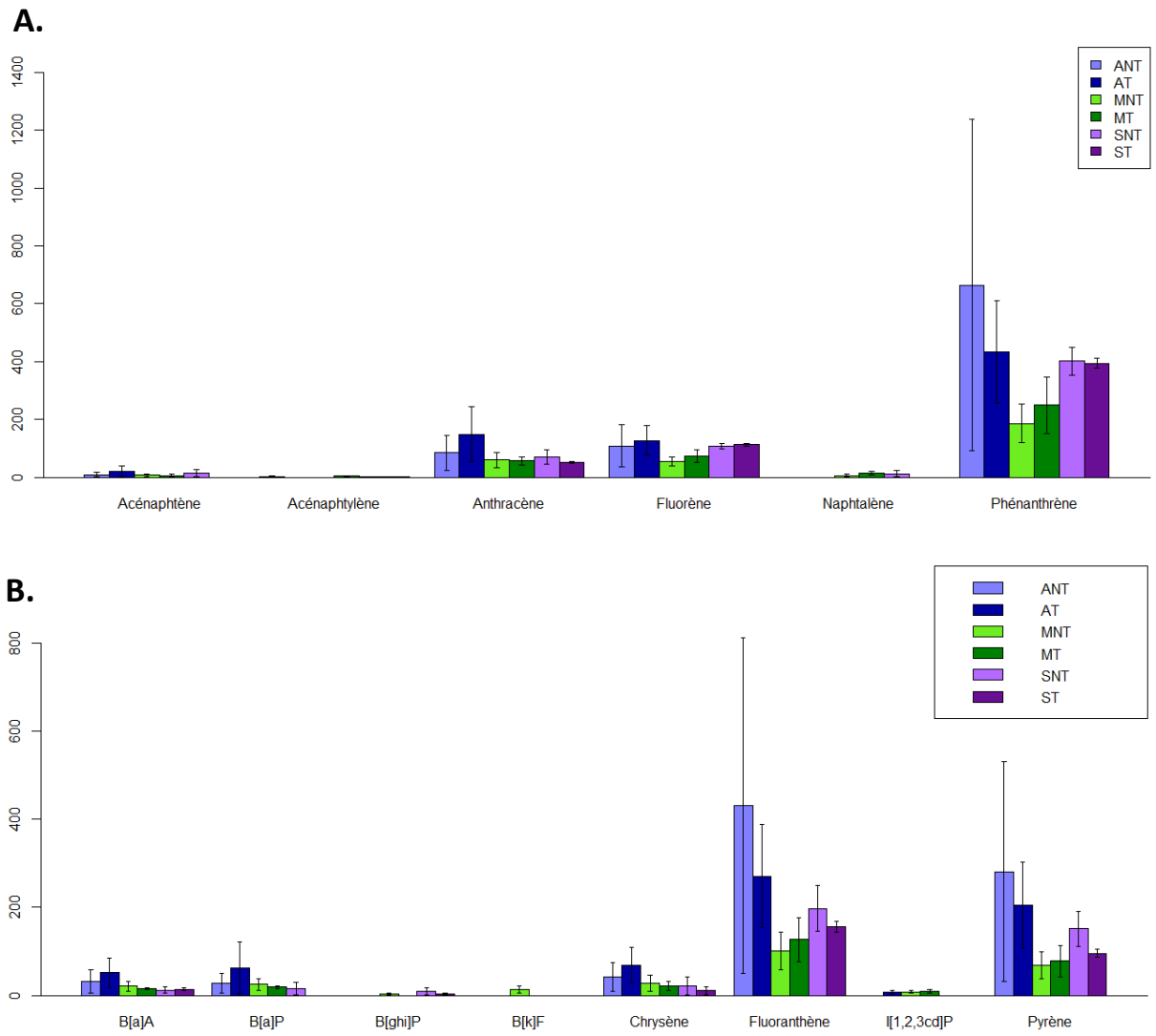


**<u>Figure 6</u> : Répartition des HAPs détectés dans les plantes pour les LMW HAPs (A) et les HMW HAPs (B).**

ANT, Buddleja non traités ; AT, Buddleja traités ; MNT, Miscanthus non traités ; MT, Miscanthus traités ; SNT, Saules non traités ; ST, Saules traités.

B[a]A, Benzo[a]Anthracène ; B[a]P, Benzo[a]Pyrène ; B[ghi]P, Benzo[ghi]Périylène, B[k]F, Benzo[k]Fluoranthène ; I[1,2,3cd]P, Indéno[1,2,3cd]Pyrène.

n'ont pas pu mettre en évidence de différence entre ces deux types de plantes, probablement car l'effet « taille des plantes » était prédominant.

On ne peut cependant pas exclure que des voies de métabolisation pourrait être fonctionnelles et différentes entre ces espèces, chose que nous n'avons pas eu la possibilité de vérifier dans ce travail.

### 3.3. Les HAPs restant dans les sols après 21 mois de traitement

Les dosages de HAPs ont été réalisés sur les 30 premiers centimètres de sol. Afin de représenter une valeur moyenne de la quantité de HAPs de la parcelle, nous avons effectué 5 prélèvements que nous avons regroupés et mélangés avant d'effectuer le dosage. La détoxification naturelle et passive des sols (par atténuation naturelle, volatilisation) n'est pas prise en compte dans nos calculs étant donné que le sol « contrôle » subit lui aussi la même évolution que ceux des parcelles traitées. Pour les échantillons provenant des parcelles ayant reçu un apport de terre végétale, nous avons tenu compte de la dilution d'un facteur 3 qui a été faite lors du prélèvement. En effet, en prélevant les 30 premiers centimètres de sol, nous avons prélevé la couche de 15-20 cm de terre végétale non-polluée qui a été apportée et qui représente les deux tiers de la terre prélevée.

Les résultats présentent une grande hétérogénéité qui n'est pas surprenante étant donnée l'histoire du site. En effet, les zones qui ont été polluées sont locales et donc la teneur en HAPs n'est pas homogène sur l'ensemble des parcelles, d'où l'importance de la randomisation des trois répétitions au cours de cette expérimentation. Dans toutes les conditions, la quantité d'acénaphtylène dans le sol étant en dessous du seuil de détection, la valeur de ce HAP a été majorée au niveau du seuil de détection donné par le laboratoire. Ce HAP, qui est un des plus hydrosolubles, aurait également pu être lessivé et par conséquent se retrouver dans des couches plus profondes ou bien tout simplement ne pas être un déchet de la fabrication des revêtements de la société Axson. Etant donné que ce HAP est présent dans les plantes, cela montre qu'il est présent dans le sol mais dans une quantité inférieure au seuil de détection de la méthode de dosage utilisée. On retrouve ce HAP dans les trois espèces du site pilote que ce soit dans les parcelles traitées et non-traitées.

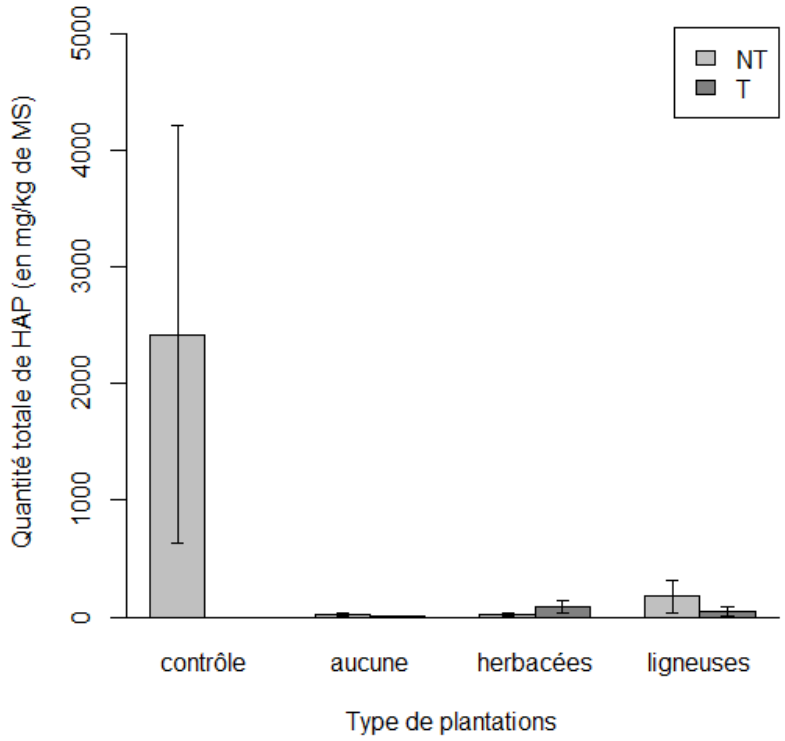


**<u>Figure 7</u> : Quantité totale des 16 HAPs dosés dans les sols pour l'ensemble des conditions étudiées.**

NT représente les parcelles n'ayant pas reçu un apport de saccharose ; T représente les parcelles ayant reçu un apport de saccharose

La quantité totale des 16 HAPs dosés dans les sols diminue de plus de 90% sur cette profondeur entre les différents traitements (apport de saccharose et type de plantation) et les parcelles contrôles (Figure 7). Aucun effet significatif n'a été détecté entre les parcelles ayant reçu un apport de saccharose et celles qui n'en ont pas eu et entre les parcelles plantées et les parcelles non plantées. L'ajout de terre végétale, lors de la mise en place du site pilote, a probablement fortement contribué à la diminution importante de la quantité totale de HAPs dans le sol, quel que soit le type de plantation (plantes herbacées, ligneuses ou aucune). Cette forte diminution des HAPs dans le sol pourrait être expliquée par l'apport de consortiums bactériens et fongiques qui sont naturellement associés au sol végétal et à l'oxygénation du sol après prélèvement du remblai, qui constitue la couche superficielle du sol pilote. En effet, il existe des techniques de dépollution, connues sous le terme de 'landfarming' (Al-Awadhi et al., 1996; Atagana, 2004; Hansen et al., 2004; Maila and Cloete, 2004), qui consistent à composter les terres polluées. Ces techniques sont efficaces, du moins pour les couches superficielles, prises en compte dans cette étude. Ce même résultat, lié à la préparation du sol, a aussi été observé par Techer et al., (2012) lors de leurs essais de phytoremédiation des HAPs en pots. L'effet stimulateur de l'introduction de plantes sur la diminution des HAPs dans le sol est largement décrit (Pradhan et al., 1998; Liste and Alexander, 2000b; Euliss et al., 2008; Técher et al., 2012). Par contre, dans l'ensemble de ces études, les sols plantés ont une diminution de leur teneur en HAPs beaucoup plus importante que les sols non-plantés. L'ensemble de ces études ont été effectuées en conditions semi-contrôlées (en serre, avec des échantillons de sols contaminés) à échelle réduite (petit volume de sol), ce qui pourrait expliquer pourquoi en l'espace de quelques mois (2-13 mois selon l'étude), on observe un effet des plantes. Vervaeke et al. (2003) et Euliss et al. (2008) ont conduit un essai en plein champ et n'ont pas pu mettre en évidence l'effet stimulateur de plantes après plus d'un an d'expérimentation.

Une autre hypothèse expliquant le fait que la quantité de HAPs restant semble supérieure dans les sols plantés que les sols non-plantés est le mécanisme de phytostabilisation. D'ailleurs, la part des HAPs stockée sans transformation par les plantes est très faible ce qui montre que la phytoaccumulation n'est pas le processus principal de la phytoremédiation des HAPs. En effet, dans ce cas, les plantes piègent les molécules au

niveau de leurs racines. Ce processus est plutôt typique de la phytoremédiation des métaux (Pulford and Watson, 2003) et n'a pas été décrit pour les HAPs.

Encore une fois, les résultats présentent un écart-type très élevé à cause l'hétérogénéité du site. En effet, de part son histoire, le site présente une pollution hétérogène sous forme de « pépites », zones dans lesquelles la teneur en HAPs est très élevées. La mise en place du site pilote a été faite de sorte que cette hétérogénéité soit minimisée. Cependant, le nombre de répétitions effectuées s'est avéré insuffisant pour contrebalancer l'hétérogénéité de la répartition de la pollution. De plus, il n'est pas certain qu'au sein d'une même parcelle la pollution soit homogène. C'est pour cela que les prélèvements de sols ont été réalisés à plusieurs endroits de façon aléatoire. Afin d'améliorer les résultats obtenus et d'éviter d'obtenir une telle hétérogénéité dans les mesures effectuées, il paraît nécessaire de multiplier le nombre de répétitions mais aussi d'augmenter le nombre d'échantillons de sol prélevés. *A posteriori*, une homogénéisation du site suite à l'apport de terre végétale par un labour profond et fragmentation du sol (herse etc.) aurait permis une meilleure répartition des polluants sur ce site expérimental.

En ce qui concerne les HAPs qui n'ont pu être détecté dans nos analyses, ni dans les sols, ni dans les plantes, ces résultats peuvent être expliqués par plusieurs processus: leur volatilisation au niveau des feuilles des plantes ou du sol, leur transformation ou même la dégradation par les plantes et/ou les micro-organismes du sol ou leur lessivage et leur non accessibilité par les racines. Des études réalisées, en parallèle par la société Sol-Environnement ont permis de révéler la présence naturelle de bactéries du genre Pseudomonas, capables de dégrader les HAPs, sur le site. L'oxygénation et la richesse de la terre végétale ajoutée au sol du site expérimental a pu favoriser leur croissance et leur activité. D'ailleurs, de nombreux micro-organismes, agissant seuls ou en consortium et vivant dans des sites pollués par les HAPs, ont déjà été identifiés et sont caractérisés par leur capacité à dégrader les HAPs (Cerniglia, 1992; Mrozik et al., 2003; Haritash and Kaushik, 2009).

**<u>Tableau 1</u> : Quantité des HAPs (en ppm) pour chaque condition testée.**
*Chaque résultat représente la moyenne des 3 répétitions.*

| | **Contrôle** | | **Sol nu** | | | | **Miscanthus** | | | | **Arbres** | | | |
|---|---|---|---|---|---|---|---|---|---|---|---|---|---|---|
| | **non traité** | | **non traité** | | **traité** | | **non traité** | | **traité** | | **non traité** | | **traité** | |
| | **Teneur en HAP (ppm)** | ***SD*** | **Teneur en HAP (ppm)** | ***SD*** | **Teneur en HAP (ppm)** | ***SD*** | **Teneur en HAP (ppm)** | ***SD*** | **Teneur en HAP (ppm)** | ***SD*** | **Teneur en HAP (ppm)** | ***SD*** | **Teneur en HAP (ppm)** | ***SD*** |
| Acénaphtylène | 0.15 | *0.00* | 0.16 | *0.00* | 0.15 | *0.00* | 0.15 | *0.00* | 0.15 | *0.00* | 0.15 | *0.00* | 0.15 | *0.00* |
| Fluoranthène | 276.40 | *210.15* | 0.66 | *0.46* | 0.29 | *0.05* | 0.57 | *0.09* | 2.24 | *1.28* | 5.33 | *4.19* | 2.11 | *1.77* |
| Benzo[b]fluoranthène | 247.89 | *172.46* | 0.95 | *0.75* | 0.31 | *0.07* | 0.59 | *0.05* | 4.10 | *2.54* | 8.05 | *5.90* | 2.30 | *1.78* |
| Benzo[k]fluoranthène | 90.20 | *59.69* | 0.40 | *0.24* | 0.15 | *0.00* | 0.22 | *0.03* | 1.62 | *1.05* | 2.67 | *1.89* | 0.81 | *0.57* |
| Benzo[a]pyrène | 217.31 | *148.95* | 0.79 | *0.61* | 0.25 | *0.05* | 0.49 | *0.07* | 3.94 | *2.69* | 6.71 | *4.95* | 1.83 | *1.39* |
| Benzo[ghi]Pérylène | 160.89 | *99.86* | 0.74 | *0.58* | 0.21 | *0.03* | 0.31 | *0.07* | 3.47 | *2.28* | 6.10 | *4.40* | 1.58 | *1.13* |
| Indéno[1,2,3cd]pyrène | 241.55 | *154.79* | 1.00 | *0.84* | 0.15 | *0.00* | 0.15 | *0.00* | 3.96 | *2.25* | 6.39 | *4.92* | 1.80 | *1.31* |
| Anthracène | 217.48 | *198.43* | 0.25 | *0.04* | 0.15 | *0.00* | 2.55 | *2.37* | 0.38 | *0.14* | 3.36 | *3.10* | 0.55 | *0.40* |
| Acénaphtène | 19.86 | *15.85* | 0.16 | *0.00* | 0.15 | *0.00* | 0.15 | *0.00* | 0.20 | *0.05* | 0.40 | *0.25* | 0.18 | *0.03* |
| Chrysène | 228.58 | *157.92* | 0.67 | *0.49* | 0.27 | *0.06* | 0.52 | *0.11* | 2.80 | *1.80* | 5.30 | *4.15* | 1.71 | *1.36* |
| Dibenzo[a,h]anthracène | 41.73 | *35.20* | 0.16 | *0.00* | 0.15 | *0.00* | 0.15 | *0.00* | 0.97 | *0.54* | 1.09 | *0.94* | 0.33 | *0.18* |
| Fluorène | 35.78 | *31.21* | 0.16 | *0.00* | 0.15 | *0.00* | 0.29 | *0.14* | 0.23 | *0.08* | 0.56 | *0.41* | 0.26 | *0.11* |
| Naphtalène | 6.33 | *4.10* | 0.16 | *0.00* | 0.15 | *0.00* | 0.15 | *0.00* | 0.20 | *0.05* | 0.30 | *0.15* | 0.10 | *0.05* |
| Pyrène | 186.01 | *136.35* | 0.60 | *0.43* | 0.22 | *0.04* | 0.47 | *0.11* | 2.25 | *1.39* | 4.50 | *3.42* | 1.76 | *1.45* |
| Phénanthrène | 295.40 | *251.49* | 0.54 | *0.22* | 0.44 | *0.06* | 1.31 | *0.79* | 1.34 | *0.64* | 4.46 | *3.67* | 1.52 | *1.15* |
| Benzo[a]anthracène | 157.39 | *110.92* | 0.43 | *0.27* | 0.17 | *0.01* | 0.30 | *0.07* | 1.79 | *1.14* | 3.22 | *2.50* | 1.15 | *0.91* |
| **total HAPs** | 2422.94 | *1786.53* | 7.79 | *4.88* | 3.37 | *0.27* | 8.38 | *3.49* | 29.63 | *17.84* | 58.60 | *44.82* | 18.14 | *13.48* |

D'autres part, plusieurs études ont montré que, dans le cadre de la phytoremédiation des HAPs, la rhizodégradation, qui combine l'action des plantes et des micro-organismes associés au système racinaire, est un des processus moteur de la détoxification des sols (Muratova et al., 2003; Kuiper et al., 2004; Abhilash et al., 2012).

Pour chacun des HAPs analysés, la quantité dans le sol des parcelles « contrôle » est significativement plus élevée que dans les autres conditions (Tableau 1). Ce résultat n'est pas dû au simple remplacement des 20 premiers centimètres constitué initialement par des gravats, par une épaisseur équivalente en terre végétale puisque les valeurs trouvées ont été corrigées en introduisant le facteur de dilution correspondant à la quantité de sol végétal rajouté ($quantité\ du\ HAP = valeur\ mesurée \times 3$). D'autre part, une attention particulière a été portée sur les méthodes de prélèvement des sols sur le terrain. La figure 8 donne la quantité de chacun des 16 HAPs dosés dans les sols pour chaque condition testée. Ce résultat montre que l'ensemble des traitements effectués (apport de terre végétale, plantations, amendements en saccharose) a permis de faire diminuer significativement la teneur des sols en HAPs.

La grande variabilité des résultats, qui traduit encore une fois très probablement l'hétérogénéité de la pollution sur le site se retrouve aussi lors de l'analyse des HAPs individuellement. La nature des HAPs dans les sols varie en fonction du traitement (type de plantation et apport en saccharose) appliqué. La comparaison du sol nu traité et non-traité nous permet d'évaluer l'effet du saccharose. Pour chaque HAP analysé, la quantité résiduelle dans le sol non traité est plus importante que dans le sol traité: l'apport de saccharose semble donc produire un effet sur le sol permettant une évolution différente des HAPs dans le sol. Le même type de réponse est observé pour les parcelles plantées avec des arbres, de façon plus marquée surtout pour les HMW HAPs. Ce résultat pourrait être dû à plusieurs facteurs :

- un développement plus important des micro-organismes dégradant les HAPs,
- une activité de ces micro-organismes favorisée par l'apport d'une nouvelle source d'énergie.

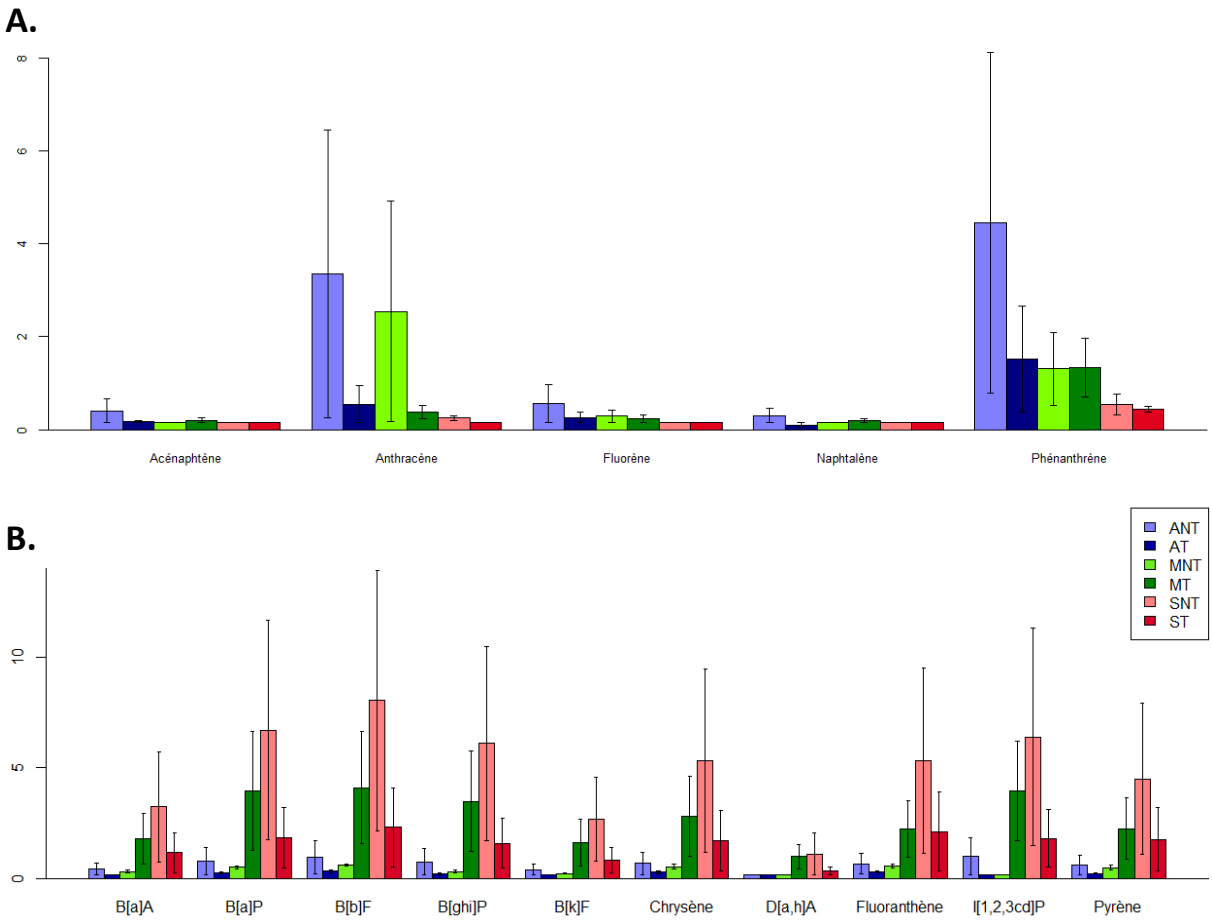


**<u>Figure 8</u> : Quantité de chaque HAP (en mg/kg de MS) détecté dans les sols en distinguant les LMW HAPs (A) et les HMW HAPs (B).**

*ANT, Arbres non traités ; AT, Arbres traités ; MNT, Miscanthus non traités ; MT, Miscanthus traités ; SNT, Sols non traités ; ST, Sols traités. B[a]A, Benzo[a]Anthracène ; B[a]P, Benzo[a]Pyrène ; B[b]F, Benzo[b]Fluoranthène ; B[ghi]P, Benzo[ghi]Périylène ; B[k]F, Benzo[k]Fluoranthène ; D[a,h]A, Dibenzo[a,h]Anthracène ; I[1,2,3cd]P, Indéno[1,2,3cd]Pyrène.*

- une meilleure interaction entre plantes et microorganismes particulièrement au niveau de la rhizosphère,
- à un meilleur développement des plantes et par conséquent une meilleure métabolisation des HAPs.

Par contre, pour le miscanthus, l'effet du saccharose diffère selon le type de HAPs : pour les LMW HAPs (Fig. 8A), le saccharose semble stimuler la disparition de ces HAPs alors que, pour les HMW HAPs (Fig. 8B), le saccharose aurait l'effet inverse et limiterait la disparition de ces HAPs du sol. Des études *in-vitro* ont montré que les exsudats racinaires du miscanthus étaient utilisés comme source d'énergie et de carbone pour le développement de la biomasse bactérienne, induisant ainsi une activité bactérienne plus importante pour la dégradation du phénanthrène et du pyrène. Une analyse de la composition des exsudats racinaires de miscanthus a permis de montrer que ce sont des molécules de la famille des flavonoïdes qui sont responsables de la biostimulation bactérienne (Técher et al., 2011). D'autre part, il est connu que le saccharose est un régulateur de la voie de biosynthèse des flavonoïdes chez les plantes (Solfanelli et al., 2006). L'apport de saccharose aurait donc pu entrainer une production de flavonoïdes qui ont été exsudés par les racines dans la rhizosphère entrainant ainsi la stimulation de l'activité bactérienne au sein des parcelles de miscanthus traitées. De plus, les LMW HAPs sont en général bien plus hydrosolubles que les HMW HAPs, ce qui les rend plus disponibles pour les bactéries qui les dégradent. Les premiers essais de biodégradation des HAPs *in-situ* ont montré que les HMW HAPs sont moins bien dégradés que les LMW HAPs (Wilson and Jones, 1993). Cette différence aurait probablement pu être exacerbée par l'apport de saccharose, en favorisant de façon directe ou indirecte (par les exsudats racinaires du miscanthus) le développement des populations bactériennes dégradant les LMW HAPs qui concurrenceraient les microorganismes dégradant les HMW PAHs.

## 4. Conclusion et perspectives

Le système mis en place lors de cette expérimentation se montre très efficace sur les couches superficielles du sol. En effet, la quantité totale des HAPs diminue largement par rapport à une parcelle non traitée (parcelles « contrôle » du site pilote).

Les dosages des HAPs dans les plantes ont permis de montrer que la phytoaccumulation des HAPs non-transformés semble être un processus mineur de la phytoremédiation des HAPs. Les plantes ne semblent pas absorber l'ensemble des 16 HAPs avec une efficacité équivalente mais sont capables d'absorber certains des LMW et des HMW HAPs.

La différence observée entre les espèces végétales se fait surtout sur la variété des HAPs absorbés et aussi sur la tolérance à ces derniers. Le miscanthus qui absorbe le plus large panel de HAPs est la plante qui a présenté le plus de difficulté à s'implanter. Le *Buddleja* semble être plus sensible car une parcelle entière n'a pas survécu après la première année et cette plante parait absorber légèrement plus de HAPs libres que les autres espèces. Enfin, le saule s'est plus facilement implanté mais semble être un peu moins performant dans sa capacité à absorber/utiliser les HAPs.

Il serait, à ce point de l'étude, intéressant de suivre l'évolution de ces végétaux sur plusieurs années. En effet, on estime que le miscanthus atteint son optimum de production de biomasse après 3 ans de culture et que les arbres ont besoin de plusieurs années afin de bien s'implanter dans le sol. Toutefois, cette expérimentation sur presque 2 ans a permis de montrer les difficultés de mise en place et de gestion d'un site de phytoremédiation.

Les plantes ont aussi permis de révéler la présence d'un HAP qui n'était pas détecté dans le sol car il était probablement en trop faible quantité. Nos résultats montrent le rôle de bio-accumulateur des végétaux, puisqu'ils ont permis de mettre en évidence la présence de molécules indétectables dans le sol, du moins avec les techniques de dosage que nous avons utilisées. Aussi, mêmes si des pollutions ne sont pas détectables dans le sol, elles peuvent se retrouver dans les végétaux qui sont cultivés dans ces sols, soulignant ainsi le rôle important de la qualité des sols agricoles et surtout des agences pour la sécurité alimentaire.

L'apport de terre végétale seule a permis de diminuer fortement la quantité de HAPs dans le sol, ce qui montre l'intérêt de cet apport non seulement pour favoriser l'implantation des végétaux, mais aussi pour apporter de nouveaux micro-organismes dans le sol pollué et oxygéner ce dernier.

L'apport de saccharose a favorisé la diminution des HAPs, notamment les HMW HAPs pour les sols non-plantés et les sols plantés d'arbres, ce qui montre le potentiel de cette technique surtout pour stimuler la bioremédiation de ces HAPs les plus récalcitrants. Toutefois, des études supplémentaires sur le devenir du saccharose dans le sol, l'impact de cet apport sur les micro-organismes et sur la gestion des apports (quantité, forme, fréquence…) paraissent nécessaires afin de comprendre et d'optimiser le système. L'installation d'un tel système de dépollution demande une vigilance constante afin de limiter le stress subit par les végétaux. D'autre part, la répartition de la pollution de façon ponctuelle rend difficiles les comparaisons entre les parcelles. Afin de mieux identifier les performances de chaque condition expérimentale, il serait pertinent de poursuivre l'expérimentation sur plusieurs années, d'analyser les couches de sol les plus profondes, la structure des systèmes racinaires pour chaque espèce végétale et d'étudier les populations microbiennes retrouvées dans chaque condition.

De ces résultats, il ressort que le saccharose modifie le comportement des plantes et probablement des micro-organismes du sol. Suivant le type de plantation (arbres, herbacées ou aucune plantation), l'effet du saccharose est différent, ce qui suggère qu'il existe un effet combiné pour ces deux paramètres : un effet du saccharose, du types de plantations et une interaction entre ces deux paramètres. L'effet entre les espèces végétales peut être de métabolisme primaire entre les plantes en C3 (les arbres) et les plantes en C4 (le miscanthus). Cependant, probablement à cause de l'hétérogénéité du site, il n'a pas été possible de vérifier statistiquement cet effet combiné des deux paramètres (plantation et apport de saccharose). D'autre part, malgré la grande variabilité, globalement, il semble que le miscanthus soit la plante qui a permis de mieux dépolluer le sol. En effet, quelque soit le HAP, sa teneur dans les sols plantés de miscanthus est moins élevée que dans les sols plantés d'arbres.

De nombreuses questions restent en suspens afin de bien déterminer le rôle de chaque paramètre de notre étude : (i) quelle est la quantité de HAPs qui a été métabolisée ou dégradée par les plantes, ii) quel(s) est(sont) le(s) mécanisme(s) prépondérant(s) impliqué(s) dans la gestion des HAPs par les plantes (stabilisation, accumulation sous des formes insolubles, volatilisation) ,(ii) quels rôles jouent les micro-organismes dans nos conditions et quelle est la part des HAPs éliminés par ces dernier dans le sol.

Afin de comprendre comment les plantes gèrent les HAPs, il est nécessaire d'approfondir les données *in-vitro* car, pour le moment, aucun modèle n'a été décrit pour les plantes. Pour l'étude des micro-organismes du sol et de leur rôle, il pourrait être judicieux de faire des analyses de métagénomiques qui permettent d'identifier les différentes populations présentes dans le sol mais aussi de suivre la dynamique de cette population.

**A.**

**B.**

**C.**

**<u>Figure Supplémentaire 1</u>** : Photographies du site avant la mise en place des parcelles expérimentales. (A.) Galette de produit pétrolier à la surface, photographie prise en juin 2010. (B) Zone fortement contaminée appelée « pépite » (entourée en rouge), photographie prise en juin 2010. (C) Vue d'ensemble du site pilote, photographie prise en décembre 2010.

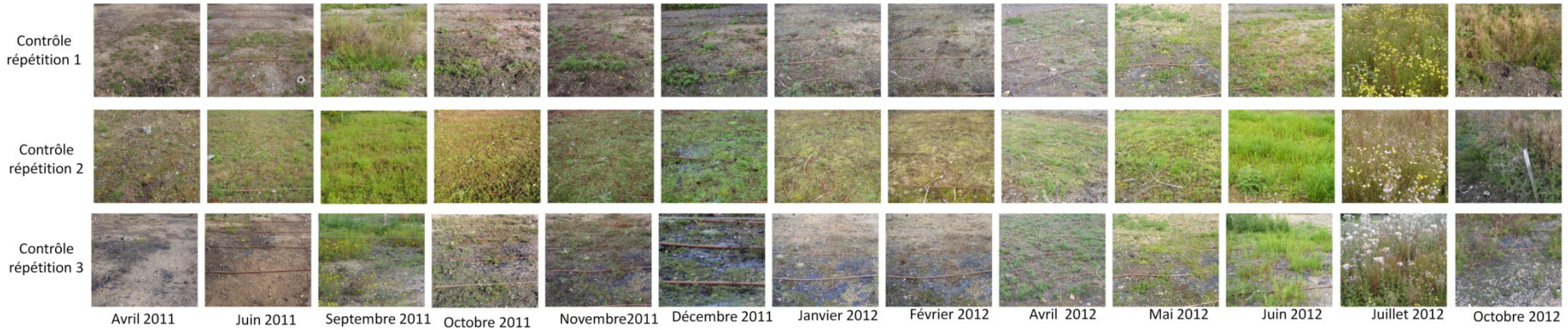


**Figure Ssupplémentaire 2** : Evolution des parcelles au cours de la durée l'expérimentation pour les parcelles contrôles

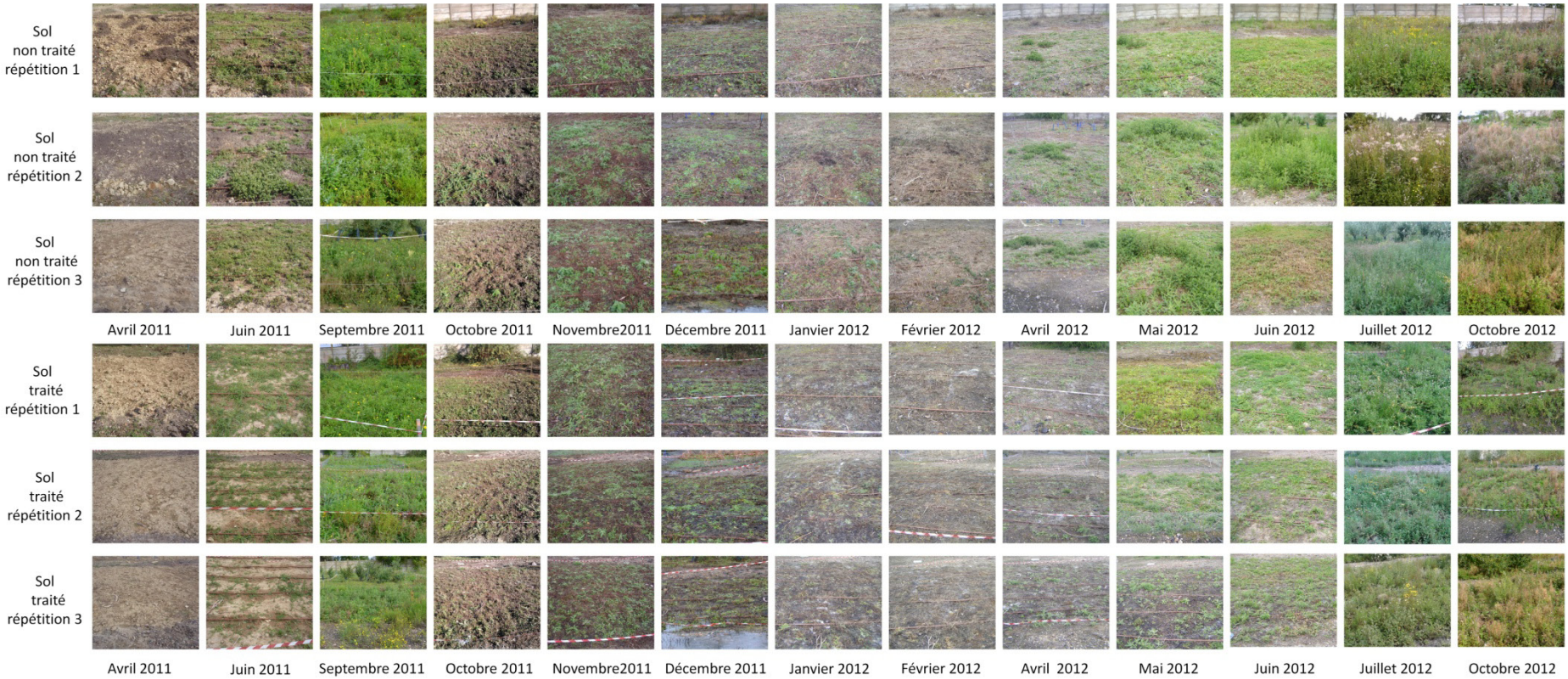


**Figure Supplémentaire 2 (suite)** : Evolution des parcelles au cours de la durée l'expérimentation pour les parcelles non-plantées avec et sans apport de saccharose

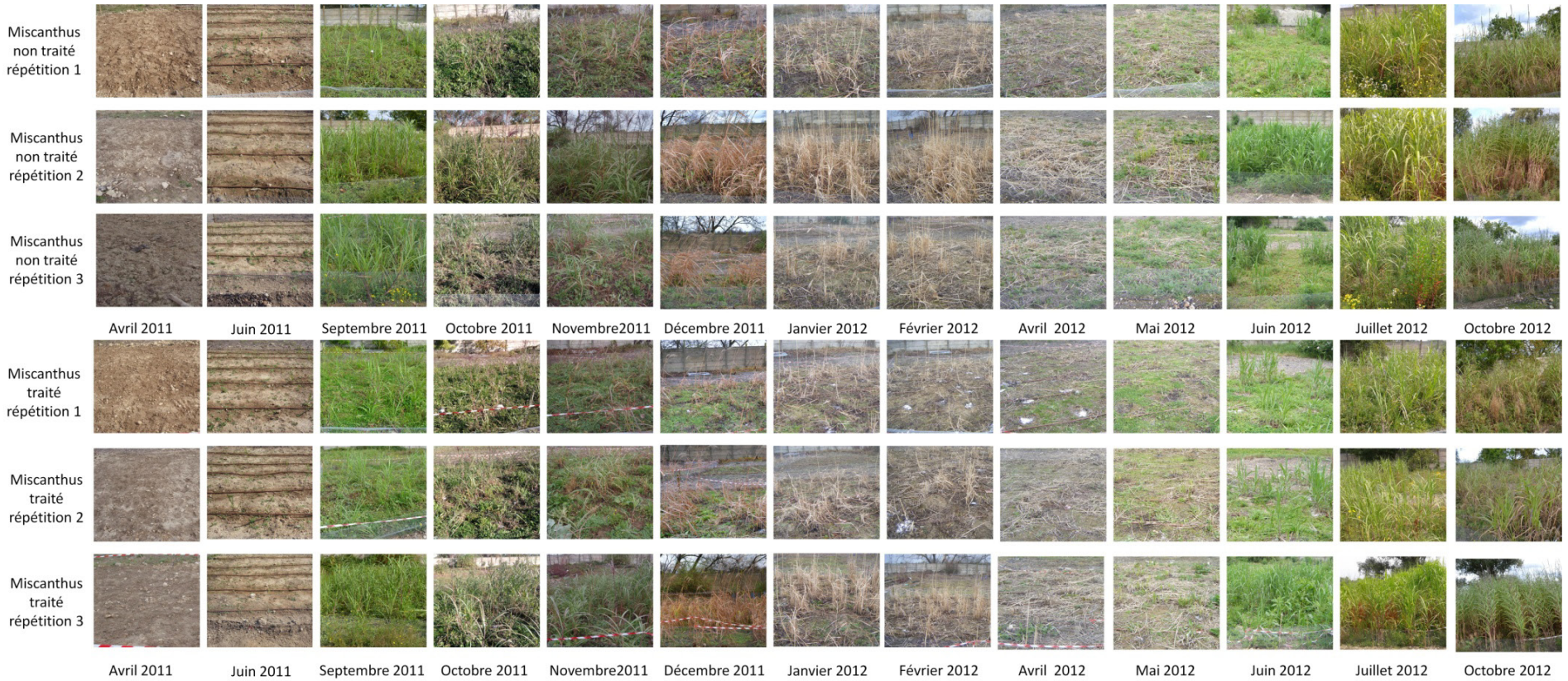


**Figure Supplémentaire 2 (suite)** : Evolution des parcelles au cours de la durée l'expérimentation pour les parcelles plantées avec du miscanthus qui ont reçu ou pas un traitement par apport de saccharose

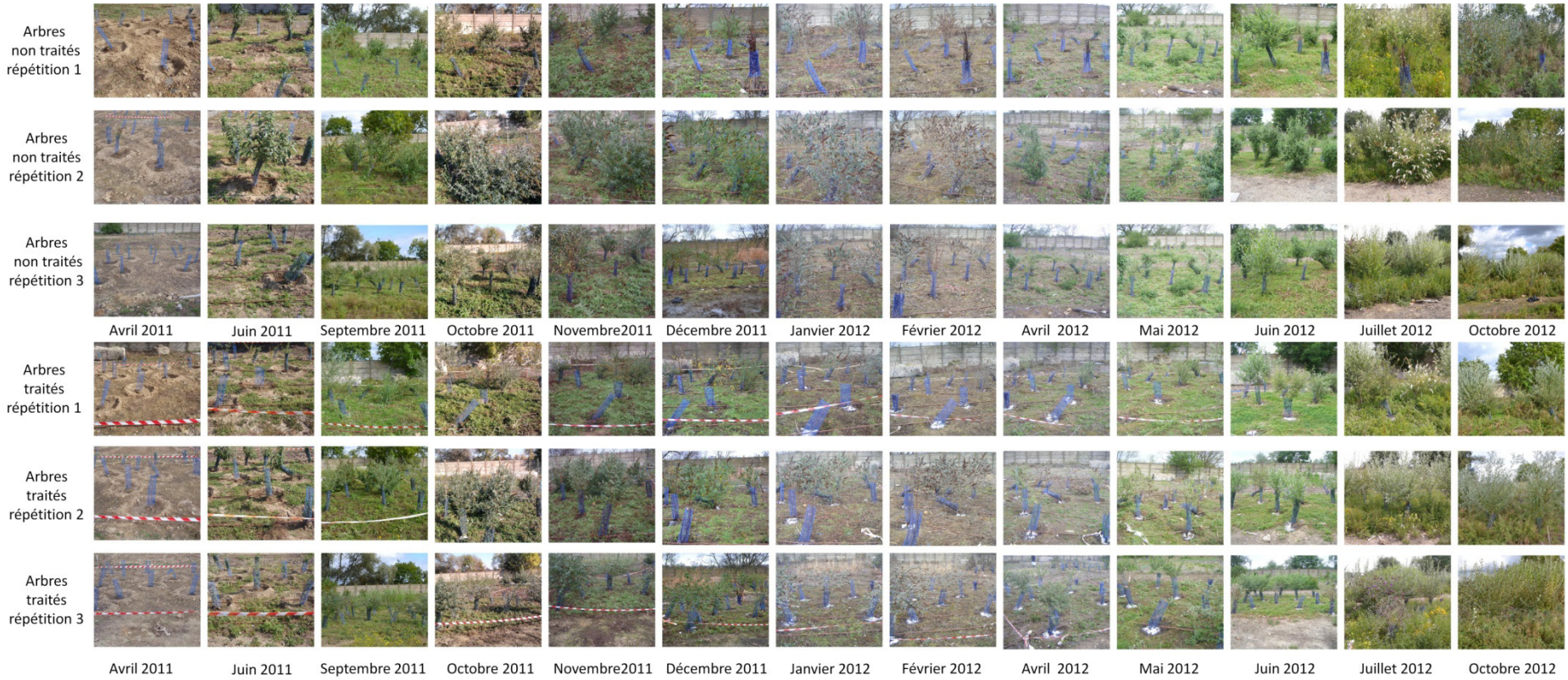


**Figure Supplémentaire 2 (suite)** : Evolution des parcelles au cours de la durée l'expérimentation pour les parcelles plantées avec des arbres (Buddleja et saules) qui ont reçu ou pas un traitement par apport de saccharose

**Figure Supplémentaire 3** : Planche des espèces identifiées sur le site pilote lors du 6ème mois d'expérimentation

| | **Nom** | **Nom commun** | **Famille** |
|---|---|---|---|
| **1** | *Cornus sanguinea* | Cornouiller sanguin | Cornacées |
| **2** | *Circium arvense* | Chardon des vignes | Astéracées |
| **3** | *Hypericum perforatum* | Millepertuis | Hypericacées |
| **4** | *Verbascum nigrum* | Molène noire | Scrophulariacées |
| **5** | *Resda lutea* | Réséda jaune | Résédacées |
| **6** | *Sambucus ebulus* | Sureau hièlbe | Caprifoliacées |
| **7** | *Carex sp* | Carex sp | Cyperacées |
| **8** | nd | nd | Astéracées |

| | **Nom** | **Nom commun** | **Famille** |
|---|---|---|---|
| **9** | *Crataegus monogyna* | Aubépine | Rosacées |
| **10** | *Acer pseudoplatanus* | Erable sycomore | Acéracées |
| **11** | *Rosa canina* | Rosier des chiens | Rosacées |
| **12** | *Geranium molle* | Géranium à feuilles molles | Géraniacées |
| **13** | *Juglans regia* | Noyer commun | Juglandacées |
| **14** | *Acer campestre* | Erable champêtre | Acéracées |
| **15** | *Rumex crispus* | Parelle crépu | Polygonacées |

**Figure Supplémentaire 3 (Suite)** : Planche des espèces identifiées sur le site pilote lors du 6ème mois d'expérimentation

| | Nom | Nom commun | Famille |
|---|---|---|---|
| **16** | *Anagallis arvensis* | Mouron rouge | Primulacées |
| **17** | *Plantago lanceolata* | Plantain lancéolé | Plantaginacées |
| **18** | *Renonculus repens* | Renoncule rampante | Renonculacées |
| **19** | *Calystegia* | Liseron | Convolvulacées |
| **20** | *Veronica persica* | Véronique de Perse | Scrofulariacées |
| **21** | nd | Fenouil/ carotte/ armoise | Apiacées |
| **22** | *Epilobium ciliatum* | Epilobe | Onagracées |
| **23** | *Persicaria maculosa* | Renouée/persicaire | Polygonacées |

| | Nom | Nom commun | Famille |
|---|---|---|---|
| **24** | *Rubus fructicosa* | Ronce | Rosacées |
| **25** | *Circium palustre* | Cirse des marais | Astéracées |
| **26** | *Dipsacus fullonum* | Cardère | Caprifiolacées |
| **27** | *Chenopodium* | nd | Chénopodiacées |
| **28** | *Betulus pendula* | Bouleau | Bétulacées |
| **29** | nd | nd | Poacées |
| **30** | *Juncus effusus* | Jonc épars | Juncacées |
| **31** | *Salix caprea* | Saule marsault | Salicacées |

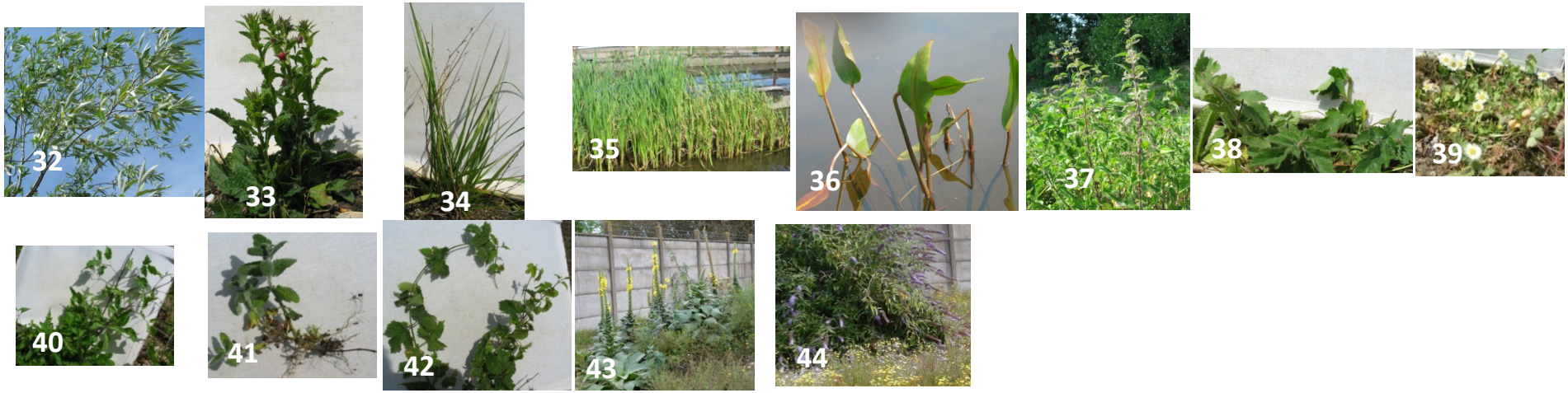


**Figure Supplémentaire 3 (Suite)** : Planche des espèces identifiées sur le site pilote lors du 6ème mois d'expérimentation

| | **Nom** | **Nom commun** | **Famille** |
|---|---|---|---|
| **32** | *Salix fragilis* | Saule fragile | Salicacées |
| **33** | nd | nd | nd |
| **34** | *Carex sp* | Carex sp | Cypéracées |
| **35** | *Typha angustifolia* | Jonc massette | Juncacées |
| **36** | *Persicaria amphibia ou Polyganum amphibium* | Renouée amphibie | Polygonacées |
| **37** | *Urtica dioica* | Ortie | Urticacées |
| **38** | *Heracleum sphondylium* | Berce | Apiacées |

| | **Nom** | **Nom commun** | **Famille** |
|---|---|---|---|
| **39** | *Bellis perennis* | Pâquerette | Astéracées |
| **40** | *Clematis vitalbas* | Clématite sauvage | Renonculacées |
| **41** | *Mentha pulegium* | Menthe pouillot | Lamiacées |
| **42** | *Humulus lupulus* | Houblon | Cannabinacées |
| **43** | *Verbascum thapsus* | Bouillon-blanc | Scrofulariacée |
| **44** | *Buddleja Davidii* | Arbres aux papillons ou *Buddleja* de David | Scrofulariacée |

# Chapitre 5 : Conclusion générale et perspectives

Jusqu'à présent les études *in-vitro* des effets des hydrocarbures aromatiques polycycliques (HAPs) sur le développement des plantes ont été réalisées pour des expositions longues (plusieurs semaines) (Alkio et al., 2005; Liu et al., 2009; Weisman et al., 2010a). Ces études permettent de comprendre les effets du phénanthrène à long terme sur les plantes mais ces effets sont modulés par le vieillissement d'*Arabidopsis* qui est, à ce stade-là, en fin de cycle de croissance. Des travaux plus récents ont mis en évidence la rapidité avec laquelle la plante est capable d'absorber et de modifier sa façon de transporter ce polluant (Zhan et al., 2010; Zhan et al., 2012), soulignant ainsi l'importance des premiers moments de contact entre la plante et le polluant. Il a donc semblé important de comprendre comment la plante était affectée à court terme (en l'espace de quelques heures).

D'autre part, bien que de nombreuses études aient mis en évidence le rôle protecteur des sucres solubles notamment du saccharose en condition de stress abiotique (Sulmon et al., 2004; Sulmon et al., 2007a; Rosa et al., 2009), l'ensemble des études sur les effets du phénanthrène sur *Arabidopsis thaliana* a été réalisé avec des milieux de cultures contenant du saccharose. Ces études ont donc montré un effet du phénanthrène modulé par celui du saccharose. En ayant travaillé avec des milieux sans sucre, l'effet protecteur des sucres en condition de stress abiotique, notamment sur la régulation des gènes de stress oxydant, a été éliminé. Ceci a permis de comprendre le réel impact des HAPs (dans notre cas, le phénanthrène) sur le développement des plantes, et le contrôle transcriptionnel et métabolique.

Les résultats que nous avons obtenus montrent que la réponse de la plante au niveau de l'expression des gènes se décompose en 3 phases : (i) une phase de perception et signalisation qui débute à 30 minutes d'incubation, (ii) une phase intermédiaire de tentative de détoxification entre 4h et 8h de traitement et enfin (iii) une phase tardive durant laquelle on observe un déficit en carbone et une inhibition de la photosynthèse après 8 à 24h de traitement. Le fonctionnement général de la plante est complètement affecté dés 8h et, à partir de 24h, le métabolisme de la plante paraît être complètement désorganisé.

Ces expérimentations ont permis de montrer que l'effet du phénanthrène sur *Arabidopsis thaliana* est très rapide et très drastique. D'autre part, à travers ces expositions

courtes au phénanthrène en absence de sucre dans le milieu de culture, nous avons pu mettre en évidence que le phénanthrène n'est pas seulement responsable d'un stress oxydant mais que ce xénobiotique affecte aussi des fonctions plus essentielles du métabolisme primaire.

Il a paru intéressant à ce stade de voir si l'apport de saccharose permet de compenser ces dommages causés par le phénanthrène.

D'un point de vue physiologique, les plantes sont moins affectées par le phénanthrène en présence de saccharose. Cet effet se retrouve aussi avec le glucose mais à un niveau moindre.

Le saccharose semble temporiser les effets du phénanthrène au niveau métabolique. Il est pris en charge et métabolisé compensant donc l'inhibition de l'activité photosynthétique. D'autre part, le saccharose pris en charge par la plante a aussi une activité régulatrice du métabolisme primaire. L'ajout du saccharose dans le milieu de culture semble limiter les dommages causés par le phénanthrène au niveau du métabolisme primaire.

En condition de stress causé par le phénanthrène, le saccharose semble moduler les gènes de réponse à un stress et stimuler de manière spécifique un groupe de gène du système antioxydant. Des études d'activités d'enzymes antioxydantes, après une exposition à court terme et dans un milieu avec ou sans sucre, permettraient de mieux cerner comment le système antioxydant est gérer dans les deux conditions. D'autre part, en réalisant l'expérience pour différents temps d'incubation comme cela a été réalisé pour l'analyse de l'effet du phénanthrène sur le transcriptome, il serait intéressant de cibler au bout de combien de temps le système antioxydant se met en place.

Cet effet protecteur du saccharose a aussi pu être observé, partiellement, sur le site pilote de phytoremédiation. En effet, les parcelles de Buddleja ayant reçu du saccharose paraissent plus résistantes et ont montré moins de symptômes de toxicité. D'autre part, l'apport de saccharose aurait permis aux plantes de mieux éliminer les HAPs, en particulier les HMW HAPs plus récalcitrants.

D'autre part, le système de détoxification des xénobiotiques décrit par Sandermann (1992) et complété par Edwards (2011) semble pouvoir être transposable aux HAPs. En effet, les familles de gènes impliquées dans ce processus sont fortement exprimées durant la phase intermédiaire pour des temps d'incubation allant de 4 à 8 heures. Ce système de détoxification parait fortement modifié par l'ajout de saccharose. En effet, l'expression de nombreux gènes impliqués dans le « green-liver » est complètement modifiée. Le saccharose semble inhiber fortement des gènes qui étaient stimulés par l'apport de phénanthrène et stimule d'autres gènes qui ne sont pas différentiellement exprimés en présence de phénanthrène. Cela suggère un système de détoxification différent lorsque le saccharose est ajouté au milieu de culture.

Grâce à l'analyse transcriptomique, des gènes potentiellement impliqués dans la détoxification des HAPs ont été identifiés. Des études supplémentaires sur l'activité des enzymes codées par ces gènes permettraient d'identifier celles qui joueraient un rôle direct dans la métabolisation de ces molécules. Un criblage à l'aide d'écotypes d'*Arabidopsis* mutés sur les gènes listés comme appartenant au xénome et étant impliqué dans la réponse aux HAPs permettrait d'identifier les gènes qui confèrent une tolérance aux HAPs. En effet un criblage des cytochromes P450 potentiellement impliqués dans la détoxification des HAPs a été lancé. Une liste de gènes a été identifiée à partir des données de nos analyses transcriptomiques mais aussi des données de Weisman. Cette étude nous permettra d'identifier les écotypes mutés sensibles, et donc de cibler les CYP impliqués directement ou indirectement dans la gestion du phénanthrène. Le mutant transparent testa 7 (tt7) muté au niveau du CYP75B1 présente un phénotype sensible en présence de phénanthrène en comparaison avec des plantes contrôles. Des essais in-vitro n'ont pas pu mettre en évidence une activité hydroxylation de cette enzyme vis-à-vis du phénanthrène. Ces résultats montrent que ce cytochrome semble plutôt exercer une action indirecte.

La spectrométrie par résonnance magnétique nucléaire (RMN) est une stratégie qui permettrait de mieux comprendre comment les plantes métabolisent/ transforment/ conjuguent les HAPs. Cette méthode est utilisée aussi bien pour l'identification de métabolites que pour faire des profils métabolomiques et des dosages de métabolites (Ratcliffe and Shachar-Hill, 2001). Mieux comprendre les processus de détoxification chez les plantes permettrait d'identifier les plantes les plus efficaces pour la phytoremédiation. Afin

de localiser le phénanthrène et ses dérivés dans les cellules végétales nous avons utilisé la technique de NanoSIMS (Multi-isotope imaging mass spectrometry) qui allie la spectrométrie de masse à de l'imagerie permettant ainsi l'identification d'isotopes tels que le carbone 13. Pour cette expérimentation, des plantules d'*Arabidopsis thaliana* ont été incubés dans du phénanthrène C13. L'analyse par NanoSIMS n'a pas permis d'identifier le signal correspondant aux carbones 13 introduits. Ceci est peut-être dû à (i) la technique de préparation des échantillons pas inclusion dans la résine qui aurait éliminé le phénanthrène libre ou (ii) un marquage insuffisant, en dessous du seuil de détection de l'appareil.

D'autre part, l'utilisation de plantes génétiquement modifiées (PGM) est une approche très intéressante d'un point de vue de la stratégie d'amélioration de la phytoremédiation. Des essais de PGM ont été réalisés en insérant un gène fongique de GST chez le tabac, améliorant ainsi l'efficacité de la plante à éliminer le naphtalène (Dixit et al., 2011). Les transporteurs actifs du phénanthrène chez le blé ont été identifiés (Zhan et al., 2010; Zhan et al., 2012). La surexpression des gènes codant pour ces protéines pourrait permettre de les multiplier et donc de stimuler l'absorption du phénanthrène par les plantes. Toutefois cette stratégie reste au stade expérimental suite à la mise en place du principe de précaution interdisant toute exploitation de PGM en condition naturelle en France. De plus, les PGM sont très mal perçues par la population européenne et plus particulièrement française. Toutefois aux Etats-Unis, en Asie et en Amérique du Sud, les PGM sont cultivées ce qui rend leur utilisation possible pour la phytoremédiation.

Enfin, la mise en place du site pilote de phytoremédiation a permis de mettre en évidence l'efficacité d'un tel système et aussi l'importance des pratiques agricoles (aération du sol, apport de terre saine) dans la diminution des taux de HAPs. Toutefois, ce travail de terrain a montré aussi la difficulté de gérer un tel site à cause la répartition hétérogène de la pollution. Toutefois ce site est représentatif des conditions de pollution des sols industriels suite à un déversement de produit ou à une gestion ancienne des déchets.

L'étude du site pilote a permis de montrer le potentiel de la phytoremédiation. En deux ans, la teneur de HAPs a bien diminué sur les 30 premiers centimètres. Il serait intéressant de faire des études complémentaires afin de voir quel système de plantation est le plus efficace sur des profondeurs plus importantes. Parmi les 3 espèces étudiées, chacune

présente des avantages et des inconvénients rendant le choix de l'espèce difficile. Afin d'obtenir le meilleur résultat, il paraît important de poursuivre l'expérimentation sur 5-10 ans afin que les plantes atteignent leur maximum de potentiel de croissance (après 3 ans pour le miscanthus, après 5 ans pour le saule par exemple) et donc soient les plus efficaces possibles dans l'élimination des HAPs du sol. De plus les conditions environnementales (arrosage, type de sol, climat…) sont déterminantes à la fois pour le choix de l'espèce et pour la mise en place du site de phytoremédiation.

Le rôle des microorganismes du sol dans la phytoremédiation du sol n'est pas à négliger. Les parcelles non-plantées ayant reçu un apport de terre végétale et donc une nouvelle population microbienne ont montré une forte diminution de leur teneur en HAPs. Il serait aussi donc intéressant d'évaluer la population microbienne du sol afin de voir comment l'apport de terre végétale mais aussi les différentes espèces végétales modifient la composition de cette population.

D'autre part, le saccharose est aussi une source de carbone pour les microorganismes et l'apport de cette molécule a probablement modifié la composition microbienne du sol en favorisant le développement ou l'activité de certaines souches.

De plus, il me parait important avant de généraliser l'application du saccharose comme amendement favorisant la phytoremédiation des HAPs d'étudier son devenir dans le sol afin d'ajuster la dose appliquée et de voir son impact sur la qualité du sol. Cependant, afin de rester dans le cadre du développement durable, il serait intéressant de voir si le même effet protecteur est obtenu en épandant des déchets issus de l'industrie sucrière comme de la mélasse ou des pulpes de betterave, permettant ainsi de valoriser les déchets de l'industrie sucrière et de ne plus utiliser des sucres raffinés destinés à l'alimentation humaine.

# Bibliographie

**Abhilash PC, Powell JR, Singh HB, Singh BK** (2012) Plant–microbe interactions: novel applications for exploitation in multipurpose remediation technologies. Trends Biotechnol **30**: 416–420

**Abramoff MD, Magalhães PJ, Ram SJ** (2004) Image processing with ImageJ. Biophotonics Int **11**: 36–42

**ADEME** (2011) Taux d'utilisation et couts des différentes techniques et filières de traitement des sols et des eaux souterraines polluées en France-Données 2008.

**Al-Awadhi N, Al-Daher R, EINawawy A, Salba MT** (1996) Bioremediation of oil-contaminated soil in Kuwait. I. landfarming to remediate oil-contaminated soil. J Soil Contam **5**: 243–260

**Alena Torres Netto EC** (2005) Photosynthetic pigments, nitrogen, chlorophyll a fluorescence and SPAD-502 readings in coffee leaves. Sci Hortic 199–209

**Alkio M, Tabuchi TM, Wang X, Colón-Carmona A** (2005) Stress responses to polycyclic aromatic hydrocarbons in *Arabidopsis* include growth inhibition and hypersensitive response-like symptoms. J Exp Bot **56**: 2983–2994

**Alkorta I, Garbisu C** (2001) Phytoremediation of organic contaminants in soils. Bioresour Technol **79**: 273–276

**Andersson BE, Henrysson T** (1996) Accumulation and degradation of dead-end metabolites during treatment of soil contaminated with polycyclic aromatic hydrocarbons with five strains of white-rot fungi. Appl Microbiol Biotechnol **46**: 647–652

**Andersson BE, Lundstedt S, Tornberg K, Schnürer Y, Öberg LG, Mattiasson B** (2003) Incomplete degradation of polycyclic aromatic hydrocarbons in soil inoculated with wood-rotting fungi and their effect on the indigenous soil bacteria. Environ Toxicol Chem **22**: 1238–1243

**Antizar-Ladislao, B., Lopez-Real, J. and Beck, A.** (2004) Bioremediation of Polycyclic Aromatic Hydrocarbon (PAH)-Contaminated Waste Using Composting Approaches. *Critical Reviews in Environmental Science and Technology*, **34**, 249–289.

**Armstrong B, Hutchinson E, Unwin J, Fletcher T** (2004) Lung Cancer Risk after Exposure to Polycyclic Aromatic Hydrocarbons: A Review and Meta-Analysis. Environ Health Perspect **112**: 970–978

**Ashraf M, Foolad MR** (2007) Roles of glycine betaine and proline in improving plant abiotic stress resistance. Environ Exp Bot **59**: 206–216

**Atagana HI** (2004) Bioremediation of creosote-contaminated soil in South Africa by landfarming. J Appl Microbiol **96**: 510–520

**Bae J-W, Park Y-H** (2006) Homogeneous versus heterogeneous probes for microbial ecological microarrays. Trends Biotechnol **24**: 318–323

**Baerson SR, Sánchez-Moreiras A, Pedrol-Bonjoch N, Schulz M, Kagan IA, Agarwal AK, Reigosa MJ, Duke SO** (2005) Detoxification and Transcriptome Response in *Arabidopsis* Seedlings Exposed to the Allelochemical Benzoxazolin-2(3H)-one. J Biol Chem **280**: 21867–21881

**Bak S, Beisson F, Bishop G, Hamberger B, Höfer R, Paquette S, Werck-Reichhart D** (2011) Cytochromes P450. Arab Book e0144

**Balabanič D, Rupnik M, Klemenčič AK** (2011) Negative impact of endocrine-disrupting compounds on human reproductive health. Reprod Fertil Dev **23**: 403–416

**Banks MK, Kulakow P, Schwab AP, Chen Z, Rathbone K** (2003) Degradation of crude oil in the rhizosphere of Sorghum bicolor. Int J Phytoremediation **5**: 225–234

**Barker L, Kühn C, Weise A, Schulz A, Gebhardt C, Hirner B, Hellmann H, Schulze W, Ward JM, Frommer WB** (2000) SUT2, a Putative Sucrose Sensor in Sieve Elements. Plant Cell Online **12**: 1153–1164

**Bezalel L, Hadar Y, Cerniglia CE** (1996a) Mineralization of Polycyclic Aromatic Hydrocarbons by the White Rot Fungus Pleurotus ostreatus. Appl Environ Microbiol **62**: 292–295

**Bezalel L, Hadar Y, Cerniglia CE** (1997) Enzymatic Mechanisms Involved in Phenanthrene Degradation by the White Rot Fungus Pleurotus ostreatus. Appl Environ Microbiol **63**: 2495–2501

**Bezalel L, Hadar Y, Fu PP, Freeman JP, Cerniglia CE** (1996b) Metabolism of phenanthrene by the white rot fungus Pleurotus ostreatus. Appl Environ Microbiol **62**: 2547–2553

**Bhargava A, Carmona FF, Bhargava M, Srivastava S** (2012) Approaches for enhanced phytoextraction of heavy metals. J Environ Manage **105**: 103–120

**Bilgin DD, Zavala JA, Zhu J, Clough SJ, Ort DR, DeLUCIA EH** (2010) Biotic stress globally downregulates photosynthesis genes. Plant Cell Environ **33**: 1597–1613

**Bizub D, Wood AW, Skalka AM** (1986) Mutagenesis of the Ha-ras oncogene in mouse skin tumors induced by polycyclic aromatic hydrocarbons. Proc Natl Acad Sci **83**: 6048–6052

**Bjoerseth A** (1983) Handbook of polycyclic aromatic hydrocarbons. Marcel Dekker,New York, NY

**Boffetta P, Jourenkova N, Gustavsson P** (1997) Cancer risk from occupational and environmental exposure to polycyclic aromatic hydrocarbons. Cancer Causes Control **8**: 444–472

**Bolouri-Moghaddam MR, Le Roy K, Xiang L, Rolland F, Van den Ende W** (2010) Sugar signalling and antioxidant network connections in plant cells. FEBS J **277**: 2022–2037

**Bonassi S, Mfrlo F, Pearce N, Puntoni R** (1989) Bladder cancer and occupational exposure to polycyclic aromatic hydrocarbons. Int J Cancer **44**: 648–651

**Boonchan S, Britz ML, Stanley GA** (2000) Degradation and Mineralization of High-Molecular-Weight Polycyclic Aromatic Hydrocarbons by Defined Fungal-Bacterial Cocultures. Appl Environ Microbiol **66**: 1007–1019

**Borsani O, Valpuesta V, Botella MA** (2001) Evidence for a Role of Salicylic Acid in the Oxidative Damage Generated by NaCl and Osmotic Stress in *Arabidopsis* Seedlings. Plant Physiol **126**: 1024–1030

**Boyes DC, Zayed AM, Ascenzi R, McCaskill AJ, Hoffman NE, Davis KR, Görlach J** (2001) Growth stage-based phenotypic analysis of Arabidopsis: a model for high throughput functional genomics in plants. Plant Cell **13**: 1499–1510

**Brazier-Hicks M, Offen WA, Gershater MC, Revett TJ, Lim E-K, Bowles DJ, Davies GJ, Edwards R** (2007) Characterization and engineering of the bifunctional N- and O-glucosyltransferase involved in xenobiotic metabolism in plants. Proc Natl Acad Sci **104**: 20238–20243

**Brennerova MV, Josefiova J, Brenner V, Pieper DH, Junca H** (2009) Metagenomics reveals diversity and abundance of meta-cleavage pathways in microbial communities from soil highly contaminated with jet fuel under air-sparging bioremediation. Environ Microbiol **11**: 2216–2227

**Callén MS, López JM, Iturmendi A, Mastral AM** (2012) Nature and sources of particle associated polycyclic aromatic hydrocarbons (PAH) in the atmospheric environment of an urban area. Environ Pollut Barking Essex 1987. doi: 10.1016/j.envpol.2012.11.009

**Carillo P, Grazia M, Pontecorvo G, Fuggi A, Woodrow P** (2011) Salinity Stress and Salt Tolerance. Abiotic Stress Plants - Mech. Adapt.

**Cerniglia CE** (1997) Fungal metabolism of polycyclic aromatic hydrocarbons: past, present and future applications in bioremediation. J Ind Microbiol Biotechnol **19**: 324–333

**Cerniglia CE** (1992) Biodegradation of polycyclic aromatic hydrocarbons. Biodegradation **3**: 351–368

**Cerniglia CE, Baalen CV, Gibson DT** (1980) Metabolism of Naphthalene by the Cyanobacterium Oscillatoria sp., Strain JCM. J Gen Microbiol **116**: 485–494

**Chambre d'Agriculture de Picardie** (2010) Fiche technique du miscanthus. http://www.chambres-agriculture-picardie.fr/no_cache/productions/energie-biomasse/cultures-biomasse/miscanthus.html?access=tlbxaaofywzjsdi&print=1

**Cheema SA, Imran Khan M, Shen C, Tang X, Farooq M, Chen L, Zhang C, Chen Y** (2010) Degradation of phenanthrene and pyrene in spiked soils by single and combined plants cultivation. J Hazard Mater **177**: 384–389

**Cheng CL, Acedo GN, Cristinsin M, Conkling MA** (1992) Sucrose mimics the light induction of *Arabidopsis* nitrate reductase gene transcription. Proc Natl Acad Sci **89**: 1861–1864

**Chiou TJ, Bush DR** (1998) Sucrose is a signal molecule in assimilate partitioning. Proc Natl Acad Sci U S A **95**: 4784–4788

**Chitwood DH, Guo M, Nogueira FTS, Timmermans MCP** (2007) Establishing leaf polarity: the role of small RNAs and positional signals in the shoot apex. Dev Camb Engl **134**: 813–823

**Choi YE, Harada E, Wada M, Tsuboi H, Morita Y, Kusano T, Sano H** (2001) Detoxification of cadmium in tobacco plants: formation and active excretion of crystals containing cadmium and calcium through trichomes. Planta **213**: 45–50

**Choudhury S, Panda P, Sahoo L, Panda SK** (2013) Reactive oxygen species signaling in plants under abiotic stress. Plant Signal. Behav. 8:

**Clavel J, Mandereau L, Limasset J-C, Hémon D, Cordier S** (1994) Occupational Exposure to Polycyclic Aromatic Hydrocarbons and the Risk of Bladder Cancer: A French Case-Control Study. Int J Epidemiol **23**: 1145–1153

**Coleman J, Blake-Kalff M, Davies E** (1997) Detoxification of xenobiotics by plants: chemical modification and vacuolar compartmentation. Trends Plant Sci **2**: 144–151

**Coruzzi GM, Zhou L** (2001) Carbon and nitrogen sensing and signaling in plants: emerging "matrix effects."Curr Opin Plant Biol **4**: 247 – 253

**Couée I, Sulmon C, Gouesbet G, Amrani AE** (2006) Involvement of soluble sugars in reactive oxygen species balance and responses to oxidative stress in plants. J Exp Bot **57**: 449–459

**Cowdrey AE** (1975) Pioneering Environmental Law: The Army Corps of Engineers and the Refuse Act. Pac Hist Rev **44**: 331–349

**Crowe ML, Serizet C, Thareau V, Aubourg S, Rouze P, Hilson P, Beynon J, Weisbeek P, van Hummelen P, Reymond P, et al** (2003) CATMA: a complete *Arabidopsis* GST database. Nucleic Acids Res **31**: 156–158

**Cunningham SD, Berti WR, Huang JW** (1995) Phytoremediation of contaminated soils. Trends Biotechnol **13**: 393–397

**Dabestani R, Ivanov IN** (1999) A Compilation of Physical, Spectroscopic and Photophysical Properties of Polycyclic Aromatic Hydrocarbons. Photochem Photobiol **70**: 10–34

**Dai C, Tian L, Zhao Y, Chen Y, Xie H** (2010) Degradation of phenanthrene by the endophytic fungus Ceratobasidum stevensii found in Bischofia polycarpa. Biodegradation **21**: 245–255

**Dejmek J, Solanský I, Benes I, Lenícek J, Srám RJ** (2000) The impact of polycyclic aromatic hydrocarbons and fine particles on pregnancy outcome. Environ Health Perspect **108**: 1159–1164

**Deng WL, Preston G, Collmer A, Chang CJ, Huang HC** (1998) Characterization of the hrpC and hrpRS operons of Pseudomonas syringae pathovars syringae, tomato, and

glycinea and analysis of the ability of hrpF, hrpG, hrcC, hrpT, and hrpV mutants to elicit the hypersensitive response and disease in plants. J Bacteriol **180**: 4523–4531

**Derudi M, Venturini G, Lombardi G, Nano G, Rota R** (2007) Biodegradation combined with ozone for the remediation of contaminated soils. Eur J Soil Biol **43**: 297–303

**Desai C, Pathak H, Madamwar D** (2010) Advances in molecular and "-omics" technologies to gauge microbial communities and bioremediation at xenobiotic/anthropogen contaminated sites. Bioresour Technol **101**: 1558–1569

**Dixit P, Mukherjee PK, Sherkhane PD, Kale SP, Eapen S** (2011) Enhanced tolerance and remediation of anthracene by transgenic tobacco plants expressing a fungal glutathione transferase gene. J Hazard Mater **192**: 270–276

**Dixon DP, Edwards R** (2010) Glutathione Transferases. Arab Book Am Soc Plant Biol. doi: 10.1199/tab.0131

**Domínguez-Solís JR, López-Martín MC, Ager FJ, Ynsa MD, Romero LC, Gotor C** (2004) Increased cysteine availability is essential for cadmium tolerance and accumulation in *Arabidopsis thaliana*. Plant Biotechnol J **2**: 469–476

**Doty SL** (2008) Enhancing phytoremediation through the use of transgenics and endophytes. New Phytol **179**: 318–333

**Dubey RS, Singh AK** (1999) Salinity Induces Accumulation of Soluble Sugars and Alters the Activity of Sugar Metabolising Enzymes in Rice Plants. Biol Plant **42**: 233–239

**Edema CU, Idu TE, Edema MO** (2011) Remediation of soil contaminated with polycyclic aromatic hydrocarbons from crude oil. Afr J Biotechnol **10**: 1146–1149

**Edwards R, Brazier-Hicks M, Dixon DP, Cummins I** (2005) Chemical Manipulation of Antioxidant Defences in Plants. *In* J. A. Callow, ed, Adv. Bot. Res. Academic Press, pp 1–32

**Edwards R, Dixon DP, Cummins I, Brazier-Hicks M, Skipsey M** (2011a) New Perspectives on the Metabolism and Detoxification of Synthetic Compounds in Plants. *In* P Schröder, CD Collins, eds, Org. Xenobiotics Plants. Springer Netherlands, pp 125–148

**Edwards R, Dixon DP, Cummins I, Brazier-Hicks M, Skipsey M** (2011b) New Perspectives on the Metabolism and Detoxification of Synthetic Compounds in Plants. *In* P Schröder, CD Collins, eds, Org. Xenobiotics Plants. Springer Netherlands, pp 125–148

**EEA** (2011a) Overview of economic activities causing soil contamination in some WCE and SEE countries (pct. of investigated sites) — European Environment Agency (EEA). http://www.eea.europa.eu/data-and-maps/figures/overview-of-economic-activities-causing-soil-contamination-in-some-wce-and-see-countries-pct-of-investigated-sites

**EEA** (2011b) Overview of contaminants affecting soil and groundwater in Europe — European Environment Agency (EEA). http://www.eea.europa.eu/data-and-maps/figures/overview-of-contaminants-affecting-soil-and-groundwater-in-europe

**Ellis MH, Dennis ES, Peacock WJ** (1999) *Arabidopsis* roots and shoots have different mechanisms for hypoxic stress tolerance. Plant Physiol **119**: 57–64

**Ende WV den, Peshev D** (2013) Sugars as Antioxidants in Plants. *In* N Tuteja, SS Gill, eds, Crop Improv. Adverse Cond. Springer New York, pp 285–307

**Ende WV den, Valluru R** (2009) Sucrose, sucrosyl oligosaccharides, and oxidative stress: scavenging and salvaging? J Exp Bot **60**: 9–18

**EPA** (1996) Superfund today- Focus on cleanup cost.

**Escalante-Espinosa E, Gallegos-Martínez ME, Favela-Torres E, Gutiérrez-Rojas M** (2005) Improvement of the hydrocarbon phytoremediation rate by Cyperus laxus Lam. inoculated with a microbial consortium in a model system. Chemosphere **59**: 405–413

**Euliss K, Ho C, Schwab AP, Rock S, Banks MK** (2008) Greenhouse and field assessment of phytoremediation for petroleum contaminants in a riparian zone. Bioresour Technol **99**: 1961–1971

**Farrar J, Pollock C, Gallagher J** (2000) Sucrose and the integration of metabolism in vascular plants. Plant Sci **154**: 1–11

**Ford C, Wilson J** (1981) Changes in Levels of Solutes During Osmotic Adjustment to Water Stress in Leaves of Four Tropical Pasture Species. Funct Plant Biol **8**: 77–91

**Foyer CH, Noctor G** (2005) Oxidant and antioxidant signalling in plants: a re-evaluation of the concept of oxidative stress in a physiological context. Plant Cell Environ **28**: 1056–1071

**Foyer CH, Noctor G** (2011) Ascorbate and Glutathione: The Heart of the Redox Hub. Plant Physiol **155**: 2–18

**FRTR** (2002) Remediation Technologies Screening Matrix and Reference Guide, Version 4.0. US Army and EPA, USA

**Furuno S, Foss S, Wild E, Jones KC, Semple KT, Harms H, Wick LY** (2012) Mycelia Promote Active Transport and Spatial Dispersion of Polycyclic Aromatic Hydrocarbons. Environ Sci Technol **46**: 5463–5470

**Furuno S, Päzolt K, Rabe C, Neu TR, Harms H, Wick LY** (2010) Fungal mycelia allow chemotactic dispersal of polycyclic aromatic hydrocarbon-degrading bacteria in water-unsaturated systems. Environ Microbiol **12**: 1391–1398

**Gagnot S, Tamby J-P, Martin-Magniette M-L, Bitton F, Taconnat L, Balzergue S, Aubourg S, Renou J-P, Lecharny A, Brunaud V** (2008) CATdb: a public access to *Arabidopsis* transcriptome data from the URGV-CATMA platform. Nucleic Acids Res **36**: D986–D990

**Galili G** (1995) Regulation of Lysine and Threonine Synthesis. Plant Cell **7**: 899–906

**Gammon MD, Santella RM** (2008) PAH, genetic susceptibility and breast cancer risk: an update from the Long Island Breast Cancer Study Project. Eur J Cancer Oxf Engl 1990 **44**: 636–640

**Gan S, Lau EV, Ng HK** (2009) Remediation of soils contaminated with polycyclic aromatic hydrocarbons (PAHs). J Hazard Mater **172**: 532–549

**Gawronski S, Gawronska H** (2007) PLANT TAXONOMY FOR PHYTOREMEDIATION. *In* N Marmiroli, B Samotokin, M Marmiroli, eds, Adv. Sci. Technol. Biol. Decontam. Sites Affect. Chem. Radiol. Nucl. Agents. Springer Netherlands, pp 79–88

**Ge Y, Dudoit S, Speed TP** (2003) Resampling-based multiple testing for microarray data analysis. Test **12**: 1–77

**Gerhardt KE, Huang X-D, Glick BR, Greenberg BM** (2009) Phytoremediation and rhizoremediation of organic soil contaminants: Potential and challenges. Plant Sci **176**: 20–30

**Germaine KJ, Keogh E, Ryan D, Dowling DN** (2009) Bacterial endophyte-mediated naphthalene phytoprotection and phytoremediation. FEMS Microbiol Lett **296**: 226–234

**Ghanem A, D'Orazio V, Senesi N** (2013) Effects of Compost Addition on Pyrene Removal from Soil Cultivated with Three Selected Plant Species. CLEAN – Soil Air Water n/a–n/a

**Ghosh M, Singh SP** (2005) A Review on Phytoremediation of Heavy Metals and Utilization of It's by Products. Appl Ecol Environ Res **3**: 1–18

**Giddings B, Hopwood B, O'Brien G** (2002) Environment, economy and society: fitting them together into sustainable development. Sustain Dev **10**: 187–196

**Gill PK, Sharma AD, Singh P, Bhullar SS** (2003) Changes in germination, growth and soluble sugar contents of Sorghum bicolor (L.) Moench seeds under various abiotic stresses. Plant Growth Regul **40**: 157–162

**Göhre V, Jones AME, Sklenář J, Robatzek S, Weber APM** (2012) Molecular crosstalk between PAMP-triggered immunity and photosynthesis. Mol Plant-Microbe Interactions MPMI **25**: 1083–1092

**Gonzali S, Loreti E, Solfanelli C, Novi G, Alpi A, Perata P** (2006) Identification of sugar-modulated genes and evidence for in vivo sugar sensing in Arabidopsis. J Plant Res **119**: 115–123

**Goodwin S, Sutter T** (2009) Microarray analysis of <i>Arabidopsis</i> genome response to aluminum stress. Biol Plant **53**: 85–99

**Guazzaroni M-E, Herbst F-A, Lores I, Tamames J, Peláez AI, López-Cortés N, Alcaide M, Del Pozo MV, Vieites JM, von Bergen M, et al** (2013) Metaproteogenomic insights beyond bacterial response to naphthalene exposure and bio-stimulation. ISME J **7**: 122–136

**Guo W-J, Bundithya W, Goldsbrough PB** (2003) Characterization of the *Arabidopsis* metallothionein gene family: tissue-specific expression and induction during senescence and in response to copper. New Phytol **159**: 369–381

**Gupta AK, Kaur N** (2005) Sugar signalling and gene expression in relation to carbohydrate metabolism under abiotic stresses in plants. J Biosci **30**: 761–776

**Gutiérrez-Alcalá G, Gotor C, Meyer AJ, Fricker M, Vega JM, Romero LC** (2000) Glutathione biosynthesis in *Arabidopsis* trichome cells. Proc Natl Acad Sci **97**: 11108–11113

**Guy CL, Huber JLA, Huber SC** (1992) Sucrose Phosphate Synthase and Sucrose Accumulation at Low Temperature. Plant Physiol **100**: 502–508

**Hansen LD, Nestler C, Ringelberg D, Bajpai R** (2004) Extended bioremediation of PAH/PCP contaminated soils from the POPILE wood treatment facility. Chemosphere **54**: 1481–1493

**Haritash AK, Kaushik CP** (2009) Biodegradation aspects of Polycyclic Aromatic Hydrocarbons (PAHs): A review. J Hazard Mater **169**: 1–15

**Harms H, Schlosser D, Wick LY** (2011) Untapped potential: exploiting fungi in bioremediation of hazardous chemicals. Nat Rev Microbiol **9**: 177–192

**Henner P, Schiavon M, Morel J-L, Lichtfouse E** (1997) Polycyclic aromatic hydrocarbon (PAH) occurrence and remediation methods. Analusis **25**: M56–M59

**Herbette S, Taconnat L, Hugouvieux V, Piette L, Magniette M-LM, Cuine S, Auroy P, Richaud P, Forestier C, Bourguignon J, et al** (2006) Genome-wide transcriptome profiling of the early cadmium response of *Arabidopsis* roots and shoots. Biochimie **88**: 1751–1765

**Hilson P, Allemeersch J, Altmann T, Aubourg S, Avon A, Beynon J, Bhalerao RP, Bitton F, Caboche M, Cannoot B, et al** (2004) Versatile Gene-Specific Sequence Tags for *Arabidopsis* Functional Genomics: Transcript Profiling and Reverse Genetics Applications. Genome Res **14**: 2176–2189

**Van Hoewyk D, Takahashi H, Inoue E, Hess A, Tamaoki M, Pilon-Smits EAH** (2008) Transcriptome analyses give insights into selenium-stress responses and selenium tolerance mechanisms in Arabidopsis. Physiol Plant **132**: 236–253

**Hsiao TC** (1973) Plant Responses to Water Stress. Annu Rev Plant Physiol **24**: 519–570

**Huang X-D, El-Alawi Y, Penrose DM, Glick BR, Greenberg BM** (2004) A multi-process phytoremediation system for removal of polycyclic aromatic hydrocarbons from contaminated soils. Environ Pollut Barking Essex 1987 **130**: 465–476

**HuiJie L, CaiYun Y, Yun T, GuangHui L, TianLing Z** (2011) Using population dynamics analysis by DGGE to design the bacterial consortium isolated from mangrove sediments for biodegradation of PAHs. Int Biodeterior Biodegrad **65**: 269–275

**Islam MA, Macdonald SE** (2004) Ecophysiological adaptations of black spruce ( Picea mariana) and tamarack ( Larix laricina) seedlings to flooding. Trees **18**: 35–42

**Jans JH, Vedder H** (2008) European Environmental Law. Europa Law Pub.

**Jedrychowski W, Galas A, Pac A, Flak E, Camman D, Rauh V, Perera F** (2005) Prenatal Ambient Air Exposure to Polycyclic Aromatic Hydrocarbons and the Occurrence of Respiratory Symptoms over the First Year of Life. Eur J Epidemiol **20**: 775–782

**Jennings AA** (2012) Worldwide regulatory guidance values for surface soil exposure to carcinogenic or mutagenic polycyclic aromatic hydrocarbons. J Environ Manage **110**: 82–102

**Jin X-F, Shuai J-J, Peng R-H, Zhu B, Fu X-Y, Tian Y-S, Zhao W, Han H-J, Chen C, Xu J, et al** (2011) Identification of candidate genes involved in responses of *Arabidopsis* to polychlorinated biphenyls based on microarray analysis. Plant Growth Regul **65**: 127–135

**Johnsen AR, Wick LY, Harms H** (2005) Principles of microbial PAH-degradation in soil. Environ Pollut **133**: 71–84

**Jones MD, Crandell DW, Singleton DR, Aitken MD** (2011) Stable-isotope probing of the polycyclic aromatic hydrocarbon-degrading bacterial guild in a contaminated soil. Environ Microbiol **13**: 2623–2632

**Jones P, Vogt T** (2001) Glycosyltransferases in secondary plant metabolism: tranquilizers and stimulant controllers. Planta **213**: 164–174

**Juhasz AL, Stanley GA, Britz ML** (2000) Degradation of High Molecular Weight PAHs in Contaminated Soil by a Bacterial Consortium: Effects on Microtox and Mutagenicity Bioassays. Bioremediation J **4**: 271–283

**Kamangar F, Strickland PT, Pourshams A, Malekzadeh R, Boffetta P, Roth MJ, Abnet CC, Saadatian-Elahi M, Rakhshani N, Brennan P, et al** (2005) High Exposure to Polycyclic Aromatic Hydrocarbons May Contribute to High Risk of Esophageal Cancer in Northeastern Iran. Anticancer Res **25**: 425–428

**Kanaly RA, Harayama S** (2000) Biodegradation of High-Molecular-Weight Polycyclic Aromatic Hydrocarbons by Bacteria. J Bacteriol **182**: 2059–2067

**Karthikeyan AS, Varadarajan DK, Jain A, Held MA, Carpita NC, Raghothama KG** (2007) Phosphate starvation responses are mediated by sugar signaling in Arabidopsis. Planta **225**: 907–918

**Katsoyiannis A, Sweetman AJ, Jones KC** (2011) PAH molecular diagnostic ratios applied to atmospheric sources: a critical evaluation using two decades of source inventory and air concentration data from the UK. Environ Sci Technol **45**: 8897–8906

**Keunen E, Peshev D, Vangronsveld J, VAN DEN Ende W, Cuypers A** (2013) Plant sugars are crucial players in the oxidative challenge during abiotic stress: extending the traditional concept. Plant Cell Environ. doi: 10.1111/pce.12061

**Kim MG, Geng X, Lee SY, Mackey D** (2009a) The Pseudomonas syringae type III effector AvrRpm1 induces significant defenses by activating the *Arabidopsis* nucleotide-binding leucine-rich repeat protein RPS2. Plant J Cell Mol Biol **57**: 645–653

**Kim S-J, Kweon O, Cerniglia CE** (2009b) Proteomic applications to elucidate bacterial aromatic hydrocarbon metabolic pathways. Curr Opin Microbiol **12**: 301–309

**Kim S-J, Kweon O, Jones RC, Freeman JP, Edmondson RD, Cerniglia CE** (2007) Complete and integrated pyrene degradation pathway in Mycobacterium vanbaalenii PYR-1 based on systems biology. J Bacteriol **189**: 464–472

**Koch K** (2004) Sucrose metabolism: regulatory mechanisms and pivotal roles in sugar sensing and plant development. Curr Opin Plant Biol **7**: 235 – 246

**Kolb M, Harms H** (2000) Metabolism of fluoranthene in different plant cell cultures and intact plants. Environ Toxicol Chem **19**: 1304–1310

**Kotterman MJJ, Vis EH, Field JA** (1998) Successive Mineralization and Detoxification of Benzo[a]pyrene by the White Rot FungusBjerkandera sp. Strain BOS55 and Indigenous Microflora. Appl Environ Microbiol **64**: 2853–2858

**Krapp A, Berthomé R, Orsel M, Mercey-Boutet S, Yu A, Castaings L, Elftieh S, Major H, Renou J-P, Daniel-Vedele F** (2011) *Arabidopsis* roots and shoots show distinct temporal adaptation patterns toward nitrogen starvation. Plant Physiol **157**: 1255–1282

**Kuiper I, Lagendijk EL, Bloemberg GV, Lugtenberg BJJ** (2004) Rhizoremediation: a beneficial plant-microbe interaction. Mol Plant-Microbe Interactions MPMI **17**: 6–15

**Küpper H, Lombi E, Zhao FJ, McGrath SP** (2000) Cellular compartmentation of cadmium and zinc in relation to other elements in the hyperaccumulator *Arabidopsis* halleri. Planta **212**: 75–84

**Kvesitadze E, Sadunishvili T, Kvesitadze G** (2009) Mechanisms of Organic Contaminants Uptake and Degradation in Plants. World Acad Sci Eng Technol **55**: 458

**Landa P, Storchova H, Hodek J, Vankova R, Podlipna R, Marsik P, Ovesna J, Vanek T** (2010) Transferases and transporters mediate the detoxification and capacity to tolerate trinitrotoluene in Arabidopsis. Funct Integr Genomics **10**: 547–559

**Lao S-H, Loutre C, Brazier M, Coleman JO., Cole DJ, Edwards R, Theodoulou FL** (2003) 3,4-Dichloroaniline is detoxified and exported via different pathways in *Arabidopsis* and soybean. Phytochemistry **63**: 653–661

**Larcher W** (2003) Physiological Plant Ecology: Ecophysiology and Stress Physiology of Functional Groups. Springer

**Launen LA, Dutta J, Turpeinen R, Eastep ME, Dorn R, Buggs VH, Leonard JW, Häggblom MM** (2007) Characterization of the indigenous PAH-degrading bacteria of Spartina dominated salt marshes in the New York/New Jersey Harbor. Biodegradation **19**: 347–363

**Layton A, Smart AE, Chauhan A, Ripp SA, Williams D, Burton W, Moser S, Phillips JR, Palumbo AV, Sayler G** (2012) Ameliorating Risk: Culturable and Metagenomic Monitoring of the 14 Year Decline of a Genetically Engineered Microorganism at a Bioremediation Field Site. OMICS J. Bioremediation Biodegrad. 9:

**Lebas G** (2012) Etude du métabolisme carboné et azoté de Miscanthus x giganteus. Université de Picardie Jules Verne, France

**Lei A-P, Hu Z-L, Wong Y-S, Tam NF-Y** (2007) Removal of fluoranthene and pyrene by different microalgal species. Bioresour Technol **98**: 273–280

**Lichtenthaler H, Wellburn A** (1983) Determinations of total carotenoids and chlorophylls a and b of leaf extracts indifferent solvents. Biochem Soc Trans **603**: 591–592

**Lily MK, Bahuguna A, Dangwal K, Garg V** (2009) Degradation of Benzo [a] Pyrene by a novel strain Bacillus subtilis BMT4i (MTCC 9447). Braz J Microbiol **40**: 884–892

**Liste H-H, Alexander M** (2000a) Accumulation of phenanthrene and pyrene in rhizosphere soil. Chemosphere **40**: 11–14

**Liste H-H, Alexander M** (2000b) Plant-promoted pyrene degradation in soil. Chemosphere **40**: 7–10

**Liu H, Weisman D, Ye Y, Cui B, Huang Y, Colón-Carmona A, Wang Z** (2009) An oxidative stress response to polycyclic aromatic hydrocarbon exposure is rapid and complex in *Arabidopsis thaliana*. Plant Sci **176**: 375 – 382

**Lloyd JC, Zakhleniuk OV** (2004) Responses of primary and secondary metabolism to sugar accumulation revealed by microarray expression analysis of the *Arabidopsis* mutant, pho3. J Exp Bot **55**: 1221–1230

**Loh K-C, Cao B** (2008) Paradigm in biodegradation using Pseudomonas putida—A review of proteomics studies. Enzyme Microb Technol **43**: 1–12

**Loreti E, Poggi A, Novi G, Alpi A, Perata P** (2005) A Genome-Wide Analysis of the Effects of Sucrose on Gene Expression in *Arabidopsis* Seedlings under Anoxia. Plant Physiol **137**: 1130–1138

**Loutre C, Dixon DP, Brazier M, Slater M, Cole DJ, Edwards R** (2003) Isolation of a glucosyltransferase from *Arabidopsis thaliana* active in the metabolism of the persistent pollutant 3,4-dichloroaniline. Plant J **34**: 485–493

**Luch A** (2005) The carcinogenic effects of polycyclic aromatic hydrocarbons. Imperial College Press, Hackensack, NJ

**Lurin C, Andrés C, Aubourg S, Bellaoui M, Bitton F, Bruyère C, Caboche M, Debast C, Gualberto J, Hoffmann B, et al** (2004) Genome-wide analysis of *Arabidopsis* pentatricopeptide repeat proteins reveals their essential role in organelle biogenesis. Plant Cell **16**: 2089–2103

**Ma B, He Y, Chen H, Xu J, Rengel Z** (2010) Dissipation of polycyclic aromatic hydrocarbons (PAHs) in the rhizosphere: synthesis through meta-analysis. Environ Pollut Barking Essex 1987 **158**: 855–861

**MacGregor DR, Deak KI, Ingram PA, Malamy JE** (2008) Root System Architecture in *Arabidopsis* Grown in Culture Is Regulated by Sucrose Uptake in the Aerial Tissues. Plant Cell Online **20**: 2643–2660

**Maila MP, Cloete TE** (2004) Bioremediation of petroleum hydrocarbons through landfarming: Are simplicity and cost-effectiveness the only advantages? Rev Environ Sci Biotechnol **3**: 349–360

**Mallick S, Chatterjee S, Dutta TK** (2007) A novel degradation pathway in the assimilation of phenanthrene by Staphylococcus sp. strain PN/Y via meta-cleavage of 2-hydroxy-1-naphthoic acid: formation of trans-2,3-dioxo-5-(2'-hydroxyphenyl)-pent-4-enoic acid. Microbiol Read Engl **153**: 2104–2115

**Mancini R, Romano G, Sgambato A, Flamini G, Giovagnoli MR, Boninsegna A, Carraro C, Vecchione A, Cittadini A** (1999) Polycyclic Aromatic Hydrocarbon–DNA Adducts in Cervical Smears of Smokers and Nonsmokers. Gynecol Oncol **75**: 68–71

**Marmiroli N, Marmiroli M, Maestri E** (2006) PHYTOREMEDIATION AND PHYTOTECHNOLOGIES: A REVIEW FOR THE PRESENT AND THE FUTURE. *In* I Twardowska, HE Allen, MM Häggblom, S Stefaniak, eds, Soil Water Pollut. Monit. Prot. Remediat. Springer Netherlands, Dordrecht, pp 403–416

**Matsui T, Nomura Y, Takano M, Imai S, Nakayama H, Miyasaka H, Okuhata H, Tanaka S, Matsuura H, Harada K, et al** (2011) Molecular Cloning and Partial Characterization of a Peroxidase Gene Expressed in the Roots of <I>Portulaca oleracea</I> cv., One Potentially Useful in the Remediation of Phenolic Pollutants. Biosci Biotechnol Biochem **75**: 882–890

**Meßner B, Thulke O, Schäffner AR** (2003) *Arabidopsis* glucosyltransferases with activities toward both endogenous and xenobiotic substrates. Planta **217**: 138–146

**Miller RL, Garfinkel R, Horton M, Camann D, Perera FP, Whyatt RM, Kinney PL** (2004) Polycyclic aromatic hydrocarbons, environmental tobacco smoke, and respiratory symptoms in an inner-city birth cohort. Chest **126**: 1071–1078

**Mitsch WJ** (2012) What is ecological engineering? Ecol Eng **45**: 5–12

**Mittler R, Vanderauwera S, Gollery M, Van Breusegem F** (2004) Reactive oxygen gene network of plants. Trends Plant Sci **9**: 490–498

**Moya JL, Ros R, Picazo I** (1993) Influence of cadmium and nickel on growth, net photosynthesis and carbohydrate distribution in rice plants. Photosynth Res **36**: 75–80

**Mrozik A, Piotrowska-Seget Z, Łabuzek S** (2003) Bacterial degradation and bioremediation of polycyclic aromatic hydrocarbons. Pol J Environ Stud **12**: 15–25

**Murashige T, Skoog F** (1962) A Revised Medium for Rapid Growth and Bio Assays with Tobacco Tissue Cultures. Physiol Plant **15**: 473–497

**Muratova A, Hūbner T, Tischer S, Turkovskaya O, Möder M, Kuschk P** (2003) Plant--rhizosphere-microflora association during phytoremediation of PAH-contaminated soil. Int J Phytoremediation **5**: 137–151

**Narro ML, Cerniglia CE, Van Baalen C, Gibson DT** (1992) Metabolism of phenanthrene by the marine cyanobacterium Agmenellum quadruplicatum PR-6. Appl Environ Microbiol **58**: 1351–1359

**Ojajärvi IA, Partanen TJ, Ahlbom A, Boffetta P, Hakulinen T, Jourenkova N, Kauppinen TP, Kogevinas M, Porta M, Vainio HU, et al** (2000) Occupational exposures and pancreatic cancer: a meta-analysis. Occup Environ Med **57**: 316–324

**Panz K, Miksch K** (2012) Phytoremediation of explosives (TNT, RDX, HMX) by wild-type and transgenic plants. J Environ Manage **113**: 85–92

**Parlement Français** (2008) LOI n° 2008-757 du 1er août 2008 relative à la responsabilité environnementale et à diverses dispositions d'adaptation au droit communautaire dans le domaine de l'environnement.

**Pasternak T, Rudas V, Potters G, Jansen MAK** (2005) Morphogenic effects of abiotic stress: reorientation of growth in *Arabidopsis thaliana* seedlings. Environ Exp Bot **53**: 299–314

**Paul MJ, Foyer CH** (2001) Sink regulation of photosynthesis. J Exp Bot **52**: 1383–1400

**Paul MJ, Pellny TK** (2003) Carbon metabolite feedback regulation of leaf photosynthesis and development. J Exp Bot **54**: 539–547

**Peng R-H, Xiong A-S, Xue Y, Fu X-Y, Gao F, Zhao W, Tian Y-S, Yao Q-H** (2008) Microbial biodegradation of polyaromatic hydrocarbons. FEMS Microbiol Rev **32**: 927–955

**Perera FP, Li Z, Whyatt R, Hoepner L, Wang S, Camann D, Rauh V** (2009) Prenatal Airborne Polycyclic Aromatic Hydrocarbon Exposure and Child IQ at Age 5 Years. Pediatrics **124**: e195–e202

**Peshev D, Vergauwen R, Moglia A, Hideg É, Ende WV den** (2013) Towards understanding vacuolar antioxidant mechanisms: a role for fructans? J Exp Bot ers377

**Pilon-Smits E** (2005) Phytoremediation. Annu Rev Plant Biol **56**: 15–39

**Pirooznia M, Nagarajan V, Deng Y** (2007) GeneVenn - A web application for comparing gene lists using Venn diagrams. Bioinformation **1**: 420–422

**Pradhan SP, Conrad JR, Paterek JR, Srivastava VJ** (1998) Potential of Phytoremediation for Treatment of PAHs in Soil at MGP Sites. J Soil Contam **7**: 467–480

**Price J, Laxmi A, Martin SKS, Jang J-C** (2004) Global Transcription Profiling Reveals Multiple Sugar Signal Transduction Mechanisms in Arabidopsis. Plant Cell Online **16**: 2128–2150

**Provart T. and Z** (2003) A Browser-based Functional Classification SuperViewer for *Arabidopsis* Genomics. Curr Comput Mol Biol 271–272

**Pucciariello C, Parlanti S, Banti V, Novi G, Perata P** (2012) Reactive oxygen species-driven transcription in *Arabidopsis* under oxygen deprivation. Plant Physiol **159**: 184–196

**Pulford ID, Watson C** (2003) Phytoremediation of heavy metal-contaminated land by trees—a review. Environ Int **29**: 529 – 540

**Rahmani F, Hummel M, Schuurmans J, Wiese-Klinkenberg A, Smeekens S, Hanson J** (2009) Sucrose Control of Translation Mediated by an Upstream Open Reading Frame-Encoded Peptide. Plant Physiol **150**: 1356–1367

**Rai VK** (2002) Role of Amino Acids in Plant Responses to Stresses. Biol Plant **45**: 481–487

**Ramel F, Sulmon C, Bogard M, Couée I, Gouesbet G** (2009) Differential patterns of reactive oxygen species and antioxidative mechanisms during atrazine injury and sucrose-induced tolerance in *Arabidopsis thaliana* plantlets. BMC Plant Biol **9**: 28

**Ramel F, Sulmon C, Cabello-Hurtado F, Taconnat L, Martin-Magniette M-L, Renou J-P, Amrani AE, Couée I, Gouesbet G** (2007) Genome-wide interacting effects of sucrose and herbicide-mediated stress in *Arabidopsis thaliana*: novel insights into atrazine toxicity and sucrose-induced tolerance. BMC Genomics **8**: 450

**Ramel F, Sulmon C, Serra A-A, Gouesbet G, Couée I** (2012) Xenobiotic sensing and signalling in higher plants. J Exp Bot **63**: 3999–4014

**Ramesh A, Walker SA, Hood DB, Guillén MD, Schneider K, Weyand EH** (2004) Bioavailability and Risk Assessment of Orally Ingested Polycyclic Aromatic Hydrocarbons. Int J Toxicol **23**: 301–333

**Ramon M, Rolland F, Sheen J** (2008) Sugar Sensing and Signaling. Arab Book e0117

**Ratcliffe RG, Shachar-Hill Y** (2001) Probing Plant Metabolism with Nmr. Annu Rev Plant Physiol Plant Mol Biol **52**: 499–526

**Ravindra K, Sokhi R, Van Grieken R** (2008) Atmospheric polycyclic aromatic hydrocarbons: Source attribution, emission factors and regulation. Atmos Environ **42**: 2895–2921

**Rehmann L, Prpich GP, Daugulis AJ** (2008) Remediation of PAH contaminated soils: Application of a solid–liquid two-phase partitioning bioreactor. Chemosphere **73**: 798–804

**Rentz JA, Alvarez PJJ, Schnoor JL** (2005) Benzo[a]pyrene co-metabolism in the presence of plant root extracts and exudates: Implications for phytoremediation. Environ Pollut **136**: 477–484

**Richardson MD, Karcher DE, Purcell LC** (2001) Quantifying Turfgrass Cover Using Digital Image Analysis. Crop Sci **41**: 1884–1888

**Roitsch T** (1999) Source-sink regulation by sugar and stress. Curr Opin Plant Biol **2**: 198–206

**Rolland F, Moore B, Sheen J** (2002) Sugar Sensing and Signaling in Plants. Plant Cell **14**: s185–s205

**Rosa M, Prado C, Podazza G, Interdonato R, Gonzalez JA, Hilal M, Prado FE** (2009) Soluble sugars: Metabolism, sensing and abiotic stress: A complex network in the life of plants. Signal Behav **4**: 288–393

**Rozen S, Skaletsky H** (2000) Primer3 on the WWW for general users and for biologist programmers. Methods Mol Biol Clifton NJ **132**: 365–386

**Rundle A, Tang D, Hibshoosh H, Estabrook A, Schnabel F, Cao W, Grumet S, Perera FP** (2000) The relationship between genetic damage from polycyclic aromatic hydrocarbons in breast tissue and breast cancer. Carcinogenesis **21**: 1281–1289

**Russo L, Rizzo L, Belgiorno V** (2012) Ozone oxidation and aerobic biodegradation with spent mushroom compost for detoxification and benzo(a)pyrene removal from contaminated soil. Chemosphere **87**: 595–601

**Rybicki BA, Neslund-Dudas C, Nock NL, Schultz LR, Eklund L, Rosbolt J, Bock CH, Monaghan KG** (2006) Prostate cancer risk from occupational exposure to polycyclic aromatic hydrocarbons interacting with the GSTP1 Ile105Val polymorphism. Cancer Detect Prev **30**: 412–422

**Rylott EL, Budarina MV, Barker A, Lorenz A, Strand SE, Bruce NC** (2011) Engineering plants for the phytoremediation of RDX in the presence of the co-contaminating explosive TNT. New Phytol **192**: 405–413

**Salt DE, Blaylock M, Kumar NPBA, Dushenkov V, Ensley BD, Chet I, Raskin I** (1995) Phytoremediation: A Novel Strategy for the Removal of Toxic Metals from the Environment Using Plants. Nat Biotechnol **13**: 468–474

**Samanta SK, Singh OV, Jain RK** (2002) Polycyclic aromatic hydrocarbons: environmental pollution and bioremediation. Trends Biotechnol **20**: 243–248

**Sandermann Jr. H** (1992) Plant metabolism of xenobiotics. Trends Biochem Sci **17**: 82–84

**Sandermann Jr. H, Scheel D, Trenck T v. d.** (1984) Use of plant cell cultures to study the metabolism of environmental chemicals. Ecotoxicol Environ Saf **8**: 167–182

**Saraswathy A, Hallberg R** (2002) Degradation of pyrene by indigenous fungi from a former gasworks site. FEMS Microbiol Lett **210**: 227–232

**Sarret G, Harada E, Choi Y-E, Isaure M-P, Geoffroy N, Fakra S, Marcus MA, Birschwilks M, Clemens S, Manceau A** (2006) Trichomes of Tobacco Excrete Zinc as Zinc-Substituted Calcium Carbonate and Other Zinc-Containing Compounds. Plant Physiol **141**: 1021–1034

**Sattler SE, Mene-Saffrane L, Farmer EE, Krischke M, Mueller MJ, DellaPenna D** (2006) Nonenzymatic Lipid Peroxidation Reprograms Gene Expression and Activates Defense Markers in *Arabidopsis* Tocopherol-Deficient Mutants. Plant Cell **18**: 3706–3720

**Schamfuß S, Neu TR, Harms H, van der Meer JR, Tecon R, Wick LY** (2013a) Mycelial Networks Enhance the Bioavailability of PAH in Water Unsaturated Environments. Environ. Sci. Technol.

**Schamfuß S, Neu TR, van der Meer JR, Tecon R, Harms H, Wick LY** (2013b) Impact of Mycelia on the Accessibility of Fluorene to PAH-Degrading Bacteria. Environ Sci Technol **47**: 6908–6915

**Schneider J, Grosser R, Jayasimhulu K, Xue W, Warshawsky D** (1996) Degradation of pyrene, benz[a]anthracene, and benzo[a]pyrene by Mycobacterium sp. strain RJGII-135, isolated from a former coal gasification site. Appl Environ Microbiol **62**: 13–19

**Schnoor JL, Licht LA, McCutcheon SC, Wolfe NL, Carreira LH** (1995) Phytoremediation of Organic and Nutrient Contaminants. Environ Sci Technol **29**: 318A–323A

**Schober W, Lubitz S, Belloni B, Gebauer G, Lintelmann J, Matuschek G, Weichenmeier I, Eberlein-König B, Buters J, Behrendt H** (2007) Environmental polycyclic aromatic hydrocarbons (PAHs) enhance allergic inflammation by acting on human basophils. Inhal Toxicol **19 Suppl 1**: 151–156

**Schreiber R, Altenburger R, Paschke A, Küster E** (2008) How to deal with lipophilic and volatile organic substances in microtiter plate assays. Environ Toxicol Chem SETAC **27**: 1676–1682

**Shim D, Kim S, Choi Y-I, Song W-Y, Park J, Youk ES, Jeong S-C, Martinoia E, Noh E-W, Lee Y** (2013) Transgenic poplar trees expressing yeast cadmium factor 1 exhibit the characteristics necessary for the phytoremediation of mine tailing soil. Chemosphere **90**: 1478–1486

**Singleton DR, Hunt M, Powell SN, Frontera-Suau R, Aitken MD** (2007) Stable-isotope probing with multiple growth substrates to determine substrate specificity of uncultivated bacteria. J Microbiol Methods **69**: 180–187

**Singleton DR, Jones MD, Richardson SD, Aitken MD** (2012) Pyrosequence analyses of bacterial communities during simulated in situ bioremediation of polycyclic aromatic hydrocarbon-contaminated soil. Appl Microbiol Biotechnol. doi: 10.1007/s00253-012-4531-0

**Singleton DR, Powell SN, Sangaiah R, Gold A, Ball LM, Aitken MD** (2005) Stable-Isotope Probing of Bacteria Capable of Degrading Salicylate, Naphthalene, or Phenanthrene in a Bioreactor Treating Contaminated Soil. Appl Environ Microbiol **71**: 1202–1209

**Sitaras IE, Bakeas EB, Siskos PA** (2004) Gas/particle partitioning of seven volatile polycyclic aromatic hydrocarbons in a heavy traffic urban area. Sci Total Environ **327**: 249–264

**Sivaraman L, Leatham MP, Yee J, Wilkens LR, Lau AF, Marchand LL** (1994) CYP1A1 Genetic Polymorphisms and in Situ Colorectal Cancer. Cancer Res **54**: 3692–3695

**Sivitz AB, Reinders A, Ward JM** (2008) *Arabidopsis* Sucrose Transporter AtSUC1 Is Important for Pollen Germination and Sucrose-Induced Anthocyanin Accumulation. Plant Physiol **147**: 92–100

**Skipsey M, Knight KM, Brazier-Hicks M, Dixon DP, Steel PG, Edwards R** (2011) Xenobiotic Responsiveness of *Arabidopsis thaliana* to a Chemical Series Derived from a Herbicide Safener. J Biol Chem **286**: 32268–32276

**Smith LE, Denissenko MF, Bennett WP, Li H, Amin S, Tang M, Pfeifer GP** (2000) Targeting of Lung Cancer Mutational Hotspots by Polycyclic Aromatic Hydrocarbons. J Natl Cancer Inst **92**: 803–811

**Smith MR** (1990) The biodegradation of aromatic hydrocarbons by bacteria. Biodegradation **1**: 191–206

**Ana Sofia Duque AMDA** (2013) Abiotic Stress Responses in Plants: Unraveling the Complexity of Genes and Networks to Survive. doi: 10.5772/52779

**Solfanelli C, Poggi A, Loreti E, Alpi A, Perata P** (2006) Sucrose-Specific Induction of the Anthocyanin Biosynthetic Pathway in Arabidopsis. Plant Physiol **140**: 637–646

**Sulmon C, Gouesbet G, Amrani AE, Couée I** (2006) Sugar-induced tolerance to the herbicide atrazine in *Arabidopsis* seedlings involves activation of oxidative and xenobiotic stress responses. Plant Cell Reports **25**: 489–498

**Sulmon C, Gouesbet G, Binet F, Martin-Laurent F, El Amrani A, Couée I** (2007) Sucrose amendment enhances phytoaccumulation of the herbicide atrazine in *Arabidopsis thaliana*. Environ Pollut **145**: 507–515

**Sulmon C, Gouesbet G, Couée I, Amrani AE** (2004) Sugar-induced tolerance to atrazine in *Arabidopsis* seedlings: interacting effects of atrazine and soluble sugars on psbA mRNA and D1 protein levels. Plant Sci **167**: 913–923

**Sulmon C, Gouesbet G, El Amrani A, Couee I** Involvement of the ethylene-signalling pathway in sugar-induced tolerance to the herbicide atrazine in *Arabidopsis thaliana* seedlings. J Plant Physiol **164**: 1083–1092

**Syed K, Doddapaneni H, Subramanian V, Lam YW, Yadav JS** (2010) Genome-to-function characterization of novel fungal P450 monooxygenases oxidizing polycyclic aromatic hydrocarbons (PAHs). Biochem Biophys Res Commun **399**: 492–497

**Szabados L, Savouré A** (2010) Proline: a multifunctional amino acid. Trends Plant Sci **15**: 89–97

**Tadege M, Dupuis I, Kuhlemeier C** (1999) Ethanolic fermentation: new functions for an old pathway. Trends Plant Sci **4**: 320–325

**Taguchi G, Ubukata T, Nozue H, Kobayashi Y, Takahi M, Yamamoto H, Hayashida N** (2010) Malonylation is a key reaction in the metabolism of xenobiotic phenolic glucosides in *Arabidopsis* and tobacco. Plant J **63**: 1031–1041

**team RDC** (2013) R: a language and environment for statistical computing. R foundation for statistical computing, Vienna, Austria

**Técher D, Laval-Gilly P, Henry S, Bennasroune A, Formanek P, Martinez-Chois C, D'Innocenzo M, Muanda F, Dicko A, Rejšek K, et al** (2011) Contribution of Miscanthus x giganteus root exudates to the biostimulation of PAH degradation: An in vitro study. Sci Total Environ **409**: 4489–4495

**Técher D, Laval-Gilly P, Henry S, Bennasroune A, Martinez-Chois C, D'Innocenzo M, Falla J** (2012) Prospects of Miscanthus x giganteus for PAH phytoremediation: A microcosm study. Ind Crops Prod **36**: 276–281

**Techer D, Martinez-Chois C, Laval-Gilly P, Henry S, Bennasroune A, D'Innocenzo M, Falla J** (2012) Assessment of Miscanthus × giganteus for rhizoremediation of long term PAH contaminated soils. Appl Soil Ecol **62**: 42–49

**Thimm O, Bläsing O, Gibon Y, Nagel A, Meyer S, Krüger P, Selbig J, Müller LA, Rhee SY, Stitt M** (2004) MAPMAN: a user-driven tool to display genomics data sets onto diagrams of metabolic pathways and other biological processes. Plant J Cell Mol Biol **37**: 914–939

**Thum KE, Shin MJ, Palenchar PM, Kouranov A, Coruzzi GM** (2004) Genome-wide investigation of light and carbon signaling interactions in Arabidopsis. Genome Biol **5**: R10

**Timpa JD, Burke JJ, Quisenberry JE, Wendt CW** (1986) Effects of Water Stress on the Organic Acid and Carbohydrate Compositions of Cotton Plants. Plant Physiol **82**: 724–728

**Trzesicka-Mlynarz D, Ward OP** (1995) Degradation of polycyclic aromatic hydrocarbons (PAHs) by a mixed culture and its component pure cultures, obtained from PAH-contaminated soil. Can J Microbiol **41**: 470–476

**Al-Turky AI** (2009) Microbial polycyclic aromatic hydrocarbons degradation in soil. Res J Environ Toxicol **3**: 1–8

**UE** (2004) Directive 2004/35/CE.

**UN** (1992) Report of the United Nations conference on Envrionment and Development.

**Valluru R, Ende WV den** (2008) Plant fructans in stress environments: emerging concepts and future prospects. J Exp Bot **59**: 2905–2916

**Vavrek MC, Campbell WJ** (2002) Identification of Plant Traits That Enhances Biodegradation of Oil.

**Venny, Gan S, Ng HK** (2012) Modified Fenton oxidation of polycyclic aromatic hydrocarbon (PAH)-contaminated soils and the potential of bioremediation as post-treatment. Sci Total Environ **419**: 240–249

**Verslues PE, Zhu J-K** (2005) Before and beyond ABA: upstream sensing and internal signals that determine ABA accumulation and response under abiotic stress. Biochem Soc Trans **33**: 375–379

**Vervaeke P, Luyssaert S, Mertens J, Meers E, Tack FM., Lust N** (2003) Phytoremediation prospects of willow stands on contaminated sediment: a field trial. Environ Pollut **126**: 275–282

**Vieira Dos Santos C, Rey P** (2006) Plant thioredoxins are key actors in the oxidative stress response. Trends Plant Sci **11**: 329–334

**Vilchez-Vargas R, Junca H, Pieper DH** (2010) Metabolic networks, microbial ecology and "omics" technologies: towards understanding in situ biodegradation processes. Environ Microbiol **12**: 3089–3104

**Wang K, Zhang J, Zhu Z, Huang H, Li T, He Z, Yang X, Alva A** (2012a) Pig manure vermicompost (PMVC) can improve phytoremediation of Cd and PAHs co-contaminated soil by Sedum alfredii. J Soils Sediments **12**: 1089–1099

**Wang MC, Chen YT, Chen SH, Chang Chien SW, Sunkara SV** (2012b) Phytoremediation of pyrene contaminated soils amended with compost and planted with ryegrass and alfalfa. Chemosphere **87**: 217–225

**Wang P, Song C-P** (2008) Guard-cell signalling for hydrogen peroxide and abscisic acid. New Phytol **178**: 703–718

**Wang Z, Liu Z, Yang Y, Li T, Liu M** (2012c) Distribution of PAHs in tissues of wetland plants and the surrounding sediments in the Chongming wetland, Shanghai, China. Chemosphere **89**: 221–227

**Ward MH, Sinha R, Heineman EF, Rothman N, Markin R, Weisenburger DD, Correa P, Zahm SH** (1997) Risk of adenocarcinoma of the stomach and esophagus with meat cooking method and doneness preference. Int J Cancer **71**: 14–19

**Warshawsky D, Cody T, Radike M, Reilman R, Schumann B, LaDow K, Schneider J** (1995) Biotransformation of benzo[a]pyrene and other polycyclic aromatic hydrocarbons and heterocyclic analogs by several green algae and other algal species under gold and white light. Chem Biol Interact **97**: 131–148

**Watts AW, Ballestero TP, Gardner KH** (2006) Uptake of polycyclic aromatic hydrocarbons (PAHs) in salt marsh plants Spartina alterniflora grown in contaminated sediments. Chemosphere **62**: 1253–1260

**Weisman D, Alkio M, Colón-Carmona A** (2010) Transcriptional responses to polycyclic aromatic hydrocarbon-induced stress in *Arabidopsis thaliana* reveal the involvement of hormone and defense signaling pathways. BMC Plant Biol **10**: 59

**Wilson SC, Jones KC** (1993) Bioremediation of soil contaminated with polynuclear aromatic hydrocarbons (PAHs): A review. Environ Pollut **81**: 229–249

**Wind J, Smeekens S, Hanson J** (2010) Sucrose: Metabolite and signaling molecule. Phytochemistry **71**: 1610–1614

**Wu J, Omokawa H, Hatzios KK** (1996) GlutathioneS-Transferase Activity in Unsafened and Fenclorim-Safened Rice (Oryza sativa). Pestic Biochem Physiol **54**: 220–229

**Xu J, Su Z-H, Chen C, Han H-J, Zhu B, Fu X-Y, Zhao W, Jin X-F, Wu A-Z, Yao Q-H** (2012) Stress responses to phenol in *Arabidopsis* and transcriptional changes revealed by microarray analysis. Planta **235**: 399–410

**Xu SY, Chen YX, Wu WX, Wang KX, Lin Q, Liang XQ** (2006) Enhanced dissipation of phenanthrene and pyrene in spiked soils by combined plants cultivation. Sci Total Environ **363**: 206–215

**Yi H, Crowley DE** (2007) Biostimulation of PAH Degradation with Plants Containing High Concentrations of Linoleic Acid. Environ Sci Technol **41**: 4382–4388

**Zhan X, Zhang X, Yin X, Ma H, Liang J, Zhou L, Jiang T, Xu G** (2012) H(+)/phenanthrene symporter and aquaglyceroporin are implicated in phenanthrene uptake by wheat (Triticum aestivum L.) roots. J Environ Qual **41**: 188–196

**Zhan X-H, Ma H-L, Zhou L-X, Liang J-R, Jiang T-H, Xu G-H** (2010) Accumulation of phenanthrene by roots of intact wheat (Triticum acstivnm L.) seedlings: passive or active uptake? BMC Plant Biol **10**: 52

**Zhanf X-X, Cheng S-P, Zhu C-J, Sun S-L** (2006) Microbial PAH-Degradation in Soil: Degradation Pathways and Contributing Factors. Pedosphere **16**: 555–565

**Zhang J, Yin R, Lin X, Liu W, Chen R, Li X** (2010) Interactive Effect of Biosurfactant and Microorganism to Enhance Phytoremediation for Removal of Aged Polycyclic Aromatic Hydrocarbons from Contaminated Soils. J Heal Sci **56**: 257–266

**Zrenner R, Stitt M, Sonnewald U, Boldt R** (2006) Pyrimidine and purine biosynthesis and degradation in plants. Annu Rev Plant Biol **57**: 805–836

**Zurbriggen MD, Carrillo N, Hajirezaei M-R** (2010) ROS signaling in the hypersensitive response. Plant Signal Behav **5**: 393–396

VU :

**Le Directeur de Thèse**
(Nom et Prénom)

VU :

**Le Responsable de l'École doctorale**

**VU pour autorisation de soutenance**

**Rennes, le**

**Le Président de l'Université de Rennes 1**

**Guy CATHELINEAU**

**VU après soutenance pour autorisation de publication :**

**Le Président de Jury,**
(Nom et Prénom)